



CSCE

**3RD AUGUST
2023**

PROCEEDINGS BOOK

**5TH CONFERENCE ON SUSTAINABILITY IN CIVIL
ENGINEERING**



EDITOR-IN-CHIEF

DR. MAJID ALI

EDITORS

ENGR. IQBAL AHMAD

ENGR. SHAHEED ULLAH

ISBN 978-969-23344-4-0

**CAPITAL UNIVERSITY OF SCIENCE AND TECHNOLOGY, ISLAMABAD,
DEPARTMENT OF CIVIL ENGINEERING**

Publication Note

This book has been produced from files received electronically by the individual authors. The publisher makes no representation, express or implied, with regard to accuracy of the information contained in this book and cannot accept any legal responsibility or liability for any errors or omissions that may have been made. All titles published by 5th Conference on Sustainability in Civil Engineering and Capital University of Science and Technology (CUST), Islamabad, Pakistan publishers are under copyright protection said copyrights being the property of their respective holders. All Rights Reserved. No part of this book may be reproduced or transmitted in any form or by any means, graphic, electronic or mechanical, including photocopying, recording, taping or by any information storage or retrieval system, without the permission in writing from the publisher.

August 3, 2023

Published By

Department of Civil Engineering

Capital University of Science and Technology, Islamabad, Pakistan

ISBN: 978-969-23344-4-0

www.csce.cust.edu.pk

www.cust.edu.pk

Foreword

Welcome to the CSCE 2023, 5th Conference on Sustainability in Civil Engineering (CSCE'23) was held by Department of Civil Engineering, Capital University of Science and Technology, Islamabad, Pakistan. The main focus of CSCE'23 was to highlight sustainability related to the field of civil engineering. It aimed to provide a platform for civil engineers from academia as well as industry to share their practical experiences and different research findings in their relevant specializations. We hope all the participants experienced a remarkable opportunity for the academic and industrial communities to address new challenges, share solutions and discuss future research directions. The conference accommodated several parallel sessions of different specialties, where the researchers and engineers interacted and enhanced their understanding of sustainability in the civil engineering dynamics.

This year, we had nine wonderful and renowned keynote speakers for this edition of CSCE. We had received 133 manuscripts from different countries around the world including UK, Ireland, Canada, Australia, Italy, Cyprus, China, Kazakhstan, Nigeria, Malaysia, KSA, and Pakistan. All papers had undergone a comprehensive and critical double-blind review process. The review committee was comprised of 57 PhDs serving in industry and academia of UK, Ireland, USA, Australia, New Zealand, Singapore, Hong Kong, Poland, Italy, Chile, Malaysia, China, Oman, Bahrain, KSA, and Pakistan. After the screening and review process, 56 papers were presented in conference. Among 56 papers, 18 opted for MDPI proceedings. The remaining 38 papers are included in this proceedings book.

We are grateful to all the reviewers and keynote speakers who have dedicated their precious time to share their expertise and experience. With this opportunity, we would also like to express our gratitude to everyone, especially all the faculty and staff at the Capital University of Science and Technology for their great support and participation. In this regard, the participation and cooperation of all authors, presenters and participants are also acknowledged, without whom this conference would not have been possible. Last but not least, an appreciation to our advising and organizing committees whose hard work and dedication has made this day possible.

Conference Chair of CSCE'23

Dr. Majid Ali

*Capital University of Science & Technology,
Islamabad, Pakistan*

Technical Committee Members

Dr. Shunde Qin	Jacobs Sutton Coldfield, UK
Dr. Furqan Qamar	WSP, UK
Dr. Afaq Ahmed	University of Memphis, USA
Dr. Mohsin Shehzad	WSP, New Zealand
Dr. Claudio Oyarzo-Vera	UCSC College of Engineering, Chile
Dr. Munir Ahmed	DAR, KSA
Dr. Rabee Shamass	London South Bank University, UK
Dr. Mehran Khan	University College Dublin, Ireland
Dr. Piotr Smarzewski	Military University of Technology, Poland
Dr. Jincheng Liu	Nanyang Technological University, Singapore
Dr. Nicola Fontana	Universita Degli Studi del Sannio, Italy
Dr. Muhammad Shakeel	Hong Kong UST, Hong Kong
Dr. Anas Bin Ibrahim	MARA University of Technology, Malaysia
Dr. Noor Aina Misnor	Universiti Pertahanan Nasional, Malaysia
Dr. Li Li	Northwest A&F University, China
Dr. Mohsin Usman Qureshi	Sohar University, Oman
Dr. Umar Farooq	Islamic University of Madinah, KSA
Dr. Uneb Gazder	University of Bahrain, Bahrain
Dr. Irfan Yousuf	CC & EC, World Bank Group, Pakistan
Dr. Hassan Farooq	DD Consultancy Directorate, Pakistan
Dr. M Zia ur Rehman Hashmi	Global Change Impact Studies Centre, Pakistan

Dr. Hassan Nasir	WSSP, Peshawar, Pakistan
Dr. Shahid Nasir	FE Pvt. Ltd, Islamabad, Pakistan
Dr. Rao Arsalan Khushnood	Tunnelling Inst. of Pak. (TIP), Islamabad, Pakistan
Dr. Hammad Anis Khan	NUST, Islamabad, Pakistan
Dr. Imran Hashmi	NUST, Islamabad, Pakistan
Dr. Habib Ur Rehman	UET, Lahore, Pakistan
Dr. Noor Muhammad Khan	UET, Lahore, Pakistan
Dr. Ammad Hassan	UET, Lahore, Pakistan
Dr. Khurram Rashid	UET, Lahore, Pakistan
Dr. Qaisar Ali	UET, Peshawar, Pakistan
Dr. Amjad Naseer	UET, Peshawar, Pakistan
Dr. Ayub Elahi	UET, Taxila, Pakistan
Dr. Faisal Shabbir	UET, Taxila, Pakistan
Dr. Naveed Ahmad (Transportation)	UET, Taxila, Pakistan
Dr. Naveed Ahmad (Geotech)	UET, Taxila, Pakistan
Dr. Usman Ali Naeem	UET, Taxila, Pakistan
Dr. Jawad Hussain	UET, Taxila, Pakistan
Dr. Faheem Butt	UET, Taxila, Pakistan
Dr. Irshad Qureshi	UET, Taxila, Pakistan
Dr. Muhammad Usman Arshid	UET, Taxila, Pakistan
Dr. Farrukh Arif	NED, Karachi, Pakistan
Dr. Tahir Mehmood	COMSATS, Wah, Pakistan

Dr. Ahsen Maqsoom	COMSATS, Wah, Pakistan
Dr. Hassan Ashraf	COMSATS Wah, Pakistan
Dr. Adnan Nawaz	COMSATS, Wah, Pakistan
Dr. Muhammad Faisal Javed	COMSATS, Abbottabad, Pakistan
Dr. Rashid Farooq	IIU, Islamabad, Pakistan
Dr. Zeeshan Alam	IIU, Islamabad, Pakistan
Dr. Mudasser Muneer Khan	BZU, Multan, Pakistan
Dr. M. Shoaib	BZU, Multan, Pakistan
Dr. Anwar Khitab	MUST, Pakistan, Pakistan
Dr. Salman Ali Suhail	University of Lahore, Pakistan
Dr. Shoukat Ali Khan	Abasyn, Peshawar, Pakistan
Dr. Sabahat Hassan	HITEC University, Taxila, Pakistan
Dr. Jehangir Durrani	Iqra National University, Peshawar, Pakistan
Dr. Khursheed Ahmed	KIU, Gilgit, Pakistan

Advisory Committee

Dr. M. Mansoor Ahmed

(Vice-Chancellor CUST Islamabad)

Patron

Dr. Imtiaz Ahmed Taj

(Dean Faculty of Engineering)

General Advisor

Dr. Ishtiaq Hassan

(Head of Civil Engineering Department)

Principle Advisor

CSCE Industrial Partners for its 5th Edition



Global Climate-Change
Impact Studies Centre



Engineering & Design
Consultants



City Engineering
Consultants



MKAI Climate Consulting



ZAC Engineers



MARK Associates



Naqvi & Siddiquie

Organizing Committee

Dr. Majid Ali
Chair

Dr. M. Ashraf Javid
Co – Chair

Engr. Shaheed Ullah
Conference Secretary – I

Engr. Iqbal Ahmad
Conference Secretary – II

Keynote Speakers

Dr. Wajiha Shahzad

Massey University, New Zealand

Unlocking the Potential of Offsite Construction for Developing Economies

Dr. Afaq Ahmed

University of Memphis, USA

State of The Art Techniques for Structural Health Monitoring of Structures

Dr. Hamza Farooq Gabriel

NUST, Islamabad, Pakistan

Sustainable Green Eco-Technologies for the Wastewater Treatment

Dr. Hossein Derakhshan

QUT, Australia

Seismic Vulnerability Assessment of Unreinforced Masonry Buildings

Dr. Anwar Khitab

MUST, Mirpur, Pakistan

Carbon Storage in Building Materials for a Greener Future

Dr. Imran Muhammad

Massey University, New Zealand

Prosperous Cities Transition - How Do Pakistani Cities Thrive in Future by Adopting Transit Oriented Development (TOD) Model?

Dr. Mizan Ahmed

Curtin University, Australia

Sustainable Use of High-Performance-Fiber-Reinforced Cementitious Composites.

Dr. Robert Evans

Nottingham Trent University, UK

The Use of Ground Penetrating Radar (GPR) to Improve Sustainability in Pavement Engineering Projects

Dr. Sajjala Sreedhar Reddy

University of Nizwa, Oman

Role of Civil Engineering in Sustainable Development

TABLE OF CONTENTS

PAPER ID	TITLE	PAGE NO.
PAPER ID. 23-106:	Synthesis and Dispersion Mechanism of Nanomaterials in Cement-Based Composites: A State-Of-The-Art Review	1
PAPER ID. 23-107:	Improved Compressive Performance of Bio-Induced Sisal Fibers Reinforced Concrete	7
PAPER ID. 23-108:	Developing High Performance Concrete Using Jute Fibers	15
PAPER ID. 23-109:	Response Surface Methodology Based Optimized Mix Design for Self-Compacting Concrete Blended with Metakaolin Waste	21
PAPER ID. 23-110:	Reliability of Cores Test Result at Elevated Temperature in Case of Normal Strength Concrete	27
PAPER ID. 23-111:	Structural Performance of E-Waste Concrete Reinforced with Different Fibres	35
PAPER ID. 23-112:	Effect of Indigenous Volcanic Ash as Partial Replacement of Cement on Mechanical Properties of Concrete at Elevated Temperature	41
PAPER ID. 23-113:	The Effect of Plastic Fibers On the Mechanical Properties, Ductility and Environmental Performance of Concrete – A Review	47
PAPER ID. 23-116:	Exploring the Potential of Moss Concrete as An Eco-Friendly Solution to Mitigate Urban Heat Island Effect	56
PAPER ID. 23-124:	Enhanced Performance of Brick Aggregate Concrete Using Partial Substitution of Sand with Waste Glass and Flax Fibre Intrusion	64
PAPER ID. 23-125:	Assessing the Flexural Strength of a Beam Using Waste Plastic as a Partial Substitute for Coarse Aggregate	72
PAPER ID. 23-126:	Bacterial Self-Healing for Sustainable Concrete: A Comparative Study of Vegetative and Spore-Forming Bacteria	78
PAPER ID. 23-128:	Effect of Bentonite & Polypropylene Fibers On Fresh and Hardened Properties of Fly Ash Based Geopolymer Concrete	86
PAPER ID. 23-130:	Performance of Self-Compacting Concrete with Incorporation of Silica Fume and Coal Bottom Ash	94
PAPER ID. 23-133:	Effect of Heat on Self-Compacting Concrete with Partial Substitution of Foundry Sand as Fine Aggregate and Addition of Propylene Fibers	101
PAPER ID. 23-135:	Concrete Evolution: An Analysis of Recent Advancements and Innovations	108
PAPER ID. 23-137:	Durability Characteristics of Self-Compacting Concrete with Partial Substitution of Foundry Sand as Fine Aggregate and Addition of Propylene Fibers	116
PAPER ID. 23-201:	Predicting the Residual Flexural Capacity of Fire Exposed Reinforced Concrete Beams Using Gene Expression Programming	123

PAPER ID	TITLE	PAGE NO.
PAPER ID. 23-202:	Strength Prediction of Various Beams Through the Artificial Neural Network	131
PAPER ID. 23-206:	Exploring Vibration Measurement Precision: A Comparative Analysis of a DIY, Low-Cost Acceleration Measurement Unit Versus A Premium Standard Accelerometer System	139
PAPER ID. 23-214:	Innovative Solutions for Sustainable Building Strengthening: Glass Fiber Reinforced Concrete	145
PAPER ID. 23-303:	Critical Factors Influencing the Adoption of The Build Operate Transfer (BOT) System in The Gulf Areas: A Comprehensive Review	152
PAPER ID. 23-401:	Application of Nonstationary in Climate Variability – A Case Study of South Punjab, Pakistan	157
PAPER ID. 23-402:	Designing the Remote and Sustainable Water Management System	162
PAPER ID. 23-405:	Scour Reduction Around Bridge Abutments Using Industrial By-Products as A Countermeasures-An Experimental Approach	170
PAPER ID. 23-407:	Bridge Pier Scour Reduction Investigation using Different Vegetation Elements as Countermeasure	176
PAPER ID. 23-408:	Experimental Investigation of Square-Shaped Sacrificial Piles on Scour Depth of Compound Bridge Pier	181
PAPER ID. 23-501:	Investigating the Effect of Shear Rate in The Shear Thinning Behaviour of Waste Plastic-Modified Asphalt Binder	189
PAPER ID. 23-502:	Construction, Conflict, Claim, And Compensation (4C) – Case Study – Faizabad Highway Interchange Project Islamabad, Pakistan	196
PAPER ID. 23-504:	Effects of Different Aggregate Gradations on Rutting Susceptibility of Hot Mix Asphalt (HMA)	203
PAPER ID. 23-505:	Road Accident Prevention Using Sustainable Methods	210
PAPER ID. 23-506:	Model-Based Relationship Between Risk-Taking Behaviour of Motorcyclists and Its Corresponding Factors. A Case Study at Srinagar Highway Islamabad After Making It Signal-Free Alignment	217
PAPER ID. 23-508:	Application of Plastic Aggregates in Asphalt Mix Paving for Sustainable Environment	225
PAPER ID. 23-510:	Optimizing Traffic Flow at Sangjani Toll Plaza in Islamabad: A Simulation Study using Different Lane Patterns	232
PAPER ID. 23-601:	Impact of Silica Fume and Biochar Treatment on The Mechanical Characteristics of Low Plastic Soils	238
PAPER ID. 23-605:	Slope Stability Analysis and Design Using Numerical Techniques: A Case Study	244

PAPER ID	TITLE	PAGE NO.
PAPER ID. 23-609:	Evaluation of Strength Parameter of Indigenous Soil under Varying Surcharge Load	250
PAPER ID. 23-705:	Treatment of Domestic Wastewater with Anaerobic Fluidized Membrane Bioreactor (An-FMBR) And Control of Membrane Fouling with Addition Of GAC	257



SYNTHESIS AND DISPERSION MECHANISM OF NANOMATERIALS IN CEMENT-BASED COMPOSITES: A STATE-OF-THE-ART REVIEW

^a Hassan Amjad, ^b Farhan Ahmad*

a: NICE, SCEE, NUST, H/12 Campus, Islamabad, 44000, Pakistan, hassanamjaduet@gmail.com

b: School of Engineering, Design and Built Environment, Western Sydney University, Australia, F.ahmad@westernsydney.edu.au

* Corresponding author: Email ID: F.ahmad@westernsydney.edu.au

Abstract- Nanomaterials have emerged as a promising avenue for enhancing the reinforcement of cementitious materials, revolutionizing the concrete industry. Incorporating nanoparticles into concrete has shown significant improvements in mechanical performance, including increased strength and resilience. This paper provides a comprehensive overview of recent studies on the synthesis and dispersion of nanomaterials in cementitious materials, encompassing graphene oxide, graphene, nano-titanium oxide, CNTs, nano-alumina, nano-clay, nano-kaolin, nano-silica, and nano-ferric oxide. The findings highlight the advancements in nanomaterial integration and their profound impact on concrete properties. Additionally, the review identifies the challenges associated with nanoparticle dispersion and discusses techniques such as ultrasonication and the use of surfactants to improve dispersion in cement composites, thereby enhancing mechanical and photocatalytic properties.

Keywords- Nanomaterials, Synthesis, Dispersion mechanism, Cementitious composites

1 Introduction

Nanomaterials have revolutionized the concrete industry, offering immense potential to enhance reinforcement in cementitious materials [1]. Incorporating innovative nanoparticles and fibers into concrete has resulted in significant improvements in mechanical performance, increasing strength and resilience. Nanomaterials such as nano-silica, nano-clay, carbon nanofibers, carbon nanotubes (CNTs), nano-titanium dioxide, graphene oxide, and nano-graphite platelets have been successfully employed to reinforce cementitious composites [2]–[7]. These nanomaterials have led to the development of cementitious composites with exceptional properties, including energy absorption and resistance to crack propagation. Challenges arise from agglomeration due to van der Waals forces, impacting the workability of cement; however, nanoparticles can fill voids, resulting in a dense microstructure and adding self-cleaning and air-purifying properties [8], [9].

Researchers have extensively investigated the integration of nanomaterials with cement-based composites to enhance their structural performance. Jamal et al. [10] studied the effect of synthesized nanomaterials such as nano-silica, nano alumina, graphene oxide, and carbon nanotube on the mechanical performance of concrete and found that the strength properties were significantly improved. Further, they recommended the dosages of nano-silica (1-4%), nano alumina (1-3%), graphene oxide (0.05-0.1%), and carbon nanotube (0.1-0.5%) for practical applications in the concrete industry. Similarly, Du et al. [11] found that the synergistic performance of nano-silica and nano-iron oxide significantly improved concrete performance and used the ultrasonication technique for uniform dispersion of nanomaterials. Nano-silica accelerates cement hydration and acts as a nucleation seed for calcium-silicate-hydrate (C-S-H), improving mechanical performance, workability, and durability [8], [9]. Nano-alumina enhances mechanical strength, with a small amount significantly increasing compressive resistance [12]. Nano- Fe_2O_3 has also shown promise in enhancing compressive strength at optimal dosages [13]. TiO_2 nanoparticles enhance the photocatalytic properties of concrete, enabling pollutant degradation [14]. Graphene family nanoparticles improve structural strength, robustness, and self-sensing capabilities [15], [16]. Carbon nanotubes offer low electrical resistance and self-sensing abilities, enabling strain detection for structural health monitoring



systems [17], [18]. The overall performance of nanomaterials in cement-based composites primarily depends on their production techniques along with their homogenous and uniform dispersion within the matrix.

This review focuses on recent studies exploring the synthesis and dispersion of nanomaterials, including graphene oxide, graphene, nano-titanium oxide, CNTs, nano-alumina, nano-clay, nano-kaolin, nano-silica, and nano-ferric oxide, in cementitious materials. The condensed content provides a comprehensive overview of advancements in nanomaterial integration and their impact on concrete properties.

2 Comprehensive Examination of Research Endeavor

2.1 Synthesis of Nanomaterials

The synthesis of nanomaterials has been a dynamic field of research and development since the inception of nano-engineering in the 1960s. Nanoparticles have a greater impact on fillers compared to micro-based materials due to their smaller size, as stated by Gutierrez et al. [19]. According to their study, any substance can be converted into nanoparticles. The production process of nanoparticles significantly affects the integrity and composition of the base materials, and two methods have been established as shown in Figure 1 [18], [20]. One approach is the top-to-down method [21], while the other is the bottom-to-up method [22]. The choice of methodology depends on factors such as suitability, cost-effectiveness, and comprehension of nano behaviour [23]. Milling is a commonly employed top-to-down method, and the choice of milling technique is based on the accessibility and feasibility of the equipment required, as it allows for instant modifications exempt from the imperative of additional chemical or electromechanical equipment. The top-to-down method entails scaling down macro structures to the nanoscale while retaining their characteristics and molecular structural arrangement [24]. This is achieved through etching and mechanical attrition processes to reduce bulk materials into nanoparticles. Many large industries utilize this technique as it enables the production of affordable nanoparticles in large quantities and is simple to sustain due to the use of electromechanical equipment with minimal chemical modifications. The contemporary method in nanomanufacturing is a different name utilized for the top-to-down method. Even so, this approach may result in inconsistent or variable uniformity and quality of the final nanoparticles. Though, the characteristics of nanoparticles can be improved through modification of milling processes including the number and types of balls employed, milling speed, and types of jars used [21], [25]. Numerous nanoparticles, including nanograins, nanoalloys, nano quasicrystal line materials, and nanocomposites, have been produced via high-energy ball milling. This method was initially developed in 1970 by John Benjamin for obtaining oxides nanoparticles using superalloys. He used it to modify and reinforced an alloy product for elevated-temperature applications [26]. The distortion and shaping of particles during milling are influenced by factors such as plastic deformation, fracture, and cold welding. Additionally, milling involves mixing particles or components to develop new degrees in material structure. The resulting nanoparticles from the milling process often exhibit flake-like shapes, although enhancements may be made based on the choice of balls and milling method. Nonetheless, in the field of concrete, the predominant means of producing nanomaterials, including nano silica, nano clay, and nano alumina, involve bottom-up synthesis methods. The bottom-to-up techniques involve the production of materials at the molecular level, through fabrication or self-fabrication processes. It is additionally recognized as molecular manufacturing or molecular nanotechnology, encompassing applications such as chemical formulations and synthesis [26]. The bottom-up technique in chemical synthesis offers precise control and design of nanoparticles in terms of their size and shape. Unlike top-down techniques, this method results in more uniform and well-organized nanoparticle structures, with atoms or molecules arranged in an orderly and crystalline manner. Various methods such as chemical reactivity, optical absorption, and electronic conductivity can be employed in this technique [18], [27]. Notably, the bottom-up technique also allows for significant modifications in surface energies and morphologies, enabling size reduction and precise creation of surface atoms. This versatile technique finds broad applications, including enhancing catalytic capability, sensing capabilities, and developing innovative pigments and paints with self-healing and self-cleaning properties. However, it should be acknowledged that the bottom-up technique is primarily applicable in laboratory settings and may entail high operational costs, require specialized knowledge in chemical applications, and have limited applicability in certain contexts [28], [29]. Despite these limitations, the bottom-up technique remains highly effective in producing nanoparticles for cutting-edge biotechnology and electronic components applications, showcasing its potential for advanced nanomaterial manufacturing. Thus, it is evident that there are two viable techniques, with the bottom-up technique offering precise control and design capabilities, for manufacturing nanomaterials to create novel cement-based composites.

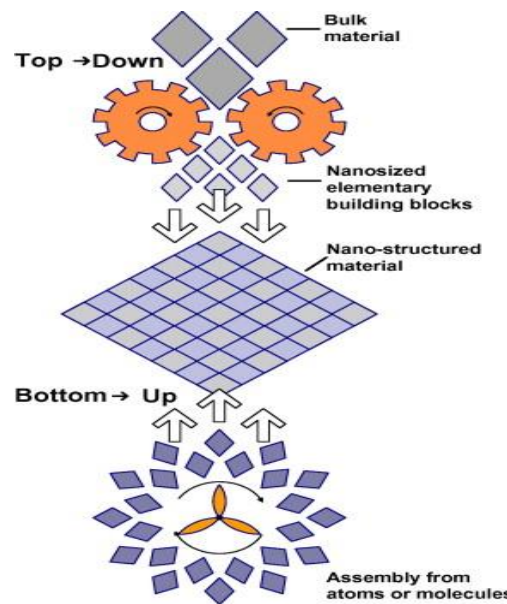


Figure 1. Nanomaterial production: top-down vs. bottom-up techniques [18]

2.2 Dispersion Mechanisms of Nanomaterials

Nanomaterials, characterized by their ultrafine particulates, high compaction, and greater surface area, are prone to agglomeration due to the strong van der Waals forces that affect their dispersion within cementitious composites [15]. Achieving adequate dispersion of nanoparticles is crucial for maximizing the capability of these additives and enhancing the performance of cementitious materials, but it remains a significant challenge in the field of cement composites [30]. Despite the importance of quantifying the extent of nanomaterial dispersion in cement matrices, there is currently no universally accepted technique for this purpose. Most research relies on indirect methods that evaluate the mechanical properties of cement composites to assess whether agglomeration has occurred. This is because non-uniform distributed nano additives in the matrix can form clumps, or flocs due to attractive electrostatic attraction, leading to detrimental effects on the mechanical characteristics of cement composites. For instance, achieving homogeneous dispersion of hydrophobic carbon nanotubes (CNT) in cement composites is particularly challenging [31], [32]. Rocha and Ludvig [32], found that CNT agglomeration and a decrease in the improved mechanical performance of cementitious material could happen if the CNT dosage in the matrix exceeds 0.05 weight percent (wt%). In their research, CNT was dispersed in a non-aqueous isopropanol medium using ultrasonication for 2 hours, without undergoing surface treatment to improve its dispersibility.

Covalent and non-covalent techniques are commonly utilized to functionalize carbon nanotubes (CNTs) to promote their dispersion and prevent aggregation [31], [33]. Chemical functionalization entails introducing functional groups onto the surface of CNTs, consequently enhancing their binding capacity to the cement matrix and improving their dispersion in cement composites. However, some researchers have noted that this approach may also weaken the mechanical properties of CNTs, thereby potentially compromising the performance of the composites [34]. As a result, non-covalent functionalization techniques that involve the use of other nanomaterials in combination with CNTs or surface treatments with surfactants, such as superplasticizers, have gained popularity [34]–[36]. For instance, Meng et al. [29] reported that incorporating polycarboxylate ether superplasticizer as a surfactant can enhance the dispersion of multi-walled CNTs (MWCNTs) and reduce their tendency to agglomerate in water. The dispersion process of MWCNTs with the addition of cyclodextrin-modified polycarboxylate superplasticizer, demonstrates a twin phenomenon of electrostatic repulsion and steric hindrance, preventing aggregation of CNTs. Additionally, Stynoski et al. [33] found that the dispersion stability of CNTs was significantly improved after functionalization with nano silica.

In the realm of cement composites, superplasticizers are commonly employed as dispersants for nanomaterials, as reported in various studies [37], [38]. Perez-Nicolas et al. [37] investigated the zeta potential of nano-additives distribution and found that limited water-reducing agents (based on naphthalene) revealed effective dispersion of nano-TiO₂ when



mechanically stirred for 20 minutes in water. The zeta potential analysis revealed that the amalgamation of this water-reducing agent and nano-TiO₂ resulted in the most negative value, indicating strong electrostatic repulsion. Furthermore, Qian et al. [38] studied the compatibility of nano clay with polycarboxylate ether superplasticizer and determined that there was an optimal dosage of polycarboxylate ether for a fixed amount of nano clay, which facilitated favourable dispersion in cement paste and prevented agglomeration. Specifically, a mixture of 0.2 wt% polycarboxylate ether and 0.5 wt% nano clay resulted in notable advancements in both the thixotropy and yield stress properties of the cement matrix. Ultrasonication is a distinct technique commonly employed to improve the uniform distribution of nano-additives in cement composites, often in conjunction with the use of a superplasticizer as a surfactant [38], [39] [15]. Ahmad and Qureshi [15] utilized a natural surfactant, namely acacia gum (AG), for the dispersion of nano graphite platelets (NGPs) as shown in Figure 2. They maintained a constant quantity of NGPs while varying the amount of AG, with NGPs to AG ratios ranging from 1:0 to 1:1 in intervals of 0.2 as depicted in Table 1.

Table 1: Variation of NGPs to AG ratios for dispersion [13]

Sample Type	NGPs: AG
S1	1:0
S2	1:0.2
S3	1:0.4
S4	1:0.6
S5	1:0.8
S6	1:1

Each ratio of NGPs to AG was subjected to mechanical sonication for 45 minutes to achieve a dispersion solution, followed by characterization using ultraviolet-visible (UV-Vis) spectroscopy. The optimal dosage was found to be an NGPs/AG ratio of 0.6:1, based on the maximum light absorbance observed during UV-Vis spectroscopy. To assess the photocatalytic properties of various cement samples, Yousefi et al. [39] studied the dispersal of nano-TiO₂ in cement mixtures, comparing the impact of manual stirring and sonication. Their findings revealed that without ultrasonication, significant agglomeration of nano-TiO₂ occurred. Furthermore, ultrasonic dispersion of the nano-TiO₂ improved the photocatalytic capabilities of the cement samples.

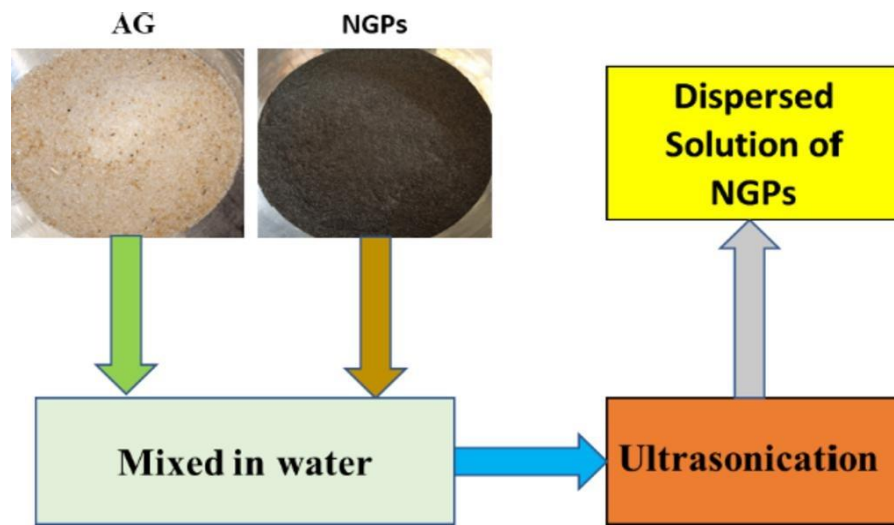


Figure 2: Dispersion of NGPs with acacia gum (AG) as a natural surfactant followed by 45 minutes of ultrasonication [13]

3 Conclusions

Nanomaterials have revolutionized the material's world by reinforcing the matrix of the composite at the nano level, thereby introducing enhanced mechanical and durability resilience in cement-based composites. The effectiveness of nanomaterials primarily depends on their production techniques and dispersion mechanisms. The following conclusions were drawn based on the review of the literature:



- 1 Nanoparticles can be synthesized using top-to-down and bottom-to-up methods. The top-to-down method enables large-scale production but lacks precise control and design capabilities. On the other hand, the bottom-to-up technique offers precise control and design but may have higher costs and limited applicability. Both methods have their advantages and are used in different contexts, with the top-to-down method being more common in industries and the bottom-to-up technique more prevalent in laboratory settings.
- 2 The effectiveness of nanomaterials in mitigating the degradation of cementitious composites largely depends upon the dispersion of nanomaterials in CBMs. Surfactant use, ultrasonic application, and functionalization of nanomaterials are frequently used applied methods to disperse nanomaterials.
- 3 Achieving proper dispersion of nanoparticles in cementitious materials is challenging due to agglomeration and quantifying nanomaterial dispersion lacks a universally accepted technique. Future, research work might be recommended to be carried out to establish an innovative approach for uniform and homogeneous dispersion of nanomaterials.

Acknowledgment

The authors would like to thank every person/department who helped thorough out the research work, particularly Dr. Rao Arsalan Khushnood and Engr. Farhan Ahmad. The careful review and constructive suggestions by the anonymous reviewers are gratefully acknowledged.

References

- [1] F. Ahmad *et al.*, "Performance Evaluation of Cementitious Composites Incorporating Nano Graphite Platelets as Additive Carbon Material," *Mater. (Basel, Switzerland)*, vol. 15, no. 1, Dec. 2021, doi: 10.3390/ma15010290.
- [2] N. Hamed, M. S. El-Feky, M. Kohail, and E.-S. A. R. Nasr, "Effect of nano-clay de-agglomeration on mechanical properties of concrete," *Constr. Build. Mater.*, vol. 205, pp. 245–256, 2019, doi: <https://doi.org/10.1016/j.conbuildmat.2019.02.018>.
- [3] Y. Ding, Z. Chen, Z. Han, Y. Zhang, and F. Pacheco-Torgal, "Nano-carbon black and carbon fiber as conductive materials for the diagnosing of the damage of concrete beam," *Constr. Build. Mater.*, vol. 43, pp. 233–241, 2013, doi: <https://doi.org/10.1016/j.conbuildmat.2013.02.010>.
- [4] Atta-ur-Rehman, J. H. Kim, H. G. Kim, A. Qudoos, and J.-S. Ryou, "Effect of leaching on the hardened, microstructural and self-cleaning characteristics of titanium dioxide containing cement mortars," *Constr. Build. Mater.*, vol. 207, pp. 640–650, 2019, doi: <https://doi.org/10.1016/j.conbuildmat.2019.02.170>.
- [5] M. Azeem and M. Azhar Saleem, "Role of electrostatic potential energy in carbon nanotube augmented cement paste matrix," *Constr. Build. Mater.*, vol. 239, p. 117875, 2020, doi: <https://doi.org/10.1016/j.conbuildmat.2019.117875>.
- [6] S. Sharma and N. Kothiyal, "Influence of graphene oxide as dispersed phase in cement mortarmatrix in defining the crystal patterns of cement hydrates and its effect on mechanical, microstructural and crystallization propertis," *RSC Adv.*, vol. 5, 2015, doi: 10.1039/C5RA08078A.
- [7] K. Snehal, B. B. Das, and M. Akanksha, "Early age, hydration, mechanical and microstructure properties of nano-silica blended cementitious composites," *Constr. Build. Mater.*, vol. 233, p. 117212, 2020, doi: <https://doi.org/10.1016/j.conbuildmat.2019.117212>.
- [8] S. Chuah, Z. Pan, J. G. Sanjayan, C. M. Wang, and W. H. Duan, "Nano reinforced cement and concrete composites and new perspective from graphene oxide," *Constr. Build. Mater.*, vol. 73, pp. 113–124, 2014, doi: <https://doi.org/10.1016/j.conbuildmat.2014.09.040>.
- [9] F. Pacheco-Torgal and S. Jalali, "Nanotechnology: Advantages and drawbacks in the field of construction and building materials," *Constr. Build. Mater.*, vol. 25, no. 2, pp. 582–590, 2011, doi: <https://doi.org/10.1016/j.conbuildmat.2010.07.009>.
- [10] J. A. Abdalla, R. A. Hawileh, A. Bahurudeen, Jittin, K. I. Syed Ahmed Kabeer, and B. S. Thomas, "Influence of synthesized nanomaterials in the strength and durability of cementitious composites," *Case Stud. Constr. Mater.*, vol. 18, p. e02197, 2023, doi: <https://doi.org/10.1016/j.cscm.2023.e02197>.
- [11] X. Du *et al.*, "Modification mechanism of combined nanomaterials on high performance concrete and optimization of nanomaterial content," *J. Build. Eng.*, vol. 64, p. 105648, 2023, doi: <https://doi.org/10.1016/j.jobe.2022.105648>.
- [12] B. J. Zhan, D. X. Xuan, and C. S. Poon, "The effect of nanoalumina on early hydration and mechanical properties of cement pastes," *Constr. Build. Mater.*, vol. 202, pp. 169–176, 2019, doi: <https://doi.org/10.1016/j.conbuildmat.2019.01.022>.
- [13] X. Du *et al.*, "Modification mechanism of combined nanomaterials on high performance concrete and optimization of nanomaterial content," *J. Build. Eng.*, vol. 64, no. November 2022, p. 105648, 2023, doi: 10.1016/j.jobe.2022.105648.
- [14] S. Kamaruddin and D. Stephan, "Quartz-titania composites for the photocatalytical modification of construction materials," *Cem. Concr. Compos.*, vol. 36, no. 1, pp. 109–115, 2013, doi: 10.1016/j.cemconcomp.2012.08.007.
- [15] F. Ahmad, M. I. Qureshi, and Z. Ahmad, "Influence of nano graphite platelets on the behavior of concrete with E-waste plastic coarse aggregates," *Constr. Build. Mater.*, vol. 316, no. August 2021, p. 125980, 2022, doi: 10.1016/j.conbuildmat.2021.125980.



5th Conference on Sustainability in Civil Engineering (CSCE'23)

Department of Civil Engineering

Capital University of Science and Technology, Islamabad Pakistan



- [16] R. A. Khushnood, A. Arif, N. Shaheen, A. G. Zafar, T. Hassan, and M. Akif, "Bio-inspired self-healing and self-sensing cementitious mortar using *Bacillus subtilis* immobilized on graphitic platelets," *Constr. Build. Mater.*, vol. 316, no. December 2021, p. 125818, 2022, doi: 10.1016/j.conbuildmat.2021.125818.
- [17] E. García-Macías, A. Downey, A. D'Alessandro, R. Castro-Triguero, S. Lafamme, and F. Ubertini, "Enhanced lumped circuit model for smart nanocomposite cement-based sensors under dynamic compressive loading conditions," *Sensors Actuators A Phys.*, vol. 260, pp. 45–57, 2017, doi: <https://doi.org/10.1016/j.sna.2017.04.004>.
- [18] F. Sanchez and K. Sobolev, "Nanotechnology in concrete – A review," *Constr. Build. Mater.*, vol. 24, no. 11, pp. 2060–2071, 2010, doi: <https://doi.org/10.1016/j.conbuildmat.2010.03.014>.
- [19] K. Sobolev and M. Ferrada Gutiérrez, "How Nanotechnology Can Change the Concrete World," in *Progress in Nanotechnology*, John Wiley & Sons, Ltd, 2009, pp. 113–116. doi: <https://doi.org/10.1002/9780470588260.ch16>.
- [20] K. Sobolev and M. F. Gutiérrez, "How nanotechnology can change the concrete world : Part two of a two-part series," *Am. Ceram. Soc. Bull.*, vol. 84, pp. 16–19, 2005.
- [21] H. Abdoli, H. R. Farnoush, H. Asgharzadeh, and S. K. Sadrnezhaad, "Effect of high energy ball milling on compressibility of nanostructured composite powder," *Powder Metall.*, vol. 54, no. 1, pp. 24–29, 2011, doi: 10.1179/003258909X12573447241662.
- [22] E. Jankowska and W. Zatorski, "Emission of Nanosize Particles in the Process of Nanoclay Blending," in *2009 Third International Conference on Quantum, Nano and Micro Technologies*, 2009, pp. 147–151. doi: 10.1109/ICQNM.2009.33.
- [23] K. Das, S. Sen, and P. Biswas, "A Review Paper – on the Use of Nanotechnology in Construction Industry," *ERN Manuf. \& Serv. Ind. Dev. Econ.*, 2020.
- [24] N. Crainic and A. T. Marques, "Nanocomposites: a State-of-the-Art Review," *Key Eng. Mater.*, vol. 230–232, pp. 650–656, 2002, doi: 10.4028/www.scientific.net/KEM.230-232.656.
- [25] T. Yadav, R. M. Yadav, and D. Singh, "Mechanical Milling: a Top Down Approach for the Synthesis of Nanomaterials and Nanocomposites," *Nanosci. Nanotechnol.*, vol. 2, pp. 22–48, Jul. 2012, doi: 10.5923/j.nnn.20120203.01.
- [26] J. S. Benjamin, "Dispersion strengthened superalloys by mechanical alloying," *Metall. Trans.*, vol. 1, no. 10, pp. 2943–2951, 1970, doi: 10.1007/BF03037835.
- [27] M. Gesoglu, E. Güneyisi, D. S. Asaad, and G. F. Muhyaddin, "Properties of low binder ultra-high performance cementitious composites: Comparison of nanosilica and microsilica," *Constr. Build. Mater.*, vol. 102, pp. 706–713, 2016, doi: <https://doi.org/10.1016/j.conbuildmat.2015.11.020>.
- [28] K. Sobolev and M. Ferrada Gutierrez, "How Nanotechnology Can Change the Concrete World," in *American Ceramic Society Bulletin*, vol. 84, 2014, pp. 113–116. doi: 10.1002/9780470588260.ch16.
- [29] B. Bhushan, *Springer Handbook of Nanotechnology*. 2017. doi: 10.1007/978-3-662-54357-3.
- [30] W. Jones, A. Gibb, C. Goodier, P. Bust, M. Song, and J. Jin, "Nanomaterials in construction – what is being used, and where?," *Proc. Inst. Civ. Eng. - Constr. Mater.*, vol. 172, no. 2, pp. 49–62, 2019, doi: 10.1680/jcoma.16.00011.
- [31] Y. Meng, B. Liao, H. Pang, J. Zhang, and L. Song, "Cyclodextrin-modified polycarboxylate superplasticizers as dispersant agents for multiwalled carbon nanotubes," *J. Appl. Polym. Sci.*, vol. 136, no. 16, p. 47311, Apr. 2019, doi: <https://doi.org/10.1002/app.47311>.
- [32] V. Rocha and P. Ludvig, "Nanocomposites Prepared by a Dispersion of CNTS on Cement Particles," *Archit. Civ. Eng. Environ.*, vol. 11, Jun. 2018, doi: 10.21307/ACEE-2018-024.
- [33] P. Stynoski, P. Mondal, E. Wotring, and C. Marsh, "Characterization of silica-functionalized carbon nanotubes dispersed in water," *J. Nanoparticle Res.*, vol. 15, no. 1, p. 1396, 2013, doi: 10.1007/s11051-012-1396-1.
- [34] B. Balasubramaniam, K. Mondal, K. Ramasamy, G. S. Palani, and N. R. Iyer, "Hydration Phenomena of Functionalized Carbon Nanotubes (CNT)/Cement Composites," *Fibers*, vol. 5, no. 4. 2017. doi: 10.3390/fib5040039.
- [35] M. S. Konsta-Gdoutos, Z. S. Metaxa, and S. P. Shah, "Highly dispersed carbon nanotube reinforced cement based materials," *Cem. Concr. Res.*, vol. 40, no. 7, pp. 1052–1059, 2010, doi: <https://doi.org/10.1016/j.cemconres.2010.02.015>.
- [36] H. Shao, B. Chen, B. Li, S. Tang, and Z. Li, "Influence of dispersants on the properties of CNTs reinforced cement-based materials," *Constr. Build. Mater.*, vol. 131, pp. 186–194, 2017, doi: <https://doi.org/10.1016/j.conbuildmat.2016.11.053>.
- [37] M. Pérez-Nicolás, J. Plank, D. Ruiz-Izuriaga, I. Navarro-Blasco, J. M. Fernández, and J. I. Alvarez, "Photocatalytically active coatings for cement and air lime mortars: Enhancement of the activity by incorporation of superplasticizers," *Constr. Build. Mater.*, vol. 162, pp. 628–648, 2018, doi: <https://doi.org/10.1016/j.conbuildmat.2017.12.087>.
- [38] Y. Qian and G. De Schutter, "Enhancing thixotropy of fresh cement pastes with nanoclay in presence of polycarboxylate ether superplasticizer (PCE)," *Cem. Concr. Res.*, vol. 111, pp. 15–22, 2018, doi: <https://doi.org/10.1016/j.cemconres.2018.06.013>.
- [39] A. Yousefi, A. Allahverdi, and P. Hejazi, "Effective dispersion of nano-TiO₂ powder for enhancement of photocatalytic properties in cement mixes," *Constr. Build. Mater.*, vol. 41, pp. 224–230, 2013.



IMPROVED COMPRESSIVE PERFORMANCE OF BIO-INDUCED SISAL FIBERS REINFORCED CONCRETE

^a Hassan Amjad, ^b Farhan Ahmad*

a: NICE, SCEE, NUST, H/12 Campus, Islamabad, 44000, Pakistan, hassanamjaduet@gmail.com

b: School of Engineering, Design and Built Environment, Western Sydney University, Australia, F.ahmad@westernsydney.edu.au

* Corresponding author: Email ID: F.ahmad@westernsydney.edu.au

Abstract- The use of calcite-precipitating bacteria and fiber reinforcement has the potential to enhance the strength and crack-healing characteristics of cementitious materials. However, their impact on the compressive response of concrete is uncertain. This study evaluates the compressive response of Sisal Fiber (SisF) reinforcement in combination with *Bacillus Subtilis* (B.St) in concrete. The results demonstrate that SisF inclusion improves ductility, peak compressive strain, post-peak compression energy, and total compression energy, leading to a 1.43 increase in the toughness index. Direct incorporation of B.St due to the Microbial-Induced Carbonate Precipitation (MICP) process results in an 8.1% increase in compressive strength compared to the control mixture. Furthermore, combining fiber reinforcement and MICP leads to a substantial 14.0% increase in compressive strength while maintaining a toughness index of approximately 1.59. The successful synthesis of MICP is confirmed through Fourier Transform Infrared analysis. These findings establish the effectiveness of SisF and B.St, in enhancing concrete's compressive performance, thereby promoting the development of more resilient and sustainable construction materials.

Keywords- Bacillus Subtilis, Compressive response, Concrete composites, Sisal fiber.

1 Introduction

The use of bacteria in bioinspired cementitious materials has shown promise in improving the mechanical performance of concrete infrastructure. By incorporating bacteria, these materials can enhance concrete by facilitating biochemical processes that result in the production of calcium carbonate (CaCc). This CaCc acts as a mineral precipitate, filling voids and cracks in the concrete's microstructure, thereby enhancing its mechanical strength and long-term durability [1]. Research has demonstrated that incorporating various strains of bacteria, such as *Bacillus Subtilis* (B.St), into concrete positively impacts its microstructure, mechanical performance, and durability [2], [3]. Studies have shown that higher volumes of B.St result in increased CaCc production and improved compressive strength [4]. Immobilization techniques using carriers like lightweight aggregates, graphite nano-platelets, and iron oxide have been used to increase the longevity of bacterial spores within cementitious composites, resulting in enhanced compressive and tensile strengths [5]–[7]. Adding fibers to bacterial concrete further enhances its performance by distributing stresses, improving toughness, and providing a protective environment for bacterial spores. Fibers like basalt fiber, polyvinyl alcohol (PVA), polypropylene (PP), flax, coconut, jute, and coir have been incorporated, leading to increased compressive strength and reduced sorptivity [3], [8]–[10].

Sisal Fiber (SisF), derived from the sisal plant leaves, has been extensively studied for its potential in enhancing cementitious materials by reinforcing fibers, making it a promising material for sustainable construction [11]–[14]. Recent findings [15] have indicated its effectiveness as an immobilizer for B.St, resulting in improvements in compressive strength and tensile resistance. However, a thorough understanding of the stress-strain profile is needed to accurately predict fracture behavior and assess many engineering properties for designing modified concrete structures. Previous work using



various bacterial strains and natural fibers has concentrated mainly on strength gains and self-healing effectiveness. According to Amjad et al. [15], compression strength increased by 14% while tensile resistance increased by 37%. The viability of several natural fibres, such as flax, coconut, and jute, as possible carriers for various strains of the *Bacillus* genus, including *Cohnii*, *Subtilis*, and *Sphaericus*, was also investigated in a related study [1]. It was discovered that these natural fibres offer improved preservation properties for immobilised bacteria because of their fibrillar and lamellar features. Coir fibre had been shown to have a 42% increase in compressive strength, indicating a substantial improvement. This research, on the other hand, presents a more comprehensive approach, assessing the compression response of bioinspired concrete supplemented with SisF and B.St as biomimetic agents.

2 Material and Methods

2.1 Preparation of the B.St

The preparation of the B.St involved the following steps as per the literature [15] with a detailed schematic method depicted in Figure 1:

- a) B.St colonies were initially cultured on agar plates and subsequently transferred to Tryptone Soya Broth.
- b) After 24 hours of shaking incubation at 37°C, the B.St cells exhibited significant growth.
- c) A sporulation medium containing magnesium sulfate heptahydrate (1.01 mM), manganese chloride (0.01 mM), ferrous sulfate (0.001 mM), potassium chloride (13.4 mM), and calcium nitrate (1.0 mM) was added to the bacterial broth solution.
- d) The mixture was further incubated for an additional 120 hours at 37°C with shaking at 150 rpm.
- e) The endospores were harvested by centrifugation at 4000 rpm and 6°C for 20 minutes.
- f) A sterile distilled water suspension was prepared for the collected endospores.
- g) The optical density of the spore solution was adjusted to a concentration of 0.5, following previous studies.

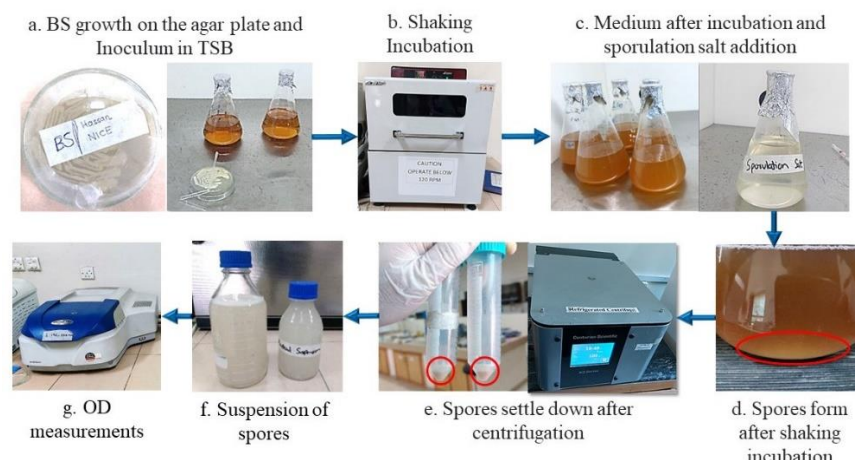


Figure 1: Preparation of the B.St

2.2 Concrete Constituents

The materials included Bestway Cement Type-1 Ordinary Portland Cement, Lawrencepur sand as the fine aggregate, and locally available Margalla crush as the coarse aggregate, meeting ASTM guidelines [16]–[19]. Table 1, and Table 2 provide the chemical constituents of the cement, properties of the fine aggregates, and properties of the coarse aggregate, respectively.



5th Conference on Sustainability in Civil Engineering (CSCE'23)

*Department of Civil Engineering
Capital University of Science and Technology, Islamabad Pakistan*



Table 1: Chemical Composition of Bestway Cement

CaO	SiO₂	Al₂O₃	Fe₂O₃	SO₃	MgO	K₂O	Na₂O
64.52	21.25	4.96	3.15	2.81	2.51	0.62	0.18

Table 2: Properties of fine and coarse aggregate

	Fineness Modulus	Absorption (%)	Bulk Specific Gravity (SSD)
Sand	2.90	2.04	2.75
Coarse aggregate	-	0.92	2.68

2.3 SisF

SisF, in the optimal size of 25 mm, was incorporated into the concrete mixture based on previous research [3], [15]. Figure 2 provides a visual of SisF:



Figure 2: Visual appearance of SisF

2.4 Mix Formulations

Four different formulations were investigated, as summarized in Table 3. In plain concrete, Mix-1 and Mix-3 had a mix design proportion of 1 for cement and 2.2 and 2.4 for fine and coarse aggregates, respectively. A water-to-cement ratio of 0.45 was chosen for the design. Fibrous mixes, Mix-2 and Mix-4, had similar proportions but included an additional superplasticizer to achieve workable mixtures within the desired slump range of 40-50 mm, as mentioned in the literature [15]. Based on the optimal dosage for concrete, 1.0 wt % SisF was incorporated into the fibrous mixes according to previous studies [12], [20]. In Mix-4, for the immobilization of bacterial spores, SisF was immersed in the biomimetic agent for one hour before being integrated into the concrete. To ensure homogeneity, calcium lactate pentahydrate, a mineral precursor, was added to all mixes. The formulations are categorized into four different mixes. The first mix, Mix-1, serves as the control mix and does not contain any SisF or biomimetic agent. In Mix-2, it is a fibrous control mix where only SisF is added at a concentration of 1.0 wt %. On the other hand, Mix-3 consists of a bacterial mix, which includes only the biomimetic agent at a concentration of 6×10^8 cells/cm³.

Table 3: Mix Design of different mixes

Materials	Mix-1	Mix-2	Mix-3	Mix-4
Cement (kg/m ³)	392	392	392	392
Fine aggregate (kg/m ³)	863	863	863	863
Coarse aggregate (kg/m ³)	941	941	941	941
Water/cement ratio	0.45	0.45	0.45	0.45
Bacterial spores content (cell/cm ³)	0	0	6×10^8	6×10^8

Lastly, Mix-4 is the fibrous bacterial mix, containing both SisF at a concentration of 1.0 wt % and the biomimetic agent at a concentration of 6×10^8 cells/cm³. These mixed formulations provide a basis for investigating the effects of different components on the experimental outcomes.



2.5 Specimen Preparation and Experimentation

All materials were carefully weighed according to the designated mix design and then dry-mixed in an electronic concrete mixer for a period of 2 to 3 minutes. Water was subsequently added, and the wet mixing process was continued for an additional 2 to 3 minutes. For each formulation, six P.C.C. cylinders measuring 100 mm in diameter and 200 mm in height and rectangular beamlets measuring 100x100x400 mm³ were cast. After casting, the samples were left to dry-cure in molds for 24 hours, under a temperature of 20±2 °C. At the end of the 24-hour curing period, the specimens were removed from their respective molds and then placed in a water curing tank, maintained at a relative humidity of 100% at room temperature (23±2°C), and left to cure for the respective days.

Standardized specimens were prepared according to ASTM-approved specifications for testing purposes. This included cylindrical specimens with a diameter of 100 mm and a height of 200 mm for evaluating the compressive response behavior. To ensure reliable results, a minimum of three specimens were prepared for each material and test. Testing of the formulated concrete mixes in compression loading was conducted to investigate strain vs stress plots, compressive strength, elastic modulus, pre and post-cracking energies, and toughness index, following ASTM C-39 guidelines [21]. In addition, Fourier-transform infrared spectroscopy (FTIR) was employed to assess any crystallographic variations in the concrete matrix resulting from microbially induced calcite precipitation (MICP).

3 Results and Discussion

3.1 Compressive Performance

Figure 3 illustrates the stress-strain plot of the investigated concrete mixtures under compression loading. The compressive strength is determined by the highest stress value obtained from the curve, while the corresponding strain value is known as the peak compressive strain (Figure 3 b). Pre-peak compression energy is calculated by integrating the response curve up to the highest stress value, while post-peak compression energy is obtained by integrating the response curve from the highest stress value to the failure point. The total compression energy, representing the area under the response curve, is derived by combining the pre-peak and post-peak compression energies. Figure 3 c shows the pre-peak, post-peak, and total compression energy of the formulated concrete mixes. The toughness index for compression, which is the ratio of total to pre-peak compression energy, is depicted in Figure 3 d to demonstrate ductility. Another significant property, the elastic modulus, is shown in Figure 3 e, which is derived using the chord technique according to ASTM C469 [22]. This technique involves establishing a chord through 40% of the peak stresses and strains at 0.05%, where the chord gradient reflects the elastic modulus of the concrete.

The behaviour of the concrete mixes is affected by the incorporation of SisF and B.St due to the composite nature of the concrete. SisF has a more ductile effect compared to B.St intrusion. While SisF has a minimal impact on compression strength (approximately 2.8%), it significantly increases the peak compressive strain (around 15.0%) in Mix-2 compared to Mix-1. This can be attributed to the confinement effect of the fiber, which delays crack formation and propagation, leading to increased peak compressive strain [23]. Mix-2 also shows significant improvements in post-peak compression energy, total compression energy, and a toughness index value of 1.43, indicating the effectiveness of fiber bridging in restraining crack widening. Mix-3, which incorporates B.St directly, exhibits an 8.1% increase in compressive strength due to the MICP process. This process fills voids and cracks, stiffening the compression behavior of the concrete and reducing the peak compression strain by 15.0%. The MICP-induced densification of the microstructure reduces compression strain and increases compressive stress [24]–[26]. The MICP does not have a prominent effect on total compression energy and compression toughness index, as it does not provide resistance to brittleness and lateral crack opening. However, the elastic modulus of Mix-3 is 22.3% higher than that of Mix-1 due to the pore refinement resulting from MICP [23].

Mix-4 exhibits stronger fiber reinforcement and MICP compared to other mixtures. The immobilization of B.St enhances both MICP potential and the interfacial bond between SisF and the cementitious matrix [15], [27]. Mix-4 shows a 14.0% increase in compressive strength and a 6.2% increase in strain compared to Mix-1. It also demonstrates significant improvements in post-peak and total compression energies, with a toughness index value of 1.59 indicating enhanced fiber reinforcement. The addition of SisF makes the behavior of Mix-4 more elastic, resulting in a 5.7% reduction in elasticity compared to Mix-1. Although these findings contradict a previous study [2] conducted on stress-strain behavior of bacterial



concrete however the results are well aligned with the literature that explored the coupled effect of fibers and microstructural densification of concrete structures [10]. However, for typical structural members as reported in the previous literature, the minimum compression capacity of 17.24 MPa is usually recommended [26].

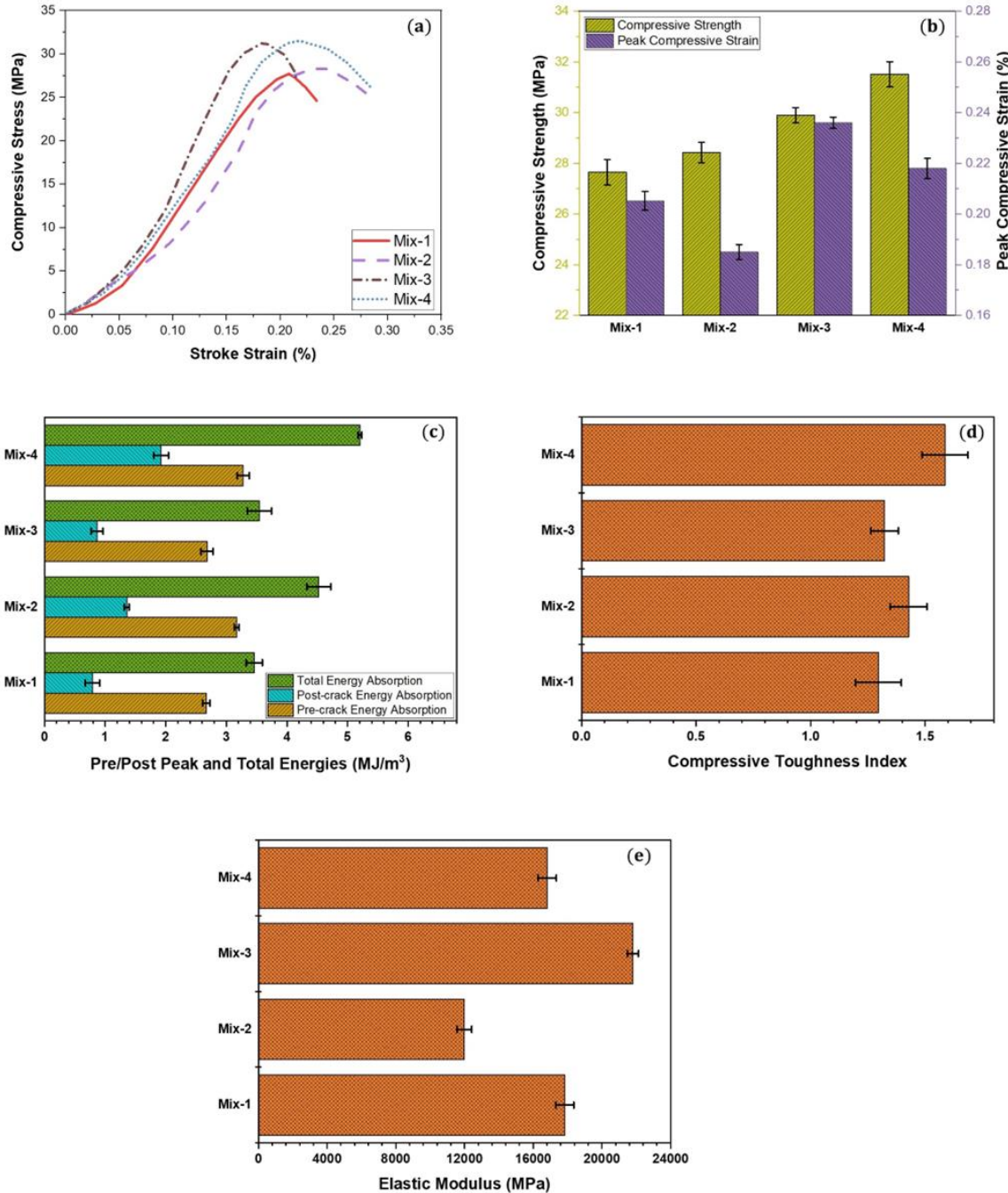


Figure 3: Compressive performance (a) compressive response behaviour (b) peak compressive strength and strain (c) pre- and post-peak compressive energies (d) compressive toughness index (e) elastic modulus



3.2 FTIR Examination

Figure 4 depicts the FTIR examination of the investigated concrete mixes to analyze the crystallographic shifts and identify molecular vibrations. Specific peaks were observed, indicating various molecular vibrations within the concrete mixture. Table 7 presents the identified molecular vibrations and their corresponding wavelengths (cm⁻¹).

The O-H stretching vibrations are represented by peaks in the range of 3425-3430 cm⁻¹. H-OH and C-H bending vibrations are observed in the range of 1640-1645 cm⁻¹. Si-O stretching vibrations are identified in the range of 1075-1080 cm⁻¹. C-O stretching vibrations are observed in the range of 970-980 cm⁻¹, and additional peaks related to molecular vibrations can be seen at 1405-1410 cm⁻¹, 870-875 cm⁻¹, and 710-715 cm⁻¹. The presence of portlandite, which is associated with O-H stretching, has been established in previous studies [28], [29]. The H-OH and C-H bending vibrations and Si-O stretching vibrations are indicative of the presence of C-S-H gel [30],[31]. The spectra of bacterial mixtures, specifically Mix-3 and Mix-4, show significant peaks related to carbonate, confirming the presence of biomineralized calcium carbonate (CaCc). These findings align with prior research on biominerization in concrete [15].

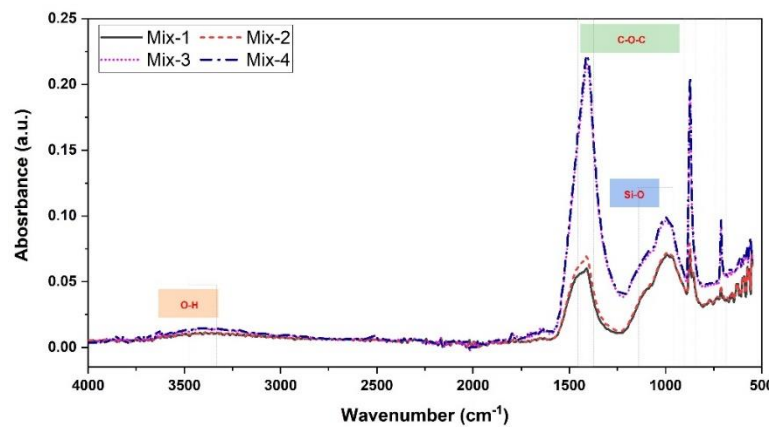


Figure 4: FTIR examination of the investigated concrete mixes

4 Conclusions

Thus using bio-triggered sisal fiber-reinforced concrete offers enhanced fracture resistance of concrete in various construction applications. It can be used in building and infrastructure construction, retrofitting existing structures, and construction in seismic-prone areas. The use of sisal fibers promotes sustainable construction practices by utilizing renewable and bio-based materials, reducing environmental impacts, and providing cost-effective solutions. The following conclusions have been derived from the experimental results:

1. The addition of B.Sb to the concrete increases its stiffness, whereas the addition of SisF increases its ductility.
2. Mix-2 containing SisF exhibits a 15% increment in peak compressive strain compared to the control mixture. Furthermore, Mix-2 demonstrates significant improvements in post-peak compression energy and total compression energy, the toughness index of the resulting concrete improved by 1.43, respectively.
3. Mix-3 containing B.St only undergoes the MICP process and exhibits an approximate 8.1% increase in compressive strength compared to the control mixture. Whereas, Mix-4 containing both fiber reinforcement and B.St shows a substantial increase of approximately 14.0% in compressive strength compared to the control mixture. Moreover, the toughness index, indicating the ratio of total to pre-peak compression energy, is approximately 1.59 for Mix-4, highlighting the enhanced toughness compared to the control mixture.
4. The FTIR examination confirms the successful synthesis of MICP.



Acknowledgment

The authors would like to thank every person/department who helped thorough out the research work, particularly the NICE and IESE department and Engr. Dr. Rao Arsalan Khushnood. The careful review and constructive suggestions by the anonymous reviewers are gratefully acknowledged.

References

- [1] R. A. Khushnood, Z. A. Qureshi, N. Shaheen, and S. Ali, "Bio-mineralized self-healing recycled aggregate concrete for sustainable infrastructure," *Sci. Total Environ.*, vol. 703, p. 135007, 2020.
- [2] N. Shaheen, R. A. Khushnood, S. A. Memon, and F. Adnan, "Feasibility assessment of newly isolated calcifying bacterial strains in self-healing concrete," *Constr. Build. Mater.*, vol. 362, no. July 2022, p. 129662, 2023.
- [3] M. Rauf, W. Khalil, R. A. Khushnood, and I. Ahmed, "Comparative performance of different bacteria immobilized in natural fibers for self-healing in concrete," *Constr. Build. Mater.*, vol. 258, p. 119578, 2020, doi: 10.1016/j.conbuildmat.2020.119578.
- [4] K. K. Sahoo, A. K. Sathyan, C. Kumari, P. Sarkar, and R. Davis, "Investigation of cement mortar incorporating *Bacillus sphaericus*," *Int. J. Smart Nano Mater.*, vol. 7, no. 2, pp. 91–105, 2016.
- [5] R. A. Khushnood, A. Arif, N. Shaheen, A. G. Zafar, T. Hassan, and M. Akif, "Bio-inspired self-healing and self-sensing cementitious mortar using *Bacillus subtilis* immobilized on graphitic platelets," *Constr. Build. Mater.*, vol. 316, no. December 2021, p. 125818, 2022, doi: 10.1016/j.conbuildmat.2021.125818.
- [6] W. Khalil and M. B. Ehsan, "Crack healing in concrete using various bio influenced self-healing techniques," *Constr. Build. Mater.*, vol. 102, pp. 349–357, 2016, doi: 10.1016/j.conbuildmat.2015.11.006.
- [7] N. Shaheen, R. A. Khushnood, W. Khalil, H. Murtaza, R. Iqbal, and M. H. Khan, "Synthesis and characterization of bio-immobilized nano/micro inert and reactive additives for feasibility investigation in self-healing concrete," *Constr. Build. Mater.*, vol. 226, no. November, pp. 492–506, 2019, doi: 10.1016/j.conbuildmat.2019.07.202.
- [8] K. Vijay and M. Murmu, "Self-repairing of concrete cracks by using bacteria and basalt fiber," *SN Appl. Sci.*, vol. 1, no. 11, pp. 1–10, 2019, doi: 10.1007/s42452-019-1404-5.
- [9] J. Feng, Y. Su, and C. Qian, "Coupled effect of PP fiber, PVA fiber and bacteria on self-healing efficiency of early-age cracks in concrete," *Constr. Build. Mater.*, vol. 228, p. 116810, 2019, doi: 10.1016/j.conbuildmat.2019.116810.
- [10] Y. Su, C. Qian, Y. Rui, and J. Feng, "Exploring the coupled mechanism of fibers and bacteria on self-healing concrete from bacterial extracellular polymeric substances (EPS)," *Cem. Concr. Compos.*, vol. 116, no. August 2020, 2021.
- [11] A. Karimah *et al.*, "A review on natural fibers for development of eco-friendly bio-composite: characteristics, and utilizations," *J. Mater. Res. Technol.*, vol. 13, pp. 2442–2458, 2021, doi: 10.1016/j.jmrt.2021.06.014.
- [12] R. Abirami, S. P. Sangeetha, K. Nadeem mishab, P. Y. Vaseem, and K. S. Sad, "Experimental behaviour of sisal and kenaf fibre reinforced concrete," *AIP Conf. Proc.*, vol. 2271, no. September, 2020, doi: 10.1063/5.0024771.
- [13] A. A. Okeola, S. O. Abuodha, and J. Mwero, "Experimental investigation of the physical and mechanical properties of sisal fiber-reinforced concrete," *Fibers*, vol. 6, no. 3, 2018, doi: 10.3390/fib6030053.
- [14] K. V. Sabarish, P. Paul, Bhuvaneshwari, and J. Jones, "An experimental investigation on properties of sisal fiber used in the concrete," *Mater. Today Proc.*, vol. 22, pp. 439–443, 2020, doi: 10.1016/j.matpr.2019.07.686.
- [15] H. Amjad, R. Arsalan Khushnood, and S. Ali Memon, "Biomimetic robust self-healing of *Bacillus Subtilis* immobilized through sisal fiber for next-generation concrete infrastructure," *Constr. Build. Mater.*, vol. 368, no. January, p. 130299, 2023, doi: 10.1016/j.conbuildmat.2023.130299.
- [16] ASTM C150, "ASTM C150/C150M - 18 Standard Specifications for Portland Cement," vol. i, pp. 1–9, 1999, doi: 10.1520/C0150.
- [17] ASTM C33, "Concrete Aggregates 1," vol. i, no. C, pp. 1–11, 2010, doi: 10.1520/C0033.
- [18] ASTM, "Método de prueba estándar para Densidad Relativa (Gravedad Específica) y Absorción de Agregado Grueso, ASTM C127-15," pp. 1–5, 2015, doi: 10.1520/C0127-15.2.
- [19] ASTM C-128-15, "Standard Test Method for Relative Density (Specific Gravity) and Absorption of Fine Aggregates, ASTM International, West Conshohocken, PA, 2015," *ASTM Int.*, vol. i, pp. 15–20, 2015, doi: 10.1520/C0128-15.2.
- [20] I. Shah, J. Li, S. Yang, Y. Zhang, and A. Anwar, "Experimental Investigation on the Mechanical Properties of Natural Fiber Reinforced Concrete," *J. Renew. Mater.*, vol. 10, no. 5, pp. 1307–1320, 2022, doi: 10.32604/jrm.2022.017513.
- [21] ASTM C-39, "Standard Test Method for Compressive Strength of Cylindrical Concrete Specimens 1 This standard is for EDUCATIONAL USE ONLY .," *Annu. B. ASTM Stand.*, no. C, pp. 1–7, 2010, doi: 10.1520/C0039.
- [22] ASTM International, "ASTM Standard C469/C469M – 14, Standard Test Method for Static Modulus of Elasticity and Poisson's Ratio of Concrete in Compression," *ASTM Int.*, 2014, doi: 10.1520/C0469.
- [23] M. Khan, M. Cao, and M. Ali, "Effect of basalt fibers on mechanical properties of calcium carbonate whisker-steel fiber reinforced concrete," *Constr. Build. Mater.*, vol. 192, pp. 742–753, 2018, doi: 10.1016/j.conbuildmat.2018.10.159.
- [24] A. Akbar, K. M. Liew, F. Farooq, and R. A. Khushnood, "Exploring mechanical performance of hybrid MWCNT and GNMP reinforced cementitious composites," *Constr. Build. Mater.*, vol. 267, p. 120721, 2021, doi: 10.1016/j.conbuildmat.2020.120721.
- [25] A. Chen, X. Han, M. Chen, X. Wang, Z. Wang, and T. Guo, "Mechanical and stress-strain behavior of basalt fiber reinforced rubberized recycled coarse aggregate concrete," *Constr. Build. Mater.*, vol. 260, p. 119888, 2020.



5th Conference on Sustainability in Civil Engineering (CSCE'23)

Department of Civil Engineering

Capital University of Science and Technology, Islamabad Pakistan



- [26] F. Ahmad, M. I. Qureshi, and Z. Ahmad, "Influence of nano graphite platelets on the behavior of concrete with E-waste plastic coarse aggregates," *Constr. Build. Mater.*, vol. 316, no. August 2021, p. 125980, 2022.
- [27] Y. Chi, P. Yang, S. Ren, and J. Yang, "Jo ur na l P re of," *Sci. Total Environ.*, p. 138954, 2020.
- [28] R. R. M. de Freitas, K. P. do Carmo, J. de Souza Rodrigues, V. H. de Lima, J. Osmari da Silva, and V. R. Botaro, "Influence of alkaline treatment on sisal fibre applied as reinforcement agent in composites of corn starch and cellulose acetate matrices," *Plast. Rubber Compos.*, vol. 50, no. 1, pp. 9–17, 2021, doi: 10.1080/14658011.2020.1816119.
- [29] A. Orue, A. Jauregi, C. Peña-Rodriguez, J. Labidi, A. Eceiza, and A. Arbelaitz, "The effect of surface modifications on sisal fiber properties and sisal/poly (lactic acid) interface adhesion," *Compos. Part B Eng.*, vol. 73, pp. 132–138, 2015.
- [30] Ahmad, F., Jamal, A., Iqbal, M., Alqurashi, M., Almoshaogeh, M., Al-Ahmadi, H. M., & E Hussein, E. (2022). Performance evaluation of cementitious composites incorporating nano graphite platelets as additive carbon material. *Materials*, 15(1), 290.
- [31] Ahmad, F., Jamal, A., Mazher, K. M., Umer, W., & Iqbal, M. (2022). Performance evaluation of plastic concrete modified with e-waste plastic as a partial replacement of coarse aggregate. *Materials*, 15(1), 175.



DEVELOPING HIGH PERFORMANCE CONCRETE USING JUTE FIBERS

^a Umer Nisar Satti, ^b Muhammad Saad Azam, ^c Daniyal Iftikhar*

a: Department of Civil Engineering, HITEC University Taxila, Pakistan, engr.umernisarsatti@gmail.com

b: Department of Civil Engineering, HITEC University Taxila, Pakistan, msaadazam.22@gmail.com

c: Department of Civil Engineering, HITEC University Taxila, Pakistan, Syed29245@gmail.com

*Umer Nisar Satti: Email ID: engr.umernisarsatti@gmail.com

Abstract- Jute fibers can be effective material to increase the strength of concrete. In Pakistan jute is easily available and cheap. To verify this aim, an experimental investigation of the flexural, tensile, compressive, rebound hammer and UPV test was performed to check the potential of jute fibers in enhancing the strength of concrete. To perform these test and to check the effect of these parameter, standard cylindrical and cube shaped specimens were prepared with different mixing ratios, and then those test results were compared to normal plain concrete. Also it had been observed that using larger cut length and higher amount jute fibers. content has ability of making round (balling) type of formation. Hence it decreases the mechanical properties of jute fibers reinforcement of concrete cement. However, shorter fiber lengths and lower fiber content led to strong structure and improved mechanical properties. Also, it had been observed that the presence of jute fibers with high amount of cement and well graded coarse aggregate resulted in greater strength of concrete.

Keywords- Concrete, Economical, Jute fibers, Specimens, Strength

1 Introduction

The construction industry is increasingly demanding building safety against heavy loads such as impact, and this requires materials with greater mechanical strength. However, cost effectiveness in construction should not be compromised. Fibers can be added to concrete to improve its mechanical properties and strength without sacrificing affordability [1]. The use of fiber is one viable and economical solution to the rust problem associated with steel reinforcement in buildings. Fiber can also enhance concretes resistance to impact loadings and the present study aims to investigate the use of jute fiber for this purpose [2]. The problem being addressed is the need for structures that can better withstand severe dynamic/impact loading. Concrete is most commonly used for construction, but it is weak in tension and requires expensive steel reinforcement. Jute fibers are a cost effective alternative to steel reinforcement and can convert crushing failure to bridging failure, providing sufficient load carrying capacity, and splitting tensile strength for concrete [3].

The present study aims to explore the overall behavior of jute fiber concrete in depth and to obtain sufficient concrete strength for better resistance against dynamic /impact loading. The raw jute fiber accessible locally, as shown in Figure 1, was used in the investigation with no pre-treatment. Different lengths of jute fibers, namely 10, 15 and 20mm were added to the concrete mixture in varied amounts. The binding substance was ordinary Portland cement with a normal consistency of 30%, an initial setting time of 02 hours and final setting time of 07 hours. The combination also included coarse materials such as sand with a fineness modulus of 2.5 and 25-mm down well-graded coarse aggregate [2].



2 Experimental Procedures

The current study evaluated the tensile strengths, flexural, compressive of concrete composites with jute fiber of ordinary concrete. A compression testing machine is used for tensile and compressive test.

2.1 Ultrasonic Pulse Velocity (UPV)

It is a nondestructive test as shown in Figure 1, that can be conducted on a concrete specimen that includes various materials like fine aggregate, coarse aggregate, and jute fibers. The UPV test is primarily used to check the reliability of concrete, including the voids, detection of cracks and other potential defects. In this test pulse of ultrasonic are passes through the specimen and it measures the time, pulse had taken to reach the structure as shown in Figure 1.b [4].

2.2 Rebound Hammer

It is a non-destructive test that may be carried out on concrete samples such cubes and cylinders that include jute fibers, fine aggregate, coarse aggregate and cement. The main purpose of this test is to determine the compressive strength of concrete. Depending on how solid the concrete surface is when the rebound hammer plunger is driven against it, determines how much the spring-controlled mass will rebound. It is believed that surface hardness and rebound are connected to the concrete's compressive strength. Divide each specimen into 10 sections, cylinder and cubes by marking on them as shown in figure 1.a. Use rebound hammer on each specimen after that take average from each specimen [5].



Figure 1: Test on Cylinder a. Ultrasonic pulse velocity (UPV) test, and b. Rebound hammer test

2.3 Testing for Compressive Strength

Compressive strength of the concrete is to evaluate the tendency to bare a static load, which tends to failure as shown in figure 2.a. The most common type of testing for concrete strength is compression; as many desired properties of concrete are correlated with its strength, concrete compressive strength is crucial for structural design [6]. Additionally, as the volume dosage rate of fiber rises in the specimens, it clearly indicates that how the compressive strength changes. AS 1012 states that specimens made for compressive strength must be about (150 mm) in diameter and (300 mm) high, although this standard only applies to aggregate with a size greater than 20 mm [7]. The stress intensity is measured qualitatively in MPa for the cube specimen (AS 1012 2002), which has 150 mm on each side. The compression test was conducted using the AS 1012.9 test method [8, 9].

2.4 Tensile Strength Testing

Tensile strength testing is mechanical test that measures a material's capacity to resist a stretching force without breaking. During the test, a sample of material is pulled until it reached to the break point as shown in figure 2.b. The maximum stress that a material can bare before it starts breaking under strain is known as its tensile strength. Tensile strength testing is mostly used in the manufacturing and construction industries to determine the strength and quality of materials like metals, polymers, and composites [6].

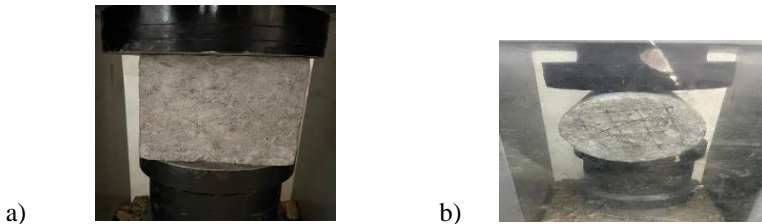


Figure 2: Test on Cube and Cylinder a. Compressive test on cube, and b. Tensile testing on cylinder

3 Research Methodology

The volume and length proportion of the jute fiber material was employed as concrete composite characteristics. Fiber lengths of 10mm, 15mm, 20mm were employed, as well as contents of 0, 0.1, 0.25 and 0.50%. Three distinct specimens were made to assess the tensile and compressive strength of: cubes (152.4 mm x152.4 mm) and cylinders (152.4 mm x 304.8 mm). The fibers were manually trimmed to specified length using a scissor and were added slowly while mixing, so the mixing was done properly before adding water to ensure equally distribution of fibers throughout the concrete (as shown in figure 3.a). This method of mixing the concrete was manually done for almost 3 minutes [2]. Once the concrete is mixed properly (as shown in figure 3.b) than it was poured into the cylinder and cube mould. Specimens were demolded after 1 day and then submerged in curing tank for 14 days. Once the curing period is finished, specimens were given 24 hours to air dry [10].

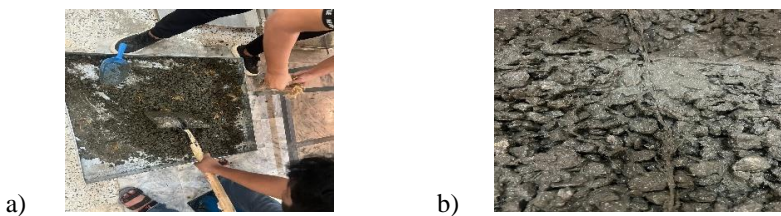


Figure 3: Test on Cube and Cylinder a. Compressive test on cube, and b. Tensile testing on cylinder

4 Results

The experimental results indicated a significant improvement in the strength properties of concrete when 0.1% by weight of 10mm jute fibers were added to the mix ratio of (1:1.5:3). The addition of jute filers resulted in an increase in both tensile strength and compressive strength when compared to conventional concrete without fibers. The incorporation of jute fibers led to a 33% increase in tensile properties, as demonstrated in Figure 5, and a 15% increase in compressive strength, as shown in Figure 4.

The average results of the rebound hammer test were 32.1, indicating that the quality of concrete was good as the value of good concrete varies from 30-40. The ultrasonic pulse velocity (UPV) values indicated that there were minimum void ratios or air pockets due to the presence of jute fibers.

These findings suggest that the addition of jute fibers to concrete can enhance its strength and durability. The results of this study provide valuable insights into the potential use of jute fibers as a reinforcement material in the construction industry.

4.1 Graphs.

Compressive strength test revealed that the addition of jute fibers increased the strength performance of the concrete. The concrete specimens with jute fibers achieved a significantly higher compressive strength compared to the control specimens. This increase can be attributed to the bridging effect provided by the jute fibers, which enhance the interfacial bonding between the cement and aggregate particles, leading to improved load transfer capabilities [11]. The tensile strength of the concrete increased with the incorporation of jute fibers. The fibers acted as reinforcement within the concrete matrix, resisting crack propagation and increasing the tensile strength.



5th Conference on Sustainability in Civil Engineering (CSCE'23)

*Department of Civil Engineering
Capital University of Science and Technology, Islamabad Pakistan*



Table 1 Strength Comparison table between conventional concrete and JFC with different mix ratios

TEST	COMPRESSION STRENGTH						SPLIT TENSILE STRENGTH					
	Ratio			1:2:4			1:1.5:3			1:2:4		
Length of jute fiber	10 mm	15 mm	20 mm	10 mm	15 mm	20 mm	10 mm	15 mm	20 mm	10 mm	15 mm	20 mm
Conventional concrete	9MPa			10MPa			3MPa			3.5MPa		
FC1 (0.1)	10.1	9.1	7.4	11.5	10.8	9.9	3.39	3.15	3.06	4.65	3.92	2.73
FC2 (0.25)	10	8.6	7.2	11.4	10.3	9.2	3.51	3.18	3.04	4.51	3.78	3.04
FC3 (0.50)	8.5	8.3	6.8	10.8	9.9	9.1	3.12	3.09	2.85	4.23	3.65	2.31

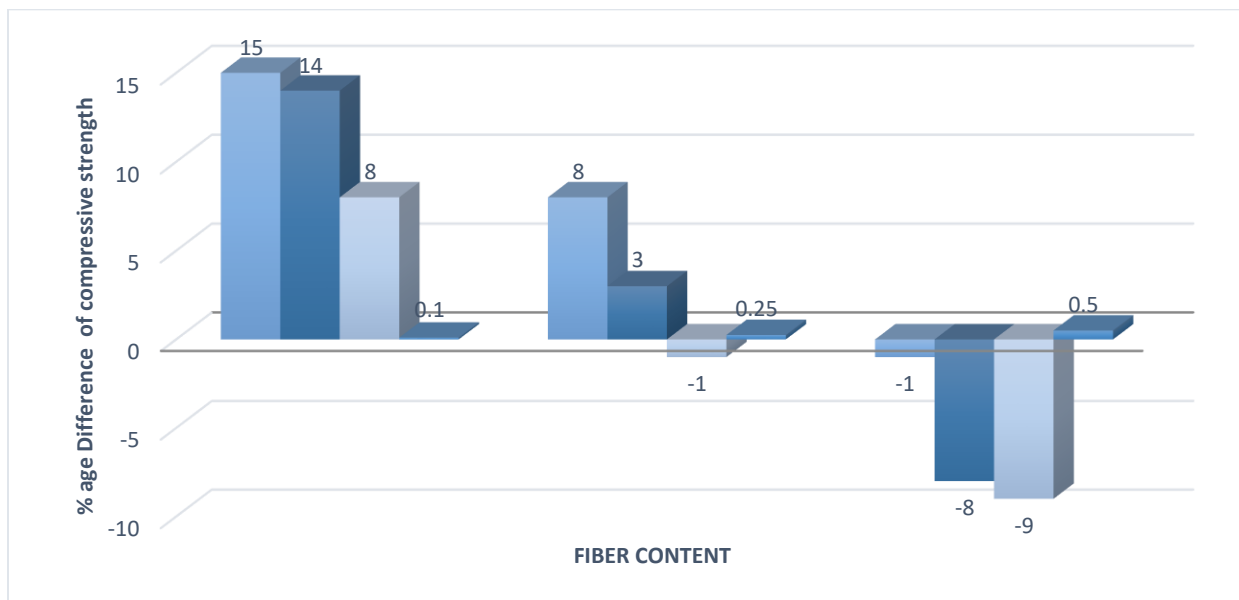


Figure 4 Comparison of Compression Value of JFC with (1:1.5:3) Mix Ratio

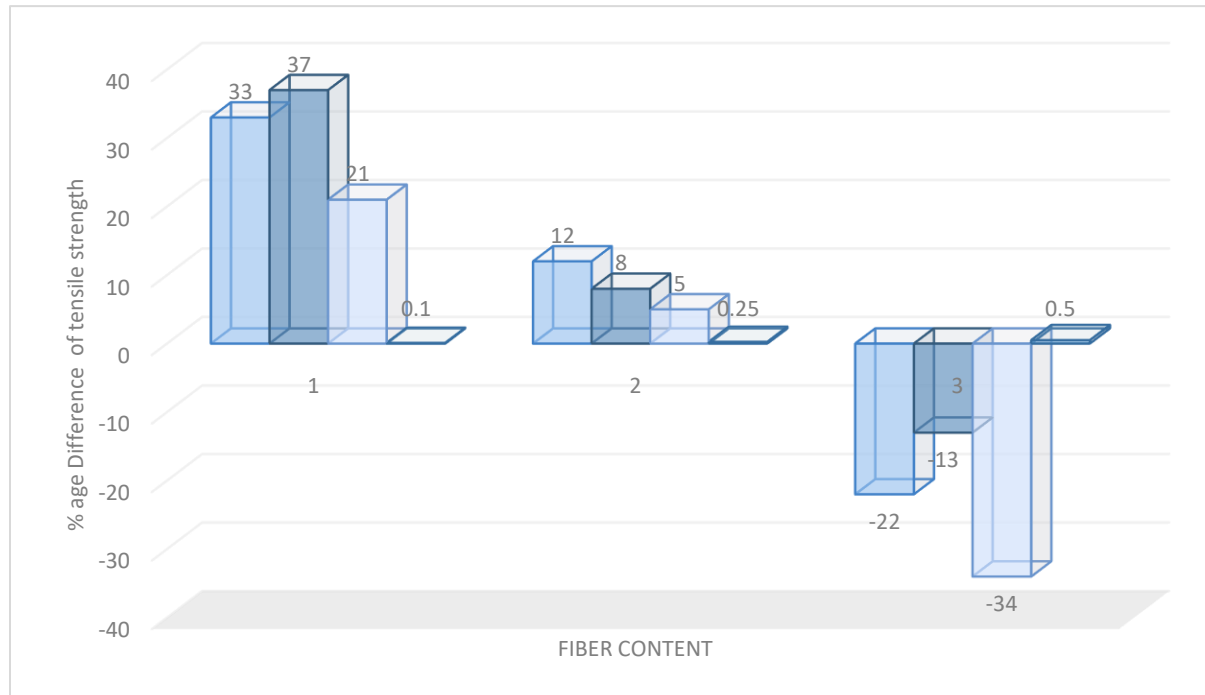


Figure 5 Comparison of Tensile Test of JFC with (1:1.5:3) Mix Ratio

5 Practical Implementation

The use of jute fibers in concrete has become increasingly popular in recent years due to the many benefits it provides. Jute fibers are a natural, renewable resource that is inexpensive and widely available. They are an eco-friendly alternative to synthetic fibers that are often used in concrete. Addition of jute fibers to concrete can improve its strength and durability. As fibers help to prevent cracking and improve the overall toughness of the concrete. This is especially important in areas that are prone to earthquakes or other natural disasters. Jute fibers can also be used to reduce the weight of concrete. This is particularly useful in construction projects where weight is a concern. The fibers can be used to create lightweight concrete that is easier handle and transport. In addition to their physical properties, jute fibers are also fire-resistant and provide good insulation properties. This makes them an ideal material for use in the construction industry.

6 Conclusions

The incorporation of 0.1% by weight of 10 mm jute fibers into concrete with a mix ratio of 1:1.5:3 resulted in significant improvements in tensile strength and compressive strength. The result concluded from this research suggest that jute fiber-reinforced concrete can be a viable and sustainable alternative for applications where increased strength is desired. The long-term durability and other properties of JFC (Jute Fiber Concert) to fully evaluate its potential for practical implementation in construction projects.

Reference

- [1] M. Aziz, P. Paramasivam, and S. Lee, "Prospects for natural fibre reinforced concretes in construction," *International Journal of Cement Composites and Lightweight Concrete*, vol. 3, no. 2, pp. 123-132, 1981.
- [2] T. Hussain and M. Ali, "Improving the impact resistance and dynamic properties of jute fiber reinforced concrete for rebars design by considering tension zone of FRC," *Construction and Building Materials*, vol. 213, pp. 592-607, 2019.
- [3] J. Ahmad, M. M. Arbili, A. Majdi, F. Althoey, A. Farouk Deifalla, and C. Rahmawati, "Performance of concrete reinforced with jute fibers (natural fibers): A review," *Journal of Engineered Fibers and Fabrics*, vol. 17, p. 15589250221121871, 2022.



5th Conference on Sustainability in Civil Engineering (CSCE'23)

Department of Civil Engineering

Capital University of Science and Technology, Islamabad Pakistan



- [4] K. Komlos, S. Popovics, T. Nürnbergrová, B. Babal, and J. Popovics, "Ultrasonic pulse velocity test of concrete properties as specified in various standards," *Cement and Concrete Composites*, vol. 18, no. 5, pp. 357-364, 1996.
- [5] K. Sanchez and N. Taranza, "Reliability of rebound hammer test in concrete compressive strength estimation," *Int. J. Adv. Agric. Environ. Eng.*, vol. 1, no. 2, pp. 198-202, 2014.
- [6] S. Tiwari, A. Sahu, and R. Pathak, "Mechanical properties and durability study of jute fiber reinforced concrete," in *IOP Conference Series: Materials Science and Engineering*, 2020, vol. 961, no. 1: IOP Publishing, p. 012009.
- [7] M. Zakaria, M. Ahmed, M. Hoque, and A. Shaid, "A comparative study of the mechanical properties of jute fiber and yarn reinforced concrete composites," *Journal of Natural Fibers*, 2018.
- [8] N. Dayananda, B. K. Gowda, and G. E. Prasad, "A study on compressive strength attributes of jute fiber reinforced cement concrete composites," in *IOP Conference Series: Materials Science and Engineering*, 2018, vol. 376, no. 1: IOP Publishing, p. 012069.
- [9] N. Bheel, T. Tafsirojjaman, Y. Liu, P. Awoyera, A. Kumar, and M. A. Keerio, "Experimental study on engineering properties of cement concrete reinforced with nylon and jute fibers," *Buildings*, vol. 11, no. 10, p. 454, 2021.
- [10] M. S. Islam and S. J. Ahmed, "Influence of jute fiber on concrete properties," *Construction and Building Materials*, vol. 189, pp. 768-776, 2018.
- [11] A. Razmi and M. Mirsayar, "On the mixed mode I/II fracture properties of jute fiber-reinforced concrete," *Construction and Building Materials*, vol. 148, pp. 512-520, 2017.



RESPONSE SURFACE METHODOLOGY BASED OPTIMIZED MIX DESIGN FOR SELF-COMPACTING CONCRETE BLENDDED WITH METAKAOLIN WASTE

*^aAbdul Aziz, ^bSyed Saqib Mehboob**

a: Department of Civil Engineering, UET, Taxila, Pakistan, engr.abdulazizwattoo@yahoo.com

b: Department of Civil Engineering, UET, Taxila, Pakistan, syed.saqib@uettaxila.edu.pk

* Corresponding author: Email ID: syed.saqib@uettaxila.edu.pk

Abstract- This study explored the fresh and hardened properties of self-compacting concrete (SCC), which is enhanced with an active combination of Metakaolin (MK) and Limestone Powder (LP). This led to the development of a method for achieving the ideal ratio of ingredients during the mix design process using optimization technique. An analysis of 16 mixing schemes is conducted using the response surface method (RSM). There are two categories of input variables: mixture variables and process variables. As mixture constituents the three ingredients of cement, metakaolin, and lime were constrained to a total of 100%. While coarse aggregate, fine aggregate, and the water-to-binder ratio were considered as process variables. By adding metakaolin and limestone powder to the SCC, the cement replacement level can range from 40 to 55%. In order to find the perfect combination, RSM optimization was employed. To understand the rheological properties of the mixture some tests like slump flow, L-box, and sieve segregation were performed. And to measure the mechanical strength, the samples were examined for the compressive strength at both 7- and 28-days. According to experimental findings, adding metakaolin at a higher concentration decreases both its workability and hardened properties.

Keywords- Mix design, Optimization, Response surface methodology, Self-compacting concrete.

1 Introduction

In the 21st century according to the United Nations annual report waste generation has potentially increased leading to environmental issues [1]. In the construction sector the excessive utilization of sand and gravel during production of concrete has not only significantly decreased natural resources but also CO₂ emissions has raised serious concerns regarding global warming [2]. From the last two decades' construction sector is considered as crucial domain and the constructional projects cannot be overlooked. Cement is a vital part of infrastructural construction activities and produced significant economic impact. According to reports worldwide approximately production of cement is three billion tons every year [3]. Therefore, the cement industry is facing exceptional challenges due to production of Ordinary Portland Cement (OPC) related to climatic changes as well as ailing economy of world in recent times. The inflation rate in prices of cement to alarming level during past few years has raised the need to explore other natural cost-effective materials for the substitution of cement [4]. To overcome these barriers, researchers are recommending utilization of eco-friendly supplementary cementitious materials (SCMs) either partially or fully for replacing OPC in concrete construction [5]. The globally campaigns are aiming to boost production and utilization of environment-friendly substantial construction material that can substitute conventional concrete materials [6]. The basic ideologies for eco-friendly environment focus



on conservation of resources, reduction of pollution, conservation of energy, reduction of waste and to protect the ecological balance of planet [7]. Keeping in view self-compacting concrete (SCC) has gained enormous popularity. The designing of SCC optimal design mix is a challenging task as a wide variety of factors affect the properties of SCC [8]. The traditional experimental design strategies for evaluation of multiple parameters affecting properties of SCC required number of trial experiments which are tedious, costly and time consuming. Hence in this study optimization technique to overcome these deficiencies Response Surface Methodology RSM has been utilized for obtaining cost and time effective eco-friendly optimized design mix for SCC. The aim of current study was to achieve optimized SCC exhibiting desirable characteristics by replacement of cement with metakaolin and limestone powder simultaneously which can be attributed to MK imparting strength property to concrete due to MK pozzolanic reaction with calcium hydroxide, enhancing ordinary Portland cement hydration and filler effect [9].

2 Experimental Procedures

2.1 Materials and Methods.

Metakaolin (Shaheen Mining Corporation); Cement (Fuji Cement Company Ltd); Limestone powder (Naeem Brothers Marble, Granite and Chakwal Stone Works); Coarse aggregate (Khanpur); Fine aggregate (Lawrencpur); Superplasticizer (Sika Pakistan). Software-Design Expert (DX®), Ver 22 (Stat-Ease, Inc., Minneapolis, USA) was employed to analyze the data for optimization.

3 Research Methodology

3.1 Concrete Mix Design and Specimen Preparation.

For finalizing the confined number of mixes, 16 No of trail mixes were carefully designed based upon L16 array by using four levels of each parameter namely cement replacement level, w/b ratio, coarse aggregate, binder content and fine aggregates shown in Table 1. The cement content was replaced by metakolin and lime powder in different proportions. Finally, 16 mixes were named for the further experimental study named as M1, M2, M3, M4, M5, M6, M7, M8, M9, M10, M11, M12, M13, M14, M15 and M16. The fresh properties tests i.e., slump flows, and L-box segregation resistance test were performed on completion of mixing time of each mixes. All tests, for fresh state properties, were conducted following the methods given by the SCC Committee of EFNARC (2005). Fresh properties of mixes tested in this experimental study are Slump flow, L-box test, and segregation resistance. The hardened properties that is compressive e strength at 7 and 28days were also studied for each mix by using laminated wooden molds in concrete laboratory. These molds were firstly cleaned and then properly oiled. After oiling, molds were placed on a clean surface and filled under their weight without compaction. After casting, the top surfaces of samples were leveled. Then, all specimens were stored at room temperature until demolding. The steel molds were removed after one day, and all specimens were placed for moist curing as per ASTM C192. The compressive strength was examined at 7 and 28 days respectively for each mix.

Table 1: Levels of parameters

L	Cement replacement %	W/B Ratio	Coarse Aggregates	Binder Content	Fine Aggregates
1	40	0.32	769.86	450	690
2	45	0.38	756.68	475	678.18
3	50	0.45	743.56	500	666.37
4	55	0.5	730.31	525	654.55

3.2 Optimization

Design Expert (DX®), Ver 22 (Stat-Ease, Inc., Minneapolis, USA) was employed to analyze the data for optimization. The factors were divided into two categories, i.e., mixture and process variables. Cement, metakaolin and lime were



5th Conference on Sustainability in Civil Engineering (CSCE'23)

*Department of Civil Engineering
Capital University of Science and Technology, Islamabad Pakistan*



included as the mixture components, constraints with the total of 100 percent. While the W/B, coarse aggregate and fine aggregate were considered as process variables. The data were entered in customized design with blank sheet adjusted to mixture components and process factors, with each of 3 variables. The details of the mixture and process components have been elaborated in Tables 2 and 3, respectively. In the mixture components, the design constraints have been given in Table 4.

Table 2: Factors for optimization

Component	Name	Units	Type	-	Minimum	Maximum
Mixture	A	%	Mixture	-	45	60
	B	%	Mixture	-	15	45
	C	%	Mixture	-	10	25
Total =						100.00
Process	D	W/B	Numeric	Continuous	0.3200	0.5000
	E	Coarse Agg.	kg/cum	Numeric	730.31	769.86
	F	Fine Agg.	kg/cum	Numeric	654.55	690.00

Table 3: Projected responses with factors for optimization

Response	Name	Units	Observations	Minimum	Maximum	Mean	Std. Dev.	Ratio
R1	Slump flow	mm	16.00	400	865	621.06	169.48	2.16
R2	Passing Ability		16.00	0.15	0.846	0.3924	0.2387	5.64
R3	Segregation resistance	%	16.00	0.88	94.48	23.91	28.53	107.36
R4	Compressive strength at 7 days	Mpa	16.00	5.97	16.39	11.25	3.79	2.75
R5	Compressive strength at 28 Days	Mpa	16.00	8.16867	21.3471	15.12	4.35	2.61

Table 4: Design constraints

Low Limit	Constraint			High Limit
45.0	\leq	A: Cement (%)	\leq	60.0
15.0	\leq	B: Metakaolin (%)	\leq	45.0
10.0	\leq	C: Lime Powder (%)	\leq	25.0
A+B+C			$=$	100.0

4 Results

The workability of each mix was investigated by using slump cone test according to ASTM C143. The main reason for decreasing in slump flow value was MK particle size because the surface area of MK was more than the cement particles. A large surface area negatively affects the fresh and rheological properties of concrete, because of its spread over a large area and obstruct the movement of fresh concrete, that is why slump flow decreased by increasing MK in SCC. The passing ability values were found in EFNARC ranges of three mixtures M4, M12 and M16 having W/B ratio 0.5. It can be attributable to water cement ratio on higher side as compared to other mixes that made SCC more flowable due to its fluidity leading to decrease in blockage [10]. Sieve segregation resistance values of mixes M3, M4 M6 M8, M11 and M16 were not in EFNARC limits due to having lesser viscosity as compared to other having dense viscosity. Both ages (7- and 28-days) compressive strength of mixes from M1 to M8 were found to be higher as compared to mixes M9 to M16 due to higher replacement of cement percentage. The increase in strength can be attributed due to the addition of mineral admixtures i.e., MK pozzolanic and micro-filling features. It can be justified by the pore size reduction and refinement of crystal structure by addition of fine particles [10].



5th Conference on Sustainability in Civil Engineering (CSCE'23)

*Department of Civil Engineering
Capital University of Science and Technology, Islamabad Pakistan*



Table:5: Mix design trials

Mix. ID	Binding content kg/cum	Cement Replaced Level %	MK %	LP %	W/B	CA kg/cum	FA kg/cum	Slump flow mm	Passing Ability	Segregation resistance %	CS at 7 days Mpa	CS at 28 Days Mpa
M1	450	40	30	10	0.32	769.86	690	545	0.160	19.76	16.20	18.82767
M2	475	40	25	15	0.38	756.68	678.18	645	0.212	1.13	15.04	19.71915
M3	500	40	20	20	0.45	743.56	666.37	800	0.345	33.40	16.39	18.88581
M4	525	40	15	25	0.5	730.31	654.55	835	0.846	60.00	14.85	18.18813
M5	500	45	30	15	0.32	756.68	654.55	415	0.308	1.32	13.46	20.20365
M6	525	45	25	20	0.38	743.56	690	770	0.257	58.18	14.61	21.34707
M7	450	45	20	25	0.45	730.31	678.18	560	0.188	5.36	14.86	18.38193
M8	475	45	35	10	0.5	769.86	666.37	747	0.470	94.48	12.03	14.42841
M9	525	50	30	20	0.32	743.56	678.18	450	0.300	0.88	8.43	13.74042
M10	450	50	25	25	0.38	730.31	666.37	590	0.150	11.56	7.69	14.16678
M11	475	50	40	10	0.45	769.86	654.55	865	0.250	54.5	7.97	11.42451
M12	500	50	35	15	0.5	756.68	690	620	0.800	11.04	10.53	12.48072
M13	475	55	30	25	0.32	730.31	666.37	400	0.380	1.70	7.85	14.070849
M14	500	55	45	10	0.38	769.86	654.55	405	0.250	1.02	6.59	8.16867
M15	525	55	40	15	0.45	756.68	690	450	0.530	2.30	5.97	8.76945
M16	450	55	35	20	0.5	743.56	678.18	840	0.833	25.98	7.46	9.1086

4.1 Optimization for Significance Mix Proportion.

The ANOVA (see Table 5) shows the model and the significant terms. The data was modeled by using the modified reduced Linear \times 2FI. No data transformation was needed for this model. The Predicted R² of 0.5801 was in a reasonable agreement with the adjusted R² of 0.7709 as the difference between above was < 0.2. The Adequate Precision ratio obtained by ANOVA was 8.072 indicated an adequate signal, as it was > 4. This model can be used to navigate the design space. The F-value of 8.21 reflected the significance of the model. There is only a 0.40% chance that an above F-value could occur due to noise. P-values < 0.05 indicated only D was significant, while A, B were not significant, yet they were involved in the significant interactions, such as AD, BE, BF and DF (see Table 4). The model terms bearing p-value > 0.10 were not significant yet included to support hierarchy. The final expressions in terms of L-Pseudo Components and Coded Factors are as follows: Slump flow (mm) = +981.62A+864.01B+277.30D-55.18E-303.37AD-444.51BE-191.80BF-161.29DF. Passing ability = +1.33A+0.2537B-0.0808C-0.3246D-3.89AB+0.9066BD+0.4144D²+0.1093F². Log₁₀



5th Conference on Sustainability in Civil Engineering (CSCE'23)

*Department of Civil Engineering
Capital University of Science and Technology, Islamabad Pakistan*



(segregation resistance (%)) = -0.7391A+0.3650B+1.69C+0.6778D+5.54AB-0.6230DF. Compressive strength at 7 days (Mpa) = +25.30A+5.81B+8.06C+3.24CF. Compressive strength at 28 Days (Mpa) = +28.27A+8.91B+14.58C-1.62D.

Table 6: ANOVA for the significance of the model

Response	Source	Sum of Squares	Df	Mean Square	F-value	p-value
Slump flow	Model (Reduced Linear \times 2FI)	3.782E+05	7	54030.76	8.21	0.0040*
	(¹)Linear Mixture	-2.079E+05	1	-2.079E+05	-31.59	1.0000
	D-W/B	1.427E+05	1	1.427E+05	21.69	0.0016*
	E-coarse aggregate	2485.20	1	2485.20	0.3777	0.5559♣
	AD	13550.61	1	13550.61	2.06	0.1892♣
	BE	40616.67	1	40616.67	6.17	0.0379*
	BF	64131.63	1	64131.63	9.75	0.0142*
	DF	80537.49	1	80537.49	12.24	0.0081*
Passing ability	Model (Quadratic \times Quadratic model)	0.8345	7	0.1192	46.57	< 0.0001*
	(¹)Linear Mixture	0.0483	2	0.0242	9.44	0.0079
	D-W/B	0.0246	1	0.0246	0.62	0.0146*
	AB	0.0955	1	0.0955	37.29	0.0003*
	BD	0.0622	1	0.0622	24.31	0.0011*
	D ²	0.3405	1	0.3405	133.03	< 0.0001
	F ²	0.0250	1	0.0250	9.75	0.0142
	Model (Quadratic \times 2FI model)	5.79	5	1.16	5.24	0.0128*
Segregation resistance	(¹)Linear Mixture	0.9523	2	0.4761	2.15	0.1669
	D-W/B	3.68	1	3.68	16.63	0.0022*
	AB	0.8292	1	0.8292	3.75	0.0816♣
	DF	1.38	1	1.38	6.23	0.0316*
Compression strength at 7-day	Model (Linear \times linear)	198.93	3	66.31	48.08	< 0.0001*
	(¹)Linear Mixture	193.80	2	96.90	70.26	< 0.0001
	CF	5.13	1	5.13	3.72	0.0778♣
	Model (Linear \times linear)	250.29	3	83.43	30.09	< 0.0001*
Compression strength at 28-day	(¹)Linear Mixture	226.05	2	113.02	40.77	< 0.0001
	D-W/B	24.24	1	24.24	8.74	0.0120*

▪ Notes: df = Degree of freedom; *significant mode or terms; ♣ non-significant terms, yet added to support hierarchy of the model

Figure 1a shows that the cement and metakaolin and the limestone powder have positive effect on slump flow. Figure 1b shows that cement and metakaolin have positive effects on the passing ability and lime powder has negative effect on the passing ability. Figure 1c represented that cement has negative effect on segregation resistance and metakaolin and lime powder has positive effect on segregation resistance. The practical implementation of the current study is that SCC can be used for casting heavily reinforced sections, places where there is no possibility to use vibratos for compacting concrete and for complicated shapes of formwork which cannot be possible to cast. Moreover, MK inclusion remarkably enhances the compressive strength at early ages. So, it can be used in-situ concrete constructions in offshore structures and tall buildings. The optimized mix design predicted by software has shown that desired features were attained at following ratio of input parameters including cement replacement level 41.22% by 22.213% metakolin and 19.088 % LP respectively keeping w/b ratio at 0.376, coarse aggregate at 736.143kg/cum, fine aggregate at 689.99kg/cum. The mix design was validating practically according to composition generated by software and it was observed that predicted responses agreed with observed responses in terms of slump flow 750.0 mm, passing ability 0.85, segregation resistance 12%, compressive strength at 7 days and 28 days 17 Mpa and 20 Mpa respectively.

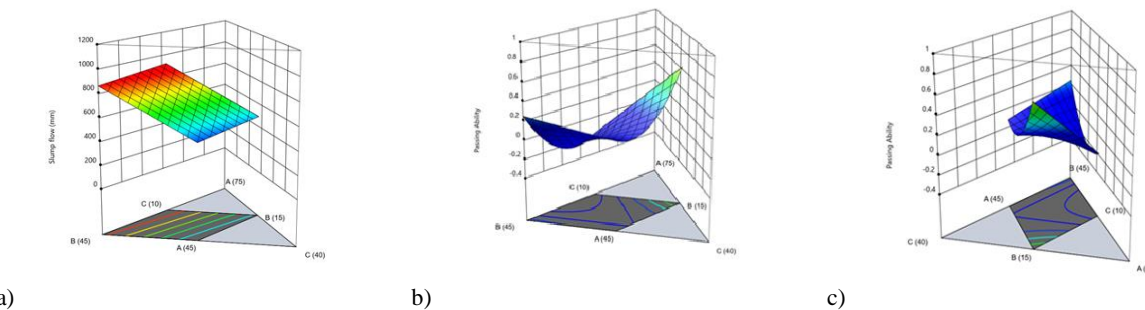


Figure 1: RSM results showing combined effect of cement, metakaolin, lime powder on various parameters like, a. slump flow, b. passing ability, and c. segregation resistance.

5 Conclusions

The optimization approach was utilized in this study by using RSM (Response surface methodology) to achieve self-compacting concrete efficiency. The study concludes that following the effective application of RSM optimization trial selected for validation study, it was determined that the desirable attributes could be attained by using an optimized mix design that included at least 41% cement replacement, followed by 22.213% replacement of metakaolin and 19.088%, lime powder, having a W/B ratio of 0.376 and containing 736143. kg/m³ of coarse aggregate and 689.99 kg/m³ of fine aggregate. The RSM regression model was employed to review self-compacting concrete properties. The ANOVA results also verified the statistically significant inclusions of all model parameters. The compressive strength of increases with increase replacement level of cement. The optimal value was achieved with replacement of cement at 41%. The similarity of predictive approach with the outcomes expected by the model leads to satisfactory experimental design adopted to measure the properties of new mixes. The results which are experimentally developed and comparison with the predicted results was nearly approximately same values. Moreover, in this study the utilization of metakaolin and lime powder as cement substitute is cost effective, sustainable and ecofriendly approach.

Acknowledgment

The authors express their heartfelt gratitude to all individuals who generously contributed to this research endeavor, with special recognition extended to the Civil Engineering department at UET Taxila for the invaluable support and assistance.

References

- [1] M. Perspectivas, "United Nations Environment Program-Global Environment Outlook GEO-3. UNEP. Fecha de consulta: Noviembre 6 de 2009," ed, 2009.
- [2] M. Behera, S. Bhattacharyya, A. Minocha, R. Deoliya, and S. Maiti, "Recycled aggregate from C&D waste & its use in concrete—A breakthrough towards sustainability in construction sector: A review," *Construction and building materials*, vol. 68, pp. 501-516, 2014.
- [3] R. Cao, Z. Fang, M. Jin, and Y. Shang, "Study on the Activity of Metakaolin Produced by Traditional Rotary Kiln in China," *Minerals*, vol. 12, no. 3, p. 365, 2022.
- [4] K. S. Devi, V. V. Lakshmi, and A. Alakanandana, "Impacts of cement industry on environment—an overview," *Asia Pac. J. Res.*, vol. 1, pp. 156-161, 2017.
- [5] S. Ibrahim and A. Meawad, "Towards green concrete: study the role of waste glass powder on cement/superplasticizer compatibility," *Journal of Building Engineering*, vol. 47, p. 103751, 2022.
- [6] R. K. Gomaa, A. Atef, and A. Mostafa, "Use of environment friendly recycled building materials in Egypt," *Journal of Al-Azhar University Engineering Sector*, vol. 17, no. 63, pp. 667-683, 2022.
- [7] A. I. Asuquo, N. O. Dan, and G. T. Effiong, "Effect of eco-friendly costs on net revenue of cement producing firms," *International Journal of Scientific and Technology Research*, vol. 9, no. 9, pp. 235-240, 2020.
- [8] B. Ramesh, V. Gokulnath, and M. R. Kumar, "Detailed study on flexural strength of polypropylene fiber reinforced self-compacting concrete," *Materials Today: Proceedings*, vol. 22, pp. 1054-1058, 2020.
- [9] M. H. R. Sobuz *et al.*, "Performance evaluation of high-performance self-compacting concrete with waste glass aggregate and metakaolin," *Journal of Building Engineering*, vol. 67, p. 105976, 2023.
- [10] S. Gao, X. Guo, S. Ban, Y. Ma, Q. Yu, and S. Sui, "Influence of supplementary cementitious materials on ITZ characteristics of recycled concrete," *Construction and Building Materials*, vol. 363, p. 129736, 2023.



RELIABILITY OF CORES TEST RESULT AT ELEVATED TEMPERATURE IN CASE OF NORMAL STRENGTH CONCRETE

^a Usman Ali*, ^b Muhammad Yaqub, ^c Tariq Ali

a: Department of Civil Engineering, UET, Taxila, Pakistan, aliusman05545@gmail.com

b: Department of Civil Engineering, UET, Taxila, Pakistan, yaqub_structure@yahoo.com

c: Department of Civil Engineering, Swedish College of Engg. and Technology Wah Cant, Pakistan, bridges.28751@gmail.com

* Usman Ali: Email ID: aliusman05545@gmail.com

Abstract- In the last decades the assessment of in situ quality of concrete and integrity of concrete elements have been tested through non-destructive approaches. Under the constant fire and earthquake risk it is very mandatory to determine the seismic performance of the existing structure and consequently, the strength of the concrete used in the construction should be known to decide for repairing and strengthening. In this instance concrete cores are taken from different places of structure and their compressive strength is determined by a test carried out on these core specimens. The core test is usually involved in the area of the concrete industry to evaluate strength and occasionally it develops a unique tool for safety assessment of concrete structures. In this study, the effect of temperature has been investigated and the reliability of the core test has been evaluated. For this purpose, the cylindrical core was extracted from Normal strength concrete (NSC) specimens that were exposed to the temperature ranging from 300 °C to 900 °C with a constant duration of 4 hr. This study compares the difference between the heated actual cylinder and the core taken from them after curing of 90 days. The difference of cylindrical control and binary mix samples and extracted core revealed that there is a 6.67% and 7.81% difference at 300 °C, while this difference was found to increase up to 8.72%, 9.81% at 500 °C Furthermore this value is recorded as 10.47%, 11.81%, and 11.97%, 13.56% at 700 °C and 900 °C respectively, whereas a total number of four (4) equation to developed through regression model for predicted strength of concrete for both cylindrical and extracted core whose R square value is 0.9666, 0.9794 and 0.9103, 0.8957 respectively.

Keywords- Normal Strength Concrete (NSC), Core Test, Temperature, Multiple Regression Model.

1. Introduction

Nowadays in the field of civil engineering concrete is a widely used material. Some reasons concrete used in construction commonly are that it is economical, easy to produce, workable, and better material but its physical and chemical properties to be changed when it is exposed to elevated temperatures causing severe deterioration and experiencing several reaction and transformation and resulting in a cement gel can breakdown and reduce the durability of concrete [1-2]. Due to elevated temperature, the strength of concrete was reduced, especially the compressive which is the main concern in any construction. Concrete compressive strength is a direct requirement for all concrete structures that are essential to resist the applied load of whatever nature. The compressive of concrete is a good index of most other properties of practical significance. During the construction, a standard test specimen was inspected to ensure the concrete quality. These samples which give the strength of concrete are prepared, cured, and tested according to the related standard specifications and codes. In another way, determination of the actual strength of concrete through the destructive method in any existing



structure is not easy for these reasons one of the most common approaches to determining in situ strength of concrete is to drill and core test [3-5].

Even though the way consists of an expansive and time-consuming process, core gives the reliable and useful results since they are tested mechanically to destruct[3]. The in situ compressive strength of the existing structure is required for the evaluation of structural safety. The in situ compressive strength of concrete is commonly determined by taking a core from different structural members and testing them in the laboratory environment but the strength of core concrete is affected due to many factors such as the core diameter, overlength ratio, coring orientation, core moisture condition at the time of testing [6-8]. During the initial evaluation, the outside of concrete may not be detected in less damaged components. In situ, and laboratory tests provide more precise information on the state and internal structure of concrete. The concrete compressive strength is the most important factor to estimate. It is critical to identify the thickness of the external layer of the member in which the concrete has been damaged to the point where it should be considered destroyed [9-11].

In the present study, the reliability of the core test has been investigated in NSC concrete after the elevated temperature in the range of (300 °C - 900 °C) and their data can be set in multiple regression models to develop the regression equation for the predicted strength of concrete. The novelty of this research on the reliability of cores at elevated temperatures in the case of normal strength is significant for several sectors because it provides an innovative approach to understanding material behavior and improving structural performance in high-temperature situations.

2. Experimental Program

2.1 Materials

The materials utilized in this investigational program along with specifications were summarized as.

2.2 Cement

The ordinary Portland cement type – I was used according to the ASTM C150 in the preparation of concrete having a fineness of 4.12%.

2.3 Fine Aggregate

A local sand from lawrancepure was used as a fine aggregate. The sieve analysis was conducted following ASTM C136 having a fineness modulus of 2.81.

2.4 Coarse Aggregate

A local coarse aggregate from Margala was used with a maximum nominal size of 12.5 mm. According to ASTM C 136, a sieve analysis was to be carried out.

2.5 Mix Proportion

Normal Strength Concrete (NSC) was used in this study. Using water-cement ratios of 0.5 and the concrete was made in the ratio of 1:2.5:2.5. To achieve the slump of 3 inches by using water reducing admixture of 0.75 by weight of cement. The addition of a calculated amount of water and admixture was added to achieve the targeted slump.

3. Research Methodology

3.1 Casting and Curing Method

The concrete ingredients (cement, sand, and aggregate) were appropriately mixed in dry conditions. Confirming the proper mixing of concrete cubes and cylinders was cast upon on standard procedure of compacting and placing in three layers. The samples were demolded after drying and then the samples were kept under control condition for 90 days. All these samples were removed from the control environment and allowed to dry at room temperature.

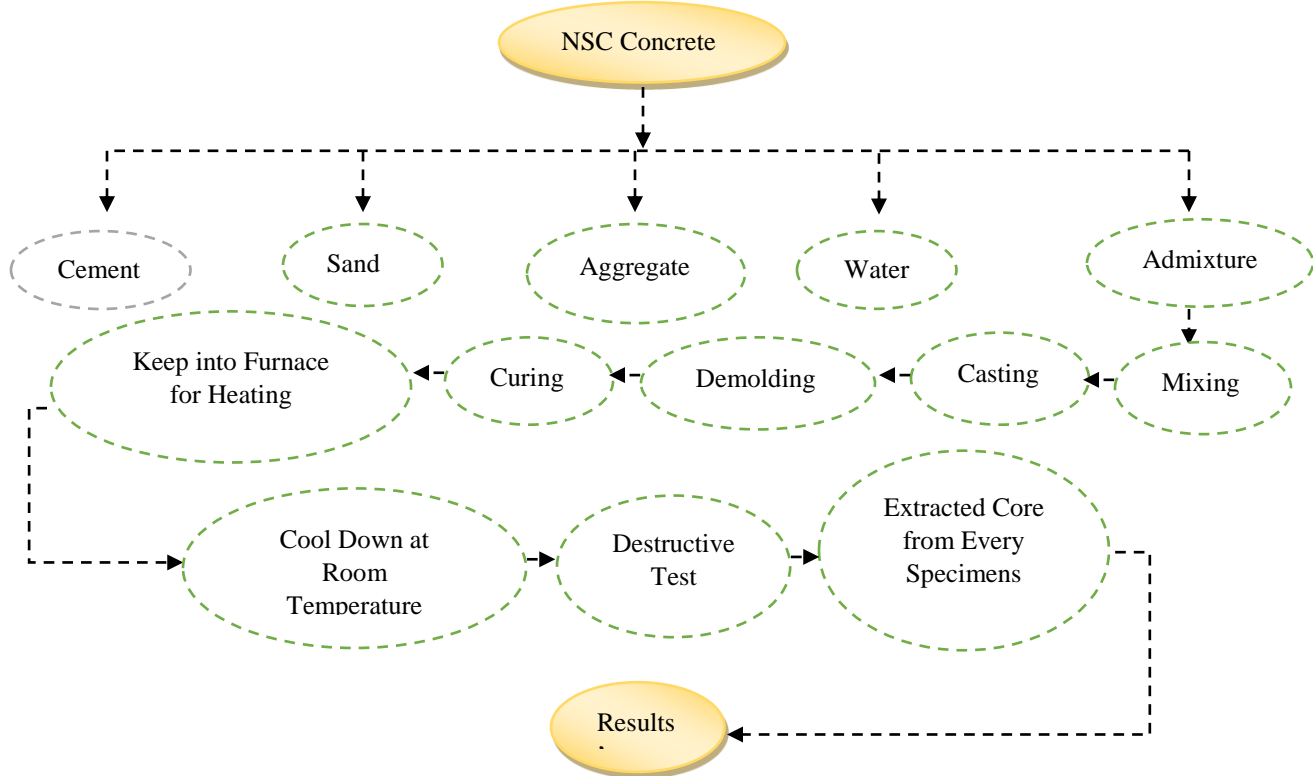


Figure 1: Methodology Flow Chart

3.2 Heating of Concrete

Locally furnace was developed to heat the specimens and its temperature was measured through thermocouples. The rising temperature of the furnace depended upon the arrangement supported by a valve and convey the appropriate thermocouples and thermostat fixed at each wanted compulsory point for a 4-hour constant duration. Throughout the mock testing, it was confirmed that the temperature rises in the furnace reached a maximum value of 1000 °C.

4. Results and Discussions

4.1 Compressive Strength After Elevated Temperature

When the concrete is exposed to higher temperatures its both physical and chemical properties are reported. Conventionally concrete can lose its strength to rising temperatures. It is evident from Figure 1 that there are NSC two groups that are experienced to the temperature the (G1) which contains pure cement and the (G2) cement replaced by fly ash.

The analysis of Figure 2 shows that when the temperature rises, the strength of concrete reduces but the G2 will perform better as compared to the G1. Due to the chemical reaction bond of cement, which is occurred from the hydration process, this bond would improve by partial replacement of pozzolanic materials[12-13].

The reduction in strength at 300 °C concerning room temperature in G1 and G2 are recorded is 28% and 22% respectively. Whereas at 500 °C the recorded reduction was 47% and 39% while at 700 °C, 900 °C the reduction was 70% and 63%, and 82% and 74% respectively. Water is present in the mix of concrete which leads to enhance strength, but this water evaporates when the temperature is going to be increased from room environmental conditions this water evaporates from the concrete which leads to slowing down the chemical reactions[14-15]. Furthermore, the reduction between G1 and G2 at 300 °C was recorded is 6% while at 500 °C, 700 °C and 900 °C the reduction was 8%, 7% and 8% respectively. It is



5th Conference on Sustainability in Civil Engineering (CSCE'23)
Department of Civil Engineering
Capital University of Science and Technology, Islamabad Pakistan



clear from Table 1 that these are regression equations that were developed through Minitab software for the predicted compressive strength of concrete. Equation 1 shows the regression of G1 and 2 shows the regression of G2 (NSC) concrete.

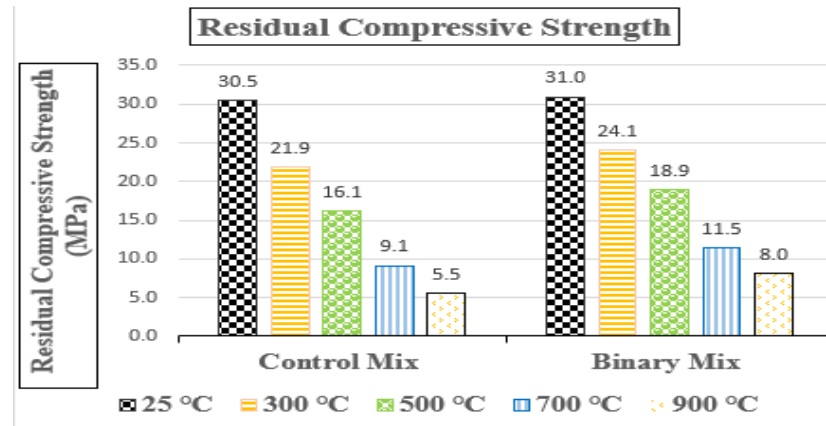


Figure 2: Residual Compressive Strength (NSC)

Table. 1 Regression Equation for The Predicted Residual Compressive Strength of Concrete (25 °C - 900 °C) NSC

Type of Concrete	Regression Equation	R Square Value	Equation No.
NSC (Control Mix)	$Y = (29.8999) - (0.0275 * \text{Fire Intensity})$	0.9666	Eq. – 1
NSC (Binary Mix)	$Y = (32.1282) - (0.0285 * \text{Fire Intensity})$	0.9794	Eq. – 2

Figure 3 depicts the comparison between the G1 (Experimental and Empirical) results. The experimental result was obtained in the laboratory. While the empirical results were calculated from the mathematical equation shown in Table 1. The difference between the G1 (Experimental and Empirical) results at 25 °C is -4.23%. While at 300 °C, 500 °C, 700 °C and 900 °C the difference was recorded as -1.17%, 0.28%, 14.60%, and 2-5.19% respectively. As per findings of tensile strength which is the function of temperature were developed by multiple regression equations our research supports the regression equation in the case of compressive strength[16].

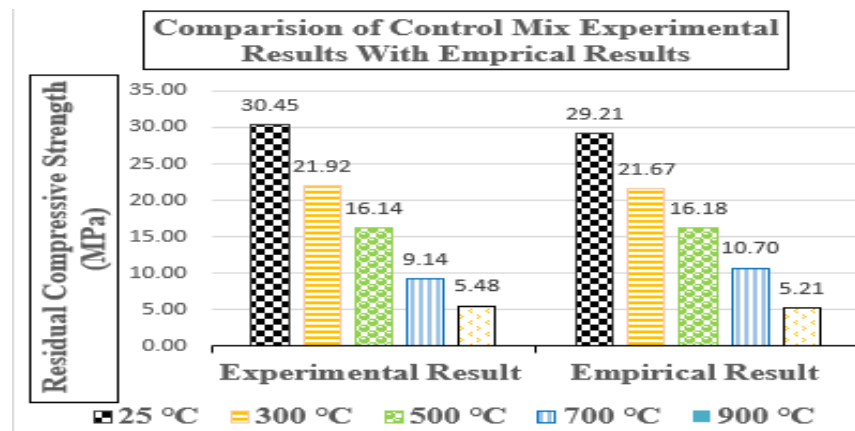


Figure 3: Comparison of Experimental and Empirical Results (NSC)

Figure 4 demonstrates the comparison between G2 (Experimental and Empirical) results. The experimental values were obtained in the laboratory while the empirical values were calculated from the mathematical equation which is clear in Table 1. The difference between G2 (Experimental and Empirical) recorded at 25 °C is 1.48%. While at 300 °C, 500 °C, 700 °C, and 900 °C difference was observed is -2.40%, -5.63%, 5.91%, and -24.39% respectively.

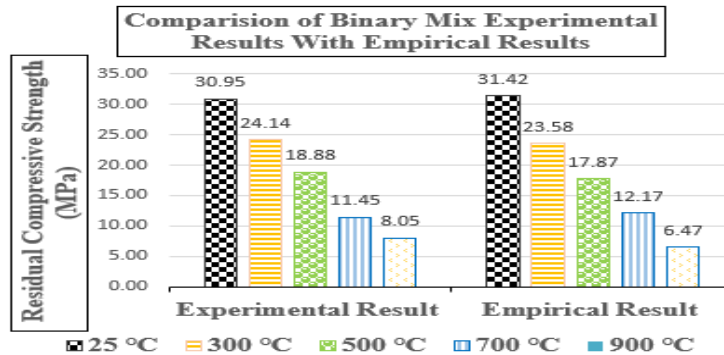


Figure 4: Comparison of Experimental and Empirical Results (NSC)

4.2 Residual Compressive Strength Using Core Method.

The core test is essential in evaluating the compressive strength, density, and permeability of concrete structures. The test determines the quality of the concrete mix, the strength of the concrete, and whether it meets the design requirements. The American Society for Testing and Materials (ASTM) provides standards for core testing procedures to ensure the accuracy and consistency of results. The core test is an integral part of the quality assurance process, and the data gathered can inform maintenance and repair decisions for concrete structures.

In conclusion, a core test is an essential tool in assessing the strength and durability of concrete structures. It provides critical information about the quality and performance of concrete, which can help identify potential issues and inform decisions regarding maintenance and repair. By following established testing procedures and guidelines, engineers and construction professionals can ensure the safety and endurance of concrete structures.

Figure 5 reveals that the residual compressive strength of concrete having a 75 x 150 mm core was extracted from a specimen. The figure shows that the strength of a concrete core can decrease with increasing temperature. The strength reduction was recorded in each temperature range concerning room temperature. The strength reduction observed at 300 °C in G1 and G2 were 31.32% and 25.43% respectively. While at 500 °C and 700 °C the reduction was 50.64%, 42.61%, and 72.48, 65.82% respectively. Similarly at 900 °C the reduction in strength recorded is 83.71% and 76.76 % respectively. Furthermore, the difference between G1 and G2 at 300 °C was observed is 5.88% while at 500 °C, 700 °C and 900 °C observed results were 8.03%, 6.66%, and 6.95% respectively. As per the aspect of core testing previous work support our work[17].

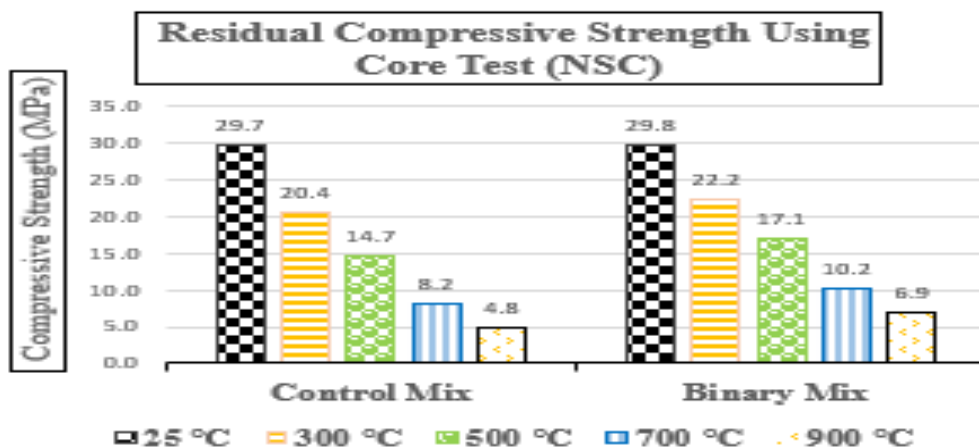


Figure 5: Residual Compressive Strength Using Core Test (NSC)



5th Conference on Sustainability in Civil Engineering (CSCE'23)
Department of Civil Engineering
Capital University of Science and Technology, Islamabad Pakistan



Table 2 communicates the regression equation of core test data which were developed through Minitab software which gives the predicted strength of concrete. Equation 3 shows the regression of G1 and 4 is the regression of G2.

Table. 2 Regression Equation for The Predicted Residual Compressive Strength of Concrete (25 °C - 900 °C) NSC

Type of Concrete	Regression Equation	R Square Value	Equation No.
NSC (Control Mix)	$Y = (24.6909) - (0.0228 * \text{Fire Intensity})$	0.9103	Eq. – 3
NSC (Binary Mix)	$Y = (26.2719) - (0.0234 * \text{Fire Intensity})$	0.8957	Eq. – 4

It is evident from Figure 6 the comparison between G1 (Experimental and Empirical) results. The experimental values were obtained in the laboratory while the empirical values were calculated from the mathematical equation which is clear in Table 2. The difference between G1 (Experimental and Empirical) recorded at 25 °C is 17.21%. While at 300 °C, 500 °C, 700 °C, and 900 °C the difference was observed is 10.59%, 7.08%, 15.69%, and 9.10% respectively. Similarly, Figure 7 communicates the differences between the G2 (Experimental and Empirical) Results. The difference observed at 25 °C was 11.10% while at 300 °C, 500 °C, 700 °C and 900 °C, the observed value was 10.88%, 12.65%, 5.63%, and 19.26% respectively.

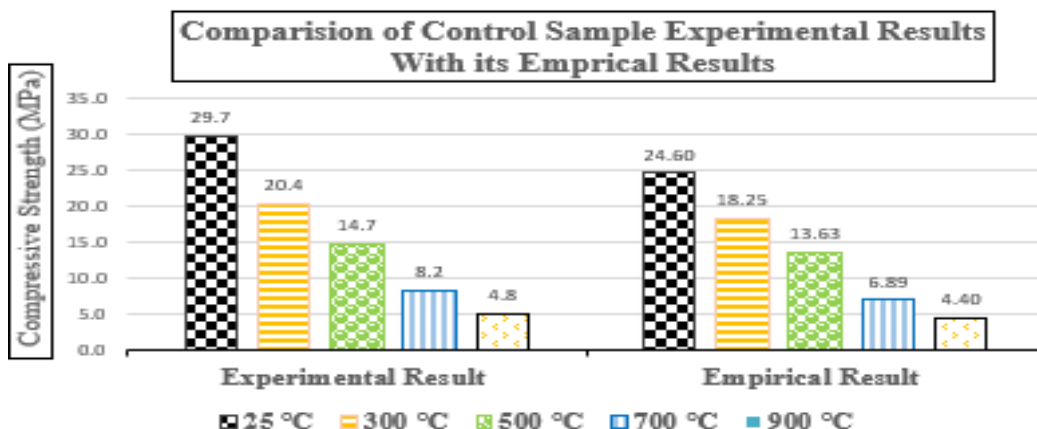


Figure 6: Comparison of Experimental and Empirical Results (NSC)

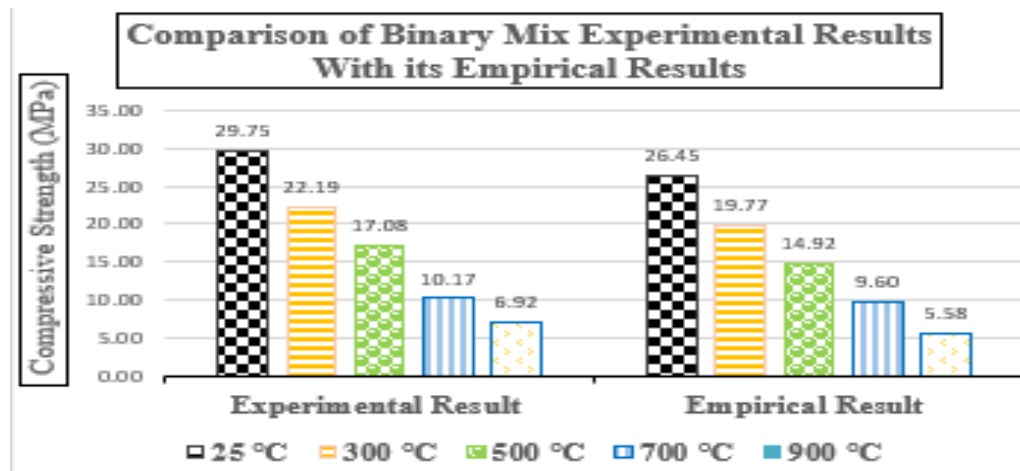


Figure 7: Comparison of Experimental and Empirical Results (NSC)



5. Practical Implementation

When a structure has been subjected to fire or high temperatures, you must evaluate the residual strength of the affected concrete. Researchers can provide insights into the performance of fire-damaged structures and aid in the decision-making process for repair, rehabilitation, or strengthening measures by investigating the reliability of cores test results at elevated temperatures.

6. Conclusions

The following conclusions can be drawn from the conducted study:

- 1 It is concluded from findings that G1 and G2 will perform relatively the same behavior at room temperature but at the higher temperature G2 perform better than G1. At room temperature, the difference between the actual and cores test in G1 and G2 is recorded as 2.58% and 4.12% respectively. Thus, the core results are very much reliable and show 100% real behavior at room temperature in connection to real testing.
- 2 The difference between the actual and core test at (300 °C – 500 °C) is relatively more as compared to room temperature which is recorded as 6.67%, 7.81%, and 8.72%, 9.81% in G1 and G2 respectively. Thus, the core results are partially reliable at medium elevated temperatures in connection to real behavior (Laboratory Destructive testing).
- 3 At higher temperatures (700 °C – 900 °C) this difference recorded between the actual and core test in G1 and G2 is 10.47%, 11.81%, and 11.97%, 13.56% respectively. Thus, the core results are not very reliable to defect the true scenario at higher elevated temperatures in connection to real testing.

7. Recommendations

It is extensively checking the behavior of concrete in binary mix condition at elevated temperature for 4 hours. It is recommended for future that check the behavior of concrete in case ternary mixes under elevated temperature for extreme exposure. Furthermore, the SEM test is also recommended before and after elevated temperature for internal behavior of the concrete.

8. Limitations

- The samples are heated with a 4-hour constant duration up to 900 °C.
- The normal strength concrete is made of many waters cement ratio, but this is made on a 0.5 water cement ratio.
- The core is taking from the specimens as per ASTM standard with a size of 75 mm x 150 mm.

9. References

- [1] S. Pul, M. Husem, M. Arslan, Y. Z.-P. of the 4th, and undefined 2011, “Investigation of relation between core and cylindrical strength of concrete specimen cured in different conditions,” *researchgate.net*, 2011, Accessed: May 25, 2023. [Online]. Available: https://www.researchgate.net/profile/Selim-Pul-2/publication/262242893_Investigation_of_relation_between_core_and_cylindrical_strength_of_concrete_specimen_cured_in_different_conditions/links/54dcbc0c0cf25b09b912c5ea/Investigation-of-relation-between-core-and-cylindrical-strength-of-concrete-specimen-cured-in-different-conditions.pdf
- [2] Q. Li, P. Liu, M. Wang, H. X.-J. of B. Engineering, and undefined 2023, “Effects of elevated temperature on the mechanical properties of concrete with aggregate of waste porcelain tile,” *Elsevier*, Accessed: Jun. 18, 2023. [Online]. Available: <https://www.sciencedirect.com/science/article/pii/S2352710222015911>
- [3] M. Tuncan, O. Ariozi, K. Ramyar, B. K.-C. and Building, and undefined 2008, “Assessing concrete strength by means of small diameter cores,” *Elsevier*, Accessed: May 25, 2023. [Online]. Available: <https://www.sciencedirect.com/science/article/pii/S0950061806003412>



5th Conference on Sustainability in Civil Engineering (CSCE'23)

Department of Civil Engineering

Capital University of Science and Technology, Islamabad Pakistan



- [4] "I.M. Nikbin, M. Eslami, D.S.M. Rezvani, An experimental... - Google Scholar." https://scholar.google.com/scholar?hl=en&as_sdt=0%2C5&q=I.M.+Nikbin%2C+M.+Eslami%2C+D.S.M.+Rezvani%2C+An+experimental+comparative+survey+on+the+interpretation+of+concrete+core+strength+results%2C+Eur.+J.+Sci.+Res.+37+%283%29+282009%29+445%2E2%80%93456%2C+ISSN+1450-216.&btnG= (accessed May 25, 2023).
- [5] F. Bartlett, J. M.-M. Journal, and undefined 1994, "Effect of core diameter on concrete core strengths," *concrete.org*, Accessed: May 25, 2023. [Online]. Available: <https://www.concrete.org/publications/internationalconcreteabstractsportal/m/details/id/4160>
- [6] A. Ergun, G. K.-G. U. J. of Science, and undefined 2012, "Assessing the relationship between the compressive strength of concrete cores and molded specimens," *dergipark.org.tr*, vol. 25, no. 3, pp. 737–750, 2012, Accessed: May 25, 2023. [Online]. Available: <https://dergipark.org.tr/en/pub/gujs/issue/7424/97476>
- [7] R. Meiningen, F. Wagner, K. H.-A. J. of T. and, and undefined 1977, "Concrete Core Strength--The Effect of Length to Diameter Ratio," *trid.trb.org*, Accessed: May 25, 2023. [Online]. Available: <https://trid.trb.org/view/60138>
- [8] F. B.-S. Safety and undefined 1997, "Precision of in-place concrete strengths predicted using core strength correction factors obtained by weighted regression analysis," *Elsevier*, Accessed: May 25, 2023. [Online]. Available: <https://www.sciencedirect.com/science/article/pii/S0167473097000209>
- [9] J. Wróblewska, R. K.-C. and B. Materials, and undefined 2020, "Assessing concrete strength in fire-damaged structures," *Elsevier*, Accessed: Jun. 18, 2023. [Online]. Available: <https://www.sciencedirect.com/science/article/pii/S0950061820311272>
- [10] V. K.-I. S. R. Notices and undefined 2014, "Properties of concrete at elevated temperatures," *downloads.hindawi.com*, 2014, doi: 10.1155/2014/468510.
- [11] J. Bao *et al.*, "A state-of-the-art review on high temperature resistance of lightweight aggregate high-strength concrete," *Elsevier*, Accessed: Jun. 18, 2023. [Online]. Available: <https://www.sciencedirect.com/science/article/pii/S2352710223004461>
- [12] M. Mohammadi, R. Moghtadai, N. S.-C. and Building, and undefined 2014, "Influence of silica fume and metakaolin with two different types of interfacial adhesives on the bond strength of repaired concrete," *Elsevier*, Accessed: Jun. 18, 2023. [Online]. Available: <https://www.sciencedirect.com/science/article/pii/S0950061813009690>
- [13] B. Behforouz, D. Tavakoli, M. Gharghani, A. A.- Structures, and undefined 2023, "Bond strength of the interface between concrete substrate and overlay concrete containing fly ash exposed to high temperature," *Elsevier*, Accessed: Jun. 18, 2023. [Online]. Available: <https://www.sciencedirect.com/science/article/pii/S2352012423001236>
- [14] M. Narmluk, T. N.-C. and concrete research, and undefined 2011, "Effect of fly ash on the kinetics of Portland cement hydration at different curing temperatures," *Elsevier*, Accessed: Jun. 18, 2023. [Online]. Available: <https://www.sciencedirect.com/science/article/pii/S0008884611000603>
- [15] J. Shen, Q. X.-C. and B. Materials, and undefined 2019, "Effect of elevated temperatures on compressive strength of concrete," *Elsevier*, Accessed: Jun. 18, 2023. [Online]. Available: <https://www.sciencedirect.com/science/article/pii/S0950061819322822>
- [16] J. van der M.-C. and B. Materials and undefined 2022, "Evaluation of concrete tensile strength as a function of temperature," *Elsevier*, Accessed: Jun. 18, 2023. [Online]. Available: <https://www.sciencedirect.com/science/article/pii/S0950061822008595>
- [17] H. A. Goaiz, H. A. Jabir, M. A. Abdulrehman, T. S. Al, and T. S. Al-Gasham, "Evaluation of lightweight Concrete Core Test Including Steel Bars," *ije.ir*, vol. 36, no. 06, pp. 1121–1128, 2023, doi: 10.5829/ije.2023.36.06c.10.



STRUCTURAL PERFORMANCE OF E-WASTE CONCRETE REINFORCED WITH DIFFERENT FIBRES

^aMuhammad Safwan Naeem, ^bMuhammad Usman Rasheed, ^cMohammad Zulqarnain

a: Department of Civil Engineering, UET, Taxila, Pakistan, msafwan.Naeem@students.uettaxila.edu.pk

b: Department of Civil Engineering, UET, Taxila, Pakistan, m.usman@uettaxila.edu.pk

c: Department of Civil Engineering, Swedish College of Engg. and Technology Wah Cant, Pakistan, engr.zulqarnain884@gmail.com

Abstract-E-waste is growing at a pace of 3-4% a year, and it is estimated that by the year 2025 its production will be increased to 55 million tons. The production of concrete in the year 2022 stood at 4.4 billion tons if we consider the percentage of aggregate at 60%-70% it comes out to be approx. 3 billion tons. The consumption of natural aggregates at this massive scale has put enormous pressure on mining resources and excessive mining has led to serious environmental and socio-economic problems. The studies so far have shown that addition of e-plastic waste as plastic aggregates results in deterioration of mechanical properties of concrete. This study aims to study the effect of addition of carbon and steel fibers on the mechanical properties E-waste concrete. Two sets of four types of concrete mixes were produced with substitution of manufactured plastic aggregate with natural concrete aggregate (NCA) up to 40% replacement levels. One set was added with carbon fibers and the other one with steel fibers. Both fibers were added in the fixed quantity of 1% by weight of binder material for each sample. The results indicated that the compressive strength of both sets of samples reduced in the range of 4-55% and 20-33% for e-waste concrete with carbon fibers and steel fibers respectively. The splitting tensile strength was reduced in the range of 5-47% and 13-32% for e-waste concrete containing carbon and steel fibers respectively.

Keywords: Fibre reinforced concrete, plastic aggregates, natural concrete aggregate (NCA) steel fibres, carbon fibres

1 Introduction

Electronic waste in crushed form has been used in various studies but there is very little research on using E-waste to produce manufactured plastic aggregates for use in concrete, the novelty of this research is that in this research manufactured plastic aggregates are used with combination of carbon and steel fibres.

Zeeshan ullah et al. [1] investigated the mechanical and durability characteristics of electronic waste concrete and discovered that for coarse aggregate replacement ratios of 10% and 20%, respectively, the compressive strength of E-waste concrete decreased in the range of 6.3%-17.1% and 23.5%-32.4%. Concrete's workability and durability were enhanced by the addition of E-waste. Sorptivity coefficient reduction, UPV values abrasion loss reduction, and enhanced performance when compared to alternative drying and wetting cycles.

C. Albano et al. [2] studied the influence of content and particle size of waste pet bottles in concrete. They found out increasing percentage of pet bottles decrease compressive strength, splitting tensile strength, modulus of elasticity and ultrasonic pulse velocity.

Semihha Akçaözoglu [3] found out that thermal coefficient, unit weight and compressive strength of concrete containing waste PET lightweight aggregate was decreased. The maximum drop in thermal conductivity was at 60% replacement of lightweight PET aggregate but compressive strength was dropped more than 80% which indicates that concrete can only be used for non-structural work.

Study conducted on review of recycled fine aggregates is cementitious composites. Results indicate mechanical properties like compressive strength, compressive and flexural strength decreases, similarly UPV also decrease.



5th Conference on Sustainability in Civil Engineering (CSCE'23)

Department of Civil Engineering

Capital University of Science and Technology, Islamabad Pakistan



Properties like water absorption, permeability and carbonation increase as percentage of plastic aggregate increase which indicates a porous concrete structure [4].

Synthetic aggregate produced by using mixture of recycled plastic made from linear low-density polyethylene (LLDPE) in powder form and red dune sand in the ratio of 70% and 30% respectively. The coarse aggregate were replaced with synthetic aggregate in the ratio of 25%, 50%, 75% and 100%. The mixes prepared with synthetic aggregate had slump reduction in the range of 11-23% as compared to control mix. The 28-day compressive strength of concrete containing synthetic aggregate decreases in the range of 15-63%, similarly the splitting tensile strength reduced in the range of 12-31% [5]. S. Bahij et al studied concrete containing different forms of plastic waste. Concrete porosity and water absorption increases. There compressive strength of concrete was reduced significantly. It was also reported that flexural strength and splitting tensile strength were also reduced [6].

The compressive strength of M20 grade concrete with coarse aggregate replaced by PCB plastic, CRT LCD Monitor, and other E-waste was compared to that of standard concrete by Saurav Dixit et al. They created four different sample kinds with varying E-waste contents (7%, 12%, 17%, and 22%). According to the study, replacing coarse aggregate with E-waste boosts concrete's compressive strength by up to 7% and up to 12% for M20 concrete. of substitution. The research suggested using e-waste as aggregate at a rate of 7-10% [7].

Aamar Danish et al added nano silica in the E-waste concrete in the range of 1-3% by the weight of binder. The purpose of research was to counter the negative effects of addition of electronic waste in the concrete on the mechanical properties. The research revealed that the compressive properties enhanced significantly [8].

A study on the sustainable reuse of E-waste in the form of coarse aggregate was conducted by S.Janani et al. In this study natural aggregates were replaced by electronic waste aggregates in the ratio of 5,10,15 and 20%. The study concluded that that plastic aggregate can be used in the replacement range of maximum 10% without having significant effect on the compressive strength of concrete [9].

2 Materials

2.1 Cement

Ordinary Portland Cement was used in preparation of concrete mixes in accordance with ASTM C150 [10].

2.2 Aggregates

Well graded coarse aggregate as per ASTM C33-03 were used in production of concrete mi along with sand as fine aggregate.

2.3 Plastic Aggregate

Plastic aggregate in the size range of 25mm to 4.5mm were used in as partial replacement of course.

2.4 Carbon Fibres

Carbon fibres in the in the mix were used as 1% by weight of binder material.

2.5 Steel Fibres

To improve flexural properties steel fibres were used as 1% of binder by weight.

Table 1 Material Properties (Steel and Carbon fibers)

Fibre Type	Length (mm)	Diameter (mm)	Aspect Ratio (L/D)	Tensile Strength (N/mm ²)
Steel Fibre	30	0.55	55	1150
Carbon Fibre	30	0.40	75	5650

Table 2 Mix Design per meter cube of concrete.

Mix ratio	Cement (kg/m ³)	Water (Liters)	Fine Aggregates (kg/m ³)	Coarse Aggregates (kg/m ³)	Admixture (superplasticizer) (kg/m ³)	Steel Fibers (kg/m ³)	Caron Fibers (kg/m ³)
1:1:2	520.78	223.93	520.78	1041.56	6.25	7.9	2.0



2.6 Admixture

To improve workability superplasticizer was used as 1% by weight of binder.

2.7 Water

Tap water free from impurities was used for producing concrete.

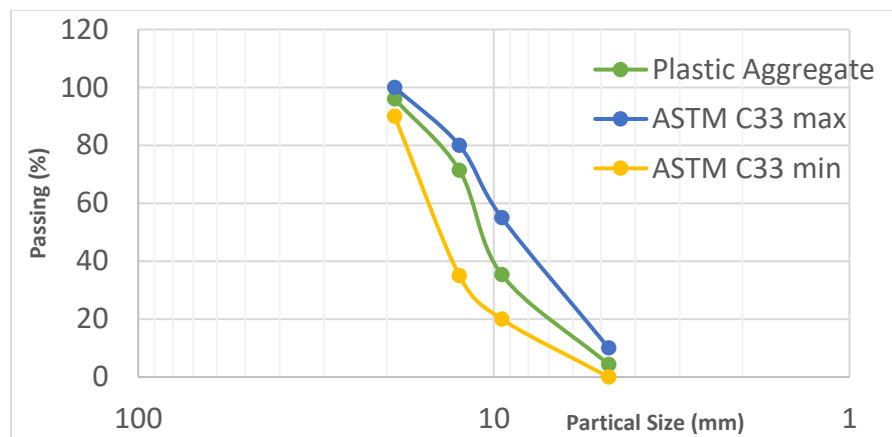


Figure 1: Gradation Curve Plastic Aggregate

3 Research Methodology

Plastic aggregates were used for replacement of coarse aggregate in varying percentages. Total 24 cylinders were cast, 12 containing different percentages of Plastic aggregate with carbon fibre and remaining 12 with steel fibres. The varying percentage of plastic aggregate were used from 10% to 40% and the ratio of fibres were kept constant as 1% of total binder content. Tested specimens having dimensions 12" height and 6" dia were prepared using concrete ratio of 1:1:2. Compressive strength and splitting tensile strength test were done on Compression Testing Machine (CTM) having loading capacity of 3000 KN. Stress-strain relationship was calculated using linear displacement sensor and strain reading at interval of 25 KN was noted. P3-stain indicator was used to measure readings from LDS at interval of 25 KN. To check the stress-strain behaviour, deflections, and maximum energy absorption of the cylinders the compressive strength test was conducted. The compressive strength test was conducted in compression testing machine (CTM).



Figure 2: Manufactured Plastic Aggregates and Carbon Fibres



Table 3: Description of Samples

Sample Designation	Description of samples
S1 PA+SF	Cylinder Specimen with Steel fibres and 10% replacement of coarse aggregate with manufactured E-waste plastic aggregates
S2 PA+SF	Cylinder Specimen with Steel fibres and 20% replacement of coarse aggregate with manufactured E-waste plastic aggregates
S3 PA+SF	Cylinder Specimen with Steel fibres and 30% replacement of coarse aggregate with manufactured E-waste plastic aggregates
S4 PA+SF	Cylinder Specimen with Steel fibres and 40% replacement of coarse aggregate with manufactured E-waste plastic aggregates
S1 PA+CF	Cylinder Specimen Carbon fibres and 10% replacement of coarse aggregate with manufactured E-waste plastic aggregates
S2 PA+CF	Cylinder Specimen with Carbon fibres and 20% replacement of coarse aggregate with manufactured E-waste plastic aggregates
S3 PA+CF	Cylinder Specimen with Carbon fibres and 30% replacement of coarse aggregate with manufactured E-waste plastic aggregates
S4 PA+CF	Cylinder Specimen with Carbon fibres and 40% replacement of coarse aggregate with manufactured E-waste plastic aggregates
S5 CCF	Control Specimen Cylinder for carbon fibres specimen 6" Diameter 12" Height

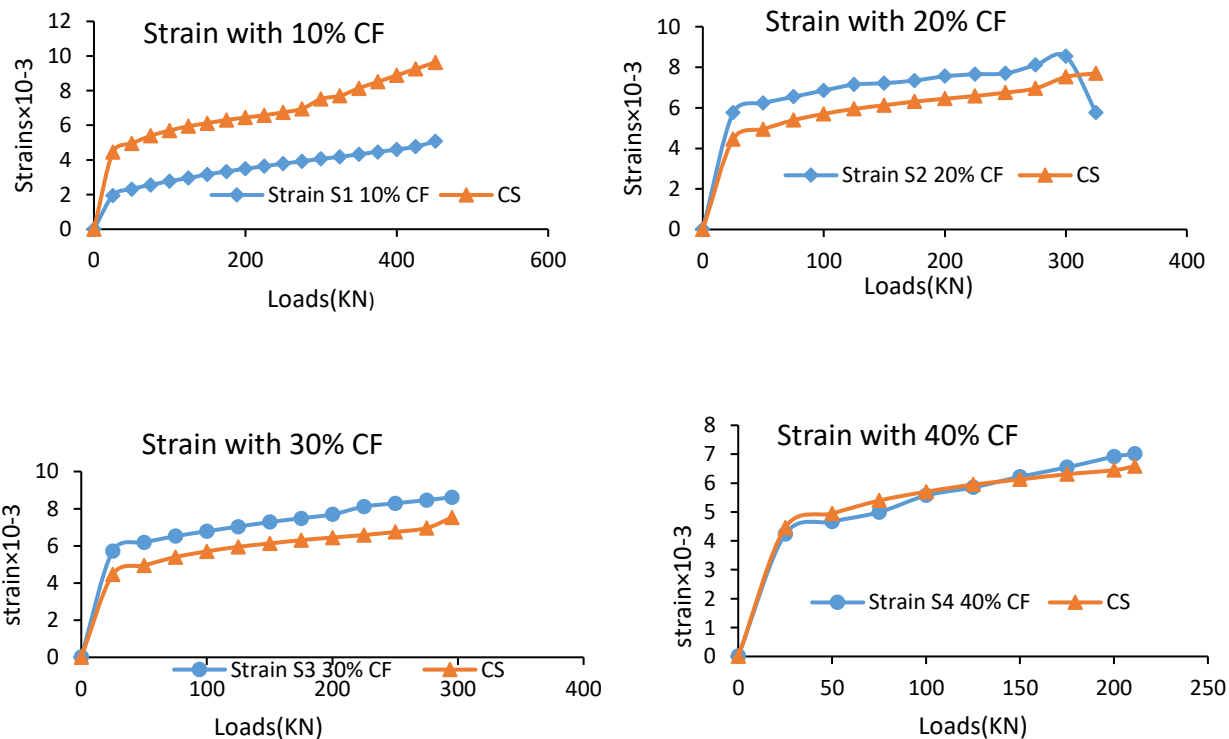


Figure 3 Loads vs Strain graphs with Carbon Fibres

4 Results and Discussions

4.1 Loads vs Strain Graphs with Carbon Fibres



The load vs strain graphs for E-waste concrete samples containing carbon fibers are shown in figure 6. The results are consistent for 20%, 30% and 40% ratios but in the case of 10% replacement sample the values of strain are quite low as compared to control specimen. If we compare these results with sample containing steel fibers, it is evident that the values of strain at same loading conditions are less.

4.2 Compressive Strength

Compressive Strength & Load vs Compressive Strength graphs is shown in Figure 7 which shows the compressive strength of both the sample sets. From the graph we can see that there is considerable reduction in compressive strength with the addition of plastic aggregates, in case of sample with steel fibers the maximus reduction in compressive strength is 32% at 40% substitution of natural aggregates with plastic aggregates. In the case of samples containing carbon fibers the loss in compressive strength is higher with maximum reduction of 55% as compared to control specimen.

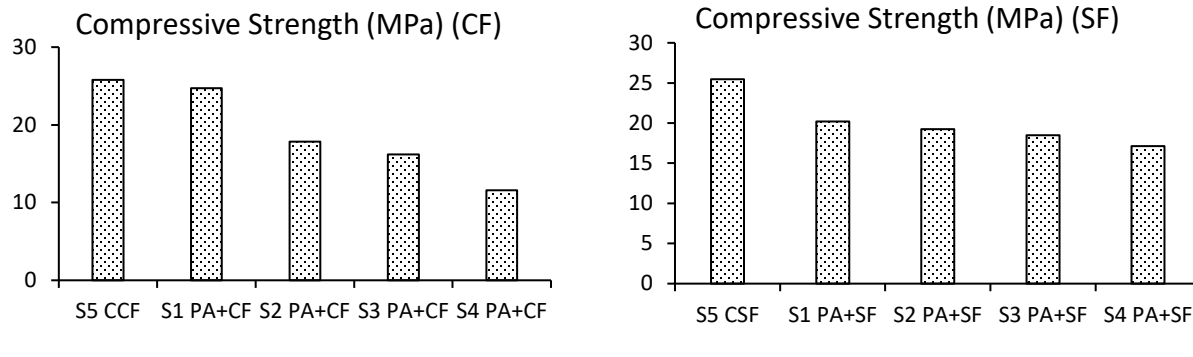
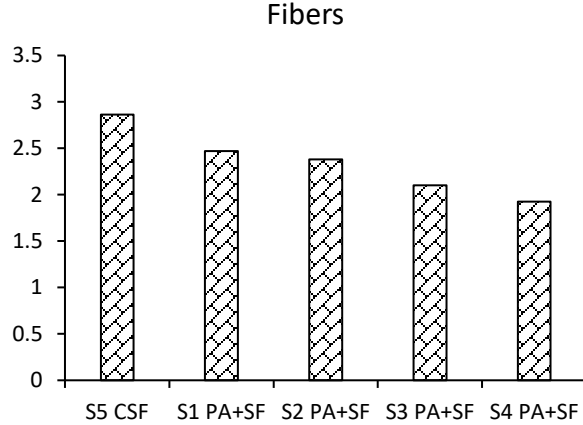


Figure 4 Compressive Strength

4.3 Splitting Tensile Strength Steel and Carbon fibres.

To check the effects of fibers on the tensile strength of concrete splitting, tensile tests were carried out. The addition of plastic aggregates decreased the tensile strength, but the percentage of tensile strength loss was less as compared to percentage of compressive strength loss. The overall tensile strength loss for steel fibers is 30% and for carbon fibers is 47%.

Splitting Tensile Strength With Steel Fibers



Splitting Tensile Strength With Carbon Fibers

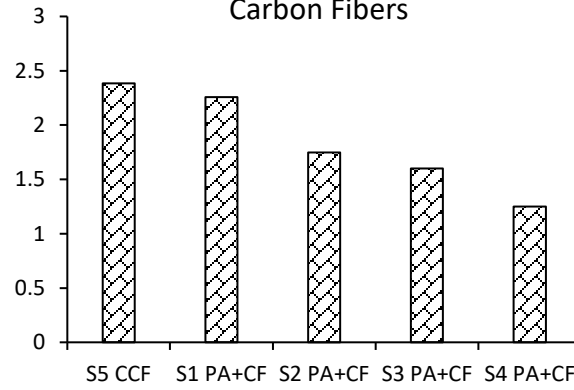


Figure 5 Splitting Tensile Strength



5th Conference on Sustainability in Civil Engineering (CSCE'23)

Department of Civil Engineering

Capital University of Science and Technology, Islamabad Pakistan



5 Relevance of Research

All the study related to use of electronic waste till this data is focused on using electronic waste as replacement material for coarse and fine aggregates as per literature very little research material is focused on improving the properties of E-waste concrete. In this research a new approach of using fibers for improving the mechanical properties is used. Research has indicated that use of fibers improves bond strength of aggregates, flexural properties, fracture toughness, ductility, and resistance to higher temperatures. If we are able to produce E-waste concrete with acceptable mechanical properties it will be a huge step forward in the direction of reuse of plastics in an effective manner. This research is also an effort to find ways to improve mechanical properties of E-waste concrete.

6 Conclusions

From the results of experiments carried out in this research following conclusions are made:

- 1 The compressive strength of E-waste concrete is directly proportional to the replacement ratio of plastic aggregate, higher the replacement more will be compressive strength loss. The addition of fibers has no significant effect in preventing compressive strength loss.
- 2 The tensile strength decreases with an increase in plastic aggregate, but addition of fibers helps reduce this strength loss. The splitting tensile strength was reduced in the range of 5-47% and 13-32% for e-waste concrete containing concrete and steel fibers respectively. Steel fibers performed better in reducing tensile strength loss.
- 3 The E-waste concrete with up to 20% replacement of natural aggregate can be used in non-structural applications.
- 4 Addition of fibers indicates a positive improvement in tensile strength of E-waste concrete.

The basic objective of this study was to study the effects of addition of carbon and steel fibers in E-waste concrete. As per above mentioned results it is quite evident that the tensile properties of E-waste concrete with fibers are improved as compared simple E-waste concrete. Further studies to optimize the concrete mix of E-waste concrete using cementitious materials to improve the compressive strength of concrete can be carried out.

REFERENCES

- [1] Z. Ullah, M. I. Qureshi, A. Ahmad, S. U. Khan, and M. F. Javaid, "An experimental study on the mechanical and durability properties assessment of E-waste concrete," *Journal of Building Engineering*, vol. 38, no. December 2020, 2021, doi: 10.1016/j.jobe.2021.102177.
- [2] P. C. Ganapathy, "An Experimental Study on Feasibility of Cinder as Partial Replacement for Coarse Aggregate," *IJSRD-International Journal for Scientific Research & Development*, vol. 4, no. 04, pp. 2321–0613, 2016.
- [3] C. Albano, N. Camacho, M. Hernández, A. Matheus, and A. Gutiérrez, "Influence of content and particle size of waste pet bottles on concrete behavior at different w/c ratios," *Waste Management*, vol. 29, no. 10, pp. 2707–2716, 2009, doi: 10.1016/j.wasman.2009.05.007.
- [4] S. Akçaözoglu, K. Akçaözoglu, and C. D. Atış, "Thermal conductivity, compressive strength and ultrasonic wave velocity of cementitious composite containing waste PET lightweight aggregate (WPLA)," *Compos B Eng*, vol. 45, no. 1, pp. 721–726, 2013, doi: 10.1016/j.compositesb.2012.09.012.
- [5] I. Almeshal, B. A. Tayeh, R. Alyousef, H. Alabduljabbar, A. Mustafa Mohamed, and A. Alaskar, "Use of recycled plastic as fine aggregate in cementitious composites: A review," *Constr Build Mater*, vol. 253, p. 119146, 2020, doi: 10.1016/j.conbuildmat.2020.119146.
- [6] A. Fahad K., G. Gurmel, K. M. Iqbal, D. Samir, K. Azzedine, and A.-O. Mansour, "Lightweight Concrete Containing Recycled Plastic Aggregates," no. Iccett, pp. 527–533, 2015, doi: 10.2991/icecett-15.2015.101.
- [7] S. Bahij, S. Omary, F. Feugeas, and A. Faqiri, "Fresh and hardened properties of concrete containing different forms of plastic waste – A review," *Waste Management*, vol. 113, pp. 157–175, 2020, doi: 10.1016/j.wasman.2020.05.048.
- [8] Aamar Danish, Togay Ozbakkaloglu, Impact of nano-silica on the mechanical properties of mortar containing e-waste plastic as fine aggregates, Materials Today: Proceedings,2023, ISSN 2214 7853, <https://doi.org/10.1016/j.matpr.2023.03.182>.
- [9] S. Janani, K. Preethi, S. Gowtham, P. Kulanthaivel, "A sustainable reuse of e waste as a partial replacement material for aggregate,Materials" Today: Proceedings,2023,ISSN 2214-7853,<https://doi.org/10.1016/j.matpr.2023.05.740>.
- [10] ASTM, "C150-Standard Specification for Portland Cement\|r," pp. 1–10, 2015, doi: 10.1520/C0150.



EFFECT OF INDIGENOUS VOLCANIC ASH AS PARTIAL REPLACEMENT OF CEMENT ON MECHANICAL PROPERTIES OF CONCRETE AT ELEVATED TEMPERATURE

^a Hashmatullah, ^b Ayub Elahi, ^c Muhammad Tausif Arshad*

a: Department of Civil Engineering, UET, Taxila, Pakistan, hashmatullah541@gmail.com

b: Department of Civil Engineering, UET, Taxila, Pakistan, ayub.elahi@uettaxila.edu.pk

c: Department of Civil Engineering, MUST, Mirpur-10250 (AJ&K), Pakistan, tausif.ce@moust.edu.pk

* Corresponding author: Email ID: hashmatullah541@gmail.com

Abstract- This study examines the repercussions of indigenous volcanic ash (IVA) as a partial substitution of cement on the concrete's mechanical properties when exposed to elevated temperatures. The study aims to explore the potential benefits and limitations of utilizing volcanic ash in concrete mixtures for applications in high-temperature environments. The research includes varying percentages of volcanic ash replacements (10%, 20%, 30% and 40%) to assess their impact on concrete's mechanical properties. The experimental program consists of conducting compressive strength tests, splitting tensile strength tests, and strength activity index tests on concrete and mortar specimens respectively. The concrete specimens are subjected to elevated temperature conditions using a controlled heating system for 2hr. The specimens mechanical properties are evaluated and compared to those of the control specimens without volcanic ash. Lower percentages of IVA replacement (10%) show better strengths as compared to the control specimens at different temperatures. However, as the volcanic ash content increases, a gradual reduction in compressive strength and splitting tensile strength is observed with increasing temperature. The findings from this research provide valuable insights into the behavior of concrete incorporating IVA at elevated temperatures. The outcomes contribute to the broader understanding of sustainable and durable concrete production using locally available volcanic ash resources.

Keywords- Compressive strength, Elevated temperature, Indigenous volcanic ash, Splitting tensile strength

1 Introduction

The extensive worldwide utilization of concrete, reaching approximately 25 gigatonnes annually, leads to a substantial environmental impact due to its high resource consumption and significant emissions [1]. While the construction industry heavily relies on ordinary Portland cement (OPC) for concrete production, the energy-intensive nature of OPC manufacturing contributes to significant environmental impacts. With global cement production ranging from 2.8 to 4.1 billion tons annually, it is projected to double by 2030. This sector alone accounts for 8-10% of anthropogenic greenhouse gas emissions, a figure that could increase to 10-15% by 2020. To address these concerns, extensive efforts have been made to develop more sustainable and durable concrete and construction products by substituting a portion of OPC with supplementary cementitious materials (SCMs) [2]–[10]. Volcanic ash, a type of natural pozzolana, demonstrates great potential as an alternative to OPC cement in the development of concrete and blended cement. Several countries have already utilized volcanic ash as a natural pozzolana. It is economically viable and can be incorporated into concrete, cement paste, and mortars. Volcanic ash utilisation as a substitute for OPC is particularly valuable owing to its ability to reduce carbon emissions, its accessibility in the region, and its beneficial pozzolanic [11]–[14]. A natural pozzolan is defined by



ASTM C618-93 as volcanic ash, which develops during volcanic eruptions [15]. To investigate the ability of the mortar, four unique proportions of VA (0, 5, 15, and 25%) were prepared as weight replacements for the cement. A series of experiments were carried out after 28, 90, and 120 days at various temperatures (25, 200, 500, and 800 °C). The findings show that substituting cement with volcanic ash can maintain a satisfactory level of compressive, tensile, and flexural strength in mortar. Compressive strength tests at various ages and temperatures show that the mortar with 15% VA replacement has better compressive strength capabilities than other proportions [16]. The incorporation of VA up to 20% in the HSC resulted in improved resistance to chloride penetrability and degradation, as well as an increase in residual strength when exposed to a high temperature of around 800°C. When the temperature was raised above 800°C, however, the durability and strength were lowered [17]. As compared to control samples, mortar specimens with 20% VA as a replacement for cement had more substantial mechanical qualities at elevated temperatures [18]. In this study, the most optimal VA concrete mixture showed a compressive strength comparable to the controlled OPC concrete. Additionally, it exhibited lower carbon emissions and greatly improved resistance against chloride penetration. The sustainability potential index analysis indicates that the most "sustainable" alternative VA concrete has a water/binder ratio of 0.33 and a VA replacement percentage of 30%[19].The incorporation of an optimal 10% of volcanic pumice powder (VPP) as a partial substitute for cement in high-strength concrete (HSC10) revealed beneficial gains in strength qualities when compared to replacement levels of 20% and 30%. The indirect tensile strength followed the same trend as the compressive strength [14]. Mechanical tests indicated that all three OPC/VA dosages, 10%, 25%, and 40%, were equally effective. However, among OPC/VA formulations, the 10–25% dosage range demonstrated the highest effectiveness[20].

The purpose of this research is to evaluate the effectiveness of using locally available volcanic ash as a partial substitute for cement in concrete, particularly in situations of high temperatures. The goal is to develop an environmentally friendly and cost-effective concrete alternative by substituting a part of ordinary OPC with natural pozzolanic ingredients. The study focuses on investigating the effect of this natural pozzolanic ingredient, IVA, on the concrete's mechanical properties at high temperatures. The research aims to validate the suitability and commercial viability of using IVA as a partial replacement for cement based on its effects on the mechanical properties of concrete under high-temperature conditions.

2 Experimental Program

Locally available ordinary Portland cement (OPC) is used in sample preparation. The physical properties of IVA and OPC cement are illustrated in Table 1, and the chemistry of OPC cement is noted in Table 2. The chemical composition of IVA and OPC cement are illustrated in Table 1. The physical properties of IVA and OPC cement are shown in Table 2. Table 3 illustrates the physical properties of both fine and coarse aggregates. The IVA used in this research was procured from Chilas (Gini), where it is readily available.

Table 1 Chemical Content of IVA & OPC

Oxides	SiO ₂	Al ₂ O ₃	Fe ₂ O ₃	CaO	MgO	SO ₃	K ₂ O	Na ₂ O	LSF	SM	Am	LOI
IVA	52.9	19.15	9.3	7.41	4.55	0.06	0.42	3.61	4.21	1.84	2.06	1.3
OPC	21.5	6	3.75	62	2.8	2.75	1	0.2	0.6

Table 2 Physical properties of IVA & OPC

Name of Property	IVA	OPC
Specific Gravity	2.67	3.07
Consistency of cement (%)	25.55	29.7
Initial setting time in minutes	175	115
Final setting time in minutes	250	243
Soundness	No Expansion	No Expansion



Table 3 Physical properties of F.A and C.A

Name of Property	(F.A)	(C.A)
Specific gravity	2.69	2.66
Absorption Capacity (%)	1.29	0.9
Fineness Modulus	2.66	

3 Research Methodology

3.1 Mix Design of Concrete

To investigate the mechanical properties of concrete. A total of five mix proportions were used. The different mix proportions are shown in Table 1. IVA0% stands for control mix containing 0% IVA, IVA10% mix containing 10% IVA, IVA20% mix containing 20% IVA, IVA 30% mix containing 30% IVA and IVA40% mix containing 40% IVA.

Table 4 Mix Design of Concrete

Concrete mix Composition					
Mixes	OPC (kg/m ³)	IVA (kg/m ³)	Water (L/m ³)	F.A (kg/m ³)	C.A (kg/m ³)
IVA0%	320	0	160	640	1280
IVA10%	288	32	160	640	1280
IVA20%	256	64	160	640	1280
IVA30%	224	96	160	640	1280
IVA40%	192	128	160	640	1280

3.2 Mixing Procedure

The tilting drum type electric concrete mixer was used for the homogenous mixing of concrete. Firstly, for one minute, the dry mixing of sand and coarse aggregate was done in the mixer. After that, cement, IVA if required, and water were added to the mixer. The ingredients were mixed in a mixer that revolved at a rate of 30 revolution/minute. The mixing process was limited to 3 minutes.

3.3 Specimen Preparation

The mortar cubes of size 50mmx50mmx50mm were prepared in accordance with ASTM C109 [21], having a mix ratio of 1:2.75 and a water to cement ratio of 0.484. 20% IVA is replaced with cement by weight in the mortar mix. The 100mm x 200mm concrete cylinders are made with a mix ratio of 1:2:4 and a water-to-cement ratio of 0.50. The percentages of 10%, 20%, 30%, and 40% IVA are replaced with cement by weight in the concrete mixes.

3.4 Heating of Concrete

The present research focuses on examining the thermal behaviour of concrete when a portion of cement is replaced with IVA. The replacement proportions of IVA with cement are 0%, 10%, 20%, 30%, and 40%. In order to investigate this, a series of concrete mixes were prepared and subjected to elevated temperatures in a furnace. Specifically, one set of concrete samples was heated to 150°C for a duration of 2 hours, while another set was exposed to temperatures of 450°C and 750°C for the same amount of time [22]. The concrete samples were allowed to cool down to room temperature after the heating process. This experimental procedure will enable the researchers to analyse and evaluate the thermal performance and behaviour of the concrete mixes at different temperatures.

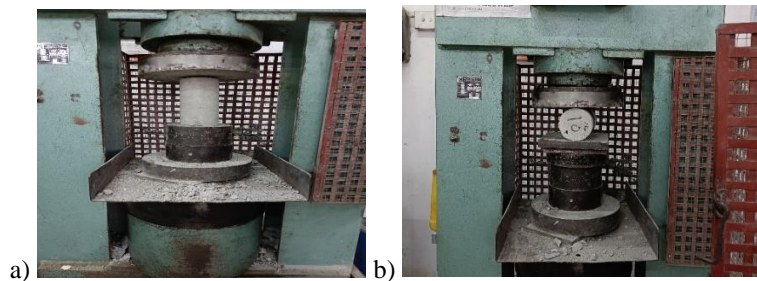


Figure 1 Testing, a. casting Compression test of cylinder, and b. Splitting tensile test

3.5 Compressive Strength

The compressive test of the specimens is conducted on cylinders of size 100mmx200mm at 28 days after exposure to different temperatures, i.e., 25°C, 150°C, 450°C, and 750°C. Figure 2a shows the relationship between the effect of different temperatures and the compressive strength of concrete for different percentages (0%, 10%, 20%, 30%, and 40%) of IVA replacement with cement. The replacement of 10% IVA with OPC cement in the specimens shows higher compressive strength compared to the control specimens after exposure to different temperatures, i.e., 25°C, 150°C, 450°C, and 750°C. At 25°C (room temperature), an increase in the compressive strength of the specimen occurs at 10% replacement of IVA with cement as compared to the control mix. It may be due to the chemical reaction of SiO₂ in IVA with CH. As a result, the amount of CH decreased and CSH (calcium silicate hydrate) increased, which improved the compressive strength of concrete. Further increase of IVA from 20% to 40% decrease in compressive strength of concrete occurs. It may be because of substituting cement with IVA, reduces the cement content in the mix [23], [24]. At 150°C, the compressive strength of some concrete mixes containing IVA increased as compared to its compressive strength at 25 °C, may be due to the formation of tobermorite. Tobermorite is a mineral formed when a chemical reaction takes place between unhydrated particles of IVA and lime at an elevated temperature [25]. The compressive strength of all mixes decreases when the temperature rises to 450 °C [26]. This decrease may be due to roughening of the pore structure of concrete. At 750 °C, all the mixes show severe loss in compressive strength, which may be due to the dissociation of CSH gel [24].

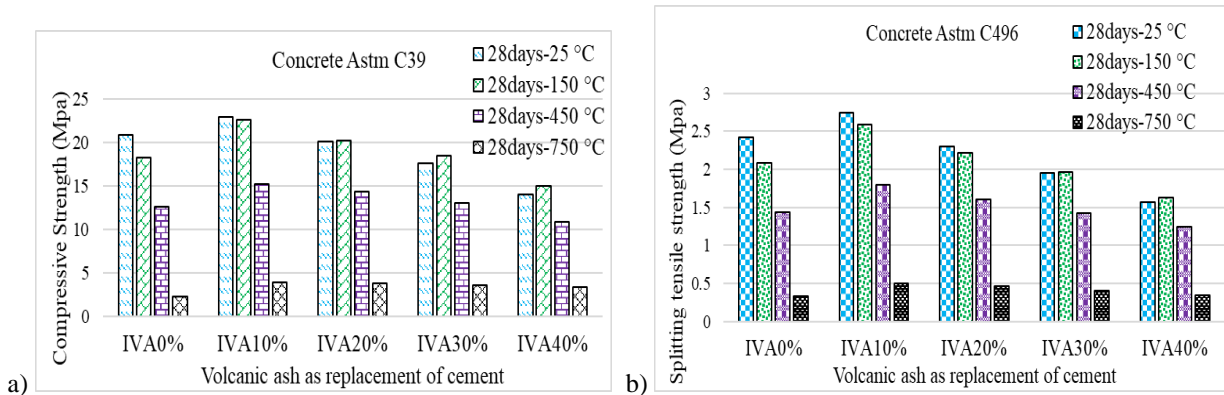


Figure 2 Results, a. Compressive strength test, and b. Splitting tensile strength test

3.6 Splitting Tensile Strength

The splitting tensile strength of concrete is performed on the cylinder of size 100mmx200mm at 28 days after exposure to different elevated temperatures, i.e., 25°C, 150°C, 450°C, and 750°C. Figure 2b shows the relationship between the effect of different temperatures and the splitting tensile strength of concrete for different percentages (0%, 10%, 20%, 30%, and 40%) of IVA replacement with cement. The effect of elevated temperatures on Splitting Tensile Strength shows a comparable trend with compressive strength. After exposure to various temperatures, i.e., 25°C, 150°C, 450°C, and 750°C, the replacement of 10% IVA with OPC cement shows higher Splitting Tensile Strength compared to the control specimens. At 25°C (room temperature), the specimen's Splitting Tensile Strength increases when 10% IVA is replaced with cement



compared to the control mix. It could be due to the chemical reaction of SiO₂ in IVA with CH [23], [24]. As a result, the amount of CH reduced while CSH increased, improving the Splitting Tensile Strength of concrete. As IVA increases from 20% to 40%, the splitting tensile strength of concrete decreases. It could be because replacing cement with IVA, decreases the cement content of the mix. At 150°C, the splitting tensile strength of a concrete mix containing IVA increased as compared to its splitting tensile strength at 25°, may be due to the formation of tobermorite. Tobermorite is a mineral that forms when unhydrated particles of IVA and lime react chemically at high temperatures. The splitting tensile strength of all mixes decreases as the temperature rises to 450 °C. This decrease may be due to roughening of the pore structure of concrete. At 750 °C, all the mixes show severe loss in splitting tensile strength, which may be due to the dissociation of CSH gel [24].

4 Discussion

In comparison to conventional concrete, IVA concrete has higher fire resistance and residual thermal characteristics. IVA concrete should be utilized in places that are more prone to catching fire to improve the structure's sustainability and lifespan. To protect the structural integrity of buildings and mitigate potential damage, it is recommended to use IVA concrete in several critical areas. These include firewalls, fire barriers, furnaces, tunnels, underground parking, kitchen areas, etc. By utilizing IVA concrete in these applications, the risk of direct structural damage can be effectively mitigated.

5 Conclusion

The study's findings lead to several key conclusions:

- 1 The strength activity index of mortar containing 20% IVA is 90.6% at 7 days and 93.9% at 28 days, exceeding the minimum threshold of 75% specified in ASTM C618.
- 2 At various elevated temperatures, the optimal amount of IVA for cement replacement is determined to be 10%. At this dosage, the compressive strength of concrete exhibits a better performance in terms of compressive strength as compared to the control specimen.
- 3 The loss in compressive strength of mix IVA10% was 0%, 1.5%, 33.7%, and 82.9%, while the loss in compressive strength of mix IVA0% was 0%, 12.4%, 39.6%, and 89.2% at various temperatures, i.e., 25°C, 150°C, 450°C, and 750°C respectively.
- 4 The splitting tensile strength accompanied the same trend as the compressive strength at 10% replacement of IVA with cement at various elevated temperatures. The loss in splitting tensile strength of mix IVA10% was 0%, 5.5%, 34.3%, and 81.8%, while the loss in splitting tensile strength of mix IVA0% was 0%, 14.1%, 40.5%, and 86.4% at various temperatures, i.e., 25°C, 150°C, 450°C, and 750°C respectively.

Recommendations

The present research investigation confirms the Viability of IVA in concrete, thereby demonstrating an efficient approach to environmental sustainability. There are some recommendations made after this investigation:

- 1 It may be possible to replace the cement quantity with calcined IVA at various temperature levels.
- 2 The combination of various locally available industrial wastes (such as fly ash, ground granulated blast furnace, etc.) can be used with IVA to produce sustainable and durable concrete.
- 3 It can also be suggested to study the durability characteristics of each concrete mix.

Acknowledgment

The authors would like to thank the Director of Postgraduate Studies and the CED at the University of Engineering and Technology Taxila, Pakistan for their assistance to provide labs and accomplish this research of M.Sc. thesis of the corresponding author.

References

- [1] A. Petek Gursel, E. Masanet, A. Horvath, and A. Stadel, "Life-cycle inventory analysis of concrete production: A critical review," *Cem. Concr. Compos.*, vol. 51, no. August 2014, pp. 38–48, 2014, doi: 10.1016/j.cemconcomp.2014.03.005.



5th Conference on Sustainability in Civil Engineering (CSCE'23)

Department of Civil Engineering

Capital University of Science and Technology, Islamabad Pakistan



- [2] W. Shen, L. Cao, Q. Li, W. Zhang, G. Wang, and C. Li, "Quantifying CO₂ emissions from China's cement industry," *Renew. Sustain. Energy Rev.*, vol. 50, pp. 1004–1012, 2015, doi: 10.1016/j.rser.2015.05.031.
- [3] H. Wang, J. Xu, X. Yang, Z. Miao, and C. Yu, "Organic Rankine cycle saves energy and reduces gas emissions for cement production," *Energy*, vol. 86, pp. 59–73, 2015, doi: 10.1016/j.energy.2015.03.112.
- [4] B. L. Damineli, F. M. Kemeid, P. S. Aguiar, and V. M. John, "Measuring the eco-efficiency of cement use," *Cem. Concr. Compos.*, vol. 32, no. 8, pp. 555–562, 2010, doi: <https://doi.org/10.1016/j.cemconcomp.2010.07.009>.
- [5] K. L. Scrivener and R. J. Kirkpatrick, "Innovation in use and research on cementitious material," *Cem. Concr. Res.*, vol. 38, no. 2, pp. 128–136, 2008, doi: <https://doi.org/10.1016/j.cemconres.2007.09.025>.
- [6] C. Ouellet-Plamondon and G. Habert, "25 - Life cycle assessment (LCA) of alkali-activated cements and concretes," F. Pacheco-Torgal, J. A. Labrincha, C. Leonelli, A. Palomo, and P. B. T.-H. of A.-A. C. Chindaprasirt Mortars and Concretes, Eds. Oxford: Woodhead Publishing, 2015, pp. 663–686. doi: <https://doi.org/10.1533/9781782422884.5.663>.
- [7] R. Kurda, J. D. Silvestre, and J. de Brito, "Life cycle assessment of concrete made with high volume of recycled concrete aggregates and fly ash," *Resour. Conserv. Recycl.*, vol. 139, no. September, pp. 407–417, 2018, doi: 10.1016/j.resconrec.2018.07.004.
- [8] V. Letelier, J. M. Ortega, E. Tarela, P. Muñoz, B. I. Henríquez-Jara, and G. Moriconi, "Mechanical performance of eco-friendly concretes with volcanic powder and recycled concrete aggregates," *Sustainability*, vol. 10, no. 9, p. 3036, 2018.
- [9] T. P. da Costa, P. Quinteiro, L. A. C. Tarelho, L. Arroja, and A. C. Dias, "Environmental assessment of valorisation alternatives for woody biomass ash in construction materials," *Resour. Conserv. Recycl.*, vol. 148, pp. 67–79, 2019.
- [10] M. U. Hossain and S. T. Ng, "Strategies for enhancing the accuracy of evaluation and sustainability performance of building," *J. Environ. Manage.*, vol. 261, p. 110230, 2020.
- [11] K. Kupwade-Patil *et al.*, "Impact of Embodied Energy on materials/buildings with partial replacement of ordinary Portland Cement (OPC) by natural Pozzolanic Volcanic Ash," *J. Clean. Prod.*, vol. 177, pp. 547–554, 2018.
- [12] K. Kupwade-Patil, S. D. Palkovic, A. Bumajdad, C. Soriano, and O. Büyüköztürk, "Use of silica fume and natural volcanic ash as a replacement to Portland cement: Micro and pore structural investigation using NMR, XRD, FTIR and X-ray microtomography," *Constr. Build. Mater.*, vol. 158, pp. 574–590, 2018, doi: 10.1016/j.conbuildmat.2017.09.165.
- [13] G. Cai, T. Noguchi, H. Degée, J. Zhao, and R. Kitagaki, "Volcano-related materials in concretes: a comprehensive review," *Environ. Sci. Pollut. Res.*, vol. 23, pp. 7220–7243, 2016.
- [14] A. M. Zeyad, B. A. Tayeh, and M. O. Yusuf, "Strength and transport characteristics of volcanic pumice powder based high strength concrete," *Constr. Build. Mater.*, vol. 216, pp. 314–324, 2019.
- [15] R. Siddique, "Properties of concrete made with volcanic ash," *Resour. Conserv. Recycl.*, vol. 66, pp. 40–44, 2012, doi: 10.1016/j.resconrec.2012.06.010.
- [16] S. A. Mohamad, R. K. S. Al-Hamid, and T. T. Khaled, "Investigating the effect of elevated temperatures on the properties of mortar produced with volcanic ash," *Innov. Infrastruct. Solut.*, vol. 5, no. 1, pp. 1–11, 2020, doi: 10.1007/s41062-020-0274-4.
- [17] K. M. Anwar Hossain, "High strength blended cement concrete incorporating volcanic ash: Performance at high temperatures," *Cem. Concr. Compos.*, vol. 28, no. 6, pp. 535–545, 2006, doi: 10.1016/j.cemconcomp.2006.01.013.
- [18] N. Khurram, K. Khan, M. U. Saleem, M. N. Amin, and U. Akmal, "Effect of Elevated Temperatures on Mortar with Naturally Occurring Volcanic Ash and Its Blend with Electric Arc Furnace Slag," *Adv. Mater. Sci. Eng.*, vol. 2018, 2018, doi: 10.1155/2018/5324036.
- [19] J. C. Liu, M. U. Hossain, S. T. Ng, and H. Ye, "High-performance green concrete with high-volume natural pozzolan: Mechanical, carbon emission and cost analysis," *J. Build. Eng.*, vol. 68, no. February, p. 106087, 2023, doi: 10.1016/j.jobe.2023.106087.
- [20] L. Presa *et al.*, "Volcanic Ash from the Island of La Palma, Spain: An Experimental Study to Establish Their Properties as Pozzolans," *Processes*, vol. 11, no. 3, p. 657, 2023, doi: 10.3390/pr11030657.
- [21] ASTM C 109/C 109M-21, "Standard test method for compressive strength of hydraulic cement mortars," *Annu. B. ASTM Stand.*, vol. 04, p. 9, 2021, doi: 10.1520/C0109.
- [22] M. N. Amin and K. Khan, "Mechanical performance of high-strength sustainable concrete under fire incorporating locally available volcanic ash in central harrat rahat, saudi arabia," *Materials (Basel.)*, vol. 14, no. 1, pp. 1–26, 2021, doi: 10.3390/ma14010021.
- [23] K. M. A. Hossain, "Blended cement using volcanic ash and pumice," *Cem. Concr. Res.*, vol. 33, no. 10, pp. 1601–1605, 2003, doi: 10.1016/S0008-8846(03)00127-3.
- [24] B. Georgali and P. E. Tsakiridis, "Microstructure of fire-damaged concrete. A case study," *Cem. Concr. Compos.*, vol. 27, no. 2, pp. 255–259, 2005, doi: 10.1016/j.cemconcomp.2004.02.022.
- [25] K. W. Nasser and H. M. Marzouk, "Properties of mass concrete containing fly ash at high temperatures," in *Journal Proceedings*, 1979, vol. 76, no. 4, pp. 537–550.
- [26] Y. N. Chan, G. F. Peng, and M. Anson, "Residual strength and pore structure of high-strength concrete and normal strength concrete after exposure to high temperatures," *Cem. Concr. Compos.*, vol. 21, no. 1, pp. 23–27, 1999, doi: 10.1016/S0958-9465(98)00034-1.



THE EFFECT OF PLASTIC FIBERS ON THE MECHANICAL PROPERTIES, DUCTILITY AND ENVIRONMENTAL PERFORMANCE OF CONCRETE – A REVIEW

^a*Arshad Qayyum**, ^b*Safeer Ullah Khattak,*

a: Department of Civil Engineering, Comsats University Islamabad, Abbottabad Campus, Pakistan, arshadkhan7446@gmail.com

b: Department of Civil Engineering, Comsats University Islamabad, Abbottabad Campus, Pakistan, safeer@cuiatd.edu.pk

* Corresponding author: Email ID: arshadkhan7446@gmail.com

Abstract- Concrete is a common building material due to its strength and durability, but it is essentially brittle, which can lead to cracking and reduced ductility under tensile loads. To enhance the ductility of concrete, different studies have been done on various fibers, including plastic fibers. This paper explores the impact of plastic fibers on the mechanical properties, ductility and environmental performance of concrete. This review paper includes different studies on plastic fiber reinforced concrete under compressive, split tensile and flexure, focusing on the effect of plastic fibers on the ductility and environmental effect of it. Different studies show that plastic fibers significantly improve the compressive, split tensile, flexure, ductility and it will also help in reducing the plastic waste. These findings have important implications for the design of concrete buildings and their construction, particularly in earthquake-prone regions, where improved ductility capacity can amplify the seismic performance of structures additionally decrease the risk of catastrophic failure. Furthermore, the use of plastic fibers as reinforcement provides a sustainable solution for managing plastic waste. Plastic fibers have low cost, high availability, and favorable mechanical properties, making them an attractive alternative to traditional fiber reinforcement materials. The use of plastic fibers into concrete can reduce the environmental impact of plastic waste. The results of this study demonstrate the potential of plastic fiber reinforced concrete to improve the ductility and concrete structure's capacity to absorb energy while providing a sustainable solution for managing plastic waste.

Keywords- Plastic Fiber Concrete, Mechanical Properties, Ductility of Plastic Fiber, Environmental Effect, Plastic Reinforced Concrete.

1 Introduction

Concrete is frequently used in building because of its high compressive strength and durability, but it is essentially brittle, which can lead to cracking and reduced ductility under tensile loads. To address this issue, different studies have explored various fiber reinforcements to improve the mechanical properties and ductility of concrete. Plastic shrinkage is a well-known phenomenon in concrete, characterized by the quick evaporation of water from the freshly laid concrete's surface. This can lead to significant shrinkage, resulting in cracking, internal warping, and external deflection, which can weaken the concrete structure [1]. According to studies on concrete, to increase the resistance to cracking, various modifications are made to the composition of mixtures. These include the use of highly absorbent polymers, particle size distribution optimization, and fiber addition. [2]. Plastic fibers have emerged as a potential alternative to traditional fiber reinforcement materials due to their high availability, low cost and favorable mechanical properties.



Plastic fibers are synthetic fibers made from different types of polymers, including polypropylene, polyester, and nylon. This paper reviews the effects of different types of fibers (steel[3], carbon[4], basalt[5], glass[6], polypropylene[7], polyvinyl alcohol[8], and plant fibers[9]) on the dynamic mechanical properties of concrete under impact loads. It also summarizes the dynamic constitutive models and numerical simulation methods for fiber-reinforced concrete[10]. They are commonly used for a variety of purposes, including textiles, packaging, and construction. Plastic waste disposal is a major environmental problem worldwide due to the health dangers and challenges involved in land filling [11]. Steel fibers have the ability to absorb energy and control cracks, which leads to improvements in both tensile strength and flexural strength of concrete [12]. The incorporation of glass fibers in concrete provides excellent strengthening effects. However, it is important to note that glass fibers exhibit poor alkali resistance [13]. Wood, sisal, coconut, sugarcane bagasse, palm, and vegetable fibers are examples of natural fibers which are cost-effective and readily accessible. However, it is worth noting that these natural fibers tend to have poor durability [14]. Compared to traditional fiber reinforcement materials such as steel and glass, plastic fibers are lightweight, non-corrosive, and easy to handle. Additionally, they have a high tensile strength and elastic modulus., which makes them ideal for use as reinforcement in concrete.

This study investigates how plastic fibers affect the ductility and strength of concrete. Different studies include testing of plain and plastic fiber reinforced concrete under tensile, compressive and flexure loading, focusing on the impact of plastic fibers on the ductility and concrete's potential to absorb energy. This study investigated the addition of Polyethylene terephthalate fiber (PET) to concrete to improve its tensile strength and ductile properties. Various fiber volumes were tested, showing reduced slump and compaction factor at higher percentages. Workability remained satisfactory up to 1.5% to 2.0% fiber addition. Higher fiber content also increased bond strength[15]. As a result, Concrete has been acknowledged as one of the possible options for developing alternative methods of utilizing the plastic waste for other purposes [16]. The results show that plastic fibers significantly improve the ductility and energy absorption capacity of concrete. This study examined waste plastic fiber reinforced concrete by varying the percentage of plastic reinforcement (0%, 0.5%, 1%, 1.5%, 2%). Mechanical properties and ductility factors were evaluated, revealing improved concrete performance with the addition of plastic [17]. This is consistent with fundamental ecological practices including preventing waste, recycling trash, avoiding landfills, extracting energy from garbage, and preserving raw materials[18]. The findings have important implications for the design and construction of concrete structures, particularly in earthquake-prone regions, where improved ductility and energy absorption capacity can enhance the seismic performance of structures and reduce the risk of catastrophic failure. On the other hand, concrete has limited properties, such as weak tensile strength, impact energy absorption, and ductility[19]. [20] They conducted research on reinforced concrete utilizing waste metalized plastic waste fibers. They discovered that the strength and IR development of concrete composites might be significantly affected by the addition of these waste fibers. Furthermore, the use of plastic fibers as reinforcement provides a sustainable solution for managing plastic waste. Several studies have shown that incorporating plastic waste from various sources (PET bottles, plastic bags, and fishing nets) as fibers in concrete beams can effectively reduce plastic waste in landfills[21]. The findings of this research demonstrate the potential of plastic fiber reinforced concrete to improve the ductility and energy absorption capacity of concrete structures while providing a sustainable solution for managing plastic waste.

2 Mechanical Properties of Plastic Fiber in Concrete

The mechanical properties of plastic fiber in concrete refer to the characteristics and behavior of concrete when reinforced with plastic fibers. These properties include the strength, ductility, energy absorption capacity, and other relevant mechanical behaviors exhibited by the composite material. Table 1 presents the findings regarding the improved mechanical properties of 28-day cured concrete incorporating plastic fiber. The results demonstrate the positive effects of plastic fiber reinforcement on the performance of the concrete. The addition of 1.5% polyethylene terephthalate (PET) fibers with an aspect ratio of 17 (AR-17) resulted in a significant increase of up to 26.3% in the compressive strength of the concrete. This enhancement indicates that the inclusion of PET fibers contributed to the concrete's ability to withstand compressive forces. Similarly, the tensile strength of the concrete increased by up to 14.48% when 1.5% PET fibers with AR-17 were incorporated. This improvement in tensile strength highlights the reinforcing effect of the fibers on the concrete's resistance to tension. The table also reveals that by adding 0.15% volume fraction (Vf) of plastic fibers confined in the tension zone, the flexural strength of the concrete increased by up to 5.26 N/mm². This increase in flexural strength suggests that the plastic fibers enhanced the concrete's ability to resist bending stresses. Moreover, the inclusion of plastic fibers improved the concrete bond strength and reduced cracks, thereby enhancing its overall



durability. Additionally, the table mentions that the typical compressive strength specified for concrete ranges from 4,000 to 5,000 psi, and it emphasizes that concrete products must undergo a curing period of 28 days before installation or use. Lastly, the table highlights that the inclusion of pozzolans and supplementary cementitious materials (SCMs) increased the strength of the concrete by 25% to 40%, further enhancing its long-term strength and durability. Overall, these findings demonstrate the positive impact of incorporating plastic fibers on the mechanical properties of 28-day cured concrete, indicating their potential to improve the overall performance and durability of concrete structures.

Table 1 Improved Mechanical Properties of 28-Day Cured Concrete Incorporating Plastic Fiber [22], [23]

Compressive Strength	Tensile Strength	Flexural Strength	Key Findings
Increased up to 26.3% using 1.5% PET with AR-17	Increased up to 14.48% using 1.5% PET with AR-17	-	Plastic fibers improved the concrete bond strength and reduced the cracks
Increased up to 8.4% using 0.15% Vf of plastic fibers	-	Increased up to 5.26 N/mm ² using 0.15% Vf of plastic fibers confined in the tension zone	Plastic fibers increased the post-crack toughness and residual strength of concrete
4,000 to 5,000 psi for typical concrete specification	-	-	Concrete products cannot be installed or used until 28 days after the date of manufacture
Increased by 25% to 40% with the inclusion of pozzolans and SCMs	-	-	Pozzolans and SCMs enhanced the long-term strength and durability of concrete

2.1 Influence of Plastic Fibers on Compressive Strength

Concrete's compressive strength may be considerably increased by adding plastic fibers. The addition of plastic fibers can increase the ability of concrete to resist compressive stresses, resulting in stronger concrete. The results demonstrate that incorporating waste plastic fibers in concrete causes a slight reduction in compressive strength, with negligible differences between M (0%) and M (5%) following 7, 14, and 28 days of curing [24]. The increase in strength is mainly due to the fiber's ability to bridge cracks that can form in the concrete. According to a study, the addition of 1.5% PET fibers and 6% Alccofine in concrete resulted in the highest compressive strength, with a decrease in strength observed beyond these percentages [25]. As a result, the fibers improve the concrete's capacity to sustain itself and increase its resistance to deformation and cracking. Additionally, plastic fibers can also improve the durability of concrete structures, as they can prevent water from penetrating the surface and reduce the potential for freeze-thaw damage.

Table 1 provides details on the various Polyethylene terephthalate fiber fiber reinforcing options for concrete's compressive strength. The properties analyzed include elastic modulus and compressive strength. The elastic modulus (Ec) is a measure of a material's stiffness or rigidity. The elastic modulus values range from 24.2 GPa to 25.9 GPa, with C2 having the lowest value and C7 having the highest. The compressive strength values are given for two different types of specimens: cubes (F(cube)) and cylinders (F(cylinder)). The age of the specimens is given as 28 days and 90 days, representing the time at which the concrete samples were tested. For the plain concrete (C1), without any fiber reinforcement, the compressive strengths are 28 MPa at 28 days and 90 MPa at 90 days, for both the cube and cylinder specimens. When fiber reinforcement is applied, the kind and length of the fibers utilized affect the compressive strengths. Two types of fibers are considered: 0.25mm fiber and 0.40mm fiber. For the 0.25mm fiber reinforcement, the compressive strengths range from 31.0 MPa to 38.7 MPa at 28 days for cube specimens. For 90-day cube specimens, the compressive strengths vary from 37.2 MPa to 40.1 MPa. The corresponding compressive strengths for 28-day cylinder specimens range from 23.3 MPa to 26.6 MPa. For the 0.40mm fiber reinforcement, the compressive strengths at 28 days for cube specimens range from 30.5 MPa to 38.7 MPa. At 90 days, the compressive strengths range from 37.7 MPa to 38.4 MPa. The compressive strengths for 28-day cylinder specimens range from 23.4 MPa to 26.2 MPa. Overall, the table demonstrates the impact of fiber reinforcement on the mechanical properties of concrete. The addition of fibers generally leads to higher compressive



strengths compared to plain concrete. The specific combination of fiber type and length influences the resulting strengths. Additionally, there are slight variations in the elastic modulus values among the different concrete properties analyzed.

Table 2 Compressive Strength of Three Concrete Mixtures (Average of Three Specimens) [26]

Concrete Property	Unit	Age	Plain	0:25mm PET Fiber			0:40mm PET Fiber		
			C1	C2	C3	C4	C5	C6	C7
Elastic modulus E_c	GPa	28	24.2	24.5	24.9	25.2	24.2	25.9	25.5
Compressive strengths $F(\text{cube})$	MPa	28	33.2	34.3	31.1	32.3	31.0	31.0	30.5
$F(\text{cube})$	MPa	90	38.1	40.1	38.4	37.7	37.2	37.7	38.7
$F(\text{cylinder})$	MPa	28	23.3	26.2	24.1	23.4	24.1	26.6	23.5

2.2 Influence of Plastic Fibers on Tensile Strength.

A material's tensile strength is determined by its capacity to withstand breaking or fracture under tensile forces. Concrete has relatively low tensile strength, and the addition of plastic fibers can improve its ability to resist tensile stresses. The study shows that the use of 30% waste plastic fiber in mortar increases the strength significantly, with the mortar strength at 90 days being more than double that of the 7 days strength [27]. The study shows that FRC with ring-shaped Polyethylene terephthalate fiber (PET) showed stronger splitting tensile strength compared to those with irregularly shaped PET and waste wire fibers because of the interlocking tensile strength of the fibers in the fiber-bridging zone. Among the ring-shaped fibers, R-10 fibers with a width of 10 mm showed the highest maximum loads, while synthetic macro-fibers had the highest splitting tensile strength. [28]. By bridging the fractures that develop as a result of tensile stresses, plastic fibers can enhance the tensile strength of concrete. By bridging these cracks, the fibers can prevent them from propagating and reduce the potential for failure. The improved tensile strength can lead to more durable concrete structures that can resist deformation and cracking.

This table 2, explains the mechanical characteristics of concrete with various fiber reinforcing choices., specifically focusing on tensile strength. The properties analyzed include elastic modulus and tensile strength. The elastic modulus (E_c) represents the stiffness or rigidity of a material. In this table, the values of elastic modulus for different concrete properties are given. The values range from 24.2 GPa to 25.9 GPa, with C2 having the lowest value and C7 having the highest. Tensile strength is a crucial property of concrete, indicating its ability to resist tension forces. It is typically measured in megapascals (MPa). The table provides tensile strength values for concrete samples at different ages and with various fiber reinforcement options. The tensile strength values are given for two types of specimens: cubes ($F(\text{cube})$) and cylinders ($F(\text{cylinder})$). The age of the specimens is given as 28 days and 90 days, representing the time at which the concrete samples were tested. For plain concrete (C1), without any fiber reinforcement, the tensile strengths are 28 MPa at 28 days and 90 MPa at 90 days for both cube and cylinder specimens. When 0.25mm fiber reinforcement is introduced, the tensile strengths vary depending on the concrete property. At 28 days for cube specimens, the tensile strengths range from 2.79 MPa to 3.08 MPa. At 90 days, the tensile strengths range from 3.32 MPa to 3.49 MPa. The tensile strengths for 28-day cylinder specimens range from 3.84 MPa to 4.35 MPa. For 0.40mm fiber reinforcement, the tensile strengths at 28 days for cube specimens range from 2.88 MPa to 3.03 MPa. At 90 days, the tensile strengths range from 3.40 MPa to 3.53 MPa. The tensile strengths for 28-day cylinder specimens range from 3.96 MPa to 4.37 MPa. Overall, the table illustrates how fiber reinforcement affects concrete's tensile strength. The addition of fibers generally leads to higher tensile strengths compared to plain concrete. The resultant strengths are influenced by the particular fiber type and length combination. The values in the table highlight the improvement in tensile strength achieved by incorporating fiber reinforcement in concrete samples, providing valuable information for construction and structural design applications.



Table 3 Compressive Strength of Three Concrete Mixtures (Average of Three Specimens except f(ctm), which is based on one load-tested prism) [26]

Concrete Property	Unit	Age	Plain	0:25mm PET Fiber			0:40mm PET Fiber		
			C1	C2	C3	C4	C5	C6	C7
Elastic modulus									
E_c	GPa	28	24.2	24.5	24.9	25.2	24.2	25.9	25.5
Tensile strengths									
F(cube)	MPa	28	2.79	3.08	2.95	2.96	3.03	2.93	2.88
F(cube)	MPa	90	3.32	3.47	3.49	3.43	3.40	3.47	3.53
F(ctm)	MPa	28	3.84	4.35	4.14	4.37	4.01	4.05	3.96

2.3 Influence of Plastic Fibers on Flexure Strength

The capacity of a material to resist bending or breaking under bending forces is referred to as flexure strength or bending strength. Plastic fibers may significantly enhance the flexural strength of concrete. According to a study by [25], Flexural strength rises with increasing PET fiber content and Alccofine %. With 1.5% fiber and 9% Alccofine, the maximum flexural strength is achieved. By boosting the material's tensile strength, the fibers can make concrete more flexibly strong., and by bridging the cracks that can form under bending stresses. The bridging of these cracks can prevent the formation of larger cracks and can reduce the potential for failure. As a result, the addition of plastic fibers can lead to more durable concrete structures that can resist deformation and cracking under bending stresses.

The ductility and flexural strength of 500 mm long prisms subjected to four-point bending are shown to be impacted by recycled HDPE (high-density polyethylene) fibers in Figure 6. A displacement-controlled power ram was used to load the material at a speed of 1 mm per minute. The load-deflection plots reveal that all prisms reached similar peak flexural loads, approximately Fcr (15.0-16.0 kN), at deflections around 0.45-0.50 mm over the 300 mm spans. However, prisms reinforced with $\varnothing 1 = 0.25$ mm fibers demonstrated slightly higher loads compared to those reinforced with $\varnothing 1 = 0.40$ mm fibers. Upon cracking, the prisms exhibited residual load levels, RL. The $\varnothing 1 = 0.25$ mm fiber-reinforced prisms achieved RL values ranging from 25% to 45% of Fcr, indicating an improved residual load capacity compared to the $\varnothing 1 = 0.40$ mm fiber-reinforced prisms, which had RL values between 13% and 32% of Fcr. As expected, a higher volume of added fibers led to a higher RL/Fcr ratio. This figure provides valuable insights into the behavior of recycled plain HDPE fiber-reinforced prisms under flexural loading. It highlights the effect of fiber diameter and volume on both peak load capacity and residual load levels, demonstrating the potential for enhancing the flexural performance and ductility of concrete structures.

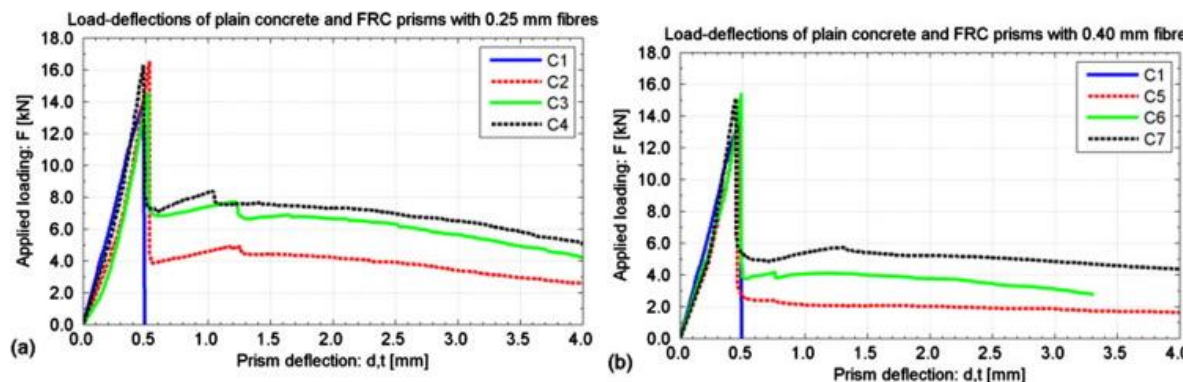


Figure 1 Flexural Strength Comparison of Plain Concrete (C1) and FRC with a) Ø 0.25 mm PET Fibers (C2-C4) and b) Ø 0.40 mm PET Fibers (C5-C7) [26]



3 The Effect of Plastic Fibers on Ductility

Ductility is an important mechanical property of construction materials such as concrete, which refers to the material's ability to undergo plastic deformation before failure. In other words, ductility measures how much a material can bend or stretch under stress without breaking. It is a crucial property for structures subjected to various types of loads and dynamic forces. Plastic macro-fibers decreased the workability of fresh concrete and increased cracking caused by plastic shrinkage. By enhancing its ductility, toughness, and flexural and tensile strength, fibers added to concrete increase the material's total strength [29]. The ductility of concrete has been discovered to be improved by the inclusion of plastic fibers. To increase the mechanical qualities of concrete, plastic fibers, which are commonly formed of materials like polypropylene, polyester, or nylon, are employed as a reinforcing material. These fibers can enhance the ductility of concrete in several ways.

Firstly, concrete's brittleness can be lessened with plastic fibers, making it less susceptible to unexpected breakdown while under stress. This is because the fibers act as tiny shock absorbers, absorbing the energy from the impact and distributing it evenly throughout the concrete matrix. As a result, the concrete becomes more resistant to cracks and fractures, and is able to undergo greater plastic deformation before failure. Secondly, the presence of plastic fibers in concrete can improve the material's post-cracking behavior. This research was done to look at the behavior of ductility, energy absorption, and impact resistance of fiber-reinforced concrete [29]. When concrete cracks under stress, the fibers help to hold the cracked surfaces together, preventing further propagation of the cracks. The impact of this is an increase in the residual strength of the material, which means that the concrete can still carry load even after cracking. This is crucial for buildings that are vulnerable to dynamic loads like earthquakes, as it allows the material to undergo a certain level of deformation without failing completely.

Finally, Plastic fibers can be added to concrete to increase its overall toughness. Concrete tends to deteriorate over time when subjected to adverse weather conditions like freeze-thaw cycles or chemical assault, decreasing its mechanical qualities. A study investigated the use of waste plastic fibers from flour sacks to enhance the performance of mortar by partially replacing sand with varying rates. According to [30], plastic shrinkage cracks in newly laid concrete can be avoided, and the post-cracking behavior of concrete can be enhanced by using synthetic fibers comprised of polyolefin, acrylic, aramid, and carbon. However, the use of plastic fibers can help to mitigate this degradation, as they act as a barrier against moisture and chemicals, preventing them from penetrating deep into the concrete matrix. The inclusion of plastic fibers to concrete has a significant impact on the material's ductility, improving its ability to undergo plastic deformation before failure. This is due to the fibers' ability to reduce brittleness, improve post-cracking behavior, and enhance overall durability. As a result, the use of plastic fibers in concrete can lead to more resilient and sustainable structures, capable of withstanding a wide range of loads and environmental conditions.

4 Environmental and Sustainability Considerations

There are a number of sustainability and environmental issues related to the usage of plastic fibers as reinforcement in concrete. First, using plastic fibers in concrete offers a long-term method of disposing of plastic waste. Less than 9% of the 335 Mt of plastic generated year worldwide, according to the report, is recycled. The majority of plastic waste ends up in landfills, leading to significant environmental concerns. The study highlights the environmental advantages of using recycled industrial plastic waste as microplastic fibers for concrete reinforcement [31]. Plastic waste is a significant environmental problem worldwide, with large amounts of plastic ending up in landfills or oceans. By using plastic fibers as reinforcement in concrete, the environmental impact of plastic waste can be reduced while providing a valuable resource for construction.

Additionally, using plastic fibers as concrete reinforcement can help cut down on carbon emissions. The production of concrete with traditional steel reinforcement requires a lot of energy and emits a lot of carbon dioxide. When used in large-scale concrete manufacturing, the strategy of partially substituting Portland cement with recovered waste plastic has the potential to minimize carbon emissions [32]. The study examined the environmental effects of utilizing recycled PET as fine aggregate in concrete and found that doing so greatly lessens both the carbon footprint and the human toxicity impact of concrete manufacturing [33]. In contrast, plastic fibers have a low carbon footprint and require less energy to produce, making them a more sustainable alternative. Finally, the use of plastic fibers in concrete can contribute to the development



of a circular economy. By incorporating plastic waste into construction materials, the value of waste materials is increased, and the need for virgin materials is reduced. This approach can help to create a more sustainable and resource-efficient construction industry.

The different stages involved in the production of plastic fiber for use in concrete. The first stage is plastic bottles being collected from landfills, indicating that these bottles are being diverted from traditional waste disposal methods. The second step is that the bottles being cleaned, which is an important step in ensuring that the material is free from contaminants that could affect the quality of the final product. Finally, the third step is the plastic bottles being converted into fibers, which are then used as a reinforcement material in concrete. The potential of recycling plastic waste into valuable products, which not only reduces the amount of plastic waste in landfills but also helps to conserve natural resources. An example of a sustainable material solution that may help in reducing the negative effects of construction activities on the environment is the use of plastic fibers in concrete. By using recycled plastic, the production of new materials can be reduced, and the environmental footprint of the construction industry can be minimized.

5 Conclusions

The research presented in this paper explores the effect of plastic fibers on the mechanical properties, ductility, and environmental performance of concrete. The findings have significant implications for sustainable construction practices and the management of plastic waste. The key conclusions from different studies are summarized as follows:

1. The inclusion of waste plastic fibers in concrete results in the higher compressive strengths achieved compared to plain concrete.
2. Concrete's split tensile strength is greatly increased by the addition of plastic fibers, indicating improved resistance to tensile stresses.
3. Plastic fibers contribute to the enhancement of flexural strength in concrete.
4. The inclusion of plastic fibers improves the ductility of concrete, making it less brittle and more resistant to cracking.
5. By utilizing recycled plastic waste as reinforcement, the environmental impact of plastic disposal in landfills or oceans can be reduced.

The study's findings show that adding plastic fibers to concrete enhances its mechanical qualities, such as ductility, flexure strength, split tensile strength, and compressive strength. Furthermore, incorporating plastic fibers offers environmental benefits by reducing plastic waste and lowering carbon emissions. These results encourage the use of environmentally friendly building techniques, where plastic fibers may be successfully used as a reinforcing material in concrete buildings.

Acknowledgment

The authors would like to thank Department of Civil Engineering Comsats University who helped thorough out the research work.

References

- [1] G. M. Sadiqul Islam and S. Das Gupta, "Evaluating plastic shrinkage and permeability of polypropylene fiber reinforced concrete," International Journal of Sustainable Built Environment, vol. 5, no. 2, pp. 345–354, Dec. 2016, doi: 10.1016/J.IJSBE.2016.05.007.
- [2] D. Shen, X. Liu, X. Zeng, X. Zhao, and G. Jiang, "Effect of polypropylene plastic fibers length on cracking resistance of high performance concrete at early age," Constr Build Mater, vol. 244, p. 117874, May 2020, doi: 10.1016/J.CONBUILDMAT.2019.117874.
- [3] D. Y. Yoo, J. J. Park, and S. W. Kim, "Fiber pullout behavior of HPFRCC: Effects of matrix strength and fiber type," Compos Struct, vol. 174, pp. 263–276, Aug. 2017, doi: 10.1016/J.COMPSTRUCT.2017.04.064.
- [4] B. Zegardlo, "Heat-resistant concretes containing waste carbon fibers from the sailing industry and recycled ceramic aggregates," Case Studies in Construction Materials, vol. 16, p. e01084, Jun. 2022, doi: 10.1016/J.CSCM.2022.E01084.



5th Conference on Sustainability in Civil Engineering (CSCE'23)

Department of Civil Engineering
Capital University of Science and Technology, Islamabad Pakistan



- [5] Y. Wang, S. Hu, and X. Sun, "Experimental investigation on the elastic modulus and fracture properties of basalt fiber-reinforced fly ash geopolymers concrete," *Constr Build Mater*, vol. 338, p. 127570, Jul. 2022, doi: 10.1016/J.CONBUILDMAT.2022.127570.
- [6] S. Ma, D. Hou, P. Bao, and D. Wang, "Influence of alkali-resistant glass fiber on seismic performance of precast ceramsite concrete sandwich wall panels," *Structures*, vol. 38, pp. 94–107, Apr. 2022, doi: 10.1016/J.ISTRUC.2022.01.081.
- [7] N. Liang, J. Mao, R. Yan, X. Liu, and X. Zhou, "Corrosion resistance of multiscale polypropylene fiber-reinforced concrete under sulfate attack," *Case Studies in Construction Materials*, vol. 16, p. e01065, Jun. 2022, doi: 10.1016/J.CSCM.2022.E01065.
- [8] D. Shen, C. Liu, M. Wang, J. Kang, and M. Li, "Effect of polyvinyl alcohol fiber on the cracking risk of high strength concrete under uniaxial restrained condition at early age," *Constr Build Mater*, vol. 300, p. 124206, Sep. 2021, doi: 10.1016/J.CONBUILDMAT.2021.124206.
- [9] M. U. Farooqi and M. Ali, "Contribution of plant fibers in improving the behavior and capacity of reinforced concrete for structural applications," *Constr Build Mater*, vol. 182, pp. 94–107, Sep. 2018, doi: 10.1016/J.CONBUILDMAT.2018.06.041.
- [10] H. Wu et al., "Dynamic mechanical properties of fiber-reinforced concrete: A review," *Constr Build Mater*, vol. 366, p. 130145, Feb. 2023, doi: 10.1016/J.CONBUILDMAT.2022.130145.
- [11] A. T. Bassam, A. Ibrahim, Hassan M. Magbool, A. Hisham, and A. Rayed, "Performance of sustainable concrete containing different types of recycled plastic," *J Clean Prod*, vol. 328, no. 15, Dec. 2021.
- [12] A. Beglarigale and H. Yazici, "Pull-out behavior of steel fiber embedded in flowable RPC and ordinary mortar," *Constr Build Mater*, vol. 75, pp. 255–265, Jan. 2015, doi: 10.1016/J.CONBUILDMAT.2014.11.037.
- [13] S. T. Tassew and A. S. Lubell, "Mechanical properties of glass fiber reinforced ceramic concrete," *Constr Build Mater*, vol. 51, pp. 215–224, Jan. 2014, doi: 10.1016/J.CONBUILDMAT.2013.10.046.
- [14] J. Torkaman, A. Ashori, and A. Sadr Momtazi, "Using wood fiber waste, rice husk ash, and limestone powder waste as cement replacement materials for lightweight concrete blocks," *Constr Build Mater*, vol. 50, pp. 432–436, Jan. 2014, doi: 10.1016/J.CONBUILDMAT.2013.09.044.
- [15] B. Sanjaykumar and S. N. Daule, "Use of Plastic Fiber in the Concrete," *SSRG International Journal of Civil Engineering (SSRG-IJCE)*, vol. 4, p. 11, 2017, Accessed: Jun. 22, 2023. [Online]. Available: www.internationaljournalssrg.org
- [16] I. Almeshal, B. A. Tayeh, R. Alyousef, H. Alabduljabbar, A. Mustafa Mohamed, and A. Alaskar, "Use of recycled plastic as fine aggregate in cementitious composites: A review," *Constr Build Mater*, vol. 253, p. 119146, Aug. 2020, doi: 10.1016/J.CONBUILDMAT.2020.119146.
- [17] R. M. P and M. S. Kumar, "An Experimental Investigation on Strength and Ductility Behavior of Waste Plastic Fiber Reinforced Concrete," 2021.
- [18] B. Bhardwaj and P. Kumar, "Waste foundry sand in concrete: A review," *Constr Build Mater*, vol. 156, pp. 661–674, Dec. 2017, doi: 10.1016/J.CONBUILDMAT.2017.09.010.
- [19] "Ultimate Failure Resistance of Concrete with Partial Replacements of Sand by Polycarbonate Plastic Waste Under Impact Load," *Civil and Environmental Research*, Feb. 2020, doi: 10.7176/cer/12-2-06.
- [20] "The feasibility of improving impact resistance and strength properties of sustainable concrete composites by adding waste metalized plastic fibres".
- [21] F. S. Khalid, J. M. Irwan, M. H. W. Ibrahim, N. Othman, and S. Shahidan, "Performance of plastic wastes in fiber-reinforced concrete beams," *Constr Build Mater*, vol. 183, pp. 451–464, Sep. 2018, doi: 10.1016/J.CONBUILDMAT.2018.06.122.
- [22] S. Anandan and M. Alsubih, "Mechanical Strength Characterization of Plastic Fiber Reinforced Cement Concrete Composites," *Applied Sciences* 2021, Vol. 11, Page 852, vol. 11, no. 2, p. 852, Jan. 2021, doi: 10.3390/APP11020852.
- [23] H. M. Adda and M. Slimane, "Study of Concretes Reinforced by Plastic Fibers Based on Local Materials," *International Journal of Engineering Research in Africa*, vol. 42, pp. 100–108, Apr. 2019, doi: 10.4028/WWW.SCIENTIFIC.NET/JERA.42.100.
- [24] L. A. Pereira De Oliveira and J. P. Castro-Gomes, "Physical and mechanical behaviour of recycled PET fibre reinforced mortar," *Constr Build Mater*, vol. 25, no. 4, pp. 1712–1717, Apr. 2011, doi: 10.1016/J.CONBUILDMAT.2010.11.044.
- [25] A. I. Al-Hadithi and N. N. Hilal, "The possibility of enhancing some properties of self-compacting concrete by adding waste plastic fibers," *Journal of Building Engineering*, vol. 8, pp. 20–28, Dec. 2016, doi: 10.1016/J.JBEE.2016.06.011.
- [26] N. Pešić, S. Živanović, R. García, and P. Papastergiou, "Mechanical properties of concrete reinforced with recycled HDPE plastic fibres," *Constr Build Mater*, vol. 115, pp. 362–370, Jul. 2016, doi: 10.1016/J.CONBUILDMAT.2016.04.050.
- [27] N. Banthia and R. Gupta, "Influence of polypropylene fiber geometry on plastic shrinkage cracking in concrete," *Cem Concr Res*, vol. 36, no. 7, pp. 1263–1267, Jul. 2006, doi: 10.1016/J.CEMCONRES.2006.01.010.
- [28] F. S. Khalid, J. M. Irwan, M. H. W. Ibrahim, N. Othman, and S. Shahidan, "Performance of plastic wastes in fiber-reinforced concrete beams," *Constr Build Mater*, vol. 183, pp. 451–464, Sep. 2018, doi: 10.1016/J.CONBUILDMAT.2018.06.122.
- [29] H. U. Ahmed, R. H. Faraj, N. Hilal, A. A. Mohammed, and A. F. H. Sherwani, "Use of recycled fibers in concrete composites: A systematic comprehensive review," *Compos B Eng*, vol. 215, p. 108769, Jun. 2021, doi: 10.1016/J.COMPOSITESB.2021.108769.
- [30] S. Yin, R. Tuladhar, F. Shi, M. Combe, T. Collister, and N. Sivakugan, "Use of macro plastic fibres in concrete: A review," *Constr Build Mater*, vol. 93, pp. 180–188, Sep. 2015, doi: 10.1016/J.CONBUILDMAT.2015.05.105.
- [31] R. Tuladhar and S. Yin, "Sustainability of using recycled plastic fiber in concrete," *Use of Recycled Plastics in Eco-efficient Concrete*, pp. 441–460, Jan. 2019, doi: 10.1016/B978-0-08-102676-2.00021-9.



5th Conference on Sustainability in Civil Engineering (CSCE'23)

Department of Civil Engineering

Capital University of Science and Technology, Islamabad Pakistan



- [32] C. E. Schaefer et al., "Irradiated recycled plastic as a concrete additive for improved chemo-mechanical properties and lower carbon footprint," *Waste Management*, vol. 71, pp. 426–439, Jan. 2018, doi: 10.1016/J.WASMAN.2017.09.033.
- [33] F. Tahir, S. Sbahieh, and S. G. Al-Ghamdi, "Environmental impacts of using recycled plastics in concrete," *Mater Today Proc*, vol. 62, pp. 4013–4017, Jan. 2022, doi: 10.1016/J.MATPR.2022.04.593.



EXPLORING THE POTENTIAL OF MOSS CONCRETE AS AN ECO-FRIENDLY SOLUTION TO MITIGATE URBAN HEAT ISLAND EFFECT

^a *Muhammad Awais* *, ^b *Safeer Ullah Khattak*

a: Department of Civil Engineering, COMSATS University Islamabad, Abbottabad Campus, Pakistan, avais.swati@gmail.com

b: Department of Civil Engineering, COMSATS University Islamabad, Abbottabad Campus, Pakistan, safeer@cuiatd.edu.pk

* Corresponding author: Email ID: avais.swati@gmail.com

Abstract- This paper explores the potential of moss concrete as an eco-friendly solution to mitigate the Urban Heat Island (UHI) effect. To mitigate UHI effects, various approaches can be implemented, such as energy efficiency improvement, green roof construction and utilization of high reflectivity materials. Moss concrete is a type of concrete that incorporates moss into its mixture to create a natural, eco-friendly building material. Mosses are known for their ability to retain moisture, and they can help regulate surface temperatures and reduce the UHI effect. Moss concrete is a type of biological concrete that is developed by growing moss on the surface of structures. The construction of moss concrete involves a conventional concrete layer that serves as the structural component of the building, a waterproof layer that acts as a barrier, and an outer layer of moss concrete designed to allow rainwater to penetrate and boost the growth of the organisms. Moss concrete has the potential to purify the air by absorbing excess carbon dioxide from the atmosphere along with storm-water management, improved water run-off quality and extension of roof life.

Keywords- Urban Heat Island effect, moss concrete, albedo, durability, eco-friendly, stormwater management.

1 Introduction

Urbanization has brought about numerous environmental challenges, including the Urban Heat Island (UHI) effect. UHI occurs when urban structures absorb and emit solar radiation, leading to increased temperatures in urban areas. Vegetation is essential in regulating surface temperatures and reducing the UHI effect [1]. Moss concrete has emerged as a potential solution to mitigate UHI due to its unique properties. A recent study was conducted to assess the impact of asphalt and concrete pavements on lowering the earth's surface temperature. The study specifically compared the albedo effects, which measure surface reflectivity, of these two pavement types in a specific application and area. The results indicated that by using concrete pavements instead of asphalt ones and increasing the average albedo, significant temperature reductions were achieved. These temperature reductions were estimated to be equivalent to removing 25-75 kgCO₂/m² [2]. Another research shows that the compressive strength of moss concrete as compared to the conventional concrete increases overtime [3]. Increasing the albedo of urban surfaces through solar reflective materials can offset temperature rise caused by global warming. Simulations showed a global cooling effect and CO₂ emission reduction of 3 × 10⁻¹⁵ K and 7 kg per 1 m² of surface, respectively [4]. This paper explores the potential of moss concrete as an eco-friendly solution to mitigate UHI and improve building materials' durability.

1.1 Moss

Moss refers to a group of non-vascular plants that belong to the division Bryophyta. These small, soft plants typically grow in dense green clumps or mats in damp or shady locations. Mosses do not have flowers or seeds and reproduce via spores. They play an important ecological role by helping to retain moisture in soil and provide habitat for insects and



other small animals. Mosses are also used for various purposes, such as landscaping, gardening, and as a decorative element in crafts and art.

1.2 Urban Heat Island Effect

The Urban Heat Island (UHI) effect is a phenomenon of heat accumulation in urban areas caused by human activities and urban construction. It can have significant impacts on urban ecological systems, altering their structure and functions, and affecting urban climates, hydrology, soil properties, atmospheric environment, material and energy cycles, and residents' health. To mitigate UHI effects, various approaches can be implemented, such as energy efficiency improvement, green roof construction, utilization of high reflectivity materials, and green land cultivation. Research using remote sensing and numerical simulation methods has provided theoretical references for improving the urban ecological environment and achieving sustainable urban development [5]. A typical Urban heat island profile is shown in (Figure 1 [6]), which shows temperature is usually higher in urban areas as compared to the rural areas.

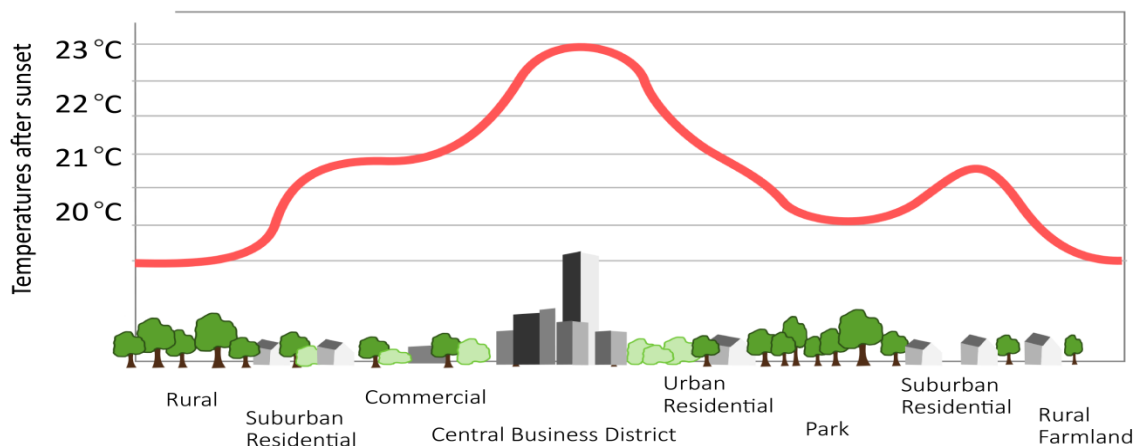


Figure 1: Urban Heat Island Profile

1.3 Green Roof Benefits

The implementation of rooftop greening is an effective option to mitigate UHI, with green roofs providing insulation and cooling the surrounding environment. Sunagoke moss has good thermal characteristics and high-speed evapotranspiration, making it a suitable afforestation plant for rooftop greening. However, industrial production of Sunagoke moss is required to meet the demand for city rooftop greening. To achieve this, plant factories are used for moss production, and a specific method of analyzing transpiration properties of Sunagoke moss has been developed to optimize the production system [7]. Another research suggests that sustainable ecological architecture refers to a form of building design that incorporates nature into all aspects of construction. Such buildings utilize living and non-living materials to create ecosystems or sustain existing habitats. The objective of ecological architecture is to explore the impact of ecological elements on buildings, their occupants, and the surrounding environment, highlighting the importance of balancing building design with nature [8].

Green roofs, which are comprised of a layer of vegetation on top of a building, offer numerous benefits including storm-water management, improved water run-off quality, improved air quality, extension of roof life, and reduction of the urban heat island effect. Extensive green roofs, which have a thin substrate layer with low-level planting such as sedum, are the preferred option for retrofitting onto existing buildings as they require minimum maintenance and are easy to install. Green roofs can also lead to building energy reduction benefits through enhanced thermal properties and insulation value. Retrofitting existing buildings with green roofs has potential for energy savings, but more research is needed to determine the extent of these benefits [9]. (Figure 2 [10]) shows a typical example of green roof.



Figure 2: Example of a typical green roof

Two types of green roofs are generally distinguished [11]: extensive and intensive as shown in Table 1:

Table 1: Types of Green Roofs

Extensive	Intensive
Low soil thickness(5-15 cm)	High soil thickness (above 15 cm)
Difficult to access	Easily accessible
Light (50-160 kg/m ²)	Heavy (more than 200 kg/m ²)
Can be maintained easily	Difficult to maintain
Less expensive	More expensive

1.4 Moss Concrete and How it is Made

Moss concrete, also known as "living concrete," is a type of concrete that incorporates moss into its mixture to create a natural, eco-friendly building material. Three species of moss namely Bryum apiculatum, Barbula indica, and Hyophila involuta commonly grow on the surface of damp cement-based materials [12].

Moss concrete is a type of biological concrete that is developed by growing moss and other organisms such as lichen and fungi on the surface of structures. The goal of this development is to help purify the air by absorbing excess carbon dioxide from the atmosphere. The construction of moss concrete involves a conventional concrete layer that serves as the structural component of the building. The next layer is a waterproof layer that acts as a barrier, separating the inner part of the building from the surface on which moss will grow. The outer layer of moss concrete is designed to allow rainwater to penetrate and boost the growth of the organisms. This layer provides water and nutrients to the moss, which is essential for its growth and survival. On the other hand, the inner portion of the concrete remains waterproofed to prevent water from seeping through to the building's interior. The waterproof layer ensures that the building's structural integrity is maintained and that the moss and other organisms do not damage the concrete structure [13].

2 Factors Affecting Growth of Moss in Concrete

Concrete with high porous surfaces has been found to be suitable for the growth of moss due to its ability to absorb and retain moisture. Moss typically requires a humid and moist environment to grow, and a porous surface can provide that environment by retaining water for longer periods. In addition, the rough surface of porous concrete provides a suitable substrate for the attachment and growth of moss spores. A study was conducted in 2018 in which different walling



materials were compared for the growth of moss and it was found that the more the porosity of a material, more will be the growth of moss [14].

3 Durability of Moss Concrete

Moss concrete has been tested for its compressive strength and showed a similar or slightly lower strength compared to conventional concrete. However, the compressive strength of moss concrete was found to increase over time due to the growth of moss within the concrete, which reinforced the material [3].

Figure 3 shows the compressive strengths of standard and moss concrete [3].

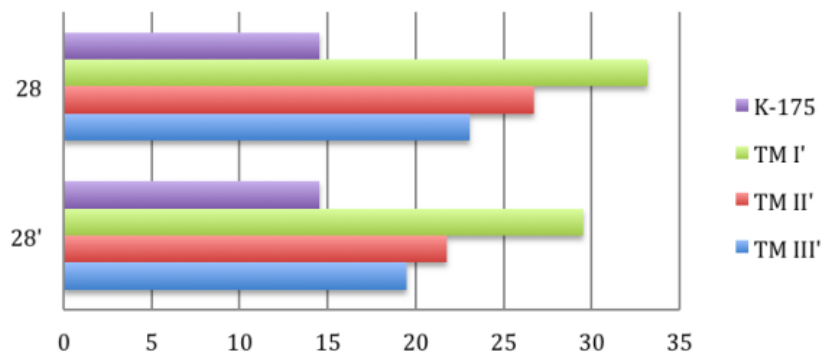


Figure 3: comparison of compressive strengths of standard concrete (K-175) vs Moss concrete (TM 1, TM 2 & TM 3)

Moss concrete offers increased resistance to acid attack and enhanced strength over time, making it a promising material for sustainable construction in urban areas. It utilizes the unique properties of moss to absorb and neutralize acidic pollutants, such as sulfur dioxide and nitrogen oxides, commonly found in urban environments. By integrating moss into concrete, it helps prevent the breakdown of calcium carbonate caused by acidic substances, maintaining the material's integrity. Additionally, as moss grows and forms a network of roots and stems within the concrete, it reinforces the structure and improves its overall strength, reducing the risk of cracking and deterioration. The combination of acid resistance and natural reinforcement makes moss concrete an ideal choice for durable and eco-friendly construction projects.

4 Protection from Rainwater and Light

Moss has been found to have a positive effect on various materials, including concrete and wood, by providing protection from rainwater and light. According to a research, when moss grows on a surface, it forms a layer of cells that can absorb and hold water, acting as a sponge. This helps to reduce the amount of water that penetrates into the material, which can cause damage over time due to freeze-thaw cycles, erosion, and other weathering effects [15]. In addition to its water-absorbing properties, moss also has the ability to absorb and filter light. Sunlight contains harmful ultraviolet (UV) radiation, which can cause degradation and fading of materials over time. Moss has been shown to be effective at filtering out a significant portion of UV radiation, reducing the amount of damage caused by sunlight exposure. Studies have also found that moss can help to reduce the surface temperature of materials, which can help to prevent cracking and other forms of damage caused by thermal stress. By absorbing and retaining moisture, moss can cool the surface of materials by as much as 10-20 degrees Celsius. Overall, the ability of moss to protect materials from water, light, and heat makes it a promising natural solution for sustainable and durable building materials.

5 Role of Moss Concrete in Storm-water Management and Temperature Regulation

Moss concrete has been shown to be effective in stormwater management due to the ability of moss to retain water and reduce runoff. Moss has a high water retention capacity and can absorb up to 20 times its dry weight in water. When used in concrete, it can absorb stormwater runoff, reducing the amount of water that enters the sewer system and reducing the risk of flooding. Additionally, the ability of moss to absorb pollutants in the air and water can help to



improve water quality. The use of moss concrete in stormwater management can also contribute to the promotion of sustainable urban drainage systems (SUDS) and green infrastructure. A study suggests that green roofs, commonly composed of vascular plants, have been used for stormwater management. However, mosses, which are primary colonizers and have numerous soil benefits, could also be valuable components. In a study evaluating three candidate moss species, it was found that mosses had high water holding capacities and delayed and reduced runoff flows. Green roofs planted solely with *Racomitrium canescens* had higher stormwater retention than vascular or medium only roofs. Moss cover also ameliorated temperature fluctuations on green roofs. These results suggest that mosses have the potential to be valuable components of green roofs for stormwater management and temperature regulation [16].

6 Effect of Moss Concrete on Albedo

Albedo refers to the measure of the reflectivity of a surface, expressed as the ratio of the reflected radiation to the total amount of incident radiation. In simpler terms, it represents the ability of a surface to reflect sunlight back into the atmosphere. A higher albedo indicates that more sunlight is reflected, which results in less absorption of solar radiation and lower surface temperatures. Conversely, lower albedo values indicate less reflection and more absorption of solar radiation, leading to higher surface temperatures. Green roofs have a high albedo, ranging from 0.7 to 0.85, which is significantly higher than conventional roofing materials. The high albedo of green roofs is due to the presence of vegetation, which reflects a large portion of the incoming solar radiation. This reduces the amount of heat absorbed by urban surfaces, lowering surface temperature and mitigating the UHI effect. The presence of vegetation also provides shading and evapotranspiration, which further helps to cool the surrounding environment [17].

Following chart shows solar reflectance (albedo) of different roofing materials [17].

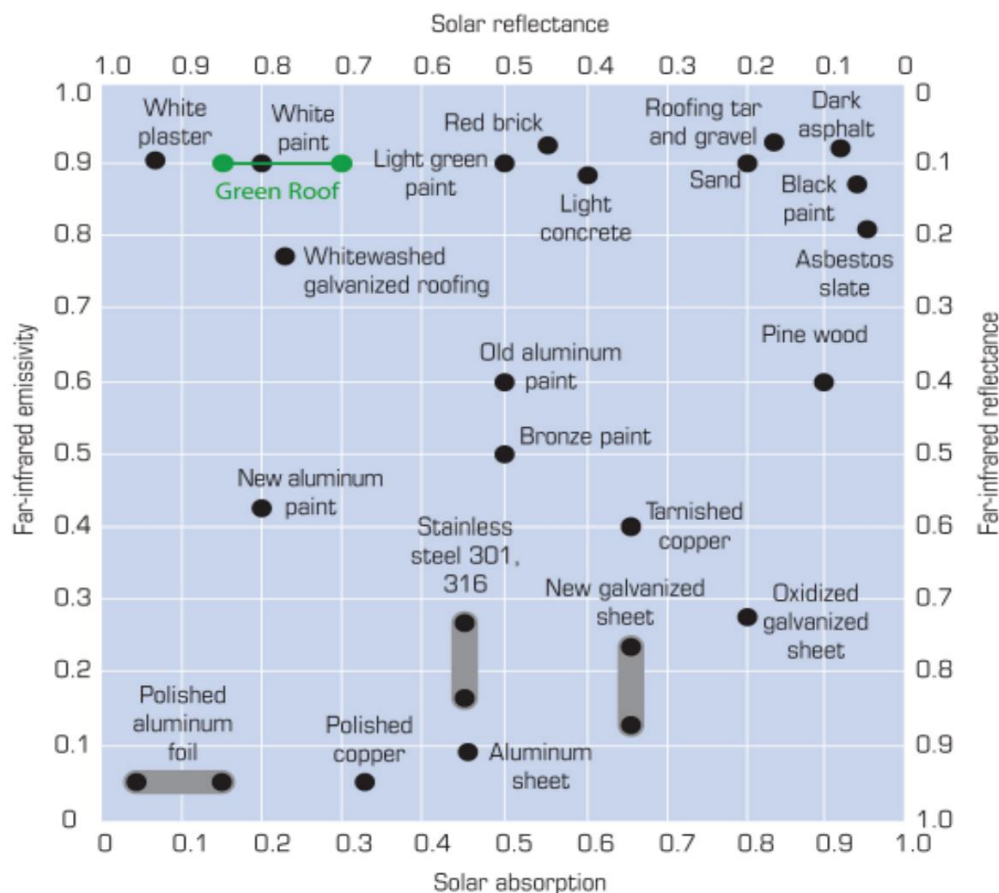


Figure 4: Data on solar reflectivity (horizontal axis) and infra-red emissivity (vertical axis) for a number of common building materials.



A recent study investigated the potential of solar reflective urban surfaces, such as white rooftops and light-colored pavements, to raise the albedo of urban areas by approximately 0.1. The aim was to assess their impact on mitigating global warming by reducing atmospheric temperature. Using a spatially explicit global climate model, long-term simulations were conducted to examine the effects of increased urban surface albedos over decades to centuries. The simulations involved increasing the albedo of all land areas within specific latitudinal ranges. The findings revealed that for each 1 m² of surface with a 0.01 albedo increase, there was a long-term global cooling effect of approximately 3×10^{-15} K. This cooling effect is equivalent to reducing CO₂ emissions by around 7 kg based on recent estimates. Additional simulations focused on increasing the albedo of urban areas alone, considering different spatial extents. These simulations showed global cooling ranging from 0.01 to 0.07 K, which corresponds to a reduction of CO₂ emissions by 25-150 billion tonnes in CO₂ equivalent [4]. Moss concrete has a high potential to improve the albedo effect due to the presence of moss, which has a high albedo. The pre-planned geometry in the panels of moss concrete provides a suitable environment for moss to grow, as it allows for adequate moisture retention and drainage. The growth of moss on the surface of the concrete helps to increase its albedo, which in turn leads to lower surface temperatures [18]. Another study found that, at minimum, green roofs have a 200% increase in albedo over conventional roofs [19]. A minimum albedo increase of 200% provides a huge potential for decreased absorption of the sun's radiation, and thus decreased warming effects on the surrounding air.

7 Disadvantages of Moss Concrete

Mosses produce oxalic acid as part of their metabolic processes, and this acid can contribute to the erosion of concrete. Oxalic acid can react with calcium ions in the concrete to form calcium oxalate crystals, which take up more space than the original calcium ions, leading to the expansion of the concrete. This expansion can cause stress on the concrete, leading to cracking, spalling, and other forms of damage. In addition, the moisture retention properties of moss can lead to increased water retention in the concrete, which can further contribute to erosion and damage over time. However, some researchers are studying ways to mitigate these effects by altering the composition of the concrete or applying coatings to protect against erosion. [15].

8 Practical Applications of Moss Concrete

The practical application of moss concrete involves utilizing moss as an integral part of the concrete mixture to enhance its properties and provide additional benefits. This innovative approach has several practical applications in construction and landscaping:

- i. Green Walls and Facades: Moss concrete can be used to create living green walls and facades, where the concrete is specifically designed to support the growth of moss. These vertical gardens offer numerous advantages, including improved air quality, thermal insulation, and visual appeal. The moss acts as a natural filter, removing pollutants from the air and reducing noise levels.
- ii. Pavements and Walkways: Moss concrete can be used in pavements and walkways, providing a visually appealing and eco-friendly alternative to traditional concrete or asphalt surfaces. The moss in the concrete mixture not only adds a touch of greenery but also helps to reduce heat island effects by absorbing and dissipating heat.
- iii. Noise Barriers and Sound Walls: Moss concrete can be incorporated into noise barriers and sound walls along highways, railways, and other noisy areas. The moss acts as a sound-absorbing material, reducing the propagation of noise and creating a more peaceful environment.
- iv. Ecological Restoration: Moss concrete can play a role in ecological restoration projects by providing a sustainable substrate for moss growth in areas that require vegetation cover. It can be used in erosion control measures, slope stabilization, and habitat creation.
- v. Urban Landscaping: Moss concrete can be used in various urban landscaping projects, such as parks, gardens, and public spaces. It adds a touch of greenery, improves aesthetics, and contributes to the overall environmental sustainability of the urban environment.



The practical application of moss concrete offers an innovative and eco-friendly approach to construction and landscaping, providing numerous benefits such as improved air quality, thermal insulation, noise reduction, and ecological restoration. It showcases the potential for integrating natural elements into the built environment, promoting sustainability and creating greener and more harmonious spaces.

9 Conclusions

In conclusion, moss concrete has emerged as an eco-friendly solution to mitigate the Urban Heat Island (UHI) effect and improve building materials' durability. Mosses, known for their ability to retain moisture, can help regulate surface temperatures and reduce the UHI effect. Moss concrete incorporates moss into its mixture, creating a natural building material that offers several advantages. Firstly, moss concrete contributes to stormwater management by absorbing and retaining water, reducing runoff and the risk of flooding. Moss has a high water retention capacity and can absorb up to 20 times its dry weight in water. By using moss concrete in construction, the amount of water entering the sewer system is decreased, improving water quality and promoting sustainable urban drainage systems (SUDS).

Secondly, moss concrete offers increased durability over time. While its initial compressive strength may be similar to or slightly lower than conventional concrete, the growth of moss within the concrete reinforces the material, enhancing its compressive strength. Moss concrete also demonstrates resistance to acid attack, preventing the breakdown of calcium carbonate and maintaining its integrity. Furthermore, moss concrete has a positive impact on temperature regulation and the reduction of the UHI effect. Moss has a high albedo, reflecting a significant portion of incoming solar radiation. By increasing the albedo of urban surfaces, moss concrete helps to lower surface temperatures and mitigate the impact of global warming. The presence of vegetation in green roofs, including moss, also provides shading and evapotranspiration, further contributing to cooling the surrounding environment. However, moss concrete does have some disadvantages. Mosses produce oxalic acid, which can contribute to the erosion of concrete. Researchers are exploring ways to mitigate these effects by altering the concrete composition or applying protective coatings. In summary, moss concrete offers an eco-friendly solution to mitigate the UHI effect and improve building materials' durability. By incorporating moss into concrete, it provides benefits such as stormwater management, enhanced durability, temperature regulation, and increased albedo. While further research is needed to address potential challenges, moss concrete shows great potential as a sustainable and effective solution for urban environments.

Acknowledgment

The authors would like to thank every person/department who helped thorough out the research work, particularly Engr. Sohaib Nazar. The careful review and constructive suggestions by the anonymous reviewers are also gratefully acknowledged.

References

- [1] N. Shishegar, "The Impacts of Green Areas on Mitigating Urban Heat Island Effect: A Review," *The International Journal of Environmental Sustainability*, pp. 12-14, 2014.
- [2] Á. Morales, A. Zaragoza M. Á. Sanjuán, "Effect of Precast Concrete Pavement Albedo on the Climate Change Mitigation in Spain," *Sustainability*, <https://doi.org/10.3390/su132011448>, vol. 13(20), p. 11448, 2021.
- [3] D. Susanto I. Chairunnisa, "Living Material as a Building Façade: The Effect of Moss Growth Toward Mechanical Performance on Pre-Vegetated Concrete Panels," *International Journal of Technology*, vol. 6(6), pp. 993-1002, 2018.
- [4] H. D. Matthews, D. Seto H. Akbari, "The long-term effect of increasing the albedo of urban areas," *Environ. Res. Lett.*, vol. 7, no. 024004, p. 10, 2012.
- [5] F. Qian, D. X. Song, K. J. Zheng L. Yang, "Research on Urban Heat island Effect," *ScienceDirect 4th International Conference on Countermeasures to Urban Heat Island (UHI)*, pp. 11-18, 2016.
- [6] Royal Meteorological Society. [Online]. <https://www.metlink.org/fieldwork-resource/urban-heat-island-introduction/>
- [7] H. Murase, H. Fukuda N. Kawakami, "Analysis of The Transpiration Properties in Sunagoke Moss," *Asia Pacific Symposium on Postharvest Research Education and Extension*, pp. 473-477, 2012.
- [8] K. Yeang, *EcoArchitecture: The Book of Ken Yeang*. New Jersey: John Wiley & Sons, 2011.
- [9] V. Stovin, S. B. M. Beck, J. B. Davison H. F. Castleton, "Green roofs; building energy savings and the potential for retrofit," *Energy and Buildings*, Volume 42, Issue 10, pp. 1582-1591, 2010.



5th Conference on Sustainability in Civil Engineering (CSCE'23)

Department of Civil Engineering
Capital University of Science and Technology, Islamabad Pakistan



- [10] University of Leeds. [Online]. <https://eps.leeds.ac.uk/cities-infrastructure-energy/doc/architecture-sustainable-buildings>
- [11] A. M. Mahalle V. Kumar, "Green Roofs for Energy Conservation and Sustainable Development: A Review," *International Journal of Applied Engineering Research ISSN 0973-4562 Volume 11, Number 4*, pp. 2776-2780, 2016.
- [12] A. Putrika, Epifit Moss Community at Universita Indonesia. Master's Thesis, 2015.
- [13] A. Dharshini B. Vennila, "A Review on Moss Concrete," *International Journal of Recent Advances in Multidisciplinary Topics*, pp. 170-171, 2023.
- [14] H. Galkanda, I. S. Ariyarathne, G. Y. Jayasinghe, R. Halwatura C. Udawattha, "Mold growth and moss growth on tropical walls. Building and Environment," *Building and Environment, Volume 137*, pp. 268-279, 2018.
- [15] M. Monte, E. Pacini M. Lisci, "Lichens and higher plants on stone: A review..," *International Biodeterioration & Biodegradation, Volume 51(1)*, vol. Volume 51(1), pp. 1-17, 2003.
- [16] J. Lambrinos, E. Schroll M. Anderson, "The potential value of mosses for stormwater management in urban environments," *Urban Ecosystems 13(3)*, pp. 319-332, 2010.
- [17] L. Parshall, G. O'Keeffe, D. Braman, D. Beattie, R. Berghage S. Gaffin, "Energy balance modeling applied to a comparison of white and green roof cooling efficiency. Green roofs in the New York Metropolitan region research report," *Retrieved March 19 2014 from http://www.statisticstutors.com/articles/debrat-green-roofs.pdf*, p. 17, 2006.
- [18] F. Capozzi, V. Spagnuolo, S. Giordano, P. Adamo A. D. Palma, "Atmospheric particulate matter intercepted by moss-bags: Relations to moss trace element uptake and land use," *Chemosphere Volume 176*, pp. 361-368, 2017.
- [19] J. Lundholm, J. S. MacIvor N. S. G. Williams, "Do green roofs help urban biodiversity conservation?," *Journal of Applied Ecology*, pp. 1643–1649, 2014.
- [20] C. Rosenzweig, L. Parshall, D. Beattie, R. Berghage, G. O'Keeffe, D. Braman S. Gaffin, "Energy Balance Modeling applied to a comparison of White and Green Roof Cooling Efficiency," *Green roofs in the New York Metropolitan region research report*, pp. 7-11, 2010.



ENHANCED PERFORMANCE OF BRICK AGGREGATE CONCRETE USING PARTIAL SUBSTITUTION OF SAND WITH WASTE GLASS AND FLAX FIBER INTRUSION

^a Hassan Amjad*, ^b Muhammad Shah Zeb

a: NICE, SCEE, NUST, H/12 Campus, Islamabad, 44000, Pakistan, hassanamjaduet@gmail.com

b: NICE, SCEE, NUST, H/12 Campus, Islamabad, 44000, Pakistan, mshahzeb895@gmail.com

* Corresponding author: Email ID: hassanamjaduet@gmail.com

Abstract- This paper addresses the growing concern over the depletion of natural resources and the environmental impact of their extraction in the construction industry. The study examined the impact of incorporating flax fiber (FF) and waste glass fine aggregates (WGFA) on the mechanical properties of recycled brick aggregate concrete. The investigation focuses on the compression, split-tensile and flexural strength of the modified concrete. The results demonstrate that the incorporation of FF and WGFA substitution can enhance the mechanical properties of brick aggregate concrete, with the 1% fiber and 50% WGFA mix showing promising results in terms of compressive strength, and the 2% fiber and 50% WGFA mix showing promising results in terms of split tensile and flexural strength.

Keywords- Concrete, Flax fiber, Mechanical properties, Recycled brick aggregate, Waste glass

1 Introduction

Concrete is widely used in construction due to its high strength and durability. As urbanization and development continue, there is an increasing demand for concrete as a construction material. However, the production of concrete alone consumes 33% of construction minerals, and the depletion of natural resources and the environmental impact caused by their extraction are significant concerns [1]. To address these concerns, alternative materials for partial or full replacement of naturally available materials in the construction industry are being explored. Recycled waste materials have been extensively researched for their potential application in concrete as substitutes for natural aggregate. Broken bricks from construction and demolition waste, which account for a significant portion of landfill waste, have been found to produce concrete with reasonably high strength and lower water permeability compared to artificial aggregate concrete. Crushed brick waste when utilized in concrete has been found to produce concrete with reasonably high strength and lower water permeability compared to artificial aggregate concrete [2]. While Gayarre et al. [3] discovered that the addition of recycled brick aggregates (ReBA) results in poor performance in terms of shrinkage and creep, it still falls within the acceptable limits for structural concrete. Additionally, Zhao et al. [4] reported that the inclusion of ReBA in concrete significantly improves its resistance against the effects of freeze and thaw actions. Thus, despite these limitations, the utilization of brick in concrete up to a certain limit as a coarse aggregate presents a sustainable approach to reducing the demand for natural resources.

Researchers have also investigated the use of discarded glass as a substitute for natural fine aggregates in concrete [5], [6]. While glass powder can improve concrete properties due to its pozzolanic characteristics, its reactivity is influenced by its size, shape, porosity, and solid phases. Silica in glass reacts with calcium hydrates ($\text{Ca}(\text{OH})_2$) to generate calcium silicate hydrate (CSH) [7]. Additionally, it has been discovered that glass exhibits pozzolanic qualities when the particle size is less than 150 μm . However, as particle size decreases, pozzolanic behaviors improve, i.e., 35 μm outperforms 150 μm [8]. Increasing the amount of waste glass (WG) aggregate up to 60% can boost compressive strength, but excessive use can weaken adhesion between the waste glass aggregate and the cement paste, leading to lower compressive strength in



concrete with waste glass aggregate [9]. Moreover, fiber-reinforced cementitious composites have proved effective in enhancing the strength and ductility of concrete. Various synthetic fibers, such as polypropylene, nylon, glass, polyester, basalt, carbon, and steel fibers, can be utilized in concrete with appropriate sizes, types, aspect ratios, and fractions with respect to volume. Nowadays, the potential of natural fibers is being studied for their use in cementitious materials [10]. One promising natural fiber for incorporation in concrete is flax fiber (FF), which is produced from the stem of the flax plant. Amjad et al. found that addition of sisal fibers can significantly enhance the resistance of concrete against tensile stresses [1]. Another study conducted by Amjad et al. also found similar results [2]. A study conducted by Fernandez [11] optimized flax fiber reinforced concrete to encourage the use of natural fibers in buildings. The study sought the optimum length and optimum ratio of FF in concrete to harvest its maximum benefits. The length of fiber was optimized at 3 cm. Tensile and compression tests were performed on cylindrical specimens and small beams were cast for a three-point bending test. Results displayed substantial enhancement occurred in the strength and toughness of FF-reinforced concrete. Similarly, Momina et al. [12] reported that the incorporation of 0.3% flax fiber with a length of 25 mm led to an approximately 4.5% enhancement in compressive strength. Thus, significant literature is available that supports that the addition of fibers in concrete can potentially improve the properties of concrete. However, literature related to the conjunction use of FF reinforcement and recycled glass powder as partial replacement of sand in ReBA concrete is not available. This study aims to investigate the mechanical properties of ReBA concrete that has glass powder as a partial replacement for sand and reinforced with FF. The mechanical properties were evaluated in terms of compressive and tensile strength.

2 Material and Experiments

The materials included Bestway Cement Type-1 Ordinary Portland Cement, Lawrencepur sand as the fine aggregate, and locally available Margalla crush as the coarse aggregate, meeting ASTM guidelines [13]–[16]. To obtain recycled brick coarse aggregate, waste bricks were obtained from the local demolished masonry structure and then were crushed in the crusher machine up to the size of 0.5 inches and down. The gradations of brick aggregates were done the same as that of natural coarse aggregates. Similarly, WG was collected from dump sites and scrap shops and then was broken down into smaller pieces and further ground into finer particles for its utilization as a partial substitution of sand, as illustrated in Figure 1. Table 1 and Table 2 provide the chemical constituents of the cement, properties of the fine aggregates, and properties of the coarse aggregate, respectively. The WG fine aggregate (WGFA) obtained was also examined through X-ray fluorescence (XRF), revealing its pozzolanic nature as depicted in Table 3 [6].

Table 1: Chemical Composition of Bestway Cement

CaO	SiO ₂	Al ₂ O ₃	Fe ₂ O ₃	SO ₃	MgO	K ₂ O	Na ₂ O
64.52	21.25	4.96	3.15	2.81	2.51	0.62	0.18

Table 2: Properties of fine aggregate and coarse aggregates

	Fineness Modulus	Absorption (%)	Bulk Specific Gravity (SSD)	Size (mm)
Sand	2.90	2.04	2.75	
WGFA	2.44	-	2.68	
Natural coarse aggregate	-	0.72	2.68	12.5
ReBA	-	13.44	1.92	12.5



Figure 1: Preparing WGFA

Table 3: Chemical composition of WGFA

SiO ₂	CaO	Al ₂ O ₃	MgO	Fe ₂ O ₃	Na ₂ O	K ₂ O	SO ₃
68.82	18.02	2.25	1.59	1.03	5.72	0.43	2.14

Based on previous literature [10], [12], the FF was cut to an optimal length of 25 mm to be used in the cementitious mix as shown in Figure 2. The FF fiber exhibits an absorption capacity of 92% and a density of 1420 kg/m³.



Figure 2: Visual of FF

2.1 Concrete Mix Proportions and Specimen Preparation

A total of 13 different concrete formulations were prepared, with one being a controlled mix without any recycled brick aggregate while the remaining having WGFA and FF as listed in Table 4. The concrete mix ratio used in all formulations was 1:1.3:1.9 (cement: fine aggregate: coarse aggregate), and the w/c was 0.45. To optimize the utilization of ReBA, the current research utilized a replacement ratio of up to 25%, which has been reported to have no significant negative effects on structural concrete [2]. All concrete mixes were supplemented with *Chemrite SP-303* superplasticizer at a weight percentage of approximately 1% to produce workable mixes.



Table 4: Concrete mix proportions

Mixes	Cement (kg/m ³)	w/c	Sand (Kg/m ³)	WGFA (Kg/m ³)	Natural Coarse Aggregate (Kg/m ³)	ReBA (Kg/m ³)	FF (Kg/m ³)
CM	439.55	0.45	571.42	-	835.15	-	-
RBCM	439.55	0.45	571.42	-	626.36	208.79	-
RBCM10WG	439.55	0.45	542.85	28.57	626.36	208.79	-
RBCM25WG	439.55	0.45	514.28	57.14	626.36	208.79	-
RBCM50WG	439.55	0.45	457.14	114.28	626.36	208.79	-
RBCM1FF	439.55	0.45	571.42	-	626.36	208.79	4.39
RBCM1FF10WG	439.55	0.45	542.85	28.57	626.36	208.79	4.39
RBCM1FF25WG	439.55	0.45	514.28	57.14	626.36	208.79	4.39
RBCM1FF50WG	439.55	0.45	457.14	114.28	626.36	208.79	4.39
RBCM2FF	439.55	0.45	571.42	-	626.36	208.79	8.78
RBCM2FF10WG	439.55	0.45	542.85	28.57	626.36	208.79	8.78
RBCM2FF25WG	439.55	0.45	514.28	57.14	626.36	208.79	8.78
RBCM2FF50WG	439.55	0.45	457.14	114.28	626.36	208.79	8.78

All materials were carefully weighed according to the designated mix design and then dry-mixed in an electronic concrete mixer for a period of 2 to 3 minutes. Water was subsequently added, and the wet mixing process was continued for an additional 2 to 3 minutes. For each formulation, eight P.C.C. cylinders measuring 100 mm in diameter and 200 mm in height and two rectangular beamlets measuring 100x100x400 mm³ were cast. After casting, the samples were left to dry-cure in moulds for 24 hours, under a temperature of 20±2 °C. At the end of the 24-hour curing period, the specimens were removed from their respective moulds and then placed in a water curing tank, maintained at a relative humidity of 100% at room temperature (23±2°C), and left to cure for the respective days.

2.2 Testing Procedure

The mechanical properties of the hardened formulated mixes were assessed in compression, tension, and flexural loadings. To determine the compressive strength, 100x200 mm³ cylindrical samples were tested using the ASTM C39 method after 28 and 120 days. Splitting tensile strength, an indirect measure of tensile strength was evaluated by following the ASTM C469 guidelines on three 100x200 mm³ cylindrical samples at 28 and 120 days. Flexural strength, which affects structural performance under bending, was also determined by utilizing the ASTM guidelines after 28 and 120 days on 100x100x400 mm³ concrete prisms.

3 Results and Discussion

3.1 Compressive Strength

Figure 4 illustrates the compression strength of all the prepared concrete mixes at the 28th and 120th days of testing age. The inclusion of ReBA leads to a reduction in compressive strength owing to the inferior morphology of the bricks, which consequently affect the compression strength [4]. An increase in compressive strength was observed with an increase in testing age which was attributed to the progressive hydration reactions and the pozzolanic nature of the WGFA. Both the 28th and 120th day compression strengths of the prepared concrete mixes demonstrated an increase in strength due to the addition of WGFA. This was attributed to the angular structure of the WGFA particles, which promotes better bonding with the adjacent cement matrix. Additionally, the pozzolanic reactivity of the WGFA may also contribute to this effect [9]. The compressive strength of the 1% fiber-reinforced concrete mixes was enhanced due to the reinforcement effect of Paper ID. 22-124



the fibers. Conversely, the compressive strength of the 2% fiber-reinforced mixes was decreased because, at higher fractions, the dispersion became much more difficult, resulting in the formation of agglomerates in the concrete mixture, thereby reducing the compression strength [17]. Among all the prepared mixtures, the mixture with 1% fiber and 50% WGFA exhibited superior performance, demonstrating the least reduction in compressive strength of approximately 3.5% and 3.1% at the 28th and 120th day of testing age, respectively, in comparison to the virgin concrete.

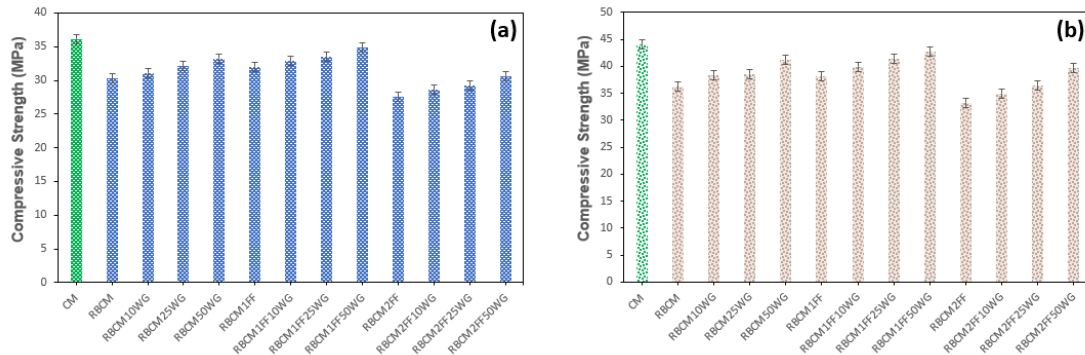


Figure 3: Compression strength of the formulated mixtures (a) 28th day (b) 120th day

3.2 Split-tensile Strength

The 28th and 120th day split tensile strength of all formulated concrete mixes is presented in Figure 4. As expected, the incorporation of recycled brick aggregate in the mixture was found to cause a reduction in split tensile strength due to the presence of voids and cracks in the brick aggregate. Results show that an enhancement in split tensile strength was observed as the testing age increased. This improvement can be attributed to the progressive hydration reactions and pozzolanic nature of waste glass fine aggregate (WGFA) used in the mixes. The results for split tensile strength were found to be similar to the ones observed for compression strength. Both the 28th and 120th day split tensile strength of the formulated concrete mixes demonstrated an increase in strength due to the addition of WGFA. This was due to the improved bond formation between the cement-WGFA interface and the pozzolanic reactivity exhibited by WGFA [9]. In contrast to the results observed for compression strength, where 2% FF-intruded mixes exhibited a decrease in split tensile strength, the split tensile strength of the formulated mixes still increased when FF content increased from 1% to 2%. This is because in the case of split tension the fiber reinforcement significantly dominates providing the confinement effect to concrete. These findings are consistent with those reported in previous literature [10], [17]. The study found that the mix with 2% FF and 50% WGFA outperformed all other formulations, exhibiting a 6.0% and 7.4% increase in split tensile strength at the 28th and 120th day of testing age, respectively, compared to the virgin concrete.

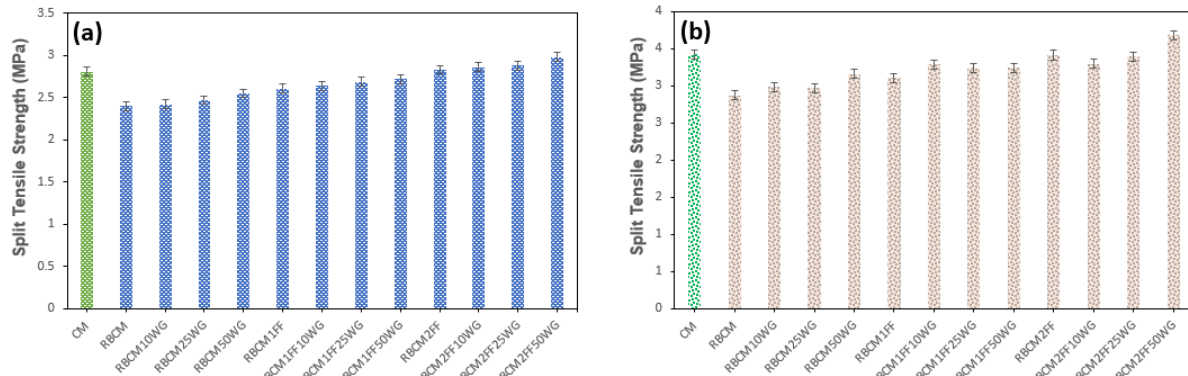


Figure 4: Split tensile strength of the formulated mixtures (a) 28th day (b) 120th day



3.3 Flexural Strength

Figure 5 presents the flexural strength of all formulated concrete mixes at the 28th and 120th days of testing age. The addition of WGFA and FF to the concrete mixes resulted in a similar trend in flexural strength as observed for split tensile strength, and the reasons explained earlier are also applicable to flexural strength. Among all the formulated mixes, the combination of 2% FF and 50% WGFA exhibited the best performance, demonstrating the least reduction in flexural strength of approximately 2.4% and 1.9% at the 28th and 120th day of testing age, respectively, compared to the virgin concrete.

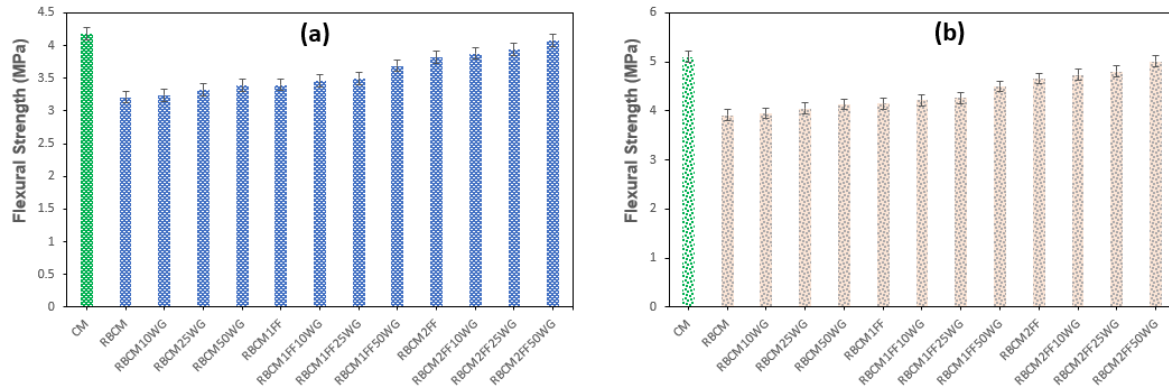


Figure 5: Flexural strength of the formulated mixtures (a) 28th day (b) 120th day

3.4 Practical Applications

The practical applications of enhancing the performance of brick aggregate concrete through the partial substitution of sand with waste glass and flax fiber intrusion are diverse and offer several benefits to construction projects. One significant advantage is the promotion of sustainable construction practices. By incorporating waste glass and flax fibers, this approach contributes to waste reduction and resource conservation. It enables the utilization of waste materials that would otherwise end up in landfills, effectively reducing the environmental burden associated with construction activities. Moreover, the addition of waste glass and flax fibers enhances the strength and durability of the concrete. Waste glass particles contribute to the overall strength of the concrete matrix, improving its load-bearing capacity. Flax fibers, on the other hand, act as reinforcement within the concrete, reducing the likelihood of cracks and enhancing its resistance to external forces, such as impact or cyclic loading. This results in more robust and long-lasting structures, reducing the need for frequent repairs or replacements. Another practical application is the improvement of thermal insulation properties. Waste glass exhibits insulating characteristics, making it suitable for applications where thermal efficiency is desired. By substituting sand with waste glass, the thermal conductivity of the concrete can be reduced, enhancing its insulation capabilities. This is particularly beneficial in regions with extreme weather conditions, as it helps regulate indoor temperatures, reduces energy consumption for heating or cooling, and contributes to energy-efficient building design. In terms of environmental impact, the use of waste glass and flax fibers helps to reduce carbon emissions and conserve natural resources. By incorporating waste materials into the concrete mix, the demand for virgin materials, is reduced. This lowers the environmental footprint associated with extraction and transportation, while also preserving natural ecosystems and minimizing habitat destruction. Furthermore, the application of waste glass and flax fibers can lead to potential cost savings. If waste glass and flax fibers are readily available as byproducts or waste materials in the local area, they can be obtained at lower costs compared to traditional raw materials. This can contribute to overall project cost reduction, making it an economically viable option for construction projects.

4 Conclusions

The following conclusions were drawn based on the findings of this research:



5th Conference on Sustainability in Civil Engineering (CSCE'23)

Department of Civil Engineering

Capital University of Science and Technology, Islamabad Pakistan



- With the inclusion of 1% FF and 50% WGFA substitution, the reduction in compressive strength was minimal at around 3.1% on the 120th day testing age.
- However, in terms of split tensile strength, the mix containing 2% fiber and 50% WGFA surpassed the virgin concrete, with an increase of 7.4% observed on the 120th day of testing.
- The reduction in flexural strength was minimal in the mix containing 2% fiber and 50% WGFA, which exhibited a decrease of approximately 1.9% on the 120th day of testing, in contrast to the virgin concrete.
- The enhanced performance of brick aggregate concrete through the partial substitution of sand with waste glass and flax fiber intrusion offers practical applications with numerous benefits for construction projects.

Thus, by incorporating waste materials and natural fibers, it promotes sustainability by reducing waste, conserving resources, and minimizing environmental impact. The addition of waste glass and flax fibers improves the strength and durability of the concrete, resulting in more robust structures with reduced maintenance needs.

It is recommended to extend this study in order to investigate the performance of this type of concrete under different environmental conditions, such as hot, cold, dry, wet, and cyclic dry-wet conditions.

Acknowledgment

The authors would like to thank every person/department who helped thorough out the research work, particularly Dr. Rao Arsalan Khushnood and Dr. Hammad Anis Khan. The careful review and constructive suggestions by the anonymous reviewers are gratefully acknowledged.

References

- [1] J. K. Steinberger, F. Krausmann, and N. Eisenmenger, "Global patterns of materials use: A socioeconomic and geophysical analysis," *Ecological Economics*, vol. 69, no. 5, pp. 1148–1158, 2010, doi: 10.1016/j.ecolecon.2009.12.009.
- [2] F. Debieb and S. Kenai, "The use of coarse and fine crushed bricks as aggregate in concrete," *Construction and Building Materials*, vol. 22, no. 5, pp. 886–893, 2008, doi: 10.1016/j.conbuildmat.2006.12.013.
- [3] F. L. Gayarre, J. S. González, C. L. C. Pérez, M. A. Serrano López, P. S. Ros, and G. Martínez-Barrera, "Shrinkage and creep in structural concrete with recycled brick aggregates," *Construction and Building Materials*, vol. 228, 2019, doi: 10.1016/j.conbuildmat.2019.116750.
- [4] Y. Zhao, J. Gao, F. Chen, C. Liu, and X. Chen, "Utilization of waste clay bricks as coarse and fine aggregates for the preparation of lightweight aggregate concrete," *Journal of Cleaner Production*, vol. 201, pp. 706–715, 2018, doi: 10.1016/j.jclepro.2018.08.103.
- [5] H. Lee, A. Hanif, M. Usman, J. Sim, and H. Oh, "Performance evaluation of concrete incorporating glass powder and glass sludge wastes as supplementary cementing material," *Journal of Cleaner Production*, vol. 170, pp. 683–693, 2018, doi: 10.1016/j.jclepro.2017.09.133.
- [6] N. Schwarz, H. Cam, and N. Neithalath, "Influence of a fine glass powder on the durability characteristics of concrete and its comparison to fly ash," *Cement and Concrete Composites*, vol. 30, no. 6, pp. 486–496, 2008, doi: 10.1016/j.cemconcomp.2008.02.001.
- [7] J. Ahmad *et al.*, "Concrete with Partial Substitution of Waste Glass and Recycled Concrete Aggregate," *Materials*, vol. 15, no. 2, p. 430, Jan. 2022, doi: 10.3390/ma15020430.
- [8] V. S. Lesovik, L. Kh. Zagorodnyuk, Z. K. Babaev, and Z. B. Dzhumaniyazov, "Analysis of the Causes of Brickwork Efflorescence in the Aral Sea Region," *Glass and Ceramics*, vol. 77, no. 7–8, pp. 277–279, Nov. 2020, doi: 10.1007/s10717-020-00287-4.
- [9] L. S. Ho and T. P. Huynh, "Recycled waste medical glass as a fine aggregate replacement in low environmental impact concrete: Effects on long-term strength and durability performance," *Journal of Cleaner Production*, vol. 368, no. February, p. 133144, 2022, doi: 10.1016/j.jclepro.2022.133144.
- [10] H. Amjad, R. Arsalan Khushnood, and S. Ali Memon, "Biomimetic robust self-healing of *Bacillus Subtilis* immobilized through sisal fiber for next-generation concrete infrastructure," *Construction and Building Materials*, vol. 368, no. January, p. 130299, 2023, doi: 10.1016/j.conbuildmat.2023.130299.
- [11] J. E. Fernandez, "Flax fiber reinforced concrete - A natural fiber biocomposite for sustainable building materials," *High Performance Structures and Materials*, vol. 4, pp. 193–207, 2002.
- [12] M. Rauf, W. Khalil, R. A. Khushnood, and I. Ahmed, "Comparative performance of different bacteria immobilized in natural fibers for self-healing in concrete," *Construction and Building Materials*, vol. 258, p. 119578, 2020, doi: 10.1016/j.conbuildmat.2020.119578.



5th Conference on Sustainability in Civil Engineering (CSCE'23)
Department of Civil Engineering
Capital University of Science and Technology, Islamabad Pakistan



- [13] ASTM C150, "ASTM C150/C150M - 18 Standard Specifications for Portland Cement," vol. i, pp. 1–9, 1999, doi: 10.1520/C0150.
- [14] ASTM C33, "Concrete Aggregates 1," vol. i, no. C, pp. 1–11, 2010, doi: 10.1520/C0033.
- [15] ASTM, "Método de prueba estándar para Densidad Relativa (Gravedad Específica) y Absorción de Agregado Grueso, ASTM C127-15," pp. 1–5, 2015, doi: 10.1520/C0127-15.2.
- [16] ASTM C-128-15, "Standard Test Method for Relative Density (Specific Gravity) and Absorption of Fine Aggregates, ASTM International, West Conshohocken, PA, 2015," *ASTM International*, vol. i, pp. 15–20, 2015, doi: 10.1520/C0128-15.2.
- [17] B. Ali, M. A. Farooq, M. H. El Ouni, M. Azab, and A. B. Elhag, "The combined effect of coir and superplasticizer on the fresh, mechanical, and long-term durability properties of recycled aggregate concrete," *Journal of Building Engineering*, vol. 59, no. July, p. 105009, Nov. 2022, doi: 10.1016/j.jobe.2022.105009.



ASSESSING THE FLEXURAL STRENGTH OF A BEAM USING WASTE PLASTIC AS A PARTIAL SUBSTITUTE FOR COARSE AGGREGATE

^a *Malik Hussain Muzaffar Awan**, ^b *Talha Malik*, ^c *Aizaz Asif*

a: Department of Civil Engineering, HITEC University Taxila, Pakistan, hussainmalik572@gmail.com

b: Department of Civil Engineering, HITEC University Taxila, Pakistan, azazasif918888@gmail.com

c: Department of Civil Engineering, HITEC University Taxila, Pakistan, talhamalik6663@gmail.com

* Corresponding author: Email ID: hussainmalik572@gmail.com

Abstract- In order to promote resource conservation, recycling plastic waste is crucial as it is durable and does not decompose. Nowadays, the concrete industry worldwide is constantly seeking to develop effective materials that are lightweight, cost-effective, and eco-friendly. To achieve the desired properties in concrete while reducing its negative effects on the environment, plastic waste can be utilized as a partial substitute for coarse aggregate. Previous research has suggested that a 10-20% replacement of coarse aggregate with plastic aggregate is ideal. This study comprised of two phases. During initial phase, concrete cylinders were examined, each containing with different proportion of plastic aggregate as a partial replacement, and favorable outcome were achieved with 20% replacement. In the second phase, three Reinforced Concrete (RC) beams were built, with two beams using 20% replacement of coarse aggregate with plastic aggregate and the third as a control specimen for comparison purposes. All beams were designed according to the ACL code and tested under third-point loading in accordance with ASTM C78/C78M to investigate their flexural behavior at midspan. The beams with partial plastic aggregate replacement exhibited almost identical flexural behavior while reducing their self-weight by 14%.

Keywords- Flexure Strength, Coarse Aggregate, Waste Plastic, concrete.

1 Introduction

Concrete, being highly versatile, is widely utilized in various forms of construction and is considered one of the most essential building materials after water [1]. During the 1960s, there was a shift towards utilizing reinforced cement concrete instead of girders, steel decking, and steel columns for both structural and non-structural components. [2]–[4]. The aggregate, consist of fine and coarse components, constitute 70% of concrete mix [3]. The presence of this particular aggregate greatly affects the weight of the concrete itself. By employing low-density aggregates, it becomes possible to decrease the overall dead load of a structure, leading to lighter burdens on supporting elements. Consequently, this can result in a reduced seismic reactive mass.

In recent years, researchers have been dedicated to identifying aggregates with low specific gravity for concrete. They have conducted tests using various materials and achieved satisfactory outcomes, such as reduced self-weight aggregates or minimum loss of strength. As a result, different types of lightweight aggregates, including expanded clay aggregate, volcanic pumice, fly ash, rice husk, and rubberized aggregate, etc. have been introduced to the concrete industry.

Numerous studies have been conducted to assess the properties of lightweight aggregates both as standalone materials and when incorporated into concrete. The effect on properties of hardened and fresh concrete having plastic aggregate is already discussed by several researchers [5]. The Researchers also discussed the effect of level of use of fine PA in place of CA



on workability [6], thermal conductivity [7], abrasion resistance [8], shrinkage [9], permeability [10], fire behaviour [11] and absorption [12]. Even some researchers reported decrease in slump of fresh concrete [13]. Polymeric material found in domestic and industrial waste, primarily rubber and plastic, have both economic and environmental impacts. These materials usually either disposed of in landfill or burned in dumps. This addresses the environmental impact, while their utilization in construction or industry addresses the economic impact.

In Pakistan 30 million tons of solid waste is generated per year, in which 9% is plastics. 9 million tonnes of plastic are thrown into ocean annually [14]. The consumption of plastic materials has witnessed a significant surge, rising from around two million tons in the 1950s to nearly four hundred and forty million tons in 2015 [15]. The excessive accumulation of plastic waste poses environmental pollution threat and indirectly contributes to issues like flooding by obstructing drainage systems, as observed in Karachi, Pakistan in 2017 (Amar Guiro, September 2017). By incorporating plastic waste as a substitute for coarse aggregate in recycling practices, not only can the detrimental effects of plastic waste be mitigated, but also the overall weight of structures can be reduced. This is facilitated by the availability and low or less density of plastic, which allows it in serving as an alternative to traditional coarse aggregate.

In recent years, construction industry has embraced recycled concrete and waste plastic aggregates to study their tension and compression properties for effective utilization. Plastic aggregates from various sources such as plastic bottles, wrapper, shopping bags and recycled rubber from tires have been successfully as partial replacement for coarse aggregates in concrete. These efforts have yielded satisfactory outcomes [16].

In this paper, three beams specimens were made for experimentation purposes. One beam was used as a specimen for comparative analysis, while the remaining beams were made with a substitution of 20% with plastic aggregates. The design of all beams adhered to the standards outlined in the ACI code and underwent testing using the third-point loading method as outlined in ASTM C78/C78M. [17-20]. Flexure strength, ductility, self-weight, and damage pattern of both types were compared.

The significance of this research lies in exploring the potential of utilizing waste plastic aggregates as a partial replacement for traditional coarse aggregates in concrete construction. This approach addresses both economic and environmental concerns by recycling plastic waste and reducing the overall weight of structures. The objective of the study is to investigate the mechanical properties, such as flexural strength, ductility, and self-weight, of concrete beams with 20% plastic aggregate substitution. By comparing these properties with the control specimens, the study aims to determine the feasibility and effectiveness of using waste plastic aggregates in concrete mix designs, contributing to sustainable and eco-friendly construction practices.

2 Experimental Procedures

Due to limited understanding of the properties of the recycled plastic aggregate taken from FF Steels (PVT.) Ltd in Islamabad, a thorough investigation was necessary to ascertain the material's various qualities essential for concrete mix design. The plastic aggregate ranged in size from 12mm to 14mm. The grading of the coarse aggregate was adjusted to replace the natural coarse aggregate with plastic aggregate. Additional properties of the plastic aggregate were documented and are presented in Table 1. Considering the desired compressive strength of 3ksi, the targeted slump range of 1 to 2 inches, and a w/c of 0.56, the following ratios have been estimated in accordance with the ACI code, considering the given qualities and specifications.

Table 1 Properties of Materials

Material	Size (inch)	Specific gravity
Courser Aggregate	1 (maximum)	2.67
Fine Aggregate	3 FM	2.6
Plastic Aggregate	0.5	0.85

Table 1 Estimated values of material ratio

% Of Plastic aggregate	Cement (lb./yd ³)	Coarse Aggregate (lb./yd ³)	Fine Aggregate (lb./yd ³)	Plastic Aggregate (lb./yd ³)	w/c
0	517.24	1240.20	1821.70	0.0	0.56
15	517.24	1240.20	1548.40	141	0.56
20	517.24	1240.20	1457.30	188	0.56



Due to the limitations in strength and workability, it is not feasible to entirely replace the coarse aggregate with plastic aggregate. Research findings suggest that replacing 15 to 22 percent of the coarse aggregate with plastic aggregate yields favorable outcomes [19]. In this particular study, the focus was on replacing 15 and 20 percent of the coarse aggregate. In this research study, a total of nine cylinders were prepared and subjected to testing in accordance with ASTM specifications. The obtained results are outlined as follows:

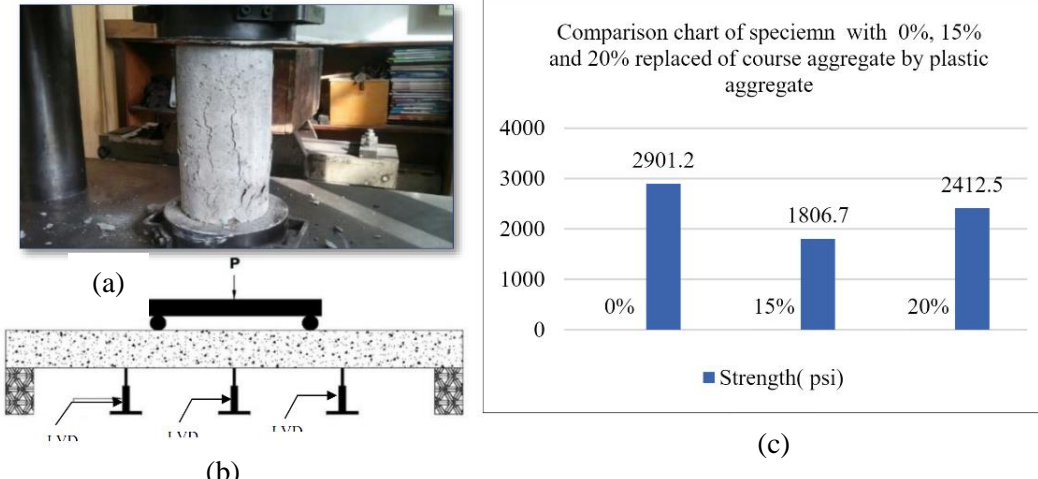


Figure 1 (a) Testing of Concrete cylinder (b) Three-point loading(c) Compressive strength of cylinder

Based on the data presented in the figure, the observed trend of decreasing compressive strength with a 15% plastic aggregate replacement and increasing compressive strength with a 20% replacement can be attributed to the complex interactions between the plastic aggregate and the other constituents of the concrete mix. At a 15% replacement level, the introduction of plastic aggregates might have caused a disruption in the overall matrix, leading to a less efficient packing arrangement and weaker bond formation between the aggregates and the cement paste. Consequently, this could have resulted in a slight decrease in compressive strength. However, at a 20% replacement level, the plastic aggregates could have facilitated better particle distribution and enhanced packing, leading to improved load transfer and interlocking within the mix. This optimized arrangement may have positively influenced the overall compressive strength, resulting in a higher value. The specific characteristics of the plastic aggregates and their interactions with the other concrete components play crucial roles in influencing this trend, making further research essential to comprehend the underlying mechanisms in detail.

1.1 Specifications of Beam Specimens

For research purposes, three beams were built, with one as control specimen (without plastic aggregate) and other two incorporating 20% plastic aggregate. All three beams were prepared using same mix proportion as the concrete cylinders. The beam specimen was 7ft long, had cross section of 6" × 9" as shown in the figure 3b and were reinforced for shear in accordance with ACI code.



Figure 2: Testing of Beam specimen



1.2 Experimental Testing of Beam Specimens

At the material testing laboratory of HITEC UNIVERSITY in Taxila, Pakistan, the three specimens underwent three-point loading tests in accordance with the ASTM C78/C78M-10 standard.

The specimens, configured as beams with a 6-foot clear span, were positioned within the test setup. Strain gauges were affixed at the location of maximum bending to monitor deflections. All specimens underwent testing using the loading criteria specified in section 2.5, employing a 0.33 factor. The load was incrementally applied at a rate of 0.2 ton per second.

In order to measure deflection, three Linear Variable Differential Transformers (LVDTs) or At the bottom of the beam, gauges were installed to measure and monitor the load and deflection. The collected data was then analyzed to assess the flexural capacity of the specimens. This information is illustrated below.

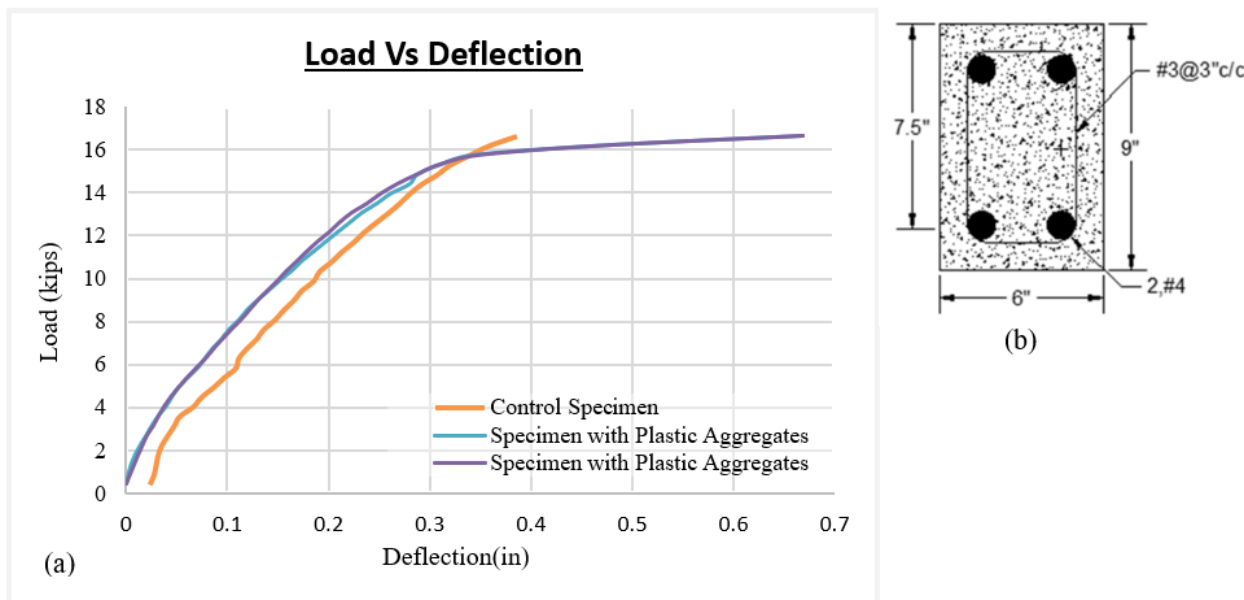


Figure 2: (a) Load vs Deflection Chart of Beam specimen (b) Cross section of beam

2 Results and Discussion

Upon comparing the lightweight specimens (with partial replacement) with the specimen for comparative analysis, it was noted that the flexural capacity of the lightweight specimens was on par with that of the control specimen.

- In contrast to the control specimen, the beams exhibited a heightened level of ductile failure.
- The replacement of 20% plastic coarse aggregate in reinforced concrete (RC) beams did not affect their flexural capacity when compared to the control specimen. However, there was a noteworthy reduction of 18 to 20% in the self-weight of the beams.
- Cracks on the tension face of the beams with partial replacement of coarse aggregate were uniformly distributed. This suggests that the presence of plastic aggregate did not lead to concentrated or localized cracking. Instead, the cracks were evenly distributed, indicating a more uniform and balanced distribution of tensile stresses within the beam. This signifies that the beams with partial replacement maintained structural integrity and exhibited improved resistance to cracking. Such uniform crack distribution is beneficial for the overall performance and durability of the beams.
- Prior to the development of flexural cracks, the beams exhibited resistance against shear forces and did not display any signs of shear cracks. This indicates the structural integrity of the beams in terms of their ability to withstand



shear stresses without exhibiting any visible indications of shear failure. The absence of shear cracks before the occurrence of flexural cracks highlights the strength and stability of the beams under applied loads.

- Based on the findings of this research and previous recommendations, it can be concluded that the practical application of plastic aggregate as a partial replacement for coarse aggregate is feasible, with an optimum replacement level of up to 20%, is feasible in the concrete. However, it is advisable to conduct further studies exploring the effects of different water-to-cement ratios (w/c) and higher percentages of plastic aggregates. These additional investigations will provide valuable insights into the behavior and performance of concrete when subjected to varying conditions of w/c and increased levels of plastic aggregate replacement.

3 Conclusions

The study demonstrated that the use of plastic aggregate as a partial replacement for coarse aggregate, up to 20%, in reinforced concrete beams resulted in beams with comparable flexural capacity to the control specimens. The lightweight beams exhibited a higher level of ductile failure and a noteworthy reduction in self-weight, showcasing their potential benefits for lightweight construction. Moreover, the presence of plastic aggregate led to uniformly distributed cracks on the tension face, indicating improved resistance to localized cracking and enhanced structural integrity. The beams also demonstrated resistance against shear forces without displaying shear cracks before the development of flexural cracks. While the practical application of plastic aggregate in concrete is feasible, further research investigating different water-to-cement ratios and higher percentages of plastic aggregate replacement is recommended to gain a deeper understanding of its behavior under varying conditions.

Acknowledgment

The authors extend their gratitude to all the individuals and departments who provided assistance throughout the research work, with special acknowledgment to the Civil Engineering department at HITEC and Engr. Inayat Ullah Khan. They also express their appreciation for the thorough review and valuable suggestions provided by the anonymous reviewers.

REFERENCES

- [1] M. Batayneh, I. Marie, and I. Asi, "Use of selected waste materials in concrete mixes," *Waste management*, vol. 27, no. 12, pp. 1870–1876, 2007.
- [2] A. Gul, B. Alam, I. U. Khan, S. A. A. Shah, S. W. Khan, and K. Shahzada, "Improving seismic capacity of dry stacked interlocking masonry structure through confinement at corners," *Soil Dynamics and Earthquake Engineering*, vol. 165, p. 107710, Feb. 2023, doi: 10.1016/j.soildyn.2022.107710.
- [3] B. Alam, K. Shahzada, I. U. Khan, and A. Gul, "Experimental assessment of diagonal shear parameters of dry stacked block masonry built with self-interlocking compressed earth blocks," *IJMRI*, vol. 1, no. 1, p. 1, 2022, doi: 10.1504/IJMRI.2022.10048224.
- [4] A. Gul, K. Khan, A. Khan, K. Shahzada, and I. Khan, "Mechanical Properties of Dry Stack Masonry using Hydraform Blocks," presented at the 1st International Conference on Advances in Civil & Environmental Engineering, UET TAXILA (1st ICACEE-2022), UET Taxila, Pakistan, Mar. 2022.
- [5] Raghavendra D, Sivakumar A. Compressive strength index of different types of light weight plastic aggregate concrete. Indian Journal of Science and Technology 2015;8:106–11.
- [6] Gromicko N, Shepard K. The History of Concrete 2006. <https://www.nachi.org/history-of-concrete.htm> (accessed November 11, 2021).
- [7] Saikia N, De Brito J. Use of plastic waste as aggregate in cement mortar and concrete preparation: A review. Construction and Building Materials 2012;34:385–401.
- [8] Pacheco-Torgal F, Ding Y, Jalali S. Properties and durability of concrete containing polymeric wastes (tyre rubber and polyethylene terephthalate bottles): An overview. Construction and Building Materials 2012;30:714–24.
- [9] Saxena R, Jain A, Agrawal Y. Utilization of waste plastic in concrete towards sustainable development: a review. J Eng Res Appl 2016;6:88–100.
- [10] Babafemi AJ, Šavija B, Paul SC, Anggraini V. Engineering properties of concrete with waste recycled plastic: a review. Sustainability 2018;10:3875.
- [11] Ismail ZZ, Al-Hashmi EA. Use of waste plastic in concrete mixture as aggregate replacement. Waste Management 2008;28:2041–7.
- [12] Saikia N, de Brito J. Mechanical properties and abrasion behaviour of concrete containing shredded PET bottle waste as a partial substitution of natural aggregate. Construction and Building Materials 2014;52:236–44.
- [13] Batayneh M, Marie I, Asi I. Use of selected waste materials in concrete mixes. Waste Management 2007;27:1870–6.



5th Conference on Sustainability in Civil Engineering (CSCE'23)

Department of Civil Engineering

Capital University of Science and Technology, Islamabad Pakistan



- [14] Choi YW, Moon DJ, Kim YJ, Lachemi M. Characteristics of mortar and concrete containing fine aggregate manufactured from recycled waste polyethylene terephthalate bottles. *Construction and Building Materials* 2009;23:2829–35.
- [15] Kou S, Lee G, Poon CS, Lai WL. Properties of lightweight aggregate concrete prepared with PVC granules derived from scraped PVC pipes. *Waste Management* 2009;29:621–8.
- [16] Wang R, Meyer C. Performance of cement mortar made with recycled high impact polystyrene. *Cement and Concrete Composites* 2012;34:975–81.
- [17] Rai B, Rushad ST, Kr B, Duggal S. Study of waste plastic mix concrete with plasticizer. *International Scholarly Research Notices* 2012;2012.
- [18] Shubbar SD, Al-Shadeedi AS. Utilization of waste plastic bottles as fine aggregate in concrete. *Kufa Journal of Engineering* 2017;8:132–46.
- [19] Akinyele J, Ajede A. The use of granulated plastic waste in structural concrete. *African Journal of Science, Technology, Innovation and Development* 2018;10:169–75.
- [20] Hama SM, Hilal NN. Fresh properties of concrete containing plastic aggregate. Use of recycled plastics in eco-efficient concrete, Elsevier; 2019, p. 85–114.



BACTERIAL SELF-HEALING FOR SUSTAINABLE CONCRETE: A COMPARATIVE STUDY OF VEGETATIVE AND SPORE-FORMING BACTERIA

^a M Abdullah Akmal, ^a Ali Raza*, ^b Syed Sohaib Ajaz

a: Department of Civil Engineering, UET, Taxila, Pakistan, mabdullahakmal12345@gmail.com

b: Department of Civil Engineering, UET, Taxila, Pakistan, ali.raza@uettaxila.edu.pk

c: Department of Civil Engineering, UET, Taxila, Pakistan, 2014civ337@student.uet.edu.pk

Abstract- Affordability and availability of concrete is driving its use in building. Hence, sustainable, and durable concrete is needed. Cracks from excessive water, creep, or shrinkage cause concrete to fail. Crack creation reduces strength, and moisture alone or with a toxic chemical like sulfur can induce steel corrosion and concrete degradation, reducing the longevity of concrete. Hence, cracks must be filled, but mechanically repairing cracks, especially micro and deep cracks, is laborious and expensive and cannot be done in structural members that are not apparent. MICCP has been studied for concrete durability. This research covers self-healing characteristics using bacterial species; the effect of bio-concrete in prisms; and a comparative study using alkali-resistant spore-forming bacteria and vegetative bacteria. For concrete to self-heal, *Bacillus subtilis* and other alkali-resistant bacteria are added during mixing. This research indicates that Spore-forming bacteria performed better than vegetative bacteria. The crack remediation due to bacterial action was confirmed by performing SEM analysis.

Keywords- Self-Healing Ability of Concrete, Vegetative Bacteria, Spore Forming Bacteria, MICCP

1 Introduction

Concrete is inexpensive and commonly used in developing countries. As cracks form in concrete over time due to shrinkage, temperature, or other factors, they reduce the material's strength and weaken it, resulting in corrosion in steel-reinforced structures. When cracks exceed the allowed limit, they have a detrimental impact on the concrete. Yet, concrete and steel bars begin to deteriorate when cracks surpass the 0.4-mm limit [1].

Various mechanical methods can be employed to fill cracks in concrete, such as manually filling the crack with epoxy resin, which is expensive and cannot be used for small or deep cracks. In addition, regular oversight is required to monitor the formation of cracks and fill them mechanically. Therefore, mechanical crack filling cannot be performed on non-visible cracks developing in structural members [2]. An essential aspect of research is the improvement of the concrete industry in terms of its durability and self-healing capabilities utilizing natural or artificial means.

The self-healing action of concrete can be achieved through two distinct methods: intrinsic and bacterial self-healing [3]. Intrinsic self-healing of concrete refers to the concrete's inherent self-healing properties that can occur in the presence of water. Calcium carbonate is formed due to the hydration of un-hydrated cement that is present in the concrete. Cement hydration produces Ca(OH)₂, which reacts with carbon dioxide in water to form CaCO₃ crystals, allowing the concrete to close itself. In general, we can say that there is no added substance or material for self-healing properties, and the entire phenomenon is natural [4]. Several scholars have reported the development of autonomous self-healing. Wang Guiming et al. [5] revealed that SEM can be used to investigate the crystalline coating's self-healing mechanism in cementitious materials., which reveals that it not only fills mortar fractures and seals pores but also repairs cracks. E. Schlangen [6] explained in his investigations that experimental and numerical studies can explain how cracks that developed in early



ages can be filled or repaired by future hydration processes. It has been found that even after one day of hydration, the sample began to regain its strength.

However, autonomous healing refers to the healing properties gained by introducing a healing substance into the cracks [7]. It has been observed that bacterial self-healing is restricted to average crack width of 0.8 mm. At this point, a crack self-heals, restoring its full strength and durability. Considering that intrinsic self-healing is limited to 0.4 mm, bacterial self-healing can provide complete results with high efficiency [8]. However, Nguyen Ngoc Tri Huynh et al. created bio-concrete to evaluate the compressive and flexural strength over largely induced artificial cracks. The cracks limit was 1-18mm and was evaluated over period of 24 hours. Their research indicated that compressive and flexural strength increased over small scale [9]. This research discusses the two most powerful healing phenomena: self-healing characteristics of alkali-resistant spore-forming bacteria and alkali-resistant vegetative bacteria. The Bacterial bio-concrete refers to the healing properties of concrete that are accomplished by employing a straightforward procedure to fill the cracks. The fundamental mechanism is accomplished by creating a concrete mixture containing a precursor such as calcium lactate ($\text{Ca}(\text{C}_3\text{H}_5\text{O}_2)_2$). When water enters the crack, bacteria start eating the Calcium lactate as food and start making calcium carbonate as a by-product, which accumulates in the crack to fill it. The microorganisms utilized in this type of concrete are alkali-resistant bacteria from the genus *Bacillus*. Bacteria from this category are the most ideal since they produce spores and can survive in harsh environments for more than 200 years. Because of its sustainable organic features, using bacteria as a healing mechanism is one of the best techniques for producing this type of concrete. Also, some precursor compounds result in an increase in concrete strength rather than a decrease in concrete strength. Microbiologically Induced Calcium Carbonate Precipitation (MICCP) has sparked a considerable interest as a viable, natural, and environmentally friendly technology for autonomous concrete repair, resulting in greater concrete durability. A substantial study has been undertaken on the use of MICCP to mend cracks in concrete [10].

2 Experimental Procedures

2.1 Materials

To test the self-healing capabilities, concrete specimens with dimensions of 500x100x100 mm were prepared. Specimens were cured for 24 hours at room temperature after molding. To evaluate the mechanical qualities, 150x300 mm cylinders were also prepared. All specimens were prepared in accordance with ASTM C31/C31M standards. Tables 1-3 provide details of the mix designs used in this research. The compositions of the concrete trials had a set parameter. The total time for mixing the concrete was set at 10 minutes.

Table 1 Types of Materials

Type	Materials
Cement	P.O 42.5 Ordinary Portland cement named “Paidar Cement” (ASTM C-150 TYPE 1)
Water	Domestic Water
Fine Aggregates	River sand, Absorption Rate; 2.5060
Coarse Aggregates	Crushed stone Aggregates, Absorption Rate; 2.29
Precursor Compound	Calcium Lactate with the specified percentage of 1% of dry weight of cement
Autogenous Compound	<i>Bacillus Subtilis</i> ; alkali resistant bacteria of genus <i>Bacillus</i> .



5th Conference on Sustainability in Civil Engineering (CSCE'23)

*Department of Civil Engineering
Capital University of Science and Technology, Islamabad Pakistan*



Table 2 Standard Consistency Value of Cement

Sr. #	Wt. of water (W ₂) gm.	%Age Wt. of water	Penetration	
			mm	mm
1	140	28		10

Table 2.1 Settling times of Cement.

Initial setting time	Final setting time
218 mins (3.64 hours)	514 mins (8.55 hours)

Table 2.2 Composition Values of Cement

Cao	SiO ₂	Al ₂ O ₃	Fe ₂ O ₃	MgO	SO ₃	Na ₂ O	P ₂ O ₅	MnO
63.5%	19%	5%	3%	2.25%	2.5%	0.4%	0.25%	0.4%

Table 3 Properties of Fine and Coarse Aggregates

Fine Aggregates	Fineness Modulus	Specific gravity (Apparent)	Water Absorption %	Apparent Density (kg/m ³)	Bulk Density (kg/m ³)	Porosity %
	2.5877	2.4903	2.5060	1345.01	1346.15	0.0651 %
Coarse Aggregates	Fineness Modulus	Specific gravity (Apparent)	Water Absorption %	Apparent Density (kg/m ³)	Bulk Density(kg/m ³)	Porosity %
	6.5588	2.81	2.29	708.56	1349.32	0.17 %

Moreover, Figure 1 and 2 shows each size level of fine and coarse aggregates.

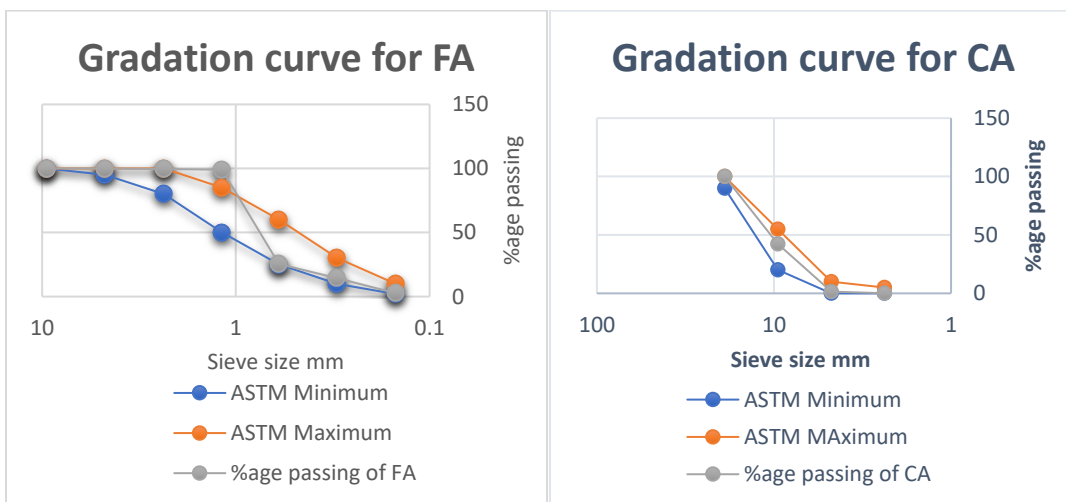


Figure 1 Gradation Curve for FA

Figure 2 Gradation Curve for CA



2.2 Bacterial Cultures Protocol

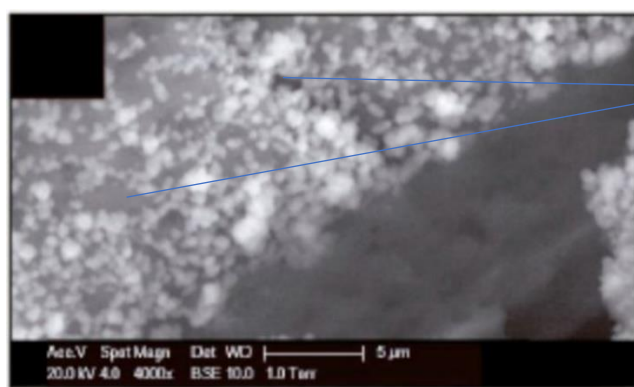
An Alkali Resistant Bacteria was selected considering the pH of concrete. As normal pH of concrete ranges from 11 to 13 which is quite high for bacteria to survive, an alkali bacterium was needed for self-healing of concrete. This research uses *Bacillus Subtilis* in both vegetative and spore forming culture for their comparative study and to evaluate healing ability of concrete as shown in figure 3. The strains of *Bacillus Subtilis* were isolated and the medium for their culture is generated. Then the culture was inoculated and incubated. After the incubation for the required amount of time, culture was diluted with N-broth medium and then it was centrifuged in falcon tubes. The OD was determined at 600nm by using spectrophotometer and pellets were dissolved in required amount of controlled distilled water to obtain the bacterial water to be used in concrete. The strains of bacteria were cultured as per specification with the concentration to be achieved as 10^6 cells/ml. The concentration at the time of synthesis was enhanced so that it can be diluted at the time of use age.



Figure 3 Bacterial Solution

2.3 Preparation Of Micro-cracks

After 24 hours of curing, three-point bending method was used to induced cracks and a smart crack gauge of 4-mm range was used to measure the width of cracks. SEM was used to bring in the images. A sample binarized image for measuring the self-healing progress is shown in Fig. 4. The bacteria self-healing of the concrete samples was ultimately characterized by measuring the overall healing area of the crack.



Cracks on
Upper layer
under
microscope.

Figure 4 SEM



3 Research Methodology

The methodology of this research involved the use of cement, sand, aggregates, precursor compound, and bacterial water in a non-encapsulated way to produce bio-concrete. The selection of cement, sand and aggregates was made through ASTM Codes involving ASTM C-150 TYPE 1, ASTM C144 and ASTM C33/C33M. Fixed mix design ratio of 1:1.5:3 and water-cement ratio of 0.49 was used to produce Samples. The precursor compound, calcium lactate was added at a specific percentage of 1% of Cement Weight to the dry mixture. The selected bacterial strain was cultured in a nutrient-rich medium, and the bacterial water was then harvested and added to the concrete mixture during the batching process. The precursor compound, typically calcium lactate or calcium acetate, was also added to the mixture to provide a source of calcium ions for the bacteria to convert into calcium carbonate. The mixture was then placed into molds and cured under optimal conditions to allow the bacteria to consume the nutrients and produce calcium carbonate, which acted as a binding agent. The bio-concrete was then tested for strength and durability using standard methods such as compressive strength, water absorption, Modulus of Rupture and Self-healing Progress. Overall, this research aimed to investigate use non-encapsulated bacterial water and precursor compounds in the production of bio-concrete, with the potential to develop sustainable and durable construction materials.

To trace the progress of bio-concrete with respect to controlling specimens, slump cone tests, compression tests, modulus of rupture tests, and scanning electronic microscopy tests were conducted. A slump cone test was conducted to determine the workability of concrete. However, results indicated that concrete had true slump, as the slump of the conventional concrete was recorded at 76 mm, while the slump for bio-concrete was 50mm, as shown in Figure 5.



Figure 5 Slump Cone Test

4 Results

4.1 Effect of Bacterial Cultures on Compressive Strength of Concrete

The compressive strength of control specimens and bio-concrete specimens was measured after 7- and 28-days curing. The size of the tested concrete cylinders was 150 x 300 mm, and an unconfined compression test was conducted.



Figure 6 Compressive Strength Setup



Figure 7 Cylindrical Specimen during Testing



The 7-day testing and 28-day testing shows an increase in compressive strength of specimens.

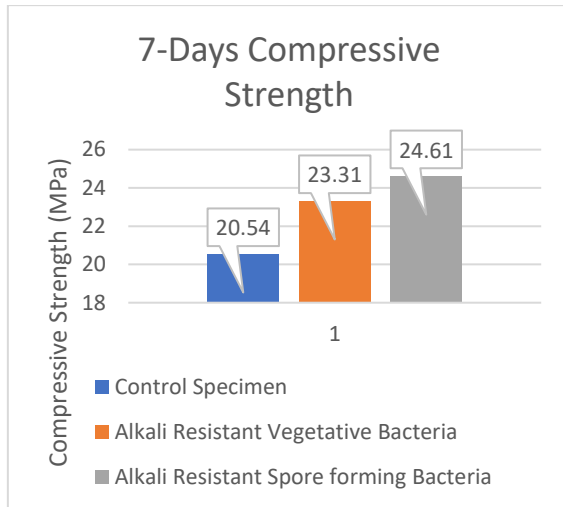


Figure 9 7-Days Compressive Strength Test

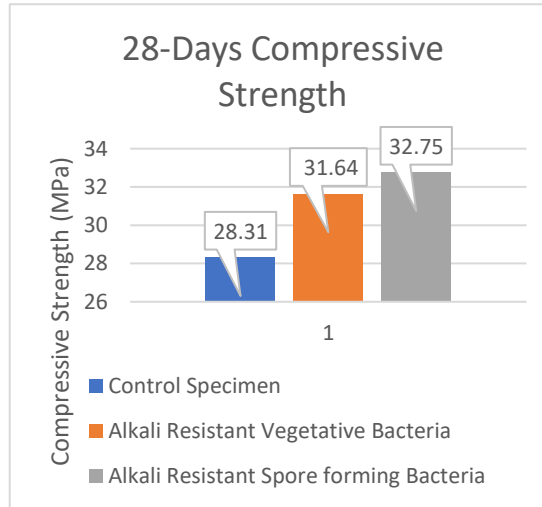


Figure 10 28-Days Compressive Strength Test

It is evident from the graphical representation of compressive strength that the Alkali Resistant Vegetative species of *Bacillus Subtilis* increases compressive strength by nearly 14% after 7 days of curing, while the Alkali Resistant Spore forming species of *Bacillus Subtilis* increases compressive strength by nearly 20%. Similarly, the compressive strength test after 28 days revealed an increase of nearly 13% for the vegetative species of *Bacillus Subtilis* and nearly 16% for the spore-forming species. This demonstrates conclusively that the use of microbes in concrete increased its compressive strength through the precipitation of calcium carbonate, as supported by a second analysis using scanning electron microscopy.

4.2 Effect of Bacterial Culture on Tensile Capacity of Concrete

The modulus of rupture test was conducted on 100 mm x 100 mm x 510 mm prisms. 28 days was the curing period for both the control and bio-concrete samples. Using the following relationship, the Modulus of Rupture was computed.

$$\text{Stress} = \frac{Pl}{bd^2}$$

The following are the results of the Modulus of Rupture test performed on prismatic specimens.



Figure 11 Prismatic Specimen after Testing

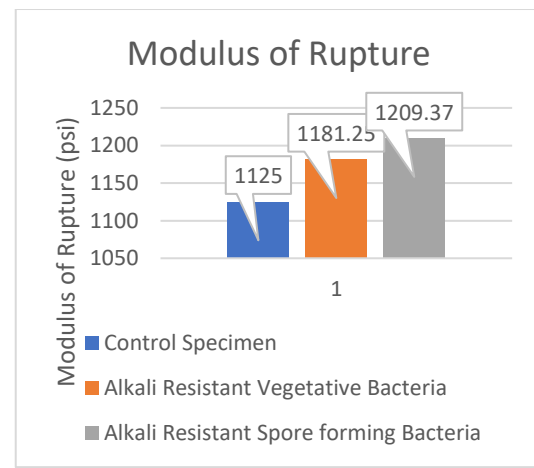


Figure 12 Test Results



The Modulus of Rupture test findings demonstrate that the use of self-healing concrete did not significantly boost the tensile capacity of the concrete. This is because, in comparison to its compressive strength, concrete's tensile strength is significantly lower, ranging from 8 to 14 percent. Since the tested prisms broke suddenly (as depicted in the image above), this explained why the concrete's tensile strength didn't improve much.

4.3 Scanning Electron Microscopy (SEM).

Scanning Electron Microscopy (SEM) was used to analyze the mineralogy of the deposited calcium carbonate caused by the induction of bacteria.

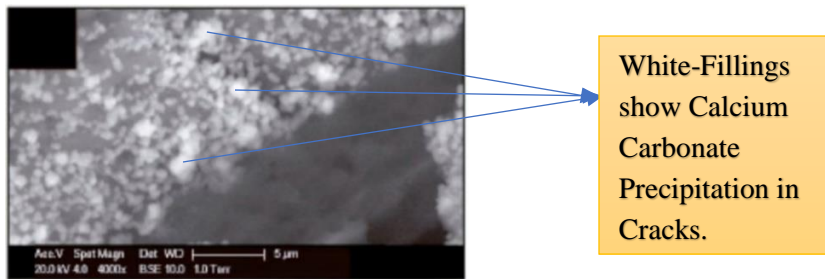


Figure 13 SEM Results (Healed Microcracks)

White Crystals, showing in Figure 13, demonstrated the concrete self-healing ability. The specimens tested for compressive strength analysis were cut into little 37×37 mm cubes and then SEM examination was done on them. The Figure 12 depicts the outcome of the SEM study. This result from the SEM confirms the filling of a microcrack and justifies the precipitation of calcium carbonate precipitation.

5 Conclusions

Following conclusions are drawn after deeply analyzing and studying the experimental results obtained by different test:

- 1 Locally developed Concrete incorporated bacteria can produce copious amount of minerals which can help in filling of cracks.
- 2 The Bio-concrete or Self-Healing concrete resulting from the application of Vegetative specie of *Bacillus Subtilis* increased the 7-days compressive strength by almost 14% while the 28-days compressive strength was increased by the percentage of almost 12%.
- 3 Similarly, the Bio-concrete or Self-Healing concrete by using Spore-forming specie of *Bacillus Subtilis* increased 7-days and 28-days compressive strength by 20% & 16% respectively.
- 4 The increase in the compressive strength is due to the accumulation of Microbiologically Induced Calcium Carbonate precipitation.
- 5 The increase in tensile strength found by Modulus of Rupture test was not much. This was because of low tensile strength of concrete and due to the abrupt failure of the specimens tested for tensile strength.
- 6 Microbiological crack remediation is more efficient in shallow cracks than in deeper cracks, primarily because the microorganisms grow more actively in the presence of oxygen.
- 7 The results from the SEM Analysis further confirms that the increase in compressive strength is due to precipitation of Calcium Carbonate and confirmed crack filling was observed.

Acknowledgment

Many people have contributed to this research and report, but the authors are grateful for the support, guidance & co-operation of their Advisor Engr Syed Saqib without whom this research & report would not have been possible. His continuous support & guidance helped us to work into & complete this research. We are honoured to acknowledge his support.

References



5th Conference on Sustainability in Civil Engineering (CSCE'23)

Department of Civil Engineering

Capital University of Science and Technology, Islamabad Pakistan



- [1] W. Ramm and M. Biscoping, "Autogenous healing and reinforcement corrosion of water-penetrated separation cracks in reinforced concrete," *Nucl. Eng. Des.*, vol. 179, no. 2, pp. 191–200, Feb. 1998, doi: 10.1016/S0029-5493(97)00266-5.
- [2] H. Rahmani and H. Bazrgar, "Effect of coarse cement particles on the self-healing of dense concretes," *Mag. Concr. Res.*, vol. 67, no. 9, pp. 476–486, May 2015, doi: 10.1680/macr.14.00158.
- [3] C. Qian, T. Zheng, X. Zhang, Y. Su, Application of microbial self-healing concrete: Case study, *Constr. Build. Mater.* 290 (2021) 123226, <https://doi.org/10.1016/j.conbuildmat.2021.123226>.
- [4] J. Wang *et al.*, "Improvement of intrinsic self-healing ability of concrete by adjusting aggregate gradation and sand ratio," *Constr. Build. Mater.*, vol. 309, p. 124959, Nov. 2021, doi: 10.1016/j.conbuildmat.2021.124959
- [5] W. Guiming and Y. Jianying, "Self-healing action of permeable crystalline coating on pores and cracks in cement-based materials," *J. Wuhan Univ. Technol. Sci. Ed.*, vol. 20, no. 1, pp. 89–92, Mar. 2005, doi: 10.1007/BF02870882.
- [6] E. Schlangen, H. Jonkers, S. Qian, and A. Garcia, "E. Schlangen, H. Jonkers, S. Qian & A. Garcia," *Fract. Mech. Concr. Struct. Adv. Fract. Mech. Concr. Oh. al.*, no. c, pp. 291–298, 2010.
- [7] C. Engineer and I. Introduction, "An Experimental Investigation on Improvement of Concrete Serviceability by using Bacterial Mineral Precipitation," vol. II, no. Iii, pp. 46–49, 2015.
- [8] M. Luo, C. Qian, and R. Li, "Factors affecting crack repairing capacity of bacteria-based self-healing concrete," *Constr. Build. Mater.*, vol. 87, pp. 1–7, Jul. 2015, doi: 10.1016/j.conbuildmat.2015.03.117.
- [9] N. N. T. Huynh, K. Imamoto, and C. Kiyoohara, "A Study on Biominerilization using Bacillus Subtilis Natto for Repeatability of Self-Healing Concrete and Strength Improvement," *J. Adv. Concr. Technol.*, vol. 17, no. 12, pp. 700–714, Dec. 2019, doi: 10.3151/jact.17.700.
- [10] Y. L. Reddy and A. Prades, "Experimental Study on the Durability of Concrete," *Mukt Shabd J.*, vol. IX, no. VI, pp. 7785–7795, 2020.



EFFECT OF BENTONITE & POLYPROPYLENE FIBERS ON FRESH AND HARDENED PROPERTIES OF FLY ASH BASED GEOPOLYMER CONCRETE

^a Shahid Zaman, ^b Rana Muhammad Waqas*, ^c Faheem Butt

a: Department of Civil Engineering, UET, Taxila, Pakistan, engr.shahid742@gmail.com

b: Department of Civil Engineering, UET, Taxila, Pakistan, rana.waqas@uettaxila.edu.pk

c: Department of Civil Engineering, UET, Taxila, Pakistan, faheem.but@uettaxila.edu.pk

* Corresponding author: Email ID: rana.waqas@uettaxila.edu.pk

Abstract- Geopolymer concrete is developed by alkaline activation of waste materials and industrial byproducts rich in silica and alumina. Bentonite is one such pozzolanic clay material that is rich in SiO₂ content. It has been extensively used as a supplementary cementitious material in conventional Ordinary Portland cement (OPC) concrete resulting more cheaper, environment friendly and durable concrete. However, a little research is reported so far to assess the performance of bentonite modified geopolymer concrete. This study investigates the individual and combined incorporation of bentonite and polypropylene (PP) fibers on the workability and mechanical properties of fly ash based geopolymer concrete. Fly ash (FA) was used as precursor to develop geopolymer concrete (GPC) mixtures. FA was replaced with bentonite at 10% wt content and PP fibers were added at three different proportions i.e., 0.5%, 0.75% and 1%. Both raw (untreated) and heat-treated (up to 200 degrees Celsius) forms of bentonite were used. The intention was to ascertain whether heat-treated bentonite can perform better than untreated bentonite when combined with various PP fibers concentrations. The mechanical properties of bentonite modified, and PP fiber reinforced GPC mixtures were evaluated. The findings showed that addition of bentonite and PP fibers significantly increased the mechanical properties of GPC mixtures. However, the contribution of heat-treated bentonite in combination with PP fibers to mechanical properties of GPC mixtures is more significant.

Keywords- geopolymer concrete, bentonite, polypropylene fibers, mechanical properties

1 Introduction

Our planet's climate is rapidly changing as a result of increased pollution and excessive CO₂ emissions into the atmosphere. All researchers are concentrating on environmentally friendly methods to protect the environment by encouraging sustainable living practices and the creation of eco-friendly technologies. In addition, the construction sector is on the lookout for eco-friendly, low-CO₂ emitting green materials. Approximately 4 billion tons of ordinary Portland cement (OPC) are used annually as a binding material in construction activities worldwide [1-2]. OPC adds 1 tons of CO₂ emission into the environment for every 1 ton it produces, which results in significant CO₂ emissions into the atmosphere. Additionally, the production of OPC requires a significant amount of raw materials. To fulfil the rising demand for infrastructure, OPC concrete manufacturing is constantly growing. The building industry is under pressure to develop OPC-based material substitutes that have similar qualities to OPC and satisfy sustainability and green material requirements [2].

The use of geopolymer concrete (GPC), which totally replaces the use of OPC and is entirely made of industrial wastes/by-products that are activated with the use of an alkaline solution, is the most efficient option to promote sustainable construction practices [3-4]. Geopolymer concrete can be considered as one emerging category of green cement adhesives



With the potential to reduce the harmful environmental effects of traditional Portland cement (OPC), such as carbon footprint and energy usage, geopolymers have recently been offered as a more environmentally friendly substitute [5–6]. Fly ash (residue of coal power plants) has been proposed as suitable precursor material to produce GPC mixtures due to its chemical composition and adequate SiO₂ and Al₂O₃ content [7–8]. It is reported that curing of GPC mixtures at elevated temperatures further improves the engineering properties. Due to the low reactivity of FA at ambient temperature, heat curing of FA-based GPC is typically carried out at a temperature of 80°C to 100°C for activation [9–10]. Furthermore, it has been established that geopolymers subjected to elevated temperature curing outperforms traditional OPC mixtures in most of the engineering properties [11–13].

There are several research available that show Class F FA has higher mechanical qualities after 24- to 48-hour heat curing. However, ambient curing of FA-based GPC does not yield the desired results because FA is not very reactive at low temperatures. Additionally, FA does not begin to geopolymerize at low temperatures. According to reports, using heat curing for GPC in worksite and field applications is not realistically viable.

The production of GPC has made considerable use of the waste products FA from coal power plants and slag from the steel and iron sectors, both of which have established high performance [14–18]. However, concerns continue to exist over the reliability of the delivery of high-quality FA, and some regions of the world have experienced FA shortages as a result of tighter regulation around coal-fired power plants. Comparatively speaking, the yearly demand for concrete for global building activities is rather high compared to the global supply of SG. In order to pursue a sustainable alternative to traditional concrete building, all available alternative raw material possibilities should be thoroughly investigated [19]. One of these ingredients is low calcium bentonite, a silica and alumina-rich naturally formed pozzolana that has been employed widely to enhance the different aspects of concrete [20]. It is an aluminophyllosilicate clay, frequently produced when volcanic ash is chemically decomposed in the presence of water. It is mostly composed of the mineral montmorillonite. Numerous studies have shown that the engineering characteristics of conventional concrete are improved when bentonite is used in replace of cement [20–28]. The sodium or calcium varieties of bentonites are typically used in industrial settings.

The swelling capacity of calcium bentonite is significantly lower than that of other forms of bentonites [20]. Attock, Jhelum, Nowshera, and Karak are just a few of the areas in Pakistan where bentonite may be found. Low calcium bentonite has been reported to be used as a partial substitute for OPC by different researchers [26 -27]. It was reported that mixes with bentonite addition do better than traditional cement concrete at different ages by using bentonite as a 0 to 21% mass replacement of OPC [26]. It was also discovered that mixtures with bentonite addition had enhanced resistance to acid assault. Bentonite's pozzolanic behaviour in the presence of the OPC has been shown by Mirza et al [27].

Low calcium bentonite has positive influences on the engineering characteristics of traditional OPC concrete, according to a review of the recent literature [21, 26, 27, 29–32]. There isn't much research, nevertheless, available on the use of bentonite to enhance the performance of GPC mixtures. Concrete is a brittle substance by nature; hence, research scholars have utilized fiber as reinforcements for concrete to increase its ductility [33–34]. PPF are great polymer fibers because they are inexpensive, light, have low thermal conductivity, and have a high elastic modulus [35]. PPF may be added to concrete to help decrease drying shrinkage and boost tensile, compressive, and flexural strength [36–37]. Researchers looked at the mechanical properties of mortars that included PPF and found that ductility was significantly improved. Until the concrete reached the optimal concentration of 1% PPF, its strength remained unchanged [38].

However, no studies have yet looked at the combined effect of heat-treated bentonite and polypropylene fibers on the performance of concrete. Previous studies have examined the effects of utilizing bentonite and polypropylene fibers independently on the qualities of concrete. In this work, we sought to examine the fresh and hardened properties of concrete when both heat-treated and untreated bentonite, as well as polypropylene fibers, were added.

2 Experimental Procedures

2.1 Materials Descriptions

FA was used as the raw ingredients for the development of the geopolymer binder. FA was replaced with bentonite at 10 wt% to develop the bentonite blended GPC mixtures. The physical and chemical composition of OPC, FA and bentonite is shown in Table 1. Other than the coarse aggregates and sand as used in conventional concrete, the precursors and alkaline Paper ID. 23-128



5th Conference on Sustainability in Civil Engineering (CSCE'23)

Department of Civil Engineering
Capital University of Science and Technology, Islamabad Pakistan



solution are the main components of GPC. The most frequently used alkaline solution in the production of GPC is a mixture of sodium hydroxide (SH) and sodium silicate (SS). The required molarity of SH was achieved by adding water and 98–99% pure SH pellets. SS solution with a SiO₂ to Na₂O ratio of 2.0 was bought from a local vendor. Bentonite clay (low calcium type) was obtained locally from Jehangir, Pakistan. Moreover, scanning electron microscopic (SEM) image of bentonite revealed spherical and thick-flake shaped particles as shown in Figure 1. Bentonite particles were found to be flaky and spherical in form. LawrencePur and Margalla, respectively, provided the fine and coarse aggregates. PPF with a 19 mm length was utilized. The properties PP fibers are presented in Table 2.

Table 1: Physical and Chemical properties of OPC, Bentonite and Fly ash

Oxides	Ordinary Portland cement	Bentonite		Fly ash
		Memon et al. work [26]	The present study	
SiO ₂	53.96	54.5	52.8	35.8
Al ₂ O ₃	32.21	20.2	16.4	20.2
Fe ₂ O ₃	2.98	8.6	5.8	11.4
MgO	1.51	4.5	1.4	1.80
CaO	4.72	7.3	4.6	14.3
Na ₂ O	0.3	1.3	0.62	1.20
K ₂ O	1.3	3.6	0.7	2.2
General properties				
Relative density (g/cm ³)	2.10	2.81	2.64	1.8
Specific surface area (cm ² /gm)	3207	4800	4900	3250
Loss on ignition (%)	1.30	5.4	9.6	0.57

Table 2: Properties of Polypropylene Fibers

Properties	Values
Tensile strength at breaking (MPa)	31 - 41
Flexural strength (MPa)	41 - 55
Elongation at break (%)	100 - 600
Tensile modulus (MPa)	1137 - 1551
Specific gravity	0.9 – 0.91

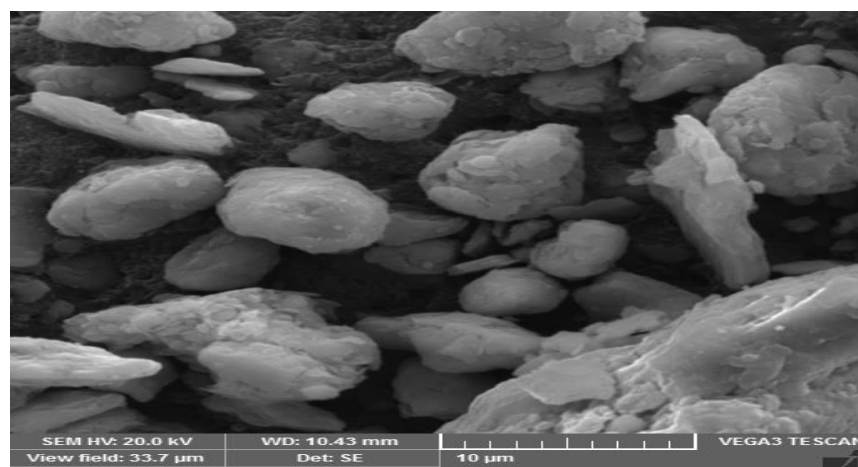


Figure 1 SEM of bentonite used in this study.



2.2 Mixture Proportions

A total of 9 mixture proportions as shown in Table 9 were prepared in this study with the aim of study the influence of untreated (raw bentonite) and treated bentonite, and PP fibers on the workability and mechanical properties of GPC mixtures. Fly ash was utilized as the precursor to develop the GPC mixes. The bentonite clay was used as substitution of FA at 10% by weight in both treated and untreated form to study the effect of bentonite clay. The optimum dosage of bentonite (10% by weight of binder) used in the present study was achieved from the literature review. GPC mixtures with 0% replacement level of bentonite were taken as the control mixes. PP fibers were added at three different proportions i.e., 0.5%, 0.75% and 1%.

Table 3: Mixture proportions used in this study.

Mix	Mix proportions (%)					Mix quantities (kg/m3)							
	ID	FA	Treated Bentonite	Un-treated Bentonite	Fibers	Sand	CA	FA	Bentonite	Alkaline solution	NaOH	Na ₂ SiO ₃	SP
M1	90	-	-	-	-	640	1201	400	-	160	53	107	6
M2	90	-	10%	-	-	643	1206	360	40	160	53	107	6
M3	90	-	10%	0.5	-	646	1212	360	40	160	53	107	6
M4	90	-	10%	0.75	-	652	1220	360	40	160	53	107	6
M5	90	-	10%	1	-	643	1206	360	40	160	53	107	6
M6	90	10%	-	-	-	646	1212	360	40	160	53	107	6
M7	90	10%	0.5	-	-	644	1208	360	40	160	53	107	6
M8	90	10%	0.75	-	-	647	1214	360	40	160	53	107	6
M9	90	10%	1	-	-	655	1225	360	40	140	53	107	6

2.3 Testing Procedures

The workability of the freshly mixed concrete mixtures was assessed by performing the slump cone test conforming ASTM C143 procedure [40]. The compressive strength of GPC mixtures was measured by testing cubes of 150mm at the age of days according to BS standard EN-12390 [41]. Concrete cylinder samples measuring 150 mm by 300 mm were tested for split tensile strength in line with ASTM C496 standards after 28 days of cure [42]. Flexural strength tests on beam specimens with dimensions of 100mm, 100mm, and 500mm were performed in accordance with ASTM C78 guidelines [43].

3 Results and Discussions

3.1 Workability

Fig. 1 displays the slump cone test results of all GPC mixes. The workability of both raw bentonite and heat-treated bentonite blended mixtures is negatively influenced by the addition of bentonite, as can be shown in Figure. As a result of the flaky shaped particles and higher specific surface area of bentonite clay as compared to fly ash round particles, the slump values of bentonite blended GPC mixes has decreased. Because bentonite clay particles have a greater specific surface area, more water or solution is needed in the mixture to thoroughly wet the particle surfaces, which makes the mixture difficult to deal with. Although adding bentonite reduces the mix's workability, the mixture is still cohesive. The earlier investigations [34, 40] have found a similar declining tendency in slump values due to bentonite addition in concrete mixes. It is significant to note that the decrease in workability is more apparent in raw bentonite blended mixes than treated blended mixes. The similar phenomenon is also reported in the previous studies [34, 40]. The decreasing trend of workability with bentonite inclusion was more pronounced for raw bentonite blended mixes. It can also be observed that



workability of fiber reinforced mixes is lower as compared to their counterparts (without fiber). Since the concentration of fibers increased internal friction in the blends with constant water to binder, the addition of PPF significantly decreased the workability.

3.2 Compressive Strength

The compressive strength of control mix and bentonite blended mixes was evaluated at the age of 28 days. Three identical specimens measuring 150x150x150 mm were tested to determine the strength of each mix. The results of compressive strength tests are shown in Figure. It can be seen that a 10% bentonite replacement led to an improvement in compressive strength for all the specimens than control mix. However, the performance of GPC mix blended with heat treated bentonite was better than un-treated bentonite blended mix. The compressive strength was improved by an extent of 10% and 18% for raw bentonite blended mix and treated bentonite blended mix respectively when compared to the control mix without bentonite. This increase in strength may be attributed to the bentonite filler and pozzolana reaction properties, which has improved the strength and led to a more compacted and refined microstructure in the concrete [25].

Furthermore, the addition of PP fibers resulted in increasing the compressive strength for all the mixes by an amount of 5-18%. The maximum increase in strength was observed for the mix with 1% addition of fibers for both untreated and treated bentonite blended mix when compared to the mix without fibers. The compressive strength of M3, M4 and M5 with 0.5%, 0.75% and 1% fibres were increased by an amount of 8%, 13% and 14% respectively when compared to control mix M2 (without fibers) for untreated bentonite blended mixes. Similarly, the compressive strength of M7, M8 and M9 mixes with 0.5%, 0.75% and 1% fibres were increased by an amount of 5%, 13% and 15% respectively when compared to control mix M6 (without fibers) for treated bentonite blended mixes. The influence of fibers was more significant for mixes with 0.5% and 0.75% fraction of fibers for both untreated and treated bentonite blended mixes.

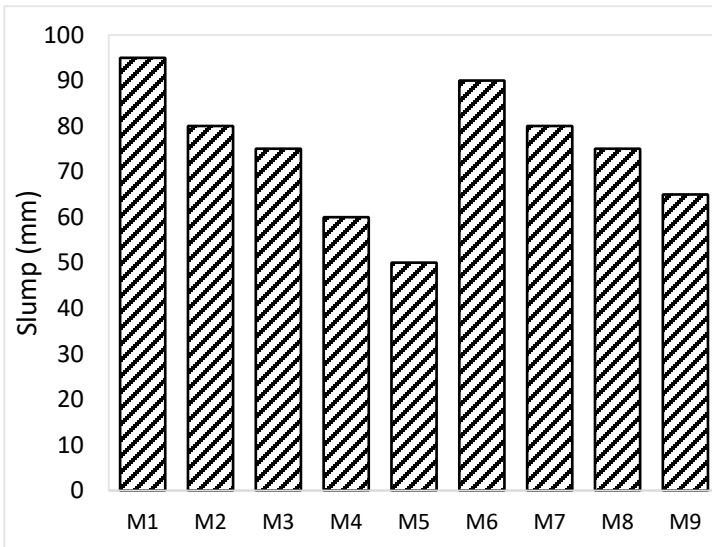


Figure 2 slump cone test results of all GPC mixes

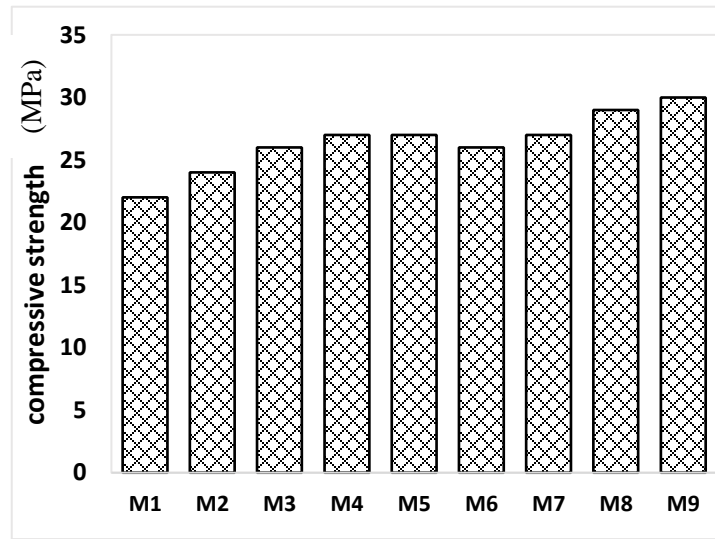


Figure 3 compressive strength of all GPC mixes

3.3 Tensile Strength

The splitting tensile strength tests on 150x300mm cylinders were carried out after 28 days of casting. Figure 8 displays the tensile strength results for the all the mixes. An increase in the tensile strength of all GPC mixes was observed with 10% bentonite (treated and raw) replacement level for all the specimens when compared to the control mix. However, the influence of bentonite on the tensile strength of GPC mixes is evident, though not huge. The tensile strength of M2 and M6 mixes containing 10% raw bentonite and treated bentonite respectively was 4% and 10% higher than the control mix (without bentonite). Furthermore, the inclusion of fibers caused a considerable increase in the tensile strength of all GPC mixes. The tensile strength of M3, M4 and M5 mixes with 0.5%, 0.75% and 1% fibres were increased by an amount of 9%, 20% and 32% respectively when compared to control mix M2 (without fibers) for untreated bentonite blended mixes.



Similarly, the tensile strength of M7, M8 and M9 mixes with 0.5%, 0.75% and 1% fibres were increased by an amount of 7%, 19% and 33% respectively when compared to control mix M6 (without fibers) for treated bentonite blended mixes.

3.4 Flexural Strength

Figure 7 shows the flexural strength value of all GPC mixes. The comparison between flexural strength values of control mix and bentonite blended mixes showed that bentonite has a positive effect on the flexural strength of all GPC mixes. It is also evident from Figure that heat treated bentonite blended specimens performed better than raw bentonite blended specimens. Additionally, the inclusion of PP fibers increased the flexural for all of the mixtures by a range of 6 to 29%. When comparing the blend of untreated and treated bentonite to the blend without fibers, the mix with a 1% addition of fibers showed the greatest gain in strength. When compared to the control mix M2 (without fibers), the compressive strength of M3, M4, and M5 (untreated bentonite blended mixes) with 0.5%, 0.75%, and 1% fibers was raised by 8%, 17%, and 27%, respectively. Similarly, as compared to control mix M6 (without fibers), the tensile strength of M7, M8, and M9 mixes (treated bentonite blended mixes) containing 0.5%, 0.75%, and 1% fibers increases by amounts of 6%, 18%, and 29%, respectively. The rough surface of the fibers, which results in a strong connection and bond in the concrete, may be to attribute for this increase in flexural strength [32, 35]. Due to their bridging influence, the fibers start to stop the crack from spreading as soon as concrete starts to cracks. This reduces the concrete's brittleness and improves its post-cracking behaviour [32, 35].

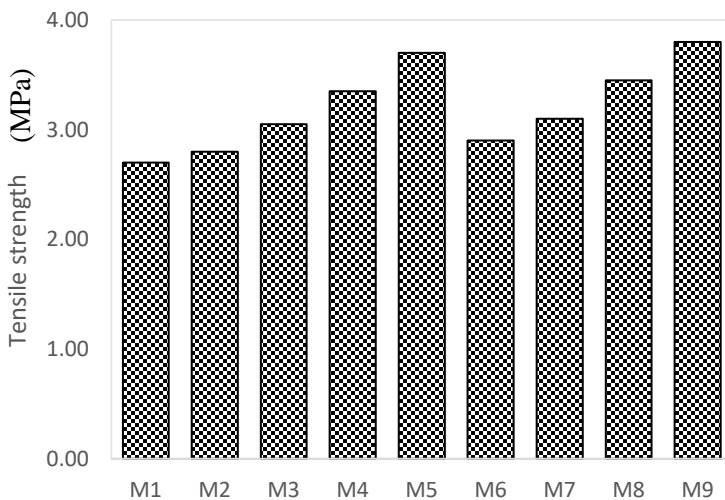


Figure 4 Tensile strength of all GPC mixes

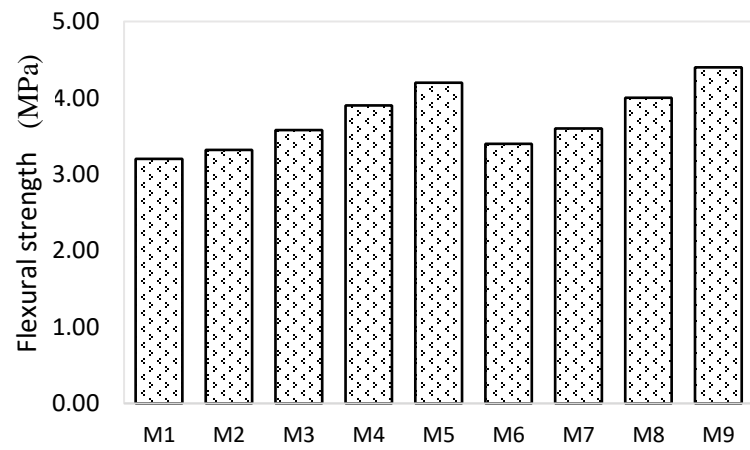


Figure 5 Flexural strength of all GPC mixes

4 Conclusions

This paper has presented the results of an experimental study conducted to evaluate the influence of bentonite and PP fibers on fresh and hardened properties. Following key conclusions have been drawn from this study:

1. The workability of both raw bentonite and heat-treated bentonite blended mixtures is negatively influenced by the addition of bentonite.
2. The decreasing trend of workability with bentonite inclusion was more pronounced for raw bentonite blended mixes.
3. Incorporation of Polypropylene fibres results in further decrease of workability.
4. A 10% bentonite replacement resulted in an improvement in compressive strength for all the specimens when compared to the control mix (without bentonite).
5. However, the performance of GPC mix blended with heat treated bentonite was superior to un-treated bentonite blended mix.
6. Furthermore, the addition of PP fibers resulted in increasing the compressive strength for all the mixes by an



5th Conference on Sustainability in Civil Engineering (CSCE'23)

Department of Civil Engineering
Capital University of Science and Technology, Islamabad Pakistan



amount of 5-18% as compared to mix without fiber.

7. The maximum increase in strength was observed for the mix with 1% addition of fibers for both untreated and treated bentonite blended mix when compared to the mix without fibers.
8. The influence of fibres on mechanical properties was more significant for mixes with 0.5% and 0.75% fraction of fibers for both untreated and treated bentonite blended mixes.
9. For each mix, the outcomes of the tensile and flexural strengths show trends that are identical to those of the compressive results. The addition of 10% bentonite improves the flexural strength and tensile strength of all GPC mixes.
10. The incorporation of PP fibres significantly increases the flexural strength and tensile strength. The inclusion of PP fibers increased the flexural and tensile strength for all the mixtures by a range of 6 to 29%. When comparing the blend of untreated and treated bentonite to the mixes without fibers, the mix with a 1% addition of fibers showed the greatest gain in strength.

5 Future Recommendations

The use of GPC in field applications is very limited. A very few practical applications of GPC in the field are reported. There is a need to develop broader and more reliable statistics on the practicality of utilizing GPC in structural applications. Further It is recommended to conduct an extensive experimental study to evaluate the long-term durability performance of PP fibres incorporated bentonite blended GPC mixes in aggressive environments, such as acidic and sulphatic environments. The behavior of GPC in extreme conditions (Fire and Corrosion environment) needs to be ascertained.

Acknowledgment

The authors acknowledge the support provided by the University of Engineering and Technology Taxila for testing of the specimens.

References

- [1] M. Zahid, N. Shafiq, M. H. Isa, and L. Gil, "Statistical modeling and mix design optimization of fly ash based engineered geopolymer composite using response surface methodology," *Journal of cleaner production*, vol. 194, pp. 483-498, 2018.
- [2] Hamada H, Alattar A, Tayeh B, Yahaya F, Adesina A. Sustainable application of coal bottom ash as fine aggregates in concrete: A comprehensive review. *Case Studies in Construction Materials*. 2022 May 6:e01109.
- [3] Ahmed HU, Mohammed AA, Rafiq S, Mohammed AS, Mosavi A, Sor NH, Qaidi S. Compressive strength of sustainable geopolymer concrete composites: a state-of-the-art review. *Sustainability*. 2021 Jan;13(24):13502.
- [4] Qaidi SM, Tayeh BA, Isleem HF, de Azevedo AR, Ahmed HU, Emad W. Sustainable utilization of red mud waste (bauxite residue) and slag for the production of geopolymer composites: A review. *Case Studies in Construction Materials*. 2022 Mar 8:e00994.
- [5] A. Palomo, M. Grutzeck, and M. Blanco, "Alkali-activated fly ashes: A cement for the future," *Cement and concrete research*, vol. 29, pp. 1323-1329, 1999.
- [6] J. Davidovits, "Geopolymers: inorganic polymeric new materials," *Journal of Thermal Analysis and calorimetry*, vol. 37, pp. 1633-1656, 1991.
- [7] K. A. Komnitsas, "Potential of geopolymer technology towards green buildings and sustainable cities," *Procedia Engineering*, vol. 21, pp. 1023-1032, 2011.
- [8] B. Singh, G. Ishwarya, M. Gupta, and S. Bhattacharyya, "Geopolymer concrete: A review of some recent developments," *Construction and building materials*, vol. 85, pp. 78-90, 2015.
- [9] Y. Fan, S. Yin, Z. Wen, and J. Zhong, "Activation of fly ash and its effects on cement properties," *Cement and Concrete Research*, vol. 29, pp. 467-472, 1999.
- [10] K. Somna, C. Jaturapitakkul, P. Kajitvichyanukul, and P. Chindaprasirt, "NaOH-activated ground fly ash geopolymer cured at ambient temperature," *Fuel*, vol. 90, pp. 2118-2124, 2011.
- [11] A. S. Parveen and D. Singhal, "Mechanical properties of geopolymer concrete: A state of the art report," in *Proceedings of the 5th Asia And Pacific Young Researchers And Graduate Symposium, Jaipur, India*, 2013.
- [12] A. Noushini, F. Aslani, A. Castel, R. I. Gilbert, B. Uy, and S. Foster, "Compressive stress-strain model for low-calcium fly ash-based geopolymer and heat-cured Portland cement concrete," *Cement and Concrete Composites*, vol. 73, pp. 136-146, 2016.
- [13] S. Wallah and B. V. Rangan, "Low-calcium fly ash-based geopolymer concrete: long-term properties," 2006.
- [14] A. S. Parveen and D. Singhal, "Mechanical properties of geopolymer concrete: A state of the art report," in *Proceedings of the 5th Asia And Pacific Young Researchers And Graduate Symposium, Jaipur, India*, 2013.
- [15] C. K. Yip, G. Lukey, and J. S. Van Deventer, "The coexistence of geopolymeric gel and calcium silicate hydrate at the early stage of alkaline activation," *Cement and concrete research*, vol. 35, pp. 1688-1697, 2005.



5th Conference on Sustainability in Civil Engineering (CSCE'23)

Department of Civil Engineering
Capital University of Science and Technology, Islamabad Pakistan



- [16] P. Nath and P. K. Sarker, "Effect of GGBFS on setting, workability and early strength properties of fly ash geopolymer concrete cured in ambient condition," *Construction and Building Materials*, vol. 66, pp. 163-171, 2014.
- [17] X. Y. Zhuang, L. Chen, S. Komarneni, C. H. Zhou, D. S. Tong, H. M. Yang, *et al.*, "Fly ash-based geopolymer: clean production, properties and applications," *Journal of Cleaner Production*, vol. 125, pp. 253-267, 2016.
- [18] B. V. Rangan, D. Sumajouw, S. Wallah, and D. Hardjito, "Reinforced low-calcium fly ash-based geopolymer concrete beams and columns," in *31st Conference on our world in concrete & structures*, 2006, pp. 16-17.
- [19] D. P. Bentz, C. F. Ferraris, S. Z. Jones, D. Lootens, and F. Zunino, "Limestone and silica powder replacements for cement: Early-age performance," *Cement and Concrete Composites*, vol. 78, pp. 43-56, 2017.
- [20] H. Murray, "Industrial clays case study," *Mining, Minerals and Sustainable Development*, vol. 64, pp. 1-9, 2002.
- [21] M. Karthikeyan, P. R. Ramachandran, A. Nandhini, and R. Vinodha, "Application on partial substitute of cement by bentonite in concrete," *International Journal of ChemTech Research*, vol. 8, pp. 384-388, 2015.
- [22] V. Grishin and L. Deryugin, "Experience in the use of bentonite-cement concrete for repairing the core of the earthfill dam of Kureiskaya HPP," *Power Technology and Engineering*, vol. 40, pp. 90-95, 2006.
- [23] M. Shabab, K. Shahzada, B. Gencturk, M. Ashraf, and M. Fahad, "Synergistic effect of fly ash and bentonite as partial replacement of cement in mass concrete," *KSCE Journal of Civil Engineering*, vol. 20, pp. 1987-1995, 2016.
- [24] D. Lima-Guerra, I. Mello, R. Resende, and R. Silva, "Use of bentonite and organobentonite as alternatives of partial substitution of cement in concrete manufacturing," *International Journal of Concrete Structures and Materials*, vol. 8, pp. 15-26, 2014.
- [25] B. Masood, A. Elahi, S. Barbhuiya, and B. Ali, "Mechanical and durability performance of recycled aggregate concrete incorporating low calcium bentonite," *Construction and Building Materials*, vol. 237, p. 117760, 2020.
- [26] S. A. Memon, R. Arsalan, S. Khan, and T. Y. Lo, "Utilization of Pakistani bentonite as partial replacement of cement in concrete," *Construction and building materials*, vol. 30, pp. 237-242, 2012.
- [27] J. Mirza, M. Riaz, A. Naseer, F. Rehman, A. Khan, and Q. Ali, "Pakistani bentonite in mortars and concrete as low cost construction material," *Applied Clay Science*, vol. 45, pp. 220-226, 2009.
- [28] W.-H. Huang, "Properties of cement-fly ash grout admixed with bentonite, silica fume, or organic fiber," *Cement and Concrete Research*, vol. 27, pp. 395-406, 1997.
- [29] J. Chamundeeswari, "Experimental Study on Partial Replacement of Cement by Bentonite in Paverblock," *International Journal of Engineering Trends and Technology*, vol. 3, pp. 41-47, 2012.
- [30] T. Akram, S. A. Memon, and M. N. Khan, "Utilization of Jehangira bentonite as partial replacement of cement," in *International Conference on Advances in Cement Based Materials and Applications in Civil Infrastructure ACBM-ACI, Lahore, Pakistan*, 2007, pp. 301-311.
- [31] O. K. Swarup, P. R. Reddy, M. A. K. Reddy, and V. R. Rao, "A Study on Durability of Concrete by Partial Replacement of Cement with Bentonite and Fly Ash," *Int. Chemtech Res*, vol. 10, pp. 855-861, 2017.
- [32] G. V. K. Reddy, V. R. Rao, and M. A. K. Reddy, "Experimental investigation of strength parameters of cement and concrete by partial replacement of cement with Indian calcium bentonite," *Technology*, vol. 8, pp. 512-518, 2017.
- [33] B. Ali, L.A. Qureshi, R. Kurda, Environmental and economic benefits of steel, glass, and polypropylene fiber reinforced cement composite application in jointed plain concrete pavement, *Composites Communications* 22 (2020), 100437.
- [34] FF Wafa, Properties & applications of fiber reinforced concrete, *Engineering Sciences* 2 (1) (1990).
- [35] Najaf E, Abbasi H, Zahrai SM. Effect of waste glass powder, microsilica and polypropylene fibers on ductility, flexural and impact strengths of lightweight concrete. *International Journal of Structural Integrity*. 2022 May 9(ahead-of-print).
- [36] M. Hsie, C. Tu, and P. S. Song, "Mechanical properties of polypropylene hybrid fiber-reinforced concrete," *Mater. Sci. Eng. A*, 2008, doi: 10.1016/j.msea.2008.05.037.
- [37] E. Prabakaran, A. Vijayakumar, J. Rooby, and M. Nithya, "A comparative study of polypropylene fiber reinforced concrete for various mix grades with magnetized water," *Mater. Today Proc.*, 2020, doi: 10.1016/j.matpr.2020.10.108ed concrete aggregate," *Constr. Build. Mater.*, vol. 23, no. 7, pp. 2606-2613, 2009.
- [38] A. Zaman, K. Shahzada, N. Tayyab, Mechanical properties of polypropylene fibers mixed cement-sand mortar, *Journal of Applied Engineering Science* 17 (2) (2019) 116–125.
- [39] P.S. Deb, P. Nath, P.K. Sarker, The effects of ground granulated blast-furnace slag blending with fly ash and activator content on the workability and strength properties of geopolymer concrete cured at ambient temperature, *Master. Des.* 62 (2014) 32–39.
- [40] ASTM C143/C143M "Standard test method for slump of hydraulic-cement concrete", ASTM Standards, 2015.
- [41] BS EN 12390-3 "Testing hardened concrete. Compressive strength of test specimens, British Standards Institution", <https://www.thenbs.com/PublicationIndex/documents/details?Pub=BSI&DocID=288816>.
- [42] ASTM C496/C496M "Standard test method for splitting tensile strength of cylindrical concrete specimens", 2017.
- [43] ASTM C78, "Standard Test Method for Flexural Strength of Concrete," Annu. B. ASTM Stand., 2016.



PERFORMANCE OF SELF-COMPACTING CONCRETE WITH INCORPORATION OF SILICA FUME AND COAL BOTTOM ASH

^aMuhammad Shawaiz Hassan, ^bFaheem Butt, ^cAyub Elahi

a: Department of Civil Engineering, UET, Taxila, Pakistan, shawaizhassan39@gmail.com

b: Department of Civil Engineering, UET, Taxila, Pakistan, faheem.but@uettaxila.edu.pk

c: Department of Civil Engineering, UET, Taxila, Pakistan, ayub.elahi@uettaxila.edu.pk

Abstract- With increasing emphasis on sustainable construction practices, supplementary cementitious materials (SCM's) used in the production of concrete has gained a lot of attention. In current study, the effects of partial Portland cement (PC) replacement with Silica Fume (SF) and Coal Bottom Ash (CBA) on the mechanical and fresh characteristics of self-compacting concrete (SCC) are investigated. By replacing PC with SF and CBA, which are industrial by-products, the environmental impact of concrete production can be reduced while improving its performance. Ten SCC mixes were examined, with varying replacement percentages: SF at 5%, 10%, and 15%; and CBA at 15%, 20%, and 25% by weight of cement content. The investigation of mechanical characteristics through compressive strength and split tensile strength tests, as well as the examination of fresh properties using the slump flow and J-ring tests, gives insightful data.

The results shows that combined incorporation of SF & CBA at 5% & 15% shows a better slump as compared to high replacement level of both the SCM's. The slump of mixes with different ratio goes on decreasing with the increasing percentage of CBA and SF although it falls in acceptable limit. Due to fineness, enhanced surface area and porosity of CBA the water demand increases which cause the decrease of workability. The 28-days Compressive strength and Spilt tensile strength are 28.56 MPa & 2.75 MPa at optimum dosage M-1(5 % SF & 15 % CBA) respectively which are less than control but significantly near control sample strength. The strength decreases with the increase of CBA & SF ratios due to slow pozzolanic reaction of CBA at early ages which however improves at later stages. Moreover, the CBA has enough potential to be employed in SSC production along with SF.

Keywords- Fresh Properties, Self-Compacting Concrete, Compressive Strength, Coal Bottom Ash, Split Tensile strength.

1. Introduction

The production of Portland cement has witnessed significant growth during the industrial revolution, but its environmental impact in terms of carbon dioxide emissions and cost implications in developing nations like Pakistan cannot be ignored. The manufacture of cement significantly increases worldwide carbon dioxide emissions, accounting for over 7% of the total, thereby exacerbating global warming [1].

The Annual Greenhouse Gas Index (AGGI) reaching 1.49 in 2021 reflects a 49% increase in the warming influence of greenhouse gas emissions [1][2]. To address these challenges and promote sustainable construction practices, the utilization of supplementary cementitious materials has gained prominence. Natural pozzolans, known for their unique



5th Conference on Sustainability in Civil Engineering (CSCE'23)

Department of Civil Engineering
Capital University of Science and Technology, Islamabad Pakistan



qualities have garnered significant attention in the construction industry [3]. Researchers are examining how admixtures affect the mechanical properties and durability in both fresh and hardened state to improve the properties of SCC [4]. The mechanical characteristics of the SCC were enhanced by the inclusion of mineral admixtures by up to 15% when compared to regular Portland cement. Up to a certain proportion of replacement, metakaolin in SCC significantly enhanced the mechanical characteristics and reduced concrete specimen absorption [5].

Concrete has been tested using Coal Bottom Ash (CBA), a by-product resulted from coal combustion in thermal power plants, in place of cement. The type of furnace and coal source employed affect the chemical composition and quality of CBA. Meeting certain standards, such as fineness requirements according to ASTM C618, is necessary to activate its pozzolanic properties [6][7]. Concrete's compressive and tensile strength along with durability, and micro structural properties are increased as a result of the reduction in CBA particle size since it has more surface area. Utilizing CBA in concrete production not only provides an economical method of disposal but also encourages sustainability by conserving natural resources [8]. In order to use CBA as pozzolanic material for its replacement against cement, its chemical composition should be in accordance with ASTM C618 for FA Class F or Class C for which the total amounts of $\text{SiO}_2 + \text{Al}_2\text{O}_3 + \text{Fe}_2\text{O}_3$ higher than 70% or 50 % respectively, while SO_3 and LOI must not exceed 5.0 and 6.0%. Moreover the combustion of Lignite or Sub-bituminous coal with a high calcium content falls in class C, while bituminous or anthracite coal with a low calcium contents falls in class F [9]. The utilizing of silica fume with FA & CBA blended cement mortars showed that blended cement with FA & CBA showed lower compressive strength than that of ordinary Portland cement while blended cement with SF showed increased strength [10]. A by-product of quartz reduction in an electric arc furnace known as Silica Fume (SF) has been widely used as a pozzolan in concrete. Its submicron particle size, ranging from 20 nm to 500 nm, contributes to enhanced compressive strength and improved durability when added in optimal quantity [11].

The inclusion of bottom ash along with fly ash in cement blends has been explored, although it leads to lower early-age compressive strength due to the slow pozzolanic reaction. SF with its large surface area and high SiO_2 content, results in increased strength development due to high rate of pozzolanic reaction. [10]. When silica fume is added to concrete, the weak area of the aggregate-cement paste interface bonds better. It aids in the development of early strength because of the higher rate of pozzolanic reaction that result in C-S-H. [12]. The partial replacement of bottom ash along with significant quantity of silica fume can increase the benefits obtained from partial replacement of cement alone with bottom ash [13]. In the past, researchers have performed experiments to study the impact of CBA replacement with cement in normal concrete, but fewer studies have been performed when it comes to SCC. This research aims to investigate the incorporation of SF and CBA in self-compacting concrete as partial replacements against cement. The study's main objective is to assess their impact on mechanical and fresh qualities, such as workability, compressive strength, and split tensile strength. The consumption of sustainable materials can be optimized; this research contributes to the development of environmentally friendly concrete with enhanced performance.

2. Experimental Procedure

2.1 Materials

This study utilizes Ordinary Portland Cement (OPC) type I, which conforms to ASTM C150 standards, as the primary binding component. OPC has specific characteristics such as an initial and final setting time of 45 minutes and 330 minutes respectively and a specific gravity of 3.1 g/cc [14]. Both CBA obtained from power plant and SF are incorporated as SCMs to enhance the concrete properties, Table 1 provides the chemical composition of OPC, CBA, and SF

Table 1 Chemical composition of OPC, CBA and SF

Chemicals	SiO ₂ (%)	TiO ₂ (%)	Al ₂ O ₃ (%)	Fe ₂ O ₃ (%)	MnO (%)	MgO (%)	CaO (%)	Na ₂ O (%)	K ₂ O (%)	P ₂ O ₃ (%)	LOI (%)
OPC	17.9	-	10.7	3.60	-	1.8	62.8	0.9	1.4	-	0.9
CBA	37.47	-	8.57	4.86	-	0.73	10.33	0.14	0.31	-	0.08
SF	94.5	-	0.09	0.10	-	0.43	0.23	-	0.93	-	2.7



For the preparation of SCC, fine aggregate (FA) sourced from Lawrencepur and coarse aggregate (CA) sourced from Kirana hills in Sargodha are utilized. The maximum size of the coarse aggregate used is 12 mm, meeting the specifications of ASTM C33/M, and satisfying the criteria set by ERNARC [15]. Table 2 provides an overview of the physical properties of both fine and coarse aggregates.

Table 2 Physical Properties of fine and Coarse Aggregate.

	FA	CA
Sp. Gravity	2.73	2.68
Water Absorption (%)	1.3	0.5
Bulk Density(Kg/m ³)	-	1612
Fineness Modulus	2.99	-

The coal-fired power station of Sitara Chemicals Industries Pvt. Ltd. in Faisalabad provided CBA that was employed in this investigation as a partial replacement for cement. The CBA sample underwent sieving through a No. 4 sieve and was subjected to both X-ray Diffraction (XRD) analyses to ensure, it met the necessary requirements as a pozzolanic material. The sample was dried and ground at Pakistan Council of Scientific & Industrial Research (PCSIR) Laboratories Peshawar until it reached the desired fineness of 45 µm or less [16]. The chemical composition of the CBA, as shown in Table 1, indicates that the sum of SiO₂, Al₂O₃ and Fe₂O₃ is 50.9%, complying with the ASTM C 618 requirements for Class C [17]. The XRD pattern, depicted in Figure 1, demonstrates the presence of both amorphous and crystalline phases with Quartz and Mullite being the predominant crystalline phases. SF, on the other hand, was obtained from a local supplier in Rawalpindi. As a result of the reduction of high quality quartz with coal in an electric arc furnace, it is an amorphous polymorph of silicon dioxide. It is typically in the form of ultrafine powder, with particle sizes ≤ 0.15 µm [18].

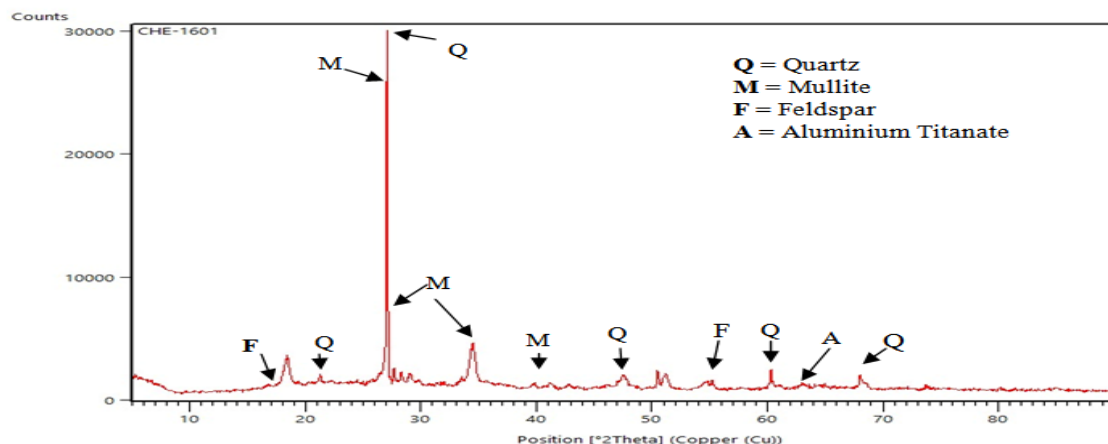


Fig.1 XRD of Coal Bottom Ash used in present study

2.2 Mix Proportions and Sample Preparation

To assess the mechanical and fresh characteristics of (SCC) ten different mixes were prepared. These mixes consisted of a control mix (CC) and nine variations with varying percentages of both SF & CBA. The compositions of the mixes were as follows: M1 (5% SF and 15% CBA), M2 (5% SF and 20% CBA), M3 (5% SF and 25% CBA), M4 (10% SF and 15% CBA), M5 (10% SF and 20% CBA), M6 (10% SF and 25% CBA), M7 (15% SF and 15% CBA), M8 (15% SF and 20% CBA), and M9 (15% SF and 25% CBA). All ingredients were precisely weighed during the batching process. To ensure uniformity and homogeneity, the mixing procedure recommended by previous studies was followed [19]. Viscocrete-3110 super plasticizer (SP) was used within the supplier's specified range to achieve the desired workability of the SCC as shown in Figure 2 (a), (b), (c). The development of the optimal SCC mixes was achieved through iterative adjustments based on the mix design. Cylindrical specimens with dimensions of 150mm x 300mm were casted to



investigate the mechanical properties as depicted in Figure 2(d).



Fig.2: Preparation of samples, (a) Dry mixing of ingredients, (b) CBA, FA & OPC, (c) Super plasticizer (SP) Viscocrete-3110, (d) freshly casted cylinders

2.3 Testing of Specimen

Self-compacting concrete (SCC) was prepared, and the fresh properties were evaluated in light of EFNARC-recommended guideline with slump cone and J-ring as shown in Figure 3 (a) (b) [20]. For the evaluation of mechanical properties, three samples were prepared for each mix to obtain average value. Compressive strength testing was conducted on 150 mm x 300 mm cylinders, following the ASTM C39 standard test method, while split tensile strength was determined according to ASTM C496. Tap water was utilized during sample preparation and curing.

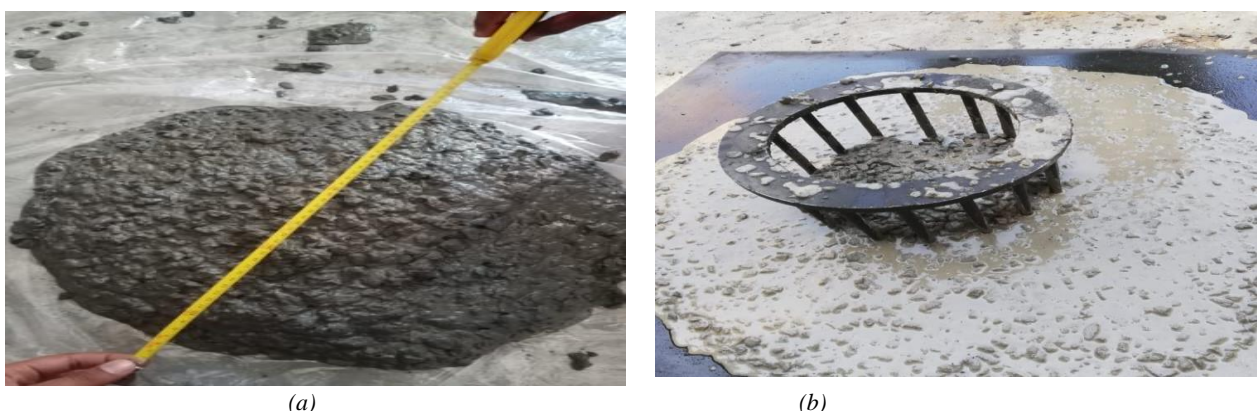


Fig 3: Evaluation of Fresh and hardened properties (a) Slump flow test (b) J-Ring test

All mixtures were kept at a constant water-to-binder ratio of 0.38, and the necessary slump was obtained by changing



the super plasticizer viscoconcrete 3110 dosage to satisfy the requirements established by EFNARC. The cured samples were stored at $23 \pm 2^\circ\text{C}$ for 28 days, immersed in clean water, and subsequently subjected to compressive and split tensile strength testing with Universal Testing Machine (UTM).

3 Results and Discussion

3.1 Slump Flow

The slump test, in accordance with ASTM C1611, was used to evaluate each mixture's workability performance [21]. The results indicated that the workability decreased with increasing amounts of both CBA and SF, with a more pronounced decrease noted at higher substitution levels, as shown in Figure 4.

However, the slump flow measurements for all the mixes fell within the range of 550-650 mm. A slump flow within the range of 500-700 mm is considered satisfactory for self-compacting concrete, as it allows for adequate flowability while avoiding segregation issues [22].

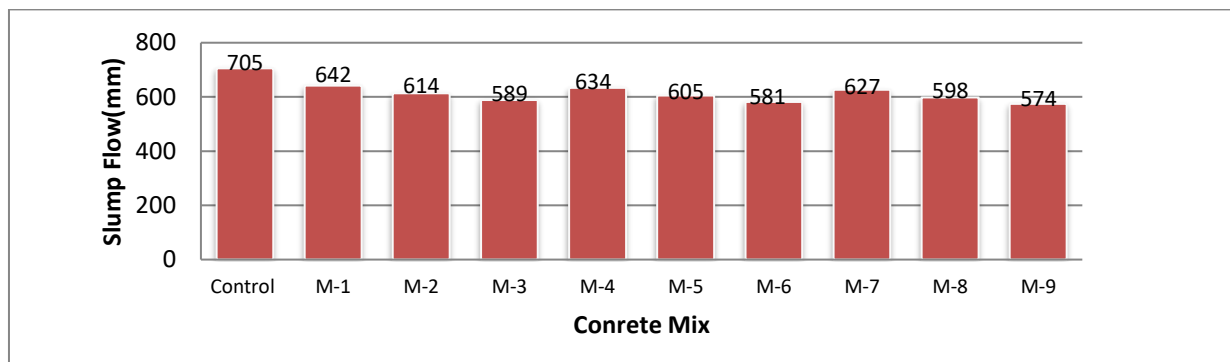


Figure 4: Slump Test Results

3.2 J-Ring

The passing ability of SCC containing CBA and SF was evaluated using the J-Ring test, which assesses the concrete's ability to flow through a confined and constricted area without vibration [20]. The inside and outside height differences between the bars of the J-Ring were measured for each mix, and the spread diameter was recorded, as shown in Figure 5 (a) and (b). The results varied for each blend. As the substitution level of both SCM's increases, height difference between the bars of the J-Ring increased and spread diameter of the concrete decreased. This can be attributed to the higher viscosity and shear stress resulting from the increased fineness and porosity of the concrete due to CBA and SF.

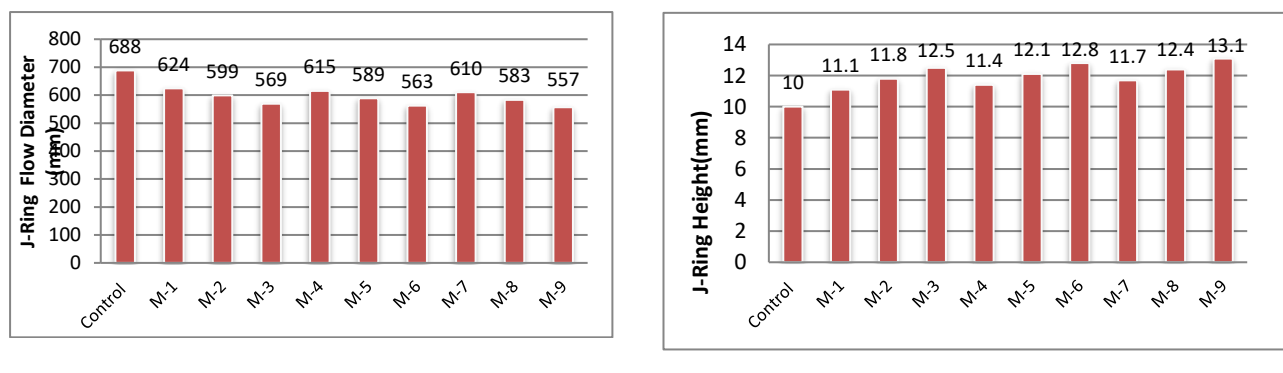


Fig.5: J-Ring Test Results, (a) J-Ring Flow Diameter Results (b) J-Ring Heights Results



3.3 Compressive Strength

Compressive strength testing was conducted following the guidelines of ASTM C-39 [24]. The results, depicted in Figure 6, illustrate the strength variations for different percentages of CBA and SF. After 28 days of curing, the mixture with 5% SF and 15% CBA had the highest strength among other however it was less than the control mix. The compressive strength began to decrease as the percentages of both replacements raise. After 28 days of curing, the lower compressive strength indicates that the pozzolanic reactivity during the early stages did not initiate properly which ultimately produce the desired C-S-H gel within concrete matrix [23]. The addition of SF at lower replacement levels demonstrated a significant increase in strength, comparable to that of the control mix. But the addition of CBA led to a reduction in compressive strength [22]. The improved strength with addition of SF is associated with micro-fillet effect and enhanced pozzolanic reactivity between SF and calcium hydroxide, leading to the development of C-S-H gel. On the other hand, the pozzolanic activity of CBA with lime is relatively low during the early stages and starts to increase significantly after 28 days [25]. The pozzolanic capacity of a material refers to its ability to react with $\text{Ca}(\text{OH})_2$, and the rate of this reaction depends on factors such as temperature, water-to-solid ratio, alkaline content, and, most importantly, the surface area of the pozzolan. After 14 days of curing, CBA's beneficial pozzolanic effect becomes more prominent, while consumption of $\text{Ca}(\text{OH})_2$ only begins to occur after 90 days of curing period [9].

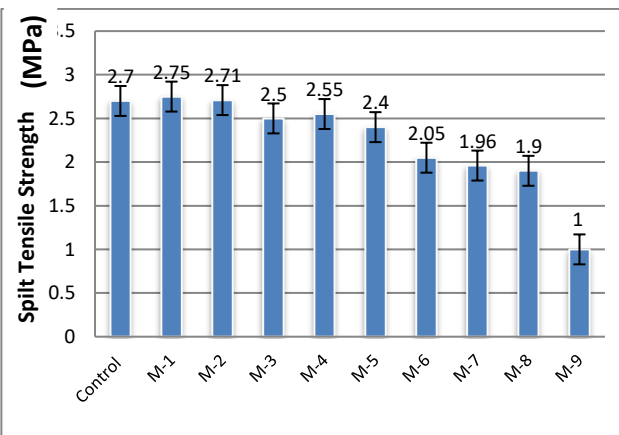
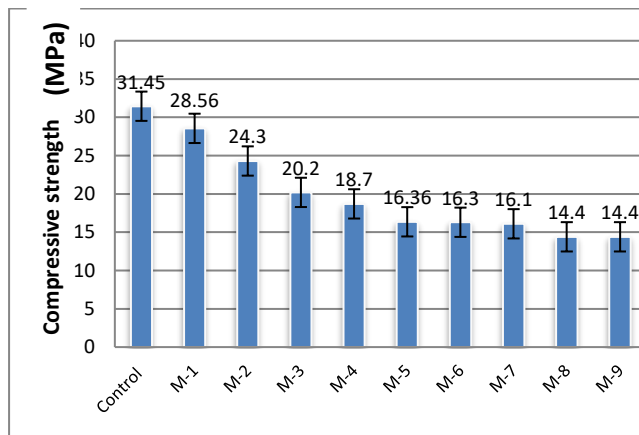


Fig 6. Compressive strength test results at 28 days Fig 7. Split Tensile strength test results at 28 days

3.4 Split tensile Strength

The split tensile strength of the SCC cylinders was evaluated following ASTM C-496. As depicted in Figure 7, the results show decline of split tensile strength with increasing percentages of both CBA and SF. The findings suggest that the inclusion of CBA and SF negatively impacts the split tensile strength. Mix M-1(5% SF and 15% CBA) had the highest split tensile strength among the evaluated mixtures after 28 days of curing period. It is important to note that the strength of the concrete begins to decrease when the amount of SF exceeds 5% and with an increasing percentage of CBA. However, a slight improvement in strength was observed at later stages of curing.

4 Conclusions

In conclusion, this study demonstrated the potential of both the SCM's (CBA &SF) as viable replacements for cement in (SCC). The findings revealed that.

- With the increase of CBA and SF percentages, the workability of the SCC mixes decreased while still meeting the required slump criteria.
- Optimum replacement levels of 5% SF and 15% CBA were identified, offering satisfactory workability and acceptable mechanical strength. Although the compressive strength and split tensile strength of these mixes were lower compared to the control mix, they were suitable for normal to medium strength concrete applications.



5th Conference on Sustainability in Civil Engineering (CSCE'23)

Department of Civil Engineering
Capital University of Science and Technology, Islamabad Pakistan



Future research should focus on investigating the long-term effects of CBA and exploring additional sources of this sustainable material. Overall, the incorporation of CBA and SF in SCC presents a promising approach for enhancing sustainability in concrete production and addressing waste management challenges.

References

- [1] Memon, S. A., et al. (2012). "Utilization of Pakistani bentonite as partial replacement of cement in concrete." **30**: 237-242.
- [2] Butler, j. and Montzka, s. (2021). The NOA Annual Greenhouse gas index (aggi). Earth system research laboratory, global monitoring division.
- [3] Wajahat, Raja, Zahoor Khan, Muhammad Yaqub, Muhammad Noman, and Rana Muhammad Waqas. 2021. "Evaluation of Mechanical and Micro structural Properties of Mortar Reinforced with Carbon Nano tubes at Elevated Temperatures." *Pakistan Journal of Engineering and Technology* 1–6
- [4] Uzal, B. and L. Turanli. 2003. "Studies on Blended Cements Containing a High Volume of Natural Pozzolans." *Cement and Concrete Research*.
- [5] Effects of Admixtures on the Self Compacting Concrete State of the Art Report S Christopher Gnanaraj1, Ramesh Babu Chokkalingam2 and G LiziaThankam3 DOI 10.1088/1757-899X/1006/1/012038.
- [6] An Overview of Fly Ash and Bottom Ash Replacement in Self-Compacting Concrete *Key Engineering Materials* Vols 594- 595 (2014) pp 465-470doi:10.4028/www.scientific.net/KEM.594-595.465.
- [7] Properties of mortar made with bottom ash and silica fume as sustainable construction materials. Article in *World Journal of Engineering* · April 2022 DOI: 10.1108/WJE-08-2021-0481.
- [8] Reviewing the role of coal bottom ash as an alternative of cement "Construction and Building Materials 233 (2020) 117276"
- [9] Potential use of Malaysian thermal power plants coal bottom ash in CONSTRUCTION.C International Journal of Sustainable Construction Engineering & Technology (ISSN: 2180-3242) Vol 3, Issue 2, 2012
- [10] Compressive strength, microstructure, and thermal analysis of autoclaved and air cured structural lightweight. concrete made with coal bottom ash and silica fume. *Materials Science and Engineering A* 527 (2010)
- [11] The effect of silica fume fineness on the improvement of Portland cement strength performance. *Construction and Building Materials* 96 (2015) 55–64
- [12] Investigation on Mechanical and Durability properties of concrete mixed with silica fumes as cementsations. Material and coal bottom ash as fine aggregate replacement material *Buildings* **2022**, 12(1), 44; <https://doi.org/10.3390/buildings12010044>.
- [13] Cementations composition containing Bottom ashes pozzolan and concretes and mortars therefrom ". United States Patent 19 Hopkins et al. USOO.5849075A 11 Patent Number: 5,849,075 (45) Date of Patent: Dec. 15, 1998. AA. C. /. C150M-20,
- [14] Standard Specification for Portland Cement," *ASTM International, West Conshohocken, PA*, 2020.
- [15] Specification and Guidelines for Self-Compacting Concrete by the European Federation of Producers and Contractors of Specialist Products for Structures" by EFNARC in February 2002
- [16] Hopkins et al. Cementations composition containing bottom ashes pozzolans and concretes and mortars.
- [17] Potential use of Malaysian thermal power plants Coal Bottom Ash in construction *International Journal of Sustainable Construction Engineering & Technology* (ISSN: 2180-3242) Vol 3, Issue 2, 2012
- [18] Micro Silica in Concrete—The Special Concrete. *International Journal of Research (IJR)* e-ISSN: 2348-6848, ISSN: 2348-795X Volume 2, Issue 08, August 2015
- [19] Fresh and rheological behavior of nano-silica and fly ash blended self-compacting concrete. *Construction and Building Materials* 95 (2015) 29–44.
- [20] The European Guidelines for Self-Compacting Concrete
- [21] A.C.1611,"StandardTestMethodforSlumpFlowofSelf-ConsolidatingConcrete
- [22] Compressive strength, water absorption, sorptivity, abrasion resistance and permeability of self-compacting Concrete containing coal bottom ash "Rafat Siddique" *Construction and Building Materials* 47 (2013) 1444
- [23] A. C39, ""Standard Test Method for Compressive Strength of Cylindrical Concrete Specimens"
- [24] The effect of fly ash and silica fume on self-compacting high performance concrete F.A. Mustapha a,b, A. Sulaiman a, R.N. Mohamed a, S.A. Umara
- [25] An investigation of bottom ash as a pozzolanic material. *Construction and Building Materials* 186 (2018) 155–162.



EFFECT OF HEAT ON SELF-COMPACTING CONCRETE WITH PARTIAL SUBSTITUTION OF FOUNDRY SAND AS FINE AGGREGATE AND ADDITION OF PROPYLENE FIBERS

^aRizwan Ghafoor, ^bMuhammad Yaqoob, ^cMuhammad Umer Malik*

a: Department of Civil Engineering, UET, Taxila, Pakistan, rizwanghafoor39@gmail.com

b: Department of Civil Engineering, UET, Taxila, Pakistan. muhammad.yaqub@uettaxila.edu.pk

c: Department of Civil Engineering, UET, Taxila, Pakistan, muhammadumermalik061@gmail.com

*Corresponding author: Email ID: rizwanghafoor39@gmail.com

Abstract- Foundry sand mainly consists of silicates, and it is used as a replacement of fine aggregate to make self-compacting concrete that is cheaper, better for the environment, and sustainable. This research study looked at how at elevated temperatures foundry sand and propylene fibers (PPF) changed the mechanical properties of self-compacting concrete. 25% cement was replaced with fly ash, fine aggregate with foundry sand at different proportions (0%, 20%, 30% & 40%) and propylene fibers in 0.75% were added. The goal was to determine the mechanical properties of above-mentioned mixes of self-compacting concrete at 25°C, 300°C, 400°C and 500°C and to compare them with normal mix self-compacting concrete. The ratio adopted for the testing is of 1:1.56:2.60 (Binder: Fine Aggregate: Coarse Aggregate). For examining the mechanical characteristics of concrete the tests carried out were splitting tensile strength, compressive strength and Flexural strength tests. Experimental results show that the mix with 25% fly ash, 20% foundry sand replacement with addition of 0.75% of propylene fibers has performed better than all other samples including the control mix at all elevated temperature.

Keywords- Foundry Sand, Elevated temperature, Heat effect, Propylene fibers, Mechanical properties.

1 Introduction

Heat is natural but sometimes it becomes accidental phenomena. Thousands of structures catch fire annually. Heat reduced the strength of concrete and made the structure unsafe. Although a lot of prevention has been taken to control the fire in buildings but still, they are under process. To make a safe structure against fire up to a certain time limit is the main purpose of the following study. When a closed room catches fire then the temperature of the structural elements gets increased with time. Concrete is an important building material that is used all over the world. Concrete comprises water, cement, sand, and small rocks. Researchers are trying to encourage builders to use natural pozzolanic materials as supplementary cementing materials (SCMs). Using SCMs, the carbon dioxide's (CO₂) amount releasing into atmosphere during the cement-making process can be kept to a minimum [1]. Natural pozzolans can be used instead of cement in concrete because they have unique properties like low permeability, less heat of hydration, high sulphate resistance, and an enhancement to the ultimate concrete strength [2].

This study investigates the use of foundry sand, an industrial byproduct that is a high-quality silica sand with consistent physical properties. Due to its exceptional heat conductivity, foundry sand has been used for millennia in the ferrous and nonferrous metal casting industries as a byproduct. Sand is an essential component of the casting of metal process, and foundries frequently recycle and reuse it until it is no longer acceptable, at that point it is known as "foundry sand." According to research by Siddique and de Schutter [3], up to 10 million tonnes of foundry sand are thrown away each year in the United States alone but may potentially be repurposed. In trials done by Siddique et al. [4], waste foundry sand was



used to replace as much as thirty percent of the normal sand in concrete. Khatib and Ellis [5], on the other hand, substituted up to 100% of the used sand with old foundry sand and noticed a decline in strength as the foundry sand percentage rose.

By nature, concrete is brittle material, hence, to improve the ductile properties of concrete, researchers have used fiber reinforcements and other materials [6,7]. PPF are excellent polymer fibers because of its low cost, lightweight, low thermal conductivity and high modulus of elasticity [8]. Incorporating PPF into concrete can assist reduce drying shrinkage and increase compressive, flexural, and tensile strength [9,10]. Afzadi et al. [11] researchers examined the mechanical properties of mortars reinforced with PPF and discovered that ductility was greatly enhanced. There was no decrease in strength up to the optimal level of 0.75% PPF.

There are different individual studies carried out to study the impact of using foundry sand as fine aggregate and polypropylene fibers on self-compacting concrete's properties, no previous study has been carried out to analyze the synergistic effect of heat on self-compacting concrete made by replacement of foundry sand as fine aggregate with addition of polypropylene fibers on the performance of concrete. This study examined the effect of heat on SCC made with foundry sand and PPF on concrete's fresh and mechanical properties.

2 Experimental Procedures

2.1 Materials with their Properties and Mix Proportions

Fly ash (FA) and ordinary Portland cement, or OPC for short, were used as the binding ingredients in this research project. OPC type 1 cement, as specified by ASTM C150, was used [12]. Locally available foundry sand was purchased from the Heavy Mechanical Complex in Taxila, Pakistan. LawrencePur and Margalla, respectively, provided the fine and coarse aggregates. 19 mm long propylene fibre was used. Tap water was used for concrete mixing and curing. The superplasticizer, Ultra-Super Plasticizer 470 was added to concrete mixtures since foundry sand and PPF make the concrete less workable. The parameters of aggregate and PPF are shown in Tables 1 and 2, whereas the parameters for fly ash and sand from foundries are shown in Table 3.

Table 1. Physical properties of fine and coarse aggregates.

Properties	Fine aggregates	Coarse aggregates
Specific gravity	2.7	2.65
Water absorption (%)	1.3	0.54
Loose density (kg/m^3)	-	1412
Rodded density (kg/m^3)	-	1550
Fineness modulus	2.99	

Table 2. Properties of Propylene Fiber.

Properties	Values
Tensile strength at breaking (MPa)	31 - 41
Flexural strength (MPa)	41 - 55
Elongation at break (%)	100 - 600
Tensile modulus (MPa)	1137 - 1551
Specific gravity	0.9 - 0.91

Table 3. Properties of Fly ash and Waste foundry sand.

Chemical Compounds	Fly ash	WFS
CaO (%)	2.92	1.65
SiO ₂ (%)	61.20	88.11
Al ₂ O ₃ (%)	28.23	0.49
Fe ₂ O ₃ (%)	3.90	2.38
MgO (%)	0.93	0.76
SO ₃ (%)	0.73	-
Na ₂ O (%)	0.01	0.95
K ₂ O (%)	1.34	0.83
TiO ₂ (%)	-	0.10
Loss on ignition (%)	0.74	4.73



The experimental schedule is shown in Table 4, which consists of comparing nine different mixes. M1 denoted the control mix having OPC as the only binder, while M2, M3 and M4 denoted the mixes containing 20%, 30% and 40% foundry sand as fine aggregate replacement respectively. Poly propylene fiber was also added in 0.75% in M2, M3 and M4 respectively.

Table 4. Mix Composition

Mix	Mix Type	Temperature (°C)	Cubes (28 days)	Beams (28 days)	Cylinders (28 days)
M1	Control Mix (SCC)	25	3	3	3
M1	Control Mix (SCC)	300	3	3	3
M1	Control Mix (SCC)	400	3	3	3
M1	Control Mix (SCC)	500	3	3	3
M2	OPC+20% F.S.W+0.75% PPF	25	3	3	3
M2	OPC+20% F.S.W+0.75% PPF	300	3	3	3
M2	OPC+20% F.S.W+0.75% PPF	400	3	3	3
M2	OPC+20% F.S.W+0.75% PPF	500	3	3	3
M3	OPC+30% F.S.W+0.75% PPF	25	3	3	3
M3	OPC+30% F.S.W+0.75% PPF	300	3	3	3
M3	OPC+30% F.S.W+0.75% PPF	400	3	3	3
M3	OPC+30% F.S.W+0.75% PPF	500	3	3	3
M4	OPC+40% F.S.W+0.75% PPF	25	3	3	3
M4	OPC+40% F.S.W+0.75% PPF	300	3	3	3
M4	OPC+40% F.S.W+0.75% PPF	400	3	3	3
M4	OPC+40% F.S.W+0.75% PPF	500	3	3	3
	Mechanical Testing		Compressive Strength	Flexural Strength	Split Tensile Strength

2.2 Concrete Mixing

Every batch of concrete was mixed in three steps. In the initial phase, aggregates and binders were combined dry. In second phase, more than half of water was added to create a uniform mixture, while the part of water remained, along with superplasticizer were then added. PPF was incorporated in the end to avoid the clumping of fibers due to more revolutions of mixer.

2.3 Specimen and Testing

During the casting of samples, one layers of concrete were applied to every sample. Using ASTM C1611 procedure, the self-compacting concrete slump flow was determined prior to specimen casting [13]. For determination of mechanical characteristics of concrete samples Compressive strength test, splitting tensile strength test, and flexural strength tests were done. Based on BS standard EN-12390 [14], 150mm x 150mm x 150mm cube specimen were casted, and then tested for compressive strength after being cured for 28 days.

After 28 days of curing, 150mm x 300mm concrete cylindrical samples were tested for the split tensile strength in accordance with ASTM C496 criteria [15]. The beam specimens measuring 100mm x 100mm x 500mm were tested for flexural strength in accordance with ASTM C78 specifications [16]. The test setup for these mechanical properties is given in Figure 1.



a)

b)

c)

d)

Figure 1 Testing formation for (a) Slump flow test (b) compressive test (c) split tensile test (d) flexural test

3 Research Methodology

Four types of mixes were prepared in Laboratory. Slump flow test was conducted firstly to determine the fresh properties of SCC, then to find out the mechanical properties' compressive strength test, flexural test and split tensile strength were done in the laboratory after 28 days curing in water tank at normal temperature. After that sample of all the mixes were taken to the oven for heating at 300°C, 400°C and 500°C for two hours. After getting cooled, these samples were taken to the Laboratory for the determination of their mechanical properties.

4 Results

4.1 Slump Flow

The workability of all the mixes was determined using slump cone apparatus based on procedure given by ASTM C1611. To create workable mixtures, varied amounts of superplasticizer were combined with a consistent water-cement ratio. Figure 2 displays the results of the workability of each mixture. The mix M2, M3, and M4 which has percentage of Foundry sand, fly ash and propylene fibers produced somewhat lower slumps than the control mix (M1). The reduction in mixes workability can be related with fineness of foundry sand as it more fine than fine aggregate. The addition of PPF to the mixtures has also significantly decreased their workability because the concentration of fibers enhances internal friction in mixtures with a constant amount of water added.

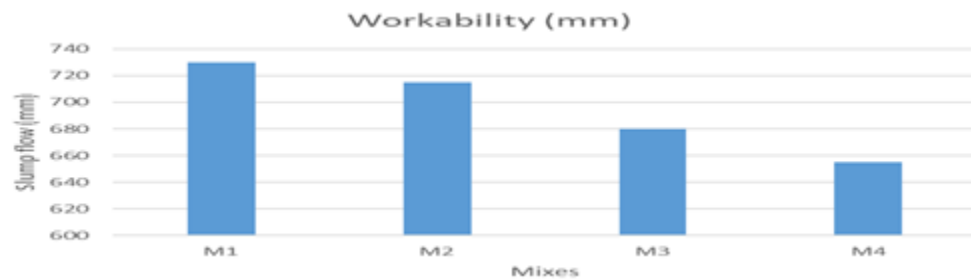


Figure 2: Slump Flow Test

4.2 Compressive Strength

According to Figure 3, which illustrates the compressive strength measurements for all the mixes, the results demonstrate that incorporating foundry sand led to enhanced compressive strength properties after a 28-day curing period. Specifically, for mixture M2, the compressive strength increased by 2.87%, 7.68%, 12.42%, 16.20% at 25°C, 300°C, 400°C and 500°C respectively, in comparison with the mix (M1) that is control mix. The enhancement in strength can be accredited to the formation of additional cementitious compounds from the pozzolanic reaction, fineness of foundry sand as well as the filler properties of fly ash, and addition of PPF to contract cracks. These properties result in a more tightly packed and finer microstructure for the concrete. The acquired results indicate that these samples performed better than control mix self-compacting concrete samples at elevated temperatures.

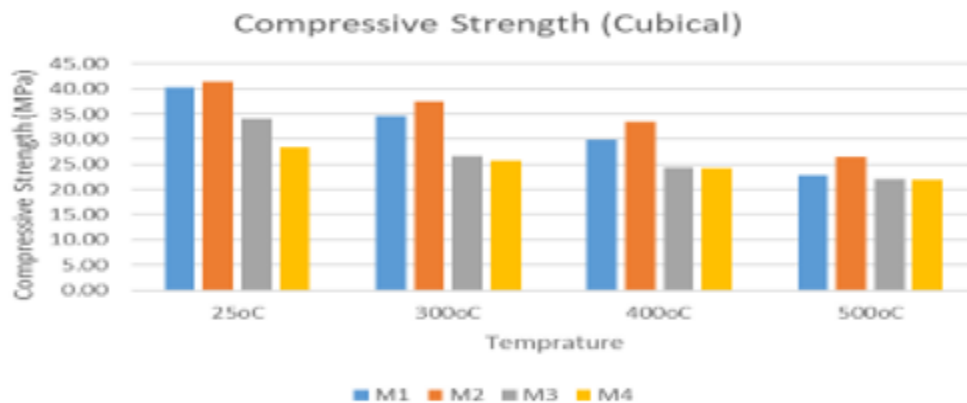


Figure 3 Compressive Strength Test

4.3 Split Tensile Strength

Figure 4 displays the split tensile strength values for all the mixtures. Following a 28-day curing period, it can be observed that the mixtures incorporating foundry sand exhibited superior performance compared to the controlled mix at elevated temperatures. Specifically, for mix M2, the splitting tensile strength increased by 3.48%, 21.38%, 21.25%, 11.89% after 28 days at 25°C, 300°C, 400°C and 500°C respectively, in comparison to mix M1. These results indicate that the inclusion of foundry sand positively influenced the split tensile strength of the concrete samples, particularly at higher temperatures. The increase in split tensile strength could possibly be explained by the coarse texture of the fibers, which enhances the adhesion and bonding between the concrete and the fibers. On the onset of cracking in concrete, the fibers begin to arrest the crack propagation due to their bridging impact, reducing the brittleness of the concrete and boosting its post-cracking behavior.

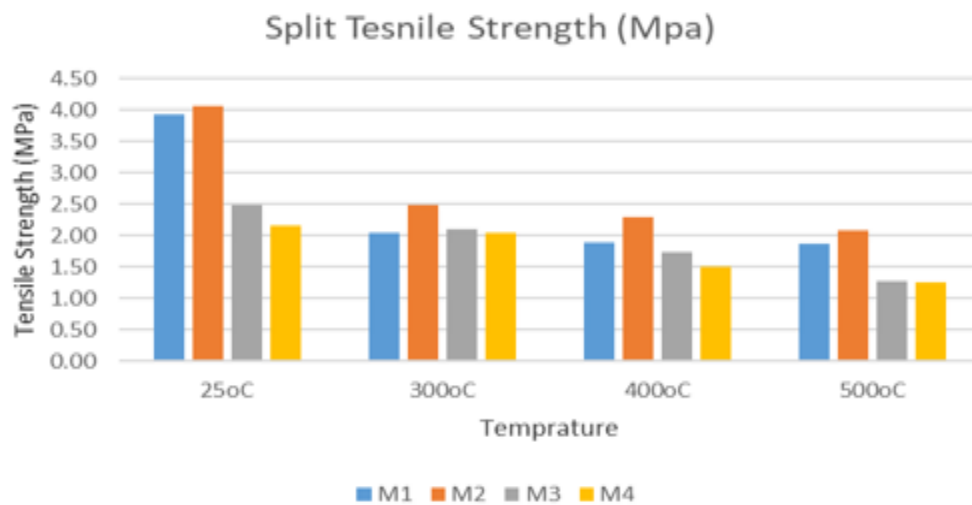


Figure 4 Split Tensile Strength Test

4.4 Flexural Strength

Figure 5 depicts the concrete's flexural strength of all specimens. Using foundry sand in self-compacting concrete enhanced flexural strength after being cured for 28 days. M2, M3 and M4 boosted the strength by 8.11%, 2.27% and 12.12% and 12.50% at 25°C, 300°C, 400°C and 500°C respectively when compared to the control mix (M1). The enhanced flexural strength results from the adherence of PPF fibers to the matrix and the enhanced bond quality, which prevents crack propagation. The incorporation of randomly mixed fibers resulted in an improvement of crack resistance, which can be attributed to the bridging effect. This effect, in turn, led to an increase in ductility and flexural strength.

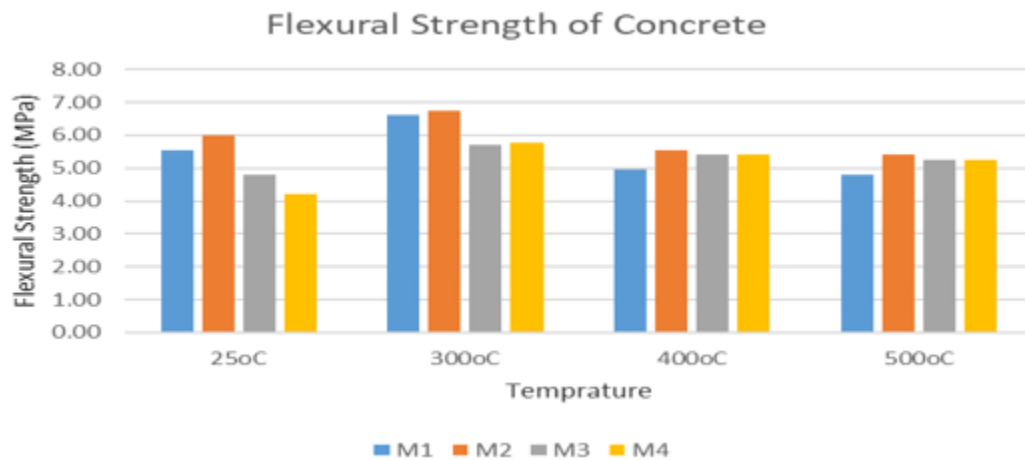


Figure 5 Flexural Strength Test

5 Conclusions

Based on the conducted experimental study, the study's findings lead to the following conclusions:

- 1- The workability of foundry sand incorporated mixes was lowered, while incorporation of Propylene fibers caused in further decrease of workability.
- 2- The addition of foundry sand as fine aggregate enhanced the mechanical characteristics (flexural, split tensile and Compressive strengths) of concrete.
- 3- By addition of 25% fly ash, 20% foundry sand as fine aggregate with addition of 0.75% propylene fibers in SCC formation, the mechanical properties like compressive, flexural and tensile strength at 25°C has been increased by 2.87%, 8.11%, and 3.48% respectively.
- 4- While at 300°C, the mechanical properties like compressive, flexural and tensile strength have been increased by 7.68%, 2.27%, and 21.38% respectively.
- 5- While at 400°C, the mechanical properties like compressive, flexural and tensile strength have been increased by 12.42%, 12.12%, and 21.25% respectively.
- 6- While at 500°C, mechanical properties like compressive, flexural and tensile strength have been increased by 16.2%, 12.50% and 11.89% respectively.
- 7- The incorporation of high dosage 30% and 40% of foundry sand content resulted in degradation of the mechanical characteristics of self-compacting concrete.

Acknowledgment

The authors express their sincere gratitude to all individuals and departments who provided support throughout the research process. Special thanks are extended to the Civil Engineering and Industrial Departments of UET Taxila, as well as Engr. Dr. Muhammad Yaqoob for their invaluable contributions and to my parents and friends for their support.

References

- [1] UN Environment, K.L. Scrivener, V.M. John, E.M. Gartner, Eco-efficient cements: Potential economically viable solutions for a low-CO₂ cement-based materials industry, Cement and Concrete Research 114 (2018) 2–26
- [2] “Use of Natural Pozzolans in Concrete (ACI 232.1R),” ACI Mater. J., 1994, doi: 10.14359/4060.
- [3] Siddique R, de Schutter G. Effect of used foundry sand on the mechanical properties of concrete. Constr Build Mater 2009;23(2):976–80.
- [4] Siddique R, Gupta R, Kaur I. Effect of spent foundry sand as partial replacement of fine aggregate on the properties of concrete. In: 22nd International conference on solid waste technology and management, Widener University, Phila. USA; 2007. p. 1386.



5th Conference on Sustainability in Civil Engineering (CSCE'23)

Department of Civil Engineering

Capital University of Science and Technology, Islamabad Pakistan



- [5] Khatib JM, Ellis DJ. Mechanical properties of concrete containing foundry sand. ACI Spec. Publication SP-200 2001:733–48.
- [6] B. Ali, L.A. Qureshi, R. Kurda, Environmental and economic benefits of steel, glass, and polypropylene fiber reinforced cement composite application in jointed plain concrete pavement, Composites Communications 22 (2020), 100437.
- [7] FF Wafa, Properties & applications of fiber reinforced concrete, Engineering Sciences 2 (1) (1990).
- [8] C. S. Das, T. Dey, R. Dandapat, B. B. Mukharjee, and J. Kumar, “Performance evaluation of polypropylene fiber reinforced recycled aggregate concrete,” Constr. Build. Mater., 2018, doi: 10.1016/j.conbuildmat.2018.09.036.
- [9] M. Hsie, C. Tu, and P. S. Song, “Mechanical properties of polypropylene hybrid fiber-reinforced concrete,” Mater. Sci. Eng. A, 2008, doi: 10.1016/j.msea.2008.05.037.
- [10] E. Prabakaran, A. Vijayakumar, J. Rooby, and M. Nithya, “A comparative study of polypropylene fiber reinforced concrete for various mix grades with magnetized water,” Mater. Today Proc., 2020, doi: 10.1016/j.matpr.2020.10.108.
- [11] A. Zaman, K. Shahzada, N. Tayyab, Mechanical properties of polypropylene fibers mixed cement-sand mortar, Journal of Applied Engineering Science 17 (2) (2019) 116–125.
- [12] ASTM C150 “ASTM C150 / C150M-19a Standard specification for Portland Cement”, 2019.
- [13] ASTM C143/C143M “Standard test method for slump of hydraulic-cement concrete”, ASTM Standards, 2015.
- [14] BS EN 12390-3 “Testing hardened concrete. Compressive strength of test specimens, British Standards Institution”, <https://www.thenbs.com/PublicationIndex/documents/details?Pub=BSI&DocID=288816>.
- [15] ASTM C496/C496M “Standard test method for splitting tensile strength of cylindrical concrete specimens”, 2017.
- [16] ASTM C78, “Standard Test Method for Flexural Strength of Concrete,” Annu. B. ASTM Stand., 2016.



CONCRETE EVOLUTION: AN ANALYSIS OF RECENT ADVANCEMENTS AND INNOVATIONS

^aAli Ajwad*

a: Doctoral Candidate, Department of Civil Engineering, University of Salerno, Italy, aajwad@unisa.it

Abstract- This comprehensive review article aims to provide a detailed overview of the significant advancements in concrete development over the past decade. It covers a wide range of aspects within concrete technology, including the emergence of novel materials, sustainable practices, durability enhancements, advanced manufacturing techniques, and emerging trends. By examining these key areas, the review aims to offer a critical analysis of the advancements, evaluating their benefits, limitations, and potential avenues for further research and improvement. Through this comprehensive exploration, the article serves as a valuable resource for researchers, engineers, and industry professionals, enabling them to stay updated on the latest trends and make informed decisions in the field of concrete technology.

Keywords- Concrete development, sustainability, durability, advanced manufacturing techniques, 3D printing, digital technologies

1 Introduction

Concrete, the most widely used construction material, has undergone significant advancements in recent years, particularly in the past decade. Intensive research and development efforts have focused on improving concrete technology by enhancing its properties, promoting sustainability, extending durability, and exploring advanced manufacturing techniques. Sustainability has been a central theme, with the utilization of alternative binders like fly ash, slag, and silica fume to reduce the carbon footprint in concrete production. This article provides an overview of these key developments, highlighting concrete's transformative journey. Its versatility has shaped the built environment, contributing to infrastructure, architectural construction, and economic growth. Advancements in self-compacting, high-performance, and fiber-reinforced concrete have enhanced structural performance, durability, and sustainability, enabling ambitious designs. Ongoing research and innovation will continue to shape the future of concrete technology and the built environment.

Concrete technology encompasses a wide range of research and advancements aimed at improving the performance, durability, sustainability, and design flexibility of concrete materials. Numerous studies conducted have explored the influence of materials like fly ash [1][2], silica fume [3][4], metakaolin [5][6], and rice husk ash [7] on concrete strength, durability, and sustainability. These studies have investigated the impact of these materials on various properties of concrete. Additionally, researchers have examined the effectiveness of various admixtures, such as superplasticizers [8] [9], viscosity-modifying admixtures (VMA) [10], and corrosion inhibitors in improving workability, rheology, and mitigating durability issues. Moreover, innovative curing methods like internal curing [11], steam curing [12] [13], and carbonation curing have been investigated to enhance early-age strength development, reduce shrinkage, and improve durability. Construction techniques like precast concrete, fiber-reinforced concrete [14], and 3D printing [15] have also been explored for their potential in improving construction efficiency, durability, and design possibilities. These studies, along with many others conducted highlight the ongoing efforts and significant advancements in concrete technology, shaping the future of sustainable and resilient construction.



1.1 Purpose, Scope, Importance and Outline of the Review

This review article examines the advancements in concrete technology over the past decade. Concrete is crucial for infrastructure and building construction, making it essential to understand the latest innovations for improved performance, durability, sustainability, and design possibilities. By exploring developments in mix design, additives, curing methods, construction techniques, and sustainable practices, this article provides a comprehensive overview. It analyzes the impact of these advancements on concrete properties, construction efficiency, environmental impact, and long-term performance. The aim is to contribute to the collective understanding, offer insights for future research, and promote progress in the field of concrete technology. This comprehensive review article examines advancements in concrete technology over the past decade, focusing on key areas such as mix design, additives, curing methods, construction techniques, and sustainable practices. It analyzes studies, research papers, and technological developments from various sources to provide a holistic overview. The impact on concrete properties, construction efficiency, sustainability, and long-term performance is assessed, along with potential implications and future directions for the field. By considering a broad range of topics, this review aims to offer a comprehensive assessment of advancements in concrete technology. This review provides a comprehensive overview of recent advancements in concrete technology. It is a valuable resource for engineers, researchers, and professionals in the construction industry to stay informed about the latest innovations. By consolidating existing knowledge, it promotes the adoption of advanced techniques, materials, and practices. The review also identifies research gaps and guides future research efforts, ultimately enhancing the performance, durability, sustainability, and design possibilities of concrete structures. This article provides a comprehensive review of advancements in concrete technology over the past decade. By analyzing key areas such as novel materials, sustainable practices, durability enhancements and advanced manufacturing techniques with the use of AI, the review offers valuable insights into the latest developments. It also identifies research gaps and suggests future directions, contributing to the advancement of the field. The review serves as a valuable resource for professionals in the construction industry.

2 State of the Art

2.1 Novel Materials

2.1.1 Ultra-High-Performance Concrete (UPHC)

Ultra-High-Performance Concrete (UHPC) has gained significant attention due to its exceptional strength, durability, and ductility which includes enhanced energy absorption capability before failure in addition to enhanced flexural strength (Figure 1). However, the high cost of raw materials and specialized manufacturing techniques associated with UHPC currently limit its widespread adoption. To overcome these challenges, further research is needed to optimize production processes, explore cost-effective alternatives for raw materials, and develop standardized mix designs that balance performance and affordability [16].

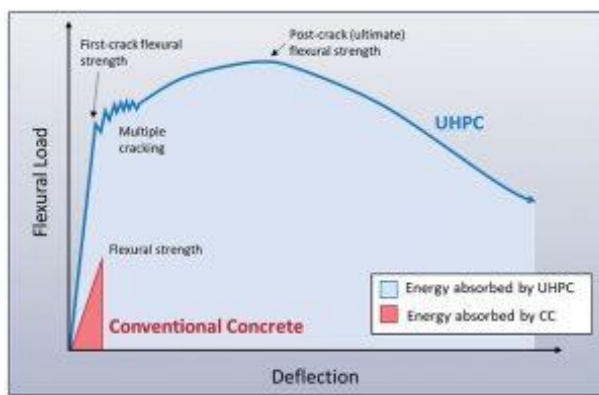


Figure 1 Load-Deflection Comparison for UPHC and Conventional Concrete (M.K. Tedros et al. [17])

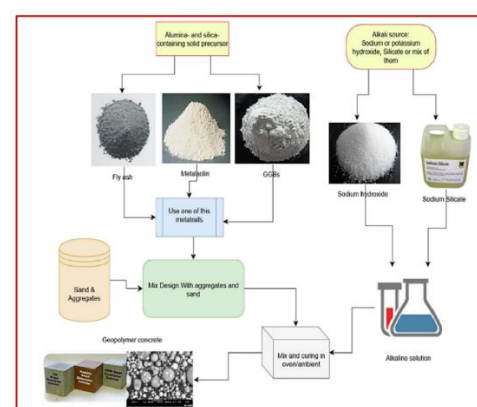


Figure 2 Geopolymer Concrete Production Process (S. Karthik, [18])



2.1.2 Geopolymer Concrete

Geopolymer concrete (Figure 2), an eco-friendly alternative to traditional cementitious materials, offers reduced carbon emissions and improved long-term durability. Although, challenges related to limited availability and variations in material properties need to be addressed. Standardization of production methods, quality control measures, and guidelines for incorporating geopolymer concrete into construction practices are essential to facilitate its wider use [19] [20].

2.1.3 High Strength Fiber-Reinforced Concrete (HSFRC)

High-Strength Fiber-Reinforced Concrete (HSFRC) combines the benefits of fiber reinforcement and high-strength concrete, resulting in improved structural performance and durability. Still, the optimal fiber type, dosage, and distribution in HSFRC require further investigation. Additionally, long-term performance studies are necessary to evaluate the durability of HSFRC structures exposed to different environmental conditions [21] [22].

2.2 Sustainable Practices

2.2.1 Supplementary Cementitious Materials (SCMs)

The utilization of Supplementary Cementitious Materials (SCMs), such as fly ash, slag, and silica fume, as partial replacements for cement in concrete production has gained traction for its potential to reduce the carbon footprint and improve long-term durability. Table 1 shows the current level of understanding and usage of numerous SCMs around the globe. Nevertheless, challenges related to variations in SCM properties and their influence on concrete performance need to be addressed. Standardization of SCM production, quality control, and guidelines for their incorporation into concrete mixes are crucial to ensure consistent quality and performance [23] [24].

Table 1 Detail of SCMs

Material	Chemistry	Volume est. (Mt/y)	In use	Comments	Reference
Coal Fly Ash – Si Rich	Si-Al	600-900	Y	Subject to Limitation of Carbon Content and Reactivity	Kumar, A., & Bhattacharjee, B. [25]
Blast Furnace Slag	CA-Si-Al	300-360	Y	Nearly fully used	Mehta, P. K., & Siddique, R. [26]
Silica Fume	Si	1-2.5	Y	Used in HPC	Hossain, K. et al. [27]
Coal Fly Ash – Ca Rich	Si-Ca-Al	100-200	Y	Subject to limitations on C, CaO, MgO content	Mehta, P. K., & Siddique, R. [28]
Limestone	CaCO ₃	300	Y	Used in combination with reactive aluminates	Bouziani, T. et al. [29]
Calcinated Clays	Si-Al	2-3	Y	Metakaolin performs best but has high water demand	Fernández-Jiménez, A. et al. [30]
Steel Slag	Ca-Si-Fe	170-250	Y	Can contain expansive components and has low reactivity	Khalifa, S., & Deja, J. [31]
Biomass Ash	Si	100-140	N	High water demand	François, R. et al. [32]
Waste Glass	Si-Na-Ca	50-100	Y	Recycling preferability	Siddique, R., & Klaus, J. [33]
Bauxite Residue	Fe-Al-Si	100-150	N	High Alkali content along with low reactivity	Zhang, X. et al. [34]
Copper Slag	Fe-Si	30-40	N	More Research Needed	Al-Jabri, K. S. et al. [35]
Other Non-Ferro Slag	Fe-Si-Ca	5-15	N	More Research Needed	Zhang, Z., & Yao, W. [36]



2.2.2 Recycled Aggregates

The use of recycled aggregates (Figure 3) in concrete production offers sustainability benefits by reducing the demand for virgin aggregates. But the challenges such as variations in the quality and availability of recycled aggregates, as well as potential detrimental effects on fresh and hardened concrete properties, need to be addressed. Improved processing techniques, quality control measures, and standardized guidelines for incorporating recycled aggregates into concrete mixes are necessary to maximize their potential [37] [38].



Figure 3 Different types of Recycled Aggregates (Makul et al., [37])

2.2.3 Incorporation of Waste Materials

The incorporation of waste materials, such as recycled plastics, glass, and rubber, into concrete shows promise for sustainability and specific property enhancements. There are still some challenges left which include the potential loss of mechanical properties, compatibility issues, and long-term durability. Further research should focus on optimizing waste material incorporation, evaluating their performance under various environmental conditions, and developing guidelines for their safe and effective utilization [39] [40].

2.3 Durability Enhancements

2.3.1 Self-healing Concrete

Self-healing concrete systems have emerged as a promising approach for crack repair and mitigating structural deterioration (Figure 4). However, achieving consistent and reliable self-healing performance, especially in real-world applications, remains a challenge. Further research should focus on improving the encapsulation and activation mechanisms of healing agents, optimizing their release, and assessing the long-term effectiveness of self-healing systems [41] [42] [43].

2.3.2 Corrosion-Resistant Concrete

Corrosion-resistant concrete has been developed to combat deterioration caused by aggressive environments and corrosive agents. While corrosion inhibitors, coatings, and electrochemical protection systems enhance durability, challenges related to long-term performance, cost, and applicability in different environmental conditions need to be addressed. Further research should explore alternative corrosion-resistant materials and develop cost-effective solutions for their widespread implementation [44] [45].

2.4 Advanced Manufacturing Techniques

2.4.1 Precast and Modular Construction

Precast and modular construction methods have gained popularity due to improved efficiency, quality control, and construction speed. However, challenges include extensive transportation and assembly processes, as well as limitations

in customization. Further research should focus on optimizing transportation logistics, developing efficient joining techniques, and expanding customization options to enhance the practicality and cost-effectiveness of precast and modular construction [46].

2.4.2 3-D Printing Technology

3D printing technology (Figure 5) has revolutionized concrete construction by enabling the fabrication of complex structures with intricate geometries. While 3D printing offers customization, material optimization, and resource efficiency, challenges related to print speed, material properties, and scale-up need to be addressed. Further research should focus on enhancing print speed, optimizing the properties of printable materials, and developing large-scale 3D printing systems for practical implementation [15] [47]. Additionally, it has been discovered that 3-D concrete printing is well on way to reduce the global energy utilization by 5% and water saving of around 20% as compared to conventional techniques [48].

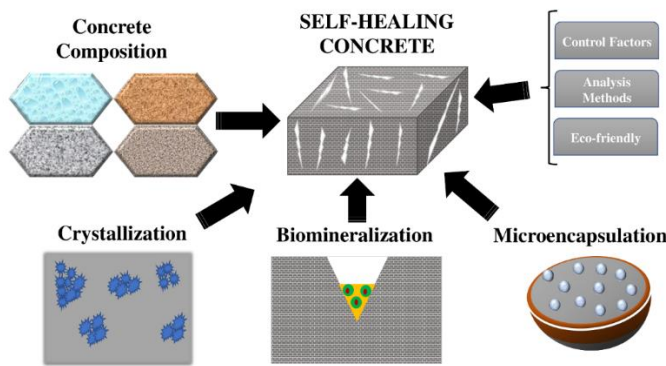


Figure 4 Self-Healing Concrete Process (Roque et al., [43])

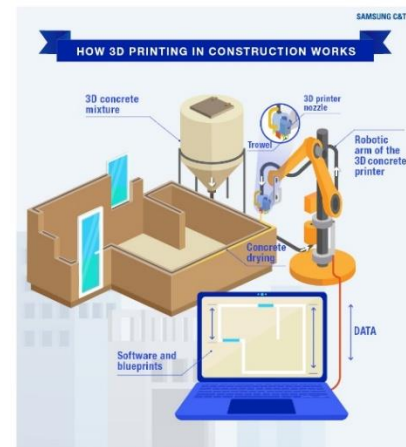


Figure 5 3-D Concrete Printing Concept [52]

2.4.3 AI in Concrete Technology

Artificial intelligence (AI) plays a crucial role in advancing concrete materials by facilitating material design and optimization, predictive modelling and simulation, and quality control and inspection. Through AI algorithms and machine learning techniques, concrete mixtures can be customized for enhanced strength, durability, and performance [49]. AI-based predictive models enable accurate simulations of concrete behavior, aiding in optimizing material compositions and structural designs. Additionally, AI-powered systems automate quality control processes, ensuring consistency and adherence to standards throughout concrete production [8] [43]. Overall, AI contributes to the development of advanced concrete materials, leading to more efficient and reliable structures in the construction industry.

3 Critical Review and Recommendations

Despite the remarkable advancements in concrete development over the last decade, several critical aspects deserve attention. Firstly, cost implications remain a challenge for some novel materials, limiting their widespread adoption. Further research is needed to optimize production processes, explore cost-effective alternatives, and develop standardized mix designs [50] [51]. Secondly, standardization and testing are essential for the successful implementation of sustainable practices, recycled materials, and SCMs. Extensive testing, standardization, and guidelines are required to ensure consistent quality, performance, and regulatory compliance [26] [53]. Collaboration between researchers, industry professionals, and regulatory bodies is crucial to develop comprehensive standards and protocols.

Thirdly, advanced manufacturing techniques, including 3D printing, face scale-up challenges and require further research to enhance their practicality, cost-effectiveness, and integration into mainstream construction practices. Strategies for optimizing production speed, material properties, and equipment reliability need to be explored to enable large-scale implementation. Lastly, the long-term performance and durability of new materials and technologies should be thoroughly investigated through field studies and monitoring to assess their reliability and address potential concerns. Continuous



monitoring, maintenance protocols, and periodic evaluation of structures are essential to ensure their long-term performance and sustainability [54] [55].

4 Conclusions and Future Recommendations

In the last decade, concrete technology has undergone remarkable advancements, encompassing novel materials, sustainable practices, durability enhancements, and advanced manufacturing techniques. These developments have the potential to bring about a revolution in the construction industry, offering improved performance, sustainability, and construction efficiency. The introduction of novel materials, such as additives, fibres, and fillers, has led to enhanced properties in concrete, including increased strength, ductility, and crack resistance. Additionally, sustainable practices have gained prominence, with the utilization of supplementary cementitious materials, recycled aggregates, and eco-friendly admixtures, contributing to reduced carbon emissions and environmental impact. The focus on durability enhancements has resulted in the development of innovative mix designs, surface treatments, and protective coatings, bolstering resistance against chemical attacks, abrasion, and environmental degradation. Advanced manufacturing techniques like 3D concrete printing and automated construction processes have opened up new avenues for design flexibility, faster construction, and cost-effectiveness. However, challenges remain, including addressing cost implications, establishing standardization, scaling up production, and ensuring long-term performance. Collaborative efforts between academia, industry, and regulatory bodies are crucial for further research and implementation, driving the future of concrete technology and enabling sustainable and resilient construction practices.

Looking ahead, there are several key areas that warrant attention and further exploration in the future of concrete technology. Firstly, continued research and development efforts are needed to optimize the performance and sustainability of novel materials. This includes investigating new types of additives, fibres, and fillers, as well as understanding their long-term behaviour and compatibility with existing construction practices. Secondly, efforts should be directed towards addressing the challenges associated with cost, standardization, and scale-up of advanced manufacturing techniques like 3D concrete printing. This involves refining the technology, improving productivity, and establishing industry-wide guidelines and regulations. Additionally, interdisciplinary collaborations between academia, industry, and regulatory bodies are crucial to foster innovation and knowledge exchange. These collaborations can drive the adoption of advanced concrete materials and practices in real-world construction projects. Lastly, the monitoring and assessment of the long-term performance and durability of advanced concrete materials and structures should remain a priority. This requires ongoing monitoring systems, maintenance protocols, and rigorous testing to ensure that the promised benefits of these advancements are sustained over time.

References

- [1]. Thomas, M., Gupta, R., & Gupta, A. (2013). Influence of fly ash on the mechanical properties of concrete: A review. *Journal of Civil Engineering and Management*, 19(6), 846-853.
- [2]. Ajwad A, Usman Ilyas, Nouman Khadim, Abdullah, Muhammad Usman, Shakir Ahmad, Bilal Zahid, & Abdul Waqar Akhtar. (2019). Assessing the Durability of Concrete with the Addition of Low Quality Fly Ash. *Scientific Inquiry and Review*, 3(1), 43-47. <https://doi.org/10.32350/sir.31.05>
- [3]. Miah, S., Sanjayan, J., & Hossain, K. M. A. (2018). Influence of silica fume on concrete properties - A critical review. *Construction and Building Materials*, 165, 399-406.
- [4]. Chakraborty, A., Ghosh, S., & Bhattacharjee, B. (2019). A review on the utilization of silica fume in cement-based materials: Engineering and durability aspects. *Construction and Building Materials*, 221, 638-656.
- [5]. Neno, F., Šafránková, M., & Pavlíková, M. (2017). Metakaolin as supplementary cementitious material in concrete: A review. *Construction and Building Materials*, 152, 1002-1019.
- [6]. Al-Hashem MN, Amin MN, Ajwad A, Afzal M, Khan K, Faraz MI, Qadir MG, Khan H. Mechanical and Durability Evaluation of Metakaolin as Cement Replacement Material in Concrete. *Materials*. 2022; 15(22):7868. <https://doi.org/10.3390/ma15227868>
- [7]. Ajwad A.,Ahmad S.,Abdullah,Jaffar S.,Ilyas U. And Adnan M. (2022) Effect of Using Rice Husk Ash as Partial Replacement of Cement on Properties of Fresh and Hardened Concrete. *Architecture, Civil Engineering, Environment*, Vol.15 (Issue 2), pp. 85-94. <https://doi.org/10.2478/acee-2022-0017>
- [8]. Aslani, F., Nejadi, S., & Wong, Y. L. (2014). Effects of superplasticizers on the workability and mechanical properties of self-compacting concrete: A review. *Construction and Building Materials*, 52, 400-411.
- [9]. Safiuddin, M., West, J. S., & Hearn, N. (2019). Recent trends on the development of self-compacting concrete: A review. *Journal of Cleaner Production*, 215, 684-706.



5th Conference on Sustainability in Civil Engineering (CSCE'23)

Department of Civil Engineering
Capital University of Science and Technology, Islamabad Pakistan



- [10].Patil, A. R., Shete, P. B., & Shewale, V. D. (2017). Viscosity modifying admixtures for concrete: A review. *Journal of Materials in Civil Engineering*, 29(12), 04017192.
- [11].Popovics, J. S., Fowler, D. W., & Stauffer, P. H. (2016). Internal curing for reducing autogenous shrinkage in high-performance concrete: A review. *Cement and Concrete Composites*, 72, 55-64.
- [12].Bentz, D. P., Weiss, W. J., & Peltz, M. A. (2018). Modeling internal curing: A review. *Cement and Concrete Composites*, 86, 35-49.
- [13].Nguyen, D. V., Yu, Q. L., & Mendis, P. (2019). A review on the effects of curing conditions on the properties of early age concrete. *Construction and Building Materials*, 195, 680-695.
- [14].Liu, J., Shen, L., & Guo, J. (2020). A review on curing methods for early-age concrete. *Construction and Building Materials*, 232, 117231.
- [15].Ajwad, A. (2018) "Production of Steel Fiber Reinforced Concrete with Different Mix Design Ratios", *Scientific Inquiry and Review*, 2(4), pp. 23-32. doi: 10.32350/sir.24.03.
- [16].GosSELIN, M., MéRY, N., & Toulemonde, F. (2018). 3D printing of concrete structures: Technology and its application. *Cement and Concrete Research*, 112, 59-67.
- [17].Van Tuan, T., OzBakkaloglu, J., & Shah, M. Y. (2019). Characteristics of ultra-high-performance fiber-reinforced concrete incorporating nanomaterials. *Construction and Building Materials*, 207, 39-54.
- [18].Tedros M.K., Sevenkar A., Berry, R. (2019) Ultra High-Performance Concrete; A Game Changer, *Building Blocks, Structure Magazine*, 6(1), 8-12.
- [19].Karthik, S., & Mohan, K. S. R. (2021). A Taguchi Approach for Optimizing Design Mixture of Geopolymer Concrete Incorporating Fly Ash, Ground Granulated Blast Furnace Slag and Silica Fume. *Crystals*, 11(11), 23-41.
- [20].Provis, J., & van Deventer, J. L. (2015). *Geopolymers: Structures, processing, properties and industrial applications*. Woodhead Publishing.
- [21].Xu, X., Wu, Q., & Gao, S. (2018). A review on the sustainability of geopolymer in the construction industry. *Journal of Cleaner Production*, 178, 649-662.
- [22].Sanjayan, V., Page, C. L., & Ngo, P. (2016). An overview of the use of high-strength fiber reinforced concrete. *Construction and Building Materials*, 110, 40-53.
- [23].Mobasher, S., Lin, K., & Alhozaimy, A. (2018). Mechanical properties and bond characteristics of ultra-high-performance fiber-reinforced concrete. *ACI Materials Journal*, 115(2), 283-292.
- [24].Almeida, R., Helene, P., & Cherif, D. (2018). *Supplementary cementitious materials: Properties, durability, sustainability*. Springer.
- [25].Shi, X., Zheng, H., & Zuo, Y. (2020). Effects of ground granulated blast-furnace slag on the properties of cement paste: A review. *Construction and Building Materials*, 263, 120640.
- [26].Kumar, A., & Bhattacharjee, B. (2016). A review on coal fly ash-based geopolymer concrete: A promising eco-friendly construction material. *Journal of Cleaner Production*, 112(Part 5), 463-482.
- [27].Mehta, P. C., & Monteiro, P. J. (2014). *Concrete: Microstructure, properties, and materials*. McGraw-Hill Education.
- [28].Hossain, K. M. A., & Lachemi, M. (2016). Mechanical properties, durability, and life-cycle assessment of sustainable self-consolidating concrete mixtures with silica fume. *Journal of Cleaner Production*, 113, 518-527.
- [29].Mehta, P. K., & Siddique, R. (2003). Sustainable concrete: Fly ash as a resource material. *Construction and Building Materials*, 17(6-7), 471-480.
- [30].Bouziani, T., Kadri, E. H., & Kenai, S. (2013). Limestone filler cement in low w/c concrete: A rational use of energy. *Construction and Building Materials*, 47, 1249-1254.
- [31].Fernández-Jiménez, A., & Palomo, A. (2005). Composition and microstructure of alkali activated fly ash/slag pastes. *Cement and Concrete Research*, 35(10), 1984-1992.
- [32].Khalifa, S., & Deja, J. (2016). Use of steel slag aggregate in asphalt concrete mixes. *International Journal of Pavement Engineering*, 17(8), 683-690.
- [33].François, R., De Schutter, G., & Taerwe, L. (2010). Hydration characteristics and pozzolanic activity of biomass fly ash in Portland cement pastes. *Cement and Concrete Composites*, 32(3), 224-230.
- [34].Siddique, M. S., Jameel, R., & Nanda, H. M. (2015). Utilization of waste plastics as a sustainable modifier for the production of concrete: A review. *Journal of Cleaner Production*, 87, 39-50.
- [35].Zhang, X., Huang, X., & Sun, D. (2012). Potential utilization of red mud as a substitute for cementitious materials in construction: A review. *Journal of Cleaner Production*, 24, 1-7.
- [36].Al-Jabri, K. S., Al-Saidy, A. H., & Taha, R. A. (2011). Effect of copper slag and cement by-pass dust addition on mechanical properties of concrete. *Construction and Building Materials*, 25(2), 933-938.
- [37].Zhang, Z., & Yao, W. (2011). Review on the utilization of nonferrous metal slag. *Journal of Wuhan University of Technology-Mater. Sci. Ed.*, 26(2), 192-198.
- [38].Tam, V.W.Y., and Gao, X.F. (2007). Microstructural analysis of recycled aggregate concrete produced from two-stage mixing approach. *Construction and Building Materials*, 21(3), 577-582.
- [39].Kou, Y., Poon, C., & Duan, Q. (2020). Properties of concrete prepared with low-grade recycled aggregates. *Construction and Building Materials*, 247, 118551.
- [40].Siddique, R., & Klaus, J. (2009). Influence of metakaolin and waste glass powder on the properties of self-compacting concrete. *Construction and Building Materials*, 23(2), 972-978.
- [41].Ismail, K., Abbas, H., & Almulhim, H. (2020). The impact of using waste glass as coarse aggregate on the mechanical properties of concrete. *Construction and Building Materials*, 303, 221-228.



5th Conference on Sustainability in Civil Engineering (CSCE'23)

Department of Civil Engineering

Capital University of Science and Technology, Islamabad Pakistan



- [41]. Yang, J., Ye, G., & Yang, Y. (2015). Self-healing concrete: From materials, properties, and mechanisms to structural applications. *Applied Materials Today*, 9, 519-539.
- [42]. Wang, Z., Li, K., & Ye, G. (2021). Mechanisms and applications of self-healing concrete: A state-of-the-art review. *Materials*, 14(12), 3336.
- [43]. Roque, B. A. C., Hidalgo-Delgado, F., Castela, A. S., Ferreira, V. M., & Camões, A. (2023). Self-Healing Concrete: Concepts, Energy Saving and Sustainability. *Energies*, 16(4), 1650. doi: 10.3390/en16041650.
- [44]. Bertolini, M. P., Redaelli, E., & Bolzoni, R. (2013). Corrosion of steel in concrete structures. Woodhead Publishing.
- [45]. Dehwah, M., Kadhum, E. H., & Bakar, M. S. A. (2020). Review on the corrosion of steel reinforcement in concrete. *Journal of Materials Research and Technology*, 9(5), 10235-10252.
- [46]. Hu, W., Huang, Q., & Li, G. (2021). Progress in research on prefabricated building technology in China: A state-of-the-art review. *Construction and Building Materials*, 307, 125534.
- [47]. Chen, X., Khoshnevis, S., & Yuan, M. (2020). 3D concrete printing: Machine, materials, and structural applications. *Advanced Engineering Materials*, 22(10), 2001110.
- [48]. Alami, A. H., Olabi, A. G., Ayoub, M., Aljaghoub, H., Alasad, S., & Abdelkareem, M. A. (2023). 3D Concrete Printing: Recent Progress, Applications, Challenges, and Role in Achieving Sustainable Development Goals. *Buildings*, 13(4), 924. doi: 10.3390/buildings13040924.
- [49]. Li, H., Bai, H., & Li, Y. (2022). An overview on ultrahigh performance concrete: Developments, properties, and application. *Journal of Materials Science*, 52(15), 8722-8749.
- [50]. Khayat, A. M., Nguyen, T. P., & Khayat, P. H. (2021). Towards performance-based specifications for concrete materials, construction, and durability. *Construction and Building Materials*, 312, 125752.
- [51]. Shaikh, M. F., Ansari, M. S., & Khan, A. U. (2022). Effect of nano-SiO₂ on strength and durability properties of cement mortar: A review. *Construction and Building Materials*, 301, 124351.
- [52]. <https://news.samsungcnt.com/features/engineering-construction/2022-08-3d-printing-brings-innovation-building-construction/>
- [53]. ACI Committee 232. (2019). Fly ash and natural pozzolans in concrete: Practitioner's guide. ACI Committee 232.
- [54]. Cramer, J., D'Ambrosia, T., & Bentz, C. (2017). NIST research on the long-term performance of concrete: A review. *Cement and Concrete Composites*, 79, 18-29.
- [55]. Ganesan, S., Ayub, M. S., & Alahakoon, V. (2022). Sustainable construction: Review of application of nanotechnology in cement-based materials. *Journal of Cleaner Production*, 318, 127515.



DURABILITY CHARACTERISTICS OF SELF-COMPACTING CONCRETE WITH PARTIAL SUBSTITUTION OF FOUNDRY SAND AS FINE AGGREGATE AND ADDITION OF PROPYLENE FIBERS

^aMuhammad Umer Malik *, ^bMuhammad Yaqub, ^cRizwan Ghafoor

a: Department of Civil Engineering, UET, Taxila, Pakistan, umermalik061@gmail.com

b: Department of Civil Engineering, UET, Taxila, Pakistan. muhammad.yaqub@uettaxila.edu.pk

c: Department of Civil Engineering, UET, Taxila, Pakistan, rizwangafoor39@gmail.com

*Corresponding author: Email ID: umermalik061@gmail.com

Abstract- Foundry sand mainly consists of silicates, and it is used as a replacement of fine aggregate to make self-compacting concrete that is cheaper, better for the environment, and more durable. This research study looked at how foundry sand and propylene fibers (PPF) changed the mechanical and durability properties of self-compacting concrete. 25% cement was replaced with fly ash, fine aggregate is replaced with foundry sand in different proportions (0%, 20%, 30% & 40%) and propylene fibers in 0.75% were added. The goal was to determine the mechanical and durability properties of above-mentioned mixes of self-compacting concrete and to compare them with normal mix self-compacting concrete. The ratio adopted for the testing is of 1:1.56:2.60 (Binder: Fine Aggregate: Coarse Aggregate). For examining the mechanical characteristics of concrete, the tests carried out were splitting tensile strength, compressive strength, and Flexural strength tests. And to examine the durability properties water absorption, acid attack and abrasion resistance tests were conducted. The normal self-compacting concrete shows less resistance towards environmental effects. Experimental results show that the mix with 25% fly ash, 20% foundry sand replacement with addition of 0.75% of propylene fibers has performed better than all other samples including the control mix against environmental effects.

Keywords- Durability properties, Foundry Sand, Fly ash, Propylene fibers, Viscocrete, Mechanical properties.

1 Introduction

Self-compacting concrete (SCC) is a special type of concrete which can be placed and consolidated under its own weight without any vibration effort due to its excellent deformability, and which at the same time is cohesive enough to be handled without segregation or bleeding. The environment can have a significant impact on the durability of concrete. Various environmental factors can affect the physical and chemical properties of concrete, leading to deterioration over time. Foundry sand mainly consists of silicates, and it is used as a replacement of fine aggregate to make self-compacting concrete that is cheaper, better for the environment, and more durable.

Concrete is an important building material that is used all over the world. Concrete comprises water, cement, sand and small rocks. Researchers are trying to encourage builders to use natural pozzolanic materials as supplementary cementing materials (SCMs). Using SCMs, the carbon dioxide's (CO₂) amount releasing into atmosphere during the cement-making process can be kept to a minimum [1]. Natural pozzolans can be used instead of cement in concrete because they have unique properties like low permeability, less heat of hydration, high sulphate resistance, and an enhancement to the ultimate concrete strength [2].



According to Gurpreet Singh and Rafat Siddique (2011), incorporating WFS (Waste Foundry Sand) as a partial replacement for sand in concrete results in increase in the USPV (Ultrasonic Pulse Velocity) values and a reduction in chloride ion penetration in concrete. These changes indicate that the concrete has achieved higher density and improved impermeability, enhanced strength properties, including compressive strength, splitting tensile strength, and modulus of elasticity [3].

Bavita Bhardwaj and Pardeep Kumar (2017) discovered that incorporating waste foundry sand (WFS) in concrete is beneficial. WFS possesses favorable material properties that contribute to the improved mechanical performance of concrete. Furthermore, the durability of concrete is enhanced when WFS is added up to an optimal level [4].

There are different individual studies carried out to study the impact of using foundry sand as fine aggregate and polypropylene fibers on self-compacting concrete's properties, no previous study has been carried out to analyze the environmental effect on durability of self-compacting concrete made by replacement of foundry sand as fine aggregate with addition of polypropylene fibers. This study examined the environmental effects on durability by i.e., Water Absorption, Acid Attack and Abrasion Resistance Tests of SCC made with foundry sand and PPF on concrete's and mechanical properties i.e., Flexural, Tensile and Compressive strength.

2 Experimental Procedures

2.1 Materials with their Properties and Mix Proportions

Fly ash (FA) and ordinary Portland cement, or OPC for short, were used as the binding ingredients in this research project. OPC type 1 cement, as specified by ASTM C150, was used [5]. Locally available foundry sand was purchased from the Heavy Mechanical Complex in Taxila, Pakistan. LawrencePur and Margalla, respectively, provided the fine and coarse aggregates. 19 mm long propylene fiber was used. Tap water was used for concrete mixing and curing. The superplasticizer, Ultra-Super Plasticizer 470 was added to concrete mixtures since foundry sand and PPF make the concrete less workable. The parameters of aggregate and PPF are shown in Tables 1 and 2, whereas the parameters for fly ash and sand from foundries are shown in Table 3.

Table 1. Physical properties of coarse and fine aggregates and waste foundry sand.

	Coarse Aggregate	Fine Aggregate	Waste Foundry Sand
Specific Gravity	2.68	2.62	2.24
Fineness Modulus	6.34	2.58	1.86
Water Absorption	0.6	1.5	1.7
Moisture Content	Nil	Nil	Nil

Table 2. Properties of Propylene Fiber.

Shape	Straight
Length (mm) l	12
Diameter (mm) d	0.019
Aspect Ratio (l/d)	631
Density (g/cm ³)	0.91
Elastic Modulus (GPa)	3.5
Tensile Strength (Mpa)	350

Table 3. Properties of Fly ash and Waste foundry sand.

1Chemical Compounds		Fly Ash		WFS
CaO %		2.92		1.65
SiO ₂		61.2		88.11
Al ₂ O ₃		28.23		0.49
Fe ₂ O ₃		3.9		2.38
MgO		0.93		0.76
SO ₃		0.73		-
Na ₂ O		0.01		0.95
K ₂ O		1.34		0.83
TiO ₂		-		0.1
Loss on Ignition (%)		0.74		0.73



The experimental schedule is shown in Table 4, which consists of comparing four different mixes. M1 denoted the control mix having OPC as the only binder, while M2, M3 and M4 denoted the mixes containing 20%, 30% and 40% foundry sand as fine aggregate replacement respectively. Poly propylene fiber was also added in 0.75% in M2, M3 and M4 respectively. Table 5 shows the mix design composition.

Table 4. No of Samples for testing

Mix	Mix Type	Disc	Cube	Cylinder	Cubes	Beams	Cylinder
M1	Control Mix (SCC)	6	6	6	3	3	3
M2	OPC (25% F.A) + 20% W.F.S + 0.75 % PPF	6	6	6	3	3	3
M3	OPC (25% F.A) + 30% W.F.S + 0.75 % PPF	6	6	6	3	3	3
M4	OPC (25% F.A) + 40% W.F.S + 0.75 % PPF	6	6	6	3	3	3
		Water Absorption	Acid Attack	Abrasion Resistance	Compressive Strength	Flexural Strength	Split Tensile Strength

Table 5. Mix Design Composition

Mix Design Proportions for M40 (1 : 1.56 : 2.60)					
Mix No.	Cement + Fly Ash	Fine Aggregate + Foundry Sand	Coarse Aggregate	w/c	Propylene Fiber
-	kg/m ³	kg/m ³	kg/m ³	-	%
M1	416.64 + 0	649.72 + 0	1082.72	0.5	0
M2	312.48 + 104.16	520 + 130	1082.72	0.5	0.75
M3	312.48 + 104.16	455 + 195	1082.72	0.5	0.75
M4	312.48 + 104.16	390 + 260	1082.72	0.5	0.75

2.2 Concrete Mixing

Every batch of concrete was mixed in three steps. In the initial phase, aggregates and binders were combined dry. In second phase, more than half of water was added to create a uniform mixture, while the part of water remained, along with superplasticizer were then added. PPF was incorporated in the end to avoid the clumping of fibers due to more revolutions of mixer.

2.3 Specimen and Testing

During the casting of samples, one layers of concrete were applied to every sample. Using ASTM C1611 procedure, the self-compacting concrete slump flow was determined prior to specimen casting [6]. For determination of mechanical characteristics of concrete samples Compressive strength test, splitting tensile strength test, and flexural strength tests were done. Based on BS standard EN-12390 [7], 150mm x 150mm x 150mm cube specimen were casted, and then tested for compressive strength after being cured for 28 days.

After 28 days of curing, 150mm x 300mm concrete cylindrical samples were tested for the split tensile strength in accordance with ASTM C496 criteria [8]. The beam specimens measuring 100mm x 100mm x 500mm were tested for



flexural strength in accordance with ASTM C78 specifications [9]. The test setup for the durability properties is given in Figure 1. For determination of durability characteristics of concrete samples water absorption, acid attack and abrasion resistance tests were done. Based on ASTM C642 [10], 100mm x 50mm circular disc specimens were casted, and then tested at 28 days and 56 days for water absorption after being cured for 28 days.

After 28 days of curing, 100mm x 100mm x 100mm concrete cubical samples were tested for 28 days and 56 days for the acid attack. The cylinder specimens measuring 100mm x 500mm were tested for abrasion in accordance with ASTM C131 [11] specifications.



a)

b)

c)

d)

Figure 1 Testing formation for (a) Slump flow test (b) Water Absorption (c) Acid Attack (d) Abrasion Resistance Test

3 Research Methodology

Four types of mixes were prepared in Laboratory. Slump flow test was conducted firstly to determine the fresh properties of SCC, then to find out the mechanical properties, compressive strength test, flexural test and split tensile strength were done and to find out the durability properties at 28 days and 56 days water absorption, acid attack and abrasion resistance in the laboratory after 28 days curing in water tank at normal temperature.

4 Results

4.1 Slump Flow

The workability of all the mixes was determined using slump flow apparatus based on procedure given by ASTM C1611. To create workable mixtures, varied amounts of superplasticizer were combined with a consistent water-cement ratio. Figure 2 displays the results of the workability of each mixture. The mix M2, M3, and M4 which has percentage of Foundry sand, fly ash and propylene fibers produced somewhat lower slumps than the control mix (M1). The reduction in mixes workability can be related with fineness of foundry sand as it more fine than fine aggregate. The addition of PPF to the mixtures has also significantly decreased their workability because the concentration of fibers enhances internal friction in mixtures with a constant amount of water added.

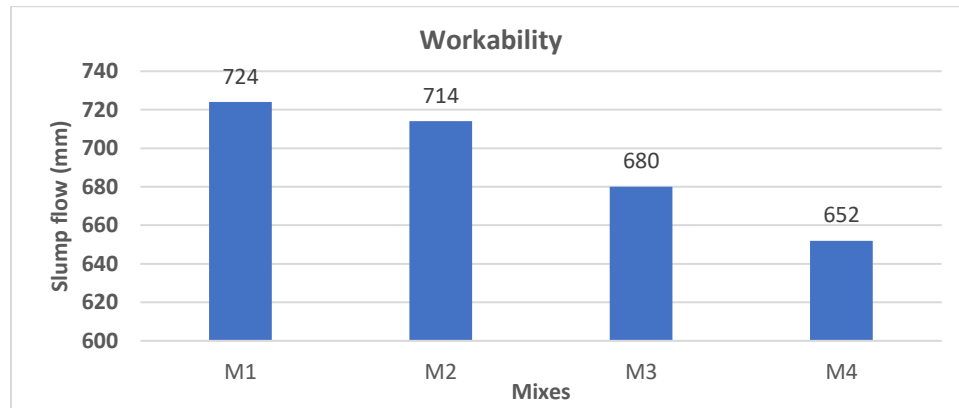


Figure 2: Slump Flow Test



4.2 Water Absorption

When it comes to durability, the water absorption of concrete is a critical parameter to consider since it indicates the level of porosity in the concrete that is accessible to water. A greater capacity for water absorption in concrete can lead to a more extensive infiltration of contaminated water, potentially having harmful chemicals, into the concrete. This can result in a shortened service life for the concrete. Water absorption testing was conducted on all four mixes after 28 and 56 days of curing. Results of this test are shown in Figure 3. From the results obtained it is noticed that water absorption was reduced by incorporation of foundry sand in the concrete. For mixture M2, the water absorption decreased by 4.2%, 10.4% at 28-day and 56-day respectively, in comparison with the mix (M1) that is control mix. The decrease in water absorption can be accredited to the formation of additional cementitious compounds from the pozzolanic reaction, fineness of foundry sand as well as the filler properties of fly ash, and addition of PPF to contract cracks.

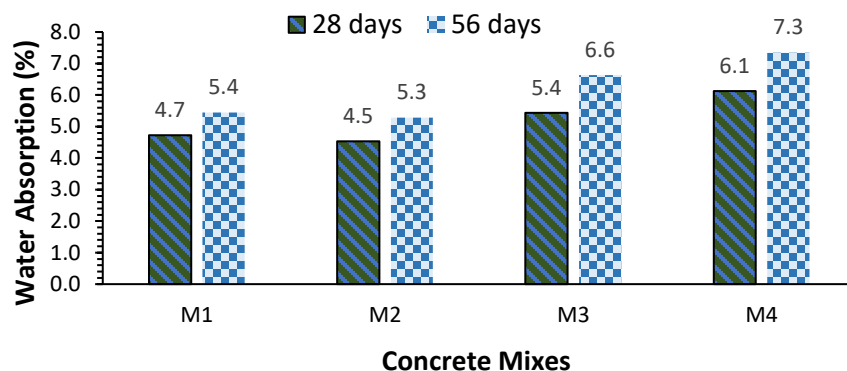


Figure 3 Water Absorption Test

4.3 Acid Attack

Figure 4 displays the weight loss incurred by all the mixes when exposed to a sulfuric acid solution for 28 and 56 days, indicating their acid attack resistance. Results show that 20% foundry sand incorporated mixes offered more resistance to weight loss against acid exposure than the control mix. After 28 and 56 days the mixes M2 resulted in 22.9% and 17.3% reduction in weight loss against abrasion respectively, when compared to the mix (M1). The control mix exhibited a higher weight loss, which may be attributed to the presence of a greater amount of calcium oxide, which can lead to the formation of gypsum, finally formation of ettringite occurs resulting in expansion and deterioration of concrete. The higher content of silicon dioxide, aluminum oxide, and ferric oxide in foundry sand may contribute to the production of more CSH gel through the pozzolanic reaction. The deterioration of concrete against acid exposure increased with time because of the deeper penetration of sulphate ions into the concrete mix resulting.

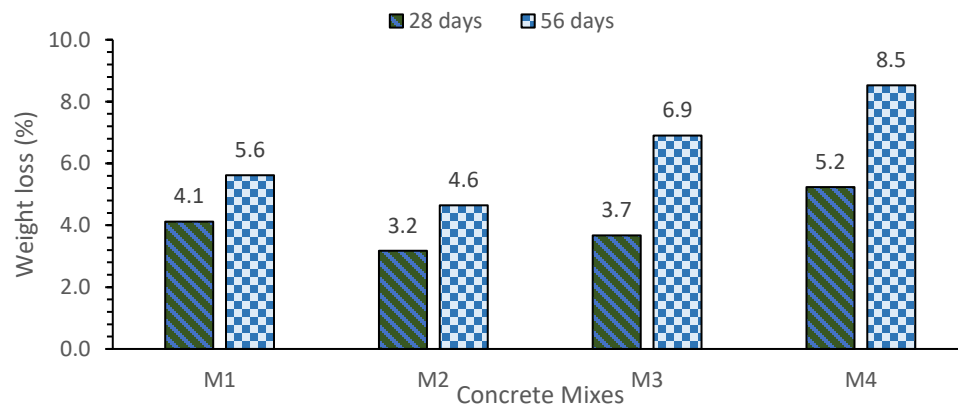


Figure 4 Acid Attack Test



4.4 Abrasion Resistance

The abrasion loss for all four mixes is shown in Figure 5. Incorporating foundry into the concrete consequences in an enhancement in the resistance of the concrete to abrasion. After 28 and 56 days the mixes M2 resulted in 40.9% and 45.8% reduction in weight loss against abrasion respectively, when compared to the mix (M1). Fig. 5 shows the specimen before and after performing the test. The pozzolanic reaction that occurs during the production of supplementary CSH gel can contribute to the development of a dense and uniform microstructure in the concrete, which may explain the increase in abrasion resistance observed in this study.

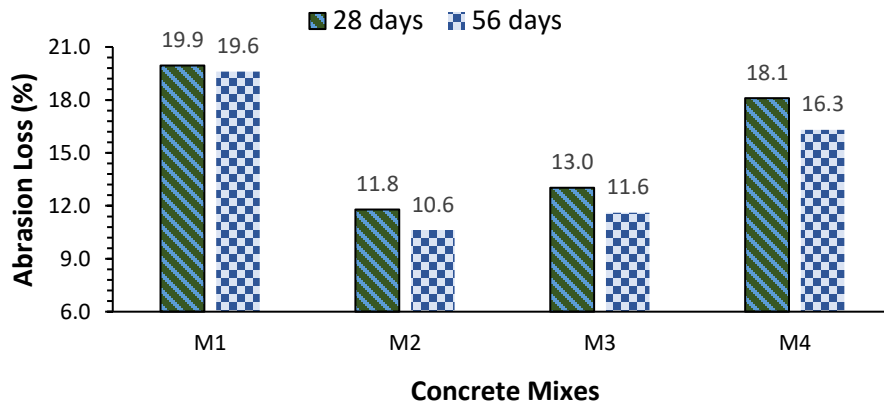


Figure 5 Abrasion Resistance Test

5 Conclusions

Based on the conducted experimental study, the study's findings lead to the following conclusions:

- 1- The workability of foundry sand incorporated mixes was lowered, while incorporation of Propylene fibers caused in further decrease of workability.
- 2- Use of foundry sand and fly ash with addition of polypropylene fiber has improved the mechanical as well as durability properties.
- 3- By addition of 25% fly ash, 20% foundry sand as fine aggregate with addition of 0.75% propylene fibers in SCC formation, the mechanical properties like compressive, flexural and tensile strength have been increased by 2.87%, 8.11%, and 3.48% respectively.
- 4- By addition of 25% fly ash, 20% foundry sand as fine aggregate with addition of 0.75% propylene fibers in SCC formation, the water absorption, acid attack and abrasion resistance has been improved by 4.2%, 22.9%, and 40.9% at 28 days and 10.4%, 17.3%, and 45.8% at 56 days, respectively.
- 5- The above results evidently shows that concrete with 25% replacement of cement with Fly ash, 20% replacement of fine aggregate with Waste Foundry Sand (WFS) and addition of 0.75% polypropylene fiber is found to be optimal mix for mechanical and durability characteristics.
- 6- The incorporation of high dosage 30% and 40% of foundry sand content resulted in degradation of the mechanical and durability characteristics of self-compacting concrete.

Acknowledgment

The authors express their sincere gratitude to all individuals and departments who provided support throughout the research process. Special thanks are extended to the Civil Engineering and Industrial Departments of UET Taxila, as well as Engr. Dr. Muhammad Yaqub for their invaluable contributions and to my parents and friends for their support.



5th Conference on Sustainability in Civil Engineering (CSCE'23)

Department of Civil Engineering

Capital University of Science and Technology, Islamabad Pakistan



References

- [1] UN Environment, K.L. Scrivener, V.M. John, E.M. Gartner, Eco-efficient cements: Potential economically viable solutions for a low-CO₂ cement-based materials industry, *Cement and Concrete Research* 114 (2018) 2–26.
- [2] “Use of Natural Pozzolans in Concrete (ACI 232.1R),” *ACI Mater. J.*, 1994, doi: 10.14359/4060.
- [3] Raffat Siddique, Effect of Used – Foundry sand on the mechanical properties of concrete, *Construction and Building Materials* 23(2009) 976-980.
- [4] Bhupendra Singh Shekhawat(2007), Utilisation of Waste Glass Powder in Concrete, *International Journal of Innovative Research in Science, Engineering and Technology*
- [5] ASTM C150 “ASTM C150 / C150M-19a Standard specification for Portland Cement”, 2019.
- [6] ASTM C143/C143M “Standard test method for slump of hydraulic-cement concrete”, *ASTM Standards*, 2015.
- [7] BS EN 12390-3 “Testing hardened concrete. Compressive strength of test specimens, British Standards Institution”, <https://www.thenbs.com/PublicationIndex/documents/details?Pub=BSI&DocID=288816>.
- [8] ASTM C496/C496M “Standard test method for splitting tensile strength of cylindrical concrete specimens”, 2017.
- [9] ASTM C78, “Standard Test Method for Flexural Strength of Concrete,” *Annu. B. ASTM Stand.*, 2016.
- [10] ASTM C642 “Standard test method for density, absorption, and voids in hardened concrete”, *ASTM Standards* (2013).
- [11] ASTM C131/C131M “Standard test method for resistance to degradation of small- size coarse aggregate by abrasion and impact in the Los Angeles machine”, 2014.



PREDICTING THE RESIDUAL FLEXURAL CAPACITY OF FIRE EXPOSED REINFORCED CONCRETE BEAMS USING GENE EXPRESSION PROGRAMMING

^a Raheel Asghar, ^b Safeer Ullah Khattak*

a: Department of Civil Engineering, COMSATS University Islamabad, Abbottabad Campus, Pakistan, raheelasghar68@gmail.com

b: Department of Civil Engineering, COMSATS University Islamabad, Abbottabad Campus, Pakistan, safeer@cuiatd.edu.pk

* Corresponding author: Email ID: raheelasghar68@gmail.com

Abstract- Reinforced concrete (RC) structures are the most commonly used ones in the construction industry; however, they exhibit a tendency of getting damaged when subjected to fire, which can cause significant deterioration and compromise their overall safety. Considering their fire susceptibility, it is critical to predict the residual flexural capacity of their structural elements especially the immediate load distributing elements i.e., RC beams in order to ensure their safety and reliability in fire hazard situations. In an effort to do so, a novel methodology was introduced by this research, utilizing gene expression programming (GEP) to accurately forecast the remaining flexural strength of RC beams after being imperiled to fire. For the evolution of GEP model, a comprehensive database consisting of 280 datapoints as reported in the past literature was used. The database incorporated seven input variables corresponding to the predetermined remnant flexural capacity output of the given beams. The performance of the proposed model was assessed using three widely recognized performance metrics: the mean absolute error, the coefficient of determination, and the root mean squared error. From the performance evaluation results, a robust correlation was found to exist between the target and predicted results with minimum error. Therefore, the proposed model can be assuredly recommended for quickly, accurately, and dependably forecasting the remnant flexural strength of RC beams after being subjected to fire.

Keywords- Fire, Gene Expression Programming, Prediction, Reinforced Concrete Beams, Residual Flexural Capacity.

1 Introduction

1.1 Background

Reinforced concrete (RC) structures are widely used in the construction industry [1], [2] due to their high strength, durability, and cost-effectiveness. However, these structures exhibit a tendency of getting damaged when subjected to fire, which can cause significant deterioration and reduce their overall load carrying capacity [3]–[6]. The reduction in load carrying capacity can compromise the safety of a structure and may lead to catastrophic failure. Among various members of these structures, beams are the most important ones since they are responsible to distribute the load of floor systems to the adjoining columns through transverse loading phenomenon [7]. Considering the importance and fire damage tendency of RC beams, it is critical to predict their residual flexural capacity when subjected to fire in order to ensure the safety and dependability of the aforementioned structures.

In the recent years, several experimental as well as data driven studies have been carried out to assess the behaviour of RC beams when imperilled to fire [8]–[11]. The experimental studies were conducted to explore the performance of these



beams whereas the data driven studies were carried out to develop predictive models for their residual strength. The experimental investigations have shown that the residual or remnant flexural strength of fire imperilled RC beams depends on various factors such as fire temperature, fire duration, beam geometry, and material characteristics [8], [10], [12]. However, they are time consuming, costly, and difficult to be conducted for every real-world situation. The data driven studies, on the other hand, were found to successfully forecast the remnant flexural strength of RC beams while avoiding these problems [11], [13]. However, they also have certain limitations as well e.g., the assumption of linear material behavior, which may not be valid for high-temperature situations. Moreover, some studies have not proposed mathematical expressions which is a big concern for their applicability to the real-world problems [11]. To overcome these limitations, genetic algorithm-based approach of gene expression programming (GEP) is often recommended [14]–[18]. It is a form of evolutionary algorithm which has been successfully applied in various fields, including civil engineering, to model complex systems and predict their behaviour under different conditions [19], [20].

In short, forecasting the remaining flexural strength of RC beams is critical to ensure the safety and serviceability of RC structures in fire hazard situations. Traditional methods employed for this purpose have shown some substantial limitations. Therefore, this research aims to develop predictive model for the remnant flexural strength of fire subjected RC beams utilizing GEP. It also aims to provide a simple mathematical expression for future implementation of the intended model. It is further extended to evaluate and validate the performance of intended model to ensure its precision and prediction accuracy.

1.2 Gene Expression Programming

GEP is an evolutionary algorithm which is based on genetic programming. It involves the use of linear chromosomes to represent a tree-like structure of genes. These genes are thereafter articulated in the form of arithmetical expressions or computer programs [14], [21]–[24]. The overall working procedure of GEP can be divided into four basic steps: the generation of preliminary populace, the execution, the fitness evaluation, and the creation of ensuing populations of GEP programs or the derivation of optimal solutions in the form of arithmetical or mathematical equations. All these steps of GEP algorithm are illustrated in Figure 1 [14].

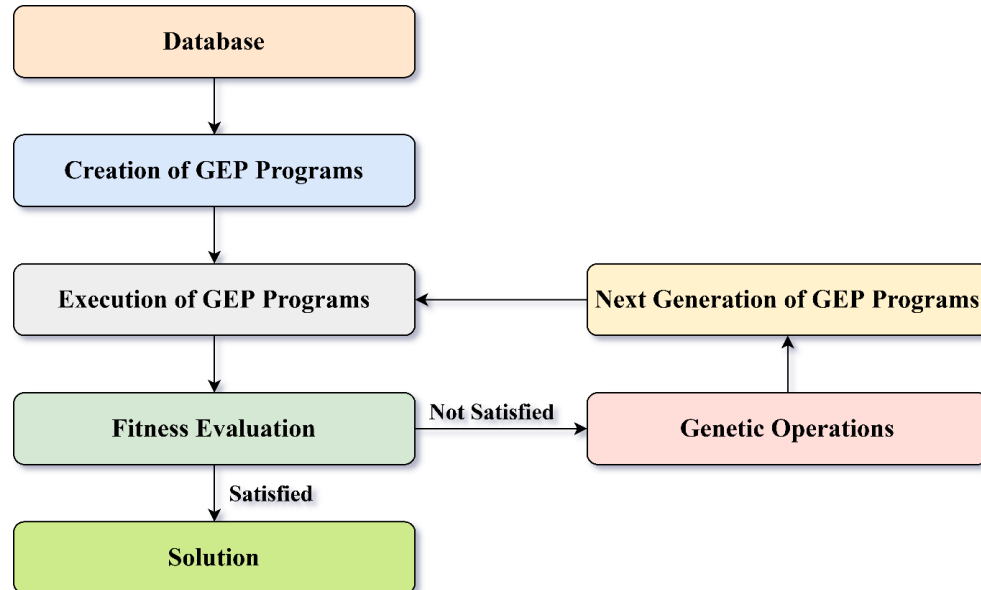


Figure 1: Working Algorithm of GEP

The GEP algorithm begins by randomly generating a population of chromosomes (or GEP programs) from the database, each of which consists of a fixed number of genes, arranged in a linear sequence [14]. After the generation of preliminary populace of chromosomes or GEP programs, they are executed, following which, their fitness is assessed using predefined fitness or performance assessment metrics. If the fitness (or performance) assessment results meet the concluding bench



mark, the GEP algorithm concludes, and the optimal solution is presented as an arithmetical or mathematical expression [14]. However, if the fitness (or performance) assessment results fail to meet the concluding bench mark, the whole process is repeated by the generation of an ensuing populace of chromosomes or GEP programs employing the genetic operations of selection, crossover, mutation, and replacement [14].

In summary, GEP is a powerful artificial intelligence (or machine learning) based data processing tool that uses genetic algorithms to evolve computer programs or mathematical expressions. It has the ability to efficiently determine the high-quality solutions by using a combination of genetic operators and fitness-based selection. Considering all its advantageous attributes, this research intends to utilize GEP for accurately predicting the residual flexural strength of RC beams under standard fire conditions.

2 Research Methodology

The evolution of a diagnostic model for estimating the remnant flexural capacity or strength of fire imperilled RC beams consists of three fundamental steps: the creation or selection of a thorough catalogue representing the datapoints of given phenomenon, the identification of model's input and output variables or parameters, and the fruition of the intended GEP model. These steps are further elaborated upon in the succeeding subsections.

2.1 Database

A comprehensive database describing the fire performance of RC beams assembled by Hakan Erdem [11] was selected to evolve the diagnostic model for estimating (or forecasting) the residual flexural strength of aforementioned beams. It consisted of 280 datapoints with 260 exhibiting the fire damage whereas 20 without exhibiting fire damage. The thorough elaboration of the statistical properties of this database is presented in Table 1. It shows the standard deviation, mean, and range of the various input and output variables. The width, depth, area of steel, concrete cover, fire exposure time, and compressive strength of the concrete of RC beams were found to be ranging between 250 to 1000 mm, 280 to 380 mm, 226 to 1527 mm², 20 to 90 mm, 0 to 120 minutes, and 13 to 20 MPa respectively. Analysing the statistical characteristics for width and depth, the aforementioned beams in the given database were revealed to be extending from very small cross sections to the very large ones. This shows the comprehensive and inclusive nature of the selected database. The yield strength of the reinforcing steel was however found to be constant at 365 MPa throughout the database (representing single grade of steel). It was not neglected from the database because of its greater importance towards the fire behaviour of RC beams. These statistical characteristics especially the range of parameters in the database must be regarded as the boundary limits of proposed model to which it can be applied.

Table 1: Description of the Statistical Properties of Database

Parameter	Symbol	Unit	Type	Maximum	Minimum	Mean	STD
Width	B	mm	Input	1000	250	430	302.78
Depth	D	mm	Input	380	280	320	49.08
Area of Steel	A _{st}	mm ²	Input	1526.81	226.19	722.25	390.06
Concrete Cover	C _c	mm	Input	90	20	34	28.05
Fire Exposure Time	T	min	Input	120	0	56.07	38.81
Compressive Strength	f _{c'}	MPa	Input	20	13.33	17.33	3.27
Yield Strength	f _y	MPa	Input	365	365	365	0.00
Residual Flexural Capacity	M _r	KN-m	Output	202.63	0.69	13.10	26.23

STD: Standard Deviation.



2.2 Model Parameters

The selection of input variables against the preestablished residual flexural strength output of RC beams (under standard fire conditions) was done on the basis of their statistical and structural importance. The statistical importance was determined in terms of p -value calculated using linear regression and analysis of variance (ANOVA) whereas the structural importance was determined based on the engineering knowledge. Employing this strategy, seven input variables were selected to predict the single residual flexural capacity output variable. A detailed description including the name, symbol, measuring unit, and type of all these variables (either the input or output) is presented in Table 1.

2.3 Model Development

The development of remnant flexural strength prediction model of RC beams subjected to standard fire was done utilizing tremendously flexible and efficient GEP based data modelling software GeneXproTools 5.0. The modelling process was initiated by importing an organized Microsoft Excel's database of the given phenomenon consisting of seven input variables against the preestablished output variable to this software. For effective and robust data modelling, the given database consisting of 280 datapoints was randomly split-up into two groups: the training database, consisting of 70% of the total datapoints and testing/validating database, consisting of 30% of the total datapoints [11], [25]. The performance or fitness of GEP models was assessed on the basis of three well-known performance metrics (as recommended by some antecedent research studies [14], [19], [25]): determination metric (R^2), root mean squared error metric ($RMSE$), and mean absolute error metric (MAE). These performance (or fitness) metrics can be computed using equation (1), (2), and (3) respectively [26]. In the aforementioned equations, X describes the known output variable, Y describes the estimated (or forecasted) output variable, and p describes the number of datapoints. Based on the results obtained for these performance (or fitness) metrics, the model owning best fitness was presented for imminent estimating or forecasting the remnant flexural strength of fire imperiled RC beams.

$$R^2 = \left[\frac{p \sum_{i=1}^p (X_i Y_i) - (\sum_{i=1}^p X_i)(\sum_{i=1}^p Y_i)}{\sqrt{[p \sum_{i=1}^p X_i^2 - (\sum_{i=1}^p X_i)^2][p \sum_{i=1}^p Y_i^2 - (\sum_{i=1}^p Y_i)^2]}} \right]^2 \quad (1)$$

$$RMSE = \sqrt{\frac{1}{p} \sum_{i=1}^p (Y_i - X_i)^2} \quad (2)$$

$$MAE = \frac{1}{p} \sum_{i=1}^p |Y_i - X_i| \quad (3)$$

3 Results

The results of the research on the predictive modelling of residual flexural strength of RC beams subjected to standard fire can be divided into three parts i.e., the formulation, validation, and performance evaluation of aforementioned capacity prediction model. A comprehensive and in-depth insight into all these parts has been provided in the succeeding subsections.

3.1 Residual Flexural Capacity Prediction Model

The remnant flexural strength prediction model of RC beams imperilled to standard fire was developed using GEP based GeneXproTools 5.0. This software offers the results in the form of expression trees which are tree like data structures with each node representing a unique expression. The expression tree obtained for this model was found to be a combination of three sub-expression trees which were linked via division operation. To make this model applicable to the scenarios of real physical world, this expression tree was decrypted into the mathematical expressions as presented in equations (4)-(6). All the symbols involved in these equations have been described in Table 1.



$$M_r = \frac{2.19X_1X_2}{B} \quad (4)$$

$$X_1 = D + 4A_{st} - 7.29C_c \quad (5)$$

$$X_2 = \frac{Bf'_c}{f_y(4.23 + T)} - \frac{1.53TB}{C_c f_y(4.23 + T)} \quad (6)$$

3.2 Model Validation

To ensure the strength and accuracy of the GEP models, it is common practice to perform sensitivity and parametric analysis [14], [25]. The sensitivity analysis assesses the impact of individual input variables on the output of the GEP model whereas the parametric analysis investigates the effects of varying the model parameters on its performance. The results of both the aforementioned analyses have been presented in the succeeding subsections for a comprehensive understanding.

3.2.1 Sensitivity Analysis

Sensitivity analysis is used to investigate the relative impact (or benefaction) of input parameters (or variables) towards the overall model development. It was conducted on the basis of procedure presented by Asghar et. al. [14]. From the sensitivity analysis results as presented in Figure 2, T was found to be the most significant input parameter of the proposed model followed by C_c and f'_c whereas B was found to be the least significant one. These results were discovered to be in good agreement with that presented by Hakan Erdem [11] which validates the robustness of this model.

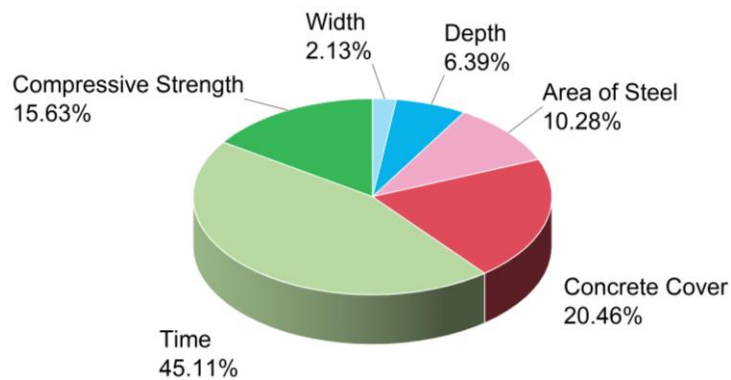


Figure 2: Contribution of Input Parameters to the Development of Proposed Model

3.2.2 Parametric Analysis

Parametric analysis is used to explore the impact of certain variation in the input parameter on the predicted output of the given model. It was conducted on the basis of procedure laid out by Asghar et. al. [14]. From the parametric analysis results as presented in Figure 3, the remnant flexural strength of RC beams imperilled to fire was found to be increasing with the increase in B , D , A_{st} , and f'_c whereas decreasing with the increase in T . It is because the beams with lesser B and D experiences more concentrated effect of fire (or heat), the beams with greater A_{st} , and f'_c can better mitigate the fire hazard conditions due to their superior performance characteristics, whereas the beams with prolonged T can lead to the increase in temperature attained by their concrete and reinforcement. The residual flexural strength of the aforementioned beams was also found to exhibit a direct relationship with C_c which is because a thicker clear concrete cover provides enhanced insulation by slowing down the transfer of heat from the surroundings to the steel reinforcement. This slowing down of heat transfer allows it to stay cooler for a longer period of time, therefore, reducing the risk of premature failure and exhibiting higher residual flexural strength. The parametric analysis results were found to be in good agreement with that presented by Hakan Erdem [11] which validates the robustness of the proposed model.

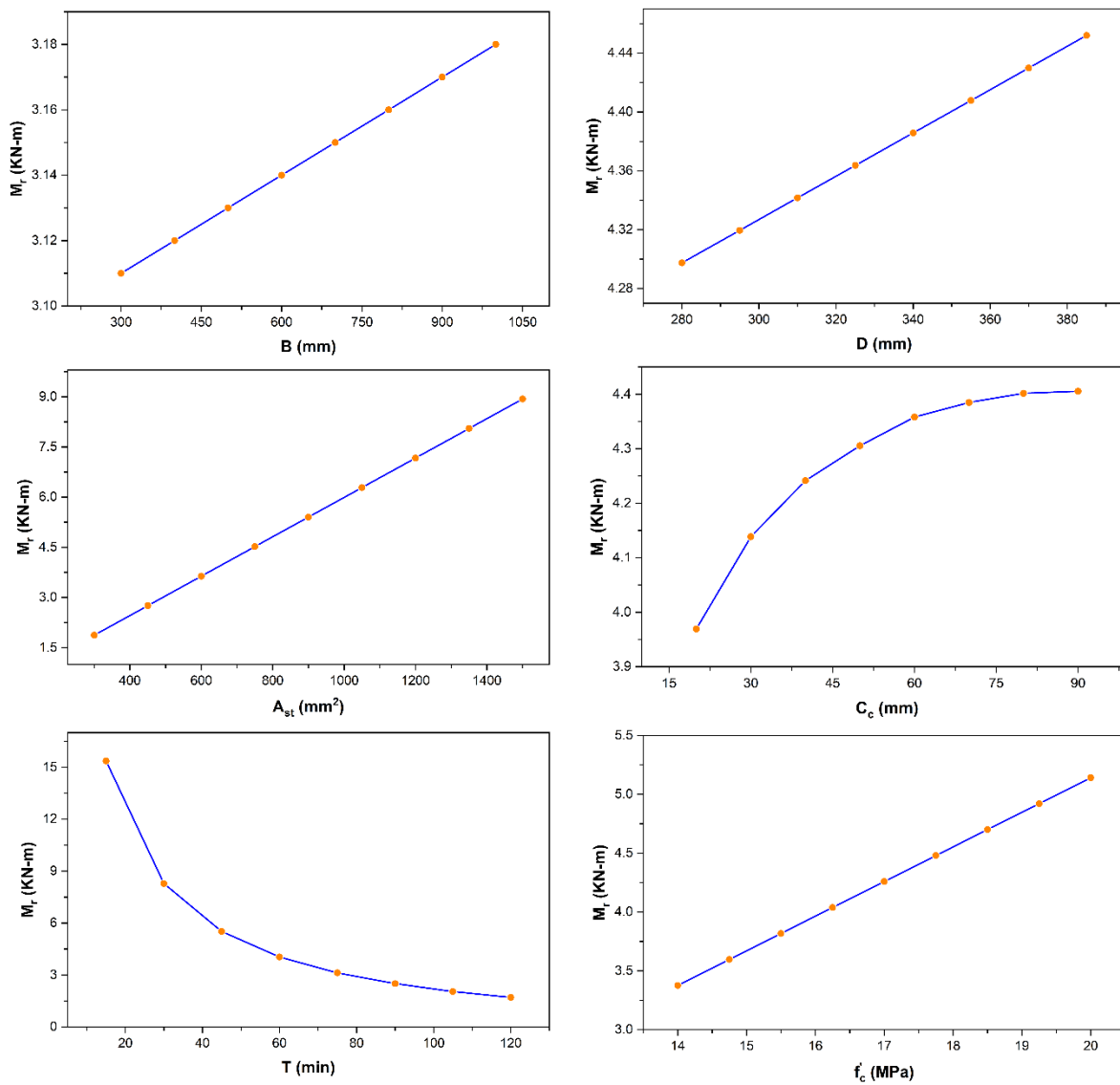


Figure 3: Parametric Analysis Results of Proposed Model

3.3 Performance Evaluation

The performance (or fitness) of proposed residual flexural strength estimation (or forecasting or prediction) model of fire exposed RC beams was evaluated based on three well-known performance (or fitness) indicators i.e., R^2 , $RMSE$, and MAE . Among these fitness indicators, R^2 was determined in decimal points whereas $RMSE$ and MAE were determined in KN-m. From the performance evaluation results as presented in Figure 4, these performance indicators were found to be 0.9737, 4.16, and 2.13 correspondingly for training database whereas 0.9813, 1.80, and 1.36 correspondingly for testing or validating database. Analysing these fitness metrics (or indicators), it was found that a robust (or strong) relationship (or association) exists between the target and predicted results. Moreover, the error between them was also found to be at its lowest. This shows the higher precision and prediction accuracy of proposed model. Conscientiously assessing the results of performance evaluation and model validation, the proposed model is highly recommended to be used for determining the remnant flexural capacity or strength of fire imperilled RC beams for future real-world scenarios or applications.

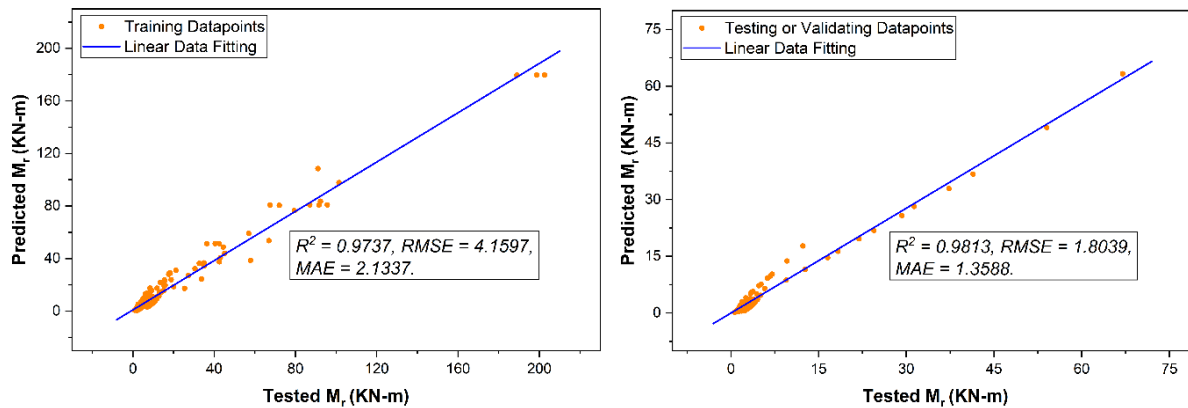


Figure 4: Performance Evaluation Results of Proposed Model

4 Conclusions

This article presented a novel gene expression programming (GEP) based research which has established the potential and practical relevance of the GEP in accurately estimating (or forecasting) the residual (or remnant) flexural strength of fire imperilled RC beams, contributing to the field of structural engineering and fire safety. On the basis of the findings of this research, the conclusions drawn are presented below.

- 1 The proposed model offers a unique way of computing the remaining flexural strength of RC beams after being imperilled to fire while avoiding the complex structural and mathematical calculations.
- 2 The model as proposed by this research was discovered to be accurate and precise in predicting the remnant flexural strength of RC beams imperilled to fire.
- 3 The trend of output with the input variables of the model as proposed by this research was discovered to be in consonance with the results obtained from experimental methods. This validates its ability to capture the underlying physical processes of the given phenomenon.
- 4 Fire exposure time was found to be the most significant input parameter of the proposed model followed by clear cover and concrete's compressive strength.

Analyzing the performance or fitness scrutinization results, the model evolved by this research can be assuredly recommended for quickly, accurately, and dependably forecasting the remnant flexural strength of RC beams after being imperilled to fire.

Acknowledgment

The authors would like to thank everyone who have helped in carrying out this research, particularly Engr. Dr. Muhammad Faisal Javed. The careful review and constructive suggestions by the anonymous reviewers are gratefully acknowledged.

References

- [1] R. Asghar, A. Shahzad, S. U. Amjad, and A. Akhtar, "Comparative Study on the Seismic Performance of Bare Frame and Infilled Frame RC Structures with Brick Masonry and Low Strength Concrete Block Masonry Infills," in Proceedings of the 2nd Conference on Sustainability in Civil Engineering CSCE'20, Islamabad, Pakistan, 2020, p. 8.
- [2] R. Asghar, A. Shahzad, S. U. Amjad, and A. Akhtar, "Experimental Determination of the Mechanical Properties of Brick Masonry and Low Strength Concrete Block Masonry," in Proceedings of the 2nd Conference on Sustainability in Civil Engineering CSCE'20, Islamabad, Pakistan, 2020, p. 6.
- [3] D. P. Thanaraj, A. N. P. Arulraj, and K. Al-Jabri, "Investigation on structural and thermal performance of reinforced concrete beams exposed to standard fire," Journal of Building Engineering, vol. 32, p. 101764, Nov. 2020, doi: 10.1016/j.jobe.2020.101764.
- [4] A. Shishegaran, M. Moradi, M. A. Naghsh, B. Karami, and A. Shishegaran, "Prediction of the load-carrying capacity of reinforced concrete connections under post-earthquake fire," J. Zhejiang Univ. Sci. A, vol. 22, no. 6, pp. 441–466, Jun. 2021, doi: 10.1631/jzus.A2000268.



5th Conference on Sustainability in Civil Engineering (CSCE'23)

Department of Civil Engineering
Capital University of Science and Technology, Islamabad Pakistan



- [5] V. K. R. Kodur and A. Agrawal, "Effect of temperature induced bond degradation on fire response of reinforced concrete beams," *Engineering Structures*, vol. 142, pp. 98–109, Jul. 2017, doi: 10.1016/j.engstruct.2017.03.022.
- [6] M. H. Bhuiyan and S. Ahmed, "Post-Fire Residual Capacity of Reinforced Concrete Beam," in *Advances in Civil Engineering*, S. Arthur, M. Saitoh, and S. K. Pal, Eds., in *Lecture Notes in Civil Engineering*. Singapore: Springer, 2022, pp. 117–126. doi: 10.1007/978-981-16-5547-0_13.
- [7] R. Asghar, M. A. Khan, R. Alyousef, M. F. Javed, and M. Ali, "Promoting the green Construction: Scientometric review on the mechanical and structural performance of geopolymers concrete," *Construction and Building Materials*, vol. 368, p. 130502, Mar. 2023, doi: 10.1016/j.conbuildmat.2023.130502.
- [8] M. Esfahani, M. Hoseinzadeh, M. Shakiba, F. Arbab, M. Yekrangi, and G. Pachideh, "Experimental investigation of residual flexural capacity of damaged reinforced concrete beams exposed to elevated temperatures," *Engineering Structures*, vol. 240, p. 112388, Aug. 2021, doi: 10.1016/j.engstruct.2021.112388.
- [9] B. Cai, B. Li, and F. Fu, "Finite Element Analysis and Calculation Method of Residual Flexural Capacity of Post-fire RC Beams," *Int J Concr Struct Mater*, vol. 14, no. 1, p. 58, Sep. 2020, doi: 10.1186/s40069-020-00428-7.
- [10] V. K. R. Kodur and A. Agrawal, "An approach for evaluating residual capacity of reinforced concrete beams exposed to fire," *Engineering Structures*, vol. 110, pp. 293–306, Mar. 2016, doi: 10.1016/j.engstruct.2015.11.047.
- [11] H. Erdem, "Predicting the moment capacity of RC beams exposed to fire using ANNs," *Construction and Building Materials*, vol. 101, pp. 30–38, Dec. 2015, doi: 10.1016/j.conbuildmat.2015.10.049.
- [12] Y. Y. Xu, B. Wu, M. Jiang, and X. Huang, "Experimental Study on Residual Flexural Behavior of Reinforced Concrete Beams after Exposure to Fire," *Advanced Materials Research*, vol. 457–458, pp. 183–187, 2012, doi: 10.4028/www.scientific.net/AMR.457-458.183.
- [13] B. Cai, G. Pan, and F. Fu, "Prediction of the Postfire Flexural Capacity of RC Beam Using GA-BPNN Machine Learning," *Journal of Performance of Constructed Facilities*, vol. 34, no. 6, p. 04020105, Dec. 2020, doi: 10.1061/(ASCE)CF.1943-5509.0001514.
- [14] R. Asghar et al., "Predicting the Lateral Load Carrying Capacity of Reinforced Concrete Rectangular Columns: Gene Expression Programming," *Materials*, vol. 15, no. 7, Art. no. 7, Jan. 2022, doi: 10.3390/ma15072673.
- [15] A. Nafees et al., "Predictive Modeling of Mechanical Properties of Silica Fume-Based Green Concrete Using Artificial Intelligence Approaches: MLPNN, ANFIS, and GEP," *Materials*, vol. 14, no. 24, Art. no. 24, Jan. 2021, doi: 10.3390/ma14247531.
- [16] H. A. Shah, S. K. U. Rehman, M. F. Javed, and Y. Iftikhar, "Prediction of compressive and splitting tensile strength of concrete with fly ash by using gene expression programming," *Structural Concrete*, vol. 23, no. 4, pp. 2435–2449, 2022, doi: 10.1002/suco.202100213.
- [17] M. A. Khan, S. A. Memon, F. Farooq, M. F. Javed, F. Aslam, and R. Alyousef, "Compressive Strength of Fly-Ash-Based Geopolymer Concrete by Gene Expression Programming and Random Forest," *Advances in Civil Engineering*, vol. 2021, p. e6618407, Jan. 2021, doi: 10.1155/2021/6618407.
- [18] A. Ahmad, K. Chaiyasan, F. Farooq, W. Ahmad, S. Suparp, and F. Aslam, "Compressive Strength Prediction via Gene Expression Programming (GEP) and Artificial Neural Network (ANN) for Concrete Containing RCA," *Buildings*, vol. 11, no. 8, Art. no. 8, Aug. 2021, doi: 10.3390/buildings11080324.
- [19] M. F. Iqbal et al., "Prediction of mechanical properties of green concrete incorporating waste foundry sand based on gene expression programming," *Journal of Hazardous Materials*, vol. 384, p. 121322, Feb. 2020, doi: 10.1016/j.jhazmat.2019.121322.
- [20] F. E. Jalal, Y. Xu, M. Iqbal, M. F. Javed, and B. Jamhiri, "Predictive modeling of swell-strength of expansive soils using artificial intelligence approaches: ANN, ANFIS and GEP," *Journal of Environmental Management*, vol. 289, p. 112420, Jul. 2021, doi: 10.1016/j.jenvman.2021.112420.
- [21] D. Mohammadzadeh S., S.-F. Kazemi, A. Mosavi, E. Nasseralshariati, and J. H. M. Tah, "Prediction of Compression Index of Fine-Grained Soils Using a Gene Expression Programming Model," *Infrastructures*, vol. 4, no. 2, Art. no. 2, Jun. 2019, doi: 10.3390/infrastructures4020026.
- [22] D.-P. N. Kontoni et al., "Gene Expression Programming (GEP) Modelling of Sustainable Building Materials including Mineral Admixtures for Novel Solutions," *Mining*, vol. 2, no. 4, Art. no. 4, Dec. 2022, doi: 10.3390/mining2040034.
- [23] Y. Murad, A. Ashteyat, and R. Hunaiyat, "Predictive model to the bond strength of FRP-to-concrete under direct pullout using gene expression programming," *Journal of Civil Engineering and Management*, vol. 25, no. 8, Art. no. 8, Aug. 2019, doi: 10.3846/jcem.2019.10798.
- [24] C. Ferreira, *Gene Expression Programming: Mathematical Modeling by an Artificial Intelligence*. Springer, 2006.
- [25] F. E. Jalal, Y. Xu, M. Iqbal, B. Jamhiri, and M. F. Javed, "Predicting the compaction characteristics of expansive soils using two genetic programming-based algorithms," *Transportation Geotechnics*, vol. 30, p. 100608, Sep. 2021, doi: 10.1016/j.trgeo.2021.100608.
- [26] "Measures of Fit for Regression." <https://www.geosoft.com/GeneXproTools/AnalysesAndComputations/MeasuresOfFit/Regression.htm> (accessed Jun. 11, 2023).



STRENGTH PREDICTION OF VARIOUS BEAMS THROUGH THE ARTIFICIAL NEURAL NETWORK

^a Muhammad Mahtab Ahmad*, ^b Ayub Elahi

a: Department of Civil Engineering, UET, Taxila, Pakistan, mahtabahmad010@gmail.com

b: Department of Civil Engineering, UET, Taxila, Pakistan, ayub.elahi@uettaxila.edu.pk

* Corresponding author: Email ID: mahtabahmad010@gmail.com

Abstract- This study aims to compare of first crack load and flexural strength of reinforced concrete beams without stirrups obtained from the conventional model developed using the current design code (ACI building code) with the non-conventional problem solver, i.e., an Artificial Neural Network (ANN). For this purpose, 110 sample data of reinforced concrete beams without stirrups reinforcement obtained from published research data are used to train Multilayer Backpropagation Neural Network through MATLAB. This work enables the development of a knowledge-based structural analysis model capable of predicting RC structural responses. The results obtained from the ANN model are closer to the experimental results of the conventional model. The coefficient of determination obtained from the comparison of these results is 0.945.

Keywords- Reinforced Concrete, Soft Computing, Artificial Neural Network, Ultimate Limit State, Finite Element, Multilayer Back Propagation, Nonlinear Finite Element Analysis, The Central Nervous System,

1 Introduction

Researchers and engineers have proposed essential theories [1–3] and techniques [4] to accurately forecast the behaviour of reinforced concrete (RC) structure elements at the ultimate limit state (ULS), ensuring safety and cost-effectiveness. Soft Computing (SC) methods [5–7], such as Artificial Neural Networks (ANNs) and Genetic Algorithms [8], have emerged as powerful computational tools that deviate from traditional analysis procedures and offer improved accuracy. ANNs provide precise and economical solutions with minimal analysis time, making them more efficient than conventional numerical procedures like the finite element (FE) method. To analyse RC structures effectively, accurate prediction of the nonlinear behaviour of individual components is crucial. ANNs rely on heuristic approaches rather than strict mechanics, and their calibration process must consider critical factors, including essential design parameters [9]. Experimental studies using scaled models [2, 10, 11] provide the database for the ANN model, capturing the behaviour and load-carrying capacity of RC members. However, the input values from these studies may not represent the design parameters used in full-scale RC members, limiting the precision of ANN predictions. Nonlinear Finite Element Analysis (NLFEA) and physical models using RC design codes [2, 10] [12] can offer valuable insights but may require re-calibration and have limitations in predicting full-scale RC members [13]. The main objective of this research is to train an ANN model to accurately predict structural properties (e.g., flexural strength, shear strength, and first crack load value) of RC beams based on key design parameters approaching the ULS. The study utilizes Multilayer Back Propagation (MBP) Neural Networks and MATLAB [12, 13] to develop an open-source analysis tool allowing users to modify parameters and solve a broader range of engineering problems. The proposed framework comprises several components: (1) analysis of relevant test data to create databases for developing the ANN model, (2) focus on the architectural formation of the ANN model, (3) training the ANN model, and (4) developing a function to expand the ANN model's application for predicting RC structure response, even in cases where available experimental databases lack design parameters or inadequately represent them [16].



1.1 Artificial Neural Network Morphology

Artificial Neural Networks (ANNs) are computational models inspired by the biological neural networks found in human and animal brains. They are designed to process information, learn from it, identify patterns, and make predictions, like the biological nervous system. ANNs have a wide range of applications in natural language processing, image recognition, and data prediction. The structure of an ANN consists of interconnected neurons organized into layers, including an input layer, one or more hidden layers, and an output layer. Each neuron is connected to others through weighted links. These weights determine the significance of the input values. The values from the neurons in each layer are summed with bias values, and this process is repeated for subsequent layers, forming a network that processes and transmits information. Activation functions define the relationship between neurons in consecutive layers. The output of a neuron in one layer becomes the input for the neurons in the next layer. Initially, the weights are assigned randomly, but during the training process, iterations are performed to adjust the weight values to achieve accurate output predictions. Equation (1 & 2) provides an analytical expression for the summation of weights [20].

$$x_j = \sum(y_i W_{ji}) + b_j \quad \text{Equation (1)}$$

$$y_j = f(x_j) \quad \text{Equation (2)}$$

In the above Equations, x_j represents the output from a specific neuron, y_k represents the results received from applying the activation function $f(x_j)$, W_{ji} represent weights coefficients used between interconnected neuron, b_j is the bias value for the neuron, and "j" and "i" represent the number of layers and neurons in each network, respectively.

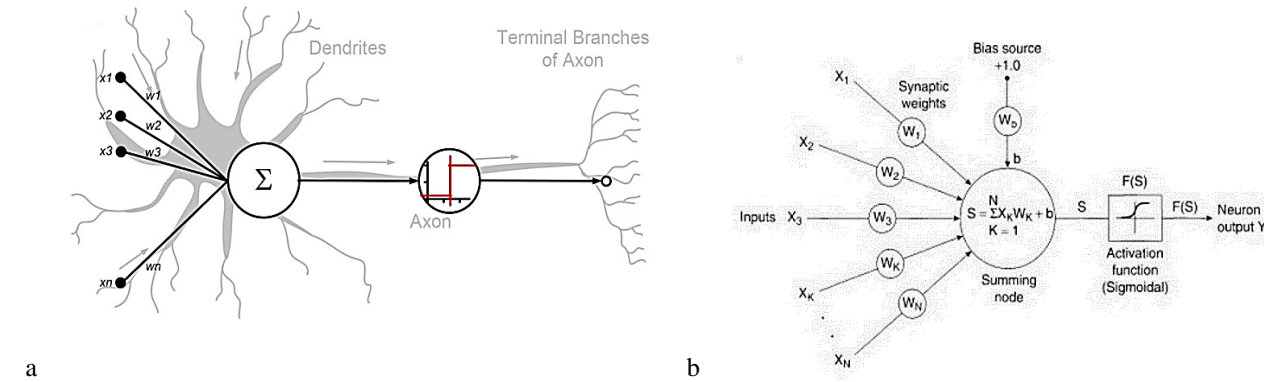


Figure 1 a) Biological and Artificial Neural Network Morphology, b) Structure of ANN model[20]

2 Artificial Neural Network Model Formation

2.1 Multilayered Backpropagation ANN Model Structure

The Multilayered Backpropagation Neural Network (MBNN) model is widely used to predict the behaviour of reinforced concrete structures [19]. The visual representation of MBNN is shown in Figure 3 (b). It operates in two phases: free forward calculation and Error Signal Backpropagation. In the first phase, input parameters from the sample database are fed into the input layer neurons. Weights are multiplied with inputs, and biases are summed to produce neuron outputs. An activation function introduces nonlinearity. This process continues through hidden layers, and their outputs serve as inputs for the output layer, generating predictions. Predicted results are compared with target values in the database, calculating the error [21, 22]

$$E = \frac{1}{2} \sum(X_j - Y_j)^2 \quad \text{Equation (3)}$$

The error signal obtained from the previous phase is used to adjust the weights and biases of the MBNN. This involves changing the network architecture, such as the number of neurons or layers, and increasing the cycles. The feedforward process is repeated to minimize errors and optimize the network for accurate results [20]. The "Gradient Descent" method is employed, where weight adjustments depend on the error function "E" and learning rate " η " [16]. Correction is calculated using equation (4).

$$\Delta W_{ji} = -\eta \frac{\delta E}{\delta W_{ji}} \quad \text{Equation (4)}$$

As from equation 4, if a higher learning rate value is applied, then abrupt changes in the value of weights would come out during each iteration if higher values of weights are used initially; this would lead to a prolonged process to achieve an optimised neural network model. On the other hand, with a small value of learning rate and small values of weights initially



applied, training cycles are increased with prolonged training time but can proceed to a more optimised Neural Network model.

2.2 Transfer Function

Activation functions in an ANN model play a vital role in processing and transmitting information between layers. The choice of activation function depends on the problem and input parameter normalization. Different functions are applied between layers. For instance, the "log-sigmoid" function is used between the input and hidden layers when data is normalized between 0 and 1. When normalization yields result between -1 and 1, the "linear" function is used for the last two layers. In decision-making cases, the "hyperbolic tangent" function can be used between all layers, with "Gaussian" for the output layer and "hyperbolic tangent" for the hidden layer. Activation function selection has no strict rule, and each has advantages and limitations. Sigmoid provides non-linearity and an output range of 0 to 1 but faces vanishing gradients and output saturation. Tanh introduces non-linearity, has zero-centred output, stronger gradients, and vanishing gradients and no finite bounds. ReLU is popular in deep learning due to sparsity, efficiency, and avoiding vanishing gradients, but can lead to dead neurons and lacks an upper bound. Softmax is used in multi-class classification for class probabilities but can be sensitive to large inputs and assumes class independence. Consider these factors to select appropriate activation functions based on task and network architecture, ensuring optimal performance and stability in the ANN model.

2.3 MBNN Model Creation

For predicting flexural strength, shear strength, and first crack load in beams, the Multilayer Back Propagation neural network (MBPNN) is selected. Previous studies indicate that the network's performance depends on factors such as sample database size, number of hidden layers and neurons, and initial weights and biases. Activation functions, error functions, and learning algorithms are also critical in determining the learning rate and performance. Literature suggests optimizing the neural network for improved performance and fast learning rate [20, 23],

1. Initial values for weights and biases should be assigned between -0.5 and 0.5.
2. In the hidden layer number of neurons should be double the amount neurons in the input layer
3. The activation function for the first two layers (input layer and hidden layer) should use used sigmoid activation function, while the output layer hyperbolic tangent activation function should be used.

Determining the ideal number of hidden layers and neurons in an artificial neural network is challenging and crucial for its predictive capabilities. Increasing layers or neurons can improve pattern learning but may be overfitted without proper regularization. Reducing complexity can lead to underfitting. Cross-validation and grid search techniques are used to find optimal configurations. Cross-validation divides the dataset, and trains and evaluates the network multiple times, comparing performance across configurations. Grid search explores hyperparameter combinations to select the best configuration based on validation set performance. Both approaches aim for a balanced architecture maximizing prediction accuracy. Optimal architecture depends on the dataset and problem, requiring careful evaluation and experimentation.

2.4 Sample Database

110 Sample databases were included in this network training testing and validation process. Data is based on a simply supported beam without shear reinforcement, whose sampling was done in UET Taxila concrete laboratory. The ranges of the database are listed in the table below.

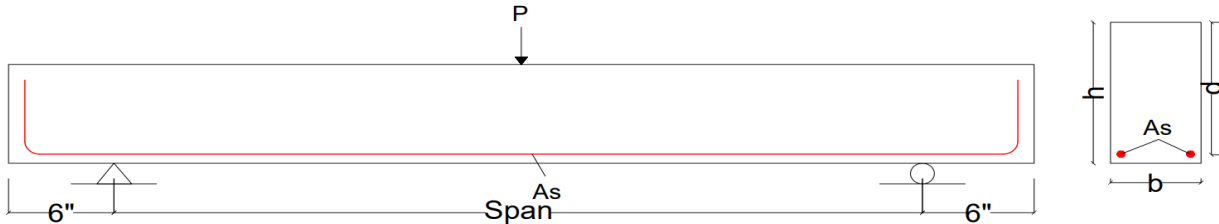


Figure 2 Beam cross Section details.

Table 1 Range of sample database for network training

Units	b inch	d inch	Av/d	p ₁ %	a ₁	f _y psi	f _c psi	L inch	M _f lb.in	P _{cr} lb.
Max	7	12.5	6	2.057	2.91	77222	8339	126	1047084	54574
Min	6	10.5	1	0.349	0.37	70727	7697	21	95400	2160
SD	0.502	1.004	1.588	0.582	0.768	2599.74	157.47	33.35	237180.73	10268.58
Avg.	6.5	11.5	3.5	1.099	1.389	74286	8024.29	85.5	483318.08	12606.42
COV	0.077	0.087	0.454	0.529	0.553	0.035	0.0196	0.39	0.49	0.815



2.5 Data Processing

ANN performance relies on the quality of the database. To optimize the network, it's crucial to normalize the database for efficient training. After training, data can be denormalized for comparison with target values. Normalization converts values to unitless form, ensuring consistency. Database normalization between upper and lower values prevents slow learning. MATLAB's Neural Network Toolbox provides functions for normalization. Performing normalization before data loading allows for greater control. In the mentioned model, data is normalized between 0.1 and 1 using equation (5).

$$x' = \frac{(x - x_{min})}{(x_{max} - x_{min})} (u - l) + l \quad \text{Equation (5)}$$

Where x' is the new normalized value, x is the original value, u is the upper limit for normalization, and l is the lower limit for normalization.

2.6 Division of Database

Data is split into three subsets: training, validation, and testing. The training subset is used for weight and bias adjustments through gradient updates. The validation subset calculates the error function and supports backpropagation during training. The testing subset evaluates different network models and compares errors with the validation process. If discrepancies arise, the dataset division is adjusted to minimize differences. Our model assigns 70% for training, 15% for validation, and 15% for testing. MATLAB's "dividerand" command randomizes the database division for optimized efficiency.

2.7 The Functionality of ANN Model

ANN model is trained as a multi-layer model that is coded in MATLAB using the Levenberg-Marquardt algorithm with the free forward back-propagation method [4, 19, 20]. The key aspects of training are summarized as

- 1) The training process involves dividing the database into three subsets using a random method. 70% of the data is used for training, 15% for validation, and the remaining 15% for testing.
- 2) 1000 epochs/cycle are selected to train the ANN model, and the training is stopped if either of the following conditions is met: (a) a maximum of 100 validation failures occur, or (b) the minimum performance learning slope becomes 10^{-8} .
- 3) The error value of the correlation factor (R), the mean absolute error (MAE), and the mean squared error (MSE) are used to select the optimized ANN model [21–23]. These measures are expressed analytically by equations (6)–(8) respectively, as referenced from the literature.

$$R = \frac{\sum_{i=1}^n (X_i - \bar{X})(Y_i - \bar{Y})}{\sum_{i=1}^n (X_i - \bar{X})^2 \sum_{i=1}^n (Y_i - \bar{Y})^2} \quad \text{Equation (6)}$$

$$MSE = \frac{\sum_{i=1}^n (X_i^2 - Y_i^2)}{n} \quad \text{Equation (7)}$$

$$MAE = \frac{\sum_{i=1}^n |X_i - Y_i|}{n} \quad \text{Equation (8)}$$

here $\bar{X} = \frac{\sum_{i=1}^n X_i}{n}$ and $\bar{Y} = \frac{\sum_{i=1}^n Y_i}{n}$ which are averages of measured (Y_i) and predicted (X_i) outputs while n is the number of sample data in the database. While to get an optimised ANN model, the value of "R" should be highest, approaching 1, while the values of "MSE" and "MAE" should be lowest.

While to overcome the problem of overfitting gradient descent methodology is used to converge values of weights and biases, while at the same time, early stopping criteria as defined in the functionality of ANN is employed to avoid overfitting.

3 Research Methodology

Concrete waste is produced due to research work, participating in global warming to some extent as concrete is also a source of temperature increase. To overcome this on behalf of previous sample data, one of the soft computing techniques, an Artificial neural network, is used to get optimised sample data results to reduce the number of physical concrete beam sample creations. For this research work, the methodology adopted is displayed in the flow chart in Figure 3 (a) to develop a green and economical solution.

4 Results and Discussion

The ANN model's results are compared using regression curves and the coefficient of determination. Regression values range from 0.92 to 0.97, and the coefficient of determination is above 0.94, indicating a good fit and training the model three times yields optimised results. The regression analysis listed in Figure 5 shows precise predictions for the first crack

load ($R=0.981$ for training and 0.967 overall) and flexural strength ($R=0.997$ for training and 0.977 overall). These results confirm the accuracy of the ANN model in predicting these structural properties.

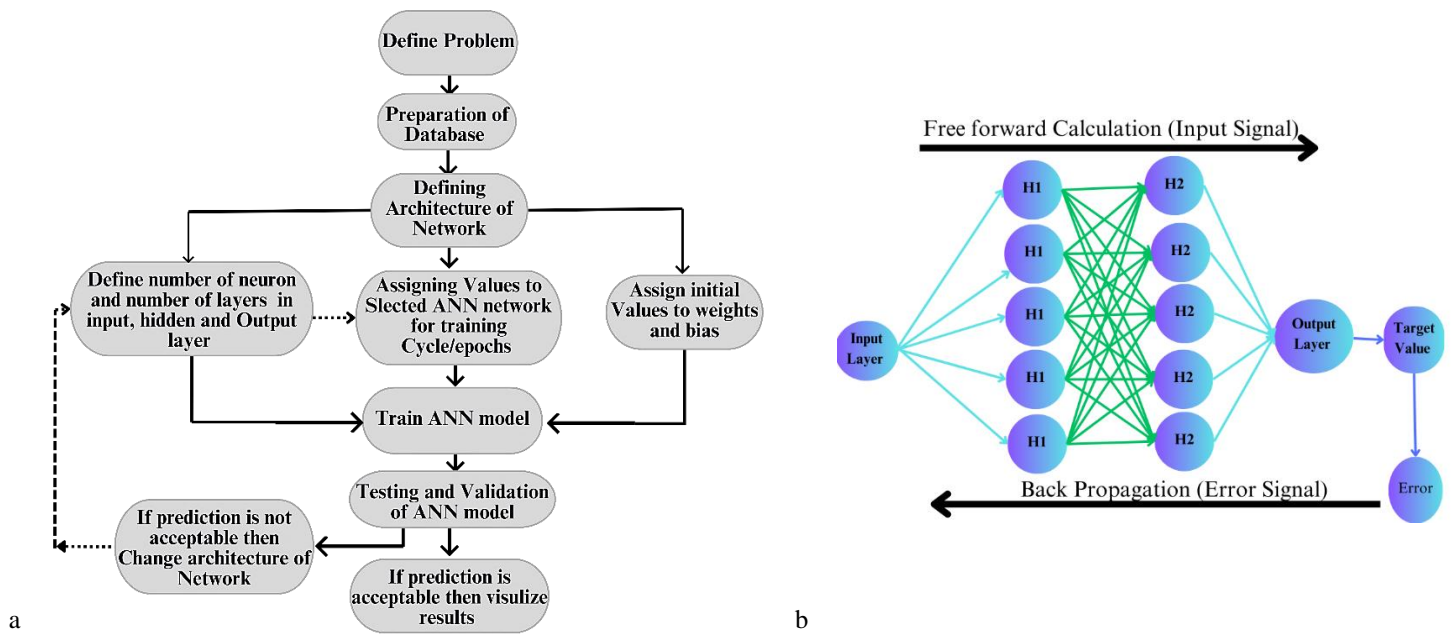


Figure 3 a) Research Methodology Layout, b) Multilayer Back-propagation Neural Network Structure

Table 2 a) Error checks for the first cracking load model, b) Error checks for the Flexural Strength model

First Cracking Load ANN model	
MSE	0.0019
MAE	0.0315
R	0.96735
R^2 (Coefficient of determination)	0.9404

Flexural Strength ANN model	
MSE	0.0017441
MAE	0.0234
R	0.97764
R^2 (Coefficient of determination)	0.9756

4.1 Behaviour of First Crack Load based on a/d.

The first cracking load decreases as the shear span to adequate depth (a/d) ratio increases, while keeping the reinforcement ratio constant at 0.349%. Experimental results (Figure 5a) show that for an "a/d" ratio of 1, the load is 28.1 Kip, and for an "a/d" ratio of 6, the load reduces to 2.16 kip. This decreasing trend is due to the increased span length with a higher "a/d" ratio while keeping the depth constant. Comparisons between experimental, ANN, and theoretical results confirm the decreasing trend. ANN predictions achieve a coefficient of determination of 0.9404, indicating accurate predictions based on input parameters.

4.2 Behaviour of first crack load based on reinforcement ratio.

The first cracking load initially increases with a higher reinforcement ratio (%) for a constant shear span to an effective depth ratio ($a/d=1$) (Figure 5b). However, after reaching a reinforcement ratio of 0.984%, the load decreases for the beam samples. This trend differs from the decreasing trends observed in the same sample's experimental, ANN, and theoretical results. The increase in the first cracking load with a higher reinforcement ratio is due to the steel strength and bond with concrete, enhancing the load-carrying capacity. Excessive reinforcement, however, leads to brittle failure and a decrease in load-carrying capacity.

4.3 Behaviour of Flexural Strength based on a/d.

The Flexural Strength of the reinforced concrete beam with constant steel reinforcement ratio (ρ) 0.349% and varying shear span to effective depth ratio (a/d) shows a decreasing trend with an increase in a/d . The same trend was observed in the case of ANN-predicted results. The prediction accuracy of ANN results is checked by finding the coefficient of determination by comparing predicted results against specific input data with experimental results of that input data physical model that is 0.9756.



4.4 Behaviour of Flexural Strength based on reinforcement ratio.

Experimental results with a constant shear span to effective depth ratio (a/d) demonstrate an increase in flexural strength up to a reinforcement ratio of 0.984%. Beyond this point, the flexural strength shows marginal changes. Similarly, the ANN-predicted results exhibit the same trend, closely matching the experimental data. This suggests that the ANN model is effective for predicting the flexural strength or ultimate load of reinforced concrete members.

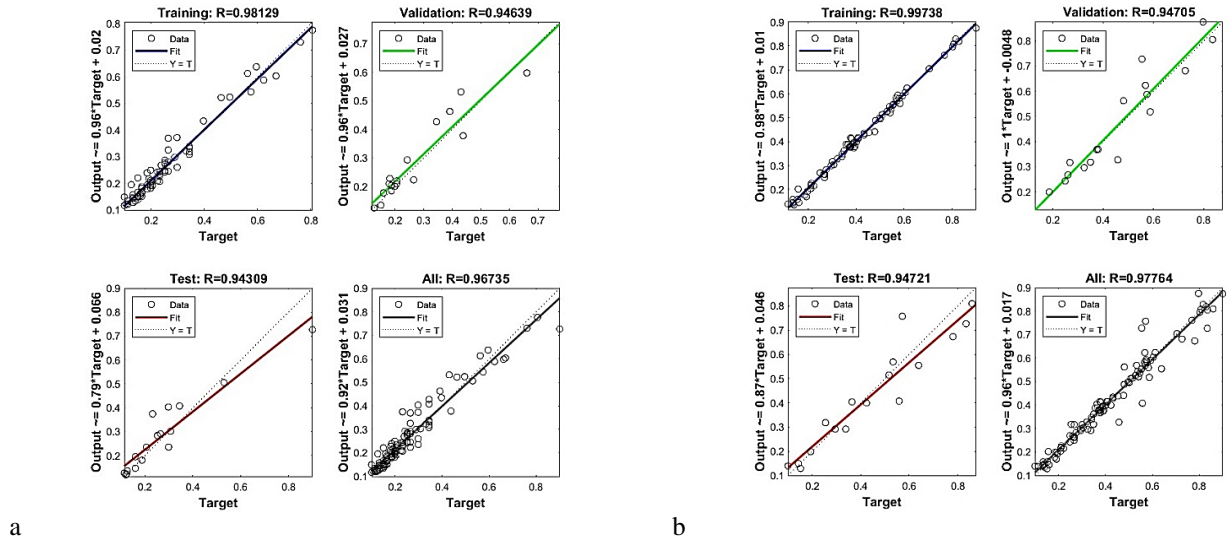


Figure 4 a) ANN model results for First crack load prediction, b) ANN model Results for Flexural Strength prediction

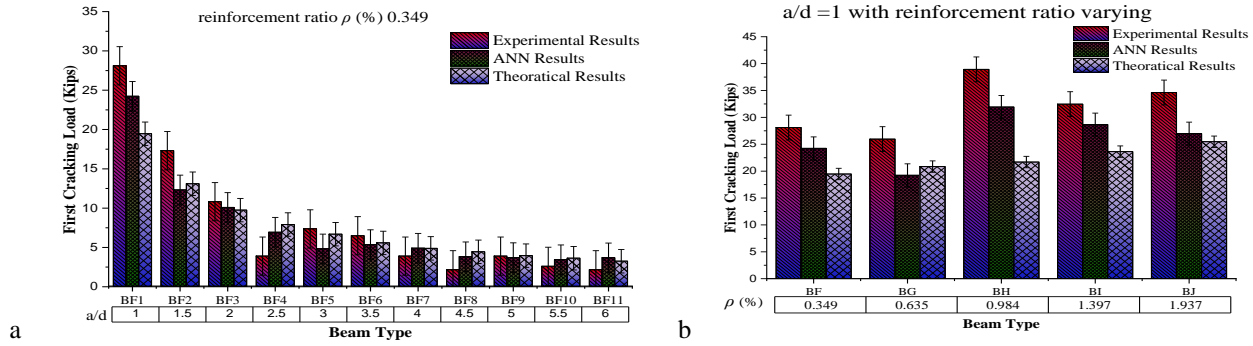


Figure 5 a) Comparison of First Cracking Load results with increasing a/d ratio by ρ (%) constant, b) Comparison of First Cracking Load results by increasing ρ (%) by keeping a/d ratio constant.

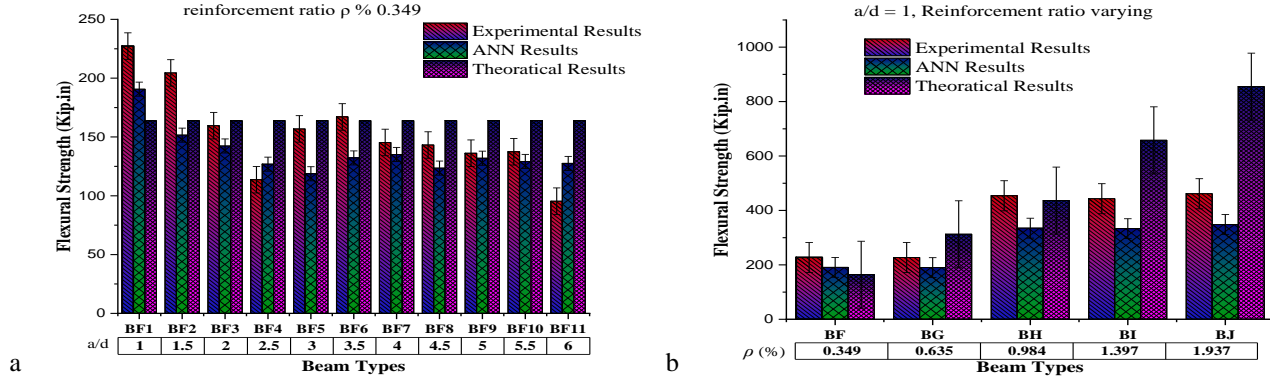


Figure 6 a) Comparison of Flexural Strength results with increasing a/d ratio by keeping ρ (%) constant, b) Comparison of Flexural Strength results by increasing ρ (%) by keeping a/d ratio constant.



5 Conclusions

This study explains the development of a knowledge-based structural analysis model capable of predicting RC structural responses. The ANN model was developed based on the Multilayer Backpropagation neural network methodology, which enables the prediction of the behaviour of nonlinear elements. Input parameters are selected based on physical model preparation, and the predicted results are compared with the experimental results of the physical model. Predicted results are close to the experimental results.

1. The linear correlation coefficient "R" for the first cracking load is 0.96735, and the coefficient of determination " R^2 " for the First Cracking Load is 0.9404, close to 1, showing precise and close to experimental results.
2. The linear correlation coefficient "R" for the Flexural Strength is 0.97764, and the coefficient of determination " R^2 " for the Flexural Strength is 0.9756, close to 1, showing precise and close to experimental results

Unlike the conventional method for predicting the structural response of reinforced concrete members, Soft Computing Techniques, i.e. ANN model, can predict the behaviour of RC structural members with simple or complex geometry under different loading conditions. As soon as the ANN model is trained based on the concerned sample database can predict accurate prediction of the RC structural member accurately without concerning material behaviour and mechanics of the underlying member at the ultimate limit state (ULS).

5.1 Future Work Direction

ANN model can be used with professional design software for nonlinear analysis to predict the response of structural members at ultimate limit state under simple or complex loading without requiring analysis time and predicting accurate results compared to conventional current design codes.

Acknowledgement

I wish to express my gratitude to my research supervisor, Prof. Dr. Ayub Elahi for his ample guidance and encouragement to me during this research proceedings.

References

- [1] B. S. Institution, *Eurocode 2: Design of concrete structures: Part 1-1: General rules and rules for buildings*. British Standards Institution, 2004.
- [2] A. C. Institute, "Building Code Requirements for Structural Concrete (ACI 318-08) and Commentary: An ACI Standard," American Concrete Institute, 2008.
- [3] K. Maruyama, "JSCE Standard Specifications for Concrete Structures 2007, Codes in Structural Engineering-Developments and Need for International Practice," in *Joint IABSE-fib Conference Dubrovnik 2010*, 2010, pp. 315–322.
- [4] A. Ahmad, N. D. Lagaros, and D. M. Cotsovos, "Neural Network-Based Prediction: The Case of Reinforced Concrete Members under Simple and Complex Loading," *Applied Sciences*, vol. 11, no. 11, p. 4975, 2021.
- [5] V. Chandwani, V. Agrawal, and R. Nagar, "Applications of soft computing in civil engineering: a review," *Int J Comput Appl*, vol. 81, no. 10, 2013.
- [6] S. K. Das, A. Kumar, B. Das, and A. P. Burnwal, "On soft computing techniques in various areas," *Comput. Sci. Inf. Technol*, vol. 3, no. 59, p. 166, 2013.
- [7] S. Talatahari, V. P. Singh, A. H. Alavi, and F. Kang, "Soft computing methods in civil engineering," vol. 2015. Hindawi, 2015.
- [8] R. R. Yager and L. A. Zadeh, *Fuzzy sets, neural networks and soft computing*. John Wiley & Sons, Inc., 1994.
- [9] B. Z. Dehkordi, R. Abdipour, S. Motaghehd, A. K. Charkh, H. Sina, and M. S. Shahid Zad, "Reinforced concrete frame failure prediction using neural network algorithm," *Journal of Applied Sciences*, vol. 12, no. 5, pp. 498–501, 2012.
- [10] B. S. En, "1-1. Eurocode 2: Design of concrete structures—Part 1-1: General rules and rules for buildings," *European Committee for Standardization (CEN)*, 2004.
- [11] M. D. Kotsovov, "Compressive force-path method," *Switzerland: Springer*, 2013.
- [12] Y. O. Özkilic, C. Aksoylu, and M. H. Arslan, "Experimental and numerical investigations of steel fiber reinforced concrete dapped-end purlins," *Journal of Building Engineering*, vol. 36, p. 102119, 2021, doi: <https://doi.org/10.1016/j.jobe.2020.102119>.
- [13] G. Balaji and R. Vetturayashudharsanan, "Experimental investigation on flexural behaviour of RC hollow beams," *Mater Today Proc*, vol. 21, pp. 351–356, 2020, doi: <https://doi.org/10.1016/j.matpr.2019.05.461>.
- [14] M. H. Beale, M. T. Hagan, and H. B. Demuth, "Neural network toolbox," *User's Guide, MathWorks*, vol. 2, pp. 77–81, 2010.
- [15] H. N. Koivo, "Neural networks: Basics using matlab neural network toolbox," *Author Website*, 2008.
- [16] A. Ahmad, G. Kotsovou, D. M. Cotsovos, and N. D. Lagaros, "Assessing the accuracy of RC design code predictions through the use of artificial neural networks," *International Journal of Advanced Structural Engineering*, vol. 10, pp. 349–365, 2018.



5th Conference on Sustainability in Civil Engineering (CSCE'23)

Department of Civil Engineering

Capital University of Science and Technology, Islamabad Pakistan



- [17] D. Anderson and G. McNeill, "Artificial neural networks technology," *Kaman Sciences Corporation*, vol. 258, no. 6, pp. 1–83, 1992.
- [18] I. A. Basheer and M. Hajmeer, "Artificial neural networks: fundamentals, computing, design, and application," *J Microbiol Methods*, vol. 43, no. 1, pp. 3–31, 2000.
- [19] D. Svozil, V. Kvasnicka, and J. Pospichal, "Introduction to multi-layer feed-forward neural networks," *Chemometrics and intelligent laboratory systems*, vol. 39, no. 1, pp. 43–62, 1997.
- [20] A. Ahmad, D. M. Cotovos, and N. D. Lagaros, "Framework for the development of artificial neural networks for predicting the load carrying capacity of RC members," *SN Appl Sci*, vol. 2, pp. 1–21, 2020.
- [21] A. Ahmad, M. Elchalakani, N. Elmesalami, A. El Refai, and F. Abed, "Reliability analysis of strength models for short-concrete columns under concentric loading with FRP rebars through Artificial Neural Network," *Journal of Building Engineering*, vol. 42, p. 102497, 2021, doi: <https://doi.org/10.1016/j.jobe.2021.102497>.
- [22] M. Kaczmarek and A. Szymańska, "Application of artificial neural networks to predict the deflections of reinforced concrete beams," *Studia Geotechnica et Mechanica*, vol. 38, Jul. 2016, doi: 10.1515/sgem-2016-0017.
- [23] U. Naik and S. Kute, "Span-to-depth ratio effect on shear strength of steel fiber-reinforced high-strength concrete deep beams using ANN model," *International Journal of Advanced Structural Engineering*, vol. 5, no. 1, p. 29, 2013, doi: 10.1186/2008-6695-5-29.
- [24] F. Giordano, M. La Rocca, and C. Perna, "Input variable selection in neural network models," *Communications in Statistics- Theory and Methods*, vol. 43, no. 4, pp. 735–750, 2014.
- [25] M. H. Beale, M. T. Hagan, and H. B. Demuth, "Neural Network Toolbox™, User's Guide, MATLAB® R2015a, The MathWorks," Inc., Natick, MA, USA, vol. 410, 2015.
- [26] J. Utans, J. Moody, S. Rehfuss, and H. Siegelmann, "Input variable selection for neural networks: Application to predicting the US business cycle," in *Proceedings of 1995 Conference on Computational Intelligence for Financial Engineering (CIFEr)*, IEEE, 1995, pp. 118–122.
- [27] A. Krogh and J. Vedelsby, "Neural network ensembles, cross validation, and active learning," *Adv Neural Inf Process Syst*, vol. 7, 1994.



EXPLORING VIBRATION MEASUREMENT PRECISION: A COMPARATIVE ANALYSIS OF A DIY, LOW-COST ACCELERATION MEASUREMENT UNIT VERSUS A PREMIUM STANDARD ACCELEROMETER SYSTEM

^a Usama Bin Tariq, ^b Basit Tanveer, ^c Nawab Khan,

a: Department of Civil Engineering, UET, Taxila, Pakistan, usamakhan40.uk@gmail.com

b: Department of Civil Engineering, UET, Taxila, Pakistan, basittanveer68@gmail.com

c: Department of Civil Engineering, UET, Taxila, Pakistan, nawabjaveed6@gmail.com

* Corresponding author: Email ID: usamakhan40.uk@gmail.com

Abstract- This study focuses on the fabrication and utilization of a low-cost acceleration measurement unit in the construction industry. The ADXL 345 Accelerometer is integrated with an Arduino Mega 2560 microcontroller to facilitate monitoring and recording of readings. The accelerometer captures acceleration along three axes and is connected to the microcontroller. While the low-cost acceleration measurement unit offers approximate measurements, it is subject to certain limitations. The research highlights the importance of creating affordable sensors in scenarios where premium sensors are not readily available or cost-effective. To evaluate the accuracy of the developed prototype, a comparison is made against a premium acceleration measurement unit (AMUs) comprising MEMS type accelerometer 4030 by TE Connectivity controlled by the DAQ System7000 by Vishay Intertechnology, Inc. USA. The relative error is calculated with respect to a finite element model. The obtained results demonstrate that the relative error is not significantly high, thereby indicating the potential reliability of the acceleration measurement unit.

Keywords- Accelerometer, Arduino, Dynamic response, Monitoring and recoding

1 Introduction

Accelerometers play a vital role in various technical domains, including aerospace engineering, civil engineering, and electronics. These devices are primarily used to measure accelerations along one or more axes. Accelerometers are used in the building sector to monitor and evaluate the response of the structure to seismic activity, wind forces, and vibrations. Accelerometers are carefully positioned in key areas of a building to collect continuous data on structural behaviour for post-event and real-time analysis [1].

For assessing a building's structural performance, integrity, and safety, precise acceleration measurements are essential for vibrational analysis techniques. This collected data provides insightful information about how structures behave dynamically under various loading scenarios. It helps reduce the risk of damage and failure by assisting in the design of structures that can withstand anticipated loadings and accelerations. Computed results from the analysis of dynamic acceleration data include displacement, velocity, and frequency. These measurements make it easier to evaluate how structures respond, spot potential weaknesses, confirm design presumptions, and make the necessary adjustments to maintain structural integrity.

However, the cost of acceleration measurement sensors is frequently out of reach, particularly in developing nations like Pakistan. There is a pressing need to develop/fabricate low-cost, in-house acceleration measurement units that can be used across various industries in order to address this issue and make such sensors available. These devices can still offer useful



information and act as a cost-effective solution, even though their accuracy and precision might not be as good as those of high-end sensors [2].

A study [3] examines the use of an inexpensive Arduino-based vibration measurement system for structural health monitoring. They mentioned the drawbacks of inexpensive components and how they affect measurement accuracy. When choosing such systems, the authors stress the importance of carefully considering the trade-off between cost and accuracy. The experimental validation of vibration-based energy harvesting for structural health monitoring with Arduino-based systems is presented by Kaur and Bhalla in 2015 [4]. In addition to highlighting the significance of precise vibration measurement for effective energy harvesting, they also express concern about the potential shortcomings of inexpensive Arduino units in achieving the necessary level of accuracy. Tomaneng et al. propose an advanced Arduino-based seismic monitoring system in 2022 [5], with the goal of improving vibration measurement accuracy. They incorporate sophisticated signal processing algorithms and noise reduction techniques to overcome the drawbacks of inexpensive Arduino units. A study [6] offers a soft-gauge solution based on the low-cost triple-axis accelerometer MMA7361L and LabVIEW software for lift vibration analysis with national standards precision. The MMA7361L and NI USB6009 3-dimensional vibration signals are fed into a soft-gauge programmed in LabVIEW to filter, and the fast Fourier transform (FFT) is used to determine the power spectral density (PSD) and spectrogram of vibrations of filtered vibration signals. [7] in paper used inkjet-printed sensor in the mesoscale to investigate its behavior in low-frequency domain (20Hz). This frequency fits its applications in the field of seismic monitoring. Based on results and performances authors encourage the use of all-inkjet-printed sensor because of low cost and disposable features.

The aforementioned literature review showcases several studies that have examined and compared low-cost and premium Arduino-based systems for vibration measurement.

This study focuses on the fabrication of a low-cost acceleration measurement unit and compares the results with a finite element model and measurements from a MEMS type accelerometer 4030 by TE Connectivity connected to a DAQ System7000 by Vishay Intertechnology, Inc. USA. The measurements are displayed and recorded using the Arduino Mega 2560 in conjunction with the ADXL 345 3-axis acceleration measurement sensor. The outcomes of this research have significant implications for various departments, given the diverse applications of this sensor.

2 Experimental Procedures

There were numerous in-depth discussions with relevant technology experts prior to the creation of the new prototype.

The choice of an appropriate accelerometer was given careful thought throughout the procedure. The sensitivity requirements, frequency range, size, price, and environmental conditions of the intended application are just a few of the variables that affect the selection of an accelerometer [8]. The ADXL 345 accelerometer was decided upon for this study in accordance with these factors. With variable sampling rates up to 100Hz, this accelerometer can detect acceleration in three dimensions. The ADXL345 is a small and energy-efficient component that is frequently used in electronic devices, such as smartphones, tablets, and game controllers, to detect changes in orientation and movement.

2.1 Arduino Mega 2560

The Arduino Mega 2560 is a reliable platform for displaying and storing information in computer memory. It employs the ATmega2560, an 8-bit AVR-based microcontroller with 256 KB of flash memory for storing program code, 8 KB of SRAM for storing data, and 4 KB of EEPROM for nonvolatile storage. The Arduino Mega 2560 is an improved version of the original Arduino boards, with an increased number of features and capabilities than the Arduino Uno. It is especially useful for projects that require many I/O pins, a large amount of program memory, and advanced functionality. The Arduino Mega 2560 is frequently used in projects requiring enhanced processing power and communication capabilities, such as robotics, automation, data recording, and other applications.

Features of Arduino Mega 2560:

- Microcontroller
- Digital I/O Pins
- Analog Inputs
- Communication Interfaces
- Memory Expansion
- Additional I/O



- Power Supply

Fusion 360, a program renowned for its sophisticated 3D modelling capabilities, is used to create the enclosure (see Figure 1b) for the Arduino and accelerometer. It makes it possible to design the casing in a precise and unique way. Once the design is complete, a CNC (Computer Numerical Control) machine is used to precisely cut the required acrylic sheets to the required sizes.

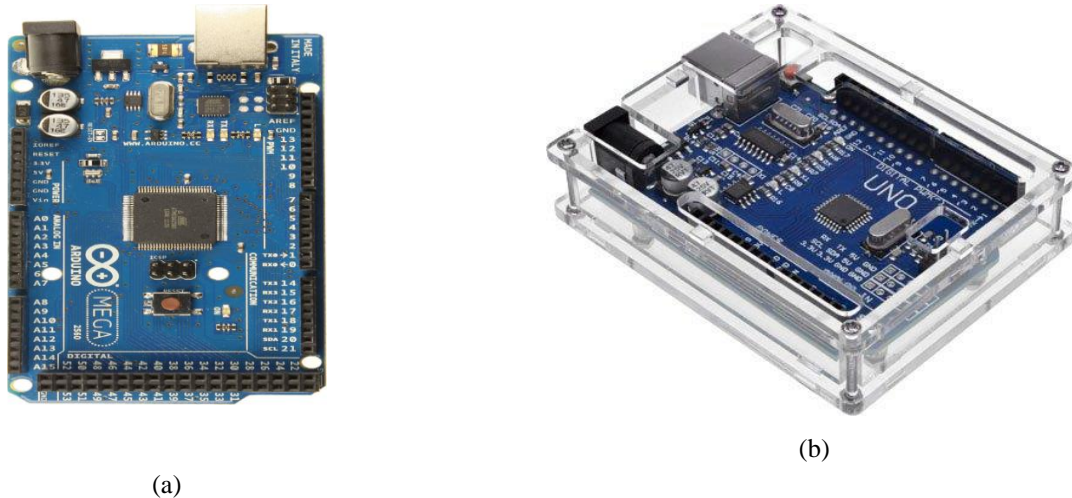


Figure 1: Prototype assemblage (a) Arduino Mega 2560 board (b) Acrylic casing

2.2 Steel Frame Test Model

The premium acceleration sensor (MEMS Accelerometer by TE Connectivity) and the prototype are both attached to the top of the model. Finger-tap force is used to cause vibrations in the steel frame while samples are being collected for a predetermined amount of time. 'Coolterm' software is utilized to save the data. The readings collected are displayed using the Arduino IDE software. The chosen accelerometer's accuracy is within $\pm 3g$ range. Using Finite Element Method (FEM), response time history and power amplitude of the steel frame are conducted to obtain a structural response set of data. This data is then compared with the readings from the premium and prototype acceleration measurement units to determine the relative inaccuracy.

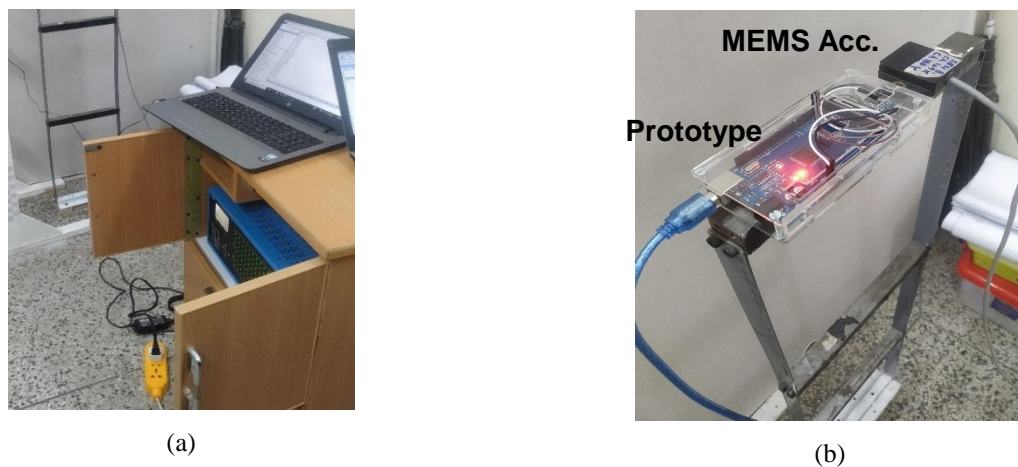


Figure 2: Testing setup (a) DAQ System7000 (b) Prototype and MEMS (4020) acceleration measurement unit mounted on steel frame model



3 Research Methodology

The results of the experiment (see Section 4) and analyzed through the utilization of graphs representing the power spectrum and time response. The power spectrum is a mathematical representation that illustrates the distribution of a signal's power or energy across different frequencies. It is obtained by subjecting the signal to a mathematical operation called the Fourier transform, which decomposes the signal into its constituent frequencies. By examining the power spectrum, valuable insights can be gained regarding the frequency composition of the signal under investigation.

On the other hand, the time-based response of a system or signal depicts its behavior over time in response to a specific input or stimulus. It represents the output of the system as a function of time when subjected to a particular input. This temporal response provides significant information about the dynamic characteristics of the system, including its transient response, stability, and other inherent qualities.

The power spectrum makes it possible to identify and characterize frequency components that make up the signal, highlighting dominant frequencies or potentially interesting spectral features. On the other hand, the temporal response demonstrates how the system or signal develops and changes over time, providing essential information about its transient behaviour, damping properties, and general dynamic response.

4 Results

Figures 3(a) and 3(b) are time history response graphs which give a visual representation of the structure's response to vibrations. It is clear from the graphs that the Premium Acceleration Measurement Unit displayed higher acceleration values than the Prototype. Particularly, at 12.5 seconds into the test, the Prototype recorded its highest acceleration reading of 0.183 g. The System7000, on the other hand, recorded a maximum acceleration reading of 0.199 g. These numbers demonstrate how the two systems' acceleration measurements differ from one another.

The System7000 consistently showed higher acceleration values than the Prototype over the length of the 50-second test. This shows that throughout the testing period, the premium measurement unit consistently recorded higher acceleration levels. The premium system appears to be better able to detect and record weaker magnitudes of acceleration based on the higher values it recorded.

When assessing the efficiency and dependability of the prototype acceleration measurement unit, it needs to take these conclusions into account. It is advised to conduct additional research and testing to determine the Prototype's limitations and possible areas for development, especially with regard to precisely measuring acceleration values.

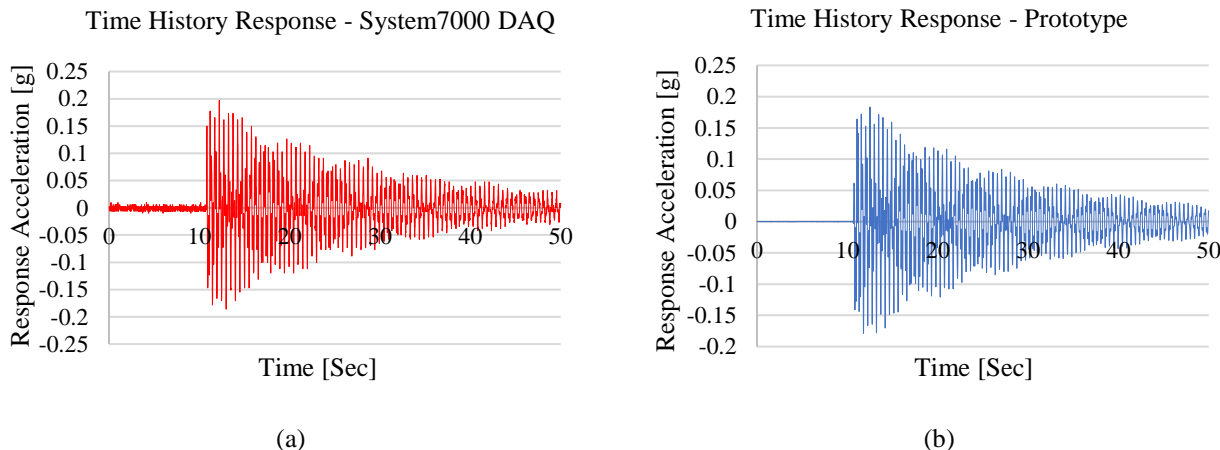


Figure 3: Time history model response (a) System7000 DAQ (b) Prototype

Figure 4 illustrates the frequency content and power distribution of the signal received from the vibrating structure. The graph shows the relationship between frequency, which represents the speed at which the signal oscillates, and power spectrum, which represents the distribution of power or energy across various frequencies. Applying the Fourier



transform, which breaks the signal down into its component frequencies, yields the power spectrum. The estimated modal frequencies of the test model are presented in the Table 1.

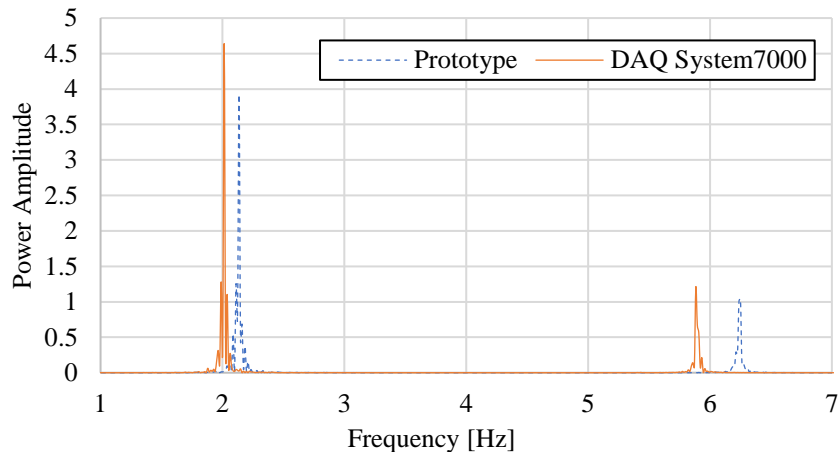


Figure 4: Frequency vs Power Spectrum

Table 1: Dynamic characteristics

Mode (Hz)	FE Results	Prototype	System7000-DAQ
1	1.97	2.14 (+9%)	2.01 (+2%)
2	5.93	6.25 (+5%)	5.88 (-1%)

Note: Parentheses percentage difference is calculated w.r.t to FE Results.

When compared to the results from the Finite Element Model (FEM), the results analysis provides important information about the relative error and accuracy of the prototype and the System 7000-DAQ.

The prototype displays a relative error of 9% at Mode 1, which deviates from the FEM results by about 9%. The System7000, on the other hand, shows a relative error of 2%, which indicates a closer alignment with the FEM results. According to these results, the System7000 produces measurements that are more accurate than the prototype at Mode 1.

About Mode 2, the prototype shows a relative error of 5%, which denotes a minimal departure from the FEM findings of 5%. The System7000, on the other hand, displays a negative relative error of -1%, which indicates a slight underestimation in comparison to the FEM results. It is notable that a negative relative error implies that the System7000 is marginally more accurate than the prototype at Mode 2 than the FEM results.

5 Conclusions

The outcomes of the experiment show that, up to a point, both inexpensive and expensive acceleration measurement units can measure vibrations effectively. However, there have been some apparent differences in terms of their precision and dependability.

- A cost-effective option, the low-cost prototype unit showed limitations in terms of accuracy and sensitivity. As a result of measurement errors and instrument sensitivity, the readings were less accurate.
- The expensive premium acceleration measurement unit displayed superior performance in terms of accuracy and precision. Its high-quality parts, cutting-edge signal processing procedures, and improved noise reduction techniques made its vibration measurements more reliable and precise.
- The premium unit is suitable for applications where accuracy is crucial because it can pick up even the smallest changes in vibration patterns and finer details.



5th Conference on Sustainability in Civil Engineering (CSCE'23)

Department of Civil Engineering

Capital University of Science and Technology, Islamabad Pakistan



It is crucial to take the particular needs of the project or application into account when choosing between inexpensive and expensive units. The inexpensive unit might be an option if cost is the main consideration, and the application allows for some margin of error. The premium unit is recommended, despite its higher price, for applications that call for exceptional accuracy and dependability.

The comparison's conclusion emphasizes the compromises between cost and effectiveness in vibration measurement. Understanding the advantages and disadvantages of each choice and choosing the ideal Arduino Mega unit in accordance with their unique requirements will help engineers and researchers make well-informed choices.

References

- [1] A. Villarroel, G. Zurita, and R. Velarde, "Development of a low-cost vibration measurement system for industrial applications," *Machines*, vol. 7, no. 1, p. 12, 2019.
- [2] D. Caballero-Russi, A. R. Ortiz, A. Guzmán, and C. Canchila, "Design and Validation of a Low-Cost Structural Health Monitoring System for Dynamic Characterization of Structures," *Applied Sciences*, vol. 12, no. 6, p. 2807, 2022.
- [3] S. Komarizadehasl, F. Lozano, J. A. Lozano-Galant, G. Ramos, and J. Turmo, "Low-cost wireless structural health monitoring of bridges," *Sensors*, vol. 22, no. 15, p. 5725, 2022.
- [4] N. Kaur and S. Bhalla, "Combined energy harvesting and structural health monitoring potential of embedded piezo-concrete vibration sensors," *Journal of Energy Engineering*, vol. 141, no. 4, p. D4014001, 2015.
- [5] S. D. G. Tomaneng, J. A. P. Docdoc, S. A. Hierl, and P. D. Cerna, "Towards the Development a Cost-effective Earthquake Monitoring System and Vibration Detector with SMS Notification Using IOT," *International Journal of Engineering and Manufacturing*, vol. 12, no. 6, p. 22, 2022.
- [6] B. Ando, S. Baglio, C. O. Lombardo, V. Marletta, and A. Pistorio, "A Low-Cost Accelerometer Developed by Inkjet Printing Technology," *IEEE Transactions on Instrumentation and Measurement*, vol. 65, no. 5, pp. 1242–1248, May 2021, doi: <https://doi.org/10.1109/tim.2015.2490998>.
- [7] M. Vannoni and S. Straulino, "Low-cost accelerometers for physics experiments," *European Journal of Physics*, vol. 28, no. 5, pp. 781–787, Jul. 2007, doi: <https://doi.org/10.1088/0143-0807/28/5/001>.
- [8] C. Ratcliffe, D. Heider, R. Crane, C. Krauthauer, M. K. Yoon, and J. W. Gillespie Jr, "Investigation into the use of low cost MEMS accelerometers for vibration based damage detection," *Composite Structures*, vol. 82, no. 1, pp. 61-70, 2008.



INNOVATIVE SOLUTIONS FOR SUSTAINABLE BUILDING STRENGTHENING: GLASS FIBER REINFORCED CONCRETE

Faheem Ahmad Gul

a: School of Civil and Architectural Engineering, Nanchang Institute of Technology, Nanchang 330099, China,
faheem@nit.edu.cn

* Corresponding author: Email ID: faheem@nit.edu.cn

Abstract- Steel-reinforced Glass Fiber Reinforced Concrete (SGFRC) is a promising alternative to conventional construction materials, offering enhanced structural performance and sustainability. This paper presents a review of recent research on SGFRC in construction. By integrating fine glass fibers (GF) into steel-reinforced concrete matrix, SGFRC demonstrates remarkable tensile strength, flexural performance, and durability, enabling resilient and long-lasting structures. The eco-friendly nature of glass fibers further contributes to construction sustainability by reducing carbon footprints. This study explores manufacturing techniques and formulation strategies to optimize SGFRC properties for strengthening, energy-efficient, and environmentally conscious buildings. Experimental examinations, including flexural strength (FS), pre-crack/post-crack/total energy absorption, and toughness index, compare SGFRC with steel-rebar-reinforced plain concrete (SPC). Both adopt a mix design ratio of 1:2:4 (Cement: Sand: Aggregates) with a water-cement ratio of 0.7. GFRC incorporates 5% of 5cm lengthy GF by mass of cement, leading to reduced density and slump. Findings highlight SGFRC's superiority in FS and other flexural strength properties, emphasizing GFRC's significance for enhancing structural performance and promoting sustainable construction practices.

Keywords- Construction Sustainability, Enhanced Structural Performance, Steel-reinforced Glass Fiber Reinforced Concrete (SGFRC), Strengthening Building Structures.

1 Introduction

In the field of construction materials, the quest for sustainable alternatives to conventional materials has become increasingly vital to address the challenges posed by environmental concerns and resource scarcity [1]. One promising solution that has garnered significant attention is Steel-reinforced Glass Fiber Reinforced Concrete (SGFRC) [2]. This innovative composite material offers a compelling combination of enhanced structural performance and sustainability, making it a potential game-changer in the construction industry [3]. The following paper presents a review of recent research on SGFRC in construction, shedding light on its unique properties and contributions to sustainable building practices.

SGFRC's exceptional attributes can be attributed to the incorporation of fine glass fibers (GF) into the steel-reinforced concrete matrix. This integration bestows the concrete with remarkable flexural strength, improved tensile performance, and exceptional durability, enabling the construction of resilient and long-lasting structures that can withstand the test of time and environmental challenges [4][5][6]. Moreover, the eco-friendly nature of GF plays a significant role in enhancing the overall sustainability of the construction industry. By reducing carbon footprints, SGFRC demonstrates its commitment to environmentally conscious construction practices [7].

As the significance of sustainability grows in the construction sector, understanding and optimizing the properties of SGFRC become paramount. The research presented in this study offers novelty and significant contributions to the field of construction materials and sustainable building practices. This study takes a deep dive into various manufacturing techniques and formulation strategies employed to maximize the performance of SGFRC [8][9]. Architects and engineers



will gain valuable insights from these findings, enabling them to design energy-efficient and environmentally conscious buildings that align with sustainable construction principles [10]. The study's key focus on enhancing the pre and post-cracking behaviors of SGFRC in pursuit of a sustainable approach to strengthening building structures is a notable aspect of the research. Moreover, the exceptional impact resistance and good ductility of glass fibers distinguish them among artificial fibers [11], adding to the novelty of the study. By evaluating the long-term serviceability of strengthened, long-lasting structures, this research addresses a critical aspect of sustainability in construction. The experimental exploration of flexural strength, energy absorption, and toughness index contributes valuable knowledge to the potential of GFRC reinforced with steel rebar for achieving both structural strengthening and sustainable construction goals. Through an advanced understanding of SGFRC's mechanical properties, this study endeavors to make a significant contribution to the realization of more resilient and eco-conscious building solutions.

2 Experimental Procedures

2.1 Primary Materials

Steel-rebar-reinforced plain concrete (SPC) and steel-reinforced glass fiber reinforced concrete (SGFRC) are composed of several key ingredients. These include Ordinary Portland cement, locally sourced sand, aggregates, potable water, and a specific mass percentage of glass fibers relative to the amount of cement used in the mixture.

2.2 Glass Fibers Preparation

Obtaining glass fibers of the required length can be a laborious and time-consuming process, as they are commonly available in the form of glass sheets. In order to achieve the desired length, glass fibers are carefully pulled out from the sheet and then precisely chopped to the required length of 5 cm. Figure 1 provides a visual representation of this process, showcasing the glass fibers after they have been pulled from the sheet and cut to the specified length.



Figure 1: Prepared Glass Fibers

2.3 Development of Concrete Mixtures and Casting Techniques

The mix-design, water-cement ratio, and fiber addition for steel-rebar-reinforced plain concrete (SPC) and steel-reinforced glass fiber reinforced concrete (SGFRC) are provided in Table 1. To compensate for the added fiber mass, an equal measure (mass) of aggregate is deducted from the total mass of aggregates. All materials are added based on the mass of cement. The concrete mix is prepared using a drum-type concrete mixer. All ingredients, including water, are placed in the mixer,



and it is rotated for a duration of five minutes to ensure thorough mixing.

In the preparation of GFRC, the ingredients of the concrete, along with the fibers, are added to the mixer layer by layer to prevent the formation of lumps. Approximately two-thirds of the required water is added, based on the water-cement ratio of 0.7, which is the same as that used for PC. The concrete mixer undergoes rotation for three minutes initially. Afterward, the remaining one-third of the water is introduced to the GFRC mixture, and the drum-type concrete mixer continues to rotate for an additional two minutes. The workability of the GFRC is observed, and it is ensured that the added water is sufficient to achieve the desired workability. Before pouring the GFRC into molds, a slump cone test is performed to assess the consistency of the mixture.

The GFRC mixture is introduced into molds in a series of three layers, and each layer undergoes compaction with 25 blows from a steel rod. To promote self-compaction and remove air voids, the molds are lifted to a height of approximately 200-300 mm and then dropped onto the floor. After a pouring duration of 24 hours, the specimens are demolded. All specimens are subsequently immersed in water at room temperature for a curing period of 28 days before testing.

Table 1 Mix-design, Water-cement ratio and Glass Fibers Content of SPC and SGFRC

Mixes	Mix-design ratio (Cement:Sand:Aggregate)	Water-cement ratio	Glass Fibers by Mass of Cement (%)	Fibers Cut Length (cm)
SPC	1:2:4	0.7	--	--
SGFRC	1:2:4	0.7	5	5

2.4 Casting of Beam-lets and Reinforcement Details

For both Steel-Rebar-Reinforced Plain Concrete (SPC) and Steel-Reinforced Glass Fiber Reinforced Concrete (SGFRC), beam-lets with dimensions of 102 mm width, 102 mm depth, and 457 mm length were cast. To compare the flexural properties of the two materials, a total of four beam-lets are cast, with two beam-lets for SPC and two beam-lets for SGFRC with steel rebars.

For each composite, the average of the results obtained from the two specimens is considered as the final value. The reinforcement details for both SPC and SGFRC, including steel rebars, are provided in Figure 2.

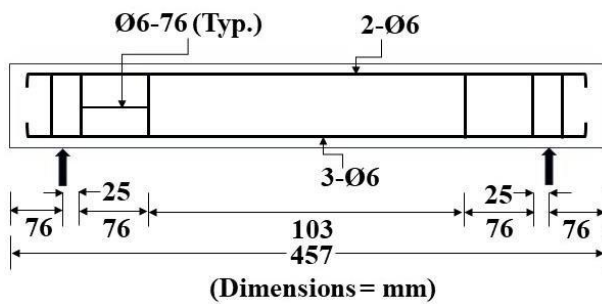


Figure 2: Details of beam under consideration

3 Research Methodology

To assess the workability and flow characteristics of fresh concrete in both plain concrete (PC) and glass fiber reinforced concrete (GFRC) mixes, the slump cone test is conducted following ASTM C143/C143M-15a [12] guidelines. This standardized test allows for a fair comparison of workable behavior under identical mix designs and water-cement ratios. The test helps to attribute any differences in workability to the presence of glass fibers in the GFRC mixture, aiding in evaluation during casting and placement processes.

The densities of steel-rebar-reinforced plain concrete (SPC) and steel-reinforced glass fiber reinforced concrete (SGFRC) beam-lets are computed using ASTM C138/C138M-16 [13]. An electric weighing balance is used to measure the masses, Paper ID. 23-214



and volumes are calculated manually based on dimensions. These ASTM standards ensure accurate density values for both SPC and SGFRC, facilitating quantitative material property comparison.

To determine the flexural strength of SPC and SGFRC beam-lets, ASTM C78/C78M-15b [14] is conducted. A servo-hydraulic testing machine subjects the reinforced beam-lets to a flexural test, measuring deflections with a dial gauge. The loading rate of 100-250 pounds/second are used in all tests. It may be noted that the loading rate was controlled manually. The test data provides parameters like first crack load (P_f), maximum-load (P_m), ultimate-load (P_u), maximum deflection (Δ), crack strength at ultimate-load, and failure modes, offering insights into the strength characteristics and behavior of the composites.

Additionally, various performance indicators are determined, such as the flexural strength (FS), energy-absorption up to first crack (E_f), energy absorption from first crack to maximum-load (E_m), energy-absorption from maximum-load to ultimate-load (E_u), total energy-absorption (TE), and total toughness index (TTI). These parameters offer a comprehensive understanding of the materials' flexural performance and energy-absorption capacities.

4 Results and Analysis

4.1 Density and Slump of Concrete

The slump of plain concrete (PC) and glass fiber reinforced concrete (GFRC) are given in the third column of Table 2. It is observed that the slump of GFRC is less than that of PC by 20 mm for the same water-cement ratio i.e. 0.7. Thus, the slump of GFRC is reduced by 50% compared to that of PC. As predicted, the decrease in the slump of GFRC is observed due to the presence of glass fibers. Similarly, the observed density of the steel rebar reinforced GFRC is reduced by 91 kg/m³ as compared to that of steel rebar reinforced PC. The percentage reduction in the density of steel rebar reinforced GFRC is 3.83% when compared with steel rebar reinforced PC. This reduction is due to the presence of glass fibers (less dense in nature) to the concrete.

Table 2 Slump and Densities of PC and GFRC

Mixes	Water-cement ratio	Slump (mm)	Density (kg/m ³)
PC	0.7	40	2375
GFRC	0.7	20	2284

4.2 Behavior of Beam-lets During Flexural Strength Test

4.2.1 Load-deflection Behavior of Beam-lets with Rebars

Figure 3 illustrates the recorded mid-span load-deflection curves of SPC and SGFRC, both of which have flexural reinforcement consisting of 3-Ø6 bars and shear reinforcement of Ø6-76 mm. In Figure 4, the cracks observed during testing of the beam-lets of SPC and SGFRC with flexural reinforcement of 3-Ø6 and shear reinforcement of Ø6-76 mm include the first crack, maximum-load cracks, and ultimate-load cracks. It is noted that before appearance of first crack, the load-deflection curve is increased linearly. The area under the load-deflection curve shows energy absorption of the tested beam-lets. The flexural strength test is employed to observe the behavior of SPC and SGFRC beam-lets. This study reveals specific data, such as length of first crack and the number of cracks at both the maximum-load and ultimate-load. The first crack of SPC and SGFRC is observed at 91.1% and 85.1%, respectively, of their respective highest load. The first crack dimensions in SPC are relatively larger when compared to the corresponding SGFRC specimens. Furthermore, an increase in flexural reinforcement is found to reduce the length of the first crack. Specifically, the length of the first crack is approximately 70 mm for SPC and 57 mm for SGFRC specimens. At maximum-load, the amount of cracks and their dimensions are more for SPC beam-lets as compared to that of SGFRC beam-lets. At ultimate-load, the number of cracks and their dimensions are further larger than that of noted at the maximum-load. The study reveals that SGFRC outperformed SPC in reducing the number and size of cracks, showcasing the significant improvement brought about by



the incorporation of glass fibers in the concrete. These findings have promising implications for sustainable construction, as the enhanced performance of SGFRC in reinforced concrete flexural members can contribute to improved seismic performance and greater durability [15].

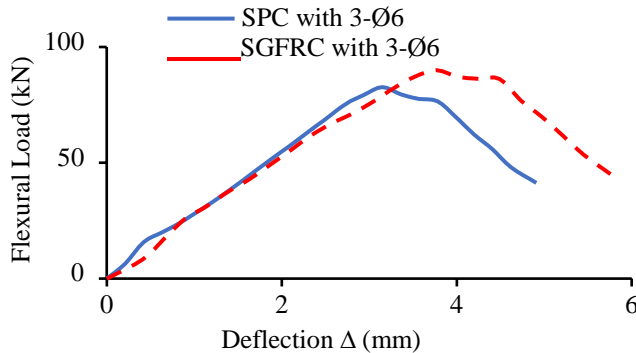


Figure 3: Deflection curve of beam-lets under load

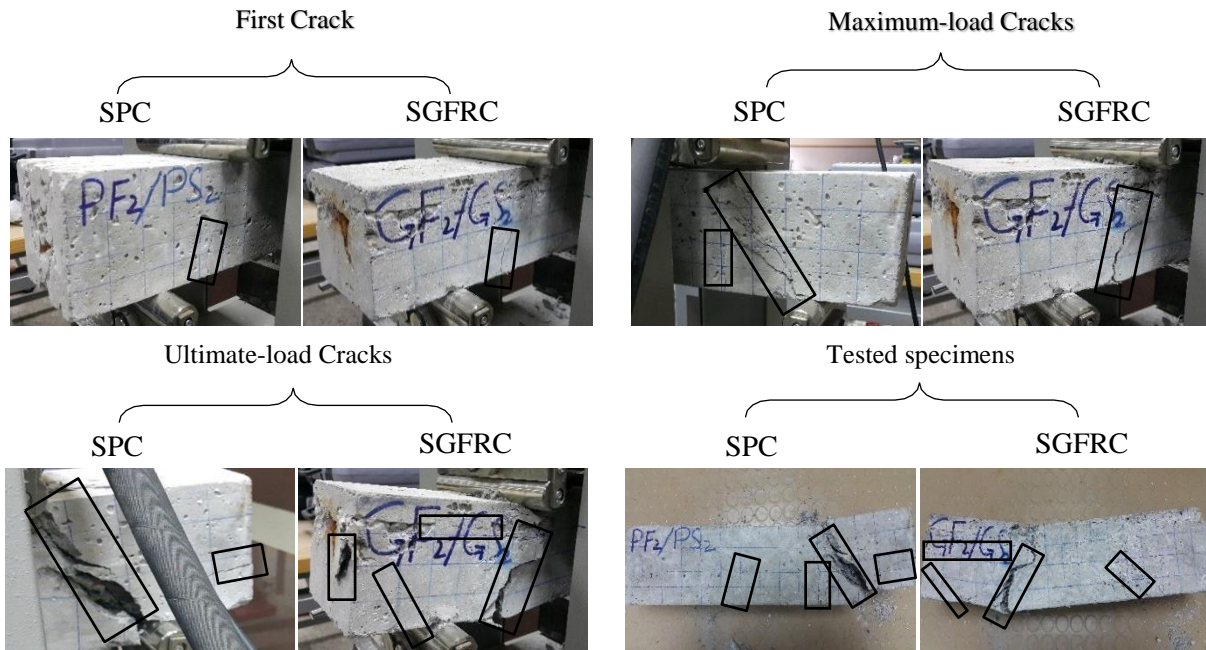


Figure 4: Behavior of beam-lets with flexural rebars reinforcement (3-Ø6) and shear rebars reinforcement (Ø6-76 mm)

4.2.2 Effect of Steel Reinforcement on Strength, Energy Absorption and Toughness Index

Table 3 presents the flexural strength (F.S), energy absorption, and toughness index data of the beam-lets (SPC and SGFRC) with flexural rebar reinforcement of 3-Ø6 and shear rebar reinforcement of Ø6-76 mm. It can be noted that Table 3 presents the averaged values obtained from two beam-lets. The calculated values of F.S for the SPC and SGFRC are 18.0 MPa and 19.6 MPa, respectively. It is increased in SGFRC by 8.9% as compared with that SPC. The calculated values of energy absorption (E_f) up to first crack load of SPC and SGFRC are 104.1 kN.s and 121.7 kN.s, respectively. The E_f of SGFRC is increased by 17.6 kN.s (16.9%) as compared with that SPC. Similarly, the calculated values of energy absorption from first crack to maximum-load (E_m) of SPC and SGFRC are 33.3 kN.s and 60.8 kN.s, respectively. The E_m of SGFRC is increased by 27.5 kN.s (82.6%) in contrast to that of SPC. Likewise, the calculated values of energy absorption from maximum-load to ultimate-load (E_u) of SPC and SGFRC beam-lets are 115.1 kN.s and 145.9 kN.s, respectively. The E_u of SGFRC is increased by 30.8 kN.s (26.8%) in comparison to that of SPC. The T.E is calculated by



summing the values of E_f , E_m , and E_u , which is same as the area under the load-deflection curve from zero to the P_u . The T.E of SPC and SGFRC are 252.5 kN.s and 328.3 kN.s, respectively. The T.E of SGFRC is increased by 75.8 kN.s (30%) as compared to that of SPC. The calculated values of total toughness index (T.T.I) of SPC and SGFRC are 2.43 and 2.7, respectively. The T.T.I of SGFRC is increased by 0.27 (11.1%) as compared to that SPC. It may be noted that the F.S, E_f , E_u , TE, TTI are increased due to the presence of glass fiber. The utilization of SGFRC offers a promising approach to enhance the seismic performance of flexural members while promoting sustainable construction practices. The notable improvements in flexural strengths, energy absorptions, and total toughness index achieved through SGFRC demonstrate its potential in increasing the ductility and seismic energy absorption capacity of these structural elements. By incorporating environmentally-friendly GF into the concrete matrix, we not only bolster the earthquake resistance of the flexural members but also contribute to the overall sustainability of the construction industry [16]. These advancements signify a step towards creating resilient and eco-conscious structures that can withstand seismic forces while minimizing their environmental impact.

Table 3 Comparison of strength, energy absorption and toughness index of beams-lets with flexural rebar reinforcement (3-Ø6) and shear rebar reinforcement (Ø6-76 mm)

Specimens	F.S (MPa)	E_f (Up to P_f) (kN.s)	E_m (P_f to P_m) (kN.s)	E_u (P_m to P_u) (kN.s)	T.E (kN.s)	T.T.I (-)
SPC	18.0	104.1	33.3	115.1	252.5	2.43
SGFRC	19.6	121.7	60.8	145.9	328.3	2.70

5 Conclusions and Recommendations

Based on the findings from the experimental work conducted on steel-reinforced glass fiber reinforced concrete (SGFRC) beam-lets, the following conclusions can be drawn regarding the flexural strength and post-cracking behavior in comparison to steel-rebar-reinforced plain concrete (SPC):

1. Workability: GFRC demonstrates a significant 50% reduction in workability compared to plain PC due to the interlocking nature of glass fibers, hindering particle movement during mixing and placing [17][18]. Thus, careful mix design and construction processes are vital for achieving the desired workability and proper compaction of the GFRC mixture.
2. Density: SGFRC shows a 3.83% decrease in density due to the lower-density glass fibers [5] promotes sustainable construction. It lowers material consumption, conserving resources and reducing environmental impacts during concrete production. The lighter composite also enhances transportation and installation energy efficiency, resulting in reduced carbon emissions and environmental impact. SGFRC's sustainability benefits make it an eco-friendly alternative, supporting environmentally conscious and resource-efficient construction practices.
3. Energy Absorption: The notable 30% increase in total energy absorption in SGFRC compared to SPC indicates its enhanced ability to withstand and dissipate energy, making it beneficial for structural performance of strengthened buildings [3]. This higher energy absorption capacity can contribute to safer and more resilient structures, aligning with sustainable construction principles that prioritize long-term durability and safety.
4. Toughness Index: SGFRC exhibits an 11.1% increase in toughness, providing improved crack resistance and longer-lasting structures [19], aligning with sustainable construction practices.

In conclusion, steel-reinforced GFRC offers advantages and challenges for sustainable construction. Despite reduced workability and density, it shows remarkable improvements in energy absorption and toughness, making it promising for resilient structures. Further research on glass fiber content optimization and combined reinforcements is needed to fully leverage GFRC's potential for enhancing seismic performance and eco-friendly structures in alignment with sustainable principles. Acknowledging this pilot study's limitations in the number of tested beams, we aim to establish a foundation for future comprehensive research to draw more robust conclusions.



Acknowledgment

The author would like to express their sincere gratitude to all individuals who provided valuable assistance and support throughout the course of this experimental research. Their contributions have been instrumental in the successful completion of this study.

References

- [1] M. N. Amin, K. Khan, M. Sufian, Q. M. S. Al-Ahmad, A. F. Deifalla, and F. Alsharari, "Predicting parameters and sensitivity assessment of nano-silica-based fiber-reinforced concrete: a sustainable construction material," *Journal of Materials Research and Technology*, vol. 23, pp. 3943–3960, 2023.
- [2] O. Zaid, J. Ahmad, M. S. Siddique, F. Aslam, H. Alabduljabbar, and K. M. Khedher, "A step towards sustainable glass fiber reinforced concrete utilizing silica fume and waste coconut shell aggregate," *Scientific Reports*, vol. 11, no. 1, p. 12822, 2021.
- [3] J. Blazy, R. Blazy, and Ł. Drobiec, "Glass Fiber Reinforced Concrete as a Durable and Enhanced Material for Structural and Architectural Elements in Smart City—A Review," *Materials*, vol. 15, no. 8, p. 2754, 2022.
- [4] K. Chandramouli, P. S. R. S. Rao, P. Narayanan, and P. Sravana, "Strength properties of glass fiber concrete," *ResearchGate*, vol. 5, no. 4, 2010.
- [5] M. Khan and M. Ali, "Use of glass and nylon fibers in concrete for controlling early age micro cracking in bridge decks," *Construction and Building Materials*, vol. 125, pp. 800–808, 2016.
- [6] J. A. Purkiss, "Some Mechanical Properties of Glass Reinforced Concrete at Elevated Temperatures," pp. 230–241, 1985.
- [7] M. Sandanayake, "Environmental Impacts of Construction in Building Industry—A review of knowledge advances, gaps and future directions," *Knowledge*, vol. 2, no. 1, pp. 139–156, 2022.
- [8] C. Zhang, Z. Zhu, S. Wang, and J. Zhang, "Macro-micro mechanical properties and reinforcement mechanism of alkali-resistant glass fiber-reinforced concrete under alkaline environments," *Construction and Building Materials*, vol. 368, p. 130365, 2023.
- [9] P.-S. Shin, J.-H. Kim, K. L. DeVries, and J.-M. Park, "Manufacturing and qualitative properties of glass fiber/epoxy composite boards with added air bubbles for airborne and solid-borne sound insulation," *Composites Science and Technology*, vol. 194, p. 108166, 2020.
- [10] B. H. Mohammed, A. F. H. Sherwani, R. H. Faraj, H. H. Qadir, and K. H. Younis, "Mechanical properties and ductility behavior of ultra-high performance fiber reinforced concretes: Effect of low water-to-binder ratios and micro glass fibers," *Ain Shams Engineering Journal*, vol. 12, no. 2, pp. 1557–1567, 2021.
- [11] Y. Lv, "Experiment Investigation on Mechanical Property of Glass Fiber Reinforced Concrete," *Advanced Materials Research*, vol. 915–916, pp. 784–787, Apr. 2014.
- [12] ASTM C143 / C143M-15a, Standard Test Method for Slump of Hydraulic-Cement Concrete, ASTM International, West Conshohocken, PA, 2015, www.astm.org
- [13] ASTM C138 / C138M-16, Standard Test Method for Density (Unit Weight), Yield, and Air Content (Gravimetric) of Concrete, ASTM International, West Conshohocken, PA, 2016, www.astm.org
- [14] ASTM C78 / C78M-15b, Standard Test Method for Flexural Strength of Concrete (Using Simple Beam with Third-Point Loading), ASTM International, West Conshohocken, PA, 2016, www.astm.org
- [15] B. Ali, L. A. Qureshi, S. H. A. Shah, S. U. Rehman, I. Hussain, and M. Iqbal, "A step towards durable, ductile and sustainable concrete: Simultaneous incorporation of recycled aggregates, glass fiber and fly ash," *Construction and Building Materials*, vol. 251, p. 118980, 2020.
- [16] H. Tahir et al., "Optimisation of Mechanical Characteristics of Alkali-Resistant Glass Fibre Concrete towards Sustainable Construction," *Sustainability*, vol. 15, no. 14, p. 11147, 2023.
- [17] M. Madhkhan and R. Katirai, "Effect of pozzolanic materials on mechanical properties and aging of glass fiber reinforced concrete," *Construction and Building Materials*, vol. 225, pp. 146–158, 2019
- [18] Y. M. Ghugal and S. B. Deshmukh, "Performance of Alkali-resistant Glass Fiber Reinforced Concrete," *Journal of Reinforced Plastics and Composites*, vol. 25, no. 6, pp. 617–625, 2006.
- [19] A. B. Kizilkanat, N. Kabay, V. Akyüncü, S. Chowdhury, and A. H. Akça, "Mechanical properties and fracture behavior of basalt and glass fiber reinforced concrete: An experimental study," *Construction and Building Materials*, vol. 100, pp. 218–224, 2015.



CRITICAL FACTORS INFLUENCING THE ADOPTION OF THE BUILD OPERATE TRANSFER (BOT) SYSTEM IN THE GULF AREAS: A COMPREHENSIVE REVIEW

^a*Muhammad Junaid Yamin**, ^b*Saidu Abdulai Koroma*

a: Construction Engineering and Management Department, KFUPM, KSA, g202203880@kfupm.edu.sa

b: Construction Engineering and Management Department, KFUPM, KSA, g202211660@kfupm.edu.sa

Abstract- The Build-Operate-Transfer (BOT) model has gained significant attention worldwide as a solution for major public infrastructure development. The Gulf Cooperation Council (GCC) countries, renowned for their government surpluses and oil reserves, are particularly interested in implementing the BOT model to drive economic development and diversification and transform the region into a trade and financial center. However, there is a research gap in understanding the critical factors influencing the adoption of BOT in the GCC region. This paper aims to address this gap by identifying these factors, assessing their impact on project performance, and proposing measures to ensure the success of BOT systems. Through a comprehensive literature review, this study identifies government support, risk allocation, local financial market conditions, project selection, and a strong private consortium as crucial factors for BOT project success. The research methodology involves data collection through a systematic literature review and data analysis using the Likert Scale method. The results of this study provide valuable insights for decision-makers in both the public and private sectors, enabling them to make informed decisions and improve the efficiency of BOT projects in the construction industry. By understanding these critical factors, stakeholders can optimize project outcomes and contribute to the overall development and diversification goals of the GCC region.

Keywords- Build Operate Transfer (BOT) system, Contractual agreements, Infrastructure, GCC

1 Introduction

The concept of BOT gathered attention after the global need for major public infrastructural development has become an increasingly demanding. The basis of a sustainable and fruitful society is based on impressive economic growth and an increase in population which has led to significant demand for public infrastructure [11] Countries in the Gulf Cooperation Council (GCC) region, known for their government surpluses and oil reserves, are keen on implementing BOT as a financial model to transform the region into a trade and financial center and achieve economic development and diversification [2]

Sarvari et al. (2019) as cited by Asad M, and Mahoud M, (Asad & Mahoud, n.d.) defined “BOT as an arrangement of contract in which the private sector finances a public infrastructure's design, construction, operation, and maintenance for a particular concession period, and at the end of it transfers the ownership to the government”.

Several studies have been conducted to identify the critical factors influencing BOT implementation, particularly in the GCC region. [2]. The COVID-19 pandemic and oil price levels have further motivated the Gulf region to explore BOT as a means to address their energy and infrastructure needs [3]. Stakeholders' interests and effective project delivery are



crucial for the success of BOT projects. Factors such as legal concerns, government support, project clarity, and equitable deals for all parties play a significant role.[4]

However, there is a research gap in understanding the common critical factors affecting BOT adoption in the GCC region. To fill this gap, the study aims to identify these factors, assess their impact on project performance, and propose measures to ensure the success of BOT systems. The findings can guide decision-makers in both the public and private sectors to make informed decisions and improve the efficiency of BOT projects in the construction industry.

1.1 Literature Review

Study has shown that, BOT contracts are difficult to win. The process is, however, burdensome and it requires time, money, experience, and political influence. Given this, the type of project delivery involves higher risk, and making decisive decisions is complex. The evolution of this PDS has changed over time, and its implementation has been considered getting better. Due to the extensive research in this area, the government (public sector) and private sector (Consortium) have minimized disputable endings by having clear knowledge of meeting in an agreeable term. There are lots of critical success factors (CSFs) that are very significant for BOT investors to adopt if they want to continue winning BOT contracts [5]

Amongst the many other factors, there are some important factors that both parties will agree upon. These crucial elements include choosing the appropriate project [7], the consortium's strength, the advantage of the technical solution, the differentiation of the financial package, the guarantee, and entrepreneurship and leadership. If these factors are integrated and given trending attention, the possibility of winning a BOT contract will be enhanced [5]. Moreover, the evaluation of achieving success in the construction industry is based on the appropriate selection criteria for project adoption [5].

Considering the GCC region, there will be slightly different from each country, depending on their operational environment, policies, and legal restriction which is likely the same. However, Studies and discussions about CSFs for BOT projects within the GCC region have been previously done. Five main CSF dimensions, including "economic viability," "sound financial package," appropriate risk allocation via reliable contractual arrangements," "reliable concessionaire consortium with strong technical strength," and "favourable investment environment," have been to categorize CSFs of public-private partnership projects like BOT. [1]. Furthermore, a study was done in Kuwait to identify the critical factor for the implementation of the BOT system by considering a major infrastructural project. Government representatives and concessionaires both concur that effective project management is a key component of BOT project success. This finding might be interpreted in the context of developing and funding various socioeconomic programs as:" Shadadiyah The expansion of the tourism industry on Failaka Island, Bubian Island, the Shadadiyah University Campus (investment in human capital), and the Jaber Al Ahmed AlSabah Hospital" [6]

Several studies have shown that Kingdom of Saudi Arabia haven't participated in the BOT contracts actively in past years but now, Saudi government have shown interest in these kinds of projects to overcome the difference between mining sector, religious tourism, and development on the national level.[12]

2 Research Methodology

The research methodology encompasses two distinct stages, namely Data Collection and Data Analysis. These stages are crucial in ensuring a comprehensive and systematic approach to the research process.

2.1 Stage 1: Data Collection

The first stage is comprised of collecting data through reviewing literature from 15 different articles on relevant to BOT project delivery. To understand the underlying critical factors affecting the adoption of the BOT project delivery system in the GCC region, this study implemented a partial systematic literature review on the critical factors affecting the success and failure factors of selected papers that are published in top construction engineering journals. About 16 critical factors based on occurrences within the GCC region were identified. These success factors indicate the prevailing factors that are ubiquitous in the GCC region which helped in explaining the extent to which the factors were going to affect the adoption of the BOT project delivery system and the mitigating measures for a successive BOT system.



2.2 Stage 2: Data Analysis

In the second stage of methodology, the collected data was analyzed using a Likert Scale method. Sixteen (16) critical success factors were selected as common factors affecting the adoption of the BOT project delivery system in the GCC region. Amongst these factors, the occurrence and/or frequency at which these factors are affecting the implementation of BOT in the GCC countries are highlighted based on several published papers related to this type of project delivery system. The scaling method helped to represent an interval level of measurement that had given a clear interpretation of the level of importance of the factors in a sequential means whilst adopting BOT projects. The scale ranges from 6 and above as extremely critical, 4-5 as Moderately Critical, and 1-3 as Least critical.

3 Results

The data collection showed that the Government Role/Support is extremely critical for the adoption of BOT projects within the GCC region. Factors like the Local Financial Market, Project Selection, and Strong Private Consortium are significantly considered in the adoption of this type of project delivery system.

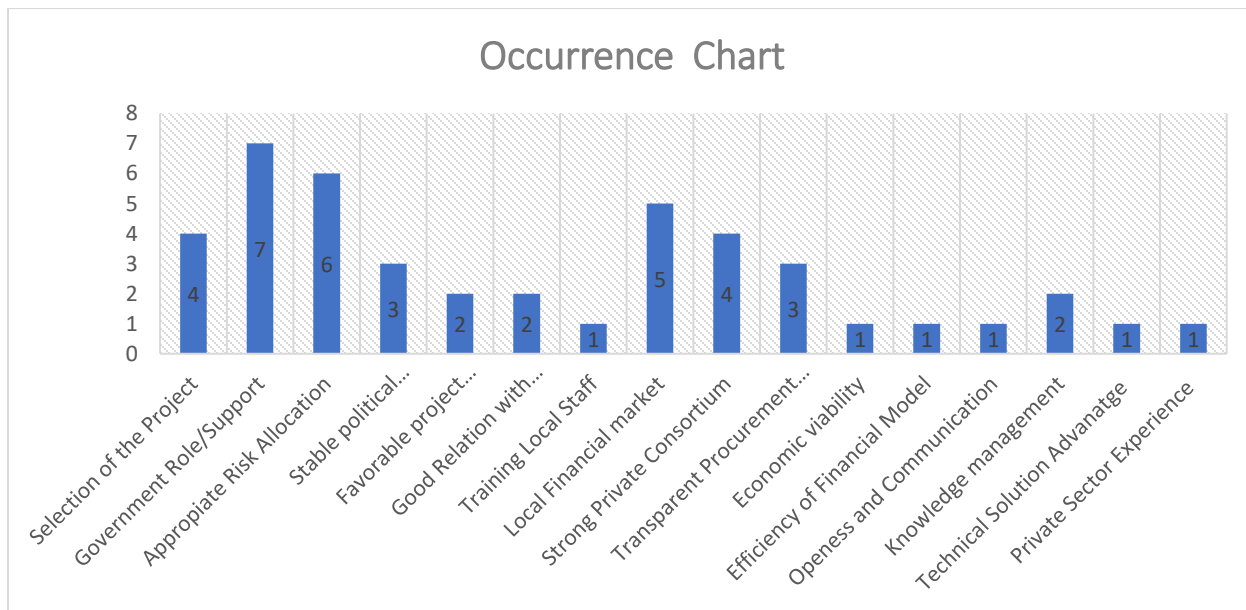


Figure 1: Success factors on the scale of occurrence

The research findings highlight the crucial factors influencing the adoption of BOT projects in the GCC region. According to the Likert Scale ratings, the Government role/support and Appropriate Risk Allocation are rated as extremely critical, scoring 6 and above. These factors play a pivotal role in ensuring the success and effectiveness of the BOT model in the region.

On the other hand, factors such as the Local Financial Market, Selection of project, and Strong Private Consortium receive a rating of 4-5 on the Likert Scale, indicating their moderately critical impact on the adoption of BOT projects in the GCC region. These factors, while not as crucial as the government's role and risk allocation, still hold significant influence in the overall success of BOT projects.

To ensure success in the BOT projects, the extremely critical factors are important to be known by all GULF countries to bolster their infrastructural development goal. To achieve this, the analysis above has helped in the assessment of these common factors. The extremely critical factors are:

- 1. Government Role/ Support:** The lengthy and complex process is crucial to the BOT project's success, and the continuous support of the government by providing attractive incentives to the stakeholders and private sectors to come and invest in the local market. Government must offer good return rates and provide a firm mechanism to deal with legal frameworks related to the project. [10]



Table 1 Likert Scale interval for factors affecting BOT Projects in the GCC region

Factors	Intervals	Description
- Government role/Support - Appropriate Risk Allocation	6 and above	Extremely Critical
- Local Financial Market - Selection of project - Strong Private Consortium	4-5	Moderate critical
< = 3 factors	1-3	Least Critical

2. **Appropriate risk allocation:** Allocation of risk is the most essential part of the success of the BOT project as it requires complete knowledge of identification, classification, and management of risk associated with both parties. For example, the investment risk, parties who are going to invest in the project must ensure that there is no political instability in the country, or their law must support preparing a sound environment for the projects.[10]

Furthermore, the factors of moderate significance are delineated as follows.

- I. **Local Financial Market:** The success of these types of projects immensely depends on the favorable market condition of the host country. The depth of the financial market might have a huge impact on the life of the project. All government taxation policies should be established in advance to get a clear concept of market conditions.[9]
- II. **Selection of the Project:** the selection of the project hugely impacts the success of the BOT projects. Due to constraints related to budget, the government should focus on those projects which have the highest priorities in terms of safeguarding the interest of the private and public sectors.[8]
- III. **Strong Private Consortium:** As the risk is shifted from the government to the private sector in such types of projects, the private consortium must be strong enough to bear the weightage of the project. There must be strong communication between the private sector and the host government. The strong organizational structure of the private party might play an effective role in the success of BOT projects.[8]

4 Conclusions

As the whole world is going for different approaches to developing their economies and infrastructure, GULF-related countries have also shown interest in the involvement of private sectors to contribute with the government bodies under specific contractual agreements. Due to the influence of Covid_19 and oil price levels, the GCC region must aspire to this BOT method so it would boost their energy and infrastructural needs. There have been studies on BOT methods but still, there is a huge research gap on stake holder's interest in the project. This difference between investors' expectations and project outcome generally defines the success of the project.

However, this Term paper reviewed several research on the type of project delivery that helps to give us insight into identifying the factors, the extent of the critical performance factors influencing the adoption of the BOT project, and the possible mitigating measures. This Term paper achieved that Government Role/Support and Appropriate Risk Allocation are the common factors within the GCC region that are extremely critical factors that both contracting parties should consider when implementing BOT projects. Local Financial Market, Selection of the Project, and Strong Private Consortium are moderately critical. Hence, the rest of the factors are least critical.

Acknowledgment

The authors would like to express their deepest gratitude and appreciation to the Department of Construction Engineering and Management (CEM) at King Fahd University of Petroleum and Minerals for their invaluable support and guidance throughout the research work. The careful review and constructive suggestions by the anonymous reviewers are gratefully acknowledged.



5th Conference on Sustainability in Civil Engineering (CSCE'23)

Department of Civil Engineering
Capital University of Science and Technology, Islamabad Pakistan



References

- [1] M. M. Asad and M. Mahoud, "Interrelationships of the Critical Success Factors of BOT Projects in Iran: A Grey-DEMATEL Approach."
- [2] H. Sharaffudin and A. AL-Mutairi, "Success Factors for the Implementation of Build Operate Transfer (BOT) Projects in Kuwait," International Journal of Business and Management, vol. 10, 2015
- [3] S. M. bin Jubair and J. S. K. Singh, "Critical Success Factors of Public-private Partnership (PPP) Projects in the Kingdom of Saudi Arabia," Webology, vol. 19, no. 1, pp. 1521–1540, Jan. 2022
- [4] R. Markom, E. Rabiah, and A. E. Ali, "A Legal Analysis of Successful and Problematic Build Operate and Transfer (BOT) Projects in Malaysia," 2012.
- [5] U. Z. Kahvandi, E. Saghatforoush, A. ZareRavasan, and C. Preece, "Integrated Project Delivery Implementation Challenges in the Construction Industry," Civil Engineering Journal, vol. 5, no. 8, pp. 1672–1683, Aug. 2019
- [6] H. Sharaffudin and A. AL-Mutairi, "Success Factors for the Implementation of Build Operate Transfer (BOT) Projects in Kuwait," International Journal of Business and Management, vol. 10, 2015
- [7] Z. Kahvandi, E. Saghatforoush, A. ZareRavasan, and C. Preece, "Integrated Project Delivery Implementation Challenges in the Construction Industry," Civil Engineering Journal, vol. 5, no. 8, pp. 1672–1683, Aug. 2019, doi: 10.28991/cej-2019-03091362.
- [8] T. A. Kaleel and M. Kareem, "Determine the factors that affecting on the applicability of Build Operate Transfer contracts for infrastructure in Iraq," in IOP Conference Series: Materials Science and Engineering, Jun. 2019, vol. 518, no. 2.
- [9] K. al Merri, "Critical success factors for public private partnership in the UAE: Impact of Perception on success of PPP عوامل النجاح الخامسة للشراكة بين القطاعين العام والخاص في دول الإمارات العربية المتحدة: تأثير الإدراك على نجاح مشاريع الشراكة بين القطاعين العام والخاص .by HANI SUBHI MOHD MUSTAFA," 2017
- [10] M. Alhashemi, M. Dulaimi, F. Ling, and M. Kumaraswamy, "CRITICAL SUCCESS AND FAILURE FACTORS FOR PUBLIC PRIVATE PARTNERSHIP PROJECTS IN THE UAE."
- [11] Al-Sharif, F and Kaka, A (2003) Potential of PFI/PPP as a financing source for public services projects in Saudi Arabia. In: Greenwood, D J (Ed.), 19th Annual ARCOM Conference, 3-5 September 2003, University of Brighton. Association of Researchers in Construction Management, Vol. 1, 71-80.
- [12] M. Elsayed Mohamed Omran, E. Mohamed Omran, and S. Mohammed Majed Dandan, "BOT Contracts of Saudi Arabia and Barriers of International Investment: Answer From Law and Economic Perspectives," Indian J Sci Technol, vol. 9, no. 48, Dec. 2016 doi: 10.17485/ijst/2016/v9i48/101519.



APPLICATION OF NONSTATIONARY IN CLIMATE VARIABILITY – A CASE STUDY OF SOUTH PUNJAB, PAKISTAN

^a*Muhammad Usman Khan*, ^b*Mudassar Iqbal**, ^c*Noor Muhammad Khan*

a: Centre of Excellence in Water Resources Engineering, UET., Lahore, Pakistan, usmank4773@gmail.com

b: Centre of Excellence in Water Resources Engineering, UET., Lahore, Pakistan, mudassar@cevre.edu.pk

c: Centre of Excellence in Water Resources Engineering, UET., Lahore, Pakistan, noorkhan@uet.edu.pk

*Corresponding author: Email ID: mudassar@cevre.edu.pk

Abstract- The rate of change in the planet's environment has been inconsistent. One of the main reasons is believed to be vital changes caused by human in the climate. Recent innovations in time series investigation of hydro-climatological parameters have contributed to the belief that the effects of nonstationarity are considerable enough to call the validity of conventional stationary methods into question. The goal of this study was to assess the nonstationary variability in Southern Punjab using nonstationary parameters for the historical era (1970-2015). Generalized Extreme Value, GEV, Gumbel, GUM, Normal, NOR and Lognormal, LOGNOR were used as the frequency analysis probability functions. The findings of the nonstationarity variability influences across the Southern Punjab showed a variety of variations, such as an increase or reduction in the return level of extreme rainfall. Upon an evaluation of NLLH value, GEV offered the best match compared to other distributions. In Bahawalnagar, Bahawalpur, Multan, Rahim Yar Khan, and DG Khan, the yearly nonstationary consequences for the 100-year return level were 15.2, 8.7, 58.3 18.7 and 20% respectively. The evidence also showed that extreme precipitation appears to be increasing during the historical period, which increases floods. Overall, nonstationarity variations demonstrated the importance of adopting climate change into hydraulic structure design.

Keywords- Climate change, GEV, Nonstationarity, Precipitation, Probability Distributions

1 Introduction

In meteorology, atmospheric sciences, and other closely related fields, extreme weather or climate play a fundamental role. One of the primary regulating factors affecting the world climate is solar radiation. The overall equilibrium of incoming – outgoing radiation (long wave radiations) has been thrown off due to increased aerosol and greenhouse gas concentration [1]. The presence of these elements in a place over an extended length of time controls its climate. The amount of longwave radiation emitted from the earth's surface fluctuates as a result of changes in land use patterns, such as the removal of forests, which influence carbon dioxide (CO_2) emission levels and surface albedo. [2]. The nature of precipitation is also shifting as a result of rising temperatures, with northern regions increasingly seeing more rainfall than snowfall [3]. The occurrence of summer days and soaring temperatures is increasing while the number of winter days is dwindling [4]. Aziz adopts a fixed and nonstationary recurrence technique to analysis the fluctuating irregularity in annual rainfall as well as extraordinary rainfall in Turkey. The findings have been presented in Turkey as nonstationarity influence plans, which offer information on the inconsistent nature of the severity of impacts such as effect kinds, such as an increase or reduction in the next phase of excess precipitation [5]. The number of hot and cold days as well as the frequency and intensity of hydro-climatological extremes, increased globally between 1950 and 2010. Severe extreme temperatures, droughts, flooding, and precipitation have all been more often during the past century [6]. Indicating that the characteristics (of location, shape and scale) of fundamental distributions might shift over time and contradicting the theory of stationarity



becomes incorrect, the existence of climate change and variables related to land use may modify the probability of hydrological severe occurrences [7]. Since the top and bottom tails of distributions are connected to disasters such flooding and drought, respectively, they are important for the preparation and administration of water resources [8].

Despite the possibility that the professional has never acknowledged the existence of nonstationarity in hydrological operations, they have chosen the fixed assumption as a logical approach to address assessments of future conditions of the framework based on empirical evidence [9]. Many previous researchers have shown how this dread of stationarity (such as the idea of regular intervals) could be hazardous as a result of climate transformation. Later, it is predicted that the frequency of extraordinary precipitation events would rise, and neglecting these developments will lead to the mistake of excessive events. No matter what, using limitations recognize the stationarity that accepts no change after given amount of time [10]. The idea of stationarity in hydro-climatological variables is regarded to be invalidated by large human caused shifts in the Earth's climate, which modify the means and extremes of precipitation [11]. Sertac, [12] adopted a nonstationary GEV distribution in a region where floods occur on a yearly basis. They established that nonstationary levels were lower than stationary levels. Due to this local and global development, the stationarity theory has come under heavy criticism. Keeping this in mind, several studies have attempted to investigate the viability of this idea in flood regimes in numerous geographic locations across the world considering the impact of natural climatic variation [13–15] or changes in land use [16].

The forecasting of weather is primarily used to predict the condition of the environment's changes in the near future, from a few minutes to hours, days to seasons, and it requires improved precision and reliability. Global circulation models are frequently used for generating climate predictions, which provide an overall picture of weather conditions over a longer time horizon, such as fifty or one hundred years. In this work, nonstationary variability in return levels of significant precipitation at the selected stations was measured across the historical (1970–2015) and projection (2020–2100) periods using a nonstationary frequency analysis technique. Nonstationarity analysis comprised on the normal and lognormal distributions in addition to the well-known generalized extreme value (GEV) and Gumbel distributions. In this regard, the present research shows how probability distribution functions may be used to quantify nonstationarities in return level of extreme precipitation.

2 Study Area and Data

The research was carried out in South Punjab, Pakistan (Figure 1) considering the meteorological stations Dera Ghazi, DG Khan, Multan, MTN, Bahawalnagar, BHN, Bahawalpur, BHP, and Rahim Yar Khan, RY Khan. For the historical period (1970-2015), the impacts of nonstationarities upon annual and seasonal maximum precipitation (MP) were evaluated. Although the region is primarily flat, there are a few hilly areas in the far north and south-west sides.

The observed data of daily precipitation was collected from Pakistan Meteorological Department (PMD) for the duration of 45 years (1971 to 2015).

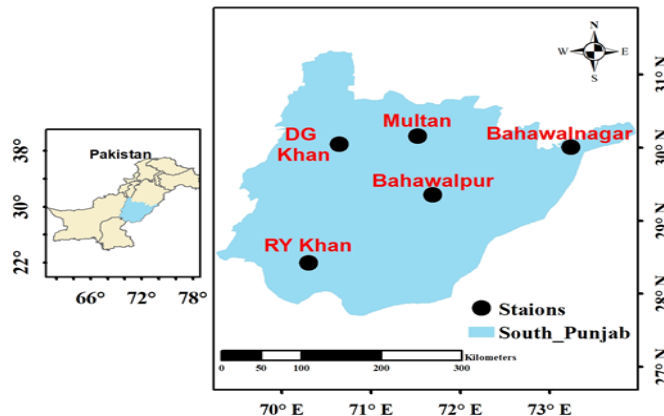


Figure 1: Geographical location of South Punjab with meteorological stations.



3 Research Methodology

3.1 Stationary and Non-Stationary Frequency Analysis.

The parameters of the GEV and GUM are designed to be time dependent by incorporating time as a covariant so that may be used under nonstationary settings [12]. This study makes use of both stationary and nonstationary (GEV, GUM, NORM, and LOGNORM) frequency analysis distributions. Equation (1) represents the GEV cumulative distribution function's nonstationarity form.

$$F(z, \theta_t) = \exp \exp \left\{ - \left[1 + \varepsilon \left(\frac{z - \mu_t}{\sigma_t} \right) \right]^{\frac{-1}{\varepsilon}} \right\} \quad (1)$$

Here, the location parameter has been modified to $\mu_t = \mu_1 + \mu_2 * t$ and the scale parameter is changed to $\sigma_t = \sigma_1 + \sigma_2 * t$. In this case, the location and scale parameters (μ_1 (μ_2) and σ_1 (σ_2)) are intercept (slope) values respectively. For a specific period of time, t serves as descriptive covariant of time, making μ_t and σ_t nonstationary. The negative log likelihood function was minimized using the MLLE to assess distributional parameters. For a stationary and non-stationary variant of the GEV distribution, the likelihood functions may be represented by equations (2) and (3), respectively.

$$l(\mu, \sigma, \varepsilon, x) = -n \log \sigma - \left(\frac{1}{\varepsilon} + 1 \right) \sum_{i=1}^n \log \log \left[1 + \varepsilon \left(\frac{x_i - \mu}{\sigma} \right) \right] - \sum_{i=1}^n \log \left[1 + \varepsilon \left(\frac{x_i - \mu}{\sigma} \right) \right]^{\frac{-1}{\varepsilon}} \quad (2)$$

$$l(\mu_t, \sigma_t, \varepsilon) = -n \log \sigma - \left(\frac{1}{\varepsilon} + 1 \right) \sum_{i=1}^n \log \left[1 + \varepsilon \left(\frac{x_i - \mu_i}{\sigma_i} \right) \right] - \sum_{i=1}^n \log \left[1 + \varepsilon \left(\frac{x_i - \mu_i}{\sigma_i} \right) \right]^{\frac{-1}{\varepsilon}} \quad (3)$$

Different packages are used to determine the estimation of parameters of the frequency analysis probability functions. In order to compute the values of the parameters of the GUM and GEV functions using the maximum likely-hood estimation (MLLE) approach, we selected the "ISMEV" package in R programming [13]. The same procedure was performed for parameter calculation of the NOR and LOGNOR functions.

In the equation, the variations of nonstationarities are expressed as percentage fluctuations between 100-year non-stationary and stationary return values.

$$\text{Nonstationary impacts} = \frac{\text{nonstationary RL} - \text{stationary RL}}{\text{stationary RL}} * 100 \quad (4)$$

An increasing (decreasing) variation of nonstationarity states the condition of higher (lower) return levels. Higher (lower) return levels indicate that the risk of an extreme event occurring during a certain return period has increased (decreased) because of nonstationarity.

4 Results

4.1 Nonstationary Variations During the Historical Period (1970–2015) Annually

Maps of the nonstationarity variations during 100-year recurrence intervals using four probability distributions for annually max precipitation is shown in fig 2 (a). With a few notable differences, the study's findings show that all four distributions have revealed comparable implications for annual AMPs. There are a number of comparable consequence outcomes across the stations that are supported to varying degrees by all four probability functions. The findings demonstrated that positive nonstationary variations have been found for every station. The nonstationary generated by the GEV and LOGNOR probability distributions is shown to be greater in relation to the remaining two stations. Generally, the nonstationary variations from all four probability distributions have been found positive throughout all the stations.

Seasonally



Figure 2 (b) depicts the fluctuations of nonstationarity during 100-year recurrence intervals using four probability distributions for seasonally max precipitation. The evaluation of seasonal maximum precipitation reveals an overall trend of nonstationarity effect from each of the four distributions. However, minor variations have been found at few stations. Seasonal trends highlight the significance of periodicity on the amount of 100-year rainfall recurrence during a historic time period under changing climatic conditions. Seasonal analysis for winter and spring MP indicated that all four distributions have more or less similar impacts of nonstationarity throughout the seasons. The results also showed the positive impacts of nonstationarity at all stations. Moreover, in spring except for GEV the other three probability distributions have a negative effect on Rahim Yar Khan. The positive nonstationary impacts of summer MP are comparable to those of annual MP. This may because of majorly annual extreme precipitation occurred during the summer season. Seasonal MP for autumn has more positive impacts (up to 65%) utilizing the GEV at all stations. Positive impacts using the Gumbel distribution (up to 63%) were identified at all stations except Bahawalnagar where negative impacts of 9% were determined. Overall, higher return level values were anticipated in the autumn, although the effects varied among stations in other seasons.

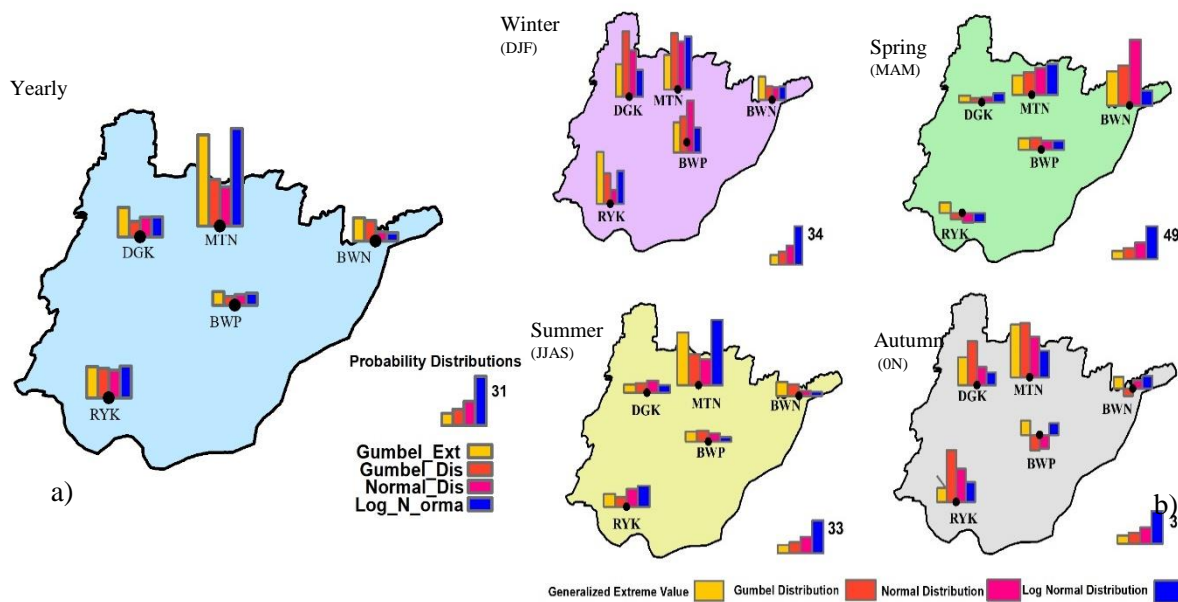


Fig:2 Fluctuations of Nonstationarity Variations during 100 – Year Recurrence Intervals Using Four Probability Distributions for Annual and Seasonal Max. Precipitation

5 Conclusions

Following conclusions can be drawn from the conducted study:

- 1 Analysis of historic data indicates that higher levels of severe precipitation were predicted over the winter at all stations. In the spring, variations of nonstationary are more prevalent in Multan and Bahawalnagar than at other sites, with the exception of Rahim Yar Khan, where negative variations of nonstationary have been observed.
- 2 The expected increasing nonstationary impacts. (10-60%) emphasized to adapt and integrate the climate change in design of hydraulic infrastructure.

The above outcomes strongly recommended nonstationary conditions to be implemented in future projects of water resources. The study, however, may be completed in the future by incorporating the other GCMs with their ensemble approach. Furthermore, nonstationarity of other meteorological variables such as temperature, required to be assessed for future research.



Acknowledgment

The authors would like to thanks Pakistan Meteorological Department for providing data for conducting the research. The authors also thankful to the Centre of Excellence in Water Resources Engineering (CEWRE) to provide research atmosphere to perform research activities.

References

- [1] IPCC (2013). Climate Change 2013: The Physical Science Basis. Contribution of Working Group I to the Fifth Assessment Report of the Intergovernmental Panel on Climate Change [Stocker, T.F., D. Qin, G.-K. Plattner, M. Tignor, S.K. Allen, J. Boschung, A. Nauels, Y. Xia, V. Bex and P.M. Midgley (eds.)]. Cambridge University Press, Cambridge, United Kingdom and New York, NY, USA, 1535 pp.
- [2] Salvati, L., Sateriano, A., and Zitti, M. (2013). Long-term land cover changes and climate variations – A country-scale approach for a new policy target. *Land Use Policy*, 30: 401-407.
- [3] IPCC (2007). Climate Change 2007: Impacts, Adaptation, and Vulnerability, Parry ML, OF Canziani, Palutikof JP, van der Linden PJ, Hanson CE (eds). Cambridge University Press: Cambridge, UK.6
- [4] D. S. Arndt, M.O. Baringer, and M.R. Johnson “Global ocean heat fluxes” [in “State of the Climate in 2009”].
- [5] Aziz, R., Yucel I, and C. Yozgatligil, (2020) "Nonstationarity impacts on frequency analysis of yearly and seasonal extreme temperature in Turkey". *Atmos Res*. <https://doi.org/10.1016/j.atmosres.2020.104875>, 2020.
- [6] Mirza, M.M.Q. (2003). Climate change and extreme weather events: can developing countries adapt? *Climate Policy*, 3: 233-248 Linnenluecke, M.K., Stathakis, A., and Griffiths, A. (2011). Firm relocation as adaptive response to climate change and weather extremes. *Global Environmental Change*, 21: 123-133.
- [7] Aziz, R., Yucel I, and C. Yozgatligil, (2020) "Nonstationarity impacts on frequency analysis of yearly and seasonal extreme temperature in Turkey". *Atmos Res*. <https://doi.org/10.1016/j.atmosres.2020.104875>, 2020.
- [8] Robert M. H. (2010). USGS “a perspective on nonstationarity and water management” Workshop on nonstationarity, hydrological frequency analysis and water management 2010, Colorado Water Institute. P5-14
- [9] Webb, J. W., and White K. D. (2010). “Nonstationarity in water management: USACE perspective” Workshop on nonstationarity, hydrological frequency analysis and water management 2010, Colorado Water Institute. P16-19
- [10] Katz, R. W. (2013). “Statistical methods for nonstationary extremes.” Chapter 2, *Extremes in a changing climate: Detection, analysis and uncertainty*, A. AghaKouchak, D. Easterling, and K. Hsu, eds., Vol. 65, Springer, New York.
- [11] Bayazit, M. *Environ. Process.* (2015). 2: 527. <https://doi.org/10.1007/s40710-015- 0081-7> Milly, P. C. D., et al. (2008). “Stationarity is dead: Whither water management?” *Science*, 319(5863), 573–574.
- [12] Sertac, O. Non-stationary Investigation of Extreme Rainfall. *Civil Engg. Journal*, 2021, 7(9).
- [13] Norrent, C.; Douguédroit, A. Monthly and daily precipitation trends in the Mediterranean (1950–2000). *Theor. Appl. Climatol.* 2006, 83, 89–106. [CrossRef]
- [14] Villarini, G.; Serinaldi, F.; Smith, J.A.; Krajewski, W.F. On the stationarity of annual flood peaks in the continental united states during the 20th century. *Water Resour. Res.* 2009, 45. [CrossRef]
- [15] Wilson, D.; Hisdal, H.; Lawrence, D. Has streamflow changed in the nordic countries?—recent trends and comparisons to hydrological projections. *J. Hydrol.* 2010, 394, 334–346. [CrossRef]
- [16] Zaman, C.Q.U.; Mahmood, A.; Rasul, G.; Afzal, M. Climate Change Indicators of Pakistan; Report No: PMD-22/2009; Pakistan Meteorological Department: Islamabad, Pakistan, 2009.
- [17] Cooley, D. (2013). Return periods and return levels under climate change. Chapter 4, *Extremes in a changing climate: Detection, analysis and uncertainty*, A. AghaKouchak, D. Easterling, and K. Hsu, eds., Vol. 65, Springer, New York. https://doi.org/10.1007/978-94-007-4479-0_4 Salas, J.D., Obeysekera, J. (2014). Revisiting the concepts of return period and risk for non-stationary hydrologic extreme events. *J. Hydrol. Eng.* 19, 554–568. [http://dx.doi.org/10.1061/\(ASCE\)HE.1943-5584.0000820](http://dx.doi.org/10.1061/(ASCE)HE.1943-5584.0000820).
- [18] Heffernan J., Stephenson A. (2012). ismev: An Introduction to Statistical Modeling of Extreme Values. R package version 1.39, Original S functions written by Janet E. Heffernan with R port and R documentation provided by Alec G. Stephenson, URL <https://CRAN.R-project.org/package=ismev>.



DESIGNING THE REMOTE AND SUSTAINABLE WATER MANAGEMENT SYSTEM

^aHadia Tariq, ^bSarwar Imtiaz, ^cErum Aamir*

a: Institute of Environmental Sciences and Engineering, NUST, H/12 Campus, Islamabad, 44000, Pakistan

b: Institute of Environmental Sciences and Engineering, NUST, H/12 Campus, Islamabad, 44000, Pakistan

c: Institute of Environmental Sciences and Engineering, NUST, H/12 Campus, Islamabad, 44000, Pakistan

* Corresponding author: Email ID: erum21@hotmail.com

Abstract- Freshwater availability is a huge issue for downstream areas but the mismanagement practices and exploitation of freshwater leading towards scarcity is an absolute crisis right now and if the mismanagement practices continue to be like that, then by the end of 2047, the world would be left with less than 500 cubic centimeters per capita of water availability leading towards absolute scarcity. To solve the water mismanagement of the capital city, National University of Science and Technology (Nust) as the case study was chosen. A pilot scale prototype was made for this project which was basically a monitoring system and can be expanded to a controlling system with few sensors and a microcontroller (Arduino UNO) was installed which was used to monitor the water level in the overhead tank, water flow from the taps and water leakage from any tap. It stored the data and calculated the total water usage and was aligned with mobile application for data viewing and storage with just an internet connection. The user was able to analyze the real-time data and the stored data anytime and anywhere just by using the mobile application and internet connection. SONAR Sensor was installed to check the water level in the tank. It showed the water in percentage. Water flow sensor was installed to measure the water flow from the tap. These sensors directly sent the data to the microcontroller which was programmed according to the sensors and then the microcontroller interpreted the data and send it to the user to its application. Prototype resembled the complete water system of a house or any commercial building. Cost benefit analysis was done to check the feasibility of the project which showed that it was the most suitable system in the conservation of the water. Hostel building was selected for this project which had 4 floors. Two SONAR sensors and 140 water flow sensors were installed. Every single tap was attached to a water flow sensor. User was able to see each tap and its data and can monitor even single tap. This study addresses SDG 6 which is clean water and sanitation and SDG 12 which is responsible consumption and production.

Keywords- Mobile application, remote sensing, SDG 6, SDG 12, sustainable solution, water management.

1 Introduction

Water is the basic necessity of life but world is constantly struck with the issue of access to clean water. There is not enough clean water, and the mismanagement practices are leading towards scarcity. 3 billion people lack access to drinking water that is safe. [1] 1/5th of the population lives in areas where water is physically scarce and 1/4th of the population lives in developing countries that face water shortages due to lack of infrastructure to transport water and weak governance, [1] so investing in improved water management and services is one prerequisite to reduce poverty and achieving sustainable economic growth. The relationship between water and poverty is a two-way street. Poor people receive direct benefits from improved water services and improved sanitation services through better health, reduced health costs, timesaving, and increase productivity. Access to adequate and safe water supply is essential for poverty reduction, yet poverty itself can be the driver of pollution and unsustainable use of water resources. 89% of people have access to drinking water 58% of people have access to water for sanitation and 60% [2]. of people have access to water for hygienic purposes. 21 million people lack access to clean water close to home. In 1947 per capita availability of water in Pakistan was 300 cubic centimeters and there was no stress of water whereas in 2017 it reduces to per capita availability of water up to 1000 cubic centimeters leading towards scarcity and extrapolating that it can be seen in the current situation that by the end of 2047 the per capita availability of water will reduce to less than 500 cubic centimeters leading towards



5th Conference on Sustainability in Civil Engineering (CSCE'23)

Department of Civil Engineering

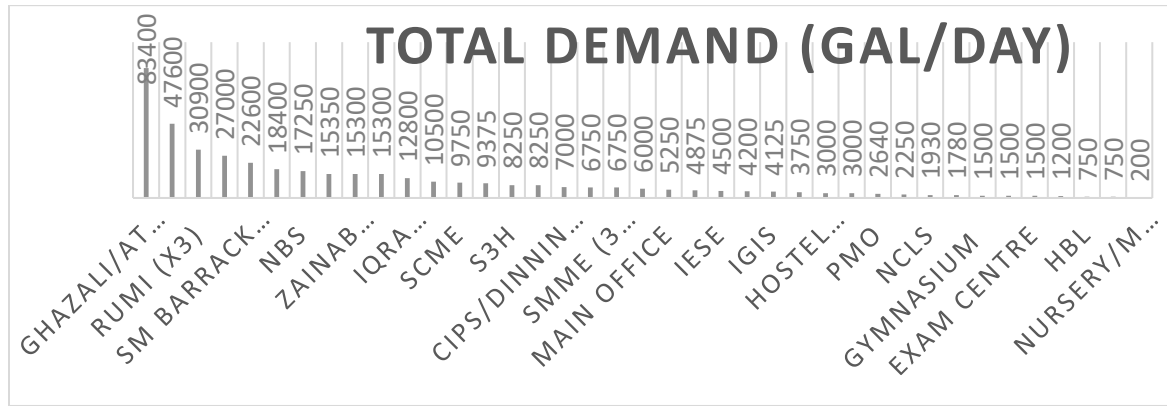
Capital University of Science and Technology, Islamabad Pakistan



absolute scarcity. [2] so to control mismanagement practices, the innovation in this project was development of mobile application with access to everyone and developing of smart water management system [1] which will be the first remote management water system in NUST.

Total water demand in National University of Science and Technology (NUST) H-12

This is the data that was collected from PMO, the graph 1 shows the water demand in respective areas, departments of NUST.



Graph 1: Total Water Demand

Objective

The objective of this project was to develop a sustainable water management system and remotely regulated water system for minimum water wastage keeping in mind future implementation on larger scale. The second objective was real time water usage data identification and accessibility for consumers and providing quantitative framework for making management decisions

2 Experimental Procedures

Construction of the Prototype

There were total of two sensors in the prototype, SONAR [3]-[4] sensor to sense the water level in the water tank and the other one was the water flow sensor which was attached to the water tap to measure the flow of the water flowing through the tap and leaving out the water tank and then there was a processor (Micro-Controller) which was the brain of the prototype which would be receiving the information from the sensors and sending it to the laptop and mobile application through its input-output peripherals.[8]

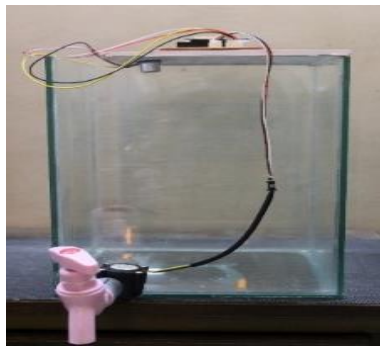


Figure 1: Prototype



2.1 The Process

2.1.1 Stage One (Sensor Stage)

The sensors were able to sense the change. SONAR [7] sensor was sensing the change in the water level and water flow sensor was sensing the flow of the water through the tap perfectly and both would give the feed to the micro-controller.

2.1.2 Stage Two (Micro-Controller Stage)

Micro-Controller decided what to do with the information. It interpreted the data and send it to the laptop and the mobile application using WIFI connection, which could remotely be accessed.

2.1.3 Stage three (Mobile Application stage)

Whoever was accessing the mobile application using its login and password, will get the notification and the data received from the sensors was showing on the mobile application.

2.1.4 Explanation of the Process

The prototype was composed of a water tank, microcontroller, SONAR Sensor, and water flow Sensor along with a water tap. The process worked in a systematic manner beginning with the sensor and then moving towards the microcontroller to receive and send the information to the user using WIFI which ultimately conveyed the command.

The sensors were programmed to do their basic job which is explained in the tabular form in Table 1. Followed by a detailed explanation and pictorial presentation.

Table 1 List of devices and their tasks

S. #	Devices	Tasks
1.	SONAR sensor	Detect the water level
2.	Water flow sensor	Measure the water flow
3.	Micro-controller	Interprets data it received

1. SONAR sensor was being used to detect the water level in the tank which ultimately detected any changes in the water level in the overhead tank with quite accuracy.
2. Water flow sensor was basically sensing the flow of water running through the tap. It measured the flow rate as well, which could be seen on the mobile application on a real-time basis. There was a few seconds delay in the information in the real-time which was not even noticeable.

2.1.5 SONAR Sensor

This was the SONAR sensor which basically was used to sense the water level in the tank. An ultrasonic sensor worked by emitting a sound wave that is above the human hearing range. It was working all the time and was sending the real time data to the micro-controller and it detected any change in the level of the water tank and fed the information to the micro-controller. [5]



Figure 2: SONAR sensor



2.1.6 Water Flow Sensor

Water flow sensor was installed just before the tap. Water flow sensor consisted of a plastic valve from which water could pass. A water rotor along with a hall effect sensor was present to sense and measure the water flow.

It basically detected the flow in the tap and measured the flow rate of the running water through the tap. It was feeding the micro-controller in real time. It was being used to get the flow rate and to calculate the total usage of water from that tap. Also, it was being used to detect the leakage in any of the tap as it was very sensitive and would sense the leakage of water from the tap and feed it to the micro-controller.

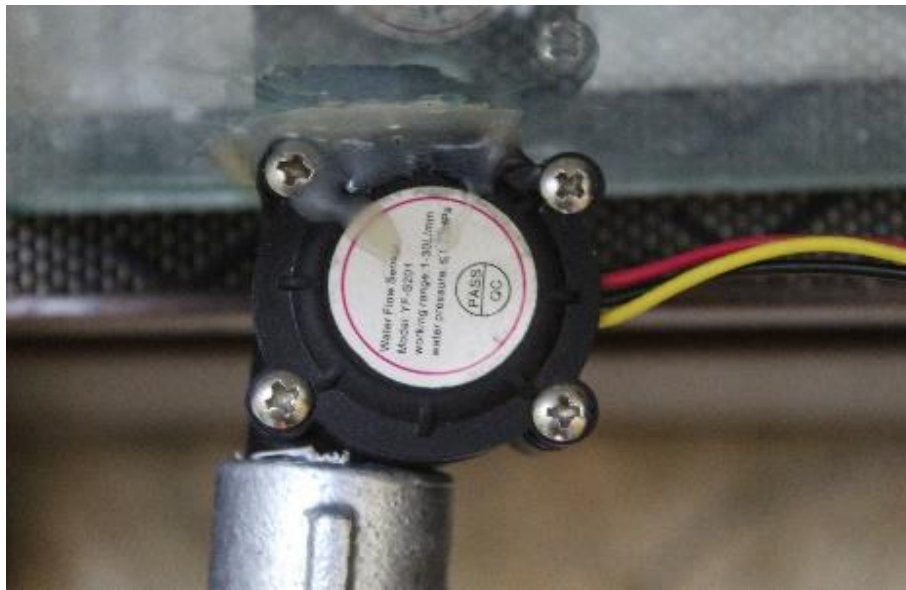


Figure 3: Water flow sensor

2.1.7 Micro-Controller

Microcontroller was embedded inside of a system to control a singular function in a device. It interpreted the data it received from its I/O peripherals using its central processor. The basic function of this microcontroller in the project was to get information from the sensors and send this information to the users/consumers wirelessly using WIFI. The mobile application was developed to show the data to the users.

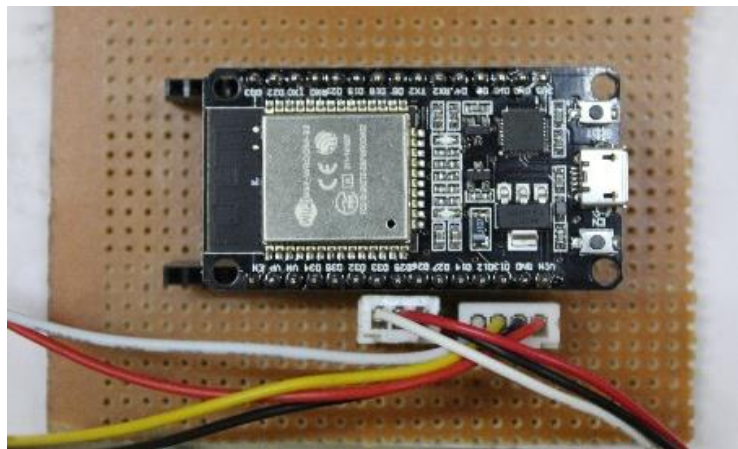


Figure 4: Microcontroller



5th Conference on Sustainability in Civil Engineering (CSCE'23)

Department of Civil Engineering

Capital University of Science and Technology, Islamabad Pakistan



2.2. Laptop's Interface

On the laptop screen the real-time data was showing. There were only two objects to show one was “Water Level in the Tank” and the other one was “Flow rate” of the water flowing from the tap. The water level was being measured in terms of percentage such that 44% of the water the water tank was filled with the water and flow was showing in L/min which was apparently 0 because no water was flowing from the tap.

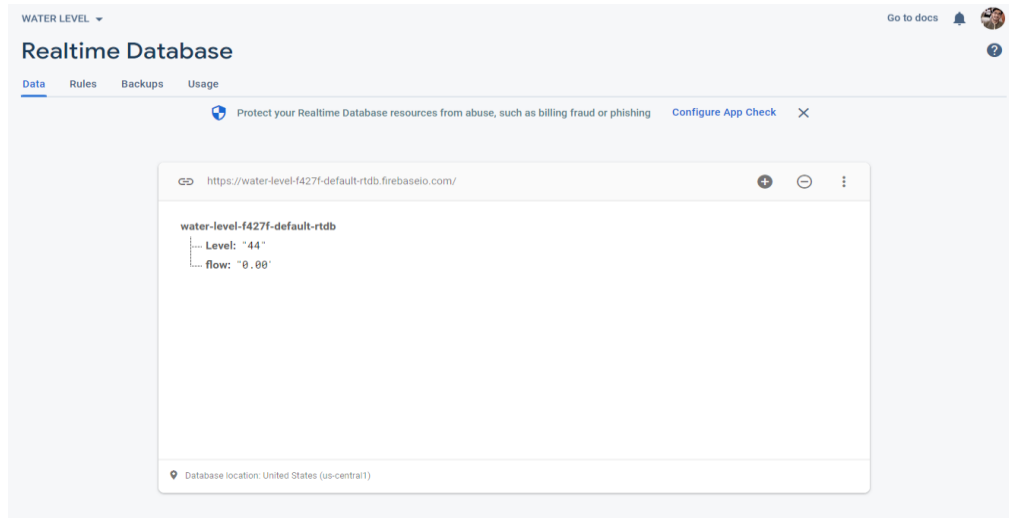


Figure 5: Laptop's Interface

2.2 Mobile Application's Interface

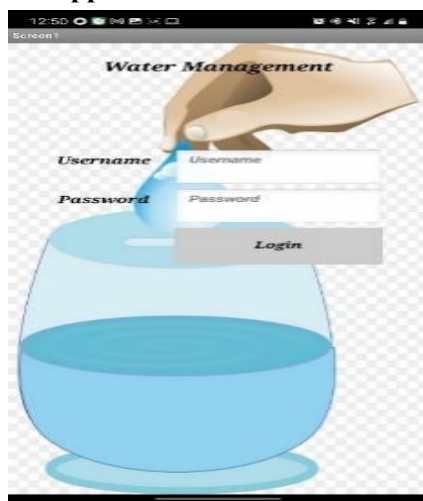


Figure 6 (a): Login Interface



Figure 6 (b): User Interface

These were the screenshots taken from the mobile phone where it can be seen in figure, user has its own login id to get into the application to get the information. While in the other figure user was getting the results from the micro-controller as can be seen water level was showing in percentages that was 44% of the water tank is filled with water or the 44% of the total water was remaining in the tank. And flow rate can also be seen which was showing in L/min.



3. Results

After several tests runs and trials, it was concluded that the device performance was very good, and assembly could be implemented in the hostel or any other building. Real-time data was received, and any leakage was detected immediately. Also, the data from the flow sensor could be stored in the laptop and so, it could determine the pattern of water usage. As water flow sensor will be installed on each tap it will show which tap is leaking. This would provide the quantitative framework to make management decisions. This will conserve water usage and will help to fight water scarcity in Pakistan. By this one could access the data from anywhere just by using the internet on the mobile phone.

This project was implemented on larger scale. Attar 1 hostel building was selected.

Distribution of Items

- Over Head Tank = 1
- Total No of Taps in Attar 1 Hostel = 140 (30 on each floor (4 floors in total) + 10 in the Dining Hall + 4 in the Kitchen + 6 miscellaneous)
- SONAR Sensors (Range 20cm - 400cm) Required for Over Head Tank = 2
- Arduino UNO (Micro-Controller) Required = 7 (1 for each Floor + 1 for the Dining Hall + 1 for the Kitchen + 1 Miscellaneous)
- Water Flow Sensors Required = 140 (There is a sensor for every single tap)
- Data Cables Required = 7 (Cable for every Micro-Controller)

Cost-Benefit Analysis:

Total cost of the prototype

Table 2: Cost of the prototype

	Item	Quantity	Per Unit Cost	Total Cost
1	Glass Sheet	6ft	600/-	3600/-
2	SONAR Sensor	1	350/-	350/-
3	Water Flow sensor	1	450/-	450/-
4	Data Cable	1	300/-	300/-
5	Arduino UNO	1	1050/-	1050/-
<i>Total</i>		5750/-		

Total cost for Attar 1 hostel

Table 3: Cost for Attar 1 Hostel

	Item	Quantity	Per Unit Cost	Total Cost
1	Arduino UNO	7	1050/-	7,350/-
2	SONAR Sensor	2	350/-	700/-
3	Water Flow sensor	140	450/-	63,000/-
4	Data Cable	8	300/-	2400/-
5	Miscellaneous			5000/-
<i>Total</i>		78,450		



5th Conference on Sustainability in Civil Engineering (CSCE'23)

Department of Civil Engineering

Capital University of Science and Technology, Islamabad Pakistan



Total Benefits

On average out of every 5 taps 2 were leaking.

There were total 140 taps in the Hostel building and considering the given statement, it had 56 leaking taps.

On average 10 drips per minute a single tap would waste 1 gallon per day.

So, 56 gallons of water was being wasted daily.

On monthly basis 1680 gallons of water was being wasted.

As one 1000 gallons water tanker costs 4000 rupees which means it costs 4 rupees per gallon.

So, it was saving

$$1680 \times 4 = 6720 \text{ Rupees per month}$$

And Wastewater treatment cost per gallon is 1.08 rupee.

$$1680 \times 1.08 = 1814 \text{ Rupees per month}$$

Total benefits in terms of money are = $6720 + 1814$

$$= 8534 \text{ Rupees per Month}$$

Break-Even Analysis

$$\text{Total Cost} = 78,450/-$$

And it was saving

$$\text{Monthly basis} = 8,534/-$$

So, it will achieve its Breakeven point within 10 months = $8,534 \times 10 = 85,340/-$

The results and Cost-Benefit Analysis clearly demonstrated that this Remotely Managed water system, will provide Economical, Environmental, and social benefits to society. This will reduce the carbon footprint in the environment. The Remotely Water Management system seems a favorable and feasible solution to the current water crises in terms of services as well as in terms of monetary value. Inadequacy of such a Water Management system causing the Water availability issue not only in the NUST but in Pakistan as well. Thus, this remote Water Management system is the most feasible solution in the current scenario.

4. Applications

This technology can have numerous applications some of them are given below.

- i. On larger scale, this technology can be used in detection of leakage in fuel tanks, large water reservoirs, institutions, hotels, restaurants, malls, and public toilets etc. for determining and checking the usage ratio
- ii. This technology can save lots of water in public places where the water use is consistent, but maintenance is irregular.
- iii. The sensor technology was a step towards the sustainable use and proper management of water resources and thus can lead to a lot of savings on indirect costs by decreasing the water required through proper management and thus, the water pumped or supplied and less water requirement would also save on electricity bills of pumping water from groundwater sources or water transmission costs.

Conflict of Interest

This study has no conflict of Interest.

References

- [1] UNESCO," [Online]. Available: <https://www.unesco.org/en/wwap>.
- [2] UNICEF," [Online]. Available: <https://www.unicef.org/pakistan/wash-water-sanitation-and-hygiene-0>.
- [2] Hjelmervik K. T. "Predicting SONAR false alarm rate inflation using acoustic modelling and a high-resolution terrain model". IEEE J. Oceanic Engineering, 35(2):278-287, (2010).
- [3] Hodges R. P. "Underwater Acoustics: Analysis, Design and Performance of SONAR". John Wiley & Sons, (2011).



5th Conference on Sustainability in Civil Engineering (CSCE'23)

Department of Civil Engineering

Capital University of Science and Technology, Islamabad Pakistan



- [4] De-Marco K. J., M. E. West, A. & Howard M. "SONAR-based detection and tracking of a diver for underwater human-robot interaction scenarios". Proc. IEEE Int. Conf. Syst., Man, and Cybernetics, 2378-2383, (2013).
- [5] Sarabia E. G., J. R. Llata, S. Robla, C. Torre-Ferrero & Oria J. P. "Accurate estimation of airborne ultrasonic time of flight for overlapping echoes". Sensors, 13:15465-15488, (2013).
- [6] Terzic J., Terzic E., Nagarajah R. & Alamgir M. "Ultrasonic Sensing Technology. In Ultrasonic Fluid Quantity Measurement in Dynamic Vehicular Applications", Springer, Heidelberg, (2013).
- [7]] Ullah I., Q. Ullah, F. Ullah & S. Shin. "Sensor-based autonomous robot navigation with distance control. J. Comput. Intelligence and Electron". Syst. 1:1-8, (2013).
- [8] Dombestein E. & Wegger K. E. "Predicting SONAR false alarm rate inflation using acoustic modelling and a high-resolution terrain model". Tech. Report 2014/00512, FFI, (2014).
- [9] Persons M. J. G., I. M Parnum, K. Allen, R. D. McCauley and Erbe C. "Detection of sharks with gemini imaging SONAR". Acoustic Australia, 42(3):185 - 189, (2014).
- [10] S. N. Kothawade, S. M. Furkhan, A. Raoof and K. S. Mhaske, "Efficient water management for greenland using soil moisture sensor," 2016 IEEE 1st International Conference on Power Electronics, Intelligent Control and Energy Systems (ICPEICES), pp. 1-4, doi: 10.1109/ICPEICES.2016.7853281, 2016.
- [11] Smith, A. "Historical development of SONAR". Retrieved July 9,2017 from <http://sciencejrank.org/pages/6289/SONAR-Historical-development-SONAR.html>, (2016).
- [12] K. Gupta, M. Kulkarni, M. Magdum, Y. Baldawa and S. Patil, "Smart Water Management in Housing Societies using IoT," 2018 Second International Conference on Inventive Communication and Computational Technologies (ICICCT), pp. 1609-1613, doi: 10.1109/ICICCT.2018.8473262, (2018).
- Urick, R. J. "Principles of Underwater Sound", 3rd Edition. New York: McGraw-Hill, (1983).
- [13] Boniel, G. J., Catarinen, C. C., Nanong, R. D., Noval, J. P., Labrador, C. J., & Cañada, J. R. (2020). "Water management system through wireless sensor network with mobile application". *HIGH-ENERGY PROCESSES IN CONDENSED MATTER (HEPCM 2020): Proceedings of the XXVII Conference on High-Energy Processes in Condensed Matter, Dedicated to the 90th Anniversary of the Birth of RI Soloukhin*, (2020). <https://doi.org/10.1063/5.0026155>.
- [14]A. Djalilov, "Study on automatic water level detection process using ultrasonic sensor," 2023.



SCOUR REDUCTION AROUND BRIDGE ABUTMENTS USING INDUSTRIAL BY-PRODUCTS AS A COUNTERMEASURES-AN EXPERIMENTAL APPROACH

*^a Rana Adnan Amir, ^a Naeem Ejaz, ^a Nadir Murtaza**

a: Department of Civil Engineering, UET, Taxila, Pakistan, ranaadnan_56@yahoo.com

b: Department of Civil Engineering, UET, Taxila, Pakistan, naeem.ejaz@uettaxila.edu.pk

c: Department of Civil Engineering, UET, Taxila, Pakistan, Nadirkhattak1122@yahoo.com

* Corresponding author: Email ID: Nadirkhattak1122@yahoo.com

Abstract- Due to the three-dimensionalities of the flow and sediment movement, the scour process around bridge elements such as piers, abutments, and spur dikes is complicated. In the present study, a laboratory investigation was carried out to determine the scouring around the bridge abutment without and with countermeasures. A wooden model of bridge abutment was embedded in a sand bed under two different values of discharge. Each experimental case was run for the time duration of two hours. The result showed that scouring around bridge abutment increases by increasing the flow discharge. The maximum scouring around the bridge was observed to be 17.92cm which was 9% greater than scouring at a flow discharge of $0.016\text{m}^3/\text{s}$. By providing an industrial by-product as a countermeasure, it was observed that scouring around the bridge abutment decreases compared to without placing any countermeasures but scouring increases by increasing the flow discharge. The maximum reduction in scouring around the bridge abutment was observed to be 33% for two different values of flow discharge compared to the without placing countermeasures cases. It was concluded that industrial by-products reduced scouring around the bridge abutment up to the maximum level and provided protection to the bridge abutment from failure.

Keywords- Scouring, bridge abutments, countermeasures, sand bed, flow discharge.

1. Introduction

The process of soil or silt being eroded or removed from around the base or foundation of a bridge is referred to as "scouring around a bridge abutment." The moving water of a river or stream, particularly during times of high-water velocity or floods, has the potential to bring about this effect. If it is not addressed, scouring has the potential to put the bridge's stability and safety at risk. Sand, gravel, and silt are examples of sediments that are typically carried by rivers. These sediments have the potential to build up around the abutments of the bridge over time. It is possible for scouring in the river as a result of the sediments being mobilized and eroded if there is an excessive sediment load or if there are changes in the sediment transport patterns of the river as shown in Figure 1.

Local scouring is an important and critical process that may occur around the piers and abutments leading to the catastrophic collapse of the bridge [1]. The process of local scour occurs in the surroundings of piers and abutments and has many similarities [2-4]. Therefore, it is necessary to assess the local scour around piers and abutments carefully and precisely. Otherwise, local scour may result in the collapse of the whole bridge structure, with the potential of a serious death toll and injuries in its aftermath [5, 6]. As the flow encounters the pier or abutment, it separates and converges downstream, forming a vortex. The downstream flow and vortices shed by the abutment may result in local scour at its



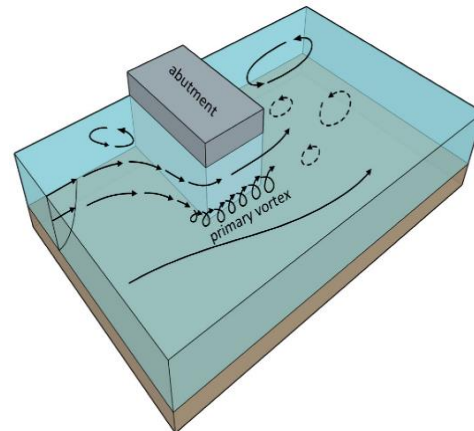
upstream face [7]. The horseshoe vortex at the base of the abutment causes the scour hole to become wider and deeper as briefly presented in Figure 1 [8, 9]. It's important to note that scours can be influenced by various factors, including flow velocity, sediment characteristics, channel geometry, and structural design. Understanding the scour mechanism is crucial for designing effective countermeasures to mitigate scours and ensure the stability of bridge structures [10].

Many hydraulic researchers have investigated the challenge of local scouring experimentally under various flow conditions. Numerous methods have been proposed and implemented based on research aiming to minimize local scours around the piers and abutments [11]. There are two categories of countermeasure techniques around the abutments for local scour: bed surface armoring and flow modification [12-14]. Bed surface armoring techniques use hard materials like riprap stones, gabions, cable-tied blocks, concrete mats, or bags to protect the bed surface materials from flow-induced destabilization and scour. The flow modification techniques either prevent the scour-inducing mechanism or shift the scour hole away from the abutment's vicinity [15]. They are spur dike, parallel-wall, or collar and hooked-collar applications on abutments used as countermeasures against abutment scour in open-channel flow scenarios [16].

Previous literature shows that different researchers proposed countermeasures for scour reduction around bridge abutments, but their proposed solution is not economical and cost-effective. Therefore, in the present study, the objective was to investigate the scour reduction under different flow discharges and to investigate the maximum scour around the bridge abutment. The present study mainly focuses on scour reduction around bridge abutments by using industrial by-products such as bricks, and ceramic material to provide economical and better countermeasures.



(a)



(b)

Figure 1. (a) bridge abutment failure caused by scouring (b) schematic figure of scouring pattern around bridge abutment

2. Experimental Procedures

Experiments were performed in an open channel placed in the water resources engineering laboratory of the Civil Engineering Department of the University of Engineering and Technology Taxila. The channel has a length of 20 meters, width of 0.96 meters, and height of 1 meter respectively as shown in Figure 2a. Flow was supplied to the channel from the underground tank through the pump. The channel flow was measured by using a compound rectangular trapezoidal sharp-crested weir provided at the end of the channel. Such discharge was permitted so that bed shear stress does not exceed the threshold. The whole study was carried out using a bed of uniform sand that has an average diameter of 'd₅₀' = 0.51 mm. The geometric standard deviation of the particle size distribution $\sigma_g = (d_{84}/d_{16})^{0.5}$ was 1.74, here d₈₄ and d₁₆ represent that the sediment sizes were finer at 84% and 16% respectively. The mean grain size of sand is d₅₀=0.51 mm. The tests were performed at two different discharges (i.e., 0.016 m³/s, 0.022 m³/s). To fulfill the short-abutment criteria i.e., La/Yc ≤ 1, the flow depth of 12cm was used in all these experiments against 14 cm abutment length as shown in Figure 2b and Figure 2c shows the scour depth and scour pattern around the bridge abutment. Flow conditions for each experimental case are summarized in Table 1.



Table 1. Hydraulics condition experiment

Discharge (m ³ /s)	Flow depth (cm)	Median Grain Size
Q	Y _m	(d ₅₀) (cm)
0.016	12	0.051
0.022	12	0.051

3. Research Methodology

All the experiments were carried out in clear water conditions. To confirm fully established velocity profiles, a vertical-wall abutment was positioned in the last one-third of the sediment bed region of the experiment portion [17]. To measure the value of discharges at trapezoidal sharp-crested weir was positioned with the help of the equation

$$Q_t = \frac{2}{3} C_{rd2} \sqrt{2g} (b^* h^{3/2}) + \frac{2}{3} C_{rd1} \sqrt{2g} (2b') h'^{3/2} + \frac{8}{15} C_{td} \sqrt{2g} (\tan \theta) h e^{5/2}$$

the end of the channel a weir was positioned with obtained by [18].

Where θ = notch angle, b = length of the weir

C_{rd} = discharge coefficient of the rectangular sharp-crested weir,

C_{td} = discharge coefficient for triangular sharp-crested weir

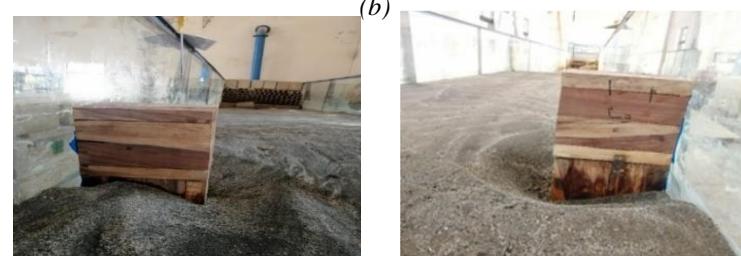
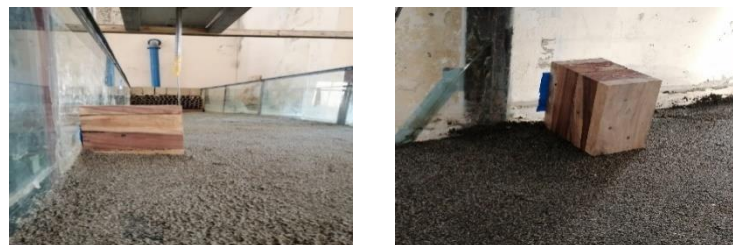
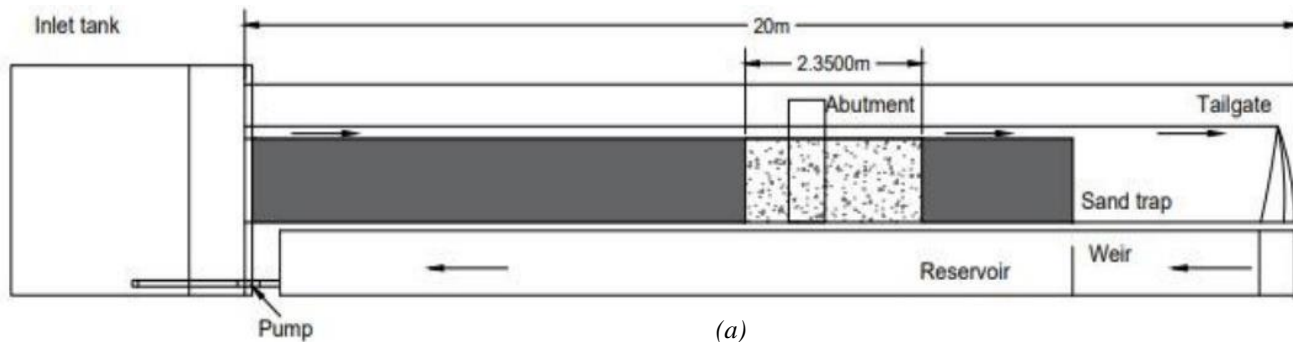


Figure 2. experimental setup of laboratory investigation (a) schematic diagram of experimental work with abutments setup (b) photograph of abutments model in a flume (c) scouring depth and pattern around abutments



4. Results

4.1. Scour Depth without Countermeasures

The scour depth around the bridge abutment has been determined under two different flow discharges. It was observed that scouring depth at the outer side of the bridge abutment increases by increasing the flow discharge as by increasing the discharge the flow velocity at the outer edge of the abutments increased that resulting sediment flow on the outer edge of the abutment. *Figure 3a* shows the scour around bridge abutments for flow discharge of $0.016\text{m}^3/\text{s}$. The maximum scour depth underflow discharge of $0.016\text{m}^3/\text{s}$ was observed to be 16.29cm as shown in *Figure 3a*.

Similarly, scouring depth around the bridge abutment underflow discharge of $0.022\text{m}^3/\text{s}$ was also determined. The maximum scour around the bridge abutment underflow discharge of $0.022\text{m}^3/\text{s}$ was observed to be 17.92cm which was 9% more than scour depth under the discharge of $0.016\text{m}^3/\text{s}$ as shown in *Figure 3b*. The results showed that by increasing the flow discharge, scour depth around bridge abutments increased by a multiple of 9%.

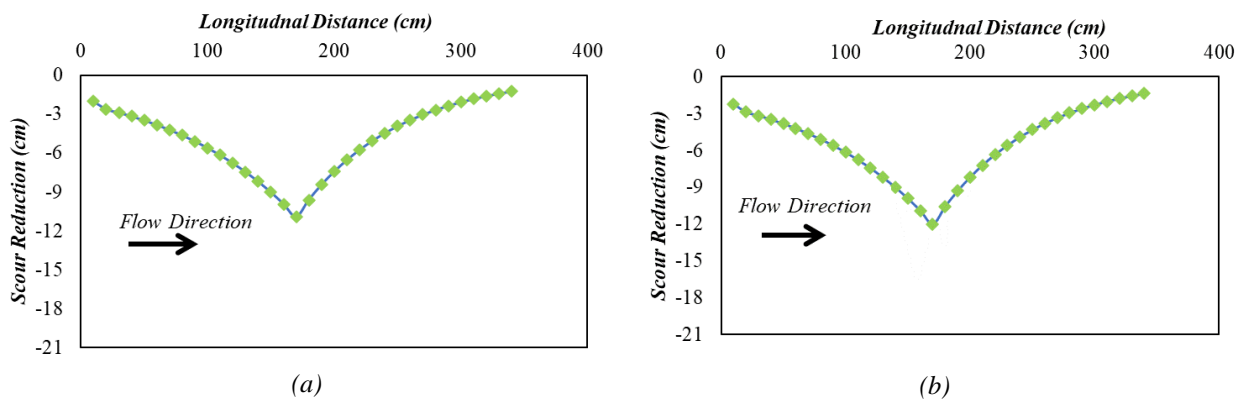


Figure 4. Scour reduction using countermeasures (a) Scour reduction under flow discharge of $0.016\text{m}^3/\text{s}$ (b) scour reduction under flow discharge of $0.022\text{m}^3/\text{s}$.

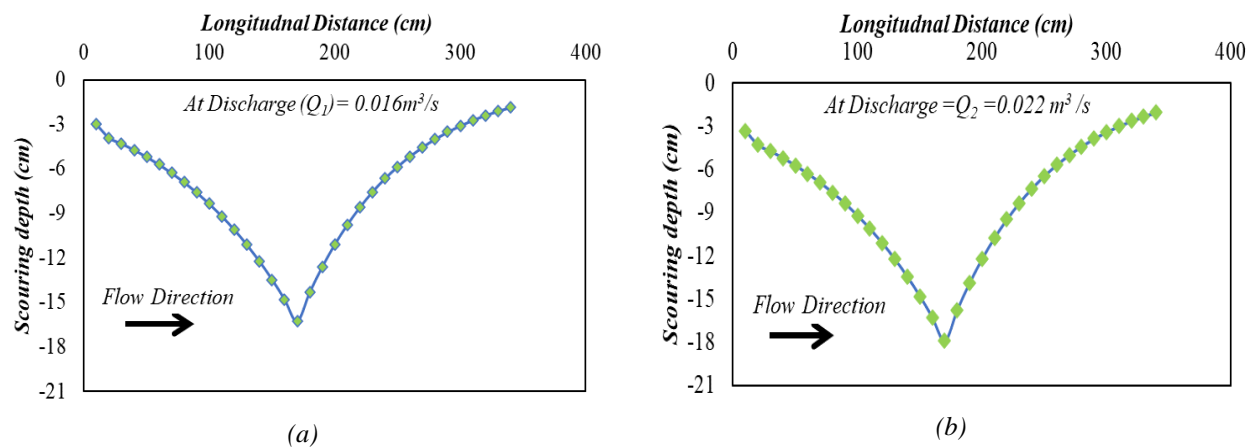


Figure 3. Scour depth around abutments without countermeasures. (a) scour depth at discharge of $0.016\text{m}^3/\text{s}$ (b) scour depth at discharge of $0.022\text{m}^3/\text{s}$.



4.2. Scour Depth with Countermeasures

The present study investigates the scour reduction around bridge abutments using industrial by-products as a countermeasure. It was observed that scour depth with countermeasures decreases for two different values of flow discharge but increases by increasing flow discharge as shown in [Figure 4a-b](#). Industrial by-products protect the bridge abutments that reduced the flow velocity around the bridge abutment resulting in a scour reduction around the bridge. The scour depth is reduced by up to 33% for two different values of flow discharge and scour reduction increases by decreasing the intensity of flow. Hence it was found that industrial by-products are efficient for scour reduction around bridge abutments.

4.3. Implementation of Study

In Pakistan, it is common practice to come across scouring or sediment erosion, both of which have the potential to cause damage to bridge abutments. Researchers from a variety of institutions have come up with a variety of potential solutions to the problem of scouring bridge abutments in the hopes of reducing the frequency with which it occurs [\[12,19,20\]](#). However, despite the fact that these preventative measures have been shown to be beneficial in lowering scour, the country's economic conditions have not been fulfilled by them. This study investigates the use of industrial by-products as a potential method for reducing the amount of scouring that occurs near bridge abutments in a way that is both cost-effective and efficient. The project will also look into ways to improve existing systems to prevent the collapse of bridge abutments.

5. Conclusions

Based on an experiment performed in the hydraulic laboratory for scour reduction around bridge abutments using industrial by-products as a countermeasure, the following conclusion has been concluded.

1. The scour depth around bridge abutments increases by increasing the flow discharge and the maximum scour depth was observed to be 17.92cm.
2. The maximum scour around the bridge abutment underflow discharge of $0.016\text{m}^3/\text{s}$ was observed to be 16.29cm.
3. Scour depth underflow discharge of $0.022\text{m}^3/\text{s}$ was observed to be 9 percent more than scour depth underflow discharge of $0.016\text{m}^3/\text{s}$.
4. The scour depth was reduced up to 33% when the industrial product is provided as a countermeasure around the bridge abutment which reduced the flow velocity around the abutment.
5. The results concluded that using industrial by-products as countermeasures would be economical and should be implemented in developing countries.

References

- [1] Bestawy, A., et al., Reduction of local scour around a bridge pier by using different shapes of pier slots and collars. *Water Supply*, 2020. 20(3): p. 1006-1015.
- [2] Chiew, Y.-M., Scour and scour countermeasures at bridge sites. *Transactions of Tianjin University*, 2008. 14(4): p. 289-295.
- [3] Singh, N.B., T.T. Devi, and B. Kumar, The local scour around bridge piers—a review of remedial techniques. *ISH Journal of Hydraulic Engineering*, 2022. 28(sup1): p. 527-540.
- [4] Chiew, Y.-M., Scour and scour countermeasures at bridge sites. *Transactions of Tianjin University*, 2008. 14: p. 289-295.
- [5] Al-Shukur, A.-H.K. and Z.H. Obeid, Experimental study of bridge pier shape to minimize local scour. *International Journal of Civil Engineering and Technology*, 2016. 7(1): p. 162-171.
- [6] Jahangirzadeh, A., et al., Experimental and numerical investigation of the effect of different shapes of collars on the reduction of scour around a single bridge pier. *PloS one*, 2014. 9(6): p. e98592.
- [7] Kothyari, U.C., R.C.J. Garde, and K.G. Ranga Raju, Temporal variation of scour around circular bridge piers. *Journal of Hydraulic Engineering*, 1992. 118(8): p. 1091-1106.
- [8] Kumar, V., K.G.R. Raju, and N. Vittal, Reduction of local scour around bridge piers using slots and collars. *Journal of hydraulic engineering*, 1999. 125(12): p. 1302-1305.
- [9] Dey, S. and R.V. Raikar, Characteristics of horseshoe vortex in developing scour holes at piers. *Journal of Hydraulic Engineering*, 2007. 133(4): p. 399-413.
- [10] Melville, B.W. and S.E. Coleman, Bridge scour. 2000: Water Resources Publication.



5th Conference on Sustainability in Civil Engineering (CSCE'23)

Department of Civil Engineering

Capital University of Science and Technology, Islamabad Pakistan



- [11] Hong-Wu, T., et al., Protection of bridge piers against scouring with tetrahedral frames. International Journal of Sediment Research, 2009. 24(4): p. 385-399.
- [12] Farooq, R. and A.R. Ghumman, Impact assessment of pier shape and modifications on scouring around bridge pier. Water, 2019. 11(9): p. 1761.
- [13] Alabi, P.D., Time development of local scour at a bridge pier fitted with a collar. 2006, University of Saskatchewan.
- [14] Osroush, M., S.A. Hosseini, and A.A. Kamanbedast, Countermeasures against local scouring around bridge abutments: combined system of collar and slot. Iranian Journal of Science and Technology, Transactions of Civil Engineering, 2021. 45: p. 11-25.
- [15] Tafarognoruz, A., R. Gaudio, and S. Dey, Flow-altering countermeasures against scour at bridge piers: a review. Journal of hydraulic research, 2010. 48(4): p. 441-452.
- [16] Karami, H., et al., Protective spur dike for scour mitigation of existing spur dikes. Journal of hydraulic research, 2011. 49(6): p. 809-813.
- [17] M. Vaghefi, M. Akbari, and A. R. Fiouz, "An experimental study of mean and turbulent flow in a 180-degree sharp open channel bend: Secondary flow and bed shear stress," KSCE Journal of Civil Engineering, vol. 20, no. 4, pp. 1582-1593, 2016.
- [18] Martinez, J., Reca, J., Morillas, M.T., and Lopez, J.G (2005) "Design and calibration of a compound sharp-crested weir", Journal of Hydraulic Engineering, Vol. 131, No. 2, pp.112-116.
- [19] Farooq, R., et al., *Optimal octagonal hooked collar countermeasure to reduce scour around a single bridge pier*. Periodica Polytechnica Civil Engineering, 2020. **64**(4): p. 1026-1037.
- [20] Farooq, R., et al., *Effects of hooked-collar on the local scour around a lenticular bridge pier*. International Journal of Sediment Research, 2023. **38**(1): p. 1-11.



BRIDGE PIER SCOUR REDUCTION INVESTIGATION USING DIFFERENT VEGETATION ELEMENTS AS COUNTERMEASURE

^a*Sajjad Hussain**, ^b*Naeem Ejaz*, ^c*Sheraz Hussain*

a: Department of Civil Engineering, UET, Taxila, Pakistan, ziadbacha001@gmail.com

b: Department of Civil Engineering, UET, Taxila, Pakistan, naeem.ejaz@uettaxila.edu.pk

c: Department of Civil Engineering, UET, Taxila, Pakistan, sheraalvi212@gmail.com

*Corresponding authore: Email ID: sh389633@gmail.com

Abstract- Due to climate change extreme weather conditions like increased heat, droughts, glaciers melting affected the natural ecosystem of our country. Flash floods mostly occurred in hilly areas of Pakistan. Scouring occurs when the flow of water around bridge piers erodes the bed material, potentially undermining the foundation of the structure. To mitigate this problem, various countermeasures have been proposed and studied. This research investigates the effectiveness of different vegetation elements as countermeasures for reducing bridge pier scour. The study comprises a comprehensive examination of two types of rigid vegetation, including wooden and steel cylinders around bridge pier in experimental flume setups. These cylinders were of circular cross-section and were installed upstream of the bridge pier, which is of circular shape. The aspect ratio (AR-ratio of width to length) of wooden and steel cylinders and the spacing between the cylinders (G/d) were changed against two different flow conditions (where G is spacing between each cylinder and d is the diameter of each cylinder). The experiments were conducted under sub critical flow conditions i.e at Froude number 0.136 and 0.187. The results showed that by decreasing the aspect ratio of cylinders, scourhole reduces effectively. The denser arrangement of cylinders obstructs the flow and results in a greater reduction of scouring on the bridge pier. Maximum scour reduction at pier is 71.7% by using vegetation cylinders of 7.46 aspect ratio and G/d ratio of 0.71. Thus, vegetation significantly contributes to scour reduction on the bridge pier. Hence, sacrificial piles with a denser arrangement are recommended for scour reduction at pier facing high river flow.

Keywords- Scouring, pier, vegetation cylinders, clear water condition, scour countermeasure.

1 Introduction

Bridge structures play a vital role in facilitating transportation networks, connecting communities, and fostering economic development. However, bridges located in waterways are susceptible to a critical issue known as bridge pier scour, which poses a significant threat to their integrity and safety. Scouring occurs when the flow of water around bridge piers erodes the bed material, potentially leading to the undermining of the bridge foundation and compromising its structural stability. As climate change and extreme weather events intensify, the risk of bridge pier scour becomes even more pronounced, necessitating innovative and sustainable solutions to address this challenge. (Kho et al., 1997)

Various countermeasures have been proposed and implemented to mitigate bridge pier scour, ranging from traditional hard engineering structures to more environmentally friendly and ecologically sensitive approaches. Among these alternative methods, the use of vegetation elements as scour-mitigating measures has gained increasing attention in recent years.



Vegetation, with its natural adaptability and root systems, can potentially provide a sustainable and environmentally beneficial solution to reduce the scouring effects around bridge piers (Breusers et al., 1977). This research aims to investigate the effectiveness of different vegetation elements as countermeasures for bridge pier scour reduction. The study involves a comprehensive examination of various vegetation types, including live plants, woody debris, and synthetic materials, to assess their potential in stabilizing the riverbed and impeding the erosive flow of water around bridge piers. By strategically deploying vegetation in experimental flume setups that simulate real-world hydraulic conditions, the performance of each vegetation element will be evaluated through systematic measurements of scour parameters (Khosronejad et al., 2012). The successful implementation of vegetation-based countermeasures offers multiple benefits beyond scour reduction. Vegetation elements can enhance ecological habitats, foster biodiversity, and improve water quality by filtering pollutants. Moreover, they are generally more cost-effective and sustainable compared to conventional hard engineering structures, which often involve significant maintenance and environmental trade-offs (DATYE & RAO, 1974).

This investigation will contribute valuable insights into the viability of vegetation-based countermeasures for bridge pier scour reduction. By understanding the hydrodynamic and ecological interactions of different vegetation elements, engineers, and policymakers can develop practical guidelines and design strategies for incorporating vegetation-based solutions into bridge construction and maintenance practices. Ultimately, this research endeavors to promote the resilience and longevity of bridge infrastructure while preserving and enhancing the natural environment in waterway settings. In summary, this investigation on bridge pier scour reduction using various vegetation elements as countermeasures holds the potential to revolutionize traditional scour mitigation practices. By exploring the advantages of vegetation-based solutions, it seeks to offer a more sustainable, cost-effective, and environmentally sensitive approach to safeguarding bridge infrastructure in waterways. Ultimately, the outcomes of this research can contribute to the development of resilient and ecologically responsible bridge design guidelines, fostering a harmonious coexistence between human-made structures and the natural environment. (Eni, 1967). The study conducts a comprehensive examination and comparison of effectiveness of two types of rigid vegetation, wooden and steel cylinders, in experimental flume setups. By testing and comparing different types of vegetation, the research contributes to a deeper understanding of how vegetation characteristics influence scour reduction.

2 Experimental Procedures

Experiments were conducted in the hydraulic laboratory of the Civil Engineering Department at the University of Engineering and Technology (UET), Taxila. All experiments were conducted in a rectangular channel with 20 meters long, 1 meter wide, and 0.75 meters deep (Fig. 1). Transparent glass and a concrete base served as the channel's side walls and bed, respectively. Sand material was used to prepare the channel bed up to a depth of 0.30 meters, having size of $d_{50} = 0.88$ mm and relative density $G=2.56$. To prevent an unchanging water level in the test portion, the sand bed needs to be properly levelled. An adjustable tailgate was put at the downstream most point of the channel to manage the water level, and a flow control valve was fixed at the channel upstream to control discharge.



Figure 1: Vegetation cylinders conditions, a. steel cylinder protection, and b. wooden cylinder protection

2.1 Vegetation Cylinders Condition

In present study, wooden vegetation cylinders with an average diameter of 7mm and steel cylinders with an average diameter of 3mm are used. The G/d arrangement of the vegetation cylinders, where G denotes the distance between each cylinder in the cross-stream direction and d denotes the diameter of a cylinder. The G/d ratio indicates the density or sparsity of vegetation. Paper ID. 23-407



cylinders. for dense arrangement its value is 0.25 and for sparse arrangement its value is 2.13. The experiment was performed with three G/D conditions (2.85,1.42,0.71) and three aspect ratios (cylinders width-length ratio)(18.5,10.6,7.46). Wx and Wy represents vegetation cylinders arrangement length and width respectively.

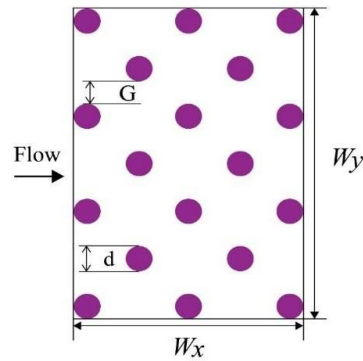


Figure 2: Vegetation cylinder conditions

3 Research Methodology

All experiments were conducted at two different discharges i.e 0.023 m³/s and 0.027 m³/s having Froude Number 0.136 and 0.187 respectively. The flow discharge was determined with a Trapezoidal weir at the end of the channel placed after the tailgate (Reca et al. 2006). Flow depth of 14cm was used in all lab experiments. All tests were carried out in clear water conditions at a threshold flow intensity (U/Uc) of less than 0.92, where U is the approach velocity of flow. The logarithmic format of the velocity profile was used to compute the critical velocity (Lauchlan and Melville 2001).

4 Results and Discussions

Initially the circular was tested without any protection. It was found that sediments creeping motion to downward flow started in the scour hole at the upstream tip of the pier. The effects of vegetation cylinders arrangement and their positions from the circular bridge pier on the normalized maximum scour depth were studied. By performing several experiments, it was showed that aspect ratio of vegetation cylinders arrangement and their G/d ratios greatly affects the scour hole. As we reduce the aspect ratio of sacrificial piles arrangement scour hole reduces on upstream face of pier. Two flow conditions were examined in this research. Scouring increases as we enhance the flow so at higher discharges scour reduction efficiency of vegetation cylinders reduces. The maximum scour depth around bridge pier were 55,51mm. The comparison of Flow Depths and Efficiencies of circular pier for the different Froude Numbers (0.136,0.187) are shown in Fig .3 and Fig. 4.

Table 1 Experimental conditions using wooden cylinders

Case	Q(m ³ /s)	h(m)	v(m/s)	AR	G/d	T(hr)	Ds(mm)	E (%)
1	0.023	0.14	0.16	3	20.84286	0
2	0.023	0.14	0.16	18.5	2.85	3	16.88	19
3	0.023	0.14	0.16	18.5	1.42	3	16.0	23.2
4	0.023	0.14	0.16	18.5	0.71	3	14.2	31.5
5	0.023	0.14	0.16	10.6	2.85	3	15	27.8
6	0.023	0.14	0.16	10.6	1.42	3	13	37.5
7	0.023	0.14	0.16	10.6	0.71	3	10	51.9
8	0.023	0.14	0.16	7.46	2.85	3	11	47.1
9	0.023	0.14	0.16	7.46	1.42	3	7	66.3
10	0.023	0.14	0.16	7.46	0.71	3	6	71.7



Table 2 Experimental conditions using steel vegetation protection

Case	Q(m^3/s)	h(m)	v(m/s)	AR	G/d	T(hr)	Ds(mm)	E (%)
11	0.023	0.14	0.16	18.5	2.85	3	17.80	14.4
12	0.023	0.14	0.16	18.5	1.42	3	16.6	20.1
13	0.023	0.14	0.16	18.5	0.71	3	14.7	30.2
14	0.023	0.14	0.16	10.6	2.85	3	15	27.8
15	0.023	0.14	0.16	10.6	1.42	3	14	32.7
16	0.023	0.14	0.16	10.6	0.71	3	11	47.1
17	0.023	0.14	0.16	7.46	2.85	3	12	61.5
18	0.023	0.14	0.16	7.46	1.42	3	8	42.3
19	0.023	0.14	0.16	7.46	0.71	3	9	66.3

The maximum scour depth (Ds) around circular bridge pier were 20.84mm and 22.91mm, respectively against Froude number 0.136 and 0.187 as shown in figure 3: a and b.

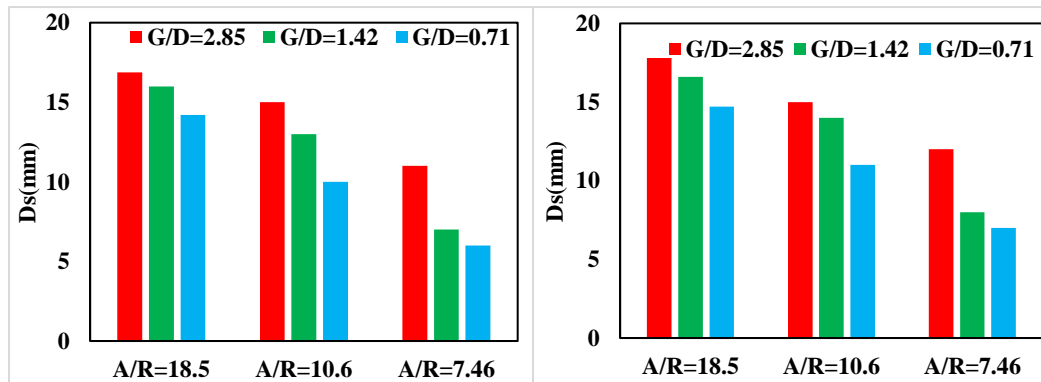


Figure 3: scour depth comparison at different aspect ratios and different G/d ratios, a. using wooden cylinders, and b. using steel cylinders

The maximum scour reduction for bridge pier with wooden vegetation arranged with aspect ratio of 7.46 and G/d ratio of 0.71 is 71.7% as shown in figure 4: a

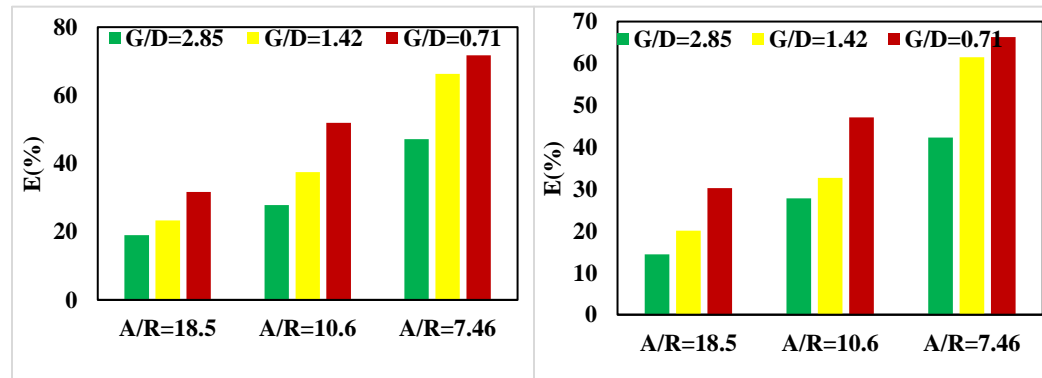


Figure 4: Scour reduction efficiency comparison at different aspect ratios and different G/d ratios, a.using wooden cylinders, b. using steel cylinders



5 Conclusions

Following conclusions can be drawn from the conducted study:

1. The Scouring depth around the bridge pier increases by increasing Froude Number in clear water condition. At Froude number 0.136 scour depth is 20.84 while at Froude number 0.187 its value is 22.91.
2. The scour depth of bridge pier is decreased by providing vegetation. At Froude number 0.136 without vegetation scour depth value is 20.84mm but it is reduced to 16.88mm by providing vegetation protection. Same is the case at Froude number 0.187, 22.91 without vegetation and 18.55 with vegetation protection.
3. The maximum scour depth reduction for bridge pier with wooden vegetation arranged with aspect ratio of 7.46 and G/d ratio of 0.71 is 71.7 %.
4. Vegetation with lower G/d ratio (denser arrangement) greatly reduces scour around bridge pier. At 2.85 G/d ratio scour depth is 16.88mm and 14.0mm at G/d ratio 0.71.
5. By performing several experiments, it was found that wooden cylinder vegetation has greater scour reduction than steel cylinders due to greater roughness coefficient.

6 Limitations of the Study

- The experiments are conducted in a controlled laboratory flume setup. While laboratory experiments provide valuable insights into the behavior of different vegetation elements, the results may not fully represent the complexities and variations present in real-world field conditions, especially in a river or stream with natural sediment transport and flow dynamics.
- The scouring process in natural rivers often involves a mixture of sediment sizes. In my research, the bed material used in the flume setup might have been of uniform size, which could influence the scouring process differently than heterogeneous sediment found in real-world rivers.
- My research focused on a single pier setup, and the effectiveness of the vegetation elements for multiple piers or bridge structures in different geometric arrangements remains unexplored. Real-world bridges often have multiple piers, and the interaction between vegetation and multiple piers could differ from the single pier case.

Acknowledgment

I want to thank my advisor Professor Dr. Naeem Ejaz for his wise counsel, suggestions, and remarks. I also want to thank the UET Taxila department of civil engineering for providing me with the research space I required to complete my study.

References

- [1] Breusers, H. N. C., Nicollet, G., & Shen, H. W. (1977). Erosion locale autour des piles cylindriques. *Journal of Hydraulic Research*, 15(3), 211–252. <https://doi.org/10.1080/00221687709499645>
- [2] DATYE, K. R., & RAO, N. S. V. (1974). *Scour Around Bridge Piers*. (DECEMBER 27-28, 1974), 37–41.
- [3] Eni. (1967). *Angewandte Chemie International Edition*, 6(11), 951–952., Mi, 5–24.
- [4] Kho, K. A. I. T. Z. E., Valentine, E., & Glendinning, S. (1997). an Experimental Study of Local Scour Around Circular Bridge Piers in Cohesive Soils. *Civil Engineering*, 1–8.
- [5] Khosronejad, A., Kang, S., & Sotiropoulos, F. (2012). Experimental and computational investigation of local scour around bridge piers. *Advances in Water Resources*, 37, 73–85. <https://doi.org/10.1016/j.advwatres.2011.09.013>
- [6] Lind, L., Nilsson, C., Polvi, L. E., & Weber, C. (2014). The role of ice dynamics in shaping vegetation in flowing waters. *Biological Reviews*, 89(4), 791-804.
- [7] Nabaei, S. F., Afzalimehr, H., Sui, J., Kumar, B., & Nabaei, S. H. (2021). Investigation of the effect of vegetation on flow structures and turbulence anisotropy around semi-elliptical abutment. *Water*, 13(21), 3108.
- [8] Miyab, N. M., Fazloula, R., Heidarpour, M., Kavian, A., & Rodrigo-Comino, J. (2022). Experimental Design of Nature-Based-Solution Considering the Interactions between Submerged Vegetation and Pile Group on the Structure of the River Flow on Sand Beds. *Water*, 14(15), 2382.



EXPERIMENTAL INVESTIGATION OF SQUARE-SHAPED SACRIFICIAL PILES ON SCOUR DEPTH OF COMPOUND BRIDGE PIER

^a Muhammad Nawaz Sharif*, ^b Usman Ghani, ^c Ghufran Ahamed Pasha

a: Department of Civil Engineering, UET, Taxila, Pakistan, muhammadnawazharif29@gmail.com

b: Department of Civil Engineering, UET, Taxila, Pakistan, usman.ghani@uettaxila.edu.pk

c: Department of Civil Engineering, UET, Taxila, Pakistan, ghufran.ahmed@uettaxila.edu.pk

* Corresponding author: Email ID: muhammadnawazharif29@gmail.com

Abstract- A non-uniform pier, also known as a compound A pier, is characterized by varying cross-sectional dimensions along its length. Depending on the exposure of their foundation to the flow field, the behavior of many bridge structures is non-uniform. There are numerous causes for the bridge's failure, including design flaws and construction errors. In contrast, scouring is the most hazardous reason. The primary objective of this experimental research is to reduce the scour depth around a compound bridge pier by using a square-shaped sacrificial pile as its countermeasure in clear water scour conditions. A constant flow rate of 30 l/s. was maintained throughout the experiment, and each trial was run for about 3 hours. Scour depth was measured using a point gauge as the measurement tool. Three experimental sets were carried out by using two, four, and six sacrificial piles on the front side of the pier in different locations for each case. The results show that by using sacrificial piles, scour depth was reduced significantly. With an increase in the number of piles and varying distances from the pier, the reduction in scour depth became increasingly noticeable. Case C-4 exhibited the most significant percentage reduction in scour depth among all the cases studied, which was 47.6%. In this case, six sacrificial piles were installed u/s of the pier at a distance equal to between 5.5.67 and 6.33 times the diameter of the pier ($D_p = 76.2$ mm).

Keywords- Compound bridge pier, Countermeasures, Sacrificial piles, and Scour depth

1 Introduction

For scientists and professionals working in the domain of hydraulic structures, understanding pier scouring around bridge piers holds great significance. Scouring is the result of a complicated vortex system. This system of vortices includes a wake vortex, a horseshoe vortex, a trailing vortex, and a bow wave vortex [1]. More than 1000 bridges have failed in the United States, with 60% of these failures attributable to scour and only 2% attributable to earthquakes [2]. Fig. 1 depicts a fundamental local scour mechanism near a bridge pier. [3].

There are two kinds of local scour countermeasures around the bridge pier: Armoring and flow-altering devices [4]. Armoring devices consist of riprap, tetrapods, dolos, cable-tied blocks, etc. Flow-altering countermeasures consist of sacrificial piles, Iowa vanes, and pier-mounted flow detectors such as collars. This research aims to examine the impact of square sacrificial piles near the compound bridge pier.

Sacrificial piles serve as a protective measure upstream of the bridge pier, shielding it from local scour. These piles redirect the fast-flowing water, creating a wake area behind the pier. The effectiveness of this approach depends on factors such as the number and size of the piles in relation to the pier, the arrangement of the piles relative to one another and the bridge pier, and the projection of the piles (i.e., whether they are partially or completely submerged) [4]. Different authors have



used sacrificial piles in their research work for pier scour reduction for instance, [5], [6], [7]. The presence of sacrificial piles reduces scour depth by up to fifty percent as stated in these studies. By using collars around multi-vent bridge piers, current deflectors, and sacrificial piles on the upstream side of bridge piers Mohammed et al., 2015 [8] concluded that local scour depth around the piers can be reduced by more than 90% as compared to the unprotected bridge piers.

Manes et al. 2015 [9] suggested a new formula based on the phenomenological theory of turbulence and empirical observations for predicting scour depth. Farooq et.al 2021 [10] examines the scour around rectangular pier under clear water conditions by applying rectangular hooked collar as a scour countermeasure. The author concluded that the most effective dimensions for hooked collar which reduces scour depth to maximum extent are width of $1.5 W_p$ and side wall height of $0.3 W_p$ (W_p is the pier width). Farooq et.al 2023 [11] investigated the effect of hooked collar around a vertical pier with a lenticular cross-section. The experimental results revealed that the equilibrium scour depth decreased with the ratio of hooked collar to the pier width when W_c (width of collar) is 2 times of the pier width.

Temporal variation and maximum scour depth were significantly affected by variations in the foundation and pier geometry [12]. In addition, when the top surface of the bridge pier is maintained below the general riverbed level, maximum scour depth was reduced as compared to uniform piers. Environmental and climate change is an emerging and necessary research in every aspect of life for the future generation [13]. Nimbalkar et al., 2022 [14] developed a scour model for a compound bridge pier which is based on artificial intelligence (AI). Scouring is a time-dependent phenomenon. Over time, the scour depth will increase until it reaches equilibrium [15].

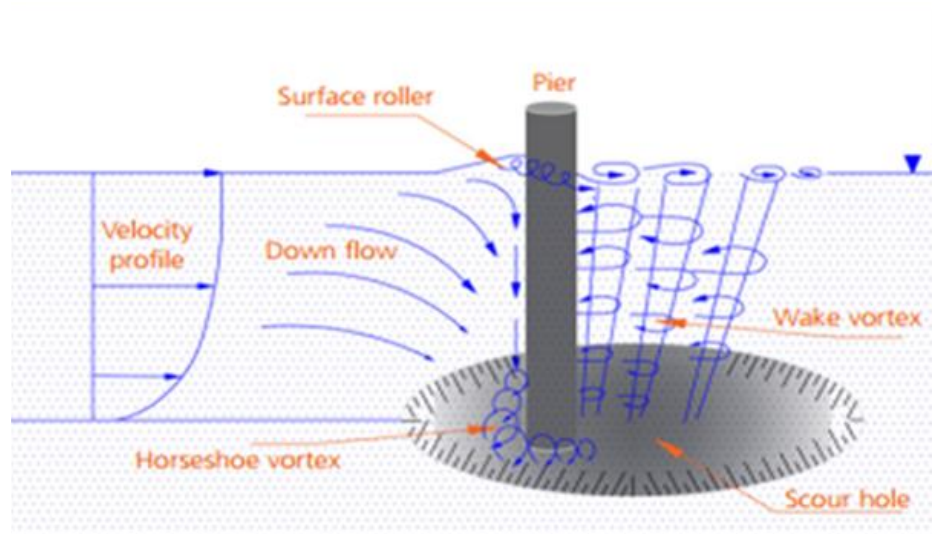


Figure 1: Local scour mechanism around a bridge pier [3].

Using an acoustic Doppler velocimeter, Kumar & Kothiyari, 2012 [16] conducted experiments on turbulence characteristics and flow patterns around circular and compound bridge piers. Melville & Raudkivi, 1996 [17] describe three scour zones for the compound bridge pier that is: In Zone 1, the foundation top lies below the scour hole's bottom, having no influence on the scour process. Zone 2 is characterized by the foundation top being inside the scour hole, leading to scour reduction. On the other hand, in Zone 3, the foundation top is above the bed level, causing increased scouring compared to a uniform pier. Moreover, scour depth is dependent on the geometry of the bridge pier and also on the size and shape of the pier's foundation diameter [18]. By investigating the effect of sacrificial piles in different configurations in front of circular bridge pier using FLOW-3D [19], the author concluded that the efficiency of sacrificial piles depends on their arrangement to be used as scour countermeasure, which influences the formation of horseshoe vortex and eventually the scouring around the pier.

From the previous studies, it can be seen that a sacrificial pile is an important technique to reduce scour around the bridge pier. Although, a lot of research has been done on uniform bridge piers combined with sacrificial piles. In the present study, a compound bridge pier with square-shaped sacrificial piles as its countermeasure was used at constant discharge under clear water conditions to investigate the impact of square sacrificial piles on scour reduction. For the design of



bridges, scour consideration is an important factor. Because failure of the bridge affects the transportation system and may cause loss of life and properties. So, it is necessary to use countermeasures such as sacrificial piles to reduce scouring and eventually protect the bridge.

2 Experimental Procedures

The experiments were conducted in a recirculating channel measuring 20 meters in length, 0.75 meters in depth, and 1 meter in width. The entire channel was made of concrete except for the walls which are made of 12 mm thick glass sheet. All the experiments were conducted in the UET Taxila Hydraulics Laboratory. In addition, the experimental work was conducted in conditions of clear water. For each test of the experimental program, the 10m length of the flume was leveled with sand using a wooden screed of equal width to the flume. Using a point gauge, the sand level was examined at random locations. The water channel was slowly filled until it reached the required depth. After turning on the pump and gradually increasing its speed until the required flow rate was reached, the tailboard was adjusted to achieve the desired water depth. After the test, the pump was turned off and the flume was slowly drained in order to preserve the scour topography. All the experiments were run for a duration of 3 hours. Because according to (Chiew and Melville) [20], After 10% of the equilibrium time, 80% of the equilibrium scour depth was achieved.

2.1 Sediment Bed

In this study, uniformly graded sand was used. The calculated geometric standard deviation was determined to be 1.21 for the sediment size $d_{50} = 0.613\text{mm}$; calculated as $\sigma_g = (d_{84}/d_{16})^{0.5}$ (d_{84} and d_{16} were the sediment sizes with a finer mass, at 84% and 16%, respectively). According to [21] if the standard deviation of soil is less than 1.3 then the sand will be classified as uniformly graded. The size of the sediment has no discernible effect on scour holes since D_p/d_{50} was > 50 ($D_p/d_{50} = 120.95$) [22]. The thickness of the sand bed was 0.203 m and was completely horizontal. The bed was properly leveled before the commencement of each trial.

2.2 Compound pier Models

The model of a compound circular pier was made up of wood. The footing top of the bridge pier model was put 25.4 mm below the general bed level, having footing diameter ($b^* = 152.4\text{ mm}$) and pier diameter ($b=76.2\text{ mm}$) such that the ratio of footing diameter to pier diameter is 2. A pictorial view of a compound circular pier has been shown in Fig. 2a. Fig. 2b illustrates the schematic diagram that represents the circular compound bridge pier, where b = the diameter of the pier, b^* = the diameter of the foundation or footing, Y = the depth of the top surface of the footing (foundation) below the channel's initial bed level and h = flow depth. The pier's average width was taken to less than one-sixth of the width of the flume to minimize the adverse effects of side walls as recommended by [23]. No changes in the bed level were observed along the contracted cross sections, suggesting the absence of any bed degradation, contraction scour appeared to be absent; this was consistent with the findings of [24]. Contraction scour is not significant when the ratio of the channel width to the pier diameter (B/D_p) equals or exceeds 10. As a result, it is safe to conclude that in the current investigation contraction effects were not present.

Table 1: Hydraulic conditions for the scour experiments.

Diameter of Pier (mm)	Diameter of foundation (mm)	Flow depth (mm)	Discharge (l/s)
76.2	152.4	127	30

2.3 Flow Conditions

To avoid incipient sediment movement at the plane sand bed with mean grain size ($d_{50} = 0.613\text{ mm}$), the flow discharge was selected to ensure that the bed shear stress remained below a critical threshold. The experiments were carried out under a constant flow discharge of $0.030\text{ m}^3/\text{sec}$. The Froude number $Fr = \frac{U}{\sqrt{gh}}$ was 0.213 where h represents the depth of flow above the sediment bed, g represents the gravitational constant and U represents the approach flow velocity. In order to ensure the condition of clear water scours, the flow intensity was consistently maintained at



approximately $U/U_c = 0.694$ in all the conducted tests. Here, U represents the velocity of the approach flow, and U_c signifies the critical velocity required for the sediment to start moving. The shields diagram was used to calculate the critical shear velocity U_{*c} for the sediments used in the current study.

In each experiment, to calculate critical velocity U_c the logarithmic average velocity equation for a rough bed was used [25].

$$\frac{U_c}{U * c} + \frac{c}{d} = 5.75 \log \left(\frac{df}{ke} \right) + 6$$

In the above equation, ' $k_e = 2d_{50}$ ', the term 'ke' represents the equivalent roughness height and d_f is the depth of flow. The clearwater condition prevails when the flow velocity U is smaller than the critical velocity U_c (i.e., $U < U_c$) and the live bed condition prevails when the flow velocity exceeds the critical flow velocity i.e. ($U > U_c$) [26].

2.4 Sacrificial Pile

A square sacrificial pile measuring 38.1 mm in dimensions was used in the study. To evaluate the efficiency of these piles, the scour depths around the pier were measured both with and without countermeasures. The reduction in scour depth under equilibrium conditions is then calculated by [27]. Table 2 and Fig. 3 depicts various arrangements of sacrificial piles.

$$R = \frac{Y_p - Y_s}{Y_p} 100 (\%) \quad (1)$$

In the absence of sacrificial piles, compound piers exhibit a maximum scour depth of Y_p , whereas compound piers with sacrificial piles show a maximum scour depth of Y_s and R is the %age reduction of scour depth. The scour depth around the compound pier was measured for each trial. The depth of scour was determined by measuring from the original sediment bed level to the maximum depth of erosion around the base of the pier.



Figure 2a: Photograph showing the model of compound circular bridge pier used in the current study



Figure 2b: Compound pier with levelled bed

Table 2: Arrangements of sacrificial piles in different cases

Case Number	Number of sacrificial piles	Distance from the pier
C-1	0	
C-2	2	5 times the pier diameter ($D_p = 76.2$ mm)
C-3	4	5 and 5.67 times the pier diameter
C-4	6	5, 5.67 and 6.33 times the pier diameter

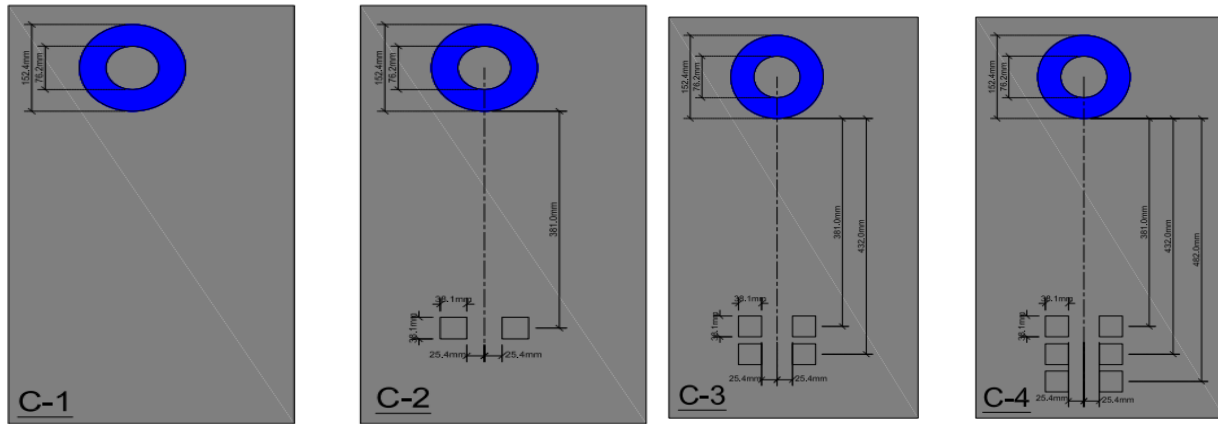


Figure 3: Various arrangements of sacrificial piles used in the lab.

3 Results

The findings revealed that the use of square-shaped sacrificial piles decreased the scour depth around the compound pier in comparison to the case without any piles. In addition, as the number of sacrifice piles increased, the depth of the scour decreased. Fig. 4 depicts the graph between maximum scour depth (mm) and no. of sacrificial piles on the u/s of the bridge pier. For case C- 2, when 2 sacrificial piles were used, scour depth reduction was observed to a minimum extent compared to the case without any piles. For C-3 when 4 sacrificial piles were used, the reduction in scour depth was more pronounced compared to C-1. The additional piles and slightly increased spacing allowed for more effective dissipation of flow energy, resulting in greater scour mitigation. Six sacrifice piles were installed upstream of the compound bridge pier for C-4, this configuration exhibited the most significant reduction in scour depth. The higher number of sacrificial piles, along with

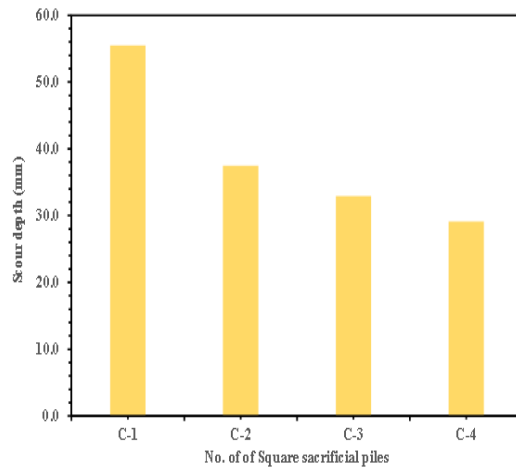
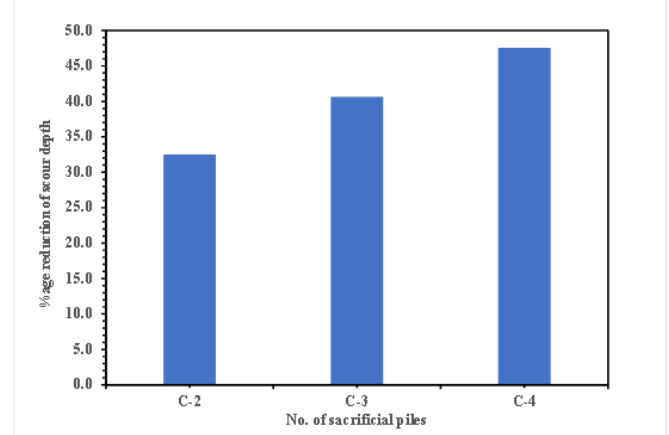


Figure 4: Scour depth Vs No. of square sacrificial piles.



the varying distances from the pier, created a more intricate

Figure 5: %age reduction of scour depth Vs No. of sacrificial piles.

flow pattern, leading to a substantial reduction in scour. The findings indicate that square-shaped sacrificial piles can effectively reduce the scour depth around a compound pier. This is due to the disruption of the flow pattern resulting from the presence of sacrificial piles, which results in a decrease in flow velocity and turbulence near the pier. Figure 5 depicts the relationship between the %age reduction of scour depth and the number of sacrificial piles. Under C-4, the maximum %age reduction in scour depth was observed, which was 47.6%. Six sacrifice piles were installed upstream of the pier in this instance at a distance equal to 5.567 & 6.33 times the pier diameter ($D_p = 76.2$ mm). Also, the minimum %age



reduction in scour depth was observed under C-2 (i.e., 32.5%). In this case, 2 sacrificial piles were installed at a distance equal to 5 times the pier diameter. The effectiveness of the scour countermeasure is influenced by the No. of sacrificial piles and their spacing distances from the pier. As more piles are used and they are placed at varying distances, a more complex flow field is created. This complex flow field dissipates energy more efficiently, leading to a greater reduction in scour depth.

3.1 Profiles of scour hole:

The longitudinal profiles of scour holes for cases C-2, C-3, & C-4 are shown in Fig. 6. From Fig. 6 it is clear that as the number of sacrificial piles increases, scour depth reduces on both the upstream and downstream side.

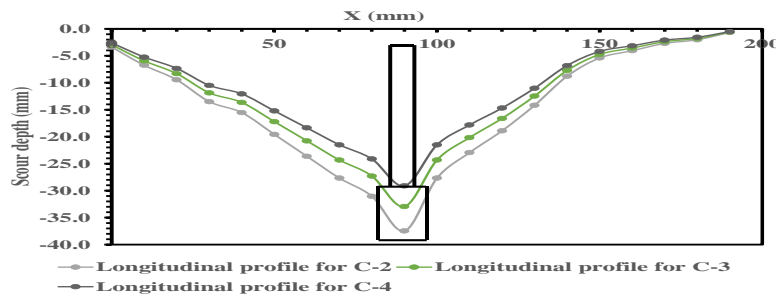


Figure 6: Longitudinal profiles of scour hole.

4 Conclusions

In this investigation, the impact of square-shaped sacrificial piles on reducing the scour depth around a compound bridge pier was evaluated.

- The maximum %age reduction of scour depth was observed under C-4 i.e., 47.6%. In this case, 6 sacrificial piles were installed upstream of the pier at a distance equal to 5,5.67 & 6.33 times the pier diameter ($D_p = 76.2$ mm).
- The minimum %age reduction of scour depth was observed under C-2 i.e., 32.5%. In this case, 2 sacrificial piles were installed upstream of the pier at a distance equal to 5 times the pier diameter ($D_p = 76.2$ mm).
- The use of sacrificial piles proved to be an efficient countermeasure against scour, and their effectiveness increased with the increasing number of piles and varying spacing distances.

5 Future Recommendations

The findings suggest that the implementation of sacrificial piles can be a viable and practical solution to alleviate scour-related issues around bridge piers and similar hydraulic structures. However, further research is needed to account for different flow conditions and pile configurations to develop more comprehensive design guidelines. Also, this study was performed on clear water scour conditions. The limitation of this research was that this study was conducted on clear water scour and not on live bed scour. In the future, the same work can also be performed for live bed scour conditions to check the efficiency of sacrificial piles on reduction of scour depth.

Acknowledgment

The authors would like to thank Prof. Dr. Usman Ghani who helped thorough out the research work, particularly Syed Ijaz Hussain Shah and the whole staff of the hydraulics lab CED.

References

- [1] C. H. Lee, C. Xu, and Z. Huang, "A three-phase flow simulation of local scour caused by a submerged wall jet with a water-air interface," *Adv Water Resour*, vol. 129, pp. 373–384, Jul. 2019, doi: 10.1016/J.ADVWATRES.2017.07.017.



5th Conference on Sustainability in Civil Engineering (CSCE'23)

Department of Civil Engineering

Capital University of Science and Technology, Islamabad Pakistan



- [2] Shirhole A.M. and R. C. Holt, “Planning for a Comprehensive Bridge Safety Program,” Transportation Research Record, Vol. 1290, pp.39-50, USA, 1991., 1991.
- [3] A. Keshavarzi, J. Ball, H. Khabbaz, C. K. Shrestha, and M. R. Zahedani, “Experimental study of flow structure around two in-line bridge piers,” Proceedings of the Institution of Civil Engineers: Water Management, vol. 171, no. 6, pp. 311–327, Dec. 2018, doi: 10.1680/jwama.16.00104.
- [4] B. W. Melville and A. C. Hadfield, “USE OF SACRIFICIAL PILES AS PIER SCOUR COUNTERMEASURES.”
- [5] F. F. Chang and M. KARIM, “AN EXPERIMENTAL STUDY OF REDUCING SCOUR AROUND BRIDGE PIERS USING PILES”.
- [6] “H.W. Shen, V.R. Schneider, S.S. Karaki, Mechanics... - Google Scholar.” https://scholar.google.com/scholar?hl=en&as_sdt=0%2C5&q=H.W.+Shen%2C+V.R.+Schneider%2C+S.S.+Karaki%2C+Mechanics+of+local+scour%2C+U.S.+Department+of+Commerce%2C+Nat.+Bureau+of+Standards%2C+Inst.+Appl.+Technol.%2C+1966&btnG= (accessed Apr. 20, 2023).
- [7] “K.K. Singh, D.V.S. Verma, N.K. Tiwari, 1995. Scour... - Google Scholar.” https://scholar.google.com/scholar?hl=en&as_sdt=0%2C5&q=K.K.+Singh%2C+D.V.S.+Verma%2C+N.K.+Tiwari%2C+1995.+Scour+protection+at+circular+bridge+piers%2C+in%3A+6th+International+Symp.+on+River+Sedimentation%2C+New+Delhi.&btnG= (accessed Apr. 20, 2023).
- [8] Y. A. Mohammed, Y. K. Saleh, and A. A. M. Ali, “Experimental investigation of local scour around multi-vents bridge piers,” Alexandria Engineering Journal, vol. 54, no. 2, pp. 197–203, Jun. 2015, doi: 10.1016/J.AEJ.2015.03.004.
- [9] C. Manes and M. Brocchini, “Local scour around structures and the phenomenology of turbulence,” J Fluid Mech, vol. 779, pp. 309–324, Aug. 2015, doi: 10.1017/jfm.2015.389.
- [10] R. Farooq, A. R. Ghuman, M. A. U. R. Tariq, A. Ahmed, A. Latif, and A. Masood, “Performance Evaluation of Scour Protection around a Bridge Pier through Experimental Approach,” Tehnički vjesnik, vol. 28, no. 6, pp. 1975–1982, Nov. 2021, doi: 10.17559/TV-20200213211932.
- [11] R. Farooq, A. H. Azimi, M. A. U. R. Tariq, and A. Ahmed, “Effects of hooked-collar on the local scour around a lenticular bridge pier,” International Journal of Sediment Research, vol. 38, no. 1, pp. 1–11, Feb. 2023, doi: 10.1016/J.IJSRC.2022.07.002.
- [12] A. Kumar, U. C. Kothiyari, and K. G. Ranga Raju, “Flow structure and scour around circular compound bridge piers - A review,” Journal of Hydro-Environment Research, vol. 6, no. 4, pp. 251–265, Dec. 2012, doi: 10.1016/j.jher.2012.05.006.
- [13] M. Qaisar, M. Yaqub, and M. N. Sharif, “An overview of study of Interfacial Transition zone of recycled aggregate concrete: A Review.”
- [14] P. Nimbalkar, P. Rathod, V. Manekar, and A. Bhalerao, “Scour model for circular compound bridge pier,” Water Supply, vol. 22, no. 5, pp. 5111–5125, May 2022, doi: 10.2166/ws.2022.125.
- [15] J. Guo, K. Kerenyi, H. Shan, Z. Xie, Y. Zhai, and L. Zhao, “Time-Dependent Scour Depth under Bridge-Submerged Flow,” pp. 105–114, Oct. 2010, doi: 10.1061/41147(392)9.
- [16] A. Kumar and U. C. Kothiyari, “Three-Dimensional Flow Characteristics within the Scour Hole around Circular Uniform and Compound Piers,” Journal of Hydraulic Engineering, vol. 138, no. 5, pp. 420–429, May 2012, doi: 10.1061/(ASCE)HY.1943-7900.0000527.
- [17] B. W. Melville and A. J. Raudkivi, “Effects of Foundation Geometry on Bridge Pier Scour,” Journal of Hydraulic Engineering, vol. 122, no. 4, pp. 203–209, Apr. 1996, doi: 10.1061/(ASCE)0733-9429(1996)122:4(203).



5th Conference on Sustainability in Civil Engineering (CSCE'23)

Department of Civil Engineering

Capital University of Science and Technology, Islamabad Pakistan



- [18] A. Sharwan and P. T. Nimbalkar, "Effects on scour for different foundation geometry of compound circular bridge piers," *International Journal of Recent Technology and Engineering*, vol. 8, no. 2, pp. 2439–2446, Jul. 2019, doi: 10.35940/ijrte.B2000.078219.
- [19] M. Nazari-Sharabian, A. Nazari-Sharabian, M. Karakouzian, and M. Karami, "Sacrificial piles as scour countermeasures in river bridges a numerical study using FLOW-3D," *Civil Engineering Journal (Iran)*, vol. 6, no. 6, pp. 1091–1103, Jun. 2020, doi: 10.28991/cej-2020-03091531.
- [20] Shriram and P. B. B. Lal, "Local scour around bridge piers," <http://dx.doi.org/10.1080/00221688709499285>, vol. 54, no. 1, pp. 36–45, Jan. 2010, doi: 10.1080/00221688709499285.
- [21] A. R. Zarrati, M. R. Chamani, A. Shafaie, and M. Latifi, "Scour countermeasures for cylindrical piers using riprap and combination of collar and riprap," *International Journal of Sediment Research*, vol. 25, no. 3, pp. 313–322, Sep. 2010, doi: 10.1016/S1001-6279(10)60048-0.
- [22] Y. M. Chiew and B. W. Melville, "Local scour around bridge piers," *Journal of Hydraulic Research*, vol. 25, no. 1, pp. 15–26, Jan. 1987, doi: 10.1080/00221688709499285.
- [23] L. E. , Frostick, S. J. , McLlland, and T. G. (Eds.) Mercer, "Users guide to physical modelling and experimentation: Experience of the HYDRALAB network. CRC press.," 2011.
- [24] F. Ballio, A. Teruzzi, and A. Radice, "Constriction Effects in Clear-Water Scour at Abutments," *Journal of Hydraulic Engineering*, vol. 135, no. 2, pp. 140–145, Feb. 2009, doi: 10.1061/(ASCE)0733-9429(2009)135:2(140).
- [25] C. S. Lauchlan and B. W. Melville, "Riprap Protection at Bridge Piers," *Journal of Hydraulic Engineering*, vol. 127, no. 5, pp. 412–418, May 2001, doi: 10.1061/(ASCE)0733-9429(2001)127:5(412).
- [26] B. W. , Melville and S. E. Coleman, "Bridge scour. Water Resources Publication.," 2000.
- [27] C. Wang, F. Liang, and X. Yu, "Experimental and numerical investigations on the performance of sacrificial piles in reducing local scour around pile groups," *Natural Hazards*, vol. 85, no. 3, pp. 1417–1435, Feb. 2017, doi: 10.1007/s11069-016-2634-0.



INVESTIGATING THE EFFECT OF SHEAR RATE IN THE SHEAR THINNING BEHAVIOUR OF WASTE PLASTIC-MODIFIED ASPHALT BINDER

^a Muhammad Ziad Bacha*, ^b Jawad Hussain, ^c Khalid Mehmood

a: Department of Civil Engineering, UET, Taxila, Pakistan, ziadbacha001@gmail.com

b: Department of Civil Engineering, UET, Taxila, Pakistan, jawad.hussain@uettaxila.edu.pk

c: Department of Civil Engineering, UET, Taxila, Pakistan, khalid.ce@must.edu.pk

Abstract- The major goal of this study was to determine how shear rate influences the shear-thinning properties of asphalt binder treated with waste plastic. The blending of asphalt and waste plastic was accomplished using a melting process. Asphalt binder is a non-Newtonian fluid that exhibits shear-thinning behavior, and the dependence of shear viscosity on shear rate is a key characteristic of its pseudo-plastic behavior. The addition of waste plastic as a modifier to asphalt binder at percentages of 16%, 18%, and 20% was found to increase the performance of the asphalt. The shear-thinning behavior of two types of bitumen grades, ARL 60/70, and ARL 80/100 was assessed through rotational viscometer testing. The experimental results demonstrated that shear rate and viscosity are inversely proportional, with an increase in the shear rate leading to a decrease in apparent viscosity. These findings indicated that waste plastic modification can impact the viscosity and shear-thinning behavior of asphalt binders.

Keywords- Brookfield Rotational Viscometer, Modified Asphalt, Shear thinning, Shear rate, Shear stress, Viscosity, Waste plastic.

1 Introduction

Asphalt binder is a crucial element in the construction of roads and highways, providing the required strength, stability, and durability to pavement [1]. However, asphalt binder's flow behaviour and viscosity undergo significant changes over time due to aging, oxidation, and weathering, which can negatively impact pavement performance[2]. To address this issue, researchers have investigated the utilization of waste plastic and waste cooking oil as a rejuvenator to improve asphalt binder's rheological properties, including stiffness and viscosity[3], [4]. According to Liu et al, [5], the flow behaviour of asphalt binder is influenced by several factors, including the shear rate. Shear rate is defined as the rate at which the material experiences shear stress or force. The relationship between shear rate and viscosity is critical for understanding the material's behaviour under different conditions.

Similar shear-thinning behavior has previously been reported in studies on waste plastic-modified asphalt binders. These studies have highlighted the influence of waste plastic content, polymer type, and processing conditions on the shear-thinning behavior. [6] The consistency of these findings across different studies further supports the understanding that waste plastic modification induces shear-thinning behavior in bitumen binders. The observed shear-thinning behavior and the associated decrease in viscosity have practical implications for asphalt applications. In road construction, for example, lower viscosity asphalt binders are desirable as they facilitate easier mixing, compaction, and coating of aggregates. [7] This characteristic can contribute to improved workability and overall performance of the asphalt mixtures. In this study, we evaluate the shear thinning behaviour of modified asphalt with waste plastic, focusing on the effect of shear rate. This study makes a novel contribution to the area by addressing a research gap on this specific topic. The relevance of this



research is that it has the potential to improve our understanding of the rheological properties of modified asphalt and provide useful insights for the development of sustainable and high-performance road-building materials.

2 Problem Statement and Objectives

With the overproduction of plastic waste, recycling it for building materials and road construction is a promising solution. However, achieving the optimal shear thinning range (viscosity in Pa. s) is crucial for effective waste plastic modification of asphalt. Failure to do so can lead to further damage of the asphalt's properties. Therefore, investigating the impact of waste plastic modification on the shear-thinning behavior of asphalt using the Brookfield rotational viscometer is essential to ensure its suitability for road construction.

The main objective of this study was to determine the impact of waste plastic modification on the shear thinning behaviour of asphalt under various shear rates. The other objectives of the research are:

- To study the effect of varying waste plastic percentages on absolute viscosity of asphalt binder; and
- To quantify the effect of shear stress and torque on the viscosity of different binders with different waste plastic percentages.

3 Materials and Methodology

3.1 Bitumen

Bitumen samples of ARL 60/70 and ARL 80/100 grades have been obtained from the MKA Asphalt facility in Islamabad, near the Margalla stop. It is advised that bitumen be stored at ambient temperatures in 5kg canisters. The bitumen samples were subjected to standard testing like penetration, ductility, and softening point. [Table 1](#) displays the assessment outcomes.

Table 1: Physical properties of Virgin bitumen

Properties		Standard code	Unit	ARL 60/70	Specification limit (minimum)
Penetration 0.1mm @ 25°C		ASTM D5	1/10 mm	61	60
Softening point (°C)		ASTM D36	°C	50	43
Ductility at 25°C		ASTM D36	Cm	103	100
Dynamic viscosity	ASTM D4402	Cp	343.5	300	

3.2 Waste Plastic

The use of waste plastic shown in [Figure 1\(a\)](#) and [\(b\)](#) in road construction has gained increasing attention as a sustainable solution for plastic waste management. Adding scrap plastic into bitumen mixtures as a partial replacement for bitumen can improve asphalt durability, including its resistance to rutting, cracking, and moisture damage. This approach can also help to reduce demand for virgin bitumen, a finite resource, and boost the long-term viability of road infrastructure. [\[8\]](#)

a) <https://www.google.com>

b) UET lab

Figure 1: a. waste plastic bottles, and b. Shredded Plastic for current study

4 Experimental work

Three samples were created for each waste plastic percentage (16%, 18%, and 20%) for all types of binders to evaluate the viability of waste plastic as a partial replacement for bitumen in the construction of roads. To guarantee appropriate mixing, the modified asphalt mixing temperature was kept between 180 and 200 °C. The waste plastic is added in shredded form, size ranges from 2.36mm to 4.75mm. Shredded waste plastic was added to the bitumen at the melting temperature of the appropriate bitumen grade, and the mixture was mechanically stirred to ensure uniform particle dispersal. The mixture was then tested with a rotational viscometer to see how it affected viscosity and shear thinning. Shredding at industrial level is done through shredding machines and then dried and heated at the shredded plastic in the drying chamber before mixing into asphalt biner.

4.1 Brookfield Rotary Viscosity Test

To measure the viscosity of asphalt modified with waste plastic, a Brookfield viscometer shown in [figure 2](#) was utilized following the ASTM D4402 standard. The experiment involved recording various parameters such as temperature, rotational speed, shear stress, shear rate, and viscosity, as outlined in [Table 2](#). The test aimed to evaluate the impact of waste plastic on the viscosity of asphalt, and the results could provide valuable insights into the feasibility of using waste plastic as a partial replacement for bitumen in road construction. Overall, the study provided a detailed methodology for assessing the rheological properties of bitumen modified with waste plastic.

Table 2: Test conditions for Brookfield rotary viscosity

Waste plastic (%)	Test temperature (°C)	Shear rate (1/s)
16%, 18%, 20%	135	1.7, 3.4, 6.8, 10.2, 13.6, 17, 20.4, 23.8, 27.2, 30.6, 34



Figure 2: Brookfield rotary viscometer



5 Results & Discussion

5.1 Discussion

Experimental work on asphalt grade 60/70 examined the impact of waste plastic modification on its behavior. The results revealed reduced viscosity and increased shear stress, indicating a thinning effect on the modified binder.[9] This behavior is attributed to the reorganization of the binder's internal structure, facilitating easier flow and lower resistance. Previous studies on waste plastic-modified asphalt binders have reported similar shear-thinning behavior, emphasizing the influence of plastic content, polymer type, and processing conditions. [10]. These consistent findings support the understanding that waste plastic modification induces shear-thinning behavior in bitumen binders. In conclusion, the experiments confirmed a clear relationship between viscosity and shear stress, demonstrating the shear-thinning behavior resulting from waste plastic modification of asphalt. The internal structure of asphalt plays a crucial role in determining its viscosity under different shear conditions. At low shear rates, the internal structure exhibits a higher resistance to deformation, leading to higher viscosity [11]. However, as the shear rate increases, the internal structure undergoes significant reorganization, promoting asphalt flow and deformation and resulting in a decrease in viscosity [12]. Understanding the shear rate-viscosity relationship and the underlying internal structure reorganization in asphalt has important implications for various applications. It allows for the optimization of asphalt mixtures, enabling the design of materials with specific flow characteristics that enhance workability and overall performance.[13] the findings presented in Figure 3 and supported by previous studies confirm the inverse connection between shear rate and viscosity in asphalt.

Figure 4 reveals a linear relationship between shear rate and shear stress for modified bitumen. The study investigated the influence of waste plastic content on shear stress at varying percentages. Notably, a significant increase in shear stress was observed at a waste plastic concentration of 20%. This implies that increasing waste plastic quantity in the binder notably affects shear stress. The observed relationship between shear rate and shear stress offers valuable insights into the rheological behavior of the modified bitumen binder, enabling the development of sustainable asphalt materials with enhanced structural and flow properties.

Figures 5 depicts the relationship between log shear rate and log viscosity for the modified binder, which shows an inverse relationship. As the log shear rate increases, the log viscosity values increase as well. This conclusion indicates that shear rate has a major impact on the shear-thinning behaviour of the asphalt binder. Higher shear rates result in lower viscosities, indicating a decrease in flow resistance. This finding emphasises the significance of shear rate in understanding the flow properties and behaviour of the modified binder, providing vital insights into its rheological features. In Figure 6, shear rate and torque display a consistent pattern: torque increases as shear rate rises. This suggests that higher rotation velocities correspond to greater shear rates unless significant shear-thinning behavior counteracts it. This relationship clarifies the rheological characteristics and informs the flow behavior of the binder under different shear conditions. Understanding this connection is crucial for developing enhanced and sustainable asphalt materials for road construction and maintenance, considering the influence of shear rate on torque.

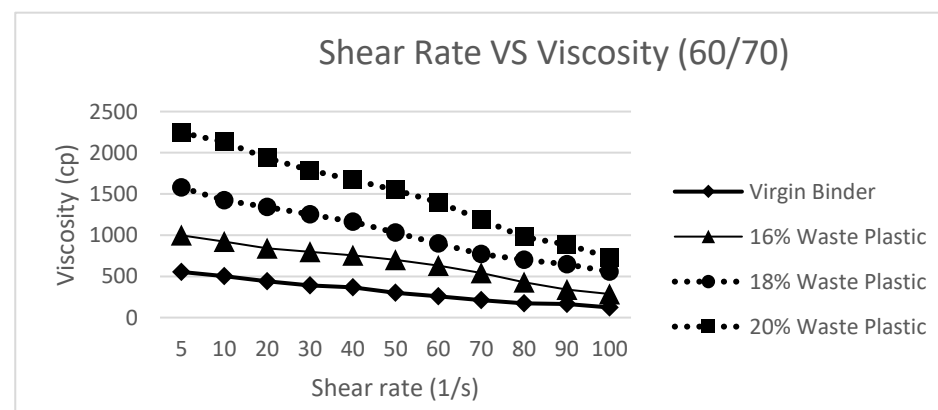


Figure 3 shear rate vs Viscosity of modified 60/70 bitumen binder.

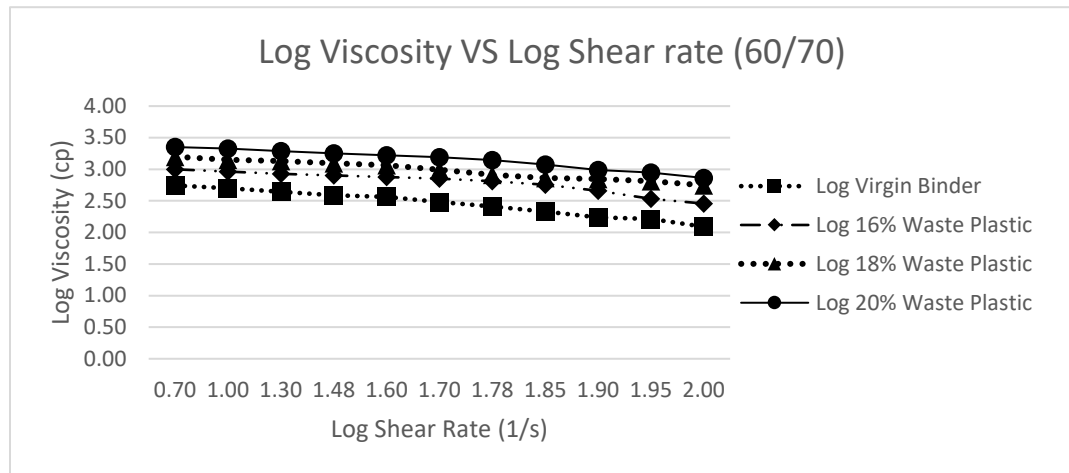


Figure 4: Shear rate vs Shear stress of modified 60/70 bitumen binder

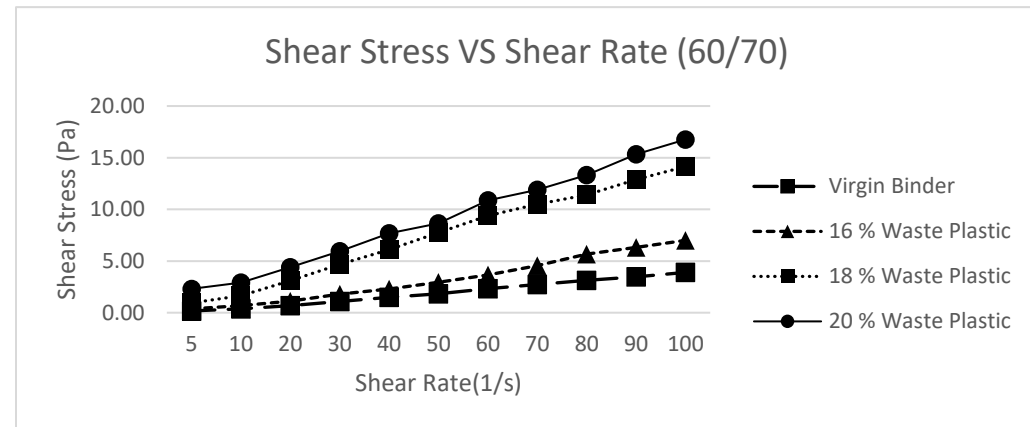


Figure 5: log Shear rate vs log viscosity of modified 60/70 bitumen binder

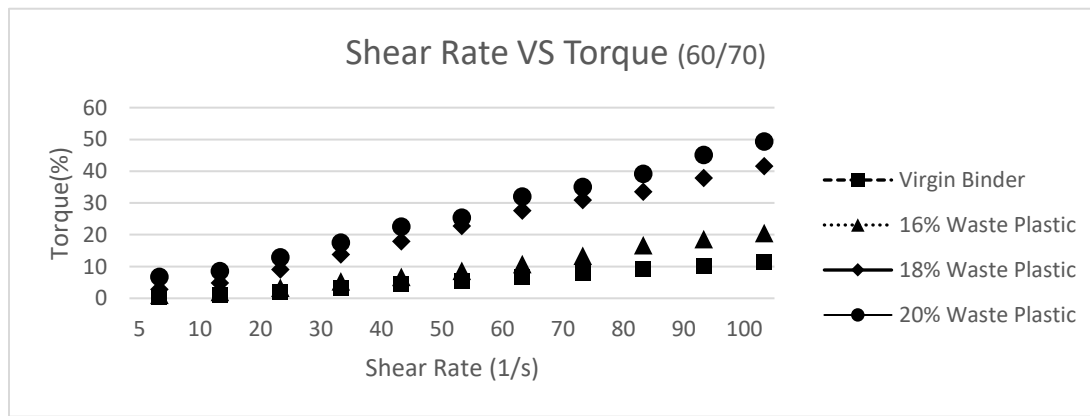


Figure 6: Shear rate vs Torque of modified 60/70 bitumen binder



5.2 Practical Implementation

The experimental work provided in the presented paper on waste plastic-modified bitumen has practical implications for asphalt binder and road building.[14] The research shows that incorporating waste plastic into bitumen reduces viscosity and increases shear stress, resulting in improved flow and workability during construction processes.[15] The research contributes to attempts to reduce environmental impact by diverting garbage from landfills and supporting the sustainable economy concept. The research findings have practical implications for facilitating the development of industry standards and guidelines for using waste plastic in asphalt binders.[16] To summarise, the research on waste plastic-modified bitumen has practical implications for improved workability, improved structural performance, customization, sustainability, and the development of industry standards in asphalt binder and road construction practises.

6 Conclusions

This study evaluated the properties of asphalt binder ARL 60/70 using a rotational viscometer, with a focus on apparent viscosity and shear-thinning behaviour. The outcomes indicated that:

1. When waste plastic was added to bitumen binders, it increased viscosity, especially at 20% concentration. On the other hand, a lowered amount of 16% approximately matched the viscosity of virgin bitumen, making it the best choice for a partial replacement.
2. However, the viscosity of all percentages i.e., 20%, 18% and 16% waste plastic-modified bitumen binders decreased as the shear rate increased. This behavior is characteristic of non-Newtonian fluids, demonstrating shear-thinning properties.
3. Increasing the shear rate resulted in higher shear stress i.e., from 0.37 to 7.0 for 16% waste plastic and for 18% waste plastic the value goes from 0.95 to 14.4, while for 20% the values range from 2.31 to 16.76.
4. The torque values also increase with the increase of shear rate for waste plastic-modified asphalt binders i.e., for 16%, the value of torque goes from 1.1 to 20.6 and for 18%, torque values are 2.8 to 41.6, while for 20% its values range from 6.8 to 49.3.

Previous and contemporary research has demonstrated that waste plastic can cause shear-thinning in asphalt binders at medium and elevated temperatures. However, its usefulness in low-temperature environments is unknown. As a result, studying the influence of waste plastic on bitumen binder rheology at minimal temperatures would provide useful insights for its usage in cold climates.

Acknowledgments

The author expresses gratitude to the Department of Civil Engineering for their invaluable support and cooperation throughout the research activity. Additionally, the author extends appreciation to the University of Engineering and Technology for funding this project, which allowed for the study to be conducted and the findings to be disseminated. The contributions of these entities were integral to the success of the research endeavour.

References

- [1] J. Chen *et al.*, ‘New innovations in pavement materials and engineering: A review on pavement engineering research 2021’, *Journal of Traffic and Transportation Engineering (English Edition)*, vol. 8, no. 6, pp. 815–999, Dec. 2021, doi: 10.1016/J.JTTE.2021.10.001.
- [2] W. Zhang, Q. Li, J. Wang, Y. Meng, and Z. Zhou, ‘Aging Behavior of High-Viscosity Modified Asphalt Binder Based on Infrared Spectrum Test’, *Materials* 2022, Vol. 15, Page 2778, vol. 15, no. 8, p. 2778, Apr. 2022, doi: 10.3390/MA15082778.
- [3] M. I. Eldeek, F. M. Jakarni, R. Muniandy, and S. Hassim, ‘Utilization of Waste Cooking Oil as a Sustainable Product to Improve the Physical and Rheological Properties of Asphalt Binder: A Review’, *Lecture Notes in Civil Engineering*, vol. 193, pp. 883–901, 2022, doi: 10.1007/978-3-030-87379-0_66/COVER.



5th Conference on Sustainability in Civil Engineering (CSCE'23)

Department of Civil Engineering

Capital University of Science and Technology, Islamabad Pakistan



- [4] O. Ukwuoma and B. Ademodi, ‘The effects of temperature and shear rate on the apparent viscosity of Nigerian oil sand bitumen’, *Fuel Processing Technology*, vol. 60, no. 2, pp. 95–101, 1999, Accessed: May 25, 2023. [Online]. Available: <https://www.academia.edu/4961537/>
The_effects_of_temperature_and_shear_rate_on_the_apparent_viscosity_of_Nigerian_oil_sand_bitumen
- [5] Liu, Hanqi, Zeiada, Waleed Al-Khateeb, Ghazi G. Shanableh, Abdallah, Samarai, Mufid, “Characterization of the shear-thinning behavior of asphalt binders with consideration of yield stress”, *Materials and Structures/Materiaux et Constructions*. 2020, Vol. 53, Issue 4, doi: 10.1617/S11527-020-01538-0, ISSN 13595997.
- [6] S. F. Kabir, R. Zheng, A. G. Delgado, and E. H. Fini, ‘Use of microbially desulfurized rubber to produce sustainable rubberized bitumen’, *Resour Conserv Recycl*, vol. 164, Jan. 2021, doi: 10.1016/j.resconrec.2020.105144.
- [7] Lingyun You, Zhengwu Long, Zhanping You, Dongdong Ge, Xu Yang, Fu Xu, Mohammad Hashemi, Aboelkasim Diab, ‘Review of recycling waste plastics in asphalt paving materials’, *Journal of Traffic and Transportation Engineering (English Edition)*, Volume 9, Issue 5, 2022, Pages 742-764, ISSN 2095-7564, <https://doi.org/10.1016/j.jtte.2022.07.002>
- [8] H. Liu, W. Zeiada, G. G. Al-Khateeb, A. Shanableh, and M. Samarai, ‘Characterization of the shear-thinning behavior of asphalt binders with consideration of yield stress’, *Materials and Structures/Materiaux et Constructions*, vol. 53, no. 4, pp. 1–13, Aug. 2020, doi: 10.1617/S11527-020-01538-0/METRICS.
- [9] M. Jasso, G. Polacco, and L. Zanzotto, ‘Shear Viscosity Overshoots in Polymer Modified Asphalts’, *Materials 2022, Vol. 15, Page 7551*, vol. 15, no. 21, p. 7551, Oct. 2022, doi: 10.3390/MA15217551.
- [10] Y. Li *et al.*, ‘Anti-rutting performance evaluation of modified asphalt binders: A review’, *Journal of Traffic and Transportation Engineering (English Edition)*, vol. 8, no. 3, pp. 339–355, Jun. 2021, doi: 10.1016/J.JTTE.2021.02.002.
- [11] M. A. Notani *et al.*, ‘Investigating the high-temperature performance and activation energy of carbon black-modified asphalt binder’, *SN Appl Sci*, vol. 2, no. 2, pp. 1–12, Feb. 2020, doi: 10.1007/S42452-020-2102-Z/FIGURES/11.
- [12] R. S. Souza, L. L. Y. Visconte, A. L. N. Da Silva, and V. G. Costa, ‘Thermal and Rheological Formulation and Evaluation of Synthetic Bitumen from Reprocessed Polypropylene and Oil’, *Int J Polym Sci*, vol. 2018, 2018, doi: 10.1155/2018/7940857.
- [13] F. S. Bhat and M. S. Mir, ‘Investigating the effects of nano Al₂O₃ on high and intermediate temperature performance properties of asphalt binder’, <https://doi.org/10.1080/14680629.2020.1778509>, vol. 22, no. 11, pp. 2604–2625, 2020, doi: 10.1080/14680629.2020.1778509.
- [14] L. A. Carrasco-Venegas, J. V. González-Fernández, L. G. Castañeda-Pérez, G. Palomino-Hernández, F. A. Dueñas-Dávila, and S. A. Trujillo-Pérez, ‘Viscosity Factor (VF) Complementary to the Statistical Indicators Associated with the Rheological Behavior of Aqueous Solutions of Polyvinyl Alcohol’, *Polymers 2023, Vol. 15, Page 1743*, vol. 15, no. 7, p. 1743, Mar. 2023, doi: 10.3390/POLYM15071743.
- [15] T. Li *et al.*, ‘Effect of fly ash on the rheological properties of potassium magnesium phosphate cement paste’, *Case Studies in Construction Materials*, vol. 17, p. e01650, Dec. 2022, doi: 10.1016/J.CSCM.2022.E01650.
- [16] Lee, Jong Sub, Sang Yum Lee, Yoon Shin Bae, and Tri Ho Minh Le. 2023. “Development of Pavement Material Using Crumb Rubber Modifier and Graphite Nanoplatelet for Pellet Asphalt Production.” *Polymers* 2023, Vol. 15, Page 727 (3): 727. <https://doi.org/10.3390/POLYM15030727>



CONSTRUCTION, CONFLICT, CLAIM, AND COMPENSATION (4C) CASE STUDY – FAIZABAD HIGHWAY INTERCHANGE PROJECT ISLAMABAD, PAKISTAN

^a *Erum Aamir**, ^b *Ismail Ghori*, ^b *Maria Aamir*,

a: Institute of Environmental Science & Engineering, NUST, H/12 Campus, Islamabad, 44000, Pakistan, erum@iese.nust.edu.pk

b: NICE, SCEE, NUST, H/12 Campus, Islamabad, 44000, Pakistan, Ismail@nice.nust.edu.pk

c: NICE, SCEE, NUST, H/12 Campus, Islamabad, 44000, Pakistan, marai2003@gmail.com

* Corresponding author: Email ID: erum@iese.nust.edu.pk

Abstract- Each individual case of construction industry dispute between the contractor and the employer is unique in its nature, but the dilemma of delays, additional costs, and claims for compensation by the contractor and disputes between the parties have been persistently perpetual, leading to further numerous, administrative, financial, contractual, technical, and contractual issues. The common factors may be aggregated under three (3) groups, namely, group-a: faulty contract documents; group-b: contractor's deficiency and failure; and group-c: beyond the control of parties (force majeure, employer's risk). reasons/common factors under group-a are attributable to the employer/client and can be mitigated at the onset of projects, the author takes the opportunity to address them briefly through the case study of one of the projects, highlighting the salient features, in a humble attempt if it could be more wisely handled by the stakeholders and beneficiaries of the construction project. A construction project of Faizabad Interchange between Islamabad and Rawalpindi has been taken up as a case study to highlight the construction industry disputes and challenges both for the contractor, client, and consultant resulting in delay, and heavy financial compensation.

Keywords- Arbitration, construction management, compensation disputes, delay, technical and contractual issues.

1. Introduction

Project Management in civil engineering projects in general and in the construction, industry has been a perpetual matter of concern for the stakeholders of the project because as defined in research and books project management is the application of information, knowledge, skills, tools, and techniques project activities to fulfill the project requirements [1-3]. However, the nature of projects is always dynamic, uncertain, unique features, elements, constraints and are different from each other [4-6].

Construction management is as plenty a count of overcoming problems as it is far from attaining effects. Such kinds of troubles include certain kinds of risks that could happen and not be foreseen by any judgmental person. The risks resulting from projects being at risk of a ramification of factors that cause value escalation and schedule overruns that have an effect on their completion. Because any risk can end up a reality, one party to a contract should go through financial and/or time losses for which they may demand remedies [7-8]. The need for remedies is what constitutes claims [9].

A claim is described as a demand for something to which a party contends, wrongly or rightly being entitled but according to which contract has not been finalized [10-11]. Researchers believe in the construction industry that states are a major source of conflict [8,11]. They are able to divert substantial methods from ongoing construction actions, yet there is an overall lack of knowledge about what states are, how they occur, and how to deal with them successfully, expeditiously, and reasonably. Because of situations and variations over claims, the construction industry is affected by an adversarial environment between contractors and clients [12]. A fruitful construction task is one that is accomplished on time, within budget, to given quality, and achieved with minimum disruption to the parties' regular operations [13-14]. To accomplish



this, allocate rights and contracts prescribed, liabilities, and duties to contracting parties in certain situations withstood during the process of construction. Disappointment in executing the allocated responsibilities can increase the likelihood of states and disputes arising [15]. It is the knowledge sufficiency and the method of harnessing the abilities of the construction group that eventually plays a role in the achievement or failure of a task [16]. To reduce claims and their rejection, parties must know the particular for declaring under each contract [17]. The fantastic principle is to review each agreement and explore evidence that the claimant should supply their claim and the procedures for completion [18]. Understanding work facets giving rise to claims is truly a skill that is to be specially acquired [19-20].

Information about the agreement terms and record keeping are fundamental for laying out authentic and genuine legitimization of guaranteed entries. Parties lawfully will undoubtedly get what they go into, and it would not be a decent guard, in the event of a case, to say they did not figure out the details of the agreement [21]. Contracting parties ought to know precisely what is required from them under an agreement prior to marking it [22]. They need to continue to review their obligations under agreements and be aware of activities that change their commitments [23]. To make a successful claim, keeping records is fundamental [24]. Regular reasons for claims include the collected effect of a progression of changes, every one of which might seem minor, yet in total affects the advancement of the works. Frequently, these impact effects are hard to decide until after a time span has passed. To capture the outcomes of a chain of occasions, great record-keeping is required [19, 20, 22].

The construction industry is the mother of all industries. The economy of a country like Pakistan is significantly dependent on construction. Nevertheless, the nature of projects is always dynamic, the construction industry involves disputes resulting from changes, variations, alterations, addition, deletion, delays, suspension, differing site conditions (unforeseen conditions), unjust enrichment by owners, etc. The main objective of this paper is to list down common factors and reasons that give rise to disputes which cause delays in the completion of the project so that may be avoided during construction. But because of the dynamic of the construction project, it is very intractable to list down all the factors preceding disputes however, some common factors and reasons that give rise to disputes may be aggregated into three groups, as elaborated below to achieve the goal of the study:

I) **Group-A Faulty Contract Documents**

- i) Faulty, ambiguous, incomplete, and unbalanced contract documents prepared in a hurry by inexperienced authors.
- ii) incomplete design/drawings and specifications.
- iii) Anomaly among drawings, items of bill of quantities, and specifications.
- iv) Delays in fulfilling the obligation of the employer/client with respect to giving possession of the site free from encumbrance, payment to the contractor, and administrative decisions.
- v) Removal and relocation of services and utilities belonging to other government or private agencies.
- vi) Subsequent significant changes in the scope of work and design/drawings.
- vii) Delays and indecision in processing the variation/change orders and rates for additional/extraneous items of work, by the consultant/project manager/the engineer.
- viii) Wrong selection of contractor on the basis of the lowest and unworkable bid price.

II) **Group-B Contractor's Deficiency and Failure**

- i) Contractor's in-house incapability with respect to project management and planning for execution of work.
- ii) Contractor's cash flow problems.
- iii) Over-commitment by contractors beyond capacity.
- iv) Lack of properly qualified and experienced personnel of contractor.
- v) Unbalanced rates.
- vi) Unpragmatic and misinterpretation of conditions of contract by an inexperienced person.

III) **Group-C Beyond The control of Parties (Force Majeure, Employer's Risk)**

These events beyond the control of parties such as:

- i) Commotion, riots, strikes, law and order situations
- ii) Unforeseeable physical condition and obstruction



- iii) Subsequent legal impediments by court orders
- iv) Exceptional adverse climatic conditions

2. Case Study – Highway Interchange Project

This is related to a roadway interchange. The construction contract period was 18 months, and the contract price was about Rs.80 million (US\$ 2 million) in the 1990s with a present-day valuation of approximately Rs. 650 million. The employer suffered from a financial loss of about more than 50% of the contract price by paying compensation against the claim.

The conditions of the contract were based on **FIDIC Fourth Edition 1987** reprinted subsequently with amendments.

I) Dispute and its Compensation

The employer/client desired that the project must be completed within the specified time period of 18 months. The whole burden for completion of work was put on the contractor and accordingly stringent and unbalanced conditions in the contract for the contractor for compliance but the employer/client lost foresight for the fulfillment of its own obligations under the contract.

The project area was infested with a large number of Services and Utilities such as gas lines, overhead power transmission lines, optic fiber lines, trees, shops, mosques, post offices, police kiosks and etc., belonging to various other government departments and private agencies.

Time was of the essence under the contract and the employer was under obligation for the removal and relocation of all the services and utilities.

Besides liquidated damages, additional punitive conditions were put in the condition for a penalty of Rs. 25,000 or US\$ 650 per day (present-day valuation of approximately Rs. 0.2 million per day) for the delay in the completion of the diversion.

But after the award of the Contract, it was found that none of the physical impediments, services/utilities were removed and relocated. During the course of construction, the design kept changing and modified perpetually for a long time, causing inordinate delays in execution. The employer/client lost about Rs.45 million (*US\$ 1.25 million*) as additional cost over a Contract Price of Rs.78 million.



Figure 1: Aerial view of Faizabad Interchange showing the clover leaf, the overhead, and the underpass.



5th Conference on Sustainability in Civil Engineering (CSCE'23)

Department of Civil Engineering
Capital University of Science and Technology, Islamabad Pakistan



II) Details

The contractual date of commencement of the project was **1st February 1993** stipulated to be completed in **18 months** on **31st July 1994** and was completed in **May 1996**.

After the award of work, it was found that the project area was infested with the following:

- i) Trees requiring legal permission from the Forest department for their cutting and removal.
- ii) Overhead power HT/LT transmission lines with poles belonging to some other government authority.
- iii) Optic fiber lines.
- iv) A large number of small public-related buildings and some other private property.
- v) Gas lines and telephone lines.

The conditions of the contract provided for the relocation of services and giving possession of the site free from all encumbrance and impediments. The physical impediments and obstructions were removed, and services were relocated, several months later after awarding of the contract as can be visualized from the tabulated information given below:

Table 1: List of physical impediments and stipulated time for their removal

S.no	Physical impediments	Time for removal and relocations
1.	Gas substation	20 months
2.	Shops	20 months
3.	Mosques	40 months
4.	Post office	28 months
5.	Police kiosks	36 months
6.	Trees	35 months
7.	Power overhead LT/HT cable	40 months
8.	Poles, telephone lines	38 months

The fallacy of affairs, unbalanced and un-pragmatic conditions of the contract were amazing, as can be seen from the following: The employer through a clause of the contract committed that all the existing structures within the contract limit shall get demolished by the employer. Through another clause of conditions of contract part-II, the employer was under obligation for relocation of Services through respective agencies being the owner of the services and utilities, and as such no extension of time was admissible to the contractor on this account.

Time was the essence of the contract and a penalty of Rs. 25,000 per day was stipulated for any delay by the contractor in the construction of the service road of the interchange. This penalty was beside the normal provision for imposing liquidated damages for overall delays. The physical obstruction and impediments lead to the employer's failure to give possession of the site free from encumbrance. Consequently, an extension of time was given.

The financial management and program of work by the contractor for a construction project with a defined period of completion attached with the penalty for delays are normally based on the stipulated period of time with some minor unforeseeable contingencies. These include inter-alia the following:

- i) Deployment of Head Office and Field Office, overhead expenses, supervisory and administrative Staff for the stipulated period.
- ii) Bank charges for various guarantees and insurance premiums for the stipulated period.
- iii) Planning the expenditure for execution and maintenance of the project for the **stipulated period** which includes the following:
 - a) Operation and maintenance of equipment and machinery for the execution of work.
 - b) Operation and maintenance of field laboratory for material testing and quality control.



5th Conference on Sustainability in Civil Engineering (CSCE'23)

Department of Civil Engineering
Capital University of Science and Technology, Islamabad Pakistan



- c) Deployment of formwork and scaffolding.
- d) Operation and maintenance of Consultant's Project Manager's Field Office and transport.

The bid price was given with the aim and intention of earning a certain amount of profit within the stipulated period, because if the amount of profit is attributed to a long period of time beyond a reasonable limit the purpose of business is affected. There exist in every contract certain terms and conditions of contract for the parties to comply with, but it is usual that the employer being the dominant party, while taking decisions/actions does not revisit and/or consult the provisions of the contract document, exercise administrative excesses and denial of the contractor's contractual rights, and committing departure from the contract giving rise to the dispute, consequently facing a loss

Arbitration.

The following factors of Bid Price were the inter-alia the following clauses:

GCC-I Clause 12.2 encountering adverse physical obstruction or condition and unforeseeable circumstances.
GCC-I Clause 26.1 obligation to comply with statutes and regulations.
GCC-I Clause 31.1 opportunity for other contractors to work
GCC-I Clause 42.1 possession of the site and access thereto free from all encumbrances
GCC-II Clause 73.9 Employer's obligation for relocation of Services and Utilities
GCC-II Clause 73.10 Diversion plan
GCC-II Clause 73.11 Employer's obligation for demolition of existing structures and buildings

Frequent changes in the design of Bridges and roads continued till October 1995 for 33 months against the stipulated original period of 18 months.

III) Admissibility of Claim for Compensation as Additional Cost & Extension of Time

The following clauses provide the admissibility of the claim for **additional cost** and extension of time due to numerous departures from the conditions of the contract by the employer.

- Clause 6.4 Delay in issuing construction drawings
- Clause 12.2 Adverse physical obstructions
- Clause 42.2 Possession of Site free from all encumbrances as per the program of work

The contractor raised an initial claim for a total amount of about **Rs. 80 million on account** of the following including general inflation.

- 7.2.1 Hire/Rental cost of "Essential plants and equipment"
- 7.2.2 Loss of profit due to insufficient cash turnover
- 7.2.4(a) Operation field laboratory
- 7.2.4(b) Monthly maintenance expenses of engineer's/employer's Office
- 7.2.5 Overhead expenses due to reduced turnover and transport
- 7.2.6 Increase in cost due to **general inflation**

Each of the clauses of the Contract prescribed the provision for:

- i) Additional cost



ii) Extension of time

The Engineer determined an amount of **Rs. 45 million (US\$ 1.2 million)** out of the Rs. 45 million, **Rs. 15 million** was paid immediately by the employer while the remaining **Rs. 30 million** was denied by the changed administration of the employer, but the honorable court order facilitated the payment.

3 Conclusions and Recommendations

It is advisable that the employer/owner of a Project while finalizing the conditions of the contract may be required to evaluate inter-alia the following:

- i) Availability of land free from all encumbrances.
- ii) Availability of final construction drawings for issuance after award of contract.
- iii) Availability of funds.
- iv) Timely appointment of the engineer/project manager.
- v) The degree of accuracy of quantities of items of works in the bill of quantity.
- vi) Extension of any Services anomaly among items of BOQ, drawings, and specifications.
- vii) Balanced conditions of contract with equity of justice.

Its highly recommended that the employer/owner of a project must take construction management and project management seriously and abide by the conditions of the contract because the same contractual and management mistakes are being repeated in almost every project in Pakistan and almost the same disputes are being observed **Islamabad Murree Dual Carriageway (IMDC) is in arbitration**, orange line of Lahore is going for arbitration with millions of extra claims and delays. Lessons learned like the timely appointment of the engineer/project manager, issuance of final construction drawings, availability of funds, etc. in the case study should be implemented on other projects to avoid dispute and delay.

References

- [1] Ghorbani A. "A Review of Successful Construction Project Managers' Competencies and Leadership Profile." *Journal of Rehabilitation in Civil Engineering*. Feb 1;11(1):76-95, 2023.
- [2] Ashkanani, S. and Franzoi, R. "Gaps in megaproject management system literature: a systematic overview", *Engineering, Construction and Architectural Management*, Vol. 30 No. 3, pp. 1300-1318. <https://doi.org/10.1108/ECAM-12-2021-1113>, 2023.
- [3] Hu, Y., Chan, A.P.C., Le, Y. and Jin, R. "From construction megaproject management to complex project management: bibliographic analysis", *Journal of Engineering Management*, Vol. 31, 04014052, doi: 10.1061/(ASCE)ME.1943-5479.0000254, 2013.
- [4] Priemus, H. and van Wee, B. "International handbook on megaprojects", *International Handbook on Mega-Projects*, Vol. 1, pp. 1-480, doi: 10.4337/9781781002308, 2013.
- [5] Ghosh B. N. ; *Scientific Methods and Social Research, Revised Edition*, Sterling Publishers Private Ltd, 1992.
- [6] Alan, A. and David, L. Book Review: Megaprojects: "The Changing Politics of Urban Public Investment", Brookings Institution Press. Copublished with the Lincoln Institute of Land Policy, Washington, DC. doi: 10.1177/1078087404267962, 2003.
- [7] Wang, T., Chan, A.P., He, Q. and Xu, J. (2020), "Identifying the gaps in construction megaproject management research: a bibliographic analysis", *International Journal of Construction Management*. doi: 10.1080/15623599.2020.1735610.
- [8] Tulu, T. "Determinants of Project Implementation Delay: The Case of Selected Projects Financed by the Development Bank of Ethiopia", St.Mary's University, Addis Ababa, 2017.
- [9] Msita K. M. I. M. "Construction Management: Claims management, East and Southern African Management Institute, Mombasa, Kenya, 1998.
- [10] Turner, J.R. and Xue, Y. "On the success of megaprojects", *International Journal of Managing Projects in Business*, Vol. 11, pp. 783-805, doi: 10.1108/IJMPB-06-2017-0062, 2018.
- [11] Hughes G. A. and Barber J. N "Building and Civil Engineering Claims in Perspective, Third Edition," *Longman scientific & technical*, 1992.
- [12] Harmon K. M. J. "Conflicts between Owners and Contractors: Proposed Intervention Process," *Journal of Management in Engineering*, Volume 19, Number 3; July, pp 121 – 125, 2003.
- [13] Ogula A. A Handbook on Educational Research. Nairobi. New Kemit Publishers. Ong, AD Bergeman, C, Bisconti TL (2004). The Role of ...; 1998.
- [14] Haltenhoff C. E. "Discussion on paper on partnering on small construction projects," *Journal of Construction Engineering and Management*, Vol. 127, No.4; July/August, pp 346 – 347, 2001.
- [15] Kannry S. J. "Construction Claim Pitfalls: Untimely Notice Can Be Fatal, "Construction Zone, Vol. 7 Issue 4 September/October 2007, p 2
- [16] Langdon D, Hackett M, Robinson I and Statham G (2007) *The Aqua Group Guide to Procurement, Tendering, and Contract Administration First Edition*, Blackwell Publishing. 2007.
- [17] FIDIC "Conditions of contract for construction for building and engineering works designed by the employer", *First Edition*, 1999.



5th Conference on Sustainability in Civil Engineering (CSCE'23)

Department of Civil Engineering

Capital University of Science and Technology, Islamabad Pakistan



- [18] Chappell D, Powell-Smith V, Sims JH. Building contract claims: John Wiley & Sons; 2008.
- [19] Zhang, M., Xue, X. and Zhang, J. "The guaranteed system for the smooth shifting of megaprojects from construction to operation: evidence from the Hong Kong-Zhuhai-Macao bridge project in China", *International Conference on Construction and Real Estate Management*, pp. 418-424, doi: 10.1061/9780784483237, 2020.
- [20] Kululanga G. K, Kuotcha W, McCaffer R, and Adum-Fotwe F. "Journal of Construction Engineering and Management," Vol. 127 No.4, July/August, pp 309 – 314, 2001.
- [21] Van Marrewijk, A., Clegg, S.R., Pitsis, T.S. and Veenswijk, M. "Managing public-private megaprojects: paradoxes, complexity, and project design", *International Journal of Project Management*, Vol. 26, pp. 591-600, doi: 10.1016/J.IJPROMAN.2007.09.007, 2008.
- [22] Wideman M. "Construction Claims Identification, Communication and Record Keeping" TUNS/Revay Seminar, *Expert Project Management – Construction Claims*, 1990. Available online: www.maxwideman.com/papers/construction/tips.htm
- [23] CCL Construction Consultants; Inc. (2009) *Construction Disputes and Claims*, Available online: <http://www.cclcc.com/services/cc.ccd/html>
- [24] Wang T. "Research on Contract Management and Claim of Construction Project" 2020.
- [25] Hassanein A. A. G. and El Nemr W. "Claims management in the Egyptian industrial construction sector: a contractor's perspective," *Journal of Engineering, Construction and Architectural Management*, Vol. 15 No. 5, October 2007, pp 456 – 468, 2008.



EFFECTS OF DIFFERENT AGGREGATE GRADATIONS ON RUTTING SUSCEPTIBILITY OF HOT MIX ASPHALT (HMA)

^a*Ashar Ahmed**, ^b*Sajjad Ali*, ^c*Syed Muhammad Noman*

a: Department of Urban and Infrastructure Engineering, NED UET, Pakistan, aahmed@cloud.neduet.edu.pk

b: Department of Civil Engineering, NED UET, Pakistan, sajjad.ali@neduet.edu.pk

c: Department of Civil Engineering, NED UET, Pakistan, syednoman@neduet.edu.pk

* Corresponding author: Email ID: aahmed@cloud.neduet.edu.pk

Abstract- This study focuses on the development of optimum job mix formula (JMF) with lower susceptibility. The effect of change in aggregate gradation in hot mix asphalt (HMA) was investigated for rut depth behaviour in flexible pavement. Samples were prepared at optimum asphalt content (OAC) which was found to be 4% through Marshall Mix Design (MMD). This optimum value was then used to find out the MMD parameters and rut resistance for various gradations. Changes in gradation were done by increasing and decreasing the percentages of coarse and fine particles. The result of this study showed that rut susceptibility increases with the change in coarser or finer aggregate percentage as compared to the control gradation, which is NHA Class A for wearing course. For a constant OAC, the sample with equal amount of coarser and finer particles showed the least rut depth. However samples that showed greater stability experienced higher rut depth which needs to be explored further.

Keywords- Hot Mix Asphalt (HMA), Marshal Mix Design (MMD), Rutting, Wheel Tracking Device (WTD)

1 Introduction

Karachi is the largest city of Pakistan [1] and comes under the category of mega-city [2]. Like other mega-cities, Karachi is also confronting with the situation of increasing population [3]. This population growth results in associated social, economic and business activities [4]. These activities need road infrastructure to meet the growing vehicular demand and fulfilment of related business tasks [5]. Road infrastructure is an important means for mobility of people and goods [6]. All commercial, business, and freight movements are mainly dependent upon it [7]. To meet the mobility demands, a strong road infrastructure is required [8]. It is the case in most developing countries that roads are subjected to higher loading than design [9]. Increase in business activities and population growth along with decrease in strength, invite road distresses. One of the major pavement distress among all is rutting [10]. The attraction towards road transportation has also increased because the railway infrastructure is deteriorating day by day in the study area. Since the last decade road infrastructure has become more than worse when 83% of load shifts to the road from rail along with an 8% annual increment in total traffic volume [11]. This extensive use of roadway causes damage and decrease in its lifespan [12].

The serviceability index is usually used to measure the comfort level provided by the transport facility [13]. Extensive use and misuse of road infrastructure causes damage and increased periodic maintenance [14]. Frequent reconstruction and maintenance activities are affecting the riding quality [15] of travelers as well. This study focuses on finding an optimum gradation and asphalt content (AC) that may help decrease the rutting susceptibility of Hot Mix Asphalt (HMA). Rutting (permanent deformation) of asphalt concrete is considered being a major form of distress [16]. It is characterized by a permanent change in the shape of the pavement or pavement layers due to cyclic wheel loading [17]. It not only affects the service life and performance of the asphalt pavement but also increases vehicle collisions resulting in loss of lives [18]. It will improve the life of the infrastructure with maximum load caring capacity and give a smooth riding surface.



Rutting occurs in the flexible pavement depending on the magnitude of the load and relative strength of the pavement layer [19]. Permanent deformation can occur in the subgrade, the base and the uppermost HMA layer [20]. Rutting in HMA layers is more common in summer [21] as compared to winter, and the pavement deformation is more likely in an aggregate base during the wet spring season [22].

Another factor that causes rutting is stress level which is the function of the magnitude of the load [23]. Application of a heavy load, environmental factors [24] and material quality [12] are some of the major factors that reduce the rutting resistance of pavement. Insufficient initial compaction on HMA, presence of voids, density and bitumen variants are also responsible for the induction of rutting in the HMA layer.

The phenomenon of rutting in the flexible pavement was found in several types of research [16]. Important factors such as the magnitude of traffic loads, loading speed, load repetition, pavement temperature and rutting resistance of asphalt mixture were also being discussed by many of the researchers [25]. For given asphalt pavement material, a deeper rut will develop under heavier traffic loads, lower traffic speed and higher pavement temperature [24]. There are two different mechanisms of rut development. The first one is associated with well-designed structures and stable materials. The permanent deformation is due to the effect of repeated load on pavement materials that are not perfectly elastic. The susceptibility of rutting depends on the stiffness. An increase in the asphalt concrete layer can better this situation [23].

Dramatic increases in the number and weight of vehicles have resulted in severe rutting on highways in Taiwan [26]. The Taiwan Area National Freeway Bureau constructed an in-service test road to investigate the effect of pavement structures and paving materials on pavement performance. A similar study was also conducted by which change in material grade can reduce the rutting effect [27]. Several laboratory tests were also used to study the rutting behaviour such as Wheel tracking device (WTD), Universal Testing Machine, [28] Marshal apparatus [27] and California Bearing ratio and stiffness test [23]. This research focuses on the examination of rutting behaviour of HMA given a constant asphalt content but varying coarse and fine aggregate composition, using laboratory tests such as WTD and Marshal Mix Design.

2 Methodology

Physical and mechanical tests were performed. The result of these tests was compared with the National Highway Authority (NHA) aggregate grading Class A for asphalt concrete wearing course. Properties of mixtures were tested according to MMD. OAC was also determined based on MMD, which was then used for all gradation changes throughout the study. There were four types of gradations. Controlled gradation (CN) is that gradation that is according to NHA Class A [29]. CN gradation has 63% coarse aggregates and 37% fine aggregates. The second gradation developed contained 70% coarse aggregates and 30% fine aggregates. These samples were termed as coarser gradation (C). The third gradation was developed by keeping the percentage of both coarse and fine aggregates to 50%. These samples were termed as finer gradation (F). The last type of gradation was termed coarser finer (CF). CF sample contained 60% coarse aggregates and 40% fine aggregates (Table 1).

Table 1: Aggregates gradation detail

Sieve Size	Gradation			
	NHA "CN"	Coarse 'C'	Finer 'F'	Coarser Finer 'CF'
		Percentage Retained		
		C=63% F=37%	C=70% F=30%	C=50% F=50%
3/4	10%	10%	10%	10%
1/2	0%	20%	10%	10%
3/8	30%	20%	20%	25%
# 4	21%	20%	10%	15%
# 8	13%	5%	20%	15%
#16	21%	20%	25%	20%
# 200	3%	3%	3%	3%
Pan	2%	2%	2%	2%



In the end, all four types of samples were being tested for rutting. Comparison of volumetric properties like stability, flow and density along with rut resistance were be analyzed and compared with NHA specification and international guidelines. Figure 1 will provide the details of the procedure followed throughout the study.

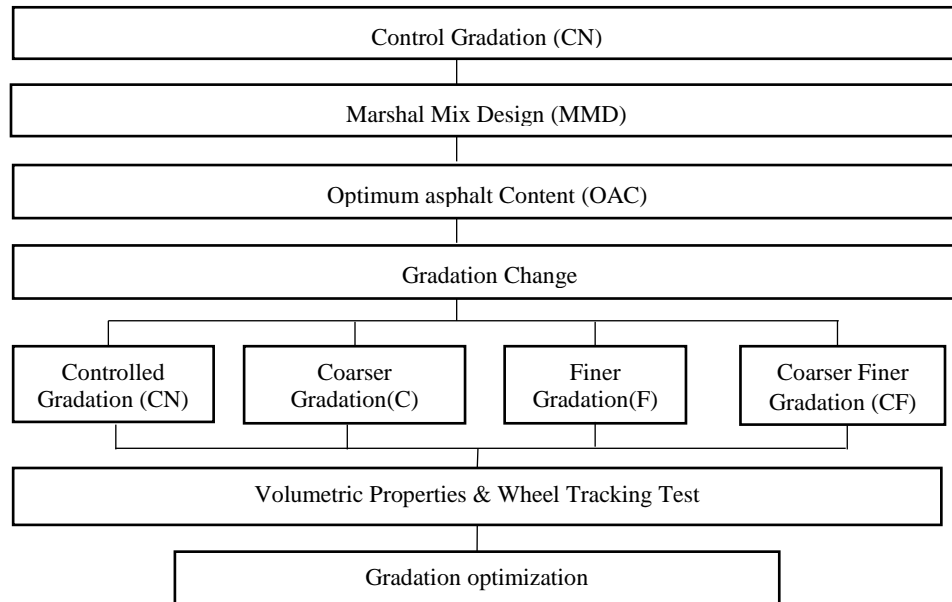


Figure 1: Flow chart of study

2.1 Experimental Program

2.1.1 Aggregates

The mixture of aggregates and asphalt was made up of three types of samples that were used, which were changed concerning their sizes. Mechanical Material properties of materials were not changed. Asphalt was the same throughout this study. Limestone was made available from local material suppliers and consistent throughout. Tests were performed on aggregates following the American Society of Testing and Materials (ASTM) and British Standard (BS). NHA and other international bodies like ASTM and BS Limitations were used for the selection of aggregates (Table 2). Aggregates were sieved and washed as per recommendation before testing as this study used variations in aggregates gradation. This variation is within the NHA gradation Class A.

Table 2: Summary of aggregates properties

Test	Standard	Result	Recommendation
Abrasion Test, (%)	ASTM C131	28.30	< 30
Specific gravity, (-)	ASTM C127	2.67	2.5 - 3.0
Absorption, (%)	ASTM C127	0.71	0.1 - 2.0
Impact value, (%)	BS 812	15.80	20 - 30
Crushing value, (%)	BS 812	20.12	< 30

2.1.2 Asphalt

Asphalt is a cementing material. It was made available from the local market. The following laboratory tests were performed. The results of those tests were being compared with the recommended values. The asphalt used was the requirements of local and international agencies (Table 3).



Table 3: Summary of asphalt testing

Test	Standard	Result	Recommendation
Penetration Grade	ASTM D5	60 - 70	60 – 70
Flash Point, (°C)	ASTM D92	130.0	120 (min)
Fire Point, (°C)	ASTM D92	290	230 (min)
Softening point, (°C)	ASTM D36	51.5	50 – 60
Specific gravity, (-)	ASTM D70	1.02	1.00 – 1.05
Consistency, (sec)	ASTM D139	>1200	1440
Viscosity , (cSt)	ASTM D2171	1323	800 – 1600
Ductility, (cm)	ASTM D113	110	>100

2.2 Test Specimens: Marshall and Rut Test

The volumetric results of mix sample were analysed. Marshal Mix Design was used to determine the properties of the mix. MMD was done for heavy traffic. Seventy-five blows on each side of the samples. Firstly, all the results were derived for CN sample type. OAC was then determined. NHA [29] guidelines provide a specification to have OAC on 4.0 % to 7.0 % air voids for wearing course. 6.0 % Air voids are taken for optimum determination. This OAC were used for all types of a mix; CN, C, F, and CF. Volumetric properties like stability and flow determined for all types of asphalt mix. After comparing mix properties, rut samples were prepared. Three rut samples were tested for each type of mix. A total of nine samples tested for rutting. These results of the rut and volumetric properties were then compared based on the mix type and percentage of aggregates. A typical specimen for rutting weight approximately 11-12 Kg depending upon the optimum density achieved. For each type of rut sample, it varies. The optimum density of each type of mix was different. That is the reason for the weight change of the rut sample for every type of mix. The size of the rut sample [Figure 2] was 300mm by 300mm and was 50mm thick. The rut sample was set for 20 mm maximum rut depth or 5000 load cycles whichever comes earlier. The testing temperature for rutting was 60°C.



Figure 2: Rut samples

3 Results and Discussion

Samples were prepared at different asphalt content using controlled gradation CN. The Asphalt content varies from 3.5% to 6.0% at 0.5% interval. After the analysis of the test result from volumetric analysis. Optimum asphalt content comes out to be 4.0%. This OAC was used to prepare the sample for volumetric assessment with gradation change from coarser to finer. The stability relation with gradation is shown in Figure 3. Stability is highest for CN gradation while lowest for C gradation. On the other hand, CF and the F gradation had lesser Stability than CN. However, all the samples have greater stability than the threshold limit, which is 680.38Kgf [30]. The percentage of air voids have reverse behaviour of stability. The lowest air voids result in the case of CN gradation. While C gradation has the highest percentage of air voids. CF and F gradations have air voids in increasing order, respectively. It was found that a higher percentage of either coarse or fine aggregates lead to a higher percentage of air voids, and the higher the air voids the lower the stability.



5th Conference on Sustainability in Civil Engineering (CSCE'23)

Department of Civil Engineering
Capital University of Science and Technology, Islamabad Pakistan

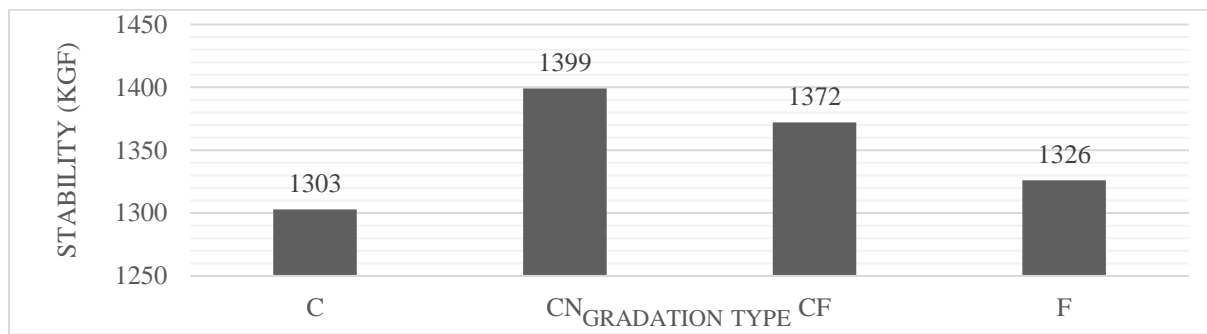


Figure 3: Relationship between stability and aggregates gradation type

The result of air voids was found opposite in nature as compared to the earlier result of gradation versus stability, that is, voids ratio increased with an increase in the percentage of same size particles. This concludes that a higher percentage of either coarser or finer particles will lead to a higher number of air voids (Figure 4). The coarser (C) and finer (F) gradations developed were experimental and hence could be the reason behind the anomalous results.

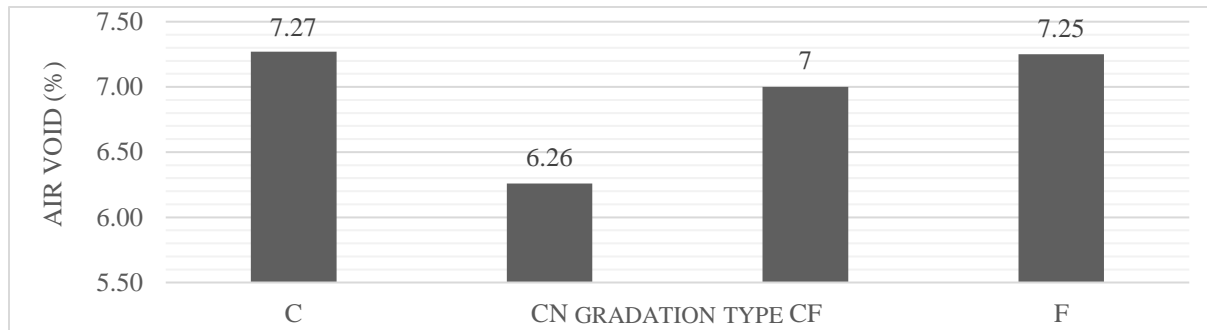


Figure 4: Relationship between air voids percentage and aggregates gradation type

In the gradation change, coarser particles were increased. The increase in the coarser particle ultimately decreases the finer portion. The study only discussed the increase in coarse aggregates. Figure 5 shows that stability increases with the increase in coarse aggregates. It is observed that for all percentages of coarse aggregates value of stability is within the range provided by the authorities [29]. A lesser percentage of coarse aggregates produced lesser stability same is the case for a higher percentage of coarse aggregates. The maximum stability values were obtained at the average region coarse aggregate gradation, the minimum percentage for coarse aggregates was 50% while the maximum was 70%.

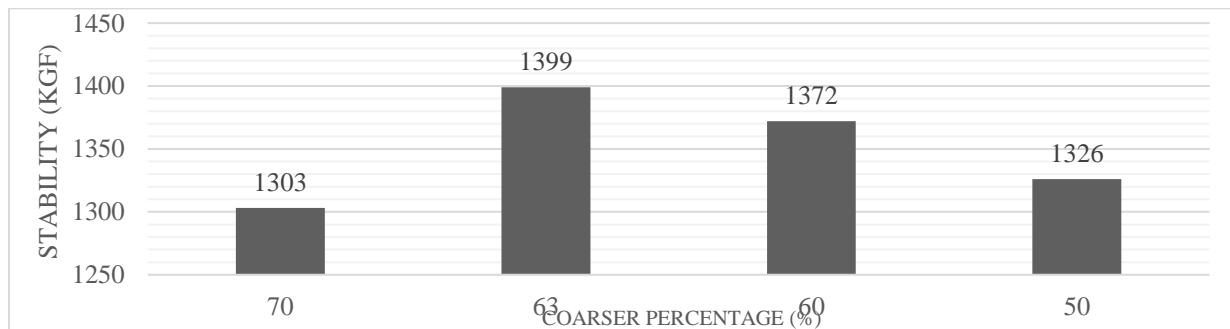


Figure 5: Relationship between stability and percentage of coarser particle

Rut test was performed through Wheel Tracking Device and the results are presented in Figure 6. The weight of material for the rut sample was calculated through optimum density. Optimum density was observed by MMD at OAC. Rut test was performed on every gradation type with replication of three samples. A total of 12 samples were tested. The



performance of the gradation type was analysed. Gradation F has higher resistance for rutting. Gradation C and CF has also shown good result. Although, CF has better resistance than C. Gradation CN crosses the limits of the rut for wearing course [30]. This is a very important finding which concludes that CN gradation type, that is NHA gradation Class A is comparatively more susceptible to rutting then gradations having more finer aggregates.

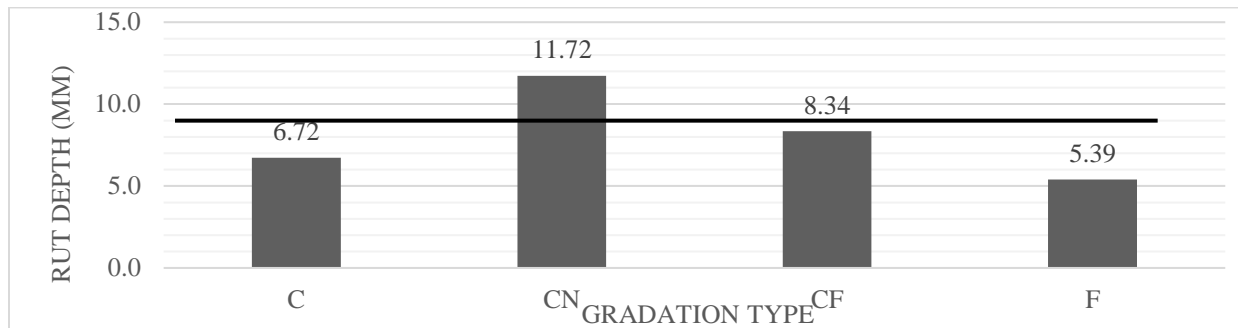


Figure 6: Relationship between rut depth and gradation types

The two extremes of coarse gradation percentage showed lesser susceptibility against rutting. It was found that finer (F) gradation produces the highest rut resistance, while 60% to 64% of coarse aggregates in the mix lead to lesser rutting resistance. This indicates that the behaviour of samples on Wheel Tracking Device is anomalous and does not conform to the usual understanding of the trend pertaining to physical parameters of HMA.

4 Conclusions and Recommendations

The study concludes that the lower the air voids percentage the higher the stability. As CN gradation has the lowest air voids percentage, it has the highest stability. Comparatively C gradation has vice versa. Stability values were within the limits for every type of gradation. The stability of NHA Class A gradation for wearing coarse, which is sample CN, was found to have the highest stability and lowest air voids. However for the same OAC the results were different for rut test. Rutting susceptibility is directly influenced by the gradation of aggregates. The sample with equal amount of coarse and fine aggregates, that is F gradation, showed least rut depth than other gradation types. Comparatively the CN sample showed highest rut depth. An OAC of 4% may have led to bleeding of asphalt in this sample and could be the possible reason behind a higher rut depth. These results lead to the conclusion that rutting susceptibility is influenced by the gradation of aggregates however OAC needs to be evaluated for each gradation type. Determination of Optimum Asphalt Content (OAC) plays an important role in determining rutting susceptibility and hence needs to be further explored. This study only focuses on OAC determined by MMD for the controlled sample, and then employed to all gradation types which led to higher rut depths for samples that showed better stability for MMD.

Acknowledgment

The authors want true acknowledgement of Mr. Talha Aqeel and Mr. Aftab Ahmed, laboratory technicians, Transportation Engineering Laboratory, Urban and Infrastructure Engineering Department, NED University of Engineering and Technology, Karachi.

References

- [1] S. Dodani, R. Mistry, A. Khwaja, M. Farooqi, R. Qureshi and K. Kazmi, "Prevalence and awareness of risk factors and behaviors of coronary heart disease in an urban population of Karachi, the largest city of Pakistan: a community survey," *Journal of Public Health*, vol. 26(3), pp. 245-249, 2004
- [2] K. Alam, T. Trautmann, and T. Blaschke, "Aerosol optical properties and radiative forcing over mega-city Karachi," *Atmospheric Research*, vol. 101 2011. doi:10.1016/j.atmosres.2011.05.007.
- [3] J. A. Cross, "Mega-cities and small towns: different perspectives on hazard vulnerability," *Global Environmental Change Part B: Environmental Hazards*, vol. 3(2), pp. 63-80, 2001. doi: 10.1016/S1464-2867(01)00020-1.
- [4] L. M. A. Bettencourt, J. Lobo, D. Helbing, C. Kühnert and Geoffrey B. West, "Growth, innovation, scaling, and the pace of life in cities," in the *Proceedings of the National Academy of Sciences*, vol. 104(17), pp. 7301-7306, 2007. doi: 10.1073/pnas.0610172104



5th Conference on Sustainability in Civil Engineering (CSCE'23)

Department of Civil Engineering
Capital University of Science and Technology, Islamabad Pakistan



- [5] A. Fraser and M. V. Cheste, "Environmental and economic consequences of permanent roadway infrastructure commitment: city road network lifecycle assessment and Los Angeles county," *Journal of Infrastructure Systems*, vol. 22(1), 2016. doi: 10.1061/(ASCE)IS.1943-555X.000027.
- [6] E.O. Akinyemi and M.H.P.Zuidgeest, "Managing transportation infrastructure for sustainable development," *Computer-Aided Civil and Infrastructure Engineering*, vol. 17(3), pp. 148-161, 2002. doi: 10.1111/1467-8667.00263.
- [7] M. Hesse and J.P. Rodrigue, "The transport geography of logistics and freight distribution," *Journal of Transport Geography*, vol. 12(3), pp. 171-184, 2004. doi: 10.1016/j.jtrangeo.2003.12.004.
- [8] C. Jeon, A. Amekudzi-Kennedy, "Addressing sustainability in transportation systems: definitions, indicators, and metrics," *Journal of Infrastructure Systems*, vol. 11 (1), pp. 31-55, 2005. doi: 10.1061/(ASCE)1076-0342(2005)11:1(31).
- [9] K. Tsunokawa, R. Islam and G. Changyu, "Optimal strategies for highway pavement management in developing countries," *Computer-Aided Civil and Infrastructure Engineering*, vol. 17(3), pp. 194-202, 2002. doi: 10.1111/1467-8667.00267.
- [10] A. Golalipour, E. Jamshidi, Y. Niazi, Z. Afsharikia and M. Khadem, "Effect of aggregate gradation on rutting of asphalt pavements," *Procedia -Social and Behavioral Sciences*, vol. 53, pp. 440-449, 2012. doi: 10.1016/j.sbspro.2012.09.895.
- [11] M. G. F. Javed, "Sustainable financing for the maintenance of Pakistan's highways," *Transport and communications bulletin for Asia and the Pacific.*, vol. 75, pp. 83-96, 2005.
- [12] M. M. Rafi, A. Qadir, S. Ali, S. Siddiqui, "Performance of hot mix asphalt mixtures made of recycled aggregates," *Journal of Testing and Evaluation*, vol.42 (2), pp. 357-367, 2014. doi:10.1520/JTE20130004.
- [13] T. Officials., AASHTO guide for design of pavement structures 1993, vol 1. Washington D.C., 1993. Available: <https://habib00ugm.files.wordpress.com/2010/05/aashto1993.pdf>
- [14] R. P. Nicolai and R. Dekker, "Optimal maintenance of multi-component systems: a review," in *Complex System Maintenance Handbook*, London: Springer, 2008, pp. 263-286. doi: 10.1007/978-1-84800-011-7_1.
- [15] Y. Ouyang and S. Madanat, "Optimal scheduling of rehabilitation activities for multiple pavement facilities: exact and approximate solutions," *Transportation Research Part A: Policy and Practice*, vol. 38 (5), pp. 347-365, 2004. doi: 10.1016/j.tra.2003.10.007.
- [16] T. F. Fwa; S. A. Tan; and L. Y. Zhu, "Rutting prediction of asphalt pavement layer using C-φ model," *Journal of Transportation Engineering*, vol. 130(5), pp. 675-683, 2004. doi: 10.1061/(ASCE)0733-947X(2004)130:5(675).
- [17] A. Saleeb, R. Liang, H. Al Qablan and D. Powers, "Numerical simulation techniques for HMA rutting under loaded wheel tester," *International Journal of Pavement Engineering*, vol. 6, 2005. doi: 10.1080/10298430500068704.
- [18] C. Chan, B. Huang and S. Richards, "Investigating effects of asphalt pavement conditions on traffic accidents in Tennessee based on the pavement management system (PMS)," *Journal of advanced transportation*, vol. 44(3), pp. 150-161, 2010. doi: 10.1002/atr.129.
- [19] D. E. Newcomb, M. Buncher and I.J. Huddleston, "Concepts of perpetual pavements," *Transportation Research Circular*, vol. 503, pp. 4-11, 2001.
- [20] M. Abu-Farsakh and Q. Chen, "Evaluation of geogrid base reinforcement in flexible pavement using cyclic plate load testing," *International Journal of Pavement Engineering*, vol. 12(3), pp. 275-288, 2011. doi: 10.1080/10298436.2010.549565.
- [21] A. Abed and A. A. Al-Azzawi, "Evaluation of rutting depth in flexible pavements by using finite element analysis and local empirical model," *American Journal of Engineering and Applied Sciences*, vol. 5(2), pp. 163-169, 2012.
- [22] I. Syed, T. Scullion and R. B. Randolph, "Tube suction test for evaluating aggregate base materials in frost-and moisture-susceptible environments," *Transportation Research Record*, vol. 1709(1), pp. 78-90, 2000. doi: 10.3141/1709-10.
- [23] J. Uzan, "Permanent deformation in flexible pavements," *Journal of Transportation Engineering*, vol. 130(1), pp. 6-13, 2004. doi: 10.1061/(ASCE)0733-947X(2004)130:1(6).
- [24] A. Qadir, U. Gazder and S. Ali, "Comparison of SBS and PP fibre asphalt modifications for rutting potential and life cycle costs of flexible pavements," *Road Materials and Pavement Design*, vol. 19(2), pp. 484-493, 2018. doi: 10.1080/14680629.2016.1259124.
- [25] T. F. Fwa, S. A. Tan and ASTM International, "Laboratory evaluation of rutting potential of asphalt mixtures," in *Effects of Aggregates and Mineral Fillers on Asphalt Mixture Performance*, R. C. Meininger, Ed. ASTM International, 1992, pp. 211-224.
- [26] J.-S. Chen, C.-H. Lin, E. Stein and J. Hothan, "Development of a mechanistic-empirical model to characterize rutting in flexible pavement," *Journal of Transportation Engineering*, vol. 130(4), pp. 515-525, 2004. doi: 10.1061/(ASCE)0733-947X(2004)130:4(519).
- [27] J. Yang, H. Zhao, J. Chen, G. Qian, W. Pan, and Y. Yang, "Study of the rutting resistance of asphalt surfacing mixtures," in proceedings of 24th Annual Southern African Transport Conference: SATC, Pretoria, South Africa, 2005, pp. 943-950.
- [28] I. Hafeez, M. A. Kamal and M. W. Mirza, "Evaluation of rutting in hma mixtures using uniaxial repeated creep & wheel tracker tests," *Pakistan Journal of Engineering and Applied Science*, pp.55-64, 2016.
- [29] N. Highway Authority, General Specifications National Highway Authority, Karachi: NHA Pakistan, 2005.
- [30] A. Ubstutye, "Mix design methods for asphalt concrete and other hot-mix types, manual series No. 2", 6th ed. The Asphalt Institute, College Park, MD, 1995.
- [31] BS812, British Standards, London: British Standards Institution (BSI).



MANHOLE RELATED ROAD ACCIDENT PREVENTION USING SUSTAINABLE METHODS

^a Ashar Ahmed*, ^b Muhammad Abeer Shaikh, ^c Bushra Aijaz

a: Department of Urban and Infrastructure Engineering, NED UET, Pakistan, aahmed@cloud.neduet.edu.pk

b: Department of Urban and Infrastructure Engineering, NED UET, Pakistan, shaikh4306588@cloud.neduet.edu.pk

c: No current Affiliation, bushra.aijaz.37@gmail.com

* Corresponding author: Email ID: aahmed@cloud.neduet.edu.pk

Abstract- Road accidents are the major cause of fatalities, injuries and property damage worldwide. The implementation of sustainable road accident prevention methods is essential to reduce the risk of accidents, promote safety and protect the environment. This research paper investigates road accidents in Karachi, particularly the impact of open manholes. Focusing on the disruptive effect of open manholes on road safety, the study addresses the issue and its implications. The paper analyzed onsite data on traffic volume and accidents, providing insights into vehicle flow rates during peak hours. The effect of open manholes on accident frequency is examined. The traffic mix at the study location comprised of 57.9% motorcycles, 28% cars and 12.4% rickshaws, while buses, tankers and trucks constituted the rest. It was found that there have been approximately 105 road accidents due to open manhole at the study location. After the recycled rubber tire has been placed, no accident occurred. This is a remarkable finding. The placement of recycled rubber tires over open manholes is a sustainable solution that is cost-effective, durable, easy to install, slip proof, more theft-proof than conventional reinforced concrete manhole covers and eco-friendly.

Keywords- Manhole, Rubber Tire, Traffic Volume, Peak Hour Factor.

1 Introduction

Road networks serve as fundamental channels, facilitating the seamless movement of numerous individuals engaged in diverse activities such as commuting, traveling, studying, and running errands. However, due to increase in exposure as a result of daily mobility, road accidents also increase. Ahmed and Aijaz [1] has indicated 28,170 fatal injuries in Pakistan in 2020 in its literature and identified major reasons for road accidents. According to the survey report published by Khurshid et al [2], 50.4% of fatalities in Karachi city; are due to the road accidents, out of which 12.9% were happened during 6:00pm till 11:59pm in 2019, which was increased in 2020 to 22%. Muhammad et al [3] have reported that 22.1% of traffic accidents have had happened in evening from 5:00pm till 9:00pm. They collected the data of 426 injured patients and recorded that 36.2% accidents were due to the vehicle slippage and 16.8% were occurred at Link Road and 75.3% on Main Road. We have identified one such region consisted of an exposed or uncovered manhole located near SSGC on the Abul Hassan Ispahani Road connecting to Main University Road, Karachi. The study area manhole is 2 ft wide and have been a reason of many vehicular accidents, especially during peak hours.

The occurrence of accidents is influenced by multifarious factors, encompassing peak traffic volumes during specific time periods, intricate traffic patterns, the quality of infrastructure, and driver conduct, including the presence of manholes along roadways. The manhole covers provides preventions to fall hazards. Manhole covers are made up of steel reinforced concrete and weighs about hundred or more kilograms to sustain the load of traffic passing over it. The



presence of numerous addicts and beggars seeking financial gain in the city has resulted in the theft and removal of manhole covers, leading to exposed manholes. Exposed manholes have become prominent contributors to road accidents. A significant number of manholes exists throughout the city, necessitating urgent attention and the implementation of a sustainable solution. There has been a lot of work towards sustainable solutions for road reparations. Abrar and Shah [4] have suggested non-woven fabric and ultra-thin asphalt overlay for repairing potholes during rehabilitation phase. Khan et al [5] has also suggested the use of rubber tires' strips in the manufacturing of manholes covers instead of conventional reinforcement. This study is one of a kind that addresses the problem pertinent to the city of Karachi. It aims to explore the various sustainable methods of mitigating road accidents due to open manholes. The installation of manhole covers that are cost-effective, environmentally friendly, and theft-resistant becomes an ideal approach. To address this challenge, rubber tires have been utilized as part of manhole covers. The placement of rubber tires as manhole covers provides visual indicator to alert drivers about manhole presence. It brings out a sustainable solution, as they can be recycled into various products such as road surfacing, and even synthetic oil. Waste rubber tire can also be used in pervious concrete, as mentioned in Bonicelli et al [6], and hence can help to minimize the need for new materials.

By deploying the recycled rubber tire on the exposed manholes, it not only warns drivers and pedestrians about the fall hazard but also a positive and low-cost solution to economy. To achieve this, an onsite survey was conducted, and responses were collected from nearby shopkeepers along the route from Abul Hasan Ispahani Road to University Road of Karachi, Pakistan. The survey included traffic volume count conducted from 5:15 pm to 7:15 pm, enabling the calculation of traffic flow rate and peak hour factors. The method adopted for traffic data collection was on-site manual count. For accident data collection, on-site interviews were conducted from the nearby shopkeepers, before and after the intervention. The subsequent sections consist of results obtained after traffic analysis results along with its discussion, followed by conclusions drawn out of this investigation.

2 Methodology

The methodology employed in this study consisted of three integral parts. The first section describes the study area followed by traffic and accident data collection and the last section explains the analysis method.

2.1 Study Area

The selected study area for this research encompassed the stretch of road from Abul Hassan Ispahani Road to Main University Road, specifically near the SSGC building. The Abul Hassan Ispahani Road facilitates around 12 educational institutes, predominantly schools. Consequently, a substantial volume of vehicles traversed this road on a regular basis. Notably, numerous manholes were present along this road, with two significant ones situated in close proximity to the UIT University and at the junction connecting Abul Hassan Ispahani Road and University Road. Our study area is the later one.

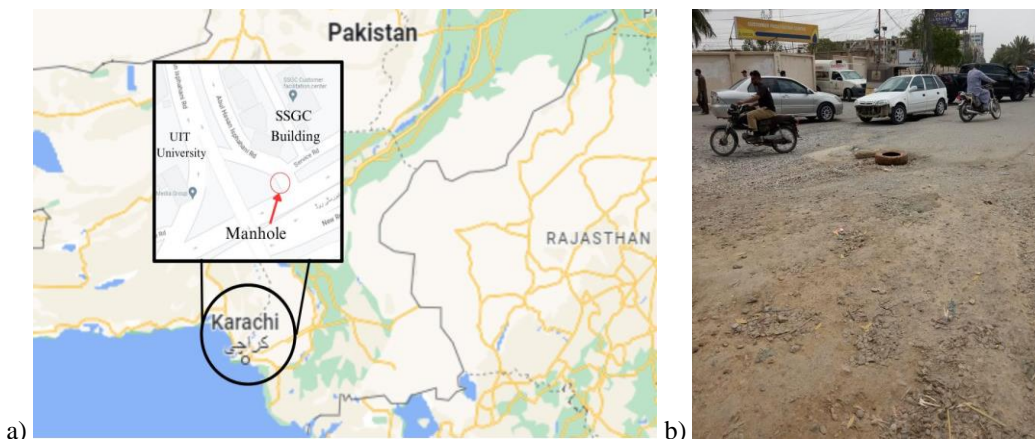


Figure 1: Study Area, a. Location of the study area (Source: Google Maps), and b. Physical condition of the road as of 01st June 2023.



5th Conference on Sustainability in Civil Engineering (CSCE'23)

Department of Civil Engineering
Capital University of Science and Technology, Islamabad Pakistan



Figure 1 depicts the location and geometry of the study area. The manhole is measured to be 2ft wide. It is situated at the curve where Abul Hassan Ispahani Road is about to join the Main University Road (Figure 1a). The curve is also connecting the service road, a U-turn and a triangular round-about. The potential dimensions of traffic movement making the study area more sensitive specially for motorcyclists, Qingqi and auto-rikshaws (Figure 1b). The presence of hawkers, baggers and pedestrians increases the chances of sudden application of brakes and turnings by the drivers, which results in greater chances of vehicle/pedestrian crashes or their fall/slippage into manhole.

2.2 Data Collection.

Data collection is the process of gathering information about the transportation system, its users, and its environment [7]. Two types of data were collected for this study; which are traffic volume and accident frequency. On-site manual count method was used to collect volume data while interview method was used to collect accident data. The authors conducted manual count of traffic moving on Abul Hasan Ispahani Road towards University Road. The two-hour traffic volume was counted from 5:15 pm to 7:15pm. The classified count was obtained through manual counting of each type of vehicle on site. The data was divided into intervals of 15 minutes for further analysis. The authors also interviewed the nearby shopkeepers to gain insights into the type and frequency of road accident at the location of study.

2.3 Traffic Analysis.

The collected traffic data was analysed for various traffic macroscopic parameters. First the distribution of traffic with respect to each mode, that is traffic mix, was analysed. It was followed by the calculations of Rate of flow and Peak Hour Factor [8]. Rate of flow represents the vehicular flow that exist for periods of time less than one hour. It is represented in units of “vehicles per hour” and can be calculated using equation (1) described as follows,

$$\text{Rate of flow} = \frac{\text{No. of vehicles}}{\text{time interval in min}} \times 60 \quad (1)$$

The Peak Hour Factor (PHF) can be collected using equation (2). PHF explains the variation of traffic occurring within an hour. It helps understand the flow of traffic on a particular location and examine the situation on site. It provides insightful information on traffic patterns and the potential influence of volume changes on the occurrence of road accidents.

$$\text{PHF} = \frac{V}{4 \times V_{m15}} \quad (2)$$

Whereas,

- PHF = Peak Hour Factor
V = Hourly Volume (vehicles)
 V_{m15} = Maximum 15-minute volume within the hour

3 Results and Discussion

3.1 Traffic Mix

The traffic mix, that is, the distribution of traffic with respect to each mode was surveyed on-site for traffic moving from Abul Hasan Ispahani Road towards University Road. The corresponding percentage for each mode of transport was calculated. The survey revealed that motorcycles made up 57.9% of all traffic passing through the location as shown in Figure 2. Cars with a share of 28.0% constituted the second largest portion, followed by rickshaws at 12.4%, while the trucks and small trucks collectively represented a minimal proportion of 0.11%.

The findings indicated that rickshaws were particularly vulnerable to accidents occurring as a result of open manholes. This observation underscores the need for effective measures to address the safety risks faced by drivers and passengers passing by the location of study.

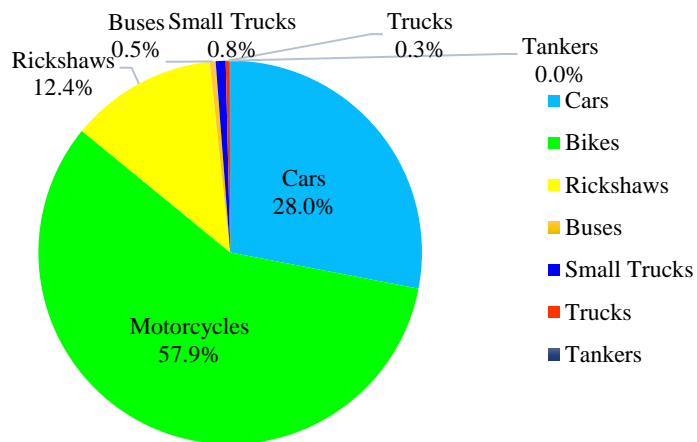


Figure 2: Traffic mix at the location of the study.

3.2 Flow Rate

Flow rate is the equivalent hourly rate at which vehicles pass through a given point or segment of a lane or roadway within a given time interval of less than one hour, usually 15 min [9]. The analysis of the flow rate at the study area indicated an upward trend. Figure 3 shows that as the time of the day is increasing the flow rate is also increasing. This is conformal with the behavior of traffic flow in the city. Since, Abul Hassan Ispahani road connects its surrounding residential areas with the University Road, this serves as the likely route for students going for evening classes at NED University and University of Karachi. The variation in the flow rate is likely due to the movement of students with respect to their evening class timings.

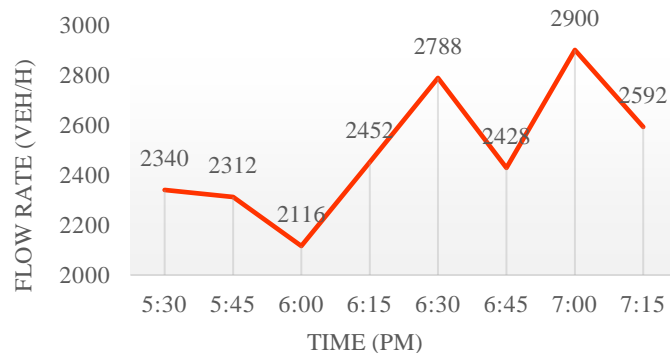


Figure 3: Traffic flow from 5:15 pm to 7:15 pm on 1 June 2023 at the location of the study.

3.3 Peak Hour Factor

The Peak Hour Factor (PHF) is one of the basic parameters used by traffic engineers to examine the macroscopic behaviour of traffic at a particular location. It is calculated on the basis of dividing an hour into four quarters, each consisting of 15-min. The total volume during a particular hour is divided by the maximum 15-min volume multiplied by 4 to obtain the PHF. The values of PHF cannot be less than 0.25 and greater than 1. The more the value is near to 1, the lesser the variation in traffic flow. The calculated PHFs are shown in Table 1.

Table 1: Peak Hour Factor

Time	PHF
Volume 5:15-6:15	0.94
Volume 6:15-7:15	0.92



The examination revealed that as the evening is approaching the variation in traffic flow is decreasing. This finding is mathematically conformal with the traffic flow behavior, as the value of PHF greater than 0.9 is an indicative of the uniformity in traffic flow.

3.4 Traffic Accidents at Study Area

According to the survey, the eyewitness at the location claimed that an average of four rickshaws and one car fell into this manhole every day as recorded in Table 2. Some of the accidents involved considerable property damage in which the front part of the rickshaw collapsed completely. No human loss or injury accident has been reported yet but it is common to have slight, sever, or even fatal accidents due open manhole if it is located on a straight segment. As per the survey, approximately 105 accidents have occurred on the site till 31st May 2023. These numbers are from the date the manhole cover was stolen, that is, 5th May 2023.

Table 2: Average accidents per day of each type of vehicle

Vehicle Type	Motorcycle	Rickshaw	Car	Bus	Small Truck	Truck	Tanker
Average accident per day	0	4	1	0	0	0	0

3.5 Sustainable Accident Prevention Methods

Road accidents involving open manhole could easily be prevented by simple methods. Conventional manhole covers contain steel reinforcements which are of high value to addicts. These conventional covers are sabotaged and stolen by addicts to extract the steel in them, in order to fulfill their needs. Unconventional manhole covers, that do not contain steel, will be of no use to them and hence will be safe from being sabotaged or stolen. One such manhole was developed at NED University in 2020 using recycled rubber tire [5]. Instead of conventional steel reinforcements, rubber tire strips were used. The load bearing capacity of the resultant tire was found to be in the range of 12.75 to 17 kN, which is higher than the conventional manhole covers available in the market. But it had some limitation like durability; since heavy traffic will be moving upon it whole day and this particular manhole cover may not support it.

To address the issue of uncovered manholes, a recycled rubber tire is proposed to be deployed as a cover. The choice of using a rubber tire cover was based on its durability, cost-effectiveness, and environmental suitability. It costs approximately PKR 1650 cheaper than sustainable manhole tires, along with they offer moderate durability in contrast to sustainable manhole cover's high durability. They do make high effectiveness and impact. Suiting them to an overall rank of 1 as presented in Table 3. Another most readily available material and the urgent solution; is the bamboo stick. In case of missing or damaged manhole cover, the first object that is used by the nearby residents or passersby is the bamboo stick as an alarming notification to the drivers. Although bamboo sticks are available at a cheaper rate than the two but they offer less durability and moderate level of effectiveness in preventing accidents.

Table 3: Sustainable Accident Prevention Methods

	Cost (PKR)	Durability	Effectiveness	Impact	Overall Rank
Sustainable Manhole Cover	2,000	High	High	High	2
Recycled Rubber Tire	350	Moderate	High	High	1
Bamboo Stick	200	Low	Moderate	Moderate	3

The onsite survey also revealed a notable decline in the number of road accidents following the implementation of rubber tire covers to secure the manholes. The rickshaws try to utilize the extra space available at the junction (curve) during peak hours, which otherwise remain empty, causing more rickshaw related accidents. The interviewers claimed that the accidents reduced to zero after the placement of rubber tires as manhole cover. The utilization of rubber tires also served as a visual indicator for drivers, alerting them about the presence of open manhole and prompting them to exercise caution. Figure 3a shows the manhole before the placement of the rubber tire. In the existing scenario speedy drivers will



get little to no chance to swerve away from its path. After intervention, as shown in Figure 3b, the manhole is noticeable to the drivers. The application of paint further improves its conspicuity specially during dark.

It is to be noted that the manhole addressed in this study does not lie in the middle of the road. It is at the corner of the road where the curve intersects the straight segment. The traffic flow and geometry of the study area indicates that vehicles do not move exactly over this manhole during off-peak hours. During peak hours only, when the traffic is near jam, the rickshaw drivers try to overtake other vehicles by utilizing the extra space available near the curve junction where this manhole is located. Placement of tire serves as an indication for potential hazard suggesting drivers to follow their usual path. This tire does not create any obstruction in the flow of traffic.



Figure 3: a) before the installation of rubber tire, b) after the installation of rubber tire.

4 Conclusions

Following conclusions can be drawn from this study:

- 1 The study location indicates that the manhole is located at a space just besides the median of the curve junction. This space is more often occupied by vehicles when the flow rate increases and the PHF is high (> 0.9).
- 2 The study findings demonstrate that there have been no accidents at the location, after the placement of the recycled rubber tire over the manhole.
- 3 The placement of rubber tire as manhole cover has deterred addicts and beggars from removing them, thus improving the safety at this specific point.
- 4 It is to be noted that mere deployment of tire over an open manhole is a temporary solution. Sustainable covers made with rubber tire strips instead of conventional steel reinforcements, is a long-term and more feasible solution.

Acknowledgment

The authors would like to acknowledge the field-work of Engr. Muhammad Shair who assisted in volume data collection, and Engr. Shahrukh and Engr. Uneeb Ahmed who arranged and placed the recycled rubber tire at the location.

References

- [1] A. Ahmed and B. Ajiaz, "A Case Study on the Potential Applications of V2V Communication for Improving Road Safety in Pakistan," *INTERACT 2023*, Apr. 2023, doi: 10.3390/engproc2023032017
- [2] A. Khurshid, A. Sohail, M. Khurshid, M. U. Shah, and A.A Jaffry, "Analysis of Road Traffic Accident Fatalities in Karachi, Pakistan: An Autopsy-Based Study", *Cureus*, vol. 13(4), e14459, 2021. <https://doi.org/10.7759/cureus.14459>
- [3] K. Muhammad, S. Shaikh, J. Ashraf, and S. Hayat, "Characteristics, reasons and patterns of Road Traffic Injuries presenting in emergency department of a tertiary care public hospital in Karachi", *Pakistan Journal of Medical Sciences*, Vol. 38 No. 4, pp. 862-867, 2022. <https://doi.org/10.12669/pjms.38.4.4490>



5th Conference on Sustainability in Civil Engineering (CSCE'23)

Department of Civil Engineering

Capital University of Science and Technology, Islamabad Pakistan



- [4] H. Abrar, M. Shah, "An Overview of Sustainable Repair Strategies for Potholes in Flexible Pavements During Rehabilitation Phase", in proceedings of the 4th Conference on Sustainability in Civil Engineering :CSCE'22, pp 368-373, Agust,2022, Islamabad, Pakistan.
- [5] S. U. Khan, A. Ahmed, S. Ali, A. Ayub, A. Shuja, and M. A. Shahid, "Use of Scrapped Rubber Tires for Sustainable Construction of Manhole Covers", *Journal of Renewable Materials*, vol. 9(5), pp. 1013–1029, 2021.
- [6] A. Bonicelli, L. G Fuentes and I. K. D. Bermejo, "Laboratory Investigation on the effects of natural fine aggregates and recycled waste tire rubber in pervious concrete to develop more sustainable pavement materials", *IOP conference Series: Materials Science and Engineering*, vol. 245(3), pp. 1-8, 2017. DOI 10.1088/1757-899X/245/3/032081.
- [7] Transportation Research Board. 2016. Highway Capacity Manual 6th Edition: A Guide for Multimodal Mobility Analysis. Washington, DC: The National Academies Press. vol.1 ch 4, pp, 2-4. DOI:10.17226/24798.
- [8] R. P. Roess, E. S. Prassas, W. R. McShane, *Traffic Engineering*, 3rd ed. Pearson/Prentice Hall, 2004, ch 5, pp. 106-117.
- [9] A. Rehman, M.M. Rathore, A. Paul, F. Saeed, and R. Ahmad, "Vehicular Traffic Optimization and Even Distribution using Ant Colony in Smart City Environment", *IET Intelligent Transport Systems*, vol. 12(7), pp.1-8. DOI:10.1049/iet-its.2017.0308



MODEL-BASED RELATIONSHIP BETWEEN RISK-TAKING BEHAVIOR OF MOTORCYCLISTS AND ITS CORRESPONDING FACTORS. A CASE STUDY AT SRINAGAR HIGHWAY ISLAMABAD AFTER MAKING IT SIGNAL-FREE ALIGNMENT

^a *Haseeb Ahsan**, ^b *Syed Bilal Ahmed Zaidi*

a: Department of Civil Engineering, UET, Taxila, Pakistan, ahsanhaseeb829@gmail.com

b: Department of Civil Engineering, UET, Taxila, Pakistan, bilal.zaidi@uettaxila.edu.pk.

* Haseeb Ahsan: Email ID: ahsanhaseeb829@gmail.com

Abstract- This study examines the factors affecting the risk-taking behavior (RTB) of motorcyclists on the Srinagar Highway in Islamabad. The reason for studying this specific area is that an abrupt change in driving behavior was observed, especially in motorcyclists. Instead of taking U-Turns, illegal crossing through the median and the use of the wrong side of the road were observed after the provision of protected U-Turns on the highway. Questionnaire-based data was collected from 350 respondents in the vicinity of the targeted area. The SPSS software was used for data screening to handle missing data. This study uses partial least squares structural equation Modelling to develop a relationship between one endogenous variable (RTB) and eight exogenous variables (demographics, arrival on time, Stress, Road Characteristics, Peer influence, special pathway for bikes, traffic rules violations, and vehicle conditions). The findings of the study show that road characteristics, peer influence, and arrival time are the most significant factors that influence the risk-taking behavior of a motorcyclist. It is suggested that instead of at-grade U-turns at the Srinagar Highway, there should be an overpass or underpass, according to the requirement. If this solution is not possible, a steel footbridge must be provided where U-Turns have been provided so that motorcyclists can cross the road easily instead of taking U-Turns. To validate the results, multinomial logistic regression was used with SPSS software. The results showed that the results obtained using the structural model were satisfactory and reliable.

Keywords- Endogenous & Exogenous variables, Footbridge, Multinomial logistic regression, Protected U-Turns, PLS-Structure Equation Modeling.

1 Introduction

Motorcycles have become a vital mode of mobility in middle-income countries and make up a significant portion of the fleet of vehicles as one entity. Although they are widely used, motorbikes still have serious safety dangers to both riders and other road users due to their high prevalence on the road and the risky driving habits of motorcycle drivers. Therefore, it is essential to identify and address the underlying factors that contribute to risky motorbike riding behaviors to reduce the incidence of accidents and promote safer travel [1]. Identifying the specific types of traffic errors and violations that contribute to motorcycle accidents is an important step in developing effective interventions to reduce the incidence of these accidents and to promote safer roadways for all users [2]. Among various causes of road accidents, two-wheeler



5th Conference on Sustainability in Civil Engineering (CSCE'23)

Department of Civil Engineering
Capital University of Science and Technology, Islamabad Pakistan



riding is a significant contributor to injuries sustained by teenagers. This group is particularly vulnerable, and understanding the factors that contribute to these injuries is crucial for developing effective preventive strategies [3].

The Capital Development Authority (CDA) implemented measures to transform the Srinagar Highway in Islamabad into a signal-free corridor. This has been achieved through the strategic integration of U-turns, despite opposition from the majority of stakeholders. The primary objective of this initiative is to alleviate traffic congestion and enhance overall traffic movement within Islamabad. The integration of U-Turns at the Srinagar Highway in Islamabad encountered resistance from Islamabad citizens. They argued that these U-Turns have led to an increase in travel duration and unnecessary fuel consumption, thereby incurring additional costs. After making the Srinagar highway signal-free alignment traffic rule violation, an increased number of accidents have been observed. Most motorcyclists used the wrong practice to cross the road through the median. They also used the wrong way to reach their destination.

It is important to study the behavior of drivers to investigate the factors that influence their behavior. These can be road characteristics, such as high-speed moving vehicles, and most motorcyclists face difficulty in taking U-Turns. There can also be a factor of increased distance for drivers to take U-Turns. Due to the increase in fuel prices, motorcyclists try to use short paths to reach their destination although it is dangerous for their life, they take a risk. So, it is important to investigate the main cause of this risky driving behavior of motorcyclists. The act of vehicles making turns and changing directions at median U-turn openings disrupts traffic flow, resulting in reduced driving speeds and diminished road capacity. Considering the distinctive physical characteristics and driving behaviors observed in such areas, the impact of median U-turns on capacity is an intriguing subject for investigation [4]. According to estimates, driver behavior has been identified as a contributing factor in approximately 90% of traffic accidents. This means that the way drivers behave on the road, including their actions, decisions, and adherence to traffic laws, plays a significant role in the occurrence of most accidents. These findings highlight the importance of promoting responsible and safe driving practices to reduce the risk of collisions and improve overall road safety [5]. A study has found that three factors affect risk-taking behavior in motorcycle riders: peer influence, confidence level, and past crash involvement. Peer influence is the most significant factor, with people who are encouraged by their friends to take risks being more likely to do so. People who are more confident in their riding skills are also more likely to take risks. Finally, people who have been in a crash in the past are more likely to take risks in the future.[6]

Our study aims to use SEM to analyze the risk-taking behavior of a motorbike user [7] stated that Structural Equation Modeling (SEM) is preferred over first-generation data analysis techniques like ANOVA and linear regression due to its ability to simultaneously analyze multiple relationships among variables, incorporate latent variables for a comprehensive understanding, assess, and account for measurement error in observed variables, evaluate model fit to assess the goodness-of-fit of the proposed model, and test complex hypotheses, including direct and indirect effects, mediation, moderation, and latent variable interactions.

This study demonstrates the previously unexplored model-based relationship between risk-taking behavior of motorcyclists and significant factors, including role violation driven by time constraints, U-turn avoidance due to road characteristics, and the influence of peer dynamics on decision-making. By understanding these relationships, policymakers and safety advocates can develop targeted interventions and strategies to reduce risk-taking behaviors among motorcyclists and promote safer riding practices. Further research in this field will contribute to the ongoing efforts to enhance road safety and protect the well-being of motorcyclists. By identifying and analyzing the complex interplay between human behavior, environmental factors, and social dynamics, this research contributes to a deeper understanding of the factors influencing road safety. The insights gained from this analysis can inform the development of road safety interventions and policies that effectively target the identified factors. By addressing these factors comprehensively, we can work towards reducing the number of road accidents, injuries, and fatalities, creating safer road environments for all.

This study investigates the relationship between risk-taking behavior of motorcyclists and significant factors, such as role violation driven by time constraints, U-turn avoidance due to road characteristics, and the influence of peer dynamics on decision-making. By understanding these relationships, policymakers and safety professionals can develop targeted interventions and strategies to reduce risk-taking behaviors among motorcyclists and promote safer riding practices.

Further research in this field will contribute to the ongoing efforts to enhance road safety and protect the well-being of motorcyclists. By identifying and analyzing the complex interplay between human behavior, environmental factors, and



social dynamics, this research contributes to a deeper understanding of the factors influencing road safety. The insights gained from this analysis can inform the development of road safety interventions and policies that effectively target the identified factors.

By addressing these factors comprehensively, we can work towards reducing the number of road accidents, injuries, and fatalities, creating safer road environments for all.

2 Research Methodology

This section outlines the steps involved in the data collection and analysis. Key aspects, such as the selection of a suitable site for data collection, development of research hypotheses, preparation and validation of a questionnaire, distribution of the questionnaire, calculation of sample size, data screening, and development of the SEM model for data analysis has been discussed in this section. A clear understanding of the methodology is essential to evaluate the credibility and accuracy of the study. The methodology flow chart is shown below in Figure 1.

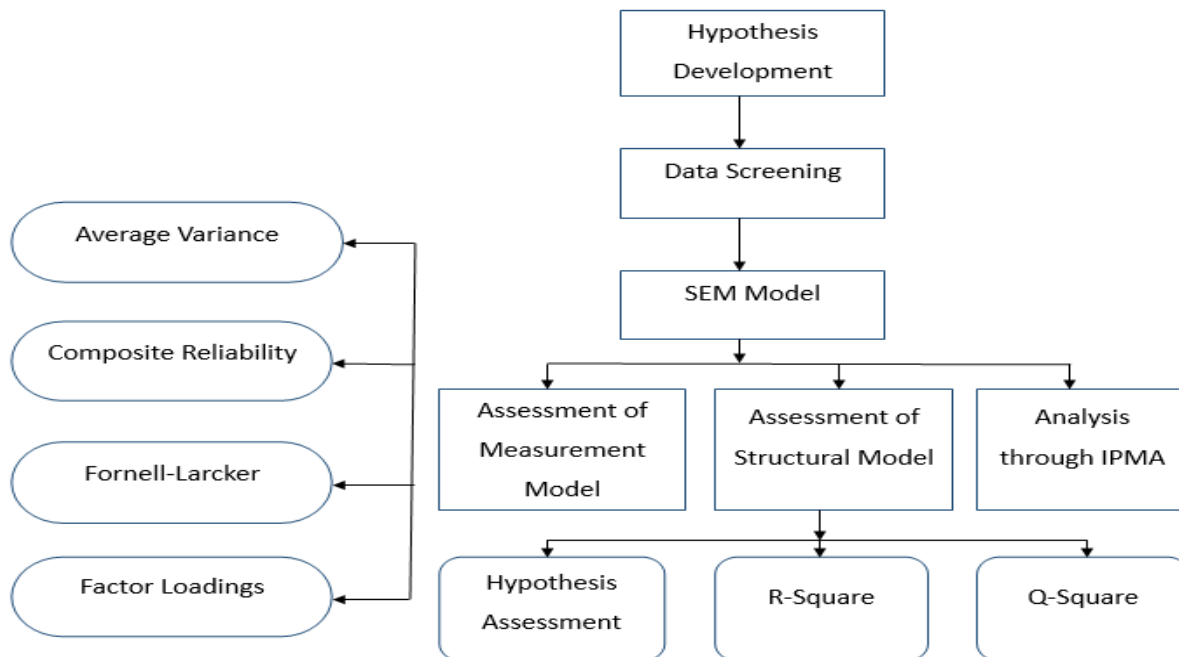


Figure 1: Methodology flow chart

In the methodology section, the study commences by formulating hypotheses to explore the influence of various exogenous variables on risk-taking behavior. The study focuses on eight specific exogenous variables, namely demographics, stress, arriving on time, road characteristics, traffic rule violations, peer influence, dedicated pathways for bikers, and vehicle condition. These variables are identified as potential factors that may affect an individual's propensity for taking risks. To collect the necessary data, a questionnaire was developed, comprising a set of structured questions tailored to the study's objectives. A diverse group of respondents provided a total of 350 responses, ensuring a wide range of perspectives. Subsequently, the collected data underwent screening and analysis using SPSS software, a widely-used tool for statistical analysis in the social sciences. This step ensured the reliability and validity of the data, facilitating a comprehensive examination of the relationships between the exogenous variables and risk-taking behavior. The analysis in this study utilized Smart PLS-4, a software tool for structural equation modeling (SEM). With Smart PLS-4, a structural equation model was constructed, consisting of a measurement model and a structural model. The measurement model was employed to assess the reliability and validity of the measured variables, ensuring the consistency and accuracy of the measurements. On the other hand, the structural model examined the relationships between the exogenous variables and risk-taking behavior, exploring how these variables influenced risk-taking. To evaluate the models' appropriateness for the study,



expert-set criteria were utilized, providing a thorough assessment of their suitability and enhancing the overall validity of the analysis

3 Data Analysis and Results

Data screening is an important step in data analysis. It includes handling missing data and outliers etc. There are different methods to handle missing data, according to our data series mean method was suitable to handle missing data. SPSS software was used to employ this method. After handling missing values, Smart-PLS Software was used to analyze the data. A structural equation model was developed using data. This model consists of two inner models, Measurement Model, and Structural Model. The structural equation model is briefly described in Figure 2 given below.

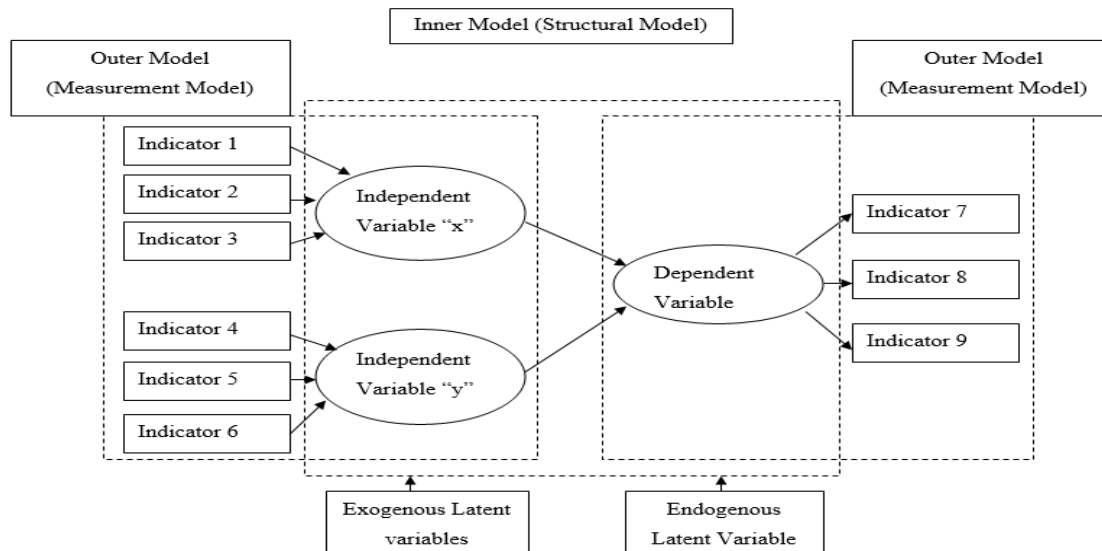


Figure 2: Structural Equation Model

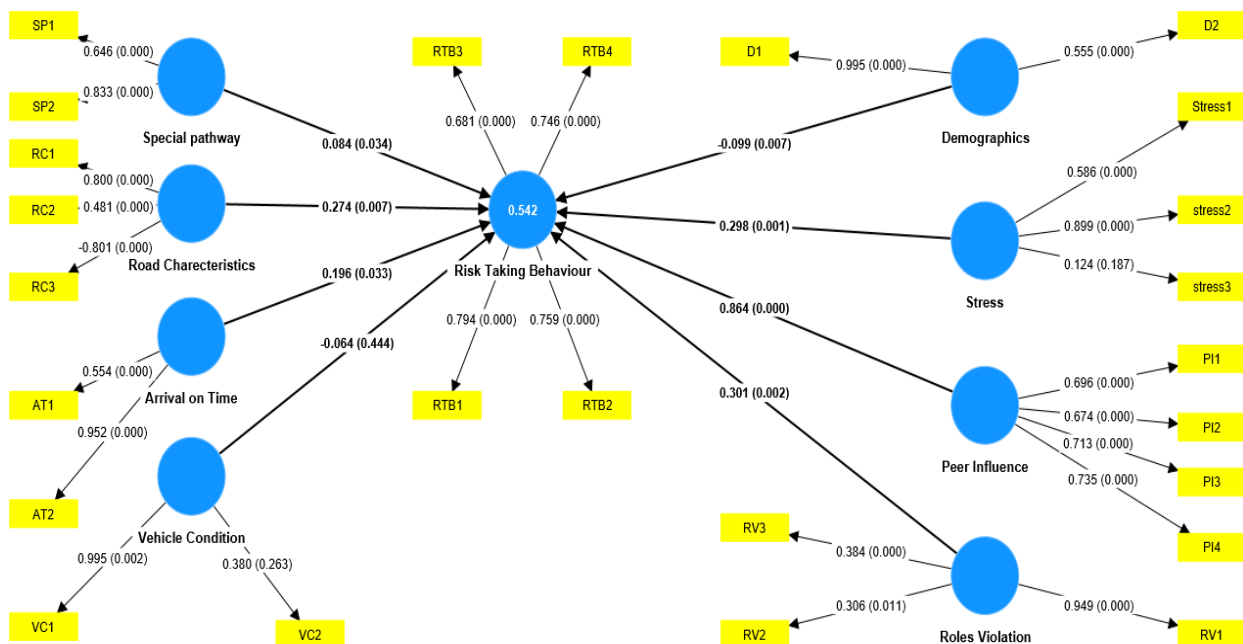


Figure 3: Structural Model Developed in Smart-PLS Software



5th Conference on Sustainability in Civil Engineering (CSCE'23)

*Department of Civil Engineering
Capital University of Science and Technology, Islamabad Pakistan*



The visual representation of the SEM model obtained from the Smart PLS software given in Figure 3 provides an overview of the relationships between exogenous and endogenous variables, along with their constructs. This representation serves as a valuable reference for understanding the conceptual framework of this study. In the first step measurement model is evaluated using different criteria set by experts. Such as average variance extracted value, composite reliability value, Fornell Larcker criteria, etc. The Average Variance Extracted (AVE) is a statistical measure used to assess the convergent validity of constructs in a research study. Generally, an AVE value greater than 0.5 is considered an acceptable threshold for establishing convergent validity. Based on the results presented by [8], the AVE values for constructs D, AT, RC, SP, and VC are reported as 0.649, 0.621, 0.504, 0.556, and 0.567, respectively. Following [9], a CR value above 0.708 was considered satisfactory. Therefore, we compared the CR values of the constructs with this threshold value. Upon evaluation, we found that constructs D (demographics), AT (arrival on time), PI (Peer Influence), and SP (a Special Pathway for Motorcyclists) had CR values above the satisfactory threshold. The CR values for these constructs are 0.774, 0.760, 0.798, and 0.711, respectively. However, constructs S (stress), RC (Road Characteristics), traffic rule violations (TRV), and vehicle conditions (VC) had CR values below the satisfactory threshold. The CR values for these constructs are 0.586, 0.163, 0.642, and 0.686, respectively. All values discussed above for average variance extracted and composite reliability are given in Table 1. Based on these findings, we can conclude that constructs D, AT, PI, and SP in the reflective measurement model demonstrated satisfactory internal consistency, as their CR values exceeded the threshold. However, constructs S, RC, TRV, and VC exhibited weaker internal consistency as their CR values fell below the threshold. These results provide insight into the reliability of the reflective measurement model. Constructs with satisfactory internal consistency can be considered reliable, whereas those with weaker internal consistency may require further investigation or refinement. The Fornell–Larcker criterion was used to assess the discriminant validity of the model. The Fornell-Larcker criterion provides guidelines for evaluating the discriminant validity of constructs in a research model. According to this criterion, the diagonal value of each construct should be larger than all the values in the corresponding column of the correlation matrix [10]. Discriminant validity was examined by assessing the AVE squared inter-correlation between constructs, following the guidelines established by [11] and [12]. Values for Discriminant Validity are given in Table 2.

Table 1: Assessment of Measurement Model Through CR & AVE Values

Variables	Composite Reliability Value	Average Variance Extracted value
Demographics	0.774	0.649
Stress	0.586	0.389
Arriving on time	0.760	0.621
Road Characteristics	0.163	0.504
Peer Influence	0.798	0.497
Special Pathway for Bikers	0.711	0.556
Implementation of traffic rules	0.642	0.402
Vehicle Condition	0.686	0.567

Table 2: Fornell-Larcker Criteria

Latent Constructs	AT	D	PI	RTB	RC	RV	SP	S	VC
AT	0.788								
D	-0.089	0.808							
PI	0.398	-0.202	0.705						
RTB	0.404	-0.288	0.649	0.746					
RC	0.208	-0.209	0.359	0.425	0.710				
RV	0.325	-0.126	0.466	0.446	0.356	0.634			
SP	0.156	-0.209	0.171	0.265	0.243	0.160	0.746		
S	0.400	-0.238	0.367	0.453	0.354	0.290	0.172	0.624	
VC	0.184	0.105	0.175	0.110	0.065	0.158	0.126	0.133	0.753

the assessment of the structural model revealed that the combination of the eight factors explained a substantial portion of the variance in RTB, with an R² value of 54.2% shown in Figure 3. Additionally, the results from Table 3 confirm that all factors, except the vehicle condition, significantly contribute to explaining RTB.



5th Conference on Sustainability in Civil Engineering (CSCE'23)

*Department of Civil Engineering
Capital University of Science and Technology, Islamabad Pakistan*



Table 3: Assessment of structural model through p-value and t value

Hypothesis	Proposed Relationship	t-statistics >1.96	p-value<0.05	Selection/Rejection
H1	Demographics → RTB	2.61	0.009	Supported
H2	Stress → RTB	3.31	0.001	Supported
H3	Arriving on time → RTB	2.05	0.040	Supported
H4	Road Characteristics → RTB	5.71	0.007	Supported
H5	Vehicle Condition → RTB	0.70	0.482	Not Supported
H6	Special Pathway → RTB	2.18	0.029	Supported
H7	Peer Influence → RTB	10.18	0.00	Supported
H8	Traffic Rules Violation → RTB	2.19	0.029	Supported

A hypothesis was developed to test the relationship between eight factors and risk-taking behavior in motorcycle riders. The hypothesis was that the eight factors would have a significant impact on risk-taking behavior, as measured by a p-value less than 0.05 and a t-value greater than 1.96.

The results of the hypothesis testing showed that seven of the eight factors were supported. The factor of vehicle condition was not supported, as the p-value of 0.482 was greater than the threshold value and the t-value of 0.70 was less than the threshold value.

The results of the hypothesis testing suggest that the seven factors of past crash involvement, confidence level, peer influence, age, gender, riding experience, and helmet use are all significant predictors of risk-taking behavior in motorcycle riders. The factor of vehicle condition was not found to be a significant predictor of risk-taking behavior.

The results of this study have implications for the development of interventions to reduce risk-taking behavior in motorcycle riders. Interventions should focus on the seven factors that were found to be significant predictors of risk-taking behavior. For example, interventions could educate riders about the risks of taking risks, provide training on how to ride safely, and encourage riders to find friends who do not encourage risky behavior.

Table 4: Results from MLR technique for assessment of model fitness.

Model Fitting Information				
Model	Model Fitting Criteria	Likelihood Ratio Tests		
	-2 Log Likelihood	Chi-Square	df	Sig.
Intercept Only	744.976			
Final	475.284	269.691	54	.000
Pseudo R-Square				
Cox and Snell				.541
Nagelkerke				.612
McFadden				.361



3.1 Use of MLR for Assessment of Model

To evaluate the fitness of our structural model, we conducted a model fitness assessment using the multinomial logistic regression (MLR) technique in SPSS. The results of the MLR analysis provided important information for evaluating the overall fit of our structural model and its ability to explain and predict the categorical outcome variables under investigation. These findings contribute to the overall assessment of model fitness and strengthen the validity of our research findings.

A p-value of less than .05 indicates a satisfactory model fit. The goodness of fit can be assessed using the Pearson and Deviance chi-square tests, with p-values greater than .05 suggesting a better fit. Likelihood ratio tests were used to ascertain the contribution of each independent variable to the dependent variable, with p-values lower than .05 shown in Table 4, indicating a significant contribution [13]. The pseudo-R² values shown in Table 4 obtained for this analysis were as follows: Cox and Snell, .541; Nagelkerke, .612; and McFadden, .361. In the case of McFadden's pseudo R², values ranging from .2 to .4 are typically considered "highly satisfactory. Cox and Snell pseudo-R², which is also derived from log-likelihoods and accounts for the sample size, cannot reach a maximum value of 1. However, Nagelkerke pseudo-R² adjusts the Cox and Snell measure to attain a value of 1 [14]. In SEM, the most commonly used method for estimation in practical applications is the minimum likelihood (ML), as highlighted by [15]. By employing ML estimation, the researchers aimed to determine the best-fitting model that would closely align the observed sample data with the expected covariances implied by the model.

4 Conclusions & Recommendations

The findings of the study highlight factors that influence risk-taking behavior:

1. Peer influence, Stress, Road characteristics, and arrival on time play important role in determining the RTB of motorcyclists.
2. From all of these influencing factors, peer influence has the most significant effect on RTB with an importance value of 0.895.
3. Motorcyclists who are encouraged by their friends to engage in overspeeding are at high risk of accidents.
4. The use of illegal road paths to reach the destination is also a significant factor that affects RTB.
5. Three U-turns have been provided at different sections of the Srinagar Highway. So, the provision of steel footbridges where U-turns have been provided can be an economical solution to minimize accident rates and they have to cover less distance comparatively.
6. It is important to educate about stress-related issues. There is a need to encourage riders to make their decision on their behalf rather than the person sitting with the driver. Both the drive and passenger must be educated about the risk and potential consequences of impaired and distracted driving behavior.

Acknowledgment

I begin by praising Allah, the Lord of all worlds, for His infinite blessings and guidance throughout my educational journey. His divine support has been instrumental in the successful completion of this thesis. I would like to express my heartfelt appreciation to my supervisor, Dr. Syed Bilal Ahmed Zaidi. His guidance, support, and expertise have played a vital role in shaping my research and enabling me to achieve this milestone. I extend my deepest thanks to my loving parents for their unwavering support and belief in my abilities. Their sacrifices, encouragement, and prayers have been my guiding light.

References

- [1] Vlahogianni, Eleni I., George Yannis, and John C. Golias. "Overview of critical risk factors in Power-Two-Wheeler safety." *Accident Analysis & Prevention* 49 (2012): 12-22.



5th Conference on Sustainability in Civil Engineering (CSCE'23)

Department of Civil Engineering

Capital University of Science and Technology, Islamabad Pakistan



- [2] Elliott, Mark A., Christopher J. Armitage, and Christopher J. Baughan. "Using the theory of planned behaviour to predict observed driving behaviour." *British Journal of social psychology* 46, no. 1 (2007): 69-90.
- [3] Varghese, Renju Rachel, Pramod Mathew Jacob, Joanna Jacob, Merlin Nissi Babu, Rupali Ravikanth, and Steph Mariyam George. "An Integrated Framework for Driver Drowsiness Detection and Alcohol Intoxication using Machine Learning." In *2021 International Conference on Data Analytics for Business and Industry (ICDABI)*, pp. 531-536. IEEE, 2021.
- [4] Tabachnick, Barbara G., and Linda S. Fidell. *Experimental designs using ANOVA*. Vol. 724. Belmont, CA: Thomson/Brooks/Cole, 2007.
- [5] Bucsuházy, Katerína, Eva Matuchová, Robert Zúvala, Pavlína Moravcová, Martina Kostíková, and Roman Mikulec. "Human factors contributing to the road traffic accident occurrence." *Transportation research procedia* 45 (2020): 555-561.
- [6] Lowry, Paul Benjamin, and James Gaskin. "Partial least squares (PLS) structural equation modeling (SEM) for building and testing behavioral causal theory: When to choose it and how to use it." *IEEE transactions on professional communication* 57, no. 2 (2014): 123-146.
- [7] Abdul Basit, Hafiz, Afaq Khattak, Qalab Abbas, Sardar Arsalan Abbas, and Arshad Hussain. "Assessment of Risk-Taking Behaviour of Young Motorcyclists at Un-Signalised Intersections—A Partial Least Square Structural Equation Modelling Approach." *Promet-Traffic&Transportation* 34, no. 1 (2022): 135-147.
- [8] Janadari, M. P. N., S. Sri Ramalu, C. Wei, and O. Y. Abdullah. "Evaluation of measurement and structural model of the reflective model constructs in PLS-SEM." In *Proceedings of the 6th International Symposium—2016 South Eastern University of Sri Lanka (SEUSL), Oluvil, Sri Lanka*, pp. 20-21. 2016.
- [9] Sarstedt, Marko, Joseph F. Hair Jr, Jun-Hwa Cheah, Jan-Michael Becker, and Christian M. Ringle. "How to specify, estimate, and validate higher-order constructs in PLS-SEM." *Australasian marketing journal* 27, no. 3 (2019): 197-211.
- [10] Wong, Ken Kwong-Kay. "Mediation analysis, categorical moderation analysis, and higher-order constructs modeling in Partial Least Squares Structural Equation Modeling (PLS-SEM): A B2B Example using SmartPLS." *Marketing Bulletin* 26, no. 1 (2016): 1-22.
- [11] De Oña, Juan, Rocío De Oña, Laura Eboli, and Gabriella Mazzulla. "Perceived service quality in bus transit service: a structural equation approach." *Transport Policy* 29 (2013): 219-226.
- [12] Hooper, Daire, Joseph Coughlan, and Michael Mullen. "Evaluating model fit: a synthesis of the structural equation modelling literature." In *7th European Conference on research methodology for business and management studies*, pp. 195-200. 2008.
- [13] Petrucci, Carrie J. "A primer for social worker researchers on how to conduct a multinomial logistic regression." *Journal of social service research* 35, no. 2 (2009): 193-205.
- [14] Tabachnick, Barbara G., and Linda S. Fidell. *Experimental designs using ANOVA*. Vol. 724. Belmont, CA: Thomson/Brooks/Cole, 2007.
- [15] Zhang, Mary F., Jeremy F. Dawson, and Rex B. Kline. "Evaluating the use of covariance-based structural equation modelling with reflective measurement in organizational and management research: A review and recommendations for best practice." *British Journal of Management* 32, no. 2 (2021): 257-272.



APPLICATION OF PLASTIC AGGREGATES IN ASPHALT MIX PAVING FOR SUSTAINABLE ENVIRONMENT

^aSaad Mehmood, ^bSyed Bilal Ahmed Zaidi*

a: Taxila Institute of Transportation Engineering, UET, Taxila, Pakistan, saad.mehmood5426@gmail.com

b: Taxila Institute of Transportation Engineering, UET, Taxila, Pakistan, bilal.zaidi@uettaxila.edu.pk

* Correspondence: saad.mehmood5426@gmail.com

Abstract- Flexible pavements use bitumen as a binder and aggregate as filler. One of the key elements of a road structure is aggregate. Researchers are looking towards alternatives to natural aggregates due to the depletion of natural resources. In this approach, plastic aggregate can be quite useful. The results of tests on asphalt mixtures using plastic aggregate derived from electronic waste as a partial replacement at 0-15% with 5% intervals demonstrate a significant result. Testing in this area revealed that while marshal stability gradually declines, performance against rut resistance significantly improves, leading to a decrease in rutting depth to from 4.78mm to 1.89mm, which demonstrated the best results at 10% partial substitution of Electronic waste plastic aggregate. Using that much percentage of Electronic waste in Flexible pavement will gradually decrease the pollution created from the Electronic waste and also contributes to the sustainability of Natural aggregates to some extent.

Keywords- Plastic aggregate, Electronic waste, modified asphalt mix, artificial aggregate.

1 Introduction

Flexible pavements use bitumen as a binder in addition to aggregates. The cost, usability, and durability of every road project depend on the caliber of the materials used and how evenly the different layers are spaced in accordance to the expected traffic loads. Aggregate is one of the essential components of a road structure. Their grade, quantity and quality play a key role in the entire service life of a pavement. Researchers are investigating innovative alternatives to natural aggregates due to the depletion of natural resources, such as reusing natural aggregates utilized in prior projects, recycling concrete waste, and creating aggregates from collected plastic.[1]

The disposal of huge quantities of poisonous and non-biodegradable waste materials poses a serious threat to the ecosystem. Many of these waste products can be adequately controlled in the construction sector by being recycled or reused. Recycling waste is important from a number of angles. It reduces environmental pollution, aids in energy conservation and recycling throughout production operations, and supports the continued use of nonrenewable natural resources.[2]

The explosive development of electronic materials over the past few decades has improved human living by revolutionizing communication, defense, and medical scientific lifestyles but presently electronic trash (Electronic waste) is developing into an unavoidable environmental concern. By using these waste products, we can maintain a healthy and sustainable ecosystem. Electronic waste is primarily produced as a result of new electronic appliance sales, including those of laptops, monitors, TVs, LE/CDs, and TVs. Additionally, the demand for aggregates in the concrete building sector is rising daily. Additionally, concrete products are depleting natural resources for aggregates. Therefore, steps should be done to recover recyclable components from Electronic waste residues in order to promote the development of sustainable Aggregate and prevent environmental contamination. Therefore, one of the potential options to ensure the sustainability of the environment is to mix Electronic waste. The electronic waste items are heated in the heating kiln below their melting point to create the electronic waste aggregates. Electronic waste aggregates are created by crushing this hot electronic debris through a particular filter size.[3]



Ahmed and Qureshi replaced 30% of the volume of NA in concrete with Electronic wastes. Additionally, concrete was strengthened by the addition of 0.75% polypropylene macro synthetic fibers. The inclusion of 0.75% macro synthetic fibers increased the compressive strength and split tensile strength values of concrete with Electronic wastes by 30% and 75%, respectively. Due to the inclusion of macro synthetic fibers, the density of concrete containing Electronic wastes somewhat increased.[4], [5]

Bituminous-mix design entails combining aggregates of varied sizes and bitumen concentrations in the best possible ratios. The wasted electronic products that are intended for reuse, resale, recycling, or disposal are referred to as electronic waste. Due to the lack of governmental control of the processing of electronic waste in poor nations, this practice may have major negative effects on public health and the environment. The utilization of recovered Electronic waste in place of coarse particles in bitumen is the subject of the current investigation.[6]

2 Problem Statement

Due to the rising demand for aggregates, natural resources are being depleted quickly, which is raising the cost of substitute materials. Aggregate availability suffers greatly as a result. Consequently, in order to stop the depletion of natural aggregates, artificial aggregates created from waste plastic, which pose a major environmental risk because it does not rapidly disintegrate naturally, should be used in place of natural aggregates.

3 Research Objectives

- Determination of Optimum bitumen Content of traditional HMA
- Optimization of Aggregates made from Electronic waste for best performance in rutting

4 Research Methodology

Electronic waste is collected from Gujranwala after a thorough review of the literature and then crushed to size range of 4.75mm-19mm with the help of crusher, and both traditional asphalt mix and modified asphalt mix with partial replacement of plastic aggregate have been put to marshal stability test and wheel tracking test. The best replacement dosage for the plastic aggregate is identified. Electronic waste aggregate is used partially in place of natural aggregate in our study up to 15% with 5% intervals. Below figure 1 is a visual representation of the research methodology:

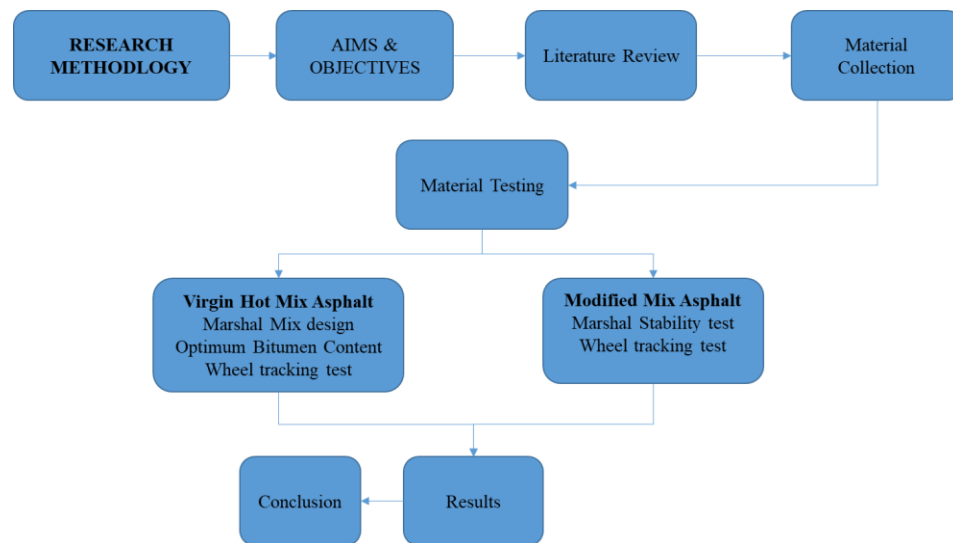


Figure 1: Research methodology



5 Results

With Hot Mix Asphalt, binder and aggregate are blended in a very specific method. The HMA's physical characteristics, which are ultimately governed by the relative proportions of these components, will determine how effectively it functions as a paved surface. As a means of testing the efficiency of modified HMA mixes, this research substitutes partially Electronic Waste plastic aggregates for natural aggregates in varying percentages (as measured by aggregate weight) in many different concrete mixes for HMA.

5.1 Sieve Analysis

To determine the particle size distribution, also known as gradation of granular materials, a sieve analysis, also known as a gradation test, is a method or procedure used in civil engineering that measures the amount of material that is stopped by each sieve as a percentage of the total mass. Gradation used in this research is NHA class B, whose gradation is shown in figure 2.

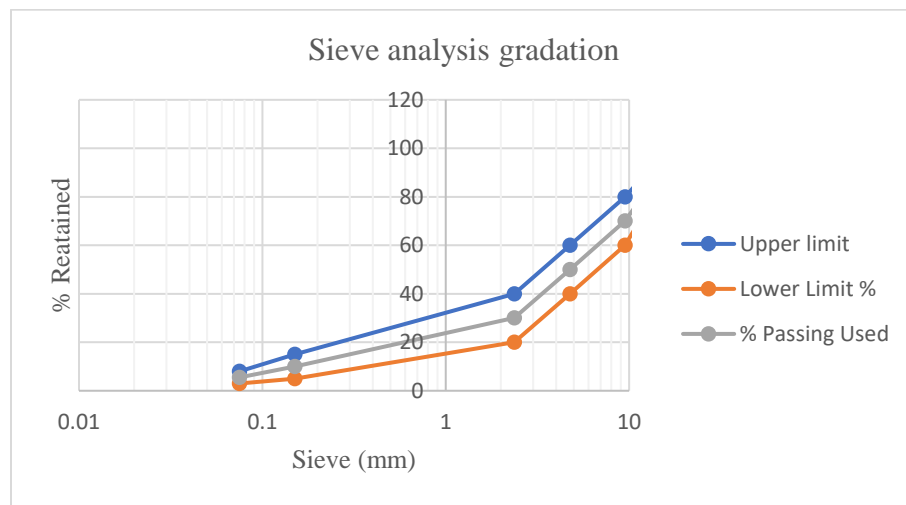


Figure 2: Sieve analysis of NHA class B

5.2 Properties of Plastic Aggregate Made from Electronic Waste

Properties of plastic aggregates characterize them and aids in understanding the behaviour of plastic aggregates made from electronic waste. Further testing is performed after knowing the specific gravity, water absorption and melting point of these aggregates. Table 1 shows the findings.

Table 1 Properties of plastic aggregates

Sr. No.	Properties of Aggregates	Test Results (Electronic waste)
1	Specific Gravity (g/cm ³)	1.34
2	Water Absorption (%)	0.15
3	Melting Point (°C)	255

5.3 Determination of Optimum Bitumen Content

Optimum bitumen content is the prime factor for designing the HMA. For determining the OBC, 3 compacted samples and one loose sample at each percent of bitumen content (3.5%, 4%, 4.5%, 5% & 5.5%) are made. Test method employed



5th Conference on Sustainability in Civil Engineering (CSCE'23)

Department of Civil Engineering
Capital University of Science and Technology, Islamabad Pakistan



for determination of OBC is Marshal Stability Method for mix design ASTM-D6927. Table 2 below shows the average value of Optimum Bitumen Content.

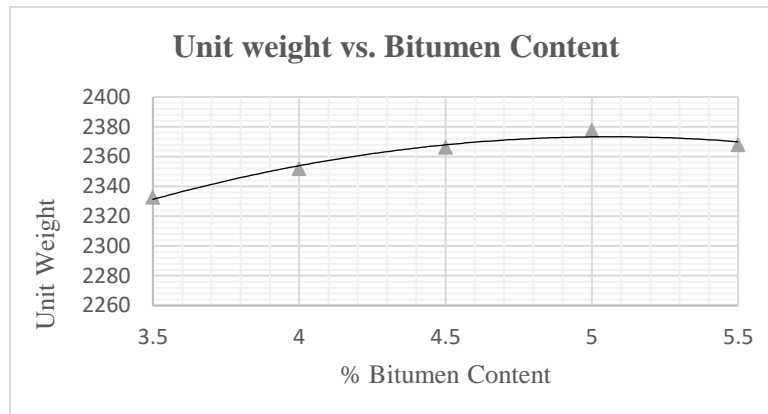


Figure 3: Unit weight vs Bitumen content

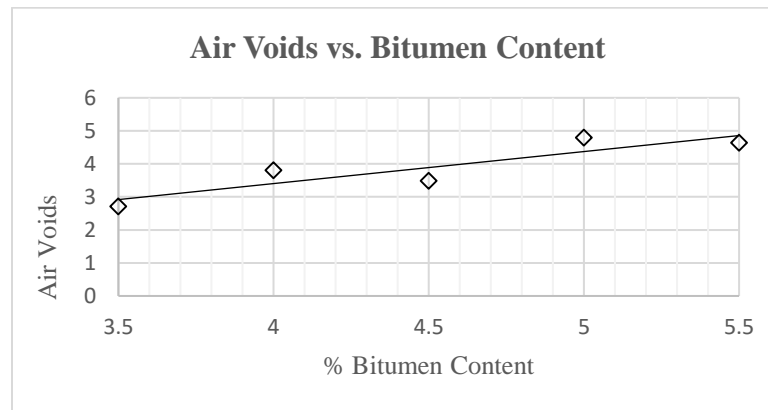


Figure 4: Air voids vs Bitumen content

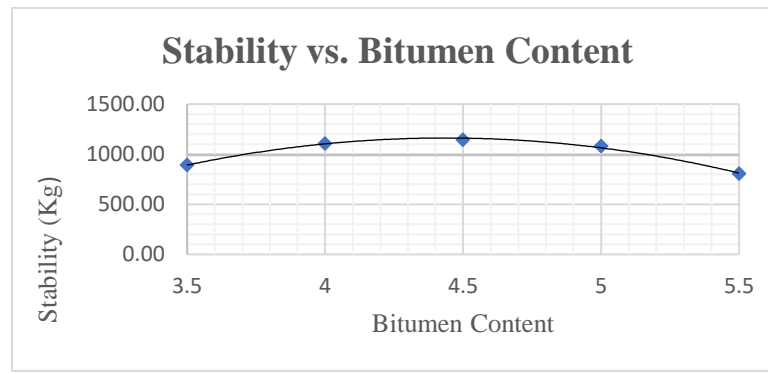


Figure 5: Stability vs Bitumen content

Table 2 Optimum bitumen content

Bitumen Content at Max Stability	4.5
Bitumen Content at 3% Air Void	3.6
Bitumen Content at Max Unit Weight	5
OBC (Optimum Bitumen Content)	4.3667



Based upon the Max. Stability, Air Voids and Max. Unit weight figure 3, figure 4 and figure 5 demonstrate the Maximum value of 4.5%, 3.6%, 5% bitumen content respectively. Computing the average of these three findings, gave the optimum bitumen content (OBC) of 4.36% as shown in table 2.

5.4 Effect of Electronic Waste on Marshall Stability

During constant deformation, the Marshall Stability load is the maximum load at which resistance occurs. Three replicates of each original and modified specimen undergone for a stability test. Plastic aggregates are partially replaced with natural aggregates ranging from 4.75mm-19mm sieve sizes. Asphalt concrete's load-resistance performance has been slightly decreased by the presence of plastic aggregate. Marshall Stability values, related to plastic content as a partial replacement of aggregates, can be seen in the table 3 below.

Table 3 Effect of Electronic waste on Marshall Stability

Marshall Stability (kg)						
0% Replacement		5% Replacement		10% Replacement		15% Replacement
1337.7	Average Value= 1288.61	1314.69	Average Value= 1277.87	1222.64	Average Value= 1253.32	1107.59
1245.66		1245.66		1280.17		1280.17
1282.48		1273.27		1257.16		1238.75

When plastic waste was added up to 5% by weight of natural aggregates, stability practically decreased with a drop of 0.8%, but if plastic content was increased up to 15%, stability was lowered by roughly 6.19%. Zero percent plastic content yields the best stability rating, while fifteen percent yields the lowest. In spite of a decline in stability with increasing plastic content (up to 15%), the value is still well within the Marshall Mix design parameters for large traffic loads (i.e., more than 1000 kg). The findings of the tests show that recycled Electronic waste plastic may be used in lieu of some of the natural aggregate in hot mix asphalt concrete. The aforesaid experimental findings are shown in the figure 6 below.

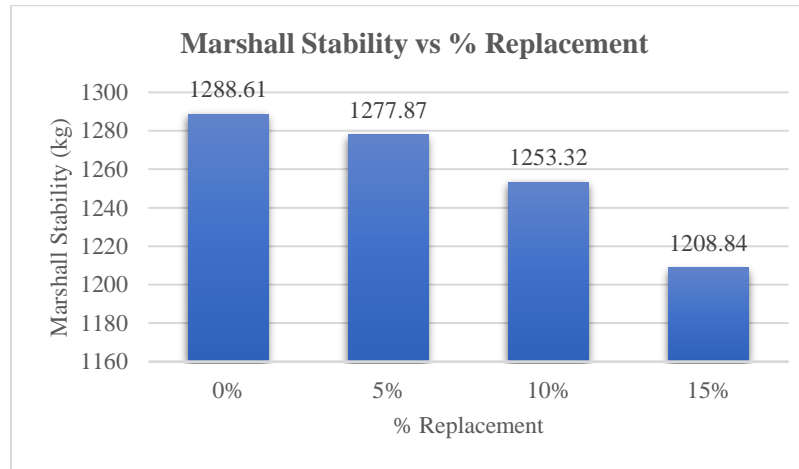


Figure 6: Effect of Electronic waste on Marshall Stability



5.5 Effects of Electronic waste on rut resistance performance

Rutting brought on by repeated loadings has long raised concerns about the performance of HMA pavement. Rutting's rate and intensity are influenced by behavioral as well as environmental factors. External factors include things like temperature, tire pressure, load, and the volume of truck traffic. Internal factors include mixture quality, bitumen, aggregate, and pavement depth. Here, 3 replicates are prepared for standard and modified HMA mixes (5%, 10% & 15%) at each percentage in which plastic aggregates are partially replaced with natural aggregates ranging from 4.75mm-19mm sieve sizes, both of which adhere to Marshall Properties are compared for their rut-resistance capabilities using wheel tracker test. Table 4 below displays the outcomes of this finding.

Table 4 Effects of Electronic waste on rut resistance performance

Rutting (mm) (10000 passes)						
0% Replacement		5% Replacement		10% Replacement		15% Replacement
4.74	Average Value = 4.78	1.99	Average Value =2.04	1.91	Average Value =1.89	9.1
4.9		2.08		1.87		10.1
4.7		2.06		1.9		9.7

Figure 7 demonstrates that the wheel tracking rate of modified HMA is lower than that of conventional HMA concrete. The maximum rut depth for conventional HMA mixes after 10,000 cycles at 55°C is 4.78 mm, whereas the maximum rut depth for modified HMA mixes at 10% replacement using same test conditions is 1.86 mm. Consequently, a typical hot mix asphalt concrete's rutting depth may be decreased by 61.08% when employing the optimal dose of plastic aggregate component in the mix. However, the data showed that modified mix was much better at resisting ruts than regular mix.

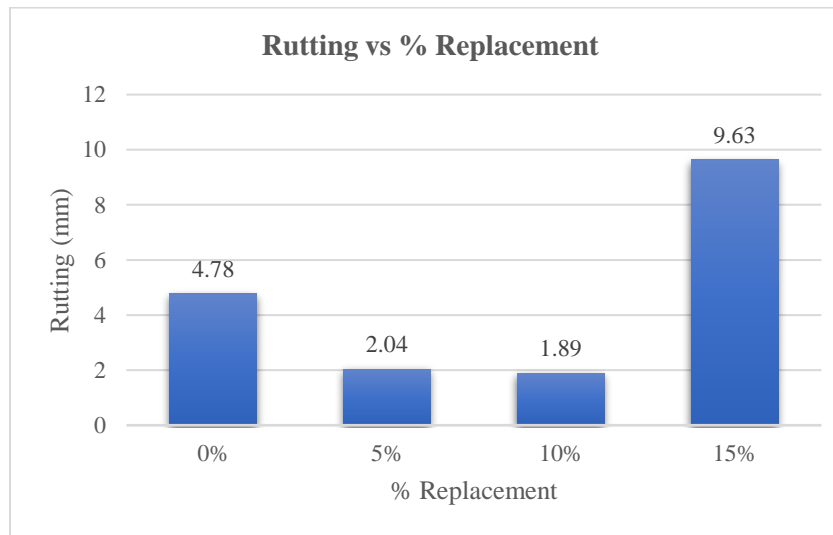


Figure 7: Effects of Electronic waste on rut resistance performance



6 Conclusions

Test results on asphalt mix with partial replacement of plastic aggregate made from Electronic waste at 0-15% replacement with 5% interval shows a considerable outcome. Testing conducted in this regard showed that marshal stability decreases continuously but performance against rut resistance increased considerably, as a result rutting depth decreased to 1.89mm, which showed the Optimum result at 10% of partial replacement of Electronic waste plastic aggregate. Beyond the 10 % content of partially replaced Electronic waste aggregate resistance to permanent deformation (rutting) reduces.

Research Study on this topic shows that with the depleting natural resources, Plastic aggregate can play an important role in sustaining the Natural aggregate to some extent, as it performed well against major problem like rutting.

Acknowledgment

I would firstly like to thank Almighty Allah for his blessings over me to complete this project. Secondly, I would like to thank my supervisor Dr. Syed Bilal Ahmed Zaidi for his continuous support and guidance during this project. I would also like to thank the Lab staff at University of Engineering and Technology, Taxila for being so helpful. Finally, I must express my very profound gratitude to my Father Mr. Sajid Mehmood and other family members for providing me with unfailing support and continuous encouragement throughout my years of study and through the process of researching and writing this thesis. This accomplishment would not have been possible without them. Thank you all.

References

- [1] S. Ullah, M. Raheel, R. Khan, and M. Tariq Khan, "Characterization of physical & mechanical properties of asphalt concrete containing low- & high-density polyethylene waste as aggregates," *Constr. Build. Mater.*, vol. 301, no. May, p. 124127, 2021, doi: 10.1016/j.conbuildmat.2021.124127.
- [2] S. Muthukumar, O. K. C. Bavithran, A. R. Nandhagopal, and T. Snehasree, "Stability study on eco-friendly Flexible pavement using E-waste and Hips," *Int. J. Civ. Eng. Technol.*, vol. 8, no. 10, pp. 956–965, 2017.
- [3] S. Ullah *et al.*, "Effect of partial replacement of E-waste as a fine aggregate on compressive behavior of concrete specimens having different geometry with and without CFRP confinement," *J. Build. Eng.*, vol. 50, no. November 2021, p. 104151, 2022, doi: 10.1016/j.jobe.2022.104151.
- [4] S. N. Abbas, M. I. Qureshi, M. Abid, M. A. U. R. Tariq, and A. W. M. Ng, "An Investigation of Mechanical Properties of Concrete by Applying Sand Coating on Recycled High-Density Polyethylene (HDPE) and Electronic-Wastes (E-Wastes) Used as a Partial Replacement of Natural Coarse Aggregates," *Sustain.*, vol. 14, no. 7, 2022, doi: 10.3390/su14074087.
- [5] A. M. A. Abdo, "Investigation the effects of adding waste plastic on asphalt mixes performance," *ARPEN J. Eng. Appl. Sci.*, vol. 12, no. 15, pp. 4351–4356, 2017.
- [6] M. K. Singh and P. Malviya, "An Experimental Study on Partial Replacement of Aggregate by E-Waste for Flexible Pavement," *Int. J. Trend Sci. Res. Dev.*, vol. Volume-3, no. Issue-3, pp. 382–384, 2019, doi: 10.31142/ijtsrd22865.



OPTIMIZING TRAFFIC FLOW AT SANGJANI TOLL PLAZA IN ISLAMABAD: A SIMULATION STUDY USING DIFFERENT LANE PATTERNS

^a Umer Sabahuddin Gill, ^b Jawad Hussain, ^c Ghulam Abbas

a: Department of Civil Engineering, UET, Taxila, Pakistan, umer.sb.gill@gmail.com

b: Department of Civil Engineering, UET, Taxila, Pakistan, jawad.hussain@uettaxila.edu.pk

c: Department of Civil Engineering, UET, Taxila, Pakistan, ghulamabbas696@yahoo.com

Abstract-Pakistan is a developing country experiencing rapid urbanization and migration of people from rural to urban areas for their daily business activities. To improve transportation for people, Pakistan constructed a Toll Plaza on the National Highway. However, toll plazas can sometimes cause traffic jams because vehicles have to stop to pay the toll, leading to a decrease in traffic flow and longer waiting times. The study aimed to reduce waiting times at toll plazas by creating a simulation model to determine the best lane pattern. Data was collected between 1:00 PM-3:00 PM in March of 2023, and VISSIM software was used for the simulation. Results showed that changing the lane pattern can significantly reduce waiting times and queue length, with waiting times being reduced by up to 95.06% and queue length by up to 67.45%. This study can be helpful in determining the best lane arrangement to reduce traffic delays at toll plazas.

Keywords: Lane pattern, Simulation model, Toll Plaza, Traffic flow, VISSIM software

1 Introduction:

Traffic congestion is one of the major problems faced by urban areas. Toll plazas are one of the critical points of a highway network where traffic is controlled for the purpose of collecting tolls. Due to the increase in the number of vehicles and inadequate infrastructure, toll plazas are becoming major sources of congestion, leading to delays, fuel wastage, and increased travel time. The Sangjani toll plaza located in Islamabad, Pakistan, is one such example where the flow of traffic is impeded due to its location and inadequate infrastructure. Various methods have been proposed to optimize the flow of traffic at toll plazas, such as the introduction of electronic toll collection (ETC) systems and the use of different lane patterns[1]. In this paper, we propose a simulation study to optimize the traffic flow at the Sangjani toll plaza using different lane patterns. Toll plazas are an essential component of road infrastructure, enabling the collection of fees for the use of roads and bridges[2]. However, toll plazas also contribute to traffic congestion, as vehicles have to slow down or stop to pay tolls, leading to increased travel time, fuel consumption, and emissions[3]. Various studies have been conducted to optimize traffic flow at toll plazas, with the aim of reducing traffic congestion and improving travel efficiency. Simulation models have been widely used to evaluate different toll plaza management practices, including lane configurations, toll collection methods, and queue management strategies[4]. One common strategy for optimizing traffic flow at toll plazas is the use of electronic toll collection (ETC) systems. ETC systems allow for faster and smoother toll collection, as vehicles do not have to stop to pay tolls[5]. Studies have shown that the use of ETC systems can significantly reduce travel time, fuel consumption, and emissions at toll plaza. Lane configurations have also been studied extensively for optimizing traffic flow at toll plazas[6]. Dedicated ETC lanes have been found to be more efficient than mixed lanes, as they reduce the number of vehicles waiting in queues and allow for faster toll collection. Dedicated cash lanes have also been found to be more efficient than mixed lanes, but less efficient than dedicated ETC lanes[7, 8]. Queue management strategies have also been studied for optimizing traffic flow at toll plazas. Dynamic pricing strategies, which adjust toll rates based on traffic conditions, have been found to be effective in reducing traffic congestion[8]. In summary, various toll plaza management practices have been studied for optimizing traffic flow and

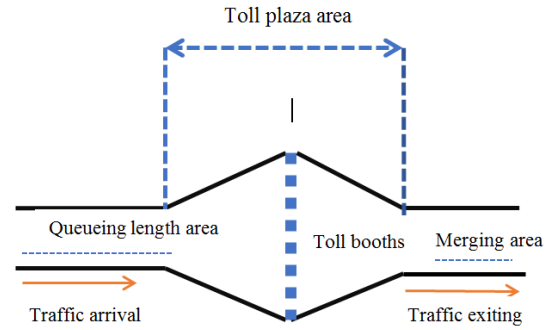
Paper ID. 23-510



reducing traffic congestion. The use of ETC systems, dedicated lanes, and queue management strategies has been found to be effective in improving travel efficiency at toll plazas. However, the effectiveness of these practices may vary depending on the specific toll plaza configuration and traffic conditions. A simulation study can provide valuable insights into the performance of different toll plaza management practices under various scenarios.



a)



b)

Figure 1: (a) Study area (b) Sangjani toll plaza layout

The Sangjani Toll Plaza is located on the Islamabad-Peshawar N-5 in the Islamabad Capital Territory of Pakistan that shown in figures 1(a) (b). The area surrounding the toll plaza is predominantly rural, with scattered villages and farmland. The Margalla Hills National Park is located to the east of the plaza, providing a scenic backdrop to the area. The toll plaza itself consists of several lanes for both electronic toll collection (ETC) and manual toll collection. It is one of the busiest toll plazas in Pakistan, serving as a major gateway for traffic travelling between Islamabad and Peshawar. The plaza is operated by the National Highway Authority (NHA) of Pakistan and is an important source of revenue for the government. However, the toll plaza has also faced criticism for causing traffic congestion and delays during peak hours. Overall, the Sangjani Toll Plaza serves as a vital transportation hub for the region, connecting major cities and providing a key source of revenue for the government.

2 Literature Review

Toll plazas are often major sources of congestion and delay in urban areas. Researchers have proposed various solutions to optimize the flow of traffic at toll plazas, including the use of ETC systems and different lane patterns[9]. Electronic toll collection (ETC) systems have been shown to significantly reduce congestion and delays at toll plazas. ETC systems use electronic sensors to detect vehicles and automatically deduct tolls from a driver's account, eliminating the need for drivers to stop and pay cash[10]. Several studies have shown that the introduction of ETC systems at toll plazas can reduce travel time, delay, and fuel consumption, thereby improving the overall efficiency of toll plaza operations. Another approach to optimizing traffic flow at toll plazas is the use of different lane patterns. This research investigated the effectiveness of different lane patterns in reducing congestion and delay at toll plaza[11]. A study evaluated the performance of different lane configurations at toll plazas and found that a combination of dedicated ETC lanes and mixed-use lanes (i.e., lanes that accept both cash and ETC payments) was the most effective in reducing delay and improving traffic flow[12]. Similarly, a study found that the use of dedicated ETC lanes and dedicated cash lanes was the most effective in reducing delay at toll plazas. Despite the existing research, there is a lack of studies that have investigated the optimal use of different lane patterns at toll plazas in Pakistan. The proposed simulation study aims to fill this gap by evaluating the performance of different lane patterns at the Sangjani toll plaza in Islamabad, Pakistan. Overall, the literature review shows that toll plazas are critical points in highway networks, and the optimization of traffic flow is essential to reduce congestion and improve efficiency. Electronic toll collection systems and different lane patterns are effective solutions that can be used to optimize the flow of traffic at toll plazas. The proposed simulation study aims to contribute to the existing literature by evaluating the effectiveness of different lane patterns at the Sangjani toll plaza in Islamabad, Pakistan.



3 Methodology

The proposed study used a simulation approach to evaluate the performance of different lane patterns in optimizing traffic flow at the Sangjani toll plaza in Islamabad, Pakistan. The simulation has been conducted using PTV Vissim, traffic simulation software widely used for modeling and simulating traffic flow in various scenarios.

3.1 Data Collection

The research process involves data collection to develop an accurate representation of the Sangjani toll plaza. The data includes the layout of the toll plaza, the number of lanes, the traffic volume, and the types of vehicles using the toll plaza. The data has been collected from the National Highway Authority (NHA) and other relevant sources as described in Table 1.

Table 1: Data collection at Sangjani toll plaza

Time(minutes)	Traffic volume	Length (m)	Cash payment	Exempted
1:00-1:15	240	0.68	217	23
1:15-1:30	254	1.03	247	7
1:30-1:45	201	1.51	167	34
1:45- 2:00	302	2.18	292	10
2:00-2:15	234	3.1	221	13
2:15-2:30	194	4.43	194	0
2:30-2:45	312	6.5	300	12
2:45-3:00	342	7.6	342	0

3.2 Model Development

The second step involves the development of a model of the Sangjani toll plaza using PTV Vissim. The model contains a representation of the physical layout of the toll plaza, the number of lanes, types of lanes and the traffic volume. The model has been calibrated and validated using real-world data collected from the toll plaza.

3.3 Lane Pattern Scenarios

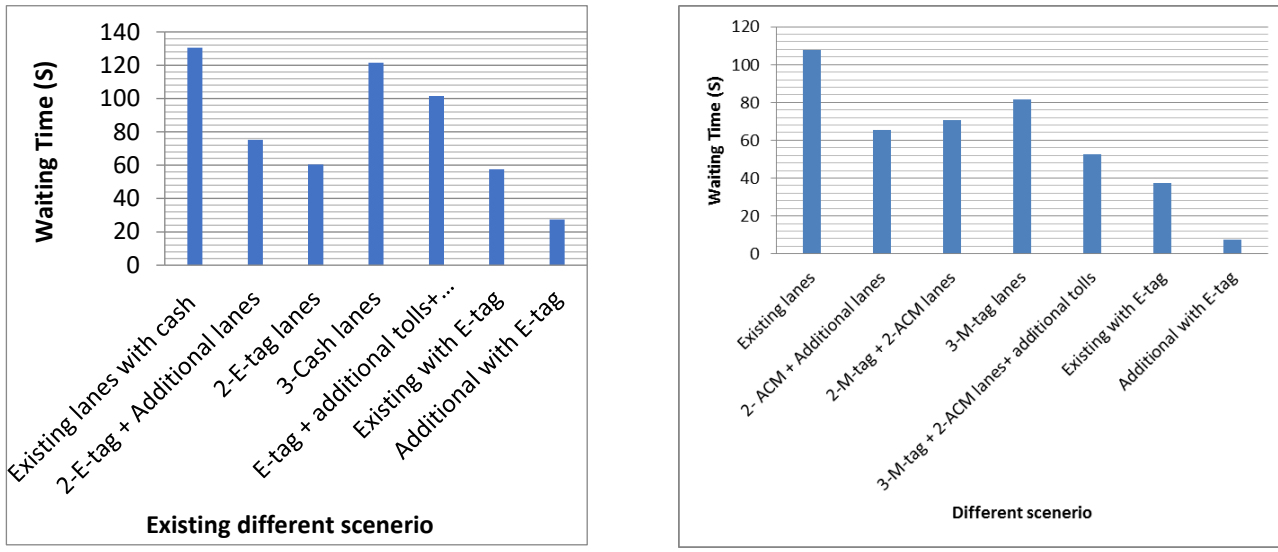
The development of different lane pattern scenarios is used to simulate and evaluate their performance. The lane pattern scenarios include a mixed pattern of cash and ETC lanes, dedicated ETC lanes, and dedicated cash lanes. Each scenario has been simulated using PTV Vissim, and the traffic volume, travel time and delay is recorded.

3.4 Performance Evaluation

Model is responsible for the evaluation of the performance of each lane pattern scenario. The performance indicators include travel time, delay, Queue length and the number of vehicles using each lane. The results have been compared across the different lane patterns, and the most effective lane pattern to be identified.

4 Results and Discussion

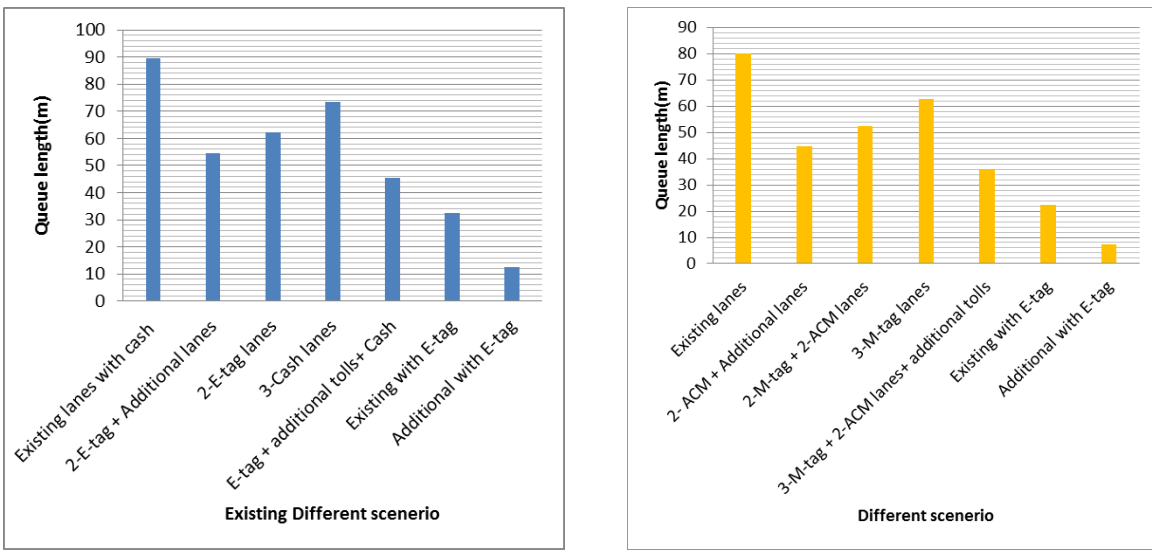
The Existing pattern of cash and ETC lanes resulted in the highest delay for vehicles using the toll plaza. This pattern caused a bottleneck at the toll plaza due to the slower cash lanes. The average delay per vehicle was recorded as 2 minutes and 10 sec. According to figure 2(a) if the lanes are not properly allocated or if there is an imbalance between cash and electronic toll collection (ETC) lanes, it can lead to longer waiting time for specific lanes. An optimal lane configuration that considers traffic patterns and payment preferences can help reduce waiting time.



a)

Figure 2: Waiting time and each lane of different scenario, (b) Waiting time and each lane of different scenario

According to (Figure 2b) those variations in the number of lanes affect waiting time, with more lanes and E-tag resulting in shorter waiting time. Optimal allocation of cash and electronic toll collection lanes reduces waiting time for different payment methods. Dedicated lanes for specific vehicles streamline traffic flow and decrease waiting time. According to these results traffic lanes management seems to be helpful to optimize waiting times and enhance toll plaza efficiency. Allocating lanes optimally based on payment methods logically leads to efficient toll collection and minimizes waiting time for specific lanes. Incorporating dedicated lanes logically streamlines traffic flow by segregating vehicles, thus reducing congestion and waiting time.



a)

Figure 3: (a) Queue length of traffic vs. existing different lanes pattern scenario, (b) Quae length of traffic vs different lanes pattern scenario

The already existing lanes pattern scenario in a simulation of traffic at a toll plaza logically impacts queue length that is shown in (figure 3a). A limited number of lanes logically lead to longer queues as vehicles have to wait for their turn to pass through the toll booths. An imbalanced lane distribution, with more cash lanes and fewer electronic toll collection (ETC) lanes, logically results in longer queues for cash transactions, causing congestion and increasing overall queue



length. The absence of dedicated lanes for specific vehicle types logically contributes to increased queue length as commercial trucks and high-occupancy vehicles merge with other traffic. Inefficient toll collection procedures logically lead to longer queues, as slow transactions and technical issues delay the process. Without regular monitoring and adjustment of the lanes pattern scenario based on traffic patterns, logical opportunities to improve queue length may be missed. Therefore, it is crucial to address these factors in order to minimize queue length and optimize traffic flow at the toll plaza.

The simulation study using PTV Vissim showed that different lane patterns can have a significant impact on the performance of the Sangjani toll plaza in Islamabad, Pakistan. The following results were observed:

The distribution of lanes for different types of payment methods also affects the queue length. If there are unequal proportions of cash lanes and electronic toll collection (ETC) lanes, as results are shown in figure 3(b), the queue length for cash lanes is longer, leading to congestion and delays. An optimal distribution of lanes based on traffic patterns and payment preferences can help balance the queue length. The presence of ETC lanes significantly impacts the queue length. ETC lanes allow for non-stop toll collection, as vehicles equipped with E-tags can pass through without stopping. This reduces the 30% queue length for ETC lanes, as vehicles can maintain a continuous flow. Efficient lane management and adequate staffing can help optimize the queue length. Toll plaza operators can actively monitor the traffic flow and adjust the number of open lanes based on real-time demand. Additionally, having sufficient toll operators and personnel at toll booths ensures smoother and quicker transactions, reducing the queue length.

5 Conclusions

- The results shows that the throughput vs. current lanes scenario are maximum 45% of the additional with E-tag lanes ,40% of the existing with E-tag lanes ,38% of the E-tag + additional toll+ cash,32% of the3- cash lanes,28% of the 2-E-tag lanes.
- Based on the results of the simulation study, it can be concluded that the dedicated ETC lane pattern and E-tag are the most effective lane pattern for optimizing traffic flow at the Sangjani toll plaza in Islamabad, Pakistan.
- This pattern allows for smoother flow of traffic through the toll plaza, reducing the delay 18% per vehicle and fuel consumption.
- The results of this study can be used by toll plaza operators and transportation planners to implement more efficient toll plaza management practices. If the existing lanes pattern scenario is not regularly monitored and adjusted based on traffic patterns, it logically contributes to 20% longer queues.
- Without proactive evaluation and optimization, opportunities to improve 63% queue length.

6 Recommendations

- It is recommended to increase the number of lanes at Sangjani Toll Plaza. This will help accommodate higher traffic volume and reduce waiting times, resulting in improved traffic flow. And in this research different lanes pattern means different types of toll collection system facilitate the transporter.
- The benefits of an optimal allocation of cash and ETC lanes. It is recommended to maintain a balanced distribution that caters to different payment preferences, reducing congestion and waiting times for both payment methods.
- It is recommended to employ proper signage, lane merging techniques, and dedicated toll plaza personnel to facilitate smoother traffic flow and minimize congestion, ultimately reducing waiting times.

References

- [1] Xiang, W., et al., *Optimizing guidance signage system to improve drivers' lane-changing behavior at the expressway toll plaza*. 2022. **90**: p. 382-396.



5th Conference on Sustainability in Civil Engineering (CSCE'23)

Department of Civil Engineering

Capital University of Science and Technology, Islamabad Pakistan



- [2] Liang, T., *Research on the environmental benefits of the cancellation of the main toll stations based on traffic simulation model*, in *Frontier Research: Road and Traffic Engineering*. 2022, CRC Press. p. 155-167.
- [3] Silveira-Santos, T., L.d.S. Portugal, and P.C.M.J.J.o.I.S. Ribeiro, *Using a Discrete-Event Simulation Model for Evaluating the Operational Performance of Toll Plazas*. 2023. **29**(1): p. 05022007.
- [4] Sewagegn, A.J.P.s.C., *OPTIMIZATION OF TOLL SERVICES USING QUEUING THEORY IN THE CASE OF ETHIOPIA*. 2022. **17**(2).
- [5] Wang, H., et al., *Analysis on Lane Capacity for Expressway Toll Station Using Toll Data*. 2022. **2022**.
- [6] Mujeeb, A., et al., *Electronic Toll Collector Framework*. 2022. **16**(1): p. 294-302.
- [7] Bari, C.S., et al., *Delay modelling at manually operated toll plazas under mixed traffic conditions*. 2022. **11**(1): p. 17-31.
- [8] Wang, J., J. Weng, and X. Wang, *Congestion Analysis of the Toll Station Based on GPS Data*, in *CICTP 2022*. 2022. p. 1608-1617.
- [9] Bains, M.S., et al., *Optimizing and modeling tollway operations using microsimulation: case study Sanand Toll Plaza, Ahmedabad, Gujarat, India*. 2017. **26****15**(1): p. 43-54.
- [10] Ramandanis, I.-D., I. Politis, and S.J.S. Basbas, *Assessing the environmental and economic footprint of electronic toll collection lanes: A simulation study*. 2020. **12**(22): p. 9578.
- [11] Ahmad, S., et al., *A Simulation-Based Study for the Optimization of Toll Plaza with Different Lane Configuration: A Case Study of Ravi Toll Plaza Lahore, Pakistan*. 2021. **11**(2): p. 157-165.
- [12] Mittal, H. and N.J.J.o.A.S. Sharma, *Operational Optimization of Toll Plaza Queue Length Using Microscopic Simulation VISSIM Model*. 2022. **13**(1): p. 418-425.



IMPACT OF SILICA FUME AND BIOCHAR TREATMENT ON THE MECHANICAL CHARACTERISTICS OF LOW PLASTIC SOILS

^a Muhammad Waleed*, ^b Moazam Sattar, ^c Ezaz Jehangir

a: NICE, SCEE, NUST, H/12 Campus, Islamabad, 44000, Pakistan, rajawaleed918@gmail.com

b: Department of Civil Engineering, UET, Taxila, Pakistan, moazam.malik59@gmail.com

c: Civil Engineering Department, Army Public College of Management & Sciences Rawalpindi, Pakistan, ezazjehangir@gmail.com

*Corresponding author: rajawaleed918@gmail.com

Abstract- Bio-cementation soil treatment technique has shown significant strength improvement in the soils. Low plastic silt soils are present in many areas of Pakistan, making the need for acceptable engineering properties to support construction activities necessary. In the current study, silica fume and biochar were used in an attempt to test the unconfined compressive strength (UCS). Several tests including the liquid limit, plastic limit, compaction test and unconfined compressive strength, were carried out on two types of soils with various additions to access the strength parameter. This study aimed to assess the impact of silica fume and biochar treatments on soil UCS results. According to the results, adding silica fume raised the UCS strength by up to 52.85%, while adding biochar enhanced it by up to 117%. Overall, this study highlights that silica fume and biochar have the potential to improve soil properties as a cost-effective and efficient solution for enhancing soil characteristics, particularly in construction projects that require compaction.

Keywords- Biochar, Unconfined compressive strength, silica fume, compaction test.

1 Introduction

Many countries, including Pakistan have a significant presence of low-plasticity silt within their territories. Liquefaction of low plasticity silt is a frequent occurrence during earthquakes, leading to infrastructure damage and the risk of loss of life and this phenomenon has been observed in various earthquakes [1]. Nevertheless, the detrimental consequences on infrastructure and the potential for loss of life are not limited solely to earthquakes. In certain cases, slope failures have been attributed not only due to earthquakes but also to substantial deformations during reconsolidation, accompanied by diminished shear strength [2]. Characterizing low-plasticity silt in laboratory settings poses significant challenges. The preparation and handling of low-plasticity silt specimens for testing purposes are particularly troublesome. This difficulty arises from the material's apparent lack of cohesion, leading to its high friability. As a result, the fabric of low-plasticity silt tends to fracture during the sampling, trimming, and preparation processes [3]. Employing soils found within the project rights-of-way presents an alternative approach that promotes the preservation of natural resources. To implement this alternative, a commonly utilized technique is soil stabilization, which involves the use of lime, hydraulic binders, chemical grouting, and soil reinforcement with geosynthetics and other similar materials this technique aims to enhance the workability and hydromechanical properties of soils, enabling their improved performance [4-7]. Soil stabilization has become a crucial aspect of construction projects such as dam and road construction. The process involves adding and blending different materials to the soil to enhance its properties, leading to long-term stability and improved shear strength



parameters. This ultimately enhances the soil's load-bearing capacity, enabling it to support the structure more effectively [8].

Al-Khalili et al. (2021) studied the effect of metakaolin and silica fume on the engineering properties of expansive soil. Their study found that adding silica fume decreased the maximum dry unit weight and the optimal moisture content increased with the addition of silica fume. The liquid limit, plastic limit, and plasticity index of the soil increased as the silica fume increased, reaching maximum values with 15% silica fume [9]. Al-Obaidi, Al-Mukhtar et al. (2020) a comparative study of silica fume and nano-silica that improve the shear strength and collapsibility of high gypseous soil was undertaken. The results of test showed that adding silica fume or nano silica fume to highly gypseous soils improved their engineering qualities, especially when the soil was saturated [10]. Bharadwaj and Trivedi (2016) conducted different experiments to check the impact of micro silica fume on engineering properties of expansive soil. During experiments the different percentages a variety of samples containing 0%, 5%, 10%, and 15% silica fume. It was found that by the addition of different percentages of silica fume, the index properties of the soil was improved [11]. The use of silica fume, phosphogypsum, and biomass ash as additives for soil improvement aims to increase the UCS of the soil, making it more suitable for construction and load-bearing purposes. These materials provide a cost-effective and sustainable approach to enhancing the strength and stability of the soil, reducing the need for extensive excavation and replacement [12]. However, it is important to consider the appropriate dosages and mix design to ensure optimal results and compatibility with specific soil types and project requirements. In the current study silica fume and biomass ash were used to improve the mechanical properties of the low-plastic soils.

2 Materials & Methodology

2.1 Materials

The soils were collected from the Tarnol and Chaklala district of Pakistan which are used in this investigation. The soil samples used in this study were disturbed and found to be silts of low compressibility (ML). The samples were obtained from a depth of 1.5 meter [13] and Table 1 lists the physical properties of soils.

Table 1 Physical properties of soils

Soil Type	Classification		Atterberg's Limits			Grain size Distribution			Moisture Density Relationship	
	AASHTO	USCS	L.L (%)	P.L (%)	P.I (%)	Sand (%)	Clay (%)	Silt (%)	MDD (kN/m ³)	OMC (%)
Chaklala	A - 4	ML	17.29	15	2.29	46	18	36	18.41	13.53
Tarnol	A - 4	ML	21.23	18.51	2.71	32	20	48	24.56	11.85

Silica fume, also known as micro silica, is a byproduct of the production of silicon metal and ferrosilicon alloys. It is a highly reactive pozzolanic material with fine particles that can fill the voids in the soil matrix [14]. When mixed with soil,



5th Conference on Sustainability in Civil Engineering (CSCE'23)
Department of Civil Engineering
Capital University of Science and Technology, Islamabad Pakistan



silica fume reacts with the calcium hydroxide present in the soil to form an additional calcium silicate hydrate (CSH) gel. This gel acts as a binder, increasing the cohesion and strength of the soil. The incorporation of silica fume can significantly enhance the UCS of the soil, making it more resistant to deformation and load-bearing and are economic and environmental constraints.

Biomass ash is a byproduct of biomass combustion processes, such as the burning of agricultural residues or wood. It contains high amounts of silica and other mineral compounds [15]. Biomass ash has been found to be effective in improving the UCS of soil due to its pozzolanic and cementitious properties. When biomass ash is added to soil, it reacts with calcium hydroxide to form additional binding compounds, similar to silica fume [16]. This reaction leads to increased strength and durability of the soil. Biomass ash is a carbon-rich material and has been recognized for its potential in carbon sequestration, soil improvement, and wastewater treatment and are economic and environmental constraints.

2.2 Methodology

Sieve Analysis: The soil underwent classification through a sieve analysis test in accordance with the ASTM D 422 standard. A 500gm soil sample was pulverized, dried in an oven, and then subjected to shaking within a set of sieves for a duration of five to ten minutes using a sieve shaker. After removing the sieve set from the shaker, the weight of the material retained on each sieve was measured separately.

Hydrometer Analysis: The hydrometer analysis method is commonly used to estimate the distribution of soil particle sizes from the #200 (0.075 mm) sieve down to approximately 0.001 mm.

Atterberg limits:

Liquid Limit: The testing procedure adhered to the ASTM D423-66 standard, employing a soil sample that had been dried in an oven and filtered through a #40 sieve. The liquid limit was ascertained by counting the number of blows required for the two sections of soil to come into contact with each other.

Plastic Limit: The plastic limit test was conducted following the guidelines of the ASTM D698-70 standard. A soil sample weighing 20 grams was mixed with water until it reached a pliable consistency and then filtered through a #40 sieve. The soil was then rolled into a ball and compressed between a glass plate and palm to form a thread with a uniform diameter of 1/8" or 3mm. The moisture content of the soil was determined by placing it in a container after it was crumbled.

Plasticity Index: The plasticity index, a significant property, is used to assess the swelling characteristics of various soils. It is determined by calculating the difference between the plastic limit and the liquid limit values.

Compaction Test: In order to assess the compaction characteristics of a soil sample, the procedures outlined in the ASTM D1557-12 standard were adhered to, and a modified proctor test was performed. The test commenced with the addition of 3% water by weight, and each subsequent trial increased the water content by 3%.

Unconfined compressive strength: The test was conducted in accordance with ASTM D 2166 (ASTM 2006) guidelines. The mold used in the test had dimensions adhering to the standard ratio of 2:1, with a height of 2.5cm and a diameter of 5cm. The soil samples were prepared based on the optimum moisture content (OMC) and maximum dry density (MDD) of the soil. The strain rate applied during the test was 1mm/min.

3 Results

3.1 Grain Size Analysis

According to the test results, Tarnol soil has 32% sand, 20% clay, and 48% silt, while Chaklala soil has 46% sand, 18% clay, and 36% silt. According to the grain size distribution, the Tarnol soil has a higher proportion of coarser particles than the Chaklala soil, while the Chaklala soil profile has a wider variety of finer particles as shown in Figure 1.

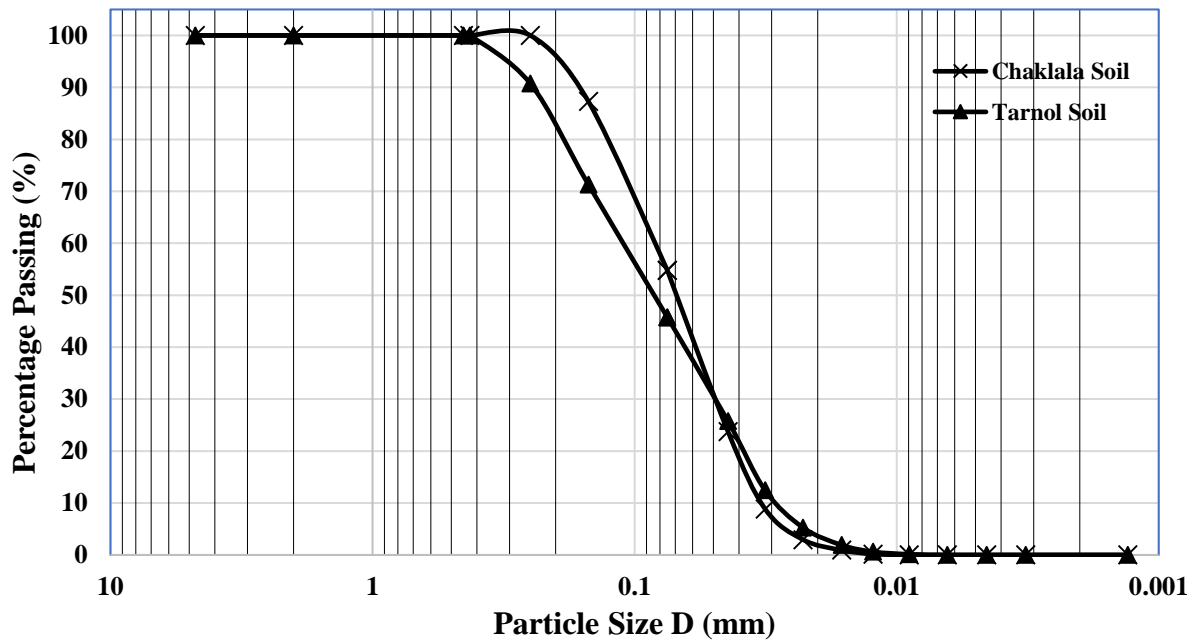


Figure 1 Gradation Curve of Chaklala and Tarnol Soil

3.2 Compaction Test Results

Figure 2 displays compaction curves for both Tarnol and Chaklala soil. The Tarnol soil has a MDD of 24.56 kN/m³ at an OMC of 11.85% while Chaklala soil has an MDD of 18.41 kN/m³ at an OMC of 13.53 %. The Tarnol soil has a higher maximum dry density than Chaklala soil, this is due to the soil profile which has a wider variety of finer particles

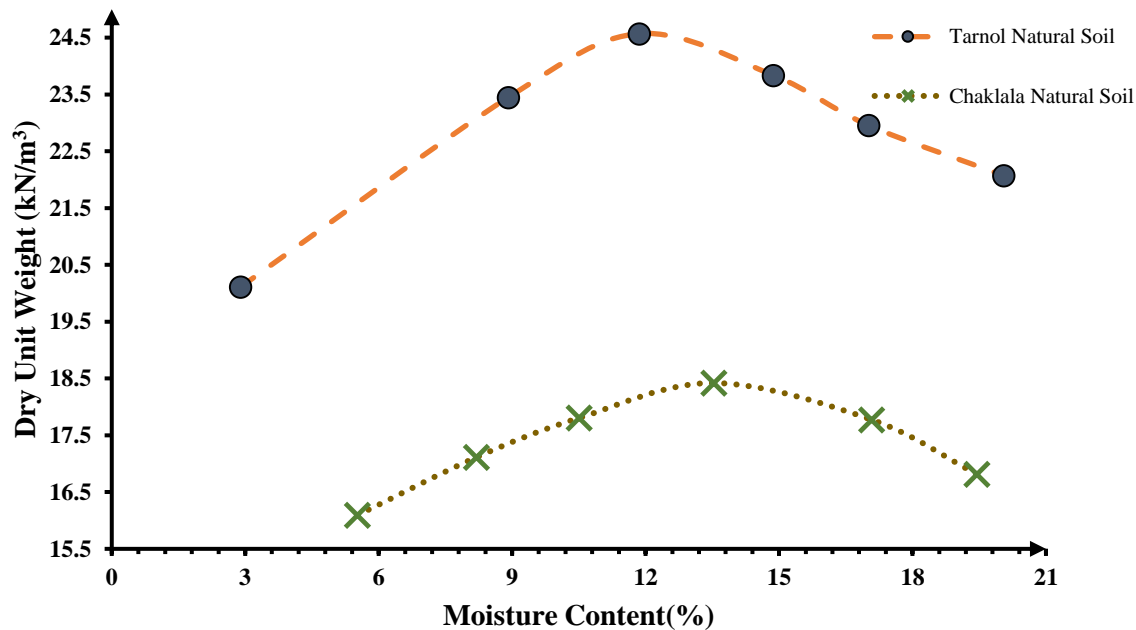


Figure 2: Moisture density relationship of soils



3.3 Unconfined compression test

Figure 3 shows the UCS of both treated and untreated soils the maximum optimum value of silica fume and biochar was calculated by using a compaction test and optimum values were used for the preparation of soil samples. The test results show that with the addition of biochar in Chaklala soil the UCS increased from 45.5 kPa to 98.75 kPa and with the addition of silica fume in Tarnol soil the UCS increased from 60.96 kPa to 93.18 kPa. The enhancement in strength is attributed to the cementitious effect of additives, which leads to better interlocking between the particles which increased its strength significantly.

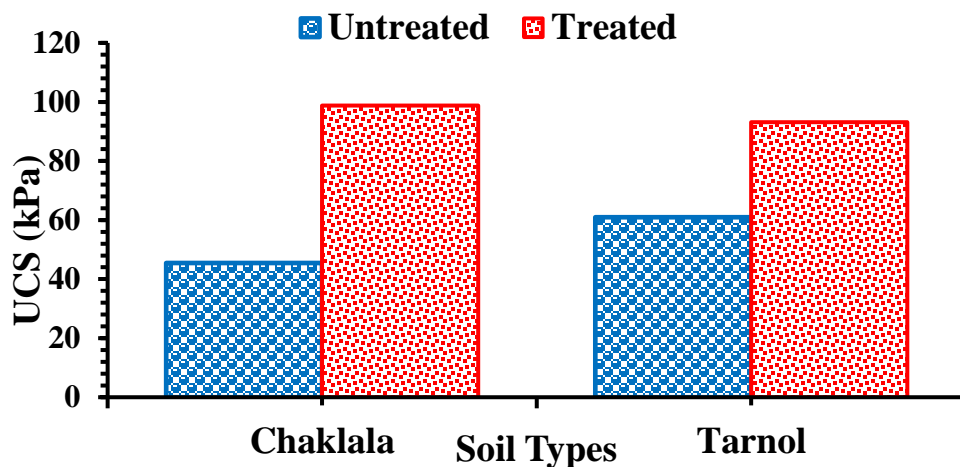


Figure 3: UCS of treated and untreated soils

4 Conclusions

After investigating the influence of silica fume and biochar on the engineering characteristics of the soils, it has been determined both these additives are suitable for modifying geotechnical and engineering properties. The following conclusions have been made based on the outcomes of the tests.

- 1 The use of silica fume and biochar stabilization has resulted in significant enhancements in the engineering characteristics of each of the two types of soil.
- 2 The Tarnol soil has an MDD of 24.56 kN/m^3 at an OMC of 11.85% while Chaklala soil has MDD of 18.41 kN/m^3 at an OMC of 13.53 %.
- 3 With the addition of biochar in Chaklala soil the UCS value increased from 45.5 kPa to 98.75 kPa and with the addition of silica fume in Tarnol soil the UCS value increased from 60.96 kPa to 93.18 kPa. The silica fume improved the UCS strength up to 52.85% and biochar increased the UCS up to 117%.

Acknowledgment

The authors would like to thank every person/department who helped thorough out the research work, particularly Attique Arshad and Dr. Zahir Uddin Khan. The careful review and constructive suggestions by the anonymous reviewers are gratefully acknowledged.

References

- [1] C. Yilmaz, V. Silva, and G. Weatherill, "Probabilistic framework for regional loss assessment due to earthquake-induced liquefaction including epistemic uncertainty," *Soil Dynamics and Earthquake Engineering*, vol. 141, p. 106493, 2021.
- [2] X. Fan *et al.*, "Earthquake-induced chains of geologic hazards: Patterns, mechanisms, and impacts," *Reviews of geophysics*, vol. 57, no. 2, pp. 421-503, 2019.



5th Conference on Sustainability in Civil Engineering (CSCE'23)
Department of Civil Engineering
Capital University of Science and Technology, Islamabad Pakistan



- [3] S. Wang and R. Luna, "Compressibility characteristics of low-plasticity silt before and after liquefaction," *Journal of materials in civil engineering*, vol. 26, no. 6, p. 04014014, 2014.
- [4] I. Chang, J. Im, and G.-C. Cho, "Introduction of microbial biopolymers in soil treatment for future environmentally-friendly and sustainable geotechnical engineering," *Sustainability*, vol. 8, no. 3, p. 251, 2016.
- [5] G. Archibong, E. Sunday, J. Akudike, O. Okeke, and C. Amadi, "A review of the principles and methods of soil stabilization," *International Journal of Advanced Academic Research/ Sciences*, vol. 6, no. 3, pp. 2488-9849, 2020.
- [6] M. K. Alhamdi and B. S. Albusoda, "A Review on Deep mixing method for soil improvement," in *IOP Conference Series: Materials Science and Engineering*, 2021, vol. 1105, no. 1: IOP Publishing, p. 012110.
- [7] H. Verma, A. Ray, R. Rai, T. Gupta, and N. Mehta, "Ground improvement using chemical methods: A review," *Heliyon*, vol. 7, no. 7, p. e07678, 2021.
- [8] H. Afrin, "A review on different types soil stabilization techniques," *International Journal of Transportation Engineering and Technology*, vol. 3, no. 2, pp. 19-24, 2017.
- [9] A. M. Al-Khalili, A. S. Ali, and A. J. Al-Taie, "Effect of metakaolin and silica fume on the engineering properties of expansive soil," in *Journal of Physics: Conference Series*, 2021, vol. 1895, no. 1: IOP Publishing, p. 012017.
- [10] A. A. Al-Obaidi, M. T. Al-Mukhtar, O. M. Al-Dikhil, and S. Q. Hannona, "Comparative study between silica fume and nano silica fume in improving the shear strength and collapsibility of highly gypseous soil," *Tikrit Journal of Engineering Sciences*, vol. 27, no. 1, pp. 72-78, 2020.
- [11] S. Bharadwaj and M. Trivedi, "Impact of micro silica fume on engineering properties of expansive soil," *Int J Sci Technol Eng*, vol. 2, no. 12, p. 435e40, 2016.
- [12] A. H. Campos Teixeira, P. R. R. Soares Junior, T. H. Silva, R. R. Barreto, and A. C. d. Silva Bezerra, "Low-Carbon Concrete Based on Binary Biomass Ash–Silica Fume Binder to Produce Eco-Friendly Paving Blocks," *Materials*, vol. 13, no. 7, p. 1534, 2020.
- [13] V. Kaushal and S. Guleria, "Geotechnical investigation of black cotton soils," *International Journal of Advances in Engineering Sciences*, vol. 5, no. 2, pp. 15-22, 2015.
- [14] C. Negi, R. Yadav, and A. Singhai, "Effect of silica fume on engineering properties of black cotton soil," *Int. J. Comput. Eng. Res.(IJCER)*, vol. 83, 2013.
- [15] B. S. Thomas, J. Yang, K. H. Mo, J. A. Abdalla, R. A. Hawileh, and E. Ariyachandra, "Biomass ashes from agricultural wastes as supplementary cementitious materials or aggregate replacement in cement/geopolymer concrete: A comprehensive review," *Journal of Building Engineering*, vol. 40, p. 102332, 2021.
- [16] N. Jiang, C. Wang, Z. Wang, B. Li, and Y.-a. Liu, "Strength characteristics and microstructure of cement stabilized soft soil admixed with silica fume," *Materials*, vol. 14, no. 8, p. 1929, 2021.



SLOPE STABILITY ANALYSIS AND DESIGN USING NUMERICAL TECHNIQUES: A CASE STUDY

^a *Ahsan Javed**, ^b *Naveed Ahmed*, ^c *Babar Khan*

a: Department of Civil Engineering, UET, Taxila, Pakistan, ahsanbhatti798@gmail.com

b: Department of Civil Engineering, UET, Taxila, Pakistan, naveed.uet28@gmail.com

c: BK Consultants (Pvt) Limited, Islamabad, Pakistan, ino@bkconsultants.com.pk

* Corresponding author: Email ID: ahsanbhatti798@gmail.com

Abstract- This case study analyses kilometer 28th of Islamabad-Murree Dual Carriage Way (IDMC) also known as National Highway (N-75) of Pakistan for its stability. The slope has high gradient, irregular shape and no vegetation cover which makes this slope susceptible to failure. The slope was analyzed with software Rocscience Slide 6.0. Based on the analysis, it was found that slope has a low factor of safety and might be unsafe. The slope was then designed using active design method. For analysis, different numerical methods i.e. Bishop's method, Janbu method simplified, Janbu method modified and Spencer method were used. Various types of supports were used individually and in combination to design the slope. Three different models were designed and analyzed having improved factor of safety from each other. From all the models, one model was finalized and declared as safest models having factor of safety greater than 2.0

Keywords- Slope Stability, Rocscience Slide 6.0, Active Design, National Highway-75 (N75).

1 Introduction

Landsliding can have significant and wide-ranging effects on both natural and human systems. Some of the effects of landsliding include loss of life and property damage, disruption of transportation networks, damage to natural habitats, soil erosion and sedimentation, flooding, economic impacts. [1] A slope fails when the driving forces overcome the resistive forces acting in the slope strata. In order to analyze the slopes for its stability, several methods have been introduced and modified over time. However, each of these methods is dependent on a number of factors i.e., type of slope, working approach, equilibrium type & assumptions. [2] Reviewing all these factors, the accuracy of one method can outperform the other.

Murree road is located near a tectonically active region of the Earth where mass movements like rock fall, rockslides and slumps cause adverse economic loss through disruption of travelling on roads. [3] Rainfall has seriously affected Islamabad Murree Dual-Carriage Way (N75) over the past few years. [4] Based on the results of a study, it can be concluded that the failure of the landslides along the Murree-Kohala road was activated by the reduction of shear strength of the slide material due to the increase in percentage of saturation, which reduced the effective normal stress along the slip surface. [3] There are major environmental impacts of landslide in Himalayan region. [5] Sohaib Naseer analyzed the slope using Limit Equilibrium and Finite Element Method using Rocscience Slide 6.0 and concluded that LE method overestimates the safety factor as compared to FE method. [6] This study was conducted in Dahr, ElBaidar – Lebanon Geometry ad visual analysis is shown in Fig. 1 (a) & (b).

In general, LE methods are used for slope stability analysis by the practicing engineers and professionals, however, similar studies show the vigorous nature of FE approach. In general, the LE and FE methods used in this study provide fairly consistent FOS. [7] LE method, being more practiced, will be used in analysis of this slope. A landslide occurred in a slope near Dahr Elbaidar in Lebanon during roads excavation work was suggested to be stabilized by means of active support system, i.e., reinforcement such as piles and nails. [8] We will be using active support system for the designing of the slope.

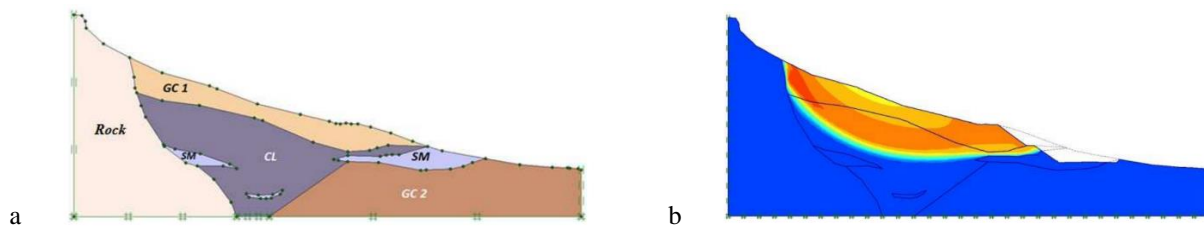


Fig 1. (a) Geometry of Slope (b) Analysis of Slope FS 2.07

Subject slope i.e., kilometer 28 of National Highway is a critical slope. It has a very steep slope at an angle of 79.69 degrees with no vegetation cover. The toe part of the slope does not have natural backfill to hold the slope. This slope has a long history of failure in the past. [9] The geographical/topographical location, seismic activity and high rainfall has been a major cause of failure of the slope. There are various software used for the analysis and design of the slopes using limit equilibrium approach [10]. We will be using Slide 6.0 in this paper due to its convenient visual representation and accurate FOS calculation. [11]

2 Research Methodology

For subject case study, boreholes were drilled at different location of the slope and samples were tested in the lab to acquire the physical properties of the slope. All the physical testing and data collection by done in collaboration with B.K Consultants. Once the soil parameters are determined, the slope is modeled with Rocscience 6.0, the slope is first analyzed for its minimum factor of safety. Based on the results, the slope is designed using active design method. Various ground improvement techniques are used with respect to support members to achieve the safest, economical, and practical model. For analysis of designed slope, Bishop's method, Janbu Method – simplified, Janbu Method – corrected and spencer method are used.

3 Experimental Analysis

The slope under study is located at kilometer 28th of Islamabad Murree National Highway (N-75). It does not have any vegetation cover and high slope gradient of 79.60 degree. Tension cracks has also developed on the road. (Fig. 2.d) The base of slope consists of Rock material; it has rocky soil strata on top of it mentioned as failure envelope in (Fig. 3.a) A distributed load of 20 kN/m² is taken as live load of traffic. This highway falls in between Murree and Islamabad having seismic zone 3 and seismic load has been applied accordingly i.e., 0.2 g horizontal and 0.1 g vertical. The slope of failure envelope is steep, and toe also does not lie on a proper slope angle or solid base, which makes it prone to failure.



Fig. 2 (a), (b), (c), (d) shows top, right side, left side and road view (with tension crack) of slope



The current geometry of the slope is shown in *Figure 2*. The slope will be analyzed for its stability using four different methods of analysis. Based on the results of Factor of Safety, the slope will be designed to achieve the safest model.

3.1 Analysis of Slope

Based on the parameters of the slope, the data was input in the software and analysed for its stability. For analysis of slope, the non-circular slip surface method was used. The properties of the materials are given as under Table 1 & 2.

Table 1: Properties of Rock

Rock		
Unit Weight	20	kN/m ³
Unconfined Compressive Strength	12000	kPa
Water Surface	None	

The Properties of identified failure envelope is given in Table 2.

Table 2: Properties of Failure Envelope

Failure Envelope		
Unit Weight	19	kN/m ³
Cohesion	50	kPa
Phi	30	degrees

The visual analysis of the slope is shown in *Fig. 3 (b)* along with the results of the same using four different approaches in *Table 3*. A filter on all the slip surfaces in applied to show only layers with FOS below 2.0.

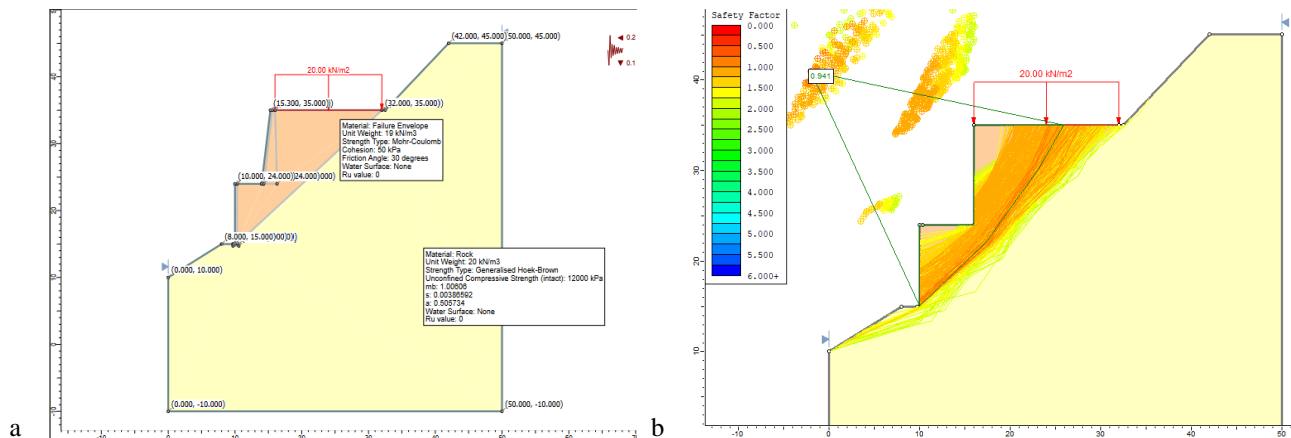


Fig 3. (a) Slope structure and coordinates (b) Analysis of Original Slope

The Table 3 shows the results of analysis of slope using four different approaches.

Table 3: Results for Analysis of Slope

Global Minimums SF			
Bishop simplified	Janbu simplified	Janbu corrected	Spencer

In *Fig 3. (b)* all yellow and brown layers are visible having FOS below 1.5. Based on these results, it is found that the slope has low factor of safety and is unsafe. It needs to be redesigned using different ground improvement techniques.



3.2 Model 1: Active Design of Slope

In model-1 of active design of slope, as shown in Fig. 4 a retaining wall of specifications given below is introduced along the steep angle of slope, in order to counter the steep angle impacts on its strength. The properties of retaining wall used are given in the Table. 4 below.

Table. 4. Properties of Ground Anchors

Retaining Wall		
Unit Weight	20	kN/m ³
Cohesion	30	kPa
Phi	35	degrees

3.3 Model 2: Active Design of Slope

In model-2 of active design of slope, as shown in Fig. 4 (a), grouted tie backs are introduced which act as ground anchors. Specifications of ground anchors are given in Table 5. Both retaining wall and ground anchors act in combination to increase the overall strength of the slope.

Table. 5. Properties of Ground Anchors

Ground Anchor		
Support Type	Grouted Tie Backs	
Tensile Strength	750	kN/m
Plate Capacity	750	kN/m
Pullout Strength		
Adhesion	15	kPa
Friction Angle	35	degrees

3.4 Model 3: Active Design of Slope

In model-3 of active design of slope, as shown in Fig 4 (b) micropiles are added in the model. The lower portion of the slope seems too steep, in order to support the toe, micropiles maybe introduced to further increase the strength of the slope. Specifications of ground anchors are given in Table 6. Retaining wall, ground anchors and micropiles act in combination to increase the overall strength of the slope.

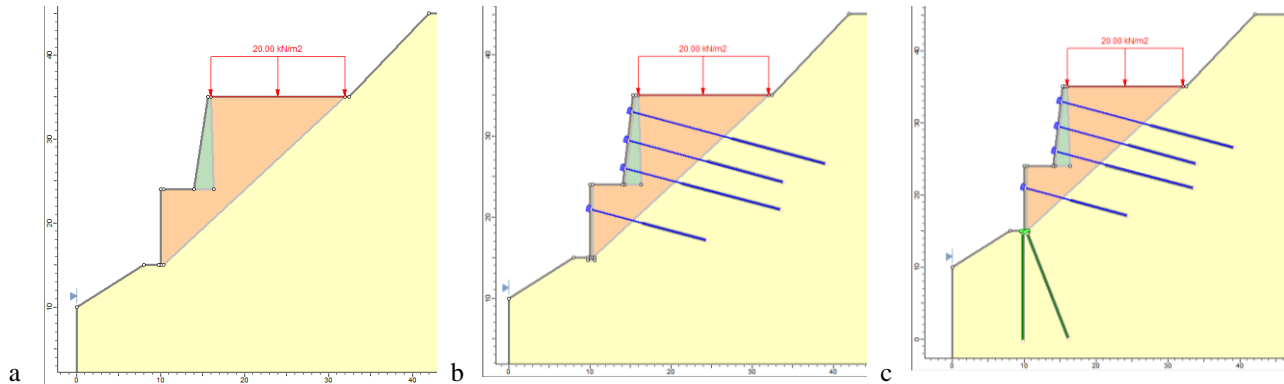


Fig 4. (a)Model 1: Existing Slope with Retaining Wall (b) Model 2: Existing Slope with retaining wall and ground anchors (c) Model 3: Existing Slope with retaining wall, ground anchors and micropiles

The properties of the micropiles are given in the Table 6.

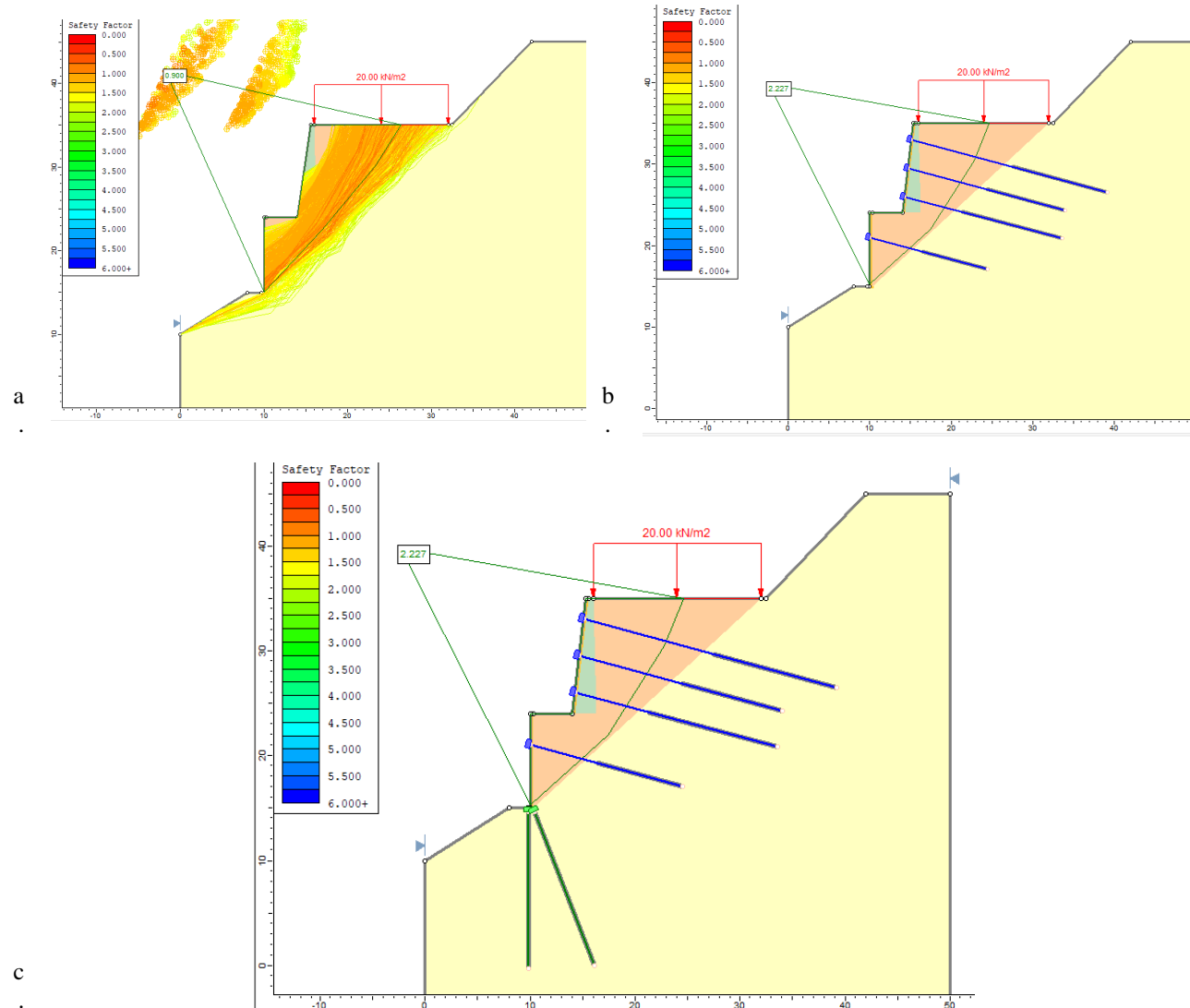
Table.6. Properties of micropiles

Micropiles		
Pile Shear Strength	30	kN
Out of place spacing	1.5	m
Force Direction	Parallel to surface	

4 Results

All the models were analyzed using Rocscience Slide 6.0. The visual analysis of models 1, 2 & 3 is shown in the Fig 5 (a), (b) & (c). A filter on all the slip surfaces in applied to show only layers with FOS below 2.0.

It can be seen in Model 1: *Fig 5 (a)*, all the yellow and brown layers have FOS below 1.5 and was unsafe. Based on these results, Model 2: *Fig 5 (b)* was designed, which on application of filter shows that no layer has FOS below 2.0 and has Global minimum SF of 2.35. However, the toe of the slope has a steep angle of slope resting on it. Model 3: *Fig 5 (c)* was designed to support the toes of the slope. It can be seen in *Table 7*, that SF using spencer method has improved from 2.60 to 2.62.


Fig 5. Analysis of (a) Model 1 (b) Model 2 (c) Model 3



5th Conference on Sustainability in Civil Engineering (CSCE'23)

Department of Civil Engineering

Capital University of Science and Technology, Islamabad Pakistan



Table 7. SF against Model 1

Global Minimums SF				
Model no.	Bishop simplified	Janbu simplified	Janbu corrected	Spencer
Model 1	0.898475	0.880255	0.900295	0.946555
Model 2	2.35709	2.15056	2.22677	2.60895
Model 3	2.35709	2.15056	2.22677	2.62366

5 Conclusions

In most of the slope cases at Islamabad Murree Dual Carriage Way (N-75), active design method is used for stability of slope. In the same way, active design method is used in this case. Active design method is most effective in stability design of the slopes which are already prone to failure because active design method acts to reduce the driving forces acting in a slope mass.

In this particular case, the slope is located in high rain fall and seismically active zone of Pakistan. The steep angle of slope, topography and rainfall conditions of area has reduced the strength of the slope. Using the active design approach and ground improvement techniques used in the design mentioned above, the strength of the slope can be improved with better slope structure and factor of safety.

Following the slope stabilization techniques used in this paper, the strength of the subject slope can be improved but findings in this research are site specific and are only applicable to this slope. For other slopes, new analysis should be carried out and based on the results the design should be made.

Acknowledgment

The authors would like to thank every person/department who helped thorough out the research work, particularly BK Consultants. They provided all the services during site visits and data collection. They also provided the manpower, and the software used in the analysis i.e., Slide software 6.0. The careful review and constructive suggestions by the anonymous reviewers are gratefully acknowledged.

References

- [1] A. N. KHAN, IMPACT OF LANDSLIDE HAZARDS ON HOUSING AND RELATED SOCIO-ECONOMIC.
- [2] A. Pourkhosrovani, "A Review of Current Methods for Slope Stability Evaluation," *Electronic Journal of Geotechnical Engineering ER*, vol. 16.
- [3] F. F. K. M. H. e. a. Ali, "Influence of Saturation on Rainfall Generated Landslides in Shale along Murree-Kohala Road, Pakistan," *JOURNAL GEOLOGICAL SOCIETY OF INDIA*, 2016.
- [4] K. A. C. A. e. a. Atta-ur-Rahman, "Causes and extent of environmental impacts of landslide hazard in the Himalayan region: a case study of Murree, Pakistan," *Natural Hazards*, 2010.
- [5] A. Khan, "Causes and extent of environmental impacts of landslide hazard in the Himalayan region: A case study of Murree, Pakistan," *Natural Hazards*, 2011.
- [6] A. Fawaz, "Slope Stability Analysis Using Numerical Modelling," *American Journal of Civil Engineering*, 2014.
- [7] S. Naseer, STABILITY ANALYSIS OF SLOPES USING LIMIT EQUILIBRIUM AND FINITE ELEMENT METHODS.
- [8] E. F. Salmi, "Slope stability assessment using both empirical and numerical methods: a case study," *Bulletin of Engineering Geology and the Environment*, 2014.
- [9] M. Akram, "Geotechnical evaluation of rock cut slopes using basic Rock Mass Rating (RMRbasic), Slope Mass Rating (SMR) and Kinematic Analysis along Islamabad Muzaffarabad Dual Carriageway (IMDC), Pakistan," *Journal of Biodiversity and Environmental Sciences*, 2018.
- [10] S. Inumula, "Stability analysis of a deep highwall slope using numerical modelling and statistical approach—a case study," *Arabian Journal of Geosciences*, 2021.
- [11] G. You, Probabilistic slope stability analysis of open pit mine using Slide 6.0, 2016.



EVALUATION OF STRENGTH PARAMETER OF INDIGENOUS SOIL UNDER VARYING SURCHARGE LOAD

^a H.Bilal*, ^b K.Riaz

a: Department of Civil Engineering, UET, Taxila, Pakistan, hazratbilal2145@gmail.com

b: Department of Civil Engineering, UET, Taxila, Pakistan, kashif.riaz@uettaxila.edu.pk

* Hazrat Bilal: Email ID: hazratbilal2145@gmail.com¹

Abstract- The study examined the result of surcharge load on subgrade soil commonly used in pavement construction in Pakistan. Soil samples of A-6 and A-2-6 types were collected from six locations in KPK and Punjab Division and classified based on AASHTO Soil Classification System. The laboratory tests were performed to define the index properties of soil samples. The ultrasonic pulse velocity technique was used to measure the resilient modulus and swelling, and CBR values were determined using overburden loads going from 2.27 to 13.8 kg. The study found that increasing surcharge weight led to an increase in ultrasonic pulse velocity and CBR values, and a decrease in soil swelling. The study also developed improved relationships for predicting the resilient modulus values based on CBR measurements, showing strong correlation with equations developed by Green and Hall and Powell et al. from the TRRL. Overall, the study provides insights into the behavior of subgrade soil under different surcharge weights and proposes improved relationships for predicting resilient modulus values, contributing to the design and construction of more reliable and efficient flexible pavements.

Keywords- CBR, Surcharge weight, MR (Resilient modulus), UPV (Ultrasonic pulse velocity), CBR-MR Relationship

1 Overview

A nation's economic progress is significantly influenced by the caliber of its road networks. The quality of the road and the effectiveness of the road pavement are significantly influenced by the strength of the subgrade soil. With rising urbanization, obtaining desired pavement strength while reducing production and construction costs is becoming more and more important. The resistance of the foundation material is assessed using a variety of tests, including the modified Proctor test, unconfined compressive strength, and California bearing ratio. In connection to the subgrade, variables including the MDD "Maximum Dry Density", the modulus of subgrade response, and the FDD "Field Dry Density" are also taken into account. The type of pavement being built determines which strength parameter should be used.

The CBR standards for subgrade soil in pavement construction are established by clients and governmental organizations. However, the industry has not established a clear standard for the usage of additional load (overburden loads) in CBR testing. The overburden pressure caused by the weight of the pavement on the earth is simulated by surcharge weight. The maximum surcharge weight allowed by the standard CBR test protocol is 4.5 kg. For pavement thicknesses of 63.5 mm, Yoder advised a surcharge weight of 2.27 kg, however the mass on soil models shouldn't be least "4.5 kg".

Contractors and construction companies take the depth of the pavement layers above the subgrade into account when calculating the surcharge weight for CBR testing. In this method, heavier surcharge weights than the CBR test's standard



5th Conference on Sustainability in Civil Engineering (CSCE'23)

Department of Civil Engineering

Capital University of Science and Technology, Islamabad Pakistan



weight are frequently used. Increased surcharge weight, however, may cause variances in soil CBR values. Investigating the impact of various surcharge weights on commonly utilized soil types for pavement building is crucial.

Razouki (Razouki, 2014) [1] conducted a study on gypsum-rich roadbed sand with 39% gypsum content, applied a 200 N surcharge loads to CBR models and subjecting them to cyclic soaking and drying processes. The research revealed that CBR values decreased during soaking but increased during drying, indicating significant deformation properties influenced by soaking duration. Jaleel's study examined sub base soil under a 4.5 kg surcharge weight, finding that prolonged soaking periods led to a decrease in the bearing ability of the sub base soil.

The "California Bearing Ratio" (CBR) and resilient modulus of gypsiferous soils were the topic of a study by (Razouki, 1999) [2] that looked at the effects of surcharge weight and soaking duration. Testing clay samples containing 33% gypsum required applying surcharge loads of 45 N, 178 N, and 312 N as well as soaking the samples for various amounts of time, ranging from 0 to 180 days. The results showed a direct correlation between surcharge weight and the predicted robust modulus, with higher surcharge weights for each soaked period demonstrating a rise in modulus. The robust modulus, however, decreased as the soaking duration increased. Additionally, (S.S.Razouki, 2002) [3] investigated how silty subgrade soil behaved when subjected to different additional loads "44.5 N, 89 N, 178 N, and 267 N" and observed that a rising in additional load led to and rise in "CBR" power.

In the field of geotechnical engineering, the UPV method is commonly employed to assess important strength parameters such as "shear modulus, elastic modulus, and Poisson's ratio" (Y.Wang, 2018) [4]. The most reliable approach for this is considered to be direct transmission. During the test, spreader and collector transducers are positioned on opposite sides of the soil models. The test involves timing the passage of waves through the soil model and measuring their amplitude (Y.Wang, 2015) [5]. Poisson's ratio and the resilient modulus can be resolving by means of the wave transmission method by calculating the shearing wave velocity (V_s) and compressive wave velocity (V_c). These velocities are obtained by dividing the length of the model (L) by the time taken (t) for the waves to traverse the soil model (D2845-08, 2000) [6]. The researcher uses the following formulae to calculate the values of the resilient modulus (MR).

$$V_c = L/T_c \quad \& \quad V_s = L/T_s \quad (1.1)$$

The Poisson's ratio (μ) is determined by employing the equation provided below.

$$\mu = (V_c^2 - 2V_s^2)/ [2(V_c^2 - V_s^2)] \quad (1.2)$$

MR "Resilient Modulus" is finding using the equation

$$M = [\rho V_s^2 (3V_c^2 - 4V_s^2)] / (V_c^2 - V_s^2) \quad (1.3)$$

Where

- L = the length covered by the pulse within the sample b/w two transducers, also known as the sample length,
- T_c, T_s = the time required for compressive waves and shearing waves to propagate through the sample, respectively,
- V_c = (velocity of compressive wave)
- ρ = (density kg/m³)
- V_s = (velocity of the shearing wave).

Focus is placed on two key goals in this study. First, it examines the effects of increased surcharge weight at various sites on the California Bearing Ratio (CBR), swell percentage, and MR "Resilient modulus" of frail and durable subgrade soils. 2nd, it compares the CBR-MR correlations discovered through laboratory research with those that are frequently used in the field. The objective is to establish if the CBR-MR relationship is constant for all subgrade soil types or if it varies with soil type. The purpose of this study is also to examine how surcharge weight affects soil swelling when it is wet.



2 Experimental Procedures

2.1 Materials

From these Six districts in KPK—Sawabi, Karak, Nowkhar, Lower Dir, Bajaur, and Mardan—were used to gather disturbed soil samples for this study. The samples were collected from a depth of roughly 1 meter below the surface of the ground. These soil samples experienced a number of tests in order to identify their index properties and assign them a classification using the AASHTO soil classification system listed in table 1. In accordance with the standards of the American Association of State Highway and Transportation Officials, the testing included wet sieve analysis and Atterberg's limits tests, such as the liquid limit and plastic limit tests.

Table 1: Geotechnical Properties of A-6 and A-2-6 Soil of Different Location

Properties	A-6 Karak	A-6 Sawabi	A-6 Nowkhar	A-2-6 Bajaur	A-2-6 L Dir	A-2-6 Mardan
Liquid Limit (L.L)	30	32	36	40	39	24
Plastic Limit (P.L)	11	17.5	12	21	22	7.7
Plasticity index (P.I)	19	14.5	24	19	17	16.3
MDD (g/cc)	1.92	1.85	1.804	1.9	1.96	1.87
OMC (%)	8.8	12	10.5	10	9	13.5

2.2 Sample Preparation

In this study, California Bearing Ratio (CBR) models were prepared according to the established test procedure. The samples consisted of A-6 and A-2-6 soils, with three samples compacted for each surcharge weight. Compaction was achieved using (10, 30, 65) blows per layer, correspondingly, with a 4.5 kg hammer and a 45 cm elevation of fall. The models were formed in 15 cm diameter of molds and compressed in five layers. To assess the swelling of the soil, the CBR model were submerged in water for 96 hours, and the percentage of soil swelling was determined using dial gauges with compassion of 0.001 cm.

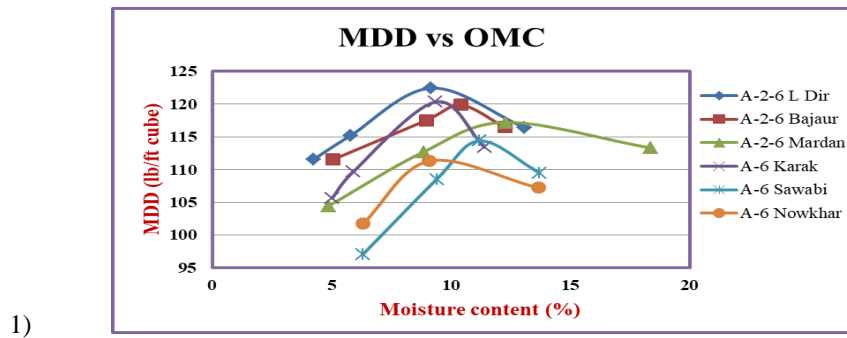
2.3 UPV (Ultrasonic Pulse Velocity)

To overcome the lack of affordable triaxial equipment in developing countries, researchers used ultrasonic pulse velocity as an alternative method to measure soil's resilient modulus. By soaking soil samples and placing transducers directly on the soil surface, compression and shear velocities were accurately determined, minimizing errors caused by steel molds and surcharge weight plates. Following the ultrasonic pulse velocity assessment, CBR testing was conducted to calculate values based on 95% of the maximum dry density. This cost-effective approach enables the estimation of resilient modulus in regions with limited triaxial equipment availability.

3 Outcome and Discussion

3.1 Modified Proctor Compaction Test (MPCT)

Moisture-Density Proctor Compaction Tests (MPCT) were performed on Two different type soil samples A-6 and A-2-6 following AASHTO T 180 standards, which utilize a 4.45-kg (10-lb.) rammer and a 457-mm (18-in.) drop. The MPCT provided numerical values for OMC (Optimum Moisture Content) and MDD (Maximum Dry Density) for each soil model. The results of the MPCT of A-6 and A-2-6 are summarized in fig 1. The relationship between moisture content and dry density for each soil is depicted graphically in (fig 1a). Based on the MDD and OMC values obtained from the MPCT, soil specimens were prepared for the soaked CBR (California Bearing Ratio) test at 95% relative compaction.



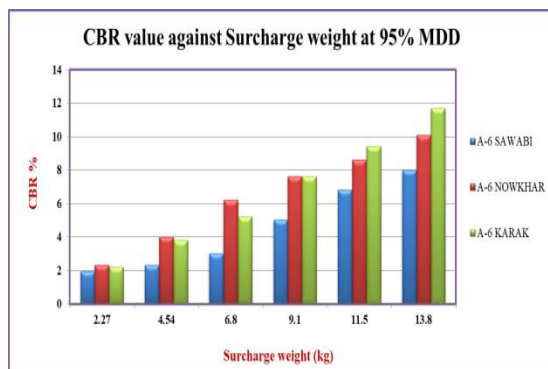
1)

Figure 1: Dry densities vs Moisture content of A-6 and A-2-6 Soil

3.2 California Bearing Ratio (CBR)

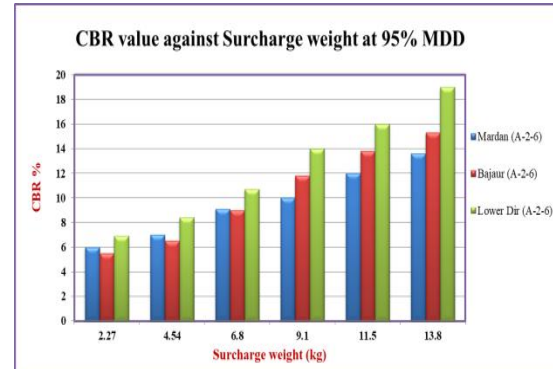
This study focuses on the impact of rising additional weight (surcharge loads) since (2.27 to 13.8 kg) on the CBR data of two soil types. The results show a significant increase in CBR data for the “A-6, A-2-6” soil as the surcharge weight increases. The CBR values for different locations 1, 2, 3 of A-6 and A-2-6 soil rise from (2.2% to 11.7%, 2.3% to 10.1%, and 1.95% to 8%) and (1, 6.9% to 19%, 5.5% to 22% and 6% to 15.5%) with rising surcharge load result presented in fig 2(a), 2(b). This rise in CBR value can be attributed to the stiffening of the soil within the California Bearing Ratio molds owing to the additional burden from the extra mass (T.Hergul, 2012) [7]. Factors such as clay mineralogy, index properties, and compactive energy also contribute to the rise in CBR values reported by (H.B.Nagaraj, 2018) [8]. The reduction in voids ratio caused by the greater additional load further enhances the strength of the soil. Overall, this study sheds light on the influence of surcharge weight on CBR values and the underlying factors affecting soil behavior (MAJEED, 2014) [9].

To compare the behavior of infirm and durable soils under the equal surcharge load, strength ratios of the “CBR” models were finded. For this purpose strength ratio indicates the comparative rise in CBR data for every increment in surcharge load compared to the CBR data found at the standard weight of 4.5 kg. The results showed in table 2 and 3.



2a)

Fig 2a: CBR % A-6 Soil of different location



2b)

Fig 2b: CBR % A-2-6 Soil of different location

Table 2: Strength Ratio CBR(S)/CBR (4.5)

Sample ID	Surcharge wt (kg)	4.5	6.8	9.1	11.5	13.8
A-6 Karak	CBR _s /CBR _{4.5}	1	1.36	2	2.47	3.07
A-6 Sawabi	CBR _s /CBR _{4.5}	1	1.30	2.17	2.95	3.47
A-6 Nowkhar	CBR _s /CBR _{4.5}	1	1.55	1.9	2.15	2.52



Table 3: Strength Ratio CBR(S)/CBR (4.5)

Sample ID	Surcharge wt (kg)	4.5	6.8	9.1	11.5	13.8
A-2-6 Dir	CBR _s /CBR _{4.5}	1	1.38	1.81	2.12	2.35
A-2-6 Bajaur	CBR _s /CBR _{4.5}	1	1.27	1.66	1.90	2.26
A-2-6 Mardan	CBR _s /CBR _{4.5}	1	1.3	1.42	1.64	1.94

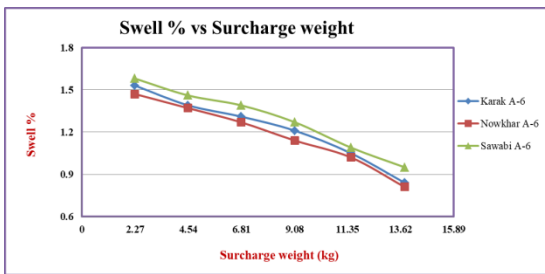
Strength Ratio is explained as CBR S/CBR 4.5 Where;

CBR (S) = "CBR" data of confirmed soil model at any functional surcharge load "S."

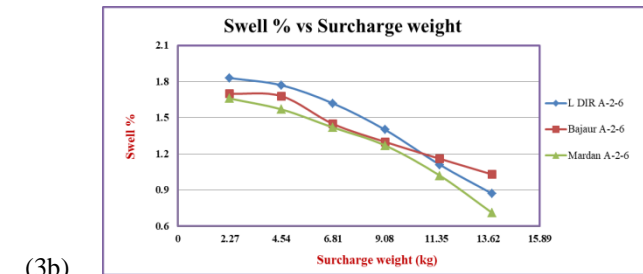
CBR (4.5) = "CBR" data of established surcharge load "4.5 kg" functional on tested soil models

3.3 Swelling Potential

One of the main aims of this research was to investigate the impact of various surcharge weights on the swelling potential of A-6 and A-2-6 soils. A comparison of the two soil types revealed that A-2-6 soil exhibited lower swelling compared to A-6 soil. The swelling data after 96 hours of soaking showed a major reduction in swell percentage as the surcharge load increased. The highest compaction effort of 65 blows per layer resulted in the least amount of swelling. For A-6 soil, the swelling potential decreased of Location 1, 2, 3 from 1.53-1.47-1.58% to 0.84-0.81-0.95% when the surcharge load increased from "2.27 to 13.8" kg as listed in fig 3(a). Similarly, for A-2-6 soil, the swelling potential decreased of Location 1, 2, 3 from 1.66-1.7-1.79% to 0.75-1.03-0.87% with the rising in overburden load since 2.27 kg to 13.8 kg as listed in fig 3(b). The higher compressive energy increased the dry density of the soil, foremost to a decrease in swell percentage. These findings align with previous research by (A.K.Mishra, 2008) [10] who observed a decrease in clayey soil swelling with rising dry density. The decrease in swell percentage can be credited to the reduction in void spaces between soil particles caused by increased compactive effort, ultimately reducing the overall voids in the clayey soil. When we utilized weak soil and increased the surcharge weight, the swelling decreased. To enhance the CBR value and minimize the potential for swelling, the surcharge weight was increased. However, in the field, the standard surcharge weight was used, resulting in greater soil swelling and deformation in the road structure. In the field, we lacked control over this aspect, whereas in the laboratory, we were able to increase the surcharge weight and effectively manage the swelling."



3(a)



(3b)

Fig 3a: Swell % of A-6 Soil

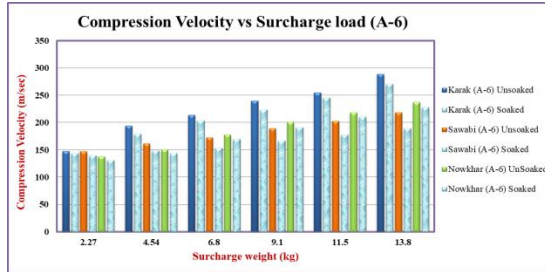
Fig 3b: Swell % of A-2-6 Soil

3.4 UPV (Ultrasonic Pulse Velocity)

The results of the "Ultrasonic Pulse Velocity Test" for A-6 and A-2-6 soils are presented in fig 4(a), 4(b). The study reveals that the velocity is higher in the dry condition compared to the soaked condition. Additionally, increasing the compaction effort to 65 blows/layer significantly increases the velocities compared to 30 and 10 blows/layer. This increase in velocity corresponds to higher CBR values, which can be attributed to greater compressed and shear wave velocities resulting from increased surcharge load. Both velocities and CBR values show an upward trend as the surcharge load increases from "2.27 to 13.8" kg. At the maximum compaction effort, A-6 soil exhibits increasing velocities and CBR values from Location 1 to 3. Similarly, A-2-6 soil demonstrates higher velocities and CBR values compared to A-6 soil. The enhanced soil stiffness under greater surcharge load contributes to the elevated compressed

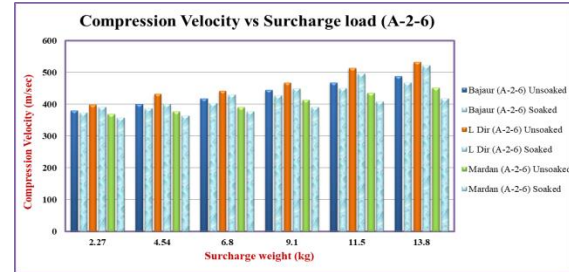


and shears wave velocities. The observed velocity increase in A-2-6 soil surpasses that of A-6 soil, and the reasons behind this difference align with previous discussion on CBR value.



4(a)

Fig 4a: Compression Velocity of A-6 soil



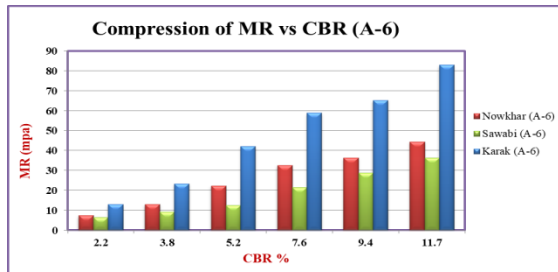
4(b)

Fig 4b: Compression Velocity of A-2-6 soil

3.5 Resilient Modulus (MR)

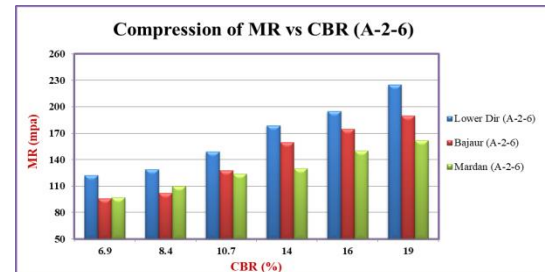
In recent research, I analyzed the CBR test value and resilient modulus of A-6 and A-2-6 soil from various locations. The CBR value assesses soil strength and bearing capacity, while the resilient modulus measures resistance to repeated loading without permanent deformation. The study found a positive correlation between CBR value and resilient modulus, indicating stronger and more resilient soils fig 5(a), 5(b). Resilient modulus is crucial for understanding soil performance under traffic loads, affecting stress and deformation distribution. By varying surcharge load, the research demonstrated that increased load elevated the resilient modulus for both soil types. These findings advance geotechnical engineering by providing insights into soil behavior under different loading conditions.

Overall, research highlights the strong correlation between the CBR value and resilient modulus, emphasizing the importance of soil strength and resilience in engineering applications. These findings can contribute to the development of more accurate design methodologies for geotechnical projects, leading to safer and more efficient infrastructures.



5(a)

Fig 5a: Resilient modulus of A-6 Soil



5(b)

Fig 5b: Resilient modulus of A-2-6 Soil

4 Conclusions

Based on the conducted study, the following conclusions can be inferred:

1. Overall, the correlation between compaction effort, compression velocity, and CBR value, indicating that increasing the compaction effort leads to higher compression rates and improved strength properties of the soil.
2. The velocity exhibited a decrease during soaking compared to the unsoaked condition. This means that when the CBR mold was soaked, its velocity decreased compared to its velocity in the unsoaked state. So the higher velocity showed higher CBR value and there is a correlation between increased velocity and improved strength properties.
3. Increasing the surcharge weight significantly improves the CBR strength ratio of "A-6 and A-2-6" soil, indicating that lower CBR silty clay can be utilized as subgrade soil with minimum pavement thickness. Additionally, both soils experience reduced swelling with higher surcharge weight. A correlation between the MR value, CBR value, and compression velocity, indicating that increasing the CBR and compression velocity leads to increased stiffness or rigidity of the material.



5th Conference on Sustainability in Civil Engineering (CSCE'23)

Department of Civil Engineering

Capital University of Science and Technology, Islamabad Pakistan



4. The variation in soil mineralogy at different locations results in differences in MR (Resilient Modulus), CBR and pulse velocity values for the same soil type

Reference

- [1] S.S. Razouki, B.M. Salem, Soaking–drying frequency effect on gypsum-rich roadbed sand, Int. J. Pavement Eng. 15 (10) (2014) 933–939, <https://doi.org/10.1080/10298436.2014.893326>.
- [2] S.S. Razouki, O.A. El-Janabi, Decrease in the CBR of a gypsiferous soil due to longterm soaking, Q. J. Eng. Geol. Hydrogeol. 32 (1) (1999) 87–89, <https://doi.org/10.1144/GSL.QJEG.1999.032.P1.07>
- [3] S.S. Razouki, A.M. Al-Shefi, Effects and observations of surcharge load on the laboratory CBR and resilient modulus values of roadbed soil, Q. J. Eng. Geol. Hydrogeol. 35 (1) (2002) 89–95, <https://doi.org/10.1144/qjegh.35.1.89>.
- [4] Y. Wang, X. Li, B. Zheng, Experimental study on mechanical properties of clay soil under compression by ultrasonic test, Eur. J. Environ. Civ. Eng. 22 (6) (2018) 666–685, <https://doi.org/10.1080/19648189.2016.1217791>.
- [5] Y. Wang, X. Li, Experimental study on cracking damage characteristics of a soil and rock mixture by UPV testing, Bull. Eng. Geol. Environ. 74 (3) (2015) 775–788, <https://doi.org/10.1007/s10064-014-0673-x>
- [6] ASTM D2845, Standard Test Method for Laboratory Determination of Pulse Velocities and Ultrasonic Elastic Constants of RocK, vol. 14, 2000
- [7] T. Hergül, An experimental study on the treatment of expansive soils by granular materials (2012).
- [8] H.B. Nagaraj, M.R. Suresh, Influence of clay mineralogy on the relationship of CBR of fine-grained soils with their index and engineering properties, vol. 15. 2018
- [9] Z. Hameed Majeed, M. Raihan Taha, I. Taha Jawad, Stabilization of soft soil using nanomaterials, Res. J. Appl. Sci. Eng. Technol., 8(4) (2014) 503–509, doi: 10.19026/rjaset.8.999.
- [10] A.K. Mishra, S. Dhawan, S.M. Rao, Analysis of swelling and shrinkage behavior of compacted clays, Geotech. Geol. Eng. 26 (3) (2008) 289–298, <https://doi.org/10.1007/s10706-007-9165-0>
- [11] AASHTO T-193, Standard Method of Test for The California Bearing Ratio, vol. 99, pp. 580–585, 2007, doi: 10.1520/d1883-07



TREATMENT OF DOMESTIC WASTEWATER WITH ANAEROBIC FLUIDIZED MEMBRANE BIOREACTOR (AN-FMBR) AND CONTROL OF MEMBRANE FOULING WITH ADDITION OF GAC

^a Kamran Manzoor*, ^b Sehrish Shoukat, ^c Sher Jamal Khan

a: NICE, SCEE, NUST, Sector H-12, Islamabad, Pakistan, kamranmunzoor@hotmail.com

b: NICE, SCEE, NUST, Sector H-12, Islamabad, Pakistan, shrishraja@gmail.com

c: NICE, SCEE, NUST, Sector H-12, Islamabad, Pakistan, sherjamal77@gmail.com

* Corresponding author: Email ID: kamranmunzoor@hotmail.com

Abstract- A lab scale Submerged Anaerobic Fluidized Membrane Bioreactor (An-FMBR) setup having Granular Activated Carbon (GAC) fluidization medium was used for the treatment of synthetic domestic wastewater and to control membrane fouling. The performance of An-FMBR having chemical oxygen demand (COD) of 517 ± 21 mg/L was investigated at various hydraulic retention times (HRTs) i.e., 12, 8, and 4 hours (h) utilizing different amounts of GAC starting with 5 g/L and increasing the concentration of GAC up to 10 g/L. First, the system was optimized in-terms of HRT without GAC addition. The optimum efficiency of the system was found at 8 h HRT in comparison with all the operating conditions tested. The COD removal of $88\% \pm 1.06\%$, $84\% \pm 0.3\%$, $63\% \pm 1.3\%$ was achieved at respective HRTs of 12, 8, and 4 h. At shorter HRT, membrane's transmembrane pressure increased more rapidly as compared to longer HRT indicating that fouling of membrane was increased at shorter HRT. After optimization of An-FMBR at 8 h HRT, GAC was added to improve the effluent quality standard and to control membrane fouling. The GAC added mainly decreased the protein in the cake layer hence helped in controlling membrane fouling for longer time. The COD removal up to 96% was achieved at 8 HRT with 10 g/L of GAC dosage. The result revealed that at optimized condition of 8 HRT and 10 g/L of GAC dosage enhanced the effluent quality and removal efficiency contributing low membrane fouling propensity.

Keywords- Anaerobic fluidized membrane bioreactor, Chemical oxygen demand, Hydraulic retention time, Granular activated carbon, Membrane fouling control

1 Introduction

Available water sources is under serious threat due to a growing global population with higher expectations for everyday life domestication, harvesting, and production. The demand for the day is to reduce the constantly growing burden on existing water supplies for sustainable growth [1]. The situation will greatly worsen where water is already in shortage such as in middle Asia. By 2025, their growth levels could decline through 6% of GDP due to water-related impacts on agriculture, health, and revenues [2]. Pakistan, once a water surplus country, is now a water deficit country due to the degradation of land and surface water supplies, the prevalence of droughts, and the change of water from agricultural to domestic and industrial use [3]. Water reuse needs time to deal with the problem of scarcity. Wastewater recycling and reuse by treatments are a possible way out of this crisis. A conventional process that succeeds in reducing organic carbon content to 95% is the activated sludge process. However, the major disadvantage of this system includes requirement of



large area, higher hydraulic retention, lower solids retention time which leads to the production of a bulk amount of sludge [4]. Both aerobic and anaerobic processes are part of the biological treatment process. Aerobic biological wastewater treatment systems utilize microbial mixed consortia to turn organic and inorganic contaminants into harmless, environmentally sustainable byproducts. Due to low building, operational, and maintenance costs with the production of biogas, the use of anaerobic systems has now increased but production of biomass is poor and post-treatment effluent is required because of high COD and nutrients and pathogenic agents [5]. Therefore, combination of membrane and biological system has an advantage over conventional process.

Membrane bioreactor is up-to-the-minute wastewater treatment process and is rapidly being employed as a novel method for biological wastewater treatment [6]. Anaerobic treatment has been proposed as an alternate approach due to generate significantly less sludge and biogas production. Anaerobic membrane bioreactors (An-MBR) have been shown to produce good characteristic effluent next to hydraulic retention times (HRT) equivalent with aerobic processes. Membranes restrict microorganism to escape from the reactor, providing for the extended solid retention times (SRT) essential to anaerobic processes along with suitable permeation rate because of separation . Membrane fouling control remains a significant issue for An-MBRs. The most widely used technique for controlling membrane fouling is biogas sparging, which involves recycling the generated biogas into the reactor for scouring effects. The energy requirements for gas sparging, which range from 0.6 to 1.6 kWh/m³, reduce the advantages of An-MBR [7]. To control the membrane fouling, the adsorption of fouling agents by the addition of powdered activated carbon was the primary focus [8]. As an alternative approach recommended utilizing fluidized the GAC particles to clean the surfaces of membrane by scouring known as a staged anaerobic fluidized membrane bioreactor (SAF-MBR) [9]. This concept was the first to demonstrate that membrane fouling could be effectively managed over an extended period using a percentage of solid medium, such as GAC [10].

In this study, lab-scale An-FMBR was utilized to treat the domestic wastewater to investigate the noteworthy aspect of this paper is its emphasis on controlling membrane fouling by adjusting HRT and GAC. Also, comparison of reactor performance, membrane fouling frequency, and energy consumption with and without GAC fluidization was also evaluated. COD, alkalinity, and volatile fatty acids (VFAs), oxidation reduction potential were also evaluated.

2 Materials and Methods

2.1 Synthetic Wastewater Characteristics.

Synthetic wastewater solution as a medium strength domestic wastewater was made using distillate water (DI) and adding into it major organic (macro) nutrients and trace (micro) nutrients [11]. The synthetic wastewater was prepared using analytical grade salts and is shown in Table 1.

Table 1 Synthetic Wastewater Characteristics

Chemical	Formula	Concentration	Unit
Dextrose (glucose)	C ₆ H ₁₂ O ₆	500	mg/L
Ammonium Chloride	NH ₄ Cl	191	mg/L
Potassium di-Hydrogen Phosphate	KH ₂ PO ₄	22	mg/L
Calcium Chloride	CaCl ₂	4.87	mg/L
Magnesium Sulphate	MgSO ₄ .7H ₂ O	4.87	mg/L
Ferric Chloride	FeCl ₃	0.5	mg/L
Cobalt Chloride	CoCl ₂	0.05	mg/L
Zinc Chloride	ZnCl ₂	0.05	mg/L
Nickel Chloride	NiCl ₂	0.05	mg/L

The pH of the low strength synthetic wastewater was maintained in the range of 6.8-7.2 using Sodium Hydrogen Carbonate (NaHCO₃) 100 mg/L.



2.2 Experimental Set-up.

A laboratory scale An-FMBR was established for this research work as shown in schematic Figure 1a and actual picture of a lab scale An-FMBR is shown in Figure 1b. Bioreactor tank has a total volume of 9.18 Litres. A 0.073 m² hollow fiber membrane of PVDF (Mitsubishi Chemical Aqua Solutions Co., Ltd., 50S0070SA, Japan) with a 0.4 μm pore size was used. The PVDF membrane component was immersed in the bioreactor's 7.18L working volume.

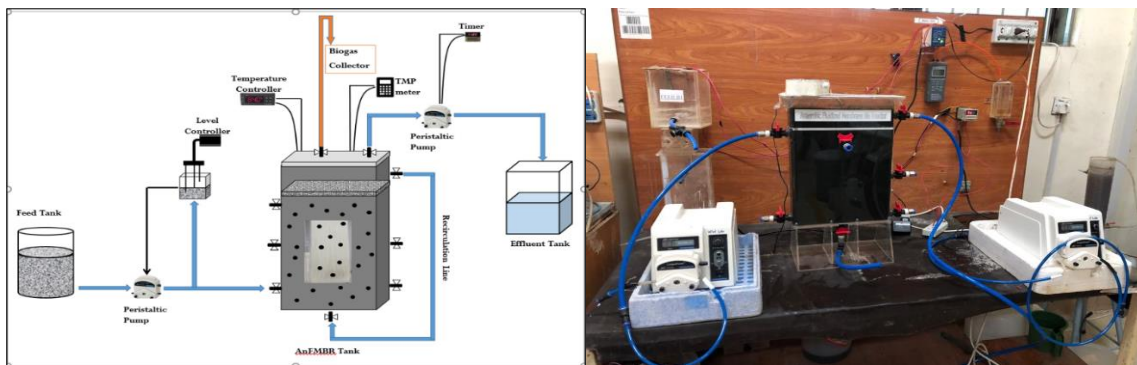


Figure 1. a. Schematic of lab scale An-FMBR, b. Actual picture of lab-scale An-FMBR setup

An An-FMBR setup consisted of a feed tank of 20L, level controller, biogas collection bag, and a permeate collection tank. Slow mixing was provided to increase the shear force on membrane in the anaerobic fluidized digestive tank using a blender (Cole Parmer, 50002-20, USA). The wastewater was fed into the An-FMBR with the help of a peristaltic pump (Longer Precision Pump Co., Ltd, BT300-2J/YZ1515X, China) maintaining the GAC fluidization. A mesh having a sieve size of 1.5 mm was provided below the recirculation line to prevent GAC from going into the recirculation line. To maintain the level of wastewater in the An-FMBR, a relay (Omron, 61F, Japan) was attached to a peristaltic pump. The temperature in the An-FMBR was kept at $35 \pm 1^\circ\text{C}$ using a controller (XMTG 131, China) along with a stainless-steel heating-rod made of stainless steel. To measure the trans membrane pressure (TMP), a TMP meter (Sper Scientific, 840099 15 PSI, USA) attached with membrane port. The permeate was extracted using a peristaltic pump by applying suction pressure to the membrane port. The membrane tank had 8 minutes' permeation and two minutes' relaxation for the membrane in the operating period with the periodic cleaning required once TMP reached close to the 30 kPa.

2.3 Experimental Conditions

The following experimental conditions were elaborated during all phases of the research. HRT of the An-FMBR process was initially maintained at 12 h, but it gradually fluctuated between 12 and 18 h because of a drop in membrane flux. The reactor was first inoculated with the seed sludge which was collected from the constructed wetland operational at NUST H-12 Islamabad, Pakistan having an ORP and pH of -336 mV and 6.9 ± 0.1 , respectively. The sludge was then allowed to acclimatize for 60 days. The influent COD concentration was maintained at 400-550 mg/L. Nitrogen was also purged at the start of every run to bubble off the oxygen gas. The procedure was conducted for 5-7 minutes to guarantee the entire anaerobic atmosphere within the reactor. After establishing the setup, the An-FMBR system was fed with synthetic wastewater comprising of glucose as a substrate. This study was conducted in 2 phases, phase 1 is to optimize HRT while phase 2 for GAC fluidization optimization. Throughout all stages, the system's anaerobic conditions were maintained by measuring pH and ORP regularly. The system was first tested for HRT optimization at 3 different HRTs i.e., 12, 8, and 4 h respectively. After optimizing the HRT at 8 h, the performance study was conducted using granular activated carbon (GAC) particles in the An-FMBR tank. The GAC particles were initially sieved through the mesh size of #10. The GAC particle size was in the range of 2-3 mm. The recirculation line was provided for the fluidization of GAC particles in the tank. In the 1st run at 8 HRT first 5g/ L GAC was added into the tank. The membrane's transmembrane pressure (TMP) was observed. After obtaining the results with 5 g/L GAC, the amount of GAC was increased to 7.5 g/L. After getting the results of An-FMBR at 7.5 g/L GAC, the amount of GAC particles was increased to 10 g/L at 8 HRT and the above-mentioned procedure was repeated.



2.4 Membrane Cleaning and Resistance Analysis

As the membrane became fouled after every filtration run, the module was withdrawn from the reactor and put in pure tap water, where it was washed through clear tap water for 1 h. The total resistance was measured by observing TMP noted throughout this hour (R_t). The cake layer that had deposited on the membrane surface was then removed using a gentle toothbrush and detergent. The membrane was then immersed in tap water for 1 h and water was run through it. The TMP during this filtration gave us the resistance caused by membrane and pore-clogging. Thus, we get resistance due to the cake layer (R_c) by deducting this resistance from the total resistance. After that, the module was immersed in a solution of 5% NaOH and 1% NaOCl for 8 h to remove organic contaminants. After being extracted from the solution, the module was dipped for 24 h in a 1% HCl solution to eliminate inorganic contaminants. To assess the resistance induced by pore-clogging, the module was dipped in tap water again and the water was run filtered through the membrane for 1 h. The TMP generated resistance due to membrane or intrinsic membrane resistance (R_m), which was subtracted from the previous resistance to produce resistance due to pore-clogging (R_p). After that, the membrane was dipped in a washing solution of NaOH and NaOCl, and the solution was circulated through it for about an hour at a flux of 6 LMH.

The total hydraulic resistance was calculated by the equation (1) during the resistance analysis:

$$R_t = \Delta P / \mu J \quad (1)$$

Where, J = operational flux ($\text{L/m}^2 \cdot \text{h}$) or LMH, ΔP = TMP (kPa), μ = viscosity of permeate or Tap water (Pa.s), it can be determined from the already available table of viscosity on internet at specific temperature R_t = total hydraulic resistance (m^{-1}).

2.5 Analytical Methods

The An-FMBR system's treatment efficiency for each condition was evaluated. Closed Reflux Method was used to measure the COD [12]. The water displacement method was used to quantify biogas from An-FMBR. A pH/ORP meter (HI 83141, Hanna Instruments Ltd., UK) was used to measure ORP and pH.

3 Results and Discussion

3.1 Start-up and Acclimatization Phase

The seed sludge was initially maintained under a mesophilic temperature of 35°C for 58 days in the An-FMBR (without membrane module) and a separate bioreactor before the start-up. Bioreactors were fed semi-continuously with low strength domestic wastewater at the same time, at HRT of 12 h. Semi-continuous feeding mode led to solve controlled pH conditions and reduced VFA production [13]. Acclimatization phase was considered complete when COD removal efficiency of system reached up to 60-65%. After completing the Acclimatization phase, a PVDF hollow fiber membrane module was inserted in the An-FMBR system, and an experimental setup was initiated.

3.2 TMP Variations & Membrane Fouling Control

TMP changes were used as a control to check the extent of biofouling in the membrane during optimization study as shown in Figure 2a.

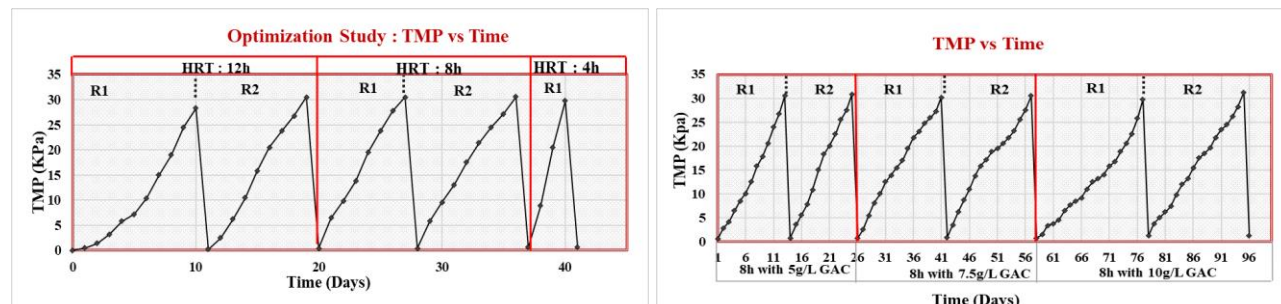


Figure 2. TMP and fouling behaviour changes in An-FMBR, a. Optimized condition, and b. performance with GAC fluidization



When the HRT was reduced, membrane fouling occurred in a short period. Initially, at 12 h of HRT for the first run, the membrane operated for 10 days without cleaning. 8 minutes of permeation period and 2 minutes of relaxation period were implied. On the 10th day, the TMP of the membrane reached up to 30 kPa, and the membrane was taken out of the system for cleaning purposes. The membrane was inserted into the system after cleaning and another run at 12 HRT started. This time membrane operated for 9 days without cleaning. At 12 h HRT membrane fouling cycle was 8 days for both runs. Reduced HRT to 4 h and increased loading rate caused significant h membrane fouling in 4 days.

During performance study, it was observed that increased GAC dosage led the membrane work for a longer period without chemical and physical cleaning. Figure 2b. shows that the membrane fouling cycle was 13 days with the dosage of 5 g/L GAC at 8 h of HRT. When 7.5 g/L GAC was added, TMP increased slowly and, membrane resistance gradually rose till day 17 when TMP reached 30 kPa. When 10 g /L of GAC was applied, TMP increased slower than 7.5 g/L and lasted for 20 days and reached 30 kPa on day 20. As the above results show, GAC supplementation could protect the membrane from rapid biofouling. Without the addition of GAC, rapid severe membrane biofouling was observed during optimization study. It was reported that the supplementation of GAC in a fluidized manner enhanced scouring effect which produced an extra shear effect and reduced membrane resistance. In this study, by increasing the amount of GAC added, better results were achieved. GAC supplementation gives better membrane performance, but the amount of GAC added is also an important in membrane fouling control, sideways with the level of expansion of GAC bed.

3.3 Optimization of HRT and COD removal Performance of An-FMBR with GAC Fluidization

To determine the operating HRT of an An-FMBR system, series of experiments were performed at 3 different HRTs i.e., 12, 8, and 4 h and organic loading rate of 1, 1.5, and 3 kg/m³.day respectively as shown in Figure 3a. After the optimization study, performance of An-FMBR was assess by adding GAC as shown in Figure 3b.

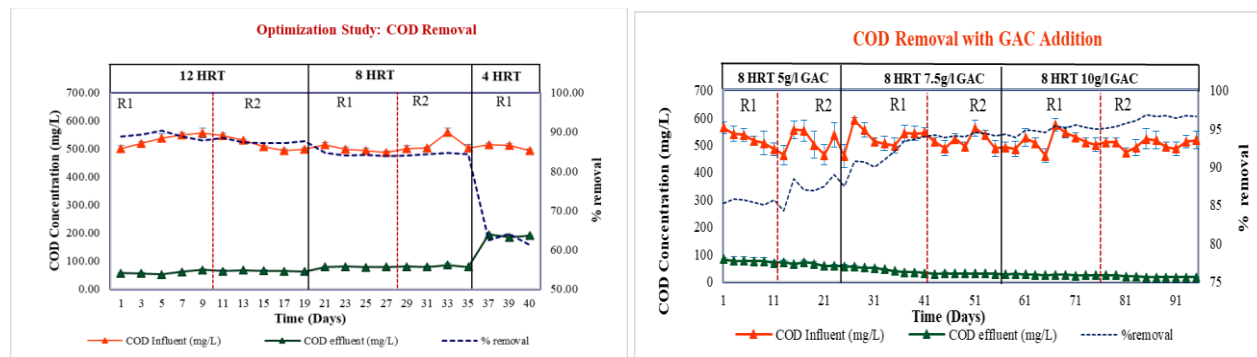


Figure 3. COD removal of An-FMBR during a. optimization of HRT, and b. performance with GAC fluidization

In optimization study, the An-FMBR showed the highest COD removal at HRT of 12 h at the lowest organic loading rate of 1 kg/m³.day and the effluent contained a COD concentration of 61 ± 3 mg/L. Reducing HRT to 8 h and increasing the loading rate to 1.5 kg/m³.day didn't significantly affect the COD removal. While HRT to 4 h and increasing the loading rate to 3 kg/m³.day showed the decreased removal efficiency. The above-mentioned results showed the decreasing trend of COD removal with an increasing loading rate. At shorter HRT biodegradation capacity of microbes become limited developed which leads to decrease in COD removal [14]. Based on the above-mentioned COD removal, the optimum HRT for the system was selected to be 8 h HRT leading to the organic loading rate of 1.5 kg/m³.day for performance study as the system didn't show significant change while reducing HRT from 12 to 8 h.

In performance study, COD removal of An-FMBR system was greatly affected by supplementation and fluidization of GAC. The impact of GAC fluidization was evaluated on membrane fouling. Different dosages of GAC were supplemented at an optimized HRT of 8 h. GAC particles of 2-3 mm were used for fluidization purposes. For each dose of GAC, 2 subsequent runs were performed. The An-FMBR showed the highest percentage of COD removal of 95.6% at an organic loading rate of 1.5 kg/m³.day with a GAC fluidization dosage of 10 g/L. The average concentration of influent and effluent COD was 510 ± 23.3 mg/L and 22 ± 1.1 mg/L respectively. When the GAC dosage was reduced to 7.5 g/L, the average percentage removal of COD was 93%. The average concentration of influent COD was 517 ± 21.7 mg/L and average



effluent contained COD concentration of 35 ± 2.5 mg/L. Further reducing the dosage of GAC supplementation to 5 g/L resulted in average percentage removal of 85.3% with an average influent COD concentration of 519 ± 33.5 mg/L and average effluent concentration of 69 ± 8.2 mg/L.

4 Conclusions

This Study focused on the feasibility of membrane fouling control by GAC supplementation and fluidization in an Anaerobic Fluidized membrane for the treatment of domestic wastewater.

1. To check the performance of lab-scale An-FMBR system, different HRTs were tested including COD removal, phosphate removal and TMP variations for membrane fouling.
2. The greater COD removal efficiency was achieved at 8h HRT and further reducing HRT greatly affected the COD removal efficiency.
3. Supplementation of GAC helped in membrane fouling control and operational time of membrane increased. Higher amount of GAC absorbed more protein from the cake layer. Decreased protein in cake layer allowed longer operational period of membrane.

5 Recommendations

Although GAC has been proven as an important factor for this study, the extent of GAC bed expansion is yet to be determined. Multiple AFMBR systems, such as side-stream, single tank with recirculation, single tank with mixers, are yet to be compared.

Acknowledgment

The authors express their gratitude for the MS Research Grant awarded by the National University of Sciences and Technology (NUST), Islamabad, Pakistan, which provided the necessary financial support for this study.

References

- [1] A.F. Ismail, P.S. Goh, Membrane science and research in Asia and the Middle East: State of the art and perspectives, *J. Membr. Sci. Res.* 5 (2019) 1–2. <https://doi.org/10.22079/JMSR.2018.96997.1226>.
- [2] Janjua, Shahmir, Ishtiaq Hassan, Shoaib Muhammad, Saira Ahmed, and Afzal Ahmed. "Water management in Pakistan's Indus Basin: challenges and opportunities." *Water Policy* 23, no. 6 (2021): 1329-1343. <https://doi.org/10.2166/wp.2021.068>.
- [3] Ishaque, Waseem, Rida Tanvir, and Mudassir Mukhtar. "Climate Change and Water Crises in Pakistan: Implications on Water Quality and Health Risks." *Journal of Environmental and Public Health* 2022 (2022).
- [4] Bera, Sweta Parimita, Manoj Godhaniya, and Charmy Kothari. "Emerging and advanced membrane technology for wastewater treatment: A review." *Journal of Basic Microbiology* 62, no. 3-4 (2022): 245-259.
- [5] L.B. Chu, F.L. Yang, X.W.B. Zhang, Anaerobic treatment of domestic wastewater in a membrane-coupled expanded granular sludge bed (EGSB) reactor under moderate to low temperature. *Process Biochemistry*. (2005) 40, 1063-1070.
- [6] N. Fallah, B. Bonakdarpour, B. Nasernejad, H.M. Moghadam, Long-term operation of submerged membrane bioreactor (MBR) for the treatment of synthetic wastewater containing styrene as volatile organic compound (VOC): Effect of hydraulic retention time (HRT). *J. hazard. materials*, (2010) 178, 718-724.
- [7] D. Martinez-Sosa, B. Helmreich, T. Netter, S. Paris, F. Bischof, H. Horn., Anaerobic submerged membrane bioreactor (AnSMBR) for municipal wastewater treatment under mesophilic and psychrophilic temperature conditions. *Bioresource Technol.*, (2011) 102, 10377-10385.
- [8] A.Y. Hu, D.C. Stuckey, Activated carbon addition to a submerged anaerobic membrane bioreactor: effect on performance, transmembrane pressure, and flux, *J. Environ. Eng.* 133 (2007) 73–80.
- [9] P. L. McCarty, J. Bae, J. Kim, Domestic Wastewater Treatment as a Net Energy Producer—Can This be Achieved? *Environ. Science Technol.* (2011) 45, 7100-7106.
- [10] J. Kim, K. Kim, H. Ye, E. Lee, C. Shin, P.L. McCarty, J. Bae, Anaerobic fluidized bed membrane bioreactor for wastewater treatment, *Environ. Sci. Technol.* 45 (2011) 576–581.
- [11] A. Aslam, S.J. Khan, H.M.A. Shahzad, Impact of sludge recirculation ratios on the performance of anaerobic membrane bioreactor for wastewater treatment, *Bioreour. Technol.* 288 (2019). <https://doi.org/10.1016/j.biortech.2019.121473>.
- [12] APHA, AWWA, WEF, 3120 B. Inductively Coupled Plasma (ICP) Method, Stand. Methods Exam. Water Wastewater, Am. Public Heal. Assoc. (2017) 1–5.



5th Conference on Sustainability in Civil Engineering (CSCE'23)

Department of Civil Engineering

Capital University of Science and Technology, Islamabad Pakistan



- [13] K. Manzoor, S.J. Khan, M. Yasmeen, Y. Jamal, M. Arshad, Assessment of anaerobic membrane distillation bioreactor hybrid system at mesophilic and thermophilic temperatures treating textile wastewater, *J. Water Process Eng.* 46 (2022) 102603. <https://doi.org/10.1016/j.jwpe.2022.102603>.
- [14] H.M.A. Shahzad, S.J. Khan, Zeshan, Y. Jamal, Z. Habib, Evaluating the performance of anaerobic moving bed bioreactor and upflow anaerobic hybrid reactor for treating textile desizing wastewater, *Biochem. Eng. J.* 174 (2021) 108123. <https://doi.org/10.1016/j.bej.2021.108123>.